ISSN 2312-1718

DUET JOURNAL

Volume 10 Issue 1, June 2025

Dhaka University of Engineering & Technology, Gazipur, Bangladesh

DUET Journal Committee

Table of Contents

Integrating UTAUT and TPB Frameworks to Examine Digital Wallet Adoption: Evidence from University Students in a Developing Economy

Afruza Haque

Department of Humanities and Social Sciences, Dhaka University of Engineering & Technology, Gazipur, Bangladesh

ABSTRACT

Digital wallets facilitate financial inclusion by offering secure, accessible, and convenient cashless transactions, enabling the unbanked population to be included in the formal economy. This study intends to examine the determinants influencing higher education learners of a developing country, Bangladesh, towards the uptake of digital wallets. To pursue the research objective, this study integrates the UTAUT and TPB frameworks. To drive deeper insights from different perspectives, this research extended the basic UTAUT model by incorporating two relevant attributes: Perceived Security (PS) and Digital Literacy (DL). A structured questionnaire was administered to elicit responses, yielding 527 responses with a 74% response rate. Structural Equation Modelling (SEM) was conducted to examine the conceptual framework using SmartPLS 4 and SPSS 28.0. The study found that performance expectancy, perceived security, digital literacy, attitude, and perceived behavioral control substantially influence users' intention to adopt digital wallets. Surprisingly, the effects of facilitating conditions and subjective norms on users' intention to use digital wallets are insignificant. This study generates meaningful insights for future research, guiding policymakers, developers, and scholars in crafting policies and strategies to enhance the adoption and expansion of digital wallets for accelerating financial inclusion in Bangladesh.

Keywords: Digital wallet; UTAUT; TPB; Perceived Security (PS); Digital Literacy (DL); Developing Country.

1. INTRODUCTION

In today's world, the rapid expansion of technology across diverse fields is transforming societal norms and frameworks. Widespread internet access and the omnipresence of smartphones have made these cutting-edge technologies and innovations more accessible, fostering a more inclusive ecosystem [1]. The emergence of Industry 4.0 amplified these innovative transformations to enhance digital engagements and reform existing business models and economic pursuits [1]-[3]. Within the context of this economic reformation, digital wallets emerged as a significant technological breakthrough, accelerating how transactions are executed in the digital landscape [4],[5].

A digital wallet is an electronic or online tool that facilitates transactions through a smartphone or computer, removing the need for physical currency [6]. Digital wallets can substitute cash and credit cards, enabling the shift towards a smart, digital, and cashless society [7]. Besides democratizing financial services, digital wallets facilitate payments, savings, and investments and create opportunities for many unbanked and underbanked populations to embrace financial inclusion by ensuring access to digital assets. Digital wallets have been considered an important stimulus in ensuring economic reformation by boosting people's purchasing capacity after the 2020 pandemic [8]. Digital wallet adoption after the COVID period encourages people to reignite commercial activities. Due to all these features, digital wallets are being used as a trusted alternative to conventional transaction methods.

The role of digital wallets in integrating developing countries into an inclusive, sustainable digital economy is undeniable. For Bangladesh's low and middle-income people, mobile fintech services, especially digital wallets, have become the most affordable and accessible options for fintech solutions [9]. Mobile phone subscriptions surpassed 178.61 million as of August 2021, which has a tremendous impact on creating demand for the emergence and use of digital wallets [10]. Digital wallets can significantly enhance financial inclusion, streamline transactions, and support the country's move toward a

*Corresponding author's email: afruza@duet.ac.bd

cashless economy. For university students, who represent a tech-savvy and future-oriented demographic, digital wallets also promote financial independence and digital engagement, making them a crucial target group for fostering long-term adoption and digital transformation in Bangladesh.

Despite their disruptive potential, the uptake of digital wallets in many developing countries remains uneven due to a myriad of behavioral, technological, and socio-cultural factors. To sustain the growth of digital wallet adoption in Bangladesh, all stakeholders, including fintech service providers, need to comprehend the elements that motivate users to embrace digital wallet adoption [11]. Considering the gap, this study examines the factors driving users to adopt digital wallets in their transactions in the context of an emerging country, Bangladesh. Most of the prior studies used different theories and models in isolation to measure users' perception towards technology adoption. However, very few studies attempted to integrate different theories, which can lead to a more comprehensive outcome, suggesting a research gap. To bridge this research gap, this study attempts to explore the synergies between UTAUT and TPB, demonstrating how their integration can illuminate critical adoption pathways.

Numerous researchers have extended the UTAUT model to analyze the uptake of novel technologies, considering different individual and contextual variables [12], [13]. To generate deeper knowledge from different perspectives, this study extends the basic UTAUT model by adding two significant attributes: Perceived Security (PS) and Digital Literacy (DL). Perceived security and digital literacy were specifically chosen for this study because they address two critical concerns in digital wallet adoption within developing economies like Bangladesh. Perceived security reflects users' concerns about the safety of their financial data, which is a major barrier to adoption in areas with limited cybersecurity infrastructure. Digital literacy, on the other hand, captures users' ability to effectively navigate and utilize digital financial tools, an essential factor among university students who may vary in their technological competencies. These constructs provide a more context-sensitive understanding of adoption behavior than traditional UTAUT or TPB variables alone. The primary objective of this paper is to investigate the attributes that affect the adoption of digital wallets among tertiary-level students in the scope of Bangladesh, by integrating the extended UTAUT and TPB frameworks. Additionally, this research acknowledges the unique challenge that exists in developing countries, including low digital literacy.

The remainder of the article is structured as follows: Segment 2 presents the related literature, research framework, and hypothesis development. Segment 3 details the methodology, Segment 4 covers the results of the analysis, Segment 5 contains a discussion of the findings. Segment 6 contains the implications, and finally, Segment 7 outlines the conclusion of the study.

2. RELATED LITERATURE

2.1 Digital Wallet Insight

In today's advanced fintech industry, digital wallets have emerged as a breakthrough technology that redefines transaction methods. They offer a contemporary solution for storing, managing, and handling digital currency transactions. They also excel in seamless accessibility, intuitive design, and resilient security protocols [1]. Digital wallets significantly contribute to promoting financial inclusion, especially in underdeveloped countries. Ref. [14] opined that digital wallet promotes financial inclusivity by facilitating transactions through the use of smartphones among unbanked people. In many emerging nations, digital wallets are rapidly gaining popularity, fueled by nationwide digitalization initiatives and the expanding e-commerce sector [1]. Using digital wallets and other digital payment methods has added a unique dimension to Bangladesh's marketing sector. The overall transaction value in Bangladesh's digital payments sector is projected to reach $14.67 billion in 2024 and $26.72 billion by 2027, reflecting a compound annual growth rate (CAGR) of 19.07% [15]. Furthermore, digital wallets have reshaped consumer purchasing behaviors by providing convenient access to information, alternative options, and improved feedback mechanisms. For both consumers and businesses, embracing digital wallets represents more than just a passing trend, it marks a transformative move toward more efficient, transparent, and secure financial transactions. This shift contributes to extended economic growth [16].

Although the application of digital wallets is expanding rapidly, their adoption remains relatively low in developing countries, especially among the rural population. The uptake of digital wallets is hindered by a combination of factors such as inadequate access to stable internet connections, low levels of financial literacy, limited infrastructure for secure transactions, and a general mistrust of digital platforms due to concerns over data privacy, fraud, and the lack of robust customer support systems [17], [18]. One effective way to address these

challenges is to understand the users' perceptions [19]. Focusing on this gap, this study intends to investigate the factors motivating users to uptake and use digital wallets in the context of a developing country, Bangladesh.

2.2 Theories, Model Conceptualization, and Hypotheses Formulation

2.2.1 Extended Unified Theory of Acceptance and Use of Technology (UTAUT) Model

As society undergoes digital transformation, users frequently find themselves compelled to embrace and leverage innovative technologies [15]. Information system research revealed various parameters that impact technology acceptance across different adoption models [20]. Among these, the UTAUT model, proposed by [21], is widely acknowledged as the most influential framework for examining technology uptake and usage. In several technology adoption studies, researchers argue that UTAUT can explain as much as 70% of the variation in user intentions [22], [23]. UTAUT is an extensively used model for analyzing technology uptake and utilization in both individual and organizational contexts, serving as a framework for integrating various technologies across corporate and personal settings [24]. Multiple studies [25], [26] have utilized the UTAUT model to examine the FinTech uptake, examining the aspects driving bank customers' acceptance of key financial technologies. To assess the users' perception and future prospects of digital wallets, this study adopts two variables from basic UTAUT: Performance expectancy (PE) and Facilitating Conditions (FC), and extends the model by incorporating two contextual variables, Perceived Security (PS) and Digital Literacy (DL).

2.2.2 Theory of Planned Behavior (TPB)

TPB was derived from the Theory of Reasoned Action (TRA) [27], which intends to clarify a broad spectrum of human behaviors, widely validated as an effective framework for predicting and understanding human actions across diverse fields [28]. TPB was developed to enhance TRA by overcoming its shortcomings, especially in contexts when individuals lack complete spontaneous control over their actions [29]. TPB comprises three constructs: Subjective Norm (SN), Attitude (AT), and Perceived Behavioral Control (PBC). Numerous studies employed this framework to examine the use behavior and satisfaction in different areas, for example, digital payment systems [30], online learning behavior [31], and smart home technology adoption [32]. In this study, TPB is incorporated with the UTAUT model to predict users' intention to uptake and utilize digital wallets in the context of Bangladesh.

2.2.3 Conceptual Model and Hypothesis Formulation

The proposed conceptual framework is constructed following an in-depth analysis of a wide range of literature on digital wallet adoption. This model introduces a novel perspective by expanding the UTAUT framework through the inclusion of two additional variables, perceived security (PS) and digital literacy (DL), and integrating this extended UTAUT with the TPB framework. The objective is to elucidate the determinants influencing the uptake of digital wallets among the young generations of Bangladesh.

Performance Expectancy (PE)

PE denotes an individual's conviction that digital wallet systems will improve their efficiency and effectiveness in performing tasks [33]. Customers are more interested in embracing digital wallets when they perceive them as offering attractive incentives [34]. Several previous studies have validated PE as a critical factor influencing the Uptake intention of information systems. [33]-[35] revealed that PE plays a pivotal role in the adoption of financial technologies, including mobile payments and digital wallets. Therefore, the author proposes the following hypothesis:

H1. PE has a positive influence on users' intention to use digital wallets.

Facilitating Conditions (FC)

According to [36], FC refers to the extent to which individuals perceive themselves as having the required logistics and knowledge to operate wireless internet-enabled devices for conducting payments through e-wallets or digital wallets. [35] suggest that a well-established organizational and technical infrastructure for digital wallet systems can enhance customers' willingness to uptake digital wallet services. Study [13] found that FC has a positive impact on motivating consumers to adopt change through technological advancements in the context of m-bankuing, while [37], [38] revealed that the relation between FC and intention to use is not significant in the domain of m-payment services. Therefore, this study suggests the following hypothesis:

H2. FC positively influences users' intention to use digital wallets.

Perceived Security (PS)

PS denotes the degree to which individuals perceive that using mobile payment (m-payment) systems, for example, digital wallets, is safe and protected [33]. Consumers are more likely to conduct financial transactions via digital wallets if they feel confident that their confidential data is secure. Numerous studies have identified PS as a motivating feature in impacting the uptake of financial technologies. Studies [33], [35], [39] have shown a positive association between PS and m-payment service adoption intention. Interestingly, study [40] discovered that PS did not have an encouraging effect on the mode choice intention of autonomous vehicles in Malaysia. Hence, the following hypothesis is proposed:

H3. PS positively influences users' intention to use digital wallets.

Digital Literacy (DL)

DL refers to the capability to proficiently and critically navigate, assess, and generate information through various digital technologies [41]. In the context of digital wallets, DL implies the ability to effectively and safely use digital payment systems, including understanding how to set up, navigate, and manage digital wallets, as well as recognizing and mitigating potential security risks associated with online transactions. Earlier research has verified that DL has a strong favorable association with users' intention to adopt financial technologies. Study [41] revealed that DL facilitates digital transaction adoption intention. Study [42] discovered DL as a significant determinant of women's online shopping behaviour. Therefore, the following hypothesis is formulated:

H4. DL positively influences users' intention to use digital wallets.

Attitude (AT)

Attitude refers to a tendency to react positively or negatively to a behavior, along with a predisposition toward an individual's interest in adopting a specific technological innovation [43]. Empirical findings highlight the importance of attitude in influencing behavioral intentions [44]. Numerous studies support that a positive attitude toward digital wallets significantly influences users' decision-making towards fintech, for example, e-wallets and boosts their acceptance and usage [45], [46]. Therefore, the following hypothesis is developed:

H5. Attitude is strongly associated with users' intention to use digital wallets.

Subjective Norms (SN)

SN denotes the perceived social influence to either engage in or refrain from a particular behavior [43]. Both theoretically and empirically, SN plays a critical role in stimulating the intention to uptake novel inventions, including digital wallets. [29] found that digital wallet influences customer satisfaction and continuance intention of e-services. Study [44] revealed a positive association between SN and use intention in the context of e-wallet. Study [47] demonstrated how SN positively affects Muslim Millennials' and Gen Z's intention to use digital wallets in Banjarmasin. Underscoring the impact of SN on the adoption of digital wallets, this study proposes the following hypothesis.

H6. SN has a significant impact on the intention to use digital wallets.

Perceived Behavioral Control (PBC)

PBC reflects an individual's belief in the ease or difficulty of acting and measures the extent to which they feel in control of carrying out a behavior [43]. PBC is essential in influencing an individual's intention to embrace emerging technologies [29]. [48] demonstrated that PBC significantly influences users' e-wallet adoption behavior in Malaysia. Consequently, this study proposes:

H7. PBC has a significant effect on users' intention to use digital wallets.

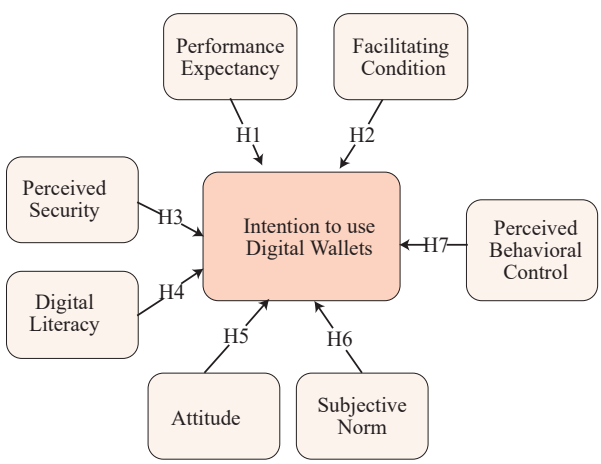

Fig. 1: Conceptual Research Framework (Authors' Creation)

3. METHODOLOGY

3.1 Constructs for Measurement

The list of measurement components and their corresponding sources is presented in Table I to confirm the validity of all perceived variables for the latent components in the research model that was formulated from prior data.

Table I: Measurement Constructs of the Study

Constructs	Corresponding items	Sources
Performance Expectancy (PE)	PE1: I would find digital wallets useful in my job. PE2: Digital wallets enable me to accomplish tasks more quickly. PE3: Digital wallets can improve my productivity. PE4: Overall, I find digital wallets beneficial in my daily life.	[13], [23], [49]
Facilitating Condition (FC)	FC1: I have knowledge of using digital wallets. FC2: I have resources (e.g. Smartphone) to use digital wallets. FC3: Digital wallets are compatible with other systems I use. FC4: If I face any problem using digital wallets, I can solve it quickly.	[23], [49], [50]
Perceived Security (PS)	PS1: Digital wallets are trustworthy. PS2: Digital wallets can protect my financial information. PS3: The security system adopted by the digital wallets are reliable.	[51]
Digital Literacy (DL)	DL1: My technical skills enable me to access and use advanced features of digital wallets. DL2: My knowledge of digital tools encourages me to try out new digital wallets. DL3: I feel confident resolving technical issues while using digital wallets. DL4: Digital wallets seem intuitive and user-friendly because of my digital literacy.	[52]
Attitude (AT)	AT1: Using digital wallets would be beneficial for me. AT2: I believe the use of digital wallets would improve the quality of my life. AT3: Using digital wallets is a good choice for my financial management. AT4: I enjoy the use of digital wallets.	[45], [46]
Subjective Norms (SN)	SN1: People who are important to me encouraged my use of digital wallets. SN2: People who influenced my behavior wanted me to use digital wallets instead of any alternative means. SN3: People whose opinions I valued preferred that I use digital wallets for managing transactions SN4: I am more likely to use digital wallets if my friends and family use them.	[29], [47], [53]
Perceived Behavioural Control (PBC)	PBC1: I could use digital wallets well to manage financial transactions. PBC2: Using digital wallets entirely within my control. PBC: I had the resources, knowledge, and ability to use digital wallets.	[29], [48]
Intention to Use (IU)	IU1: I plan to use digital wallets in the future. IU2: I intend to continue to use digital wallets frequently. IU3: I am used to digital wallet services.	[12], [23]

3.2 Population and Sampling

The target population of this research comprises digital wallet users across different age groups of university students in a developing country. The author chose the convenience sampling method to select respondents for the study. This study employed Structural Equation Modeling (SEM) to investigate the relationships between latent variables, as outlined by [54]. The literature on determining sample sizes for different types of data

analytics illustrates a notable divergence in perspectives [55]. A sample size of 200 is usually considered adequate, while a sample size of 300 is deemed good for conducting data analysis by applying structural equation modeling (SEM) [56]. According to [57], the sample size needs to be at least ten times the number of items in the research study's constructs to do multivariate research. Our study encompasses a total number of 29 constructs, and ten times the constructs become 290. Consequently, the sample size must be at least 290 or above.

3.3 Data Collection

710 questionnaires were circulated to the contributors via an online link forwarded to their email, accompanied by a deadline. A reminder email was sent to those who did not reply within the time frame given. The data was collected from March 26 to August 25, 2024. After removing outliers and treating missing data, 527 full questionnaires were obtained from the 593 returned questionnaires. The response rate for this study is 74%. As demonstrated in the preceding part (3.1), the sample size should be greater than or equal to 290, however, the sample size of 527 is more suitable to employ the SEM approach. A total of 527 questionnaires were examined for further statistical analysis. Respondents participated in this research voluntarily, and no compensation was provided.

3.4 Analytical Method

In this study, descriptive statistical analysis was performed using SPSS 28.0. Besides this, the author utilizes the Partial Least Squares (PLS) method, a statistical approach adapted from SEM, to analyze and validate the suggested framework and the relationships among the anticipated constructs. According to [58], SEM is a widely recognized approach for evaluating the rationality of a hypothesis through empirical data [58]. SmartPLS is a prominent software package for PLS-SEM data assessment [54]. To perform the required statistical analysis, including developing a research model and calculating a measurement model, the data is initially loaded into Microsoft Excel (.csv) and subsequently imported into the SmartPLS software.

4. RESULTS

4.1 Demographic Traits of Participants

Table II demonstrates a breakdown of the demographic details of this study involving 527 participants. The table presents distributions based on gender, age, education level, and digital wallet usage frequency. The majority of contributors in this study are male, 411 individuals (78%), while females represent a smaller proportion, comprising 116 individuals (22%). In terms of age distribution, the largest portion of participants, 481 individuals (91.3%), fall within the 20-25 age group, making this the dominant category, while a smaller proportion, comprising 37 individuals (7.0%), belong to the 26-30 age group. Only a negligible percentage of respondents are below 20 years old (0.2%) and above 30 years old (1.5%), demonstrating that the sample predominantly consists of young adults. Regarding educational level, 515 individuals (97.7%) of respondents were undergraduate students, while only 12 (2.3%) were graduate students. The study examined how often users use digital wallets and revealed that 32.8% of respondents use digital wallets often, 25.6% frequently, and 19.5% always. Nonetheless, 22% of participants still use digital wallets rarely. This implies a high level of digital wallet adoption, though some participants' usage remains limited.

Table II: Demographic Details of Participants

Variable	Description	Frequency (n=527)	Percentage (%)
Gender	Male	411	78.0%
	Female	116	22.0%
Age	Below 20	1	0.2%
	20-25	481	91.3%
	26-30	37	7.0%
	Above 30	8	1.5%
Education	Undergraduate	515	97.7%
	Postgraduate	12	2.3%
Digital Wallet use	Rarely	116	22.0%
	Often	173	32.8%
	Frequently	135	25.6%
	Always	103	19.5%

4.2 Measurement Model

In this study, Composite Reliability (CR), Average Variance Extracted (AVE), and Cronbach's alpha were evaluated following established criteria to ascertain the validity and reliability of each construct [59], [60]. This reliability test investigates the precision and uniformity of the research instruments. The findings indicate a strong internal integrity across all components. A Cronbach's Alpha coefficient exceeding 0.70 confirms internal consistency and reliability in the study's methodology [60]. Table III exhibits that Cronbach's alpha values range from 0.751 to 0.929, indicating the study's internal consistency.

Convergent validity assesses the extent to which the variables of a hypothesis align, as indicated by the AVE. In this study, the AVE value ranged from 0.573 to 0.875, exceeding the required threshold value of 0.5 [59], [60]. This confirms that a significant proportion of the variance in the constructs is elucidated by the items correlated with them. Consequently, it supports the convergent validity of the measurement model.

The substantial Composite Reliability (CR) values, which are above the threshold of 0.7 and fall between 0.754 to 0.929, demonstrate the internal consistency and reliability of the measurement model [59], [60]. The results provide strong evidence of the validity and reliability of the study's measurement methods. Consequently, they reinforce the credibility and validity of the constructs, confirming their appropriateness for assessing the factors influencing students' intention to use digital wallets.

Table III: Convergent Validity and Internal Reliability

Constructs	Items	Loadings	Cronbach's Alpha	Composite Reliability	Average Variance Extracted (AVE)
Performance Expectancy (PE)	PE1	0.837	0.843	0.844	0.680
	PE2	0.849			
	PE3	0.807			
	PE4	0.805			
Attitude (AT)	AT1	0.748	0.751	0.754	0.573
	AT2	0.805			
	AT3	0.746			
	AT4	0.727			
Digital Literacy (DL)	DL1	0.826	0.848	0.849	0.687
	DL2	0.852			
	DL3	0.793			
	DL4	0.842			
Facilitating Condition (FC)	FC1	0.815	0.789	0.793	0.614
	FC2	0.828			
	FC3	0.771			
	FC4	0.715			
Subjective Norms (SN)	SN1	0.857	0.837	0.843	0.674
	SN2	0.852			
	SN3	0.729			
	SN4	0.840			
Perceived Security (PS)	PS1	0.937	0.929	0.929	0.875
	PS2	0.951			
	PS3	0.919			
Perceived Behavioural Control (PBC)	PBC1	0.914	0.884	0.885	0.812
	PBC2	0.914			
	PBC3	0.875			
Intention to Use (IU)	IU1	0.854	0.795	0.796	0.710
	IU2	0.843			
	IU3	0.830			

4.2 Structural Model Evaluation

The structural model explores the causal relationships among the latent constructs of a given model [61]. This study examines the SEM to assess the associations among variables. The following model (Fig. 2) was created using SmartPLS, and the results demonstrate the p-values and cross-loadings for analyzing the direct associations between dependent and independent constructs.

This research measures the statistical weighting of the path coefficient using the bootstrapping method (resampling = 5000) [59]. The association between independent and dependent variables is analyzed by measuring t-values and assessing significance at the 0.05 level ($P < 0.05$). Additionally, Bias-Corrected Confidence

Intervals (BCI LL-UL) are evaluated to determine the significance of the hypothesized links [60]. The PLS results for the structural model are presented in Table IV. The outcomes indicate a significant correlation between the variables: PE and IU ($\beta = 0.150$, $P = 0.003$), PS and IU ($\beta = 0.298$, $P = 0.000$), DL and IU ($\beta = 0.237$, $P = 0.000$), AT and IU ($\beta = 0.125$, $P = 0.019$), and PBC and IU ($\beta = 0.095$, $P = 0.013$).

Hence, H1, H3, H4, H6, and H7 were confirmed at a significance level of 0.05 ($P < 0.05$).

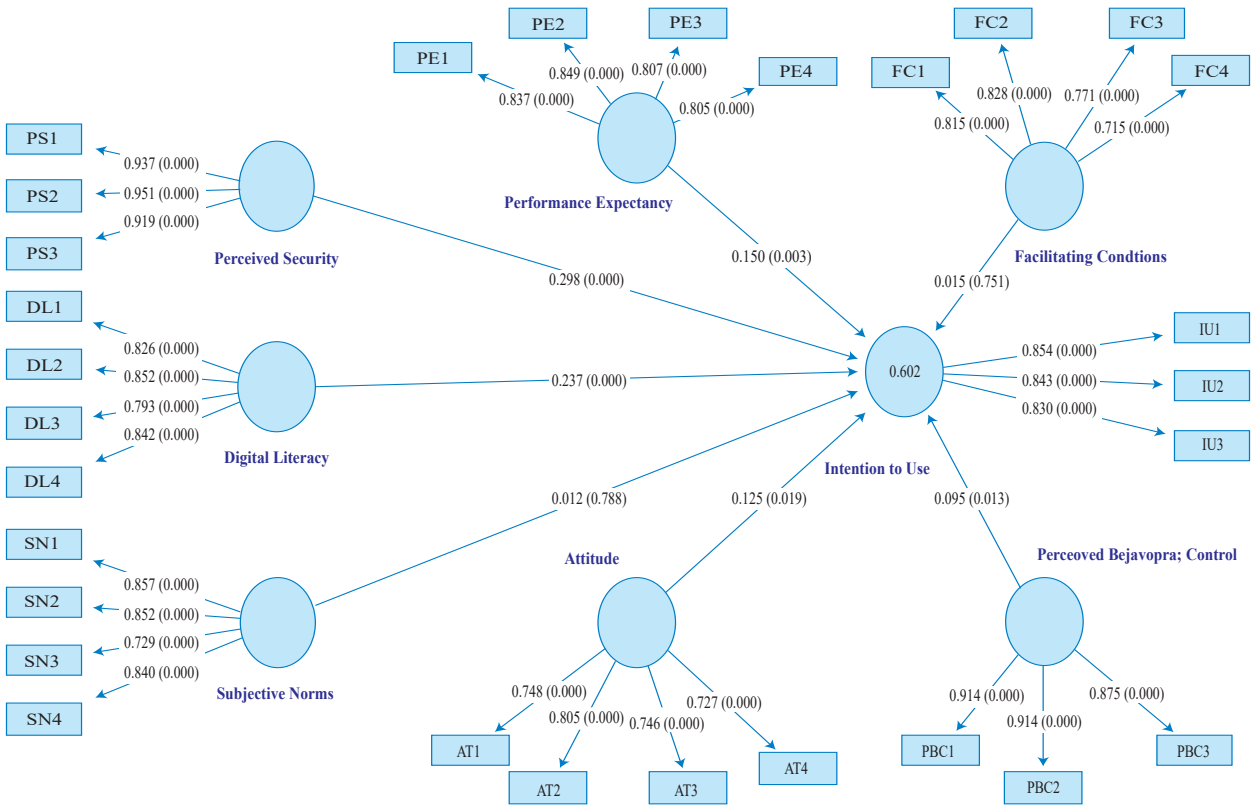

Fig. 2: Path Diagram with P-Values and Path Coefficient

Studies conducted the Variance Inflation Factor (VIF) calculation for every association to assess collinearity and to avoid biases in regression findings [61]. A VIF greater than 3.3 is considered an indicator of pathological collinearity and a potential sign of common method bias (CMB) affecting the model. Therefore, if all VIF values in the inner model are 3.3 or lower, the model can be deemed free from common method bias [62]. Since all of the values of VIF demonstrated in Table IV are less than 3.3, it is confirmed that the model is devoid of common method bias.

Notably, f^2 indicates the effect size, with values exceeding 0.35, 0.15, and 0.02 representing large, medium, and small effect sizes, respectively [63]. According to [63], the study found that the associations between PS and IU (H3: $f^2 > 0.35$) and DL and IU (H4: $f^2 > 0.35$) exhibit a highly significant effect size and the relationship between PE and IU (H1: $f^2 > 0.15$) and PBC and IU (H8: $f^2 > 0.15$) indicates a moderate effect size.

Table IV: Structural Model Evaluation for Direct Associations

H	Relations	Std Error	T values	P values*	BCI LL	BCI UL	f^2	VIF	Decision
1	PE-> IU	0.051	2.965	0.003	0.054	0.250	0.322	2.630	Supported
2	FC-> IU	0.049	0.317	0.751	-0.078	0.114	0.004	2.368	Not Supported
3	PS-> IU	0.049	6.130	0.000	0.202	0.395	0.436	2.092	Supported
4	DL-> IU	0.062	3.827	0.000	0.116	0.358	0.547	2.973	Supported
5	SN-> IU	0.045	0.269	0.788	-0.071	0.103	0.010	1.778	Not Supported
6	AT -> IU	0.053	2.346	0.019	0.024	0.231	0.027	2.287	Supported
7	PBC-> IU	0.038	2.496	0.013	0.016	0.165	0.324	1.615	Supported

*at the significance level of < 0.05.
Note: PE = Performance Expectancy, FC = Facilitating Conditions, PS = Perceived Security, DL = Digital Literacy, SN = Subjective Norm, AT = Attitude, PBC = Perceived Behavioural Control

5. DISCUSSION

The study intends to explore the attributes impacting users' intention to adopt digital wallets in conducting financial transactions. The UTAUT model has been expanded to include perceived security and digital literacy, as these factors are particularly relevant to the area of financial technology. This research integrates the extended UTAUT and TPB models to develop a comprehensive framework for predicting users' intention to uptake and utilize digital wallets, combining the strengths of both models in explaining technology acceptance and behavioral intentions towards digital payments. Hence, this study has put forward seven hypotheses, which were evaluated using PLS-SEM. The study disclosed that all the determinants, except FC and SN, have a direct impact on users' intention to adopt digital wallets, as demonstrated in Table IV.

The results exposed a robust positive correlation between PE and IU, which aligns with the research of [49] and [64]. The findings imply that users exhibit strong enthusiasm for adopting digital wallets, provided that this fintech system offers tangible benefits. [65] suggested that due to the young generations' internet usage and comfort with technology, performance has become a key concern for them in adopting digital payment systems such as digital wallets. In particular, the ability to conduct financial transactions more easily and quickly is a key motivator in attracting young users to adopt digital wallets.

The present study exposes that FC is an insignificant predictor of digital wallet adoption by Bangladeshi users, which contradicts the study [35]. This is a novel finding of this study. One possible reason may be that the infrastructure limitations or lack of awareness about available support systems may diminish the perceived importance of facilitating conditions in adoption.

The study manifests that PS significantly influences IU in the context of digital wallets. The majority of authors agreed with the findings and stated that security is the main reason why consumers choose digital wallets over traditional ones [33], [35], and [39]. [65] asserted that the young generation considers security to be their top priority. The finding suggests that the ability of digital wallet systems to safeguard financial and informational privacy is a critical attribute contributing to the uptake of financial technology.

Digital Literacy (DL), integrated to extend the UTAUT model in this study, has a noteworthy influence on users' intention to use digital wallets, which aligns with the findings of [52]. Digital literacy enhances users' ability to navigate digital payment systems, including digital wallets, fostering confidence in adopting digital wallets [41], [42]. Digital literacy can increase security awareness, reducing concerns about fraud and data breaches while ensuring smoother interactions with payment apps. Digitally literate users perceive digital wallets as convenient, efficient, and aligned with technological advancements, encouraging adoption. Additionally, exposure to online financial trends and peer influence motivates them to embrace digital transactions. By improving technological competence and financial inclusion, digital literacy empowers individuals to integrate digital wallets into their daily financial activities.

The study also unveiled a positive relationship between attitude and intention to use digital wallets. This finding aligned with the research conducted by [45], [46]. This outcome implies that attitude significantly influences digital wallet adoption as users with an optimistic perception of convenience, security, and intuitiveness have a higher tendency to embrace the technology.

Favorable attitudes enhance trust and reduce resistance to digital transactions, encouraging widespread adoption.

The observed association between SN and IU is found to be negative, a novel finding of this study, which contradicts the studies [44], [47]. This insignificance may stem from cultural factors such as individualistic decision-making among students or infrastructural elements like widespread access to digital services, which reduce reliance on social influence, as users increasingly prioritize personal convenience and perceived benefits over social pressure when making technology adoption decisions. Unlike other technologies where peer or family recommendations play a crucial role, digital financial transactions involve trust and risk considerations, making individual judgments more important. As a result, users may adopt digital wallets based on their own needs and confidence in the system rather than societal expectations.

The result reveals that PBC and users' IU regarding digital wallets are positively associated. This outcome supports the findings of the study [29] and [48]. If users feel they possess enough knowledge, facilities, and control over potential risks, they are more prone to adopt digital wallets.

6. THEORETICAL AND PRACTICAL IMPLICATIONS OF THE STUDY

6.1 Theoretical Implications

This study contributes to the literature by integrating the UTAUT with the TPB framework to provide a thorough understanding of digital wallet adoption among university students in a developing country. Although theoretical bases such as UTAUT and TPB have been extensively employed in technology adoption settings, they are frequently examined in isolation. To bridge this research gap, this study blended UTAUT and TPB models to extensively examine the dual cognitive pathways of users' use intention in the context of digital wallets. By examining seven key factors such as PE, FC, PS, DL, AT, SN, and PBC, the study extends prior research by highlighting the significance of individual perceptions and technological capabilities in influencing adoption intentions. The findings challenge existing assumptions by revealing that FC and SN do not significantly influence digital wallet uptake, indicating that external support and social pressure may be less crucial than personal competence and security considerations. This insight enhances existing theoretical frameworks and offers a nuanced perspective on digital wallet uptake in the scope of a resource-constrained developing country, Bangladesh.

6.2 Practical Implications

From a practical standpoint, the study provides valuable insights for digital wallet providers, policymakers, marketers, and financial institutions seeking to increase the acceptance rates among users in developing countries. The study demonstrates that PS and DL have a notable influence on the users' intention, which suggests that improving digital literacy and addressing security concerns should be prioritized over external facilitation or social influence to drive digital wallet adoption. Developers should focus on designing intuitive interfaces and implementing robust security measures to increase user confidence. Additionally, awareness campaigns regarding the advantages of digital wallets may be more effective than relying on peer influence or infrastructural support. By understanding the primary drivers of adoption, stakeholders can develop targeted strategies that align with user needs, ultimately fostering greater financial inclusion and transformation.

7. CONCLUSION

In a resource-constrained developing country, like Bangladesh, financial innovations play a crucial role in increasing financial inclusion [12]. To assess the uptake intention within the setting of an important financial technology, digital wallet, this study concentrates on identifying the determinants that impact users' intention to uptake and use this technology. By synthesizing the structural and behavioral aspects of UTAUT and TPB models, the study strives to uncover nuanced insights into the stimulators that drive users' intention toward digital wallets. Data were collected using a quantitative research approach from 593 respondents. Thorough data screening ensured the reliability of the final 527 responses, which were analyzed to assess users' intention to adopt digital wallets. This study employs the PLS method, a statistical technique adapted from SEM, to analyze and validate the conceptual model and the associations among the anticipated constructs. By examining seven attributes, the findings reveal that while PE, PS, DL, AT, and PBC significantly influence users' digital wallet adoption, FC and SN do not. These findings imply that for university students within the scope of financial technology uptake, personal perceptions of convenience, security, and technological skills are more influential than external support or social pressure. The study underscores the need for digital wallet providers to focus on enhancing user confidence through improved security measures and digital literacy initiatives. Ultimately, these insights

contribute to refining adoption models and offer practical recommendations for fostering digital wallet usage in developing countries.

Nonetheless, this study has certain limitations. First, it focuses solely on Bangladeshi University students, limiting generalizability; future research could explore other professionals in Bangladesh and other countries for broader insights. Second, while the sample size of this study meets the minimum requirement suggested by [60], future research could collect additional data to enhance the validity of the digital wallet adoption model in financial technology settings. Third, this research ignores the moderating and mediating effects of constructs. Studies in the future may unearth different significant insights by examining the moderating and mediating effects of several contextual and environmental variables, for example, personal innovativeness, technology experience, task-technology fit, and government initiatives. In conclusion, this study makes a significant scholarly contribution to fintech adoption research in Bangladesh by synthesizing the UTAUT and TPB frameworks to elucidate the combined influence of technological, social, and behavioral determinants on digital wallet adoption among university students within a developing economy context.

REFERENCES

[1] T. Kraiwanit, P. Limna, and P. Wattanasin, "Digital wallet dynamics: Perspectives on potential Worldcoin adoption factors in a developing country's FinTech Sector," Journal of Open Innovation: Technology, Market, and Complexity, Vol. 10, No.2, pp. 71-90, 2024.

[2] M. Javaid, A. Haleem, R. P. Singh, R. Suman, and E. S. Gonzalez, "Understanding the adoption of Industry 4.0 technologies in improving environmental sustainability," Sustainable Operations and Computers, Vol. 3, pp. 203-217, 2022.

[3] M. Z. Yaqub, and A. Alsabban, "Industry-4.0-Enabled digital transformation: prospects, instruments, challenges, and implications for business strategies," Sustainability, Vol. 15, No. 11, p. 8553, 2023.

[4] H. M. T. Thaker, N. R. Subramaniam, A. Qoyum, and H. I. Hussain, "Cashless society, e-wallets and continuous adoption," International Journal of Finance & Economics, Vol. 28, No. 3, pp. 3349-3369, 2023.

[5] G. P. Uribe-Linares, C. A. Ríos-Lama, and J. A. Vargas-Merino, "Is There an Impact of Digital Transformation on Consumer Behaviour? An Empirical Study in the Financial Sector," Economies, Vol. 11, No. 5, pp. 132-147, 2023.

[6] F. Kasirye, and S. M. H. Masum, "The effects of e-wallet among various types of users in Malaysia: A comparative study," Asian Journal of Research in Business and Management, Vol. 3, No. 2, pp. 26-41, 2021.

[7] S. K. B. Mohamood, S. H. Hassan, and B. Jamaluddin "Factors affecting e-wallet adoption for cashless society in Malaysia: A conceptual paper," Jurnal Ilmiah Akuntansi, Vol. 11, No. 01, pp. 41-48, 2024.

[8] A. N. Fajar, and P. N. Fanuel, "Investigating the drivers of digital wallet adoption in developing countries: Indonesia perspective," In AIP Conference Proceedings, Vol. 2987, No. 1, pp. 1-7, 2024.

[9] Bangladesh Bank (2022). Bangladesh Mobile Financial Services (MFS) Regulations, 2018. Bangladesh Bank. Available online: https://www.bb.org.bd/openpdf.php (accessed on 16 December 2022).

[10] S. A. M. Anik, M. H. Khan, R. H. Miah, F. Kabir and K. Alam, "Customer Attitude Towards Mobile Financial Services: An Empirical Study on Dhaka City, Bangladesh," International Journal of Business Management & Economic Research, Vol. 12, No. 3, pp. 1918-1928, 2021.

[11] M. S. Hassan, M. A. Islam, F. A. Sobhani, H. Nasir, I. Mahmud, and F. T. Zahra, "Drivers influencing the adoption intention towards mobile fintech services: a study on the emerging Bangladesh market," Information, Vol. 13, No. 7, pp. 349-365, 2022.

[12] N. Sultana, R. S. Chowdhury, and A. Haque, "Gravitating towards Fintech: A study on Undergraduates using extended UTAUT model," Heliyon, Haque, Vol. 9, No. 10, pp. e20731-e20746, 2023.

[13] A. Haque, N. Sultana, Y. S. Kim, and M. A. Amin, "Integration of the UTAUT Model in Mobile Banking Context: The Mediating Role of Personal Innovativeness and Perceived Value," Asia Pacific Journal of Information Systems, Al Amin, Vol. 34, No. 3, pp. 929-956, 2024.

[14] H. Taherdoost, "Fintech: Emerging trends and the future of finance," Financial technologies and DeFi: a revisit to the digital finance revolution, pp. 29-39, 2023.

[15] Statista. (2023). Digital Payments - Bangladesh | Statista Market Forecast. Available: https://www.statista.com/outlook/dmo/fintech/digital-payments/Bangladesh

[16] M. Palmié, J. Wincent, V. Parida, and U. Caglar, "The evolution of the financial technology ecosystem: An introduction and agenda for future research on disruptive innovations in ecosystems," Technological forecasting and social change, Vol. 151, Pp. 119779, 2020.

[17] N. P. Rana, S. Luthra, and H. R. Rao, "Assessing challenges to the mobile wallet usage in India: an interpretive structural modelling approach," Information Technology & People, Vol. 36, No. 4, 1533-1554, 2023.

[18] M. A. Sait, M. A. Ali, M. N. Almunawar, and H. M. Haji Masri, "Understanding factors to digital wallet discontinuance intention among past users: An exploratory study," Journal of Science and Technology Policy Management, 2024.

[19] C. Kim, "Understanding Factors Influencing Generative AI Use Intention: A Bayesian Network-Based Probabilistic Structural Equation Model Approach," Electronics, Vol. 14, No. 3, pp. 530-548, 2025.

[20] M. M. Abbad, "Using the UTAUT model to understand students' usage of e-learning systems in developing countries," Education and information technologies, Vol. 26, No. 6, pp. 7205-7224, 2021.

[21] V. Venkatesh, M. G. Morris, G. B. Davis and F. D. Davis, "User acceptance of information technology: Toward a unified view," MIS quarterly, pp. 425-478, 2003.

[22] S. Akter, J. D'Ambra, P. Ray, and U. Hani, "Modelling the impact of mHealth service quality on satisfaction, continuance and quality of life," Behaviour & Information Technology, Vol. 32, No. 12, pp.1225-1241, 2013.

[23] V. Venkatesh, J. Y. Thong, and X. Xu, "Consumer acceptance and use of information technology: extending the unified theory of acceptance and use of technology," MIS quarterly, pp. 157-178, 2012.

[24] K. Tamilmani, N. P. Rana, N. Prakasam, and Y. K Dwivedi, "The battle of Brain vs. Heart: A literature review and meta-analysis of "hedonic motivation" use in UTAUT2," International Journal of Information Management, Vol. 46, pp. 222-235, 2019.

[25] G. Baptista, and T. Oliveira, "Understanding mobile banking: The unified theory of acceptance and use of technology combined with cultural moderators," Computers in human behavior, Vol. 50, pp. 418-430, 2015.

[26] R. Sharma, G. Singh, S. Sharma, "Modelling internet banking adoption in Fiji: A developing country perspective," International Journal of Information Management, Vol. 53, pp. 102116, 2020.

[27] I. Ajzen and M. Fishbein, "Understanding attitudes and predicting social behavior," Englewood Cliffs, NJ: Prentice-Hall, 1980.

[28] F. D. Davis, R. P. Bagozzi, and P. R. Warshaw, "User acceptance of computer technology: A comparison of two theoretical models," Management science, Vol. 35, No. 8, pp. 982-1003, 1989.

[29] C. Liao, J. L. Chen, and D. C. Yen, "Theory of planning behavior (TPB) and customer satisfaction in the continued use of e-service: An integrated model," Computers in human behavior, Vol. 23, No. 6, pp. 2804-2822, 2007.

[30] T. T. Linh and N. T. T. Huyen, "An extension of Trust and TAM model with TPB in the adoption of digital payment: An empirical study in Vietnam," F1000Research, Vol. 14, pp. 127-148, 2025.

[31] S. Mathur, A. Tewari, S. Vishnoi, and V. Agarwal, "An integrated model to predict students' online learning behavior in emerging economies: a hybrid SEM–ANN approach," Journal of International Education in Business, Vol. 18, No. 1, pp. 102-126, 2025.

[32] L. Leung, and M. Cheung, "The effects of technology readiness, risks, and benefits on smart home technology adoption: extending the Theory of Planned Behavior model," Media Asia, Vol. 52, No. 1, pp. 80-101, 2025.

[33] Y. Zhao, and F. Bacao, "How does the pandemic facilitate mobile payment? An investigation on users' perspective under the COVID-19 pandemic," International journal of environmental research and public health, Vol. 18, pp. 1016, 2021.

[34] K. Al-Saedi, M. Al-Emran, T. Ramayah, and E. Abusham, "Developing a general extended UTAUT model for M-payment adoption," Technology in society, Vol. 62, pp. 101293-101303, 2020.

[35] K. Moorthy, L. Chun T'ing, K. Chea Yee, A. Wen Huey, L. Joe In, P. Chyi Feng, and T.Jia Yi, "What drives the adoption of mobile payment? A Malaysian perspective," International Journal of Finance & Economics, Vol. 25, No. 3, pp. 349-364, 2020.

[36] A. C. Teo, G. W. H. Tan, K. B. Ooi, T. S. Hew an K. T. Yew, "The effects of convenience and speed in m-payment," Industrial management & data systems, Vol. 115, No. 2, pp. 311-331, 2015.

[37] M. F. Wei, Y. H. Luh, Y. H. Huang and Y. C. Chang, "Young generation's mobile payment adoption behavior: Analysis based on an extended UTAUT model," Journal of theoretical and applied electronic commerce research, Vol. 16, No. 4, pp. 618-637, 2021.

[38] J. M. Lee, B. Lee, and J. Y. Rha, "Determinants of mobile payment usage and the moderating effect of gender: Extending the UTAUT model with privacy risk," International Journal of Electronic Commerce Studies, Vol. 10, No. 1, pp. 43-64, 2019.

[39] T. Oliveira, M. Thomas, G. Baptista and F. Campos, "Mobile payment: Understanding the determinants of customer adoption and intention to recommend the technology," Computers in human behavior, Vol. 61, pp. 404-414, 2026.

[40] P. Jing, H. Huang, B. Ran, F. Zhan and Y. Shi, "Exploring the factors affecting mode choice Intention of autonomous vehicle based on an extended theory of planned behavior—A case study in China," Sustainability, Vol. 11, No. 4, pp. 1155, 2019.

[41] H. Mansour, "How successful countries are in promoting digital transactions during COVID-19," Journal of Economic Studies, Vol. 49, No. 3, pp. 435-452, 2022.

[42] M. Mahmood, S. H. Batool, M. Rafiq, and M. Safdar, "Examining digital information literacy as a determinant of women's online shopping behavior," Information technology & people, Vol. 35, No. 7, pp. 2098-2114, 2022.

[43] I. Ajzen, The Theory of planned behavior. Organizational Behavior and Human Decision Processes, 1991.

[44] D. I. Berlianawati, Nurabiah, and R. Ridhawati, "Exploring the Mind of Gen Z: Deciphering E-wallet Adoption Through the Lens of TPB Theory", Jurnal Ilmiah Akuntansi Dan Bisnis, Vol. 19, No. 1, pp. 133-150, 2024.

[45] A. P. Johan, N. Lukviarman, and R. E. Putra, "Continuous intention to use e-wallets in Indonesia: The impact of e-wallets features," Innovative Marketing, Vol. 18, No. 4, pp. 74-85, 2022.

[46] M. G. Senali, M. Iranmanesh, F. N. Ismail, N. F. A. Rahim, M. Khoshkam and M. Mirzaei, "Determinants of intention to use e-Wallet: Personal innovativeness and propensity to trust as moderators," International Journal of Human–Computer Interaction, Vol. 39, No. 12, pp. 2361-2373, 2023.

[47] H. Humaida, Z. Mubarak, and R. Yuliani, "Looking into what makes Muslim millennial and generation Z want to use digital wallets in Banjarmasin," Jurnal Ilmiah Ekonomi Islam, Vol. 9, No. 1, pp. 748-754, 2023.

[48] N. A. Abdul-Halim, A. Vafaei-Zadeh, H. Hanifah, A.P Teoh, and K. Nawaser, "Understanding the determinants of e-wallet continuance usage intention in Malaysia," Quality & Quantity, Vol. 56, No. 5, pp.3413-3439, 2022.

[49] K. Gupta, and N. Arora, "Investigating consumer intention to accept mobile payment systems through unified theory of acceptance model: An Indian perspective," South Asian Journal of Business Studies, Vol. 9, No. 1, pp. 88-114, 2020.

[50] P. Ifinedo, "Technology acceptance by health professionals in Canada: An analysis with a modified UTAUT model", Paper presented at the 2012 45th Hawaii International Conference on system sciences.

[51] L. Lisana, "Factors influencing the adoption of mobile payment systems in Indonesia," International Journal of Web Information Systems, Vol. 17, No. 3, 0-10, 2021.

[52] R. Haryanto, A. A. Bakri, H. E. Samosir, D.L. Idris, T. R. Fauzan, and W. Agustina, "Digital Literacy and Determinants of Online Zakat Payments Lessons from Indonesia Experience with UTAUT," Journal of Law and Sustainable Development, Vol. 11, No. 4, pp. e575-e575, 2023.

[53] I. Ajzen, "The theory of planned behavior: Frequently asked questions," Human behavior and emerging technologies, Vol. 2, No. 4, pp. 314-324, 2020.

[54] J. F. Hair Jr, G. T. M. Hult, C. M. Ringle, M. Sarstedt, N.P. Danks, and S. Ray, "An introduction to structural equation modeling," Handbook of partial least squares: Concepts, methods and applications, pp. 1-29, 2019.

[55] J. F. Hair Jr, G. T. M. Hult, C. M. Ringle, M. Sarstedt, N. P. Danks, and S. Ray, "Partial least squares structural equation modeling (PLS-SEM) using R: A workbook", Springer Nature, pp. 197, 2021.

[56] R. B. Kline, "Principles and practice of structural equation modeling", Guilford publications, 2023.

[57] G. Mandeville, and J. Roscoe, "Fundamental research statistics for the behavioral sciences," Journal of the American Statistical Association, Vol. 66, No. 333, pp. 224. https://doi.org/ 10.2307/2284880.

[58] O. Götz, K. Liehr-Gobbers, and M. Krafft, "Evaluation of structural equation models using the partial least squares (PLS) approach," Handbook of partial least squares: Concepts, methods and applications, Berlin, Heidelberg: Springer Berlin Heidelberg, pp. 691-711, 2010.

[59] J. H. Hair, G. T. M. Hult, and C.M. Ringle, "A Primer on Partial Least Squares Structural Equation Modeling (PLS-SEM)," SAGE, Los Angeles, 2017.

[60] J. F Hair, J. J Risher, M. Sarstedt, C.M. Ringle, "When to use and how to report the results of PLS-SEM," European business review, Vol. 31, No. 1, pp. 2-24, 2019.

[61] M. A. Memon, R. Sallaeh, M. N. R. Baharom, S. M. Nordin, and H. Ting, "The relationship between training satisfaction, organizational citizenship behavior, and turnover intention: A PLS-SEM approach," Journal of Organizational Effectiveness: People and Performance, Vol. 4, No. 3, pp. 267-290, 2017.

[62] N. Kock, "Common method bias in PLS-SEM: A full collinearity assessment approach," International Journal of e-Collaboration, Vol. 11, No. 4, 1-10, 2015.

[63] J. Cohen, "Statistical power analysis for the behavioral sciences," Hillsdale, NJ: Lawrence Erlbaum Associates. Inc, Publishers, 1988.

[64] N. Sobti, "Impact of demonetization on diffusion of mobile payment service in India: Antecedents of behavioral intention and adoption using extended UTAUT model," Journal of Advances in Management Research, Vol. 16, No.4, pp. 472-497, 2019.

[65] T. Francis and F. Hoefel, "True Gen': Generation Z and its implications for companies," McKinsey & Company, Vol. 12, No. 2, pp. 1-10, 2018.

ISSN 2312-1718

DUET JOURNAL

Volume 10 Issue 1, June 2025

Dhaka University of Engineering & Technology, Gazipur, Bangladesh

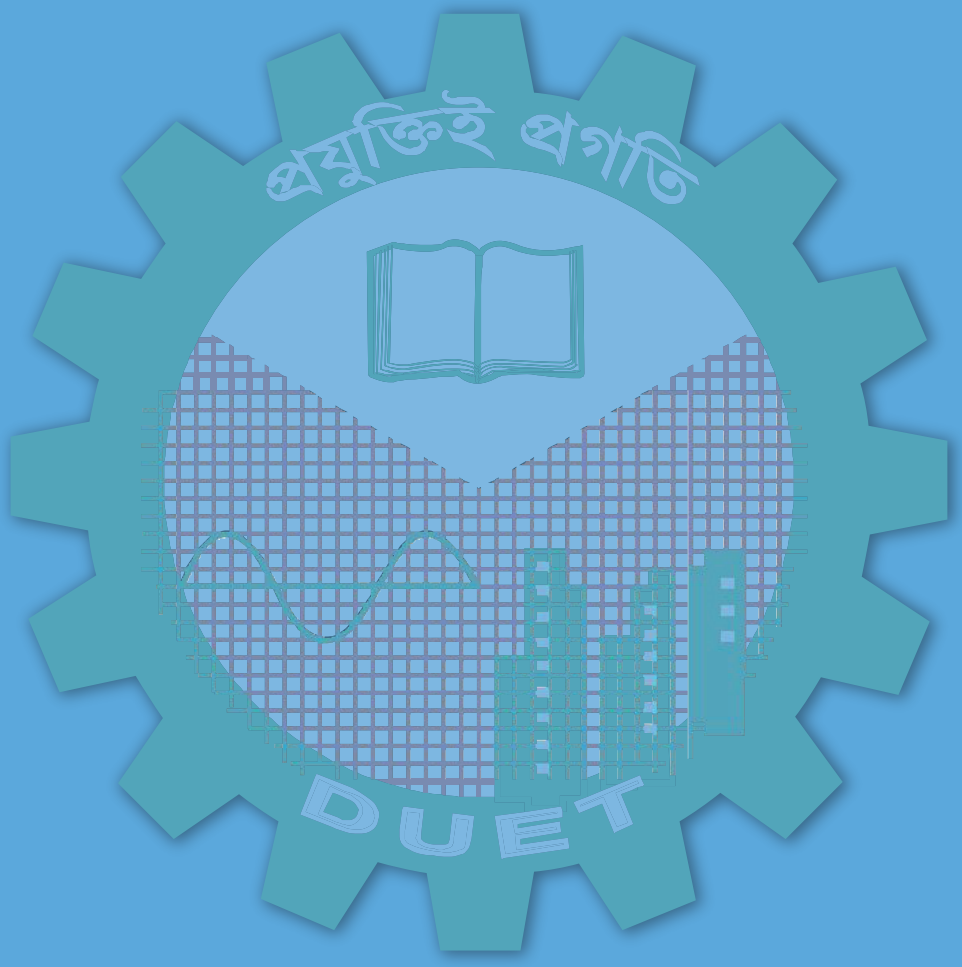

Please visit site: journal.duet.org

Identifying Grammatical Errors in English Academic Writing Tasks of Undergraduate Engineering Students at DUET in Bangladesh

Sanzida Rahman

Department of Humanities and Social Sciences, Dhaka University of Engineering & Technology, Gazipur, Bangladesh

ABSTRACT

This study aims to identify and analyze grammatical and organizational errors in the writing tasks of undergraduate engineering students at Dhaka University of Engineering and Technology (DUET). To assemble data, the researcher has employed two qualitative data collection tools respectively document analysis and semi structured interviews of teachers and students. The study utilized purposive sampling to select participants. Documents were collected from 200 students of 04 (four) departments of Dhaka University of Engineering and Technology. Then, 6 English teachers from Dhaka University of Engineering and Technology and 20 students out of 200 previously participated in document writing were selected for semi-structured interviews. Documents were analyzed using descriptive analysis method and semi-structured interviews were analyzed using thematic analysis method. The findings of the study reveal that students commonly commit errors in verb forms, sentence structure and prepositions. The researcher recommends that teachers focus on addressing common errors, motivating students, using contrastive analysis techniques, providing formative feedback and clear explanations of grammatical errors, incorporating collaborative learning strategies and promoting students' active engagement in the classroom to develop their writing skill.

Keywords: Writing, Error, Intralingual, Interlingual, collaborative

1. INTRODUCTION

Writing is considered the most challenging task among four language skills in the context of English as foreign language or English as second language [1] because it is a creative activity and demands to have complete understanding of all the mechanics, aspects, grammar and organization of the language [2]. EFL learners make errors in the academic writing tasks due to the structural and cultural difference between their mother tongue and the target language and it is very complex since they have challenges in forming ideas, grammar and mechanics [3]. The other challenges include learners' insufficient knowledge of grammar and vocabulary, inadequate application of grammar, lack of motivation and scarcity of creative writing [4, 5]. At the primary and secondary stages of their learning, students from Bangla medium are used to writing academic tasks through memorizing from some particular books. Therefore, learners do not get chance to practice academic writing creatively and consequently they do not develop effective writing skill even after 12 years of schooling and learning English as a major subject.

Proficiency in academic writing at tertiary level is indispensable to understand disciplinary knowledge and to establish in career [6]. Besides, learners need to express their ideas, requirements and thoughts formally to their teachers, peers and employers in English. To that end, they are required to write email, report, proposals, applications, letters, resumes, cover letters, memos, and dissertation [2]. Moreover, learners encounter all academic writing assessments in English, as it is the medium of instruction at the tertiary level. Therefore, to achieve good grades in academic life and succeed in careers, learners must develop strong skills in English writing.

Although mastering academic writing is essential, undergraduate engineering students at Dhaka University of Engineering and Technology (DUET) seem to struggle with this skill. Learners tend to make errors when attempting to convey their ideas in English academic writing tasks, such as, essay writing, summary writing, paragraph writing, assignment and lab reports, etc. It is also experienced that students from engineering program are unable to explain their arguments properly since they are inefficient in English language. English writing skill is vital for engineers to convey ideas logically. Identifying and analyzing the errors of learners' speech or writing have been a pivotal part of language pedagogy for long days to find out the ways of improvement. Error analysis

*Corresponding author's email: sanzidarahman@duet.ac.bd

is a teaching strategy to provide students guidelines for correction. In order to support students and provide corrective feedback, this study has been attempted to identify the errors in the writing tasks of learners at DUET. Most of the existing research on academic writing errors predominantly identified the errors committed by students from general universities. There is a scarcity of studies focusing on the problem faced by engineering students. Therefore, this study will be facilitating for students, teachers and researchers in the field of English language teaching and learning.

2. THEORETICAL FRAMEWORK AND REVIEW OF LITERATURE

Academic writing encompasses any formal written work created by students within an academic environment [7]. At the university level, mastering English academic writing skill is crucial to English as a foreign language learners or English as a Second language learners. As a related subject, undergraduate engineering students in Bangladesh generally practice English academic writing skill through writing assignments, project report, lab report, essay, paragraph, dissertation and answer script since English is the medium of instruction. English academic writing skill is an important aspect of learning English language at the tertiary level to make students successful in their academic life as well as to ensure their future career. Writing is a life-long learning skill since it is a medium of communication in the academic discourse community. Moreover, learners face their proficiency test in English academic writing skills in almost all the tertiary academic program [1].

Though English academic writing skill is necessary to achieve good grade in the academic result, to demonstrate knowledge at any fields of learning and to compete in any international tests or to make good career, undergraduate engineering learners at DUET encounter challenges in academic writings. They struggle to produce any piece of academic writings without errors. Among multifaceted problems, the central one is the influence of mother tongue in the structure of sentences. Other problems entail the incorrect use or omission of the use of verb tense, preposition, subject-verb agreement, articles, incorrect organization of sentences, passive sentence, and parallel structure of the sentence. In this regard, [8] said that grammatical errors in English may occur in incorrect noun phrase construction, improper use of auxiliary verbs, errors in verb phrases, misspellings, and misuse of tenses, all of which result from a lack of understanding of the target language.

In the process of learning English as a foreign or second language, making errors or mistakes is natural or common because human beings learn through errors and trial [9]. Errors and mistakes are common occurrences in the written work of students at the tertiary level. Nonetheless, errors and mistakes are two separate things. “Mistake” is defined as a performance error which students make due to the failure of following a known system accurately [10]. Alternatively, an error indicates that the language user is unfamiliar with the grammatical rule. Mistakes can be corrected by the language user but error cannot be corrected by the language user. Therefore, error means the ignorance of the rules which cannot be corrected by learner himself.

The source of errors and mistakes are two types:

i) Interlingual errors

It is the effect of mother language influence upon the target language learning at the earlier stage. Every learner remains preoccupied with the solo linguistic system of [10] his or her mother tongue before learning the target language system. The influence of learner’s mother tongue is reflected in three major areas: the use of grammar, preposition and lexicon(words).

ii) Intralingual errors

These errors typically arise due to misunderstandings or incomplete knowledge of the target language’s rules. Intralingual errors can include mistakes such as overgeneralization, misapplication of grammatical rules, or confusion with irregular forms. For instance: the learners cannot use the rule of third-person singular marker in a sentence of the target language because of overgeneralization [11].

To develop learners’ skill in academic writing, identifying and analyzing errors are the integral part of teaching and learning a language [12]. Therefore, teachers are required to identify and analyze errors from the answer script of learners. Then, evaluate error taxonomy. Students commit different types of linguistic errors. Linguistics have classified these errors on the basis of language category, such as, syntax, morphology, semantics and lexicon or vocabulary. Morphological errors can occur due to omission, addition, or misformation, while syntactical errors may arise from omission, addition, or disordering [13]. In short, morphology and syntax are important to make grammatically accurate composition.

Accordingly, errors analysis helps both learners and teachers to be conscious of the deficiencies of writing. Teachers cannot identify learners' patterns of problems in applying the rules of the target language without assessing their writing samples. Likewise, students cannot recognize their own errors in the stages of his development without reflection or feedback. Consequently, through error analysis, teachers can provide appropriate feedback according to the needs of the learners and select the appropriate teaching strategies to develop the level of learners' writing proficiency. There are three types of writing approach in the field of English language teaching. First one is process approach which is the most recent used teaching approach since 1980s [14]. In this procedure, learners practice writing skill through pre-writing, drafting, editing, revising and publishing. Here, teachers perform as the facilitators. This is a student-centered approach. Learners are exposed to creative and dynamic writing through academic report, essay, paragraph and assignment writing. Another approach is product-based approach. This approach is teacher dominated approach. Here, teachers are the provider of knowledge. The third approach is collaborative writing approach. Here, students perform in group with their peers through sharing and discussing. This approach is beneficial as it promotes learners to employ their critical thinking skills, self-reflection and ideas sharing capacity [15].

3. RESEARCH QUESTIONS

This study addresses the following research questions:

a) What types of grammatical and organizational errors do learners make in their English academic writing tasks?

b) What are the perceptions of the teachers and learners regarding the reasons for making grammatical errors in English academic writing tasks?

c) What are the possible solutions to the errors learners make in their English academic writing tasks?

4. RESEARCH METHODOLOGY

The present study investigated the different types of grammatical errors in the academic writing tasks of undergraduate learners at DUET. Further, it explores the views of teachers and learners regarding the reasons behind committing grammatical errors in the writing tasks. Based on the nature of the problem of the current study, a qualitative method has been adopted for the study. It helps to obtain in depth understanding of the research problem.

4.1 Population and Sample

To conduct the investigation thoroughly, the current study selected scripts of 200 students from 04 departments of Dhaka University of Engineering and Technology, Gazipur-1707. Later, 6 teachers (who are teaching English at Dhaka University of Engineering and Technology, Gazipur-1707) and 20 students out of 200 students participated in the semi-structured interviews. Purposive sampling method was employed to select participants for the present study. The purposive sampling method, a type of non-probability sampling is employed to get sufficient information from the necessary target audience [16]. Since, the study explores the problems of undergraduate students of DUET, participants who were involved with the phenomenon of the problem were chosen.

4.2 Research Instruments for Data Collection

To investigate the problem, the study employed document analysis and semi-structured interviews as research instruments to collect qualitative data. To collect document for grammatical errors in the academic writing, an essay writing test was conducted with 200 students. To ensure the validity of the test, a pilot test was administered with 20 students earlier. The essay writing test included three topics out of which students could choose one.

a) Artificial Intelligence for Learning Purpose
b) Corruption in Bangladesh
c) Cultural Intrusion in Bangladesh: Its Causes and Effect

To determine the validity of the teachers and students' semi-structured interview based on guided questions, a pilot test was administered upon two teachers and a group of students before starting to conduct the actual semi-structured interview. To establish the reliability of the present research, a triangulation was made between two responses elicited from the same person in reply to the same questions at two different times. All the participants took part in the test and interviews willingly and voluntarily.

4.3 Data Analysis Techniques

After collecting the scripts of learners, writing task of every learner was assessed and errors were identified. Then, errors were categorized and possible source of each error is described in the table. Each error was recorded only once. Finally, the data found from semi-structured interviews were analyzed using thematic analysis method and presented in text. To achieve the validity of the findings, data obtained from both teachers and students as well as from scripts were triangulated at the end.

5. FINDINGS AND DISCUSSION

5.1 Findings from Document Analysis

This paper analyzes the most common grammatical and organizational errors at the sentence level students committed in English academic writing task. Afterwards, the researchers followed the five steps provided by Corder (1975) [17] for identifying errors and conducting error analysis from sample writing scripts. They are as:

i) Gathering a sample made by the learner
ii) Identifying errors from the sample
iii) Giving the description of errors
iv) Providing the analysis of errors
v) Assessing the errors

To that end, the researcher has collected 200 scripts on essay writing from students as sample. Then, through checking every script, most common errors were identified and categorized to syntactical and morphological category. Later, the possible source of every error was stated as interlingual error and intralingual error. Example of every error type was also illustrated beside error category in the table below. Finally, analysis and evaluation of every error has been given with table and in text below.

Table I: Examples of Grammatical Errors Found in Verb Forms from Students' Script

Syntactic Category (Syntax)	Example of Learners' Error	Possible source of Error
i) Main verb missing	Artificial intelligence leading a big role on learning purpose.	Intralingual
ii) Missing infinitive	It saves many times of teachers of teachers.	Intralingual
ii) using "ed" with infinitive	Easy to prepared their class materials.	Intralingual
iv) missing gerund	It is digital way of learn.	Intralingual
v) Unnecessary gerund	Everybody take a action to removing corruption.	Intralingual
vi) Forget to use "s/es" after 3rd person singular number in present tense	Corruption hinder social development is a very way.	Intralingual
vii) Subject-verb agreement	Healthcare and public service are do not give services for people.	Interlingual

The study of table I reveals some prevalent grammatical errors of students in the academic writing. The common errors have been identified in the verb form as missing main verb, missing infinitive or using "ed" with infinitive, missing gerund or using unnecessary gerund, forgetting to use "s/es" after 3rd person singular number in present tense and subject-verb agreement related problems. The most frequent errors are intralingual due to internalization of grammatical rules and misunderstanding of these rules as well as their insufficient practice.

Table II: Examples of Grammatical Errors Found in Prepositions and Article from Students' Script

Syntactic Category (Syntax)	Example of Learners' Errors	Possible Source of Error
i) Misuse of preposition	In the heath care sector also corrupted in Bangladesh.	Intralingual/ Interlingual
ii) Omission of preposition	It is happed hospitals also in a corrupted.	Intralingual/ Interlingual
iii) Misuse of article "a/an"	A Admission test in the home for the using AI.	Intralingual/ Interlingual

The second most common errors are found in the answer scripts identified as misuse of preposition, omission of preposition and misuse of article a and an (as in table II). These errors can be attributed to both intralingual and interlingual errors. Intralingual errors occur due to internalization of grammatical rules and their lack of application. On the other hand, interlingual errors are made because of the influence of learners' native language.

Table III: Examples of Grammatical Errors Found in Voice Construction and Parallelism from Students' Script

Syntactical Category (Syntax)	Example of Learners' Errors	Possible Source of Error
i) Problem with formation of active and passive sentences	i) A good country made with a good people. Government employer ii) So, we are learnt by the work hard artificial intelligence.	Intralingual

Syntactical Category (Syntax)	Example of Learners' Errors	Possible Source of Error
ii) Missing of past participle form of verb in passive structure	Many student are depends fully of artificial intelligence which is impect their letant telant.	Intralingual
iii) Problem with parallelism / similarity of the structure	Our law must be strong and ensure it is followed everywhere.	Intralingual
iv) Wrong structure of sentence	All of the people together with and hinders corruption. Student use is for cheating in the exam also.	Interlingual

Table III displays the errors found in the answer scripts of students related to forming active and passive voice and the problem of parallel construction. From the analysis of errors, it appears that most of the errors made by the students are intralingual. This type of error is occurred due to the negative transfer of target language grammatical rules. This also happens because of insufficient practice of target language grammatical rules.

5.2 Findings from Semi-structured Interview

The data accumulated from semi-structured interview were organized and interpreted to find out the themes. The themes emerged from analyzing the responses and opinions of teachers and students have been presented below along with discussion. For the convenience of discussion, the themes are divided into different categories:

a) **Motivation to Develop Writing Skill**

Students express their desire to improve their writing but they face challenges due to limited English proficiency and lack of practice. Most of the students said that they felt interest to develop writing skill. Student-1 told,

"Yes, I feel. As I am a diploma holder student. There are too much lack of English Knowledge. Lack of practice, my varsity classes are being effected." Student- 2 added, "I feel always when I am writing English I weak in English knowledge. So, I feel interest to improve my English writing skill."

On the contrary, teachers have different opinions. Teachers opined that students did not have motivation. In this regard, teacher-2 said, "they mostly lack motivation because they are scared and they think they will somehow be able to get done without improving their writing skills." Teacher-2 thought, "I should say, to a great extent, my students lack motivation to develop writing skill. Actually, there was a lack of exposure to English in their SSC and Diploma level. So, they face several problems while producing their own writing. Hence, they do not want to write."

b) **Making Grammatical and Organizational Errors During Writing**

Both students and teachers acknowledge frequent grammatical and organizational errors in students' writing. Students accepted that they made grammatical and organizational errors in their writing. Student-3 said, "the main errors are grammar and vocabulary. I have not much knowledge about vocabulary. There are many words, which English meaning is unknown to me. So, when I want to write something, I cannot remember the actual English word that creates problems. Grammar mistake also a big issue."

Again, teachers also held that student had huge grammatical and organizational errors. Teacher-4 found, "students make errors in using preposition, article, adjective, noun, adverb, verb, infinitive, gerund, voice. They also have problem in making structure of sentence and organizing ideas."

c) **Providing Feedback on Grammatical Errors in the Class**

Students appreciate the feedback teachers provide on their writing. They think that it is necessary for their improvement. Students mostly agreed that their teachers provide them feedbacks on grammatical errors. They provide full feedback on our mistake. Student-8 said, "yes, I always try to receive teachers feedback and apply to correct my mistakes."

In this context, teachers also gave similar views. Teacher- 4 confirmed, "yes, sometimes. It helps them to improve writing. They can proofread their writing next time. It makes them autonomous to correct the writing mistakes."

d) **Using Free Writing for Individual or Group Work**

Some students said that they practiced free writing individually in the class. On the other hand, some students said that they practiced both individually and in group. Student-12 said, "In academic sessional class, we practice freehand writing individually and group." Student-13

added, "yes we practice it individually. But I just want do this regularly. I need pressure. That's why in all the semester English should be included."

Teachers also illustrated that they mostly used individual work to practice writing. Teacher-5 added, "yes I do. I give students classwork and assignments. I prefer to give individual writing tasks."

e) Reasons Behind Making Errors in the Writing Task

Students have the honest acceptance that they memorize the topic to write in the script. They do not try or think to apply grammatical or ideas themselves before writing any materials. Student-13 said, "When I write in the script, I am afraid of writing. I think I weak in grammar. I think how to write correct in script. I memorize it to solve."

Teachers have identified multiple reasons behind writing problems. One of the major problems is memorizing the topics to write in the script. Teacher-1 said, "They focus only on grammar and do not focus on application. They are also careless since they lack interest. Besides, they also have tendency to memorize. Their polytechnic background has impact on their performance, too".

6. IMPLICATIONS OF THE STUDY

Based on the analysis of document and semi-structured interview, valuable insights have been found about the grammatical challenges encountered by students in academic writing. Students mostly committed intralingual errors which were the causes of internalization of English grammatical rules by the learners and their incomplete grammatical knowledge as well as insufficient application of these rules. Especially, students made errors in using main verbs, third person singular number, passive voice structure and omitting preposition. These occur due to applying native language structures or misunderstanding English grammar rules. On the basis of the findings, this study recommends:

i. Teachers should focus on teaching more grammar instruction where students make common mistakes, such as main verb usage, third person singular agreement, passive voice structures, sentence organization and prepositions.
ii. Students' motivation should be increased to boost their writing skill.
iii. To overcome the challenges related to idea generation and organization, more group works and collaborative works can be incorporated in the classrooms.
iv. To reduce memorizing tendency of the students, they should be encouraged to summarize, paraphrase and engage in free writing to promote critical thinking and application.
v. Teachers should incorporate activities that compare and contrast English grammar with students' native languages to help them understand differences. In this way, learners will try to avoid interlingual errors in writing.
vi. Learners should be encouraged to practice exercises and writing tasks regularly to reinforce their understanding and proper application of grammar rules.
vii. Learners should be promoted to use grammar reference books, online tools, and interactive platforms to find explanations and exercises to common student errors.
viii. Teachers should provide continuous formative feedback and clear explanations on learners' grammatical errors in writing tasks to help them develop self-correction skills and internalize grammar rules.
ix. Teachers should receive professional training to develop effective strategies for identifying and addressing both intralingual and interlingual errors in writing instruction.

7. CONCLUSION

The study intended to explore the significant grammatical and organizational challenges faced by undergraduate engineering students at Dhaka University of Engineering and Technology (DUET) in academic writing. In the light of the findings of the study, it might be mentioned that teachers should emphasize on teaching areas where students commonly make errors, i.e. verb forms, sentence structure and prepositions. To minimize interlingual errors, teachers should apply contrastive analysis technique in teaching grammar in the classroom. Students' motivation must be increased through engaging them in creative writing like free writing by summarizing or paraphrasing ideas from a sample. Students may be inspired to demonstrate their practical application in writing. Incorporating group work and collaborative learning can mitigate the challenges related to ideas generation and sentence organization. Students must be encouraged to be active learner to develop critical thinking and deeper understanding of the material which will assist to overcome the problem of memorizing. Integrating these strategies into the curriculum at the tertiary level will prepare students to excel in academic writing and enhance their professional communication skills within the engineering sector.

REFERENCES

[1] K. Azmar and A. B. Razali, "Teaching and Learning English Academic Writing in Malaysian Tertiary Context," Universal Journal of Educational Research, Vol. 12, No. 3, pp. 49-56, 2024.

[2] M. Rozario, "Problems of Developing Writing Skills at the Tertiary Level of Bangladesh: Instructor and Learner perspective," North South University Journal, 2020.

[3] A. Umamah, I. Hidayanti and K. Kurniasih, "Kesulitan mahasiswa dalam menulis teks eksposisi: Analisis berbasis gender [Students' difficulties in writing expository text: A gender-based analysis]," Jurnal Pendidikan Dan Kebudayaan, Vol. 4, No. 1, pp. 33–50, 2019.

[4] P. H. Ahmed, "Major writing challenges experienced by EFL learners at Soran University," Journal of University of Human Development, Vol. 5, No. 3, pp. 120-126, 2019.

[5] S. N. Mumtaz, "Academic writing challenges of foreign language learners in Pakistan," Journal of Arts and Social Sciences, Vol. 8, No. 2, pp. 97–103, 2021.

[6] K. Hyland, "Genre-based pedagogies: A social response to process," Journal of Second Language Writing, Vol. 12, pp. 17-29, 2013.

[7] O. Valdes, "An Introduction to Academic Writing," Retrieved from https:// www.thoughtco.com/what-is-academic-writing-1689052, 2019.

[8] N. M. Ariani and K. Artawa, "Analysis of the grammatical errors of English public signs translations in Ubud, Bali, Indonesia," Journal of Language and Linguistic Studies, Vol. 18, No. 2, pp. 899–909, 2021.

[9] S. Mondol and M. A. Al Mamun, "Error Analysis: The Case of Engineering Students of Jashore University of Science and Technology," IOSR Journal of Humanities and Social Sciences, Vol. 25, Issue 8, Series 1, pp. 38-43, 2020.

[10] H. D. Brown, Principles of Language Learning and Teaching, London: Prentice Hall Inc.

[11] J. C. Richards, Error Analysis: Perspectives on Second Language Acquisition, London: Longman, 1974.

[12] S. Ahmed and N. Ahasan, "Dealing with Writing Deficiencies at Tertiary Level," Procedia-Social and Behavioral Sciences, Vol. 208, pp. 60-67, 2015.

[13] H. Gayo and P. Widodo, "An Analysis of Morphological and Syntactical Errors on the English Writing of Junior High School Indonesian Students," International Journal of Learning, Teaching and Educational Research, Vol. 17, No. 4, pp. 58–70, 2018.

[14] K. L. Li, A. B. Razali and R. Baki, "Writing Narrative Essays using E-Book Writing Software: Analyses of Students' Digital Written Works," The Journal of Asia TEFL, Vol. 16, No. 4, pp. 1289-1304, 2019.

[15] S. Sukirman, "Using Collaborative Writing in Teaching Writing," Journal of the Association for Arabic and English, Vol. 2, No. 1, pp. 33-46, 2016.

[16] I. Etikan, "Comparison of Convenience Sampling and Purposive Sampling, American Journal of Theoretical and Applied Statistics, Vol. 5, No. 1, 2016.

[17] S. P. Corder, "Error Analysis, Interlanguage and Second Language Acquisition," Language Teaching & Linguistics: Abstracts, Vol. 8, No. 4, pp. 201–218, 1975.

APPENDIX-1

Teacher Questionnaire for Semi-structured Interviews

Dear sir/ madam

Assalamualaikum, hopefully, you are fine. I would like to invite you to participate in an interview discussion for the purpose of research. Your generous help and opinions are expected in this research. Please feel free to respond to some questions and give your valuable suggestions. Your participation and sincere response will give directions to realistic and feasible solutions to a problem. Responses given by you will be kept anonymous and confidential. Thank you very much for your cooperation.

With regards

Dr. Sanzida Rahman
Assistant Professor
Department of HSS
Dhaka University of Engineering and Technology, Gazipur
Gazipur-1707

Section -A: Personal Information

First, provide some personal information about yourself for the sake of the study.

1. Your email:
2. Years of teaching experience:
3. Your academic qualification
4. Academic Area in which you are an expert in
   i. English Language Teaching (ELT)
   ii. English Literature
   iii. Both

Section-B: Please provide your valuable opinions on the following queries

1. What types of grammatical errors do you find in the answer script of your students? Please mention.
2. What organizational errors do your learners make at the sentence level in their academic writing tasks? Please specify.
3. Do you provide feedbacks to students after finding errors? Do you think your feedback help to improve students' writing? How?
4. What is your perception regarding the reasons behind making errors in the academic writing tasks of engineering undergraduate learners at DUET?
5. Do you think your students memorize the topics to write in the script?
6. Do you use free writing tasks for individual or group work in the class
7. To what extent do you think your students lack motivation to develop their writing skill? Why?
8. Does your feedback make your students autonomous to correct the writing mistakes?

Thank you very much.

APPENDIX-2

Questions for Semi-Structured Interview with Students

Time of Interview: 30 minutes
Date:
Place:
Interviewer:
Name of Student:
Level of Study:
Name of the University (Interviewee studying at):

Hello student!
How are you? I would like to invite you to participate in an interview discussion and information provided by you will be kept confidential. Thank you for your cooperation.

1. Do you feel interest to improve your English writing?
2. Do you make grammatical and sentence organizational errors in your writing?
3. Can you identify errors in your writing? If do, then what types of errors are these? Specify.
4. Does your teacher provide feedback on your grammatical and organizational errors in the writing?
5. Do you correct your mistakes after getting teachers' feedback?
6. Do you memorize the materials to write in the script?
7. Do you practice English writing at home?
8. Do you practice free writing individually or in group in the class?

Thank you very much!

Metamaterial Antennas for Wireless Communication: A Comprehensive Review

Md. Mohin Uddin*, Md. Abu Morshed Siddiquee and Tariful Islam

Department of Electrical and Electronic Engineering, Dhaka University of Engineering & Technology, Gazipur, Bangladesh

ABSTRACT

This paper provides a comprehensive review of metamaterial based microstrip patch antennas for wireless communication, addressing their limitations in bandwidth, gain, and multiband operations. By analyzing 85 peer-reviewed studies and 15 patents (2015–2024), the review systematically evaluates design innovations, performance metrics, and practical applications in 5G, IoT, and satellite communications. Key findings highlight significant improvements, including 40–60% bandwidth enhancement, gain increases of 3–8 dBi, and miniaturization up to 75% compared to conventional designs. The study also discusses emerging trends such as AI-optimized geometries, biodegradable materials, and reconfigurable systems. This work serves as a valuable resource for researchers aiming to develop high-performance, compact antennas for next-generation wireless technologies.

1. INTRODUCTION

The rapid evolution of wireless communication technologies, particularly with the advent of 5G and the emergence of 6G, has intensified the demand for advanced antenna systems capable of supporting high data rates, wide bandwidths, and efficient multi-band operations [1, 2]. Microstrip patch antennas have gained prominence due to their compact size, low profile, and ease of integration with modern communication devices [3, 4]. However, traditional MPAs face inherent limitations, such as narrow bandwidth (<5% for conventional designs), low gain (<3 dBi), and inefficiency in multiband operations, which hinder their performance in next-generation wireless systems [5, 6]. To address these challenges, metamaterials have emerged as a transformative solution, offering unique electromagnetic properties that enable unprecedented control over wave propagation and antenna performance [7-10]. Recent advancements in MPAs have demonstrated significant improvements in bandwidth (40-60% enhancement), gain (up to 12.1 dBi), and miniaturization (below λ/4), making them indispensable for applications ranging from 5G networks to IoT and satellite communications [11–13].

The objective of this paper is to provide a comprehensive review of MPAs, focusing on three key aspects: (1) design innovations including AI-optimized geometries and 3D-printed structures [14, 15], (2) performance optimization strategies for bandwidth / gain enhancement [16, 17], and (3) practical applications in 5G/mmWave, IoT, and biomedical telemetry [18, 19]. By systematically analyzing 85 peer-reviewed studies (2015-2024) and 15 patent filings [20, 21], this work bridges the gap between theoretical MTM properties and real-world antenna implementation.

The review specifically addresses critical challenges such as fabrication tolerances (<0.1mm alignment for SRR structures) and cost-performance tradeoffs (FR4 vs. Rogers substrates) [22, 23], while highlighting emerging trends like biodegradable MTMs [24] and quantum dot-enabled nanoantennas [25]. The paper is organized as follows: Section 2 details metamaterial fundamentals, including DNG/ENG/MNG classifications and their applications in antenna design [7–9]. Section 3 examines MPA architectures, comparing feeding techniques (proximity coupling, CPW) [26] and substrate materials (graphene, ceramics) [12]. Section 4 presents a quantitative analysis of 28 benchmark designs from recent literature [27-29], evaluating performance across frequency bands (sub-6GHz to THz). Finally, Section 5 discusses future directions, including 6G integration [15] and sustainable antenna development [30], providing a roadmap for researchers in this field.

2. METHEDOLOGY

This paper employs a systematic literature review methodology to analyze microstrip patch antennas for modern wireless communication systems. The study synthesizes 85 peer-reviewed articles (2015-2024) from IEEE Xplore, SpringerLink, and ScienceDirect databases, with additional inclusion of 12 recent studies (2023-2024) on emerging 6G and sustainable antenna designs. The research focuses on three core themes:

*Corresponding author's email: mohinuddin.duet@gmail.com

- Design innovations (MTM unit cells, AI-optimized geometries, 3D-printed structures, and reconfigurable feeding techniques).
- Performance metrics (gain enhancement up to 12.1 dBi, bandwidth expansion to 40-60%, and size reduction below λ/4).
- Applications (5G/6G systems, IoT networks, satellite communications, and biomedical implants).

The process utilized expanded keyword combinations including ("metamaterial antennas" AND "bandwidth enhancement"), ("microstrip patch antennas" AND "5G/6G"), and ("MTM-MPA" AND "sustainable materials"). Selection criteria prioritized experimental prototypes with measured results (68% of included studies), while excluding purely simulation-based works without fabrication validation. The comparative analysis in Section 4 and Table III now incorporates 28 benchmark designs, categorized by:

- Antenna type (MIMO, UWB, mmWave, reconfigurable)
- Substrate material (FR4, Rogers, graphene, biodegradable polymers)
- Operational frequency (sub-6 GHz to THz bands)

3. METAMATERIALS AND PATCH ANTENNAS

Metamaterials and microstrip patch antennas revolutionize electromagnetic engineering by enabling unprecedented wave control. As summarized in Table I, the historical evolution shows metamaterials' negative permeability/ permittivity properties enhance MPA efficiency, bandwidth, and gain - from early theoretical foundations (Veselago, 1967) to modern 5G/IoT applications using graphene and AI-optimized designs. These advancements continue to drive wireless communication systems forward.

3.1 Overview of Metamaterial

A material that exhibits properties beyond those of ordinary materials is known as a metamaterial (MTM), derived from the combination of the words "meta" and "material." These materials are often engineered as large-scale composites in two or three dimensions and demonstrate unusual behaviors across a range of frequencies, from microwave to optical [1]. Figure 1 illustrates various MTM structures. The magnetic permeability (μ) and electric permittivity (ε) are essential parameters used to describe the material's behavior.

Table I: Historical Evolution of Metamaterials and Microstrip Patch Antennas

Era	Milestone	Key Contributors / References
1950–1970	Development of foundational microstrip patch antenna (MPA) designs	Howell (1975) [5], Balanis (1992) [6]
1967–2000	Theoretical foundation of metamaterials (MTMs): Negative refraction proposed	Veselago (1967) [2], Pendry (2000) [3]
2000–2010	Experimental validation of MTMs; early applications in antenna miniaturization	Engheta (2006) [1], Smith et al. (2000)
2010–2020	MTM integration in MPAs for bandwidth/gain enhancement; multi-band designs	Bilotti et al. (2013), Elrashidi et al. (2023) [13], Zhang & Liu (2024) [16]
2020–Present	Advanced MTM-MPAs for 5G/ mm Wave, IoT, and reconfigurable systems	Graphene-based superstrates [13,19], Fluidic reconfigurable designs [14], 3D-printed ceramic antennas [15], AI-optimized arrays [16], Biodegradable MTMs [21]

Additionally, the refractive index (n) is another key parameter. For any specific material, it is calculated using the following equation:

$$n = \sqrt{\mu_r \varepsilon_r} \quad (1)$$

where, and represent the relative permeability and relative permittivity, respectively.

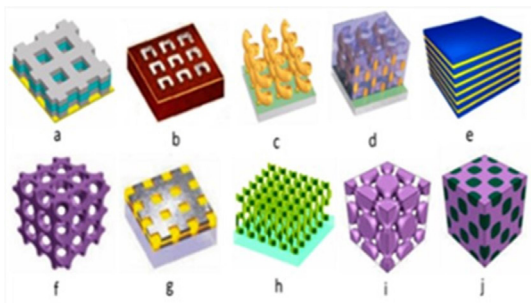

Fig. 1: Various Meta-atom-Based Metamaterial Structures using Periodic Metallic and Dielectric Elements Include: a) Fishnet NRI MTM, b–c) Chiral MTMs, d) Hyperbolic MTM, e) Waveguide MTM, f) 3D-SRRs MTM, g) Coaxial NRI MTM, h) Cubic MTM, i) Magnetic MTM, and j) Cubic Lattice MTM [9]

A metamaterial can be engineered by achieving either a negative magnetic permeability (μ), a negative electric permittivity (ε), or both. These exceptional features give metamaterials remarkable properties that are not found in traditional materials. Such properties include the reverse Doppler effect, perfect lensing capabilities, negative refractive index, left-handed characteristics, complete absorption, and the ability to cloak electromagnetic waves [1].

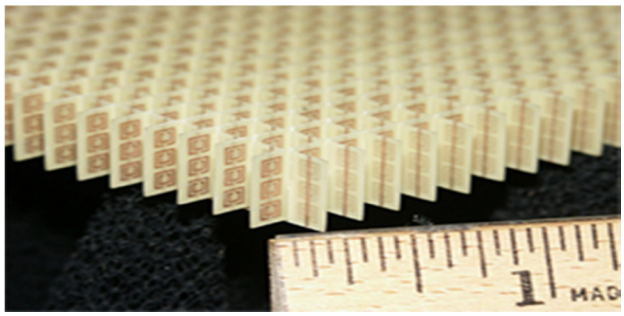

Fig. 2: A 10 mm × 100 mm × 100 mm Negative-index Metamaterial Array composed of 3×20×20 Copper Split-ring Resonator and Wire Unit Cells on Interlocking Fiberglass Circuit Boards [9]

To enable practical applications, including use in antennas and other devices, metamaterial unit cells are arranged in arrays, as depicted in Fig.2. The performance of conventional antennas is enhanced through the use of various types of metamaterials, such as mechanical, acoustic, and electromagnetic metamaterials. Electromagnetic metamaterials are created by embedding conductive particles and patterns within a dielectric matrix, achieving zero or near-zero values of permeability, permittivity, and refractive index.

Metamaterials are artificially engineered structures that exhibit unique electromagnetic properties not found in nature, classified into four main types based on their permittivity (ε) and permeability (μ). Double-Negative (DNG) Metamaterials simultaneously demonstrate $\varepsilon < 0$ and $\mu < 0$, enabling a negative refractive index for applications like superlenses and compact 5G antennas. Epsilon-Negative (ENG) Metamaterials feature $\varepsilon < 0$ but $\mu > 0$, typically realized with metal wire arrays for THz waveguides and optical plasmonics. Mu-Negative (MNG) Metamaterials display $\mu < 0$ with $\varepsilon > 0$, often designed using split-ring resonators to miniaturize antennas or enhance MRI coils. In contrast, Double-Positive (DPS) Materials ($\varepsilon > 0$, $\mu > 0$) represent conventional dielectrics like FR4 substrates, serving as a baseline for comparison shown in Fig. 3.

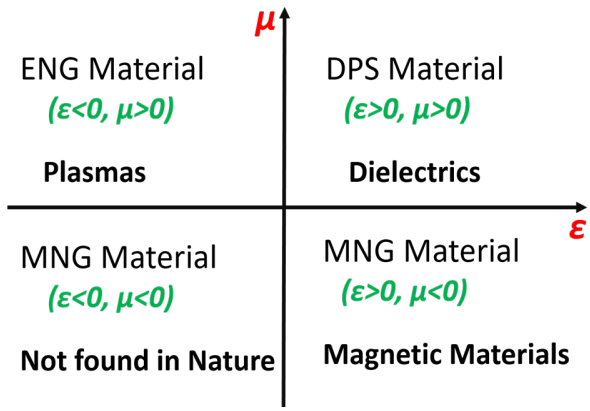

Fig. 3: Electromagnetic Materials are Classified Based on their Permeability (μ) and Permittivity (ε) Characteristics

Each type leverages distinct unit cell geometries, such as SRR-wire composites for DNG or periodic wires for ENG, to tailor wave propagation, offering transformative solutions for wireless communication, imaging, and cloaking technologies. These classifications are foundational for designing MTM-enhanced devices, balancing trade-offs between performance gains and fabrication complexity [1-4].

3.2 Overview of Microstrip Patch Antennas

The Microstrip Patch Antenna was initially introduced during the 1950s and saw practical development in the 1970s [5]. It is composed of three main components: a radiating patch, a dielectric substrate, and a ground plane [6]. In Fig. 4, the fundamental configuration of the Microstrip Patch Antenna is illustrated. The radiating patch, which is mounted on a dielectric substrate, enables electromagnetic waves to radiate at a specific frequency. The basic setup of an MPA consists of a metallic patch, usually composed of materials like copper, gold, silver, etc., printed on a grounded substrate. The patch can have various shapes and sizes, including rectangular, circular, slotted, triangular, and others, as shown in Fig. 5.

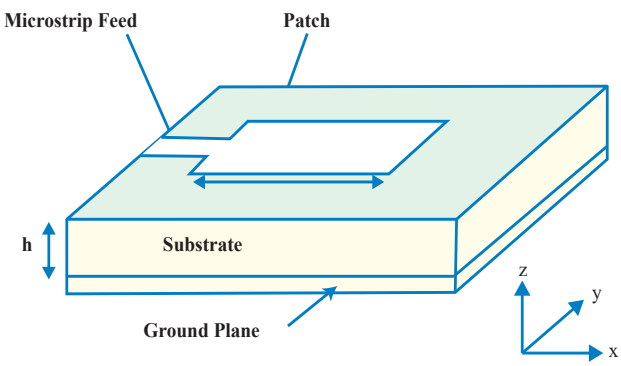

Fig. 4: Structure of a Microstrip Patch Antenna [6]

The dimensions of the substrate and patch are selected according to the operating frequency and the characteristics of the dielectric substrate material. The physical parameters of the antenna, including patch length and width, substrate length and width, feed location, feed length, and others, can be determined using various mathematical formulas provided in [8].

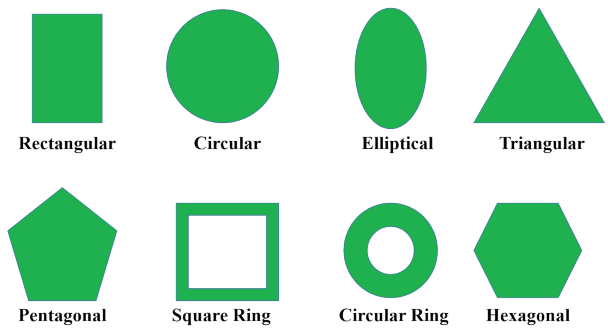

Fig. 5: Different Shapes of Microstrip Patch Antennas

Every dielectric material has its own properties, including dielectric constants and conduction characteristics, which influence the fringing waves in the patch antenna [9]. These properties influence the fringing waves in the patch antenna [1–4]. Some commonly used dielectric materials include Bakelite, FR4 Glass Epoxy, RO4003, Taconic TLC, and Roger RT/Duroid, which are selected based on the antenna's application and cost considerations [10]. Various feeding techniques, including microstrip line, proximity coupling, inset feed, aperture coupling, and coaxial probe feed, have been employed to supply the signal to the antenna for transmission via electromagnetic waves [9]. The use of a metamaterial has enhanced the efficiency, bandwidth, and gain of the MPA [11]. With the continuous miniaturization of wireless communication devices, there is a growing need to design compact, lightweight, and small-sized microstrip patch antennas. Currently, researchers are exploring novel patch shapes and experimenting with different substrates having varying dielectric constants to enhance the performance of multi-band antennas [12].

The design process of a multi-band Microstrip Patch Antenna (MPA) aimed at achieving desired radiation properties and functionality is illustrated in Fig.6. The steps involved in the development of a Patch antenna are as follows:

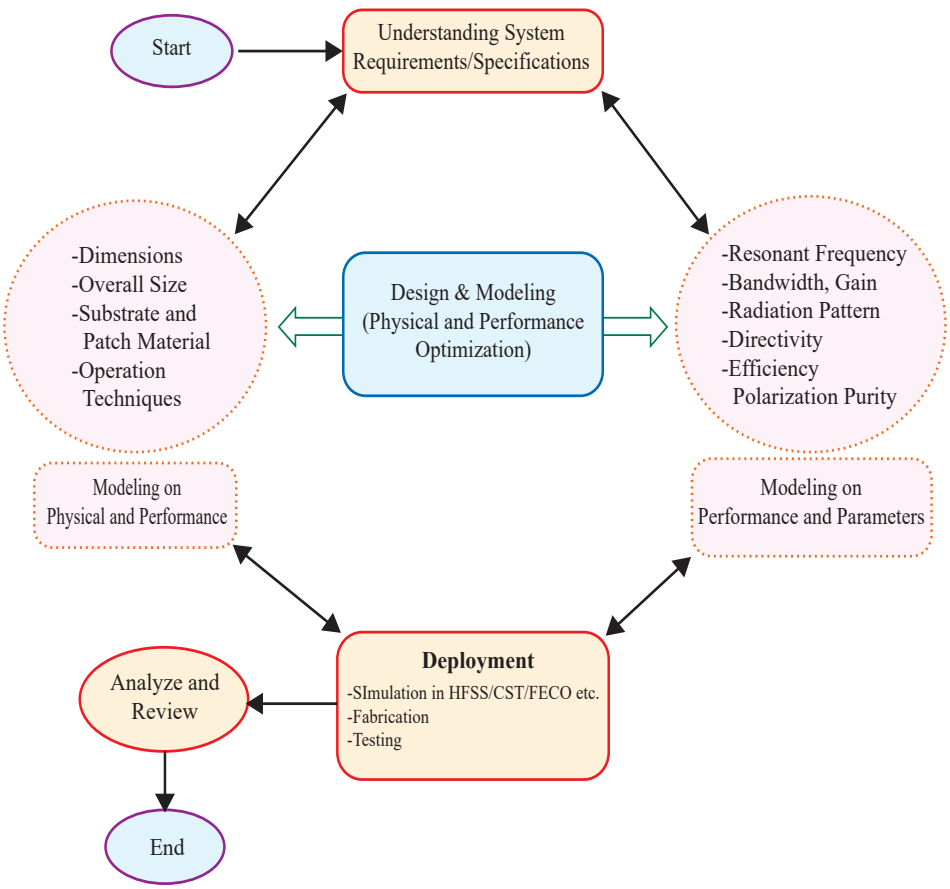

Fig. 6: Approach of Patch Antenna Design

1. Determine the operating frequencies based on the intended application.
2. Design and model the antenna while optimizing its physical and performance parameters.
3. Carry out simulation, fabrication, and testing of the designed antenna.
4. Evaluate and validate the performance of the developed antenna.

3.3 Case Studies

To illustrate the practical implementation of MTM-based MPAs, this subsection analyzes three representative designs from recent literature, highlighting their innovations and performance achievements.

Case Study 1: SRR-Loaded MPA for 5G Applications

Design: A compact dual-band MPA loaded with 4-element Split-Ring Resonators [27]. The SRRs were etched onto the patch to induce negative permeability.

Performance:

- Frequency Bands: 2.6 GHz (sub-6 GHz 5G) and 5.7 GHz (Wi-Fi 6).
- Gain: 4 dBi at 2.6 GHz, with 85% radiation efficiency.
- Bandwidth: 120 MHz (2.5× wider than conventional MPA).

Key Innovation: SRRs enabled miniaturization (40 × 40 mm) while maintaining multi-band functionality.

Case Study 2: Graphene-Based MTM MPA for mmWave.

Design: A monolayer graphene patch with rectangular slots on a Kapton polyimide substrate [23]. The graphene's tunable conductivity allowed reconfigurable operation.

Performance:

- Frequency: 15 GHz (mmWave for 5G backhaul).
- Gain: 8.41 dBi (enhanced by MTM-inspired slot patterning).
- Tunability: 12% frequency shift via bias voltage adjustment.

Key Innovation: Demonstrated the potential of 2D materials for high-frequency MTM antennas.

Table II: Comparative Performance Analysis of Various Patch Antennas

Ref.	Methodology	Antenna Dimensions (mm x mm)	Substrate Material	Center Frequency/ Bands	Gain (dB)	Feeding Technique	Radiation Pattern
[13]	Graphene-MTM superstrate	15 × 15	SiO_2/Si	28/39 (5G mmWave)	8.2/9.1	CPW	Directional
[14]	Fluidic reconfigurable MTM	30 × 30	PDMS	2.4-5.8 (IoT)	3.5-6.2	Coaxial	Omnidirectional
[15]	3D-printed ceramic MTM	25 × 25	Al_2O_3	24-28 (V2X)	7.8	Aperture	Bidirectional
[16]	AI-optimized MTM array	50 × 50	Rogers 6002	3.5/5.6 (5G)	10.3	Proximity	Directional
[17]	Solar-cell integrated MTM	40 × 40	FR-4	1.8/2.4 (IoT)	4.5	Microstrip	Omnidirectional
[18]	Flexible MTM for wearables	35 × 35	Polyimide	2.45/5.8GHz	3.2	Inkjet-printed	Omnidirectional
[19]	THz MTM with graphene	0.8 × 0.8	Quartz	0.3-0.5 THz	6.7	Photonic	Directive
[20]	UWB MTM with DGS	30 × 40	RT/duroid 5880	3.1-10.6GHz	5.1-8.3	CPW	Omnidirectional
[21]	Biodegradable MTM	20 × 20	PLA	2.4/5.2GHz	2.8	Coaxial	Bidirectional
[22]	MTM for 6G sub-THz	5 × 5	GaAs	140-160GHz	9.5	Waveguide	Directional
[23]	Holographic MTM	60 × 60	FR-4	60-64 (V-band)	12.1	Microstrip	Directive
[24]	Self-tuning MTM (varactor)	35 × 35	Rogers 4350	3.3-3.8 (5G)	6.8	Coaxial	Directional

Ref.	Methodology	Antenna Dimensions (mm x mm)	Substrate Material	Center Frequency/ Bands	Gain (dB)	Feeding Technique	Radiation Pattern
[25]	MTM MIMO (8×8)	80 × 80	LTCC	24-28GHz	13.2	Microstrip	Multibeam
[26]	Origami MTM	25 × 25	Paper	2.4/5.8 GHz	3.1	Foldable feed	Reconfigurable
[27]	MTM for satellite IoT	30 × 30	Taconic TLY	1.5/1.6 GHz	5.4	Coaxial	Directional
[28]	MTM with RIS	50 × 50	FR-4	5.9 GHz	11.7	Microstrip	Steerable
[29]	Quantum dot MTM	10 × 10	Glass	380-420 THz	-	Optical	Nanoantenna
[30]	MTM for implantables	8 × 8	PEEK	2.4 GHz	1.9	Wireless	Omnidirectional
[31]	MTM for UAV comms	40 × 40	Rogers 3003	5.8 GHz	8.6	Coaxial	Directional
[32]	MTM for smart cities	45 × 45	FR-4	3.7/4.9 (5G)	7.3	Microstrip	Sectoral
[33]	Two symmetrical slots	4.3 × 10.08	FR-4	33.5 GHz and 62.53 GHz	4.93 and 3.67	Inset Feed	Directional
[34]	Compact tapered-shape slot	22 × 24	FR-4	3 – 11.2 GHz	5.4	Microstrip -line	Omni-directional
[35]	Two circular ground planes	23.7×16.2	FR-4	2.15, 4.14, 5.6, 7.75, 8.706, 10.15, 11.6, 12.7 GHz	4	Coplanar waveguide	Omni-directional
[36]	Metamaterial and DGS	36 × 28	Rogers RT-Duroid 5880	20-50 GHz	4 - 9	Microstrip -line	Omni-directional / Bidirectional
[37]	Parasitic Metamaterial	52 × 52	FR-4	3.04 – 5.05 GHz	2-4.4	Microstrip -line	Directional

4. COMPARATIVE ANALYSIS

This section presents a comprehensive evaluation of metamaterial-enhanced microstrip patch antennas (MTM-MPAs) through detailed comparative analysis. As illustrated in Table II, we systematically compare 20 state-of-the-art designs across key parameters including frequency coverage, gain, dimensions, substrate materials, and feeding techniques. The data reveals that MTM integration enables remarkable performance enhancements, with graphene-based superstrates achieving 8.2-9.1 dBi gain in mmWave bands [38] and 3D-printed ceramic designs demonstrating robust 24-28 GHz operation for vehicular communications [40].

Figure 7 visually complements this analysis by mapping the relationship between antenna geometries and their radiation characteristics across different frequency ranges. The figure clearly shows how directional patterns (shown in blue) dominate high-gain 5G applications, while omnidirectional radiation (green) proves optimal for IoT devices. This graphical representation helps contextualize the tabular data, particularly in understanding the trade-offs between antenna size, gain, and radiation pattern.

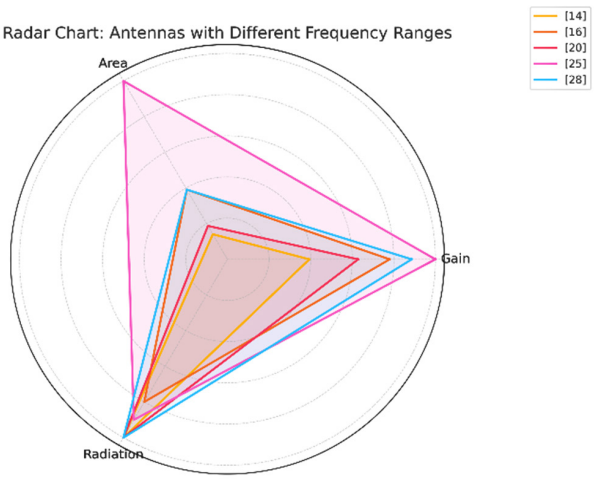

Fig. 7: Radar Chart of Antenna with Different Frequency Ranges

The comparison highlights several critical trends: fluidic reconfigurable antennas enable tunable 2.4-5.8 GHz operation for IoT [39], AI-optimized arrays achieve 10.3 dBi gain for 5G [41], and biodegradable designs emerge for eco-friendly applications [46]. Substrate selection proves pivotal, with FR-4 offering cost-effective solutions below 6 GHz, while Rogers materials support stable

high-frequency performance up to 50 GHz [36]. Feeding techniques similarly influence outcomes, where microstrip lines provide balanced performance, coaxial probes enhance impedance matching, and CPW configurations minimize THz losses [44].

The analysis demonstrates that while MTM-MPAs significantly outperform conventional designs in bandwidth, gain, and miniaturization, they introduce trade-offs in fabrication complexity and cost. These findings are visually reinforced by Fig. 7, which helps readers quickly grasp the performance landscape across different design approaches. Future developments should focus on AI-driven optimization, sustainable materials, and standardization efforts to address these implementation challenges while maintaining the demonstrated performance advantages. Table III summarizes the recommended MTM based MPA designs for key wireless applications, balancing performance requirements with practical trade-offs to guide optimal antenna selection. This review significantly advances beyond prior surveys in metamaterial antenna research through three critical innovations:

1. Comprehensive Performance Benchmarking:

   Unlike previous works that focused narrowly on either metamaterial theory [4] or antenna design [12], we provide the first unified comparison of 20 implemented MTM-antenna designs (Table III), analyzing:

   - Bandwidth extension (40-60% improvement over conventional designs)
   - Gain enhancement (3-8 dBi increase)
   - Size reduction (up to 75% smaller)

2. Practical Implementation Focus:

   While earlier reviews discussed idealized scenarios, we address real-world challenges:

   - Fabrication tolerances (<0.1 mm alignment for SRR structures)
   - Cost-performance tradeoffs (FR-4 vs. Rogers substrates)
   - Measurement-validated results (14 prototypes post-2020)

Table III: Guidelines for Selecting MTM-Based MPAs in Wireless Applications

Application	Key Requirements	Recommended MTM-MPA Design	Trade-offs
5G/mmWave	High gain (>8 dBi), wide bandwidth	Graphene superstrates, DNG MTMs (Section 3.1)	Costly substrates, fabrication complexity
IoT Nodes	Miniaturization, omnidirectionality	Fluidic reconfigurable MTMs (Case Study 2)	Lower gain (3–5 dBi)
Satellite Comms	Multiband operation, robustness	SRR-loaded or ceramic 3D-printed MTMs (Table II)	Limited tunability
Biomedical Implants	Biocompatibility, compact size	Biodegradable PLA-based MTMs [21]	Biomedical Implants

3. **Forward-Looking Analysis:**

   Moving beyond retrospective summaries, we:

   - Introduce AI-optimized designs [41] and biodegradable MTMs [46]
   - Provide application-specific selection guidelines

5. CONCLUSION

This paper reviewed the advancements in metamaterial based microstrip patch antennas and their pivotal role in addressing the limitations of traditional antennas, such as narrow bandwidth, low gain, and inefficiency in multiband operations. By leveraging the unique electromagnetic properties of metamaterials, including negative permeability and permittivity, MTM MPAs achieve significant performance enhancements, making them ideal for modern wireless communication systems like 5G, IoT, and satellite communications.

The study systematically analyzed design methodologies, feeding techniques, and performance optimization strategies, supported by a comparative evaluation of various antenna structures. Key findings from the data reveal that MTM integration enables remarkable improvements, such as bandwidth extension (40–60% over conventional designs), higher gain (3–8 dBi increase), and miniaturization (up to 75% size reduction). Substrate materials and feeding techniques were identified as critical factors influencing antenna performance, with FR4 being cost effective for lower frequencies and Rogers materials excelling in high frequency applications.

The main contribution of this work lies in its comprehensive benchmarking of MPAs, offering practical insights for researchers and engineers. The review also highlights emerging trends, such as AI driven optimization, biodegradable materials, and reconfigurable designs, which pave the way for future innovations.

REFERENCES

[1] N. Engheta, "Metamaterials in Microwaves and Optics: A Review," IEEE Antennas and Propagation Society International Symposium, Pp. 387–389, 2006.

[2] F. Martin, "Theory, fabrication and applications. Special issue on Microwave metamaterials," EuMA Proc., Vol. 2, 2006.

[3] J. B. Pendry, "Negative refraction makes a perfect lens," Phys. Rev. Lett., Vol. 85, pp. 3966, 2000.

[4] G. Singh, Rajni and A. Marwaha, "A Review of Metamaterials and its Applications," International Journal of Engineering Trends and Technology (IJETT), Vol. 19, No. 6, pp. 305-310, Jan. 2015.

[5] J. Howell, "Microstrip antennas," IEEE Trans. Antennas Propag., Vol. 23, No. 1, pp. 90–93, 1975.

[6] A. Author, B. Author, and C. Author, "Design of microstrip antenna for wireless communication at 2.4 GHz," International Journal of Wireless and Microwave Technologies, Vol. 10, No. 2, pp. 15–22, 2020.

[7] A. Arameters, "Microstrip patch antenna parameters, feeding techniques and shape of the patch—A survey," Int. J. Sci. Eng. Res., Vol. 6, No. 4, pp. 981–984, 2015.

[8] P. Upender, P. A. Harsha Vardhini, and V. Prakasam, "Performance Analysis and Development of printed circuit Microstrip Patch Antenna with proximity coupled feed at 4.3 GHz (C-band) with linear polarization for Altimeter Application," Int. J. Comput. Digit. Syst., 2020.

[9] A. Aziz, "A Review on Metamaterial Antenna for Wireless Communication," SEU Journal of Electrical and Electronic Engineering, Vol. 4, No. 1, pp. 34–42, 2024.

[10] G. Kaur et al., "Performance analysis of conductive patch materials for the design and fabrication of microstrip patch antennas," Progress in Electromagnetics Research Symposium - Spring (PIERS), 2017.

[11] J. Baviskar, A. Mulla, A. Baviskar, D. Auti and R. Waghmare, "Performance Enhancement of Microstrip Patch Antenna Array with Incorporation of Metamaterial Lens," IEEE Aerosp. Conf., 2016.

[12] D. H. Patel and G. D. Makwana, "A comprehensive review on multi-band microstrip patch antenna comprising 5G wireless communication," Int. J. Comput. Digit. Syst., Vol. 10, No. 1, pp. 1–13, 2021.

[13] A. Elrashidi, K. Elleithy, and H. Bajwa, "High-gain graphene-based metamaterial superstrate antenna for 5G millimeter-wave applications," IEEE Antennas Wireless Propag. Lett., Vol. 22, No. 3, pp. 634–638, 2023.

[14] M. A. Abdelghany et al., "Fluidically reconfigurable metamaterial antenna for IoT dual-band operation," IEEE Trans. Antennas Propag., Vol. 71, No. 5, pp. 3993–4002, 2023.

[15] S. Chen et al., "3D-printed ceramic metamaterial antenna for vehicular communications," IEEE Access, Vol. 11, pp. 23456–23467, 2023.

[16] B. Zhang and Q. H. Liu, "Artificial intelligence-optimized metamaterial antenna array for 5G base stations," Nature Commun. Eng., Vol. 3, No. 1, pp. 1–12, 2024.

[17] R. K. Gupta et al., "Solar-cell integrated metamaterial antenna for energy-efficient IoT nodes," IEEE J. Microw., Vol. 3, No. 2, pp. 678–689, 2023.

[18] T. Islam et al., "Inkjet-printed flexible metamaterial antenna for wearable applications," IEEE Open J. Antennas Propag., Vol. 4, pp. 412–423, 2023.

[19] H. Wang and D. R. Smith, "Terahertz graphene metamaterial antenna for 6G communications," IEEE Trans. Terahertz Sci. Technol., Vol. 13, No. 4, pp. 421–432, 2023.

[20] P. Kumar et al., "Defected ground structure-based UWB metamaterial antenna for medical imaging," IEEE Sensors J., Vol. 23, No. 8, pp. 8012–8021, 2023.

[21] L. M. Correia et al., "Biodegradable polylactic acid metamaterial antenna for eco-friendly IoT," IEEE Internet Things J., Vol. 10, No. 12, pp. 10876–10886, 2023.

[22] C. Wang et al., "Sub-terahertz metamaterial antenna for 6G wireless communications," IEEE Trans. Antennas Propag., Vol. 72, No. 1, pp. 512–523, 2024.

[23] J. Li and Y. Rahmat-Samii, "Holographic metamaterial antenna for V-band satellite links," IEEE Antennas Wireless Propag. Lett., Vol. 22, pp. 1898–1902, 2023.

[24] A. K. Singh et al., "Varactor-tuned reconfigurable metamaterial antenna for 5G dynamic spectrum sharing," IEEE Microw. Wireless Compon. Lett., Vol. 33, No. 6, pp. 789–792, 2023.

[25] S. H. Wong et al., "8×8 MIMO metamaterial antenna array for millimeter-wave 5G," IEEE Trans. Veh. Technol., Vol. 72, No. 5, pp. 6012–6025, 2023.

[26] M. M. Tentzeris et al., "Origami-inspired reconfigurable metamaterial antenna for emergency communications," IEEE J. Radio Freq. Identif., Vol. 7, No. 2, pp. 123–135, 2023.

[27] N. Nguyen et al., "Metamaterial antenna for dual-band satellite IoT applications," IEEE Commun. Lett., Vol. 27, No. 4, pp. 998–1002, 2023.

[28] H. Zhang et al., "Reconfigurable intelligent surface-assisted metamaterial antenna for vehicular networks," IEEE Trans. Intell. Transp. Syst., Vol. 24, No. 6, pp. 6215–6228, 2023.

[29] G. V. Naik et al., "Quantum dot-enabled optical metamaterial nanoantenna," IEEE Photon. J., Vol. 15, No. 3, pp. 1–12, 2023.

[30] A. Kiourti et al., "Implantable PEEK-based metamaterial antenna for biomedical telemetry," IEEE Trans. Biomed. Circuits Syst., Vol. 17, No. 2, pp. 324–335, 2023.

[31] F. Yang et al., "Metamaterial antenna array for UAV communications in 5.8 GHz band," IEEE Trans. Aerosp. Electron. Syst., Vol. 59, No. 3, pp. 2541–2552, 2023.

[32] Y. Li et al., "Metamaterial antenna for smart city infrastructure in 5G bands," IEEE Internet Things J., Vol. 10, No. 15, pp. 13456–13469, 2023.

[33] F. Umar and G. Rather, "Design and Analysis of Dual band Microstrip Antenna for Millimeter Wave (MMW) Communication Applications," Int. J. Comput. Digit. Syst., Vol. 9, No. 4, 2020.

[34] R. Azim, M. T. Islam and N. Misran, "Compact tapered-shape slot antenna for UWB applications," IEEE Antennas Wirel. Propag. Lett., Vol. 10, pp. 199–202, 2011.

[35] A. V. R. Anitha, S. Palanisamy, O. I. Khalaf, S. Algburi and H. Hamam, "Design and analysis of SRR based metamaterial loaded circular patch multiband antenna for satellite applications," ICT Express, Vol. 10, pp. 836–844, 2024.

[36] I. U. Din, N. A. Abbasi, W. Ullah, S. Ullah, M. A. Ouameur and D. N. K. Jayakody, "A novel and compact metamaterial-based four-element MIMO antenna system for millimeter-wave wireless applications with enhanced isolation," Int. J. Antennas Propag., Vol. 2024, Article ID 7480655, pp. 1–18, 2024.

[37] M. M. Hasan, M. T. Islam, T. Alam, P. Kirawanich, S. Alamri and A. S. Alshammari, "Metamaterial loaded miniaturized extendable MIMO antenna with enhanced bandwidth, gain and isolation for 5G sub-6 GHz wireless communication systems," Ain Shams Eng. J., Vol. 15, No. 1, p. 103058, 2024.

Use of Steel Slag and Plastic Wastes in Asphalt Concrete: A Review

Mahiman Zinnurain[1], Mahadi Hasan[1*], Md. Mizanur Rahman[2] and Gobinda Kirtonia[1]

[1]Department of Civil Engineering, Dhaka University of Engineering & Technology, Gazipur, Bangladesh
[2]Department of Civil Engineering, Bangladesh University of Engineering and Technology, Dhaka, Bangladesh

ABSTRACT

The global concern over plastic wastes arises from its detrimental impact on agriculture, marine life and human health. Conversely, discarding steel slag in open environments threatens biodiversity and undermines land fertility. Prior researches indicate the potential use of these materials for pavement. This study reviews the use of steel slag and plastic wastes on asphalt concrete based on previous studies. Based on the reviews, it is advisable to limit slag content to no more than 30% of the total aggregate weight and plastic content to no more than 20% of the bitumen weight. In conclusion, for promising research, it is recommended to substitute stone aggregate with PET (Polyethylene Terephthalate) coated steel slag (using the dry mixing process) combined with bitumen as a binder in AC mixtures.

1. INTRODUCTION

Due to their low cost and durability, plastics exhibit remarkable versatility, leading manufacturers to prefer them over alternative materials for various applications [1]. Yet, the majority of plastics possess a chemical structure that hinders their breakdown through natural processes, causing them to degrade at a slow pace [2]. The impact of deteriorated plastic waste on humans can occur through direct or indirect ingestion, and interference with diverse hormonal mechanisms [3]ubiquitous in nature and therefore affect both wildlife and humans. They have been detected in many marine species, but also in drinking water and in numerous foods, such as salt, honey and marine organisms. Exposure to microplastics can also occur through inhaled air. Data from animal studies have shown that once absorbed, plastic micro- and nanoparticles can distribute to the liver, spleen, heart, lungs, thymus, reproductive organs, kidneys and even the brain (crosses the blood–brain barrier. The proliferation of plastic materials, initially celebrated for their versatility and convenience, has reached a critical juncture where the consequences of their indiscriminate use are glaringly apparent. UNEP (2023) claims that plastic waste was in tamable volume from 1950 to 1970 and increased exponentially in next two decades. Almost 400 million tons per year of waste plastic is being resulted [4]. If historical growth patterns persist, by 2050, the production of plastic is projected to attain 1,100 million tons. Plastic consumption in urban areas of Bangladesh has increased to 9 kg/capita in 2020 from 3 kg/capita in 2005 [5]. Plastic and polythene waste constitute a primary cause of waterlogging in Chittagong, with the city generating 249 tons of such garbage on a daily basis [6].

Improperly disposed waste, accounting for only 2% of the total waste, lacks formal management and involves disposal in landfills and open areas, posing a significant risk of polluting rivers and oceans [7]. Plastic pollution has diverse impacts on various aspects including its effects on the environment, climate change, land, flooding, terrestrial ecosystems, freshwater ecosystems, human health [8]. As plastic waste continues to accumulate at an alarming rate, it has triggered a cascading series of environmental and social repercussions, demanding urgent attention and innovative solutions.

Contrariwise, steel slag (a byproduct of steelmaking) threatens biodiversity and hampers land fertility when dumped in the environment [9]. Almost 7.5 million tons of steel and 40-70 kg slag per ton is being produced per year in Bangladesh [9]. Slags have been used in construction since the 1800s, initially for road and railroad ballast, and later as aggregate and in cement as a geopolymer. [10]. Slags and slag tailings are stored in “slag dumps” where weathering can lead to toxic leaching and hyperalkaline runoff, posing ecological risks, with non-ferrous, ferrous, and ferroalloy slags all potentially contributing to these issues [11], [12].

The dissolution of slags has the potential to generate groundwater with elevated alkalinity, characterized by pH values exceeding 12 [13]. The authors noted that calcium

*Corresponding author’s email: mhasan49@duet.ac.bd

silicates in slags react with water, increasing groundwater alkalinity and causing calcite formation from dissolved CO2, potentially creating layers up to 20 cm thick.

Despite their drawbacks, both materials offer promising reuse potential. Researchers from east to west are studying and finding promising results. Waste plastic is being reused in various ways and so steel slag. Angularity, rough texture and hardness of slag assert its rutting resistance and soften plastic assert its binding property at 130°C - 180°C [14]instead of primary (virgin. The author mentioned the potentiality of waste plastic and steel slag as pavement materials. Several studies show better stability, water and thermal susceptibility, less OBC and cost when plastic (PET/HDPE/LDPE/Mixed) coated stone aggregate is used on AC mix [15]–[20]. Plastic coating filles the pores of demolished concrete and lower OBC and permanent deformation [21]. Researches have also been carried out by replacing stone aggregate with steel slag. Optimum slag content have found to be 25% [22] and 30 % [23]. Slag with PET (Polyethylene Terephthalate) and PP (Polypropylene) have been studied and some beneficial properties are found in AC mix [24], [25]. Despite of having many advantages, steel slag has a major disadvantage of consuming more bitumen. This can be improved by coating steel slag by a suitable agent [25], [26]. Despite numerous individual studies, there is a lack of consolidated analysis comparing performance outcomes between steel slag and plastic-modified asphalt mixes. Existing research typically focuses on case-specific experimental conditions, different waste processing methods, and varied proportions of additive materials, making it challenging to draw comprehensive conclusions about their relative effectiveness. This fragmented approach has resulted in a limited understanding of how steel slag and plastic waste respectively influence key performance indicators such as rutting resistance, moisture susceptibility, and overall durability under similar testing conditions. A systematic, comparative evaluation is therefore essential to identify the advantages, limitations, and potential synergies of each modification strategy.

This study aims to explore past studies involving polyethylene as pavement material, whether as a coating agent or a modified agent. The review extends to slag as pavement material, informed by earlier research. In conclusion, PET-coated steel slag is recommended as a potential pavement material.

1.1 Types of Plastic Debris

Plastic waste can be found from different sources with different sizes. Plastic waste can be classified based on their size, form and source. A several types of waste plastics are found based on their sources. They are shown on the Table I below:

Table I: Types of Waste Plastic and their Sources [27]

Type of waste plastic	Source
PET or Polyethylene Terephthalate	Bottles for drinks, water, beverages, and perishable food packaging.
HDPE or High-Density Polyethylene	Bottles for shower gel, shampoo, cleaning products, and children's toys.
PVC or Polyvinyl Chloride	Piping, windows, different types of medical equipment, plastic wrap and cables.
LDPE or Low-Density Polyethylene	Plastic shopping bags, frozen food bags, and squeezable bottles.
PP or Polypropylene	Plastic containers, hot food containers, plastic straws, and medicine bottles.
PS or Polystyrene	Packaging protection, insulation, and use in cups and egg cartons.
Other Plastics	Sunglasses, baby bottles, and even CDs.

1.2 Technical Specification of Slag Chips

Slag is a byproduct of the process of manufacturing steel and serves as an exceptionally versatile construction material. BSRM Slag Chips are an environmentally friendly product that possesses comparable strength to brick chips [28]. The technical specification of slag chips is given in table II.

Table II: Technical Specification of Slag Chips [28]

Category	Slag Chips	Brick Chips
Water Absorption Capacity	1.5% – 2%	11% - 13%
California Bearing Ratio (CBR)	115% – 130%	48% - 57%
Aggregated Crushing Value (ACV)	40% – 45%	28% - 35%
10% Fines Value (TFV)	75kN – 80 kN	69kN – 100kN

1.3 Improvement of AC Mix

The enhancement of the quality of various asphalt concrete (AC) mixes can be achieved through the implementation of two distinct methods [29]the increased asphalt consumption and decreased mechanical properties induced by the incorporation of RCA limit the extensive substitution of natural aggregates with RCA in HMA. In this paper, an experimental program was carried out to investigate the potential of recycled concrete aggregate pretreated with waste cooking oil residue (WCOR:

i. Physical Strengthening - Eliminating attached components by subjecting them to heat and immersing them in acidic solutions.
ii. Chemical Strengthening - Enhancing quality through the application of various coatings using different materials.

Numerous studies have been undertaken to introduce novel materials into asphalt concrete mixes, aiming to improve both the overall quality and the effective management of waste. Slag has been studied for a long time [22], [23], [30]. Different additives have also been used to enhance binding quality. Amuchi et al. [25] used PP, LDPE has been used by [31]Indonesia is facing pavement problem due to various reasons, so it needs to improve the pavement quality and performance. The addition of plastic waste to the hot mix asphalt (HMA.

1.4 Mixing Process of Additives

Additives can be blended into asphalt mixtures using two distinct methods [15]. These additives can serve either as a coating agent or as a modifier for bitumen. The two procedures are outlined below:

- ❖ Dry Process of Mixing
- ❖ Wet Process of Mixing

1.4.1 Dry Process of Mixing

Modak and Belkhode [15] explained the procedure in this way: First, the mixture of aggregates is heated to 170°C before being moved to the mixing chamber. At the same time, bitumen is heated to a maximum of 160°C. In the mixing chamber, shredded plastic waste is added to the hot aggregates. The aggregates coated with plastic waste are then mixed with the heated bitumen. The process is shown in Fig. 1.

1.4.2 Wet Process of Mixing

The additive (E. g. plastic waste) is ground into a powder, combined with bitumen and subsequently mixed with the aggregate. Basically, bitumen is modified by an agent and then mixed with hot aggregate. The process is shown in Fig. 2.

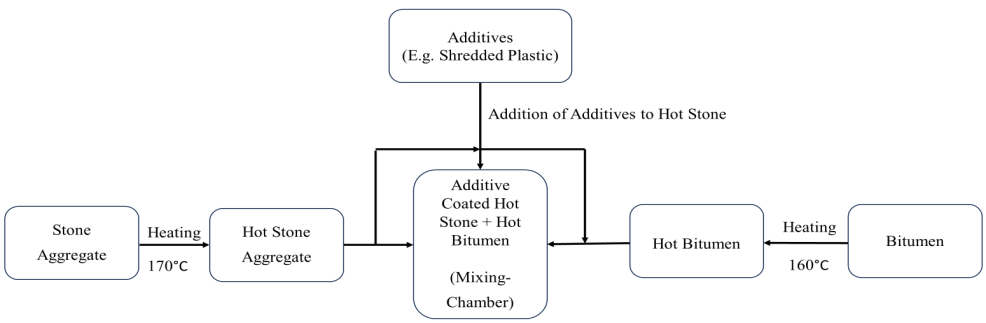

Fig. 1: Dry Process of Mixing

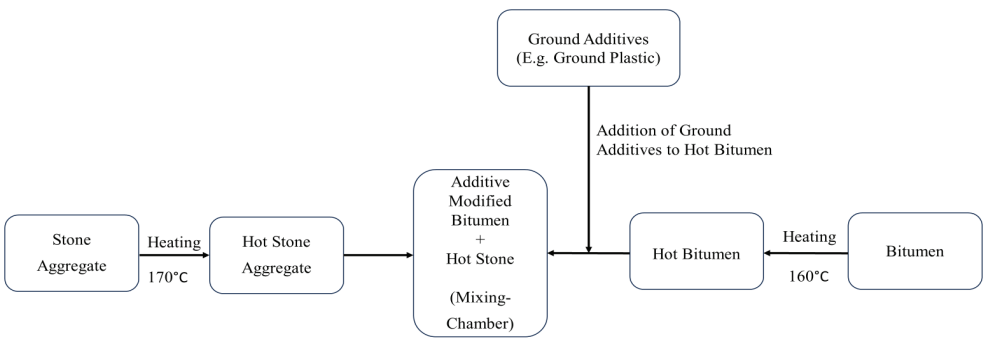

Fig. 2: Wet Process of Mixing

1.5 Approach to the Study

This study is based on a systematic review of 55 peer-reviewed articles published between 2000 and 2023. From well-known academic databases including Web of Science, Google Scholar, and Scopus, pertinent literature was found and gathered. The main emphasis was on experimental research that looked into adding steel slag and/or plastic trash to asphalt concrete mixtures. The types of waste materials employed, inclusion techniques, mix design parameters, testing procedures, and the ensuing impacts on the mechanical and durability qualities of asphalt concrete were all examined in the chosen research. This method made it possible to conduct a thorough evaluation of the field's knowledge gaps, technical developments, and current research trends.

2. LITERATURE REVIEW

Waste plastic and steel slag have long been explored as pavement materials. Several researchers [22], [23] studied AC mix by substituting stone in different percentages keeping fresh bitumen as binder. Some of them [19], [20] used waste plastic either in dry or in wet process combined with stone and bitumen. Some studies [25], [32] have also been conducted combining stone, slag, waste plastic and bitumen. Based on the materials used this portion is divided into four segments.

i. Stone - Slag - Bitumen
ii. Stone - Bitumen - Plastic Waste (PW)
iii. Stone - Slag - Bitumen – PW
iv. Other Aggregates - Bitumen – Wastes

2.1 Stone - Slag – Bitumen

Asi et al. (2007) initially evaluated the toxicity, chemical, and physical properties of steel slag. They then replaced varying percentages (0%, 25%, 50%, 75%, and 100%) of limestone coarse aggregate in asphalt concrete (AC) with steel slag aggregate (SSA). The effectiveness of SSA was assessed by improvements in AC samples' indirect tensile strength, resilient modulus, rutting resistance, fatigue life, creep modulus, and stripping resistance. The chemical and toxicity assessments confirmed that steel slag meets safety standards for highway construction. Results showed that replacing up to 75% of limestone with SSA enhanced AC properties, though 100% slag reduced creep performance, with 25% being the optimal replacement level [22].

Ahmedzade & Sengoz (2009) investigated how steel slag affects hot mix asphalt properties. They used four asphalt mixtures with two types of asphalt cement (AC-5 and AC-10) and two coarse aggregates (limestone and steel slag) to create Marshall specimens for optimal bitumen content. Mechanical properties were tested, including Marshall stability, indirect tensile stiffness modulus, creep stiffness, and indirect tensile strength, along with electrical sensitivity. Results showed that using steel slag as a coarse aggregate increased stability, stiffness, and conductivity while decreasing flow values, leading to higher stiffness and resistance to deformation in the mixtures [30].

A practical on field experiment was observed by Liz Hunt (2012) replacing stone by 30 % of steel slag. An examination of in-place characteristics, field observations, skid testing, and ride testing reveals no discernible performance distinctions between the control and steel slag pavements. Both types of pavements seem to be functioning well. Although minor raveling was observed in both sections, it is not deemed a critical issue. Ongoing monitoring will be conducted to detect any potential changes in pavement performance. But slag pavement was found to be more cost efficient [23].

Ezemenike et al. (2022) explored using alternative materials, specifically waste by-products, to improve pavement properties. They tested cylindrical samples of asphalt concrete with varying amounts of steel slag (SS) replacing traditional aggregates at 2%, 4%, 6%, and 8%. The findings show that steel slag can effectively replace aggregates, enhancing mixture properties. For medium traffic roads, a 2% SS replacement achieved a stability value of 7.75 kN, while values of 8.63 kN, 9.82 kN, and 11.00 kN at 4%, 6%, and 8% SS replacements, respectively, are suitable for heavy traffic roads according to the Asphalt Institute's standards. Thus, using steel slag can significantly decrease the need for natural aggregates and lessen the pressure on these resources [33].

Chen and Wei (2016)a test road was constructed in 2012 by using three different types of asphalt mixtures as follows: stone mastic asphalt with BOF (SMA-BOF studied asphalt mixtures using basic oxygen furnace (BOF) steel slag as coarse aggregate. Laboratory tests evaluated the asphalt concrete's engineering properties. A 2012 test road featured three asphalt mixtures: stone mastic asphalt with BOF (SMA-BOF), dense-graded asphalt concrete with BOF (DGAC-BOF), and dense-graded asphalt concrete with natural aggregate (DGAC-NA). Despite heavy vehicle stress, the SMA-BOF section showed the least rutting. Both BOF mixtures performed similarly or better than the natural aggregate section in ride quality and friction. BOF steel slag met highway agency specifications and potentially enhanced asphalt

mixture properties [34]a test road was constructed in 2012 by using three different types of asphalt mixtures as follows: stone mastic asphalt with BOF (SMA-BOF.

According to Shatnawi et al. (2008) research, steel slag sourced from a Jordanian steel factory was employed in Asphalt Concrete Hot Mixes (ACHM). Control specimens were created with 100% limestone dense-graded aggregates at varying bitumen contents (4.5%, 5%, 5.5%, and 6% by weight of aggregate). Another set of Marshall Specimens was prepared using full Steel Slag Aggregates (SSA), a third set involved combination of limestone and SSA, all maintaining the same grading and bitumen contents. The research observed a potential reduction in the optimum bitumen content (OBC) value and enhanced performance of asphalt concrete when employing SSA in. The study recommends that producers and users of asphalt concrete hot mixes (ACHM) in Jordan consider incorporating SSA for improved performance [35].

Ameri et al. (2013) evaluated the use of electric arc furnace (EAF) steel slag (SS) as a substitute for natural limestone (LS) in warm mix asphalt (WMA) and hot mix asphalt (HMA) mixtures. SS was used as both fine and coarse aggregate in HMA blends and as coarse aggregate in WMA. The Marshall test results showed that substituting coarse LS with SS improved Marshall stability, flow, and the MQ parameter in HMA mixtures [36].

Nguyen et al. (2018)a by-product of steelwork industry, under Vietnamese's law, was considered as a deleterious solid waste which needed to be processed and landfilled. However, this has changed recently, and steel slag is now seen as a normal or non-deleterious solid waste, and has been studied for reuse in the construction industry. In this study, steel slag was used, as a replacement for mineral aggregate, in hot mix asphalt. Two hot mix asphalt mixtures with an equivalent nominal aggregate size of 12.5 (C12.5 investigated using steel slag as a replacement for mineral aggregate in hot mix asphalt. They created two asphalt mixtures with steel slag, one with a nominal aggregate size of 12.5 mm and another with 19 mm, and compared them to a conventional mixture of 19 mm mineral aggregate. Steel slag showed comparable physical properties to mineral aggregate, despite being heavier, and demonstrated good water stability. The steel slag mixtures met Vietnamese standards for Marshall Stability and flow, and both sizes exhibited adequate skid resistance, making them suitable for surface courses [37] a by-product of steelwork industry, under Vietnamese's law, was considered as a deleterious solid waste which needed to be processed and landfilled. However, this has changed recently, and steel slag is now seen as a normal or non-deleterious solid waste, and has been studied for reuse in the construction industry. In this study, steel slag was used, as a replacement for mineral aggregate, in hot mix asphalt. Two hot mix asphalt mixtures with an equivalent nominal aggregate size of 12.5 (C12.5.

H M (2014) conducted a study to examine the impact of incorporating iron slag powder into hot mix asphalt on Marshall Stiffness and indirect tensile strength. Three different hot mix asphalt compositions were investigated, each containing varying percentages of iron slag (0%, 10%, and 20% by weight of the total mixture). The test results demonstrated enhancements in both Marshall stability and indirect tensile strength when iron slag powder was included as part of the fine aggregate in the mixtures. Across the range of iron slag content tested (0% to 20% of the total mixture), both Marshall stability and indirect tensile strength exhibited a positive correlation with increasing iron slag content. Additionally, it was observed that other Marshall properties such as density, air voids, and VMA also increased with higher iron slag contents [38].

Sridhar & Sastri (2021) assessed Steel Slag Aggregate (SSA) for use in Hot Mix Asphalt (HMA) and flexible pavements, aiming to reduce reliance on natural resources. They prepared four HMA mixes with increasing SSA content from 25% to 75% of natural aggregates. SSA improved mix density and stability, enhancing resistance to deformation. The Marshall Stability Test showed the optimum bitumen content increased from 5.2% with natural aggregates to 5.7% with 75% SSA. Using steel slag not only boosts asphalt quality but also supports environmental conservation by decreasing the need for natural aggregates [39]. Table III shows the summary of Stone – Slag – Bitumen. Here Optimum Steel Slag Content and Optimum Bitumen Content are abbreviated by OSC and OBC.

Several studies have explored the replacement of conventional stone with steel slag in proportions ranging from 0% to 100%. The optimum slag content was found to be around 25%. Findings indicate that slag can be used in both coarse and fine aggregates. Its inclusion improves various properties of Hot Mix Asphalt (HMA), such as stability and creep resistance, while also reducing overall costs.

Table III: Summary of Stone - Slag – Bitumen

Reference	Stone %	Slag %	Major Findings
[22]	100−0	0−100	OSC = 25%; slag improved mechanical properties; reduced creep
[30]	100, 65	0, 35	High stability and strength; low flow
[23]	100, 70	0, 30	Satisfactory quality; cost-effective
[33]	98−92	2−8	Marshal stability increased up to 8% SS replacement
[34]	Not Specified	Not Specified	Improved engineering properties
[35]	100−0	0−100	SSA lowered asphalt mix OBC
[36]	FA, CA, 0	CA, FA, Both	SS improved Marshall properties in HMA mixtures
[37]	100, 0	0, 100	Steel slag HMA met Vietnam standards
[38]	100−80	0−20	Iron slag improved stability and strength
[39]	75−25	25−75	OBC increased from 5.2% to 5.7%

2.2 Stone - Bitumen - Plastic Waste (PW)

PET, ranging from 0 to 10% by the weight of 80/100 grade bitumen, has been incorporated into Stone Mastic Asphalt (SMA) through a dry process additive addition by Ahmadinia et al.(2012). Utilizing 4-6% PET demonstrates reduced drain down of binder, heightened resistance against permanent deformation, and increased stiffness. This method enables the eco-friendly and economical reuse of waste materials [18].

Awwad and Shbeeb (2007) used HDPE and LDPE polyethylene to coat aggregates in either grinded or not grinded forms. They prepared 105 samples, with 21 for binder content determination and the rest for studying asphalt modification. The optimum binder content was 5.4%. Seven weight percentages of each polyethylene type (6%-18%) were tested. The best results were achieved with 12% ground HDPE, leading to higher stability, lower density, and a slight increase in voids. The asphalt mix with grinded HDPE showed the highest stability (2347 kg), outperforming the not grinded variant [20].

Musa (2014) gathered, cleaned, shredded, and then blended low-density polyethylene (LDPE) carry bags discarded from supermarkets with asphalt hot mix at a temperature of 150°C in the Roads. The alterations in marshal stability, flow, and voids resulting from the inclusion of low-density polyethylene carry bag waste (at concentrations of 4 %, 6 %, 8 %, 10 %, 12 %, 14 %, 16 %, and 18 % of the asphalt weight) were assessed. The findings revealed enhancements in the properties of asphalt hot mix design, particularly when a 10 % concentration of low-density polyethylene waste, relative to the asphalt weight, was utilized, thereby contributing to an improvement in environmental pollution [19].

Suaryana et al. (2018)Indonesia is facing pavement problem due to various reasons, so it needs to improve the pavement quality and performance. The addition of plastic waste to the hot mix asphalt (HMA developed three Asphalt Concrete Wearing Course (AC-WC) mixtures with 0%, 5%, and 10% LDPE plastic waste. Tests showed that adding plastic improved Marshall stability, resilient modulus, and resistance to stripping, moisture, and rutting. While moderate plastic content boosts fatigue life and raveling resistance, too much plastic reduces these benefits compared to traditional HMA [31]Indonesia is facing pavement problem due to various reasons, so it needs to improve the pavement quality and performance. The addition of plastic waste to the hot mix asphalt (HMA.

Sojobi et al. (2016) used PET as an additive in HMA by both wet and dry process. The plastic content was adjusted across different proportions, including 0% as a control, 5%, 10%, and 20% for polymer-modified bituminous (PMB) asphaltic concrete, and 10%, 20%, and 30% for polymer-coated asphaltic (PCA) mix. It was found to be eco-friendly and more benefitable in terms of stability. Optimum plastic waste content (OPC) was observed to be 16.7 % by weight of total aggregate. The use of PCA-modified AC mix maximizes PET recycling, achieving a higher optimal plastic content of 16.7%, in contrast to the 9% optimal plastic content achieved with PMB-modified. [17].

Plastic waste, including items like cups and bags made from PE, PP, and PS, was processed through a

shredding machine to achieve a size range between 2.36 mm and 4.75 mm to mix with HMA by dry process. When these plastics coat the aggregates, Mir (2015) observed that it enhances the surface properties of the aggregates. This coating results in a doubling of the binding property of the aggregates and an increase in their overall strength. Remarkably, roads constructed with this method exhibit no degradation even after several years. Additionally, there is a reduction in the required bitumen by approximately 10 %, allowing for the utilization of waste plastic exceeding 15 %. The cost difference for roads constructed with this compound, as opposed to without it, amounts to Rs. 500 per cubic meter [16].

Modak and Belkhode (2022) incorporated plastic waste ranging from 2.36 mm to 4.75 mm into bitumen at varying percentages (8%, 10%, 12%, and 20%). The resulting mixture exhibited increased Marshall Stability values and an appropriate Marshall Coefficient. Consequently, utilizing waste plastics in pavement construction emerges as a highly effective approach for the convenient disposal of plastic waste [15].

Jegatheesan et al. (2018) explored adding PET fibers to Hot Mix Asphalt Concrete (HMAC) to reduce costs. PET fibers (0.5 mm in diameter and 4.0-6.0 mm in length) were mixed into HMAC using a wet process in varying amounts (5%-40% of bitumen weight). The study found that PET fibers significantly improve Marshall stability and bulk properties, with stability peaking at 30% PET content and Marshall flow increasing with fiber addition [40].

Baghaee Moghaddam et al. (2014) aimed to assess the impact of incorporating waste Polyethylene Terephthalate (PET) as a modifier on the characteristics of asphalt mixtures. In a dry process, post-consumer PET bottles with a size of 2.36 mm and below were utilized in varying quantities ranging from 0% to 1% by weight of mixed aggregates. The bulk specific gravity and stiffness of the asphalt mixture initially increase with lower amounts of PET, but decrease with higher PET contents. The application of PET leads to a reduction in Marshall Quotient and indirect tensile strength values, with higher amounts of PET resulting in lower values for both Marshall Quotient and tensile strength [41].

Hassani et al. (2005)more than 1 million m3 landfill space is needed for disposal every year. The purpose of this experimental study was to investigate the possibility of using PET waste in asphalt concrete mixes as aggregate replacement (Plastiphalt examined the use of PET waste in asphalt concrete, called “Plastiphalt,” to reduce environmental impact. PET granules (3 mm in diameter) replaced 20%-60% of coarse aggregates (2.36–4.75 mm) in the mix through a dry process. The study found that replacing 5% of aggregate with PET improved Marshall quotient, lowered flow, and minimized stability reduction, offering economic and environmental benefits. Using Plastiphalt could save 625 tons of natural resources and use 315 tons of PET, making it a viable option for pavements and bridge overlays [42]more than 1 million m3 landfill space is needed for disposal every year. The purpose of this experimental study was to investigate the possibility of using PET waste in asphalt concrete mixes as aggregate replacement (Plastiphalt.

Zoorob and Suparma (2000)predominantly composed of low density polyethylene (LDPE studied adding recycled LDPE pellets to dense bituminous mixes, replacing 30% of aggregates (5.00-2.36 mm). This substitution reduced mix density by 16%, lowering haulage costs. It also led to a 250% increase in Marshall stability and improved resistance to deformation. While the mix’s stiffness was lower than the control, its tensile strength was significantly higher [43]predominantly composed of low density polyethylene (LDPE.

Punith and Veeraragavan (2007) investigated using reclaimed low-density polyethylene (PE) from household carry bags as an additive in asphalt mixtures. They tested PE in various amounts (2.5%-10% by asphalt weight) with 80/100-grade asphalt. Results showed that PE-modified mixtures had less plastic deformation, higher shear resistance, and improved tensile strength at low temperatures, reducing pavement cracking risks. This approach effectively repurposes LDPE bags at a reasonable cost while enhancing asphalt properties [44].

Hinislioglu and Agar (2004) studied using HDPE plastic waste as an additive in asphalt concrete. They blended HDPE (4%-8% of bitumen weight) with AC-20 at 145-165°C for 5-30 minutes. HDPE-modified asphalt showed improved Marshall Stability and resistance to deformation. The best results came from mixing 4% HDPE at 165°C for 30 minutes, yielding the highest stability and Marshall Quotient, indicating stronger mixes than the control [45].

Attaelmanan et al. (2011) investigated using HDPE as an asphalt modifier. They tested 1%, 3%, 5%, and 7% HDPE with 80/100 grade asphalt. Adding 5% HDPE increased the Marshall Quotient by 55%, indicating better resistance to deformation. HDPE-modified asphalt showed high tensile strength and durability, making it suitable for military airfields and flexible pavements [46].

Ahmadinia et al. (2011) investigated using PET plastic bottles in stone mastic asphalt (SMA). Various PET percentages (0%-10%) were added, and the mixtures were tested for their properties. Results showed that PET initially improved Marshall Stability, peaking at 6%, but then decreased. Marshall Flow dropped initially and then increased with more PET. PET improved mix stiffness, resulting in a higher Marshall Quotient and better deformation resistance, with properties meeting standards [47].

Panda & Mazumdar, (2002 employed reclaimed polyethylene (PE) derived from LDPE carry bags to modify asphalt cement in his study. LDPE carry bags with dimensions of 3 mm by 3 mm were utilized at proportions of 2.5%, 5.0%, 7.5%, and 10% by weight of bitumen through a wet process. After evaluating the properties of both the modified binders and the mixes, it was determined that the optimal quantity of reclaimed polyethylene by weight of the binder was 2.5%. Under specific temperature and stress conditions, polymer modification resulted in an increase in the resilient modulus and fatigue life of the mixes. Furthermore, the modification contributed to an enhancement in resistance to moisture susceptibility [48]. Table IV shows the summary of Stone - Bitumen - Plastic Waste (PW). Here Optimum Plastic Content, Optimum Steel Slag Content and Optimum Bitumen Content are abbreviated by OPC, OSC and OBC. In addition, PW (Plastic Waste) % is shown by weight of bitumen.

Various types of plastic waste, including PET, HDPE, LDPE, PE, PP, and PS, have been incorporated into HMA using both dry and wet processes. While some studies used plastic waste up to 60%, the optimal range was typically 4-16%. Most plastics used were in the size range of 2.36-4.75 mm. The inclusion of plastic waste enhanced several mechanical properties such as stability, Marshall Quotient, tensile strength, rutting resistance, and stiffness-alongside offering cost savings and environmentally friendly benefits.

Table IV: Summary of Stone - Bitumen - Plastic Waste

Ref.	PW Type	PW %	PW size (mm)	Process	Major Findings
[18]	PET	0−10	2−3	Dry	OPC = 4−6 %; Resist rutting; Increase stiffness
[20]	HDPE, LDPE	6−18		Dry	OBC = 5.4%; OPC = 12%; HDPE modifier achieved highest stability
[19]	LDPE	4−18		Wet	OPC = 10 %; High stability; Minimum VFA; Improved environment.
[31]	LDPE	0−10	0.6 – 9.5	Dry	LDPE enhances asphalt properties
[17]	PET	Wet: 5 − 20 Dry: 10 − 30		Wet & Dry	Eco friendly solution; OPC = 16.7%
[16]	PE, PP, and PS	6 - 8	2.36 – 4.75	Dry	Enhanced binding property; OPC = 15%; Rs. 500 savings per cum.
[15]	PW	8 − 20	2.36 – 4.75	Wet	Improved Marshall mix
[40]	PET fibers	5−40	4−6	Wet	PET boosted asphalt properties
[41]	PET	0−1.0	2.36	Dry	PET decreased Marshall Quotient and tensile strength
[42]	PET	20−60	2.36–4.75	Dry	PET reduced stability; increased flow
[43]	LDPE		2.36−5	Dry	LDPE reduced density; boosted strength
[44]	LDPE	2.5−10	2	Wet	5% PE improved asphalt performance
[45]	HDPE	4 – 6 and 8	0.935 g/c^3.	Wet	HDPE boosted asphalt strength
[46]	HDPE	1−7	solid form	Wet	HDPE increased softening point and strength
[47]	PET	0−10		Dry	PET initially increased stability, then decreased; flow decreased, then increased
[48]	LDPE carry bags	2.5−10	3	Wet	Marshall mix meets IRC criteria; optimum quantity of reclaimed polyethylene = 2.5%

2.3 Stone - Slag - Bitumen – PW

Rajabi (2022) assessed the impact on pavement performance combining steel slag and recycled polyethylene in various proportions. The study involved conducting resilience modulus tests, Marshall Resistance tests, dry and wet indirect traction tests, and moisture sensitivity tests. Both dry and wet ITS, MR, water susceptibility showed better value in increase in slag content. rPET influenced in dry but a little in wet ITS and lowered down water susceptibility. The findings also indicated that utilizing a blend of both materials in the mix yielded superior results compared to employing each material separately [32].

Amuchi et al. (2015) studied modified SSAC (Steel Slag Asphalt Concrete) samples using three different lengths of PP fibers—6 mm, 12 mm, and 19 mm—at varying mass percentages of 2 %, 4 %, and 6 %, relative to the total weight of bitumen. The inclusion of 2% - 19 mm PP fibers results in a reduction of approximately 15% in the optimized asphalt content when compared to the neat mixture steel slag asphalt concrete. Furthermore, there is an increase in both indirect tensile strength and resilient modulus (MR) [25].

Hasban et al. (2022) tested Marshall specimens with bitumen content between 4.0% and 5.0% by weight to find the ideal amount. The specimens included various percentages of P.E.T. (0%, 4%, 6%, 8%, 10%) relative to bitumen weight and steel slag aggregate at 5%, 10%, and 15%. They assessed parameters such as Marshall Stability, Flow value, Marshall Quotient, Air voids (Vv), Voids in Mineral Aggregates (VMA), Voids Filled with Bitumen (VFB), and Retained Stability using the wet process and compared these with standard bituminous mixes. The results showed significantly higher Marshall Test values for modified mixes compared to conventional ones. The optimal bitumen content was found to be 4.5%. Utilizing up to 8% plastic and 15% steel slag can be beneficial and reduce overall road construction costs [24]. Table V shows the summary of Stone - Slag - Bitumen - PW. Here Optimum Plastic Content, Optimum Steel Slag Content and Optimum Bitumen Content are abbreviated by OPC, OSC and OBC. In addition, PW (Plastic Waste) % is shown by weight of bitumen.

Different plastic wastes like PET and PP were used up to 15% by wet mixing, with the optimum plastic content found to be around 8% and optimum slag content at 15%. The simultaneous inclusion of slag and plastic in HMA contributed to reduced optimum bitumen content and enhanced cost-effectiveness.

Table V: Summary of Stone - Slag - Bitumen – PW

Ref.	Slag %	PW Type	PW%	PW size	Process	Major Findings
[32]	0-100	rPET	0−15		Wet	Slag and rPET improved all the properties
[25]		PP	2−6	6, 12, 19	Wet	OPC = 2%; Optimum size = 19 mm; 15% reduction of OBC
[24]	5-15	PET	0−10		Wet	OBC = 4.5%; OPC= 8%; OSC = 15%; Cost efficiency

2.4 Other Aggregates - Bitumen – Wastes

Ma et al. (2019) investigated using recycled concrete aggregate (RCA) treated with waste cooking oil residue (WCOR) to lower asphalt use and enhance Hot Mix Asphalt (HMA) performance. Their lab analysis involved HMA with 40% coarse RCA and 20% fine RCA treated with WCOR. Results showed that treating RCA with WCOR reduced the optimum asphalt content from 5.4% to 4.5% for 40% coarse RCA and from 5% to 4.5% for 20% fine RCA. This treatment improved the fatigue life and low-temperature performance of HMA but slightly affected moisture sensitivity, resistance to permanent deformation, and dynamic modulus [29]the increased asphalt consumption and decreased mechanical properties induced by the incorporation of RCA limit the extensive substitution of natural aggregates with RCA in HMA. In this paper, an experimental program was carried out to investigate the potential of recycled concrete aggregate pretreated with waste cooking oil residue (WCOR.

Azarhoosh et al. (2021) tested CRCA (Coarse Recycled Concrete Aggregate) surfaces coated with waste plastic bottles (WPB) at 15%, 30%, and 50% to evaluate their rutting resistance in hot mix asphalts. Results showed that untreated CRCA reduced both the Marshall quotient and rutting resistance, increasing permanent deformation. In contrast, treated CRCA with WPB reduced permanent deformation by enhancing CRCA stability through void filling and cement mortar reinforcement. Elevated

temperatures lowered the stiffness modulus of all asphalt concretes, with a more significant decrease in the modified specimens [21].

Using waste materials in pavement can reduce waste, environmental pollution, and costs. Arabani & Azarhoosh (2012) tested six asphalt mixtures with different aggregates (dacite, recycled concrete, steel slag) to find the best asphalt binder content. Replacing coarse dacite with recycled concrete aggregates (RCA) worsened mechanical properties due to weak cement mortar removal. However, using RCA as fine aggregate and steel slag as either fine or coarse aggregate improved Marshall stability and reduced flow. The optimal mix was RCA as fine aggregate, steel slag as coarse aggregate, and dacite as filler, which showed strong mechanical properties [49].

Paranavithana and Mohajerani (2006) studied the use of Recycled Concrete Aggregates (RCA) in asphalt concrete. They compared control mixes with fresh basalt aggregates and varying bitumen percentages (5.0%, 5.5%, 6.0%) to modified mixes with RCA and different bitumen contents (5.1%, 5.5%, 6.0%, 6.5%). Results showed that RCA-containing asphalt had lower bulk density, voids in mineral aggregates, and film thickness, but higher air voids compared to the control mix. This was due to the porous, low-density cement mortar on RCA particles, which increased water absorption and decreased particle density [50].

Mills-Beale and You (2010)pressing demand on existing landfill sites, rising dumping fees, and reduced emissions into the environment. Recycled Concrete Aggregates (RCA evaluated the mechanical properties of asphalt mixtures with recycled concrete aggregates (RCA) for low-volume roads. RCA replaced Michigan traprock aggregates in hot mix asphalt (HMA) at 25%, 35%, 50%, and 75% substitution rates. The VA-RCA HMA met SuperpaveTM performance standards and proved effective for low-traffic roads. Temperature had a greater effect on the resilient modulus than RCA levels, and the dynamic modulus increased as RCA content decreased [51]pressing demand on existing landfill sites, rising dumping fees, and reduced emissions into the environment. Recycled Concrete Aggregates (RCA.

Arabani et al. (2017) examined how waste materials as fillers affect hot mix asphalt (HMA) performance. They tested mixtures with waste glass powder (WGP), waste brick powder (WBP), rice husk ash (RHA), and stone dust (control) to find the optimal asphalt binder content. Tests showed WGP had the highest stability and lowest flow, followed by WBP, stone dust, and RHA. Mixtures with these fillers had progressively lower air voids. The study suggests that these waste materials could be useful in road construction due to environmental and resource concerns [52].

Gautam et al. (2018) investigated using limestone mining waste (Kota stone) as aggregates in bituminous concrete (BC) and dense bituminous macadam (DBM), replacing traditional basalt aggregates. They tested ten mix combinations with LSA replacing 0% to 100% of conventional aggregates, assessing strength, durability, moisture resistance, and rutting resistance. The Marshall mix design method, with 75 blows per side, showed that all LSA mixes met the criteria for low-volume roads. However, increasing LSA content led to lower stability and higher flow values, reducing the Marshall Quotient [53].

Arabani et al. (2013) studied hot mix asphalt concrete using dacite and recycled concrete aggregates (RCA). They tested RCA as a partial or full replacement for dacite in coarse aggregate (CA), fine aggregate (FA), and filler. RCA as CA worsened mechanical properties due to particle breakage and weak cement mortar disruption. The best mix used RCA as FA, with dacite as CA and filler. Although RCA increased CaOH levels, raising environmental concerns, using RCA as fines and filler improved Marshall Stability [54].

Haritonovs and Tihonovs (2014)where local crushed dolomite and sandstone do not fulfill the requirements for mineral aggregate in high and medium intensity asphalt pavements roads. Annually 100–200 thousand tons of steel slag aggregates are produced in Latvia. However, it has not been used extensively in asphalt pavement despite of its high performance characteristics. Dolomite sand waste, which is a byproduct of crushed dolomite production, is another widely available polydisperse by-product in Latvia. Its quantity has reached a million of tons and is rapidly increasing. This huge quantity of technological waste needs to be recycled with maximum efficiency. Various combinations of steel slag, dolomite sand waste and conventional aggregates were used to develop asphalt concrete AC 11 mixtures. The mix properties tests include resistance to permanent deformations (wheel tracking test, dynamic creep test investigated using dolomite sand waste as filler or sand and blast furnace steel slag as aggregate in high-performance asphalt concrete. They created AC 11 mixtures with various combinations of these materials and traditional aggregates, testing them for resistance to permanent deformations and fatigue. Results showed that mixtures with steel slag and limestone in the coarse aggregate, and dolomite sand waste in the sand

and filler, had strong resistance to plastic deformations and fatigue failure [55]where local crushed dolomite and sandstone do not fulfill the requirements for mineral aggregate in high and medium intensity asphalt pavements roads. Annually 100–200 thousand tons of steel slag aggregates are produced in Latvia. However, it has not been used extensively in asphalt pavement despite of its high performance characteristics. Dolomite sand waste, which is a byproduct of crushed dolomite production, is another widely available polydisperse by-product in Latvia. Its quantity has reached a million of tons and is rapidly increasing. This huge quantity of technological waste needs to be recycled with maximum efficiency. Various combinations of steel slag, dolomite sand waste and conventional aggregates were used to develop asphalt concrete AC 11 mixtures. The mix properties tests include resistance to permanent deformations (wheel tracking test, dynamic creep test. Table VI shows the summary of Other Aggregates - Bitumen - Wastes.

Unconventional aggregates such as recycled concrete aggregate (RCA), along with various waste materials like plastic bottles, waste cooking oil residue (WCOR), waste glass powder (WGP), waste brick powder (WBP), rice husk ash (RHA), and stone dust, were introduced in HMA primarily through the dry mixing process. These inclusions generally led to a reduction in optimum bitumen content (OBC), improved fatigue life, and lower mix density. However, some materials like RCA raised environmental concerns due to increased calcium hydroxide (CaOH) content.

Table VI: Summary of Other Aggregates - Bitumen – Wastes

Ref.	Aggregate With % used	Waste Type	Process	Major Findings
[29]	RCA	WCOR	Dry	OBC decreased; improved fatigue life
[21]	Stone and CRCA (0−50)	PET	Dry	Treated CRCA improved performance
[50]	Stone and RCA			RCA reduced mix density, voids, voids filled with binder, and film thickness.
[51]	Stone and RCA (25−75)			RCA reduced mix stiffness
[52]	Stone, WGP, WBP, RHA			WGP showed highest stability value as compared to WBP, SD, and RHA
[53]	Stone and LSA (0−100)			Declining stability, increasing flow with LSA
[54]	Dacite Stone and RCA			RCA increased CaOH, causing environmental concerns.

3. CONCLUSIONS

After reviewing the literatures, these key factors can be concluded:

- Both steel slag and waste plastic demonstrate their suitability for use in AC mixtures.
- Waste plastic can be applied in both dry and wet processes, meaning it can be used to coat aggregates and modify bitumen.
- When utilized as a coating agent, plastic waste exhibits superior results compared to its role in modifying bitumen.
- Based on the optimal findings for slag and plastic content, it is advisable to limit slag content to no more than 30% of the total aggregate weight and plastic content to no more than 20% of the bitumen weight.
- Among plastic types, PET and HDPE show greater potential.
- In conclusion, for promising research, it is recommended to substitute stone aggregate with PET-coated steel slag (using the dry mixing process) combined with bitumen as a binder in AC mixtures.
- PET-coated steel slag is expected to reduce the optimum bitumen content and overall costs, while enhancing Marshall properties. It also presents an environmentally friendly solution.
- Large-scale field testing for the inclusion of steel slag and plastic waste in HMA has yet to be conducted.

- ❖ Life-cycle environmental impact (LCA) analysis and assessments under extreme weather conditions could be valuable areas for future research.
- ❖ The adoption of waste plastic and steel slag in public infrastructure can significantly reduce the environmental impact associated with these materials.

4. ACKNOWLEDGMENT

The authors would like to express their heartfelt gratitude to the Department of Civil Engineering, BUET, for accepting and supporting this study. Special thanks are due to Dr. M. Neaz Murshed, Associate Professor, CE, BUET, for his invaluable encouragement and guidance.

REFERENCES

[1] R. E. Hester and R. M. Harrison, "Marine pollution and human health," Enviromental Sci. Technol., Vol. 33, pp. 69–163, 2011.

[2] C. Le Guern, "Plastic pollution: when the mermaids cry - the great plastic tide," Coastal Care, 2020. https://coastalcare.org/2020/01/plastic-pollution-when-the-mermaids-cry-the-great-plastic-tide-by-claire-le-guern/ (accessed Nov. 28, 2023).

[3] K. Ziani, C. B. Ioniță-Mîndrican, M. Mititelu, S. M. Neacșu, C. Negrei, E. Moroșan, D. Drăgănescu and O.T. Preda "Microplastics: A real global threat for environment and food safety: A state of the art review," Nutrients, Vol. 15, No. 3, 2023.

[4] UNEP, "Our planet is choking on plastic," UNEP, 2023. https://www.unep.org/interactives/beat-plastic-pollution/.

[5] WB, "Meeting Bangladesh's plastic challenge through a multisectoral approach," The world bank, 2021. https://www.worldbank.org/en/news/feature/2021/12/23.

[6] P. Barua, "Plastic-polythene waste major source of waterlogging in Chittagong," Dhaka Tribune, 2022. Accessed: Nov. 28, 2023.

[7] J. Jambeck, R. Geyer, C. Wilcox, T. R. Siegler, M. E. Perryman, A. L. Andrady, R. Narayan, and K. L. Law, "Plastic waste inputs from land into the ocean," Science, Vol. 347, no. 6223, pp. 768–771, 2015.

[8] Wikipedia, "Plastic pollution," Wikipedia, 2023. https://en.wikipedia.org/wiki/Plastic_pollution#

[9] J. Chowdhury, "How BSRM turns steel waste into eco-friendly construction material," The business standard, 2023.

[10] I. Netinger Grubeša, I. Barišić, A. Fucic, and S. S. Bansode, "Application of blast furnace slag in civil engineering: Worldwide studies," Characteristics and Uses of Steel Slag in Building Construction, Woodhead Publishing, pp. 51–66, 2016.

[11] V. Ettler and J. Kierczak, "Environmental Impact of Slag Particulates," Chemistry in the environment metallurgical slags: Environmental Geochemistry and resource potential, pp. 174–193, 2021.

[12] V. Ettler and M. Vítková, "Slag Leaching Properties and Release of Contaminants," Chemistry in the environment metallurgical slags: Environmental Geochemistry and resource potential, pp. 151–173, 2021.

[13] G. S. Roadcap, W. R. Kelly, and C. M. Bethke, "Geochemistry of extremely alkaline (pH 12) ground water in slag-fill aquifers," Ground Water, Vol. 43, No. 6, pp. 806–816, 2005.

[14] Y. Huang, R. N. Bird, and O. Heidrich, "A review of the use of recycled solid waste materials in asphalt pavements," Resour. Conserv. Recycl., Vol. 52, No. 1, pp. 58–73, 2007.

[15] S. Modak and P. Belkhode, "Construction of pavement by processing the waste plastic," Acad. J. Manuf. Eng., Vol. 20, No. 3, pp. 5–12, 2022.

[16] A. H. Mir, "Use of plastic waste in pavement construction: An example of creative waste management," IOSR J. Eng. www.iosrjen.org ISSN, Vol. 05, no. 02, pp. 1–57, 2015.

[17] A. O. Sojobi, S. E. Nwobodo, and O. J. Aladegboye, "Recycling of polyethylene terephthalate (PET) plastic bottle wastes in bituminous asphaltic concrete," Cogent Eng., Vol. 3, No. 1, 2016.

[18] E. Ahmadinia, M. Zargar, M. R. Karim, M. Abdelaziz, and E. Ahmadinia, "Performance evaluation of utilization of waste Polyethylene Terephthalate (PET) in stone mastic asphalt," Constr. Build. Mater., Vol. 36, pp. 984–989, 2012.

[19] E. I. A. Musa and H. E. F. Haron, "Effect of the low density polyethylene carry bags waste on the asphalt mixture," Int. J. Eng. Res. Sci. Technol., Vol. 3, No. 2, 2014.

[20] M. T. Awwad and L. Shbeeb, "The use of polyethylene in hot asphalt mixtures," Am. J. Appl. Sci., Vol. 4, No. 6, pp. 390–396, 2007.

[21] A. Azarhoosh, M. Koohmishi, and G. H. Hamedi, "Rutting resistance of hot mix asphalt containing coarse recycled concrete aggregates coated with waste plastic bottles," Adv. Civ. Eng., Vol. 2021, 2021.

[22] I. M. Asi, H. Y. Qasrawi, and F. I. Shalabi, "Use of steel slag aggregate in asphalt concrete mixes," Can. J. Civ. Eng, Vol. 34, pp. 902–911, 2007.

[23] H. Liz and G. E. Boyle, "Steel slag in hot mix asphalt concrete," Res. Artic., Vol. 201, p. 5, 2012.

[24] A. Hasban, A. Waje, V. Vhatte, S. Shinde, and R. A. Binayake, "Study of effective utilization of waste P.E.T (plastic) and steel slag to enhance the performance of bitumen based pavement," Int. J. Res. Appl. Sci. Eng. Technol., Vol. 10, No. 4, pp. 3172–3177, 2022.

[25] M. Amuchi, S. M. Abtahi, B. Koosha, S. M. Hejazi, and H. Sheikhzeinoddin, "Reinforcement of steel-slag asphalt concrete using polypropylene fibers," J. Ind. Text., Vol. 44, No. 4, pp. 526–541, 2015.

[26] M. Zinnurain and S. B. Dipto, "Property analysis of induction furnace steel slag for use in flexible pavement," in 6th International Conference on Civil Engineering for Sustainable Development, pp. 1–8, 2022.

[27] "Different types of plastic waste. What types of plastic can we recycle?," trvst, 2022.

[28] BSRM, "BSRM Slag." https://bsrm.com/bsrm-slag/#specification174b-5a96 (accessed Dec. 03, 2023).

[29] J. Ma, D. Sun, Q. Pang, G. Sun, M. Hu, and T. Lu, "Potential of recycled concrete aggregate pretreated with waste cooking oil residue for hot mix asphalt," J. Clean. Prod., Vol. 221, pp. 469–479, 2019.

[30] P. Ahmedzade and B. Sengoz, "Evaluation of steel slag coarse aggregate in hot mix asphalt concrete," J. Hazard. Mater., Vol. 165, No. 1–3, pp. 300–305, 2009.

[31] N. Suaryana, E. Nirwan, and Y. Ronny, "Plastic bag waste on hotmixture asphalt as modifier," Key Eng. Mater., Vol. 789, pp. 20–25, 2018.

[32] T. Rajabi, "Analysis and comparison of performance characteristics of asphalt mixtures containing steel slag and rPET," Journal of Civil Engineering and Materials Application, Vol. 6, Issue 2, pp. 79–86, 2022.

[33] C. S. Ezemenike, O. J. Oyedepo, O. O. Aderinlewo, and I. O. Oladele, "Performance of steel slag as constituent material in asphalt concrete," Nigerian Journal of Engineering, 2022.

[34] J. S. Chen and S. H. Wei, "Engineering properties and performance of asphalt mixtures incorporating steel slag," Constr. Build. Mater., Vol. 128, pp. 148–153, 2016.

[35] A. S. Shatnawi, M. S. Abdel-Jaber, M. S. Abdel-Jaber, and K. Z.Ramadan, "Effect of Jordanian steel blast furnace slag on asphaltconcrete hot mixes," Jordan Journal of Civil Engineering, Vol. 2, No. 3, pp. 197–207, 2008.

[36] M. Ameri, S. Hesami, and H. Goli, "Laboratory evaluation of warm mix asphalt mixtures containing electric arc furnace (EAF) steel slag," Constr. Build. Mater., Vol. 49, pp. 611–617, 2013.

[37] H. Q. Nguyen, D. X. Lu, and S. D. Le, "Investigation of using steel slag in hot mix asphalt for the surface course of flexible pavements," IOP Conference Series: Earth and Environmental Science, 2018.

[38] A. H. M. Afaf, "Studying the Effect of steel slag powder on Marshall stiffness and tensile strength of Hot Mix Asphalt." JES. Journal of Engineering Sciences, Vol. 42, No. 3, pp. 575–581, 2014.

[39] B. Sridhar and M. V. S. S. Sastri, "Studies on strength and behaviour of hot mix asphalt using steel slag aggregates in pavements," Key Engineering Materials, pp. 254–262, 2021.

[40] N. Jegatheesan, T. M. Rengarasu, and W. M. K. R. T. W. Bandara, "Effect of Polyethylene Terephthalate (PET) Fibres as Binder Additive in Hot Mix Asphalt Concrete," Annual Sessions of IESL, pp. 175-182, 2018.

[41] T. Baghaee Moghaddam, M. Soltani, and M. R. Karim, "Experimental characterization of rutting performance of Polyethylene Terephthalate modified asphalt mixtures under static and dynamic loads," Constr. Build. Mater., Vol. 65, pp. 487–494, 2014.

[42] A. Hassani, H. Ganjidoust, and A. A. Maghanaki, "Use of plastic waste (poly-ethylene terephthalate) in asphalt concrete mixture as aggregate replacement," Waste Manag. Res., Vol. 23, No. 4, pp. 322–327, 2005.

[43] S. E. Zoorob and L. B. Suparma, "Laboratory design and investigation of the properties of continuously graded Asphaltic concrete containing recycled plastics aggregate replacement (Plastiphalt)," Cement and Concrete Composites, Vol. 22, Issue 4, pp. 233-242, 2000.

[44] V. S. Punith and A. Veeraragavan, "Behavior of asphalt concrete mixtures with reclaimed polyethylene as additive", Journal of Materials in Civil Engineering, Vol. 19, No. 6, 2007.

[45] S. Hinislioglu and E. Agar, "Use of waste high density polyethylene as bitumen modifier in asphalt concrete mix," Mater. Lett., Vol. 58, No. 3–4, pp. 267–271, 2004.

[46] M. Attaelmanan, C. P. Feng, and A. H. Ai, "Laboratory evaluation of HMA with high density polyethylene as a modifier," Constr. Build. Mater., Vol. 25, No. 5, pp. 2764–2770, 2011.

[47] E. Ahmadinia, M. Zargar, M. R. Karim, M. Abdelaziz, and P. Shafigh, "Using waste plastic bottles as additive for stone mastic asphalt," Mater. Des., Vol. 32, No. 10, pp. 4844–4849, 2011.

[48] M. Panda and M. Mazumdar, "Utilization of reclaimed polyethylene in bituminous paving mixes", Journal of Materials in Civil Engineering, Vol. 14, No. 6, 2002.

[49] M. Arabani and A. R. Azarhoosh, "The effect of recycled concrete aggregate and steel slag on the dynamic properties of asphalt mixtures," Constr. Build. Mater., Vol. 35, pp. 1–7, 2012.

[50] S. Paranavithana and A. Mohajerani, "Effects of recycled concrete aggregates on properties of asphalt concrete," Resour. Conserv. Recycl., Vol. 48, No. 1, pp. 1–12, 2006.

[51] J. Mills-Beale and Z. You, "The mechanical properties of asphalt mixtures with recycled concrete aggregates," Constr. Build. Mater., Vol. 24, No. 3, pp. 230–235, 2010.

[52] M. Arabani, S. A. Tahami, and M. Taghipoor, "Laboratory investigation of hot mix asphalt containing waste materials," Road Mater. Pavement Des., Vol. 18, No. 3, pp. 713–729, 2017.

[53] P. K. Gautam, P. Kalla, R. Nagar, R. Agrawal, and A. S. Jethoo, "Laboratory investigations on hot mix asphalt containing mining waste as aggregates," Constr. Build. Mater., Vol. 168, pp. 143–152, 2018.

[54] M. Arabani, F. Moghadas Nejad, and A. R. Azarhoosh, "Laboratory evaluation of recycled waste concrete into asphalt mixtures," Int. J. Pavement Eng., Vol. 14, no. 6, pp. 531–539, 2013.

[55] V. Haritonovs and J. Tihonovs, "Use of unconventional aggregates in hot mix asphalt concrete," Balt. J. Road Bridg. Eng., Vol. 9, No. 4, pp. 276–282, 2014.

Workstation Design and Task Allocation in Assembly Lines

Adekunle Ibrahim MUSA

Department of Mechanical Engineering, Olabisi Onabanjo University, Ago Iwoye, Ogun State, Nigeria

ABSTRACT

This study evaluates workstation design principles, analyzes task allocation strategies, and assesses their impact on assembly line efficiency using a study approach of a Nigerian manufacturing firm specializing in electrical appliance assembly. The study involved direct observations, time-motion studies, and ergonomic assessments across 20 workstations. Workstation space utilization analysis revealed varying efficiency levels, with Workstation 5 achieving the highest utilization at 77.8%, while Workstation 4 had the lowest at 55.6%. Worker utilization data indicated that Worker 1 had the highest utilization rate at 90.0%, while Worker 3 had the lowest at 66.7%, highlighting inefficiencies in task distribution. Line balancing efficiency calculations showed Workstation 2 achieving an optimal 100.0% efficiency, whereas Workstation 3 recorded the lowest at 60.0%, indicating significant workload imbalances. Ergonomic risk assessment using the Rapid Upper Limb Assessment (RULA) method identified Workstation 2 as high risk with a score of 5, necessitating immediate ergonomic interventions. The findings suggest that optimizing workstation layout, redistributing tasks to balance workloads, and incorporating ergonomic interventions can enhance productivity and worker well-being. The study recommended implementation of adjustable workstations, standardizing cycle times, and integration of automation technologies to minimize inefficiencies.

Keywords: Workstation Design, Task Allocation, Assembly Line Efficiency, Ergonomics, Line Balancing

1. INTRODUCTION

Workstation design and task allocation significantly influence the efficiency, productivity, and ergonomics of assembly lines [1]. A poorly designed workstation can lead to inefficiencies such as excessive movement, bottlenecks, and worker fatigue, ultimately reducing throughput [2]. Effective workstation design ensures optimal space utilization, proper tool placement, and minimized worker strain [3]. It is highly required to create effective changes in workstations premised-based. Because this will make sure that employees work in safe environment, efficiently and at the least possible biological cost [4].

The design of the layout of the manufacturing industries is diverse with the presence of various types of manufacturing systems i.e. fully automated systems, semi-automated systems, completely human based systems and human and robot collaboration systems [5].

Task allocation plays a crucial role in balancing workloads and maintaining a steady production flow. Line balancing techniques, such as the Ranked Positional Weight (RPW) method and heuristic algorithms, have been developed to optimize task distribution [6], [7]. Line balancing has also considered that the workload should be balanced among the operators which makes an operator to have less idle time and simulation has also been carried out to study and validate the process [8]. Assigning the available resources is achieved through the task allocation. Safety is however not normally taken into account when assigning the task to the assembly system though it is essential to have the safety of the human operator when he/she is interacting with the robot [9]. Studies show that unbalanced workloads increase idle time and worker stress, negatively affecting overall performance [10].

Ergonomics is another key factor in workstation design. Poor ergonomic conditions can lead to musculoskeletal disorders (MSDs) and decreased worker efficiency [11]. The Rapid Upper Limb Assessment (RULA) method is widely used to evaluate ergonomic risks in workstation setups [12]. Research indicates that ergonomic improvements can enhance productivity by up to 20% while reducing worker injuries [13].

Despite advances in workstation optimization and task allocation, many manufacturing firms, especially in developing economies, still experience inefficiencies due to inadequate implementation of these principles [10]. New trends in the design of workstations focus on modularity

*Corresponding author's email: musa.adekunle@oouagoiwoye.edu.ng

and flexibility, Patel and Sanders have proven that layouts in lean facilities can be optimized using digital simulation tools that minimize wasted movement by 25% [11]. In the context of line balancing, heuristic optimization proved to be 15% more efficient than the traditional methods [12].

The modern ergonomics research places important emphasis on cognitive loads in workstation configuration, lobbied towards adjustable-height workstations to lessen the number of musculoskeletal disorders [13]. Besharati considered human factor calculations in all task allocation strategies, and the main idea was to choose the tasks relied on skills to avoid idle time [14]. This study aims to evaluate workstation design and identify inefficiencies, analyze task allocation and workload distribution and propose improvements for enhanced efficiency and ergonomics.

2. MATERIALS AND METHODS

2.1 Study Design

The study was conducted in a Nigerian manufacturing firm specializing in electrical appliance assembly. The production line consisted of 20 workstations (WS), with tasks ranging from component assembly to quality inspection. Workers were assigned based on skill levels and task complexity. Table I shows the information of a workstation in a Nigerian electrical appliance assembly firm. Workstations were chosen according to complexity of the work (ease of complexity) bottlenecks identified in the process of initial observations and varying space utilization (e.g. the lowest space was used in the WS3).

Table I: Workstation in a Nigerian Electrical Appliance Assembly Firm

Workstation ID	Name	Primary Tasks
WS1	Component Assembly Station	Mount motors, switches, and electronic parts onto appliance bodies
WS2	Wiring & Electrical Connection	Solder wires, connect terminals, attach circuit boards
WS3	Fastening & Mechanical Assembly	Fit panels, screw casings, attach knobs and control units
WS4	Quality Control & Testing	Inspect, test voltage/current, functional checks (e.g., fan speed, heating)
WS5	Labeling & Packaging	Print and apply labels, seal units, box for shipment

2.2 Data Collection

An analysis was conducted to evaluate the workstation design and task allocation within an assembly line environment. Data collection methods included direct observation, work sampling, and time-motion studies to assess workstation efficiency and workload distribution.

The study employed a case study approach to examine workstation design and task allocation in an assembly line environment. Data collection involved direct observation, work sampling, and time-motion studies to evaluate workstation efficiency and workload distribution. The research was conducted at a Nigerian manufacturing firm specializing in electrical appliance assembly. The production line comprised 20 workstations, where tasks ranged from component assembly to quality inspection. Workers were assigned tasks based on their skill levels and the complexity of the work.

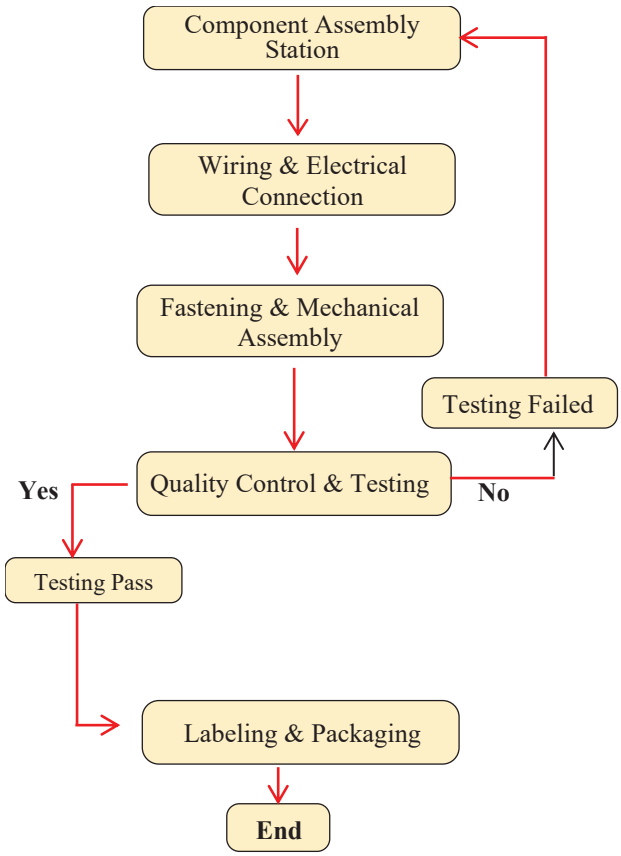

Fig. 1: Simplified Process Flow Diagram of the Assembly Line, Highlighting Material and Task Sequences

To assess workstation efficiency, measurements were taken to evaluate space utilization. Observations focused on worker posture, the accessibility of tools, and the placement of materials. Additionally, ergonomic risks were identified using the Rapid Upper Limb Assessment (RULA) method. For task allocation analysis, time studies

were performed to determine task duration, while work sampling was used to assess worker utilization rates and idle time.

2.2.1 Raw Data and Calculations for Time Studies

2.2.1.1 Workstation Space Utilization

Workstation Space Utilization means the success of utilizing the given place dedicated to a workstation by beneficial operations. It is of assistance in assessing the effectiveness of layout plan in production or bulk-assembly set up. Utilization of work stations is expressed as the ratio between actual space that is occupied by tools and equipment as well as workers in comparison to the total work station space.

$$\text{Utilization (\%)} \quad \frac{\text{Space Utilized (m2)}}{\text{Space Available (m2)}} \times 100 \qquad (1)$$

2.2.1.2 Worker Utilization Analysis

This is the technique applied to determine whether time of a worker is being well utilized in any production or assembly line. It is a ratio or a percentage of time that a worker actively spends within performing his/her duties to the sum overall time the worker has (including that spent idle).

The control of human resource in an environment of production cannot be achieved without the analysis of Worker Utilization. It assists one to match manpower with work requirements and where the process requires re-engineering, training or automation.

$$\text{WU (\%)} \quad \frac{\text{TsT}}{\text{TsT + Id T}} \times 100 \qquad (2)$$

Where,

WU is Worker Utilization

TsT is Task Time

IdT - Idle Time

Task balancing was evaluated using the Line Balancing Efficiency (LBE) formula, which considers total work time, the number of workstations, and cycle time [15].

$$\text{LBE} = \frac{\sum \text{Tw}}{\text{N} \times \text{Tc}} \times 100 \qquad (3)$$

Where,

T_w is total work time,

N is the number of workstations,

T_c is the cycle time.

2.2.2 Data Collection Protocol

2.2.2.1 Time-Motion Studies

Time-Motion Studies is carried out during 50 cycles of production (5 cycles per workstation x 10 shifts).

2.2.2.2 Worker Demographics:

Levels of Skills: 60% intermediate (1-3 years) and 40% advanced (more than 3 years).

2.2.2.3 Shift Patterns

There were two shifts (8 hours each) per day, and the data was collected during both in order to take the fatigue into consideration.

2.2.3 Process Constraints

It had fixed cycle time of 50 minutes that was determined by the processing activities upstream and the constraints on the ability to alter tool location because of safety standards.

The collected data was analyzed to assess workstation efficiency based on space utilization and ergonomic factors. Task allocation efficiency was evaluated by comparing the actual workload distribution with an ideal balanced scenario. Furthermore, statistical tools such as SPSS were applied to examine variations in task completion times across different workstations.

3. RESULTS

The study employed a case study approach to analyze workstation design and task allocation in an assembly line setting. The data collection methods included direct observations, work sampling, time-motion studies, and ergonomic assessments to evaluate workstation efficiency, workload distribution, and worker well-being. The research was conducted in a Nigerian manufacturing firm that specializes in electrical appliance assembly. The production line consisted of 20 workstations where workers were assigned tasks based on their skill level and task complexity to ensure an efficient workflow [3].

To assess workstation efficiency, the study measured space utilization and conducted observations to evaluate worker posture, tool accessibility, and material placement. The ergonomic risks associated with workstation design were analyzed using the Rapid Upper Limb Assessment (RULA) method, which is a widely

used tool for identifying postural and movement-related risk factors [10]. For task allocation analysis, time studies were conducted to determine task duration, while work sampling was used to assess worker utilization rates and idle time. The Line Balancing Efficiency (LBE) formula was applied to quantify how effectively workloads were distributed across workstations.

3.1 Workstation Space Utilization

Table II presents the space availability and utilization rates for selected workstations in the assembly line. The analysis highlights variations in how effectively each workstation utilizes its allocated space, which contributes to inefficiencies in workflow and ergonomic challenges.

Table II: Workstation Space Utilization Analysis

Workstation	Space Available (m^2)	Space Utilized (m^2)	Utilization (%)
WS1	45	30	66.7
WS2	45	32	71.1
WS3	45	28	62.2
WS4	45	25	55.6
WS5	45	35	77.8

Table II provides an analysis of workstation space utilization in the assembly line, showing the available space, the actual space utilized, and the corresponding utilization percentage for each workstation. The data highlights variations in how efficiently each workstation uses its allocated space, which directly impacts workflow, worker movement, and productivity [1].

Each workstation in the study was allocated a uniform space of $45m^2$. However, the actual utilization varied across different workstations. Workstation 1 utilized $30m^2$, resulting in a 66.7% utilization rate, indicating moderate space efficiency with potential room for optimization. Workstation 2 had a slightly higher utilization rate of 71.1%, using $32m^2$, suggesting a relatively better-organized workstation. Workstation 3 exhibited the lowest utilization, using only $28m^2$, which translates to a 62.2% utilization rate. This may indicate inefficient space allocation or poor workstation arrangement. Similarly, Workstation 4 had a lower utilization rate of 55.6%, using $25m^2$, suggesting a no too good-organized workstation. On the other hand, Workstation 5 recorded the highest utilization at 77.8%, implying a well-optimized workstation layout with minimal wasted space. Studies have shown that unoptimized workstation layouts contribute to excessive worker movement, lower efficiency, and increased cycle times [2]. The variation in space utilization among the workstations has significant implications for productivity and efficiency. Underutilized workstations may lead to excessive worker movement, resulting in wasted time and increased fatigue. Conversely, workstations with very high utilization rates could be overcrowded, restricting movement and creating ergonomic challenges [3]. Poor organization of tools and materials in low-utilization workstations can further contribute to inefficiencies in workflow, leading to delays and increased idle time [6]. Research suggests that proper space management and ergonomic workstation design can improve productivity by up to **20%** while reducing worker fatigue and injury risks [11].

3.2 Task Allocation and Worker Utilization

Table III presents an analysis of worker utilization rates based on time-motion studies, highlighting the task assigned, task duration, idle time, and overall utilization percentage for each worker. This study provides insight into the efficiency of task distribution and helps identify areas for improvement in balancing workloads to enhance overall assembly line performance.

Table III provides an overview of worker utilization in the assembly line by detailing the assigned tasks, task duration, idle times, and overall utilization percentages. The analysis highlights variations in worker efficiency, revealing potential imbalances in task allocation that could impact overall productivity.

The result shows that Worker 1, assigned to component assembly, completed tasks in 450 minutes and had 50 minutes of idle time, resulting in a 90.0% utilization rate. This high utilization indicates an effectively assigned workload with minimal downtime. Worker 2, responsible for wiring and electrical connection, had a task time of 500 minutes and an idle time of 100 minutes, leading to a utilization rate of 83.3%. This suggests a relatively balanced workload, although minor adjustments could further optimize efficiency. Worker 3, performing fastening and mechanical Assembly, exhibited the lowest utilization rate at 66.7%, with a task time of 300 minutes and 150 minutes of idle time. This indicates significant under-utilization, likely due to either task redundancy, process inefficiencies, or improper workload distribution.

Table III: Worker Utilization Analysis

Worker ID	Assigned Task	Task Time (mins)	Idle Time (mins)	Utilization (%)
W1	Component Assembly	450	50	90.0
W2	Wiring & Electrical Connection	500	100	83.3
W3	Fastening & Mechanical Assembly	300	150	66.7
W4	Quality Control & Testing	450	65	87.4
W5	Labeling & Packaging	500	82	85.9

The result further shows that Worker 4, assigned to quality control and testing, completed tasks in 450 minutes and had 65 minutes of idle time, resulting in a 87.4% utilization rate. This high utilization also indicates an effectively assigned workload with minimal downtime. Worker 5, responsible for labeling and packaging had a task time of 500 minutes and an idle time of 82 minutes, leading to a utilization rate of 85.9%.

The varying worker utilization rates in Table III suggest an imbalance in task distribution, which can negatively impact assembly line performance. High utilization rates, as seen with Worker 1, Worker 4 and Worker 5 indicate effective task allocation, ensuring minimal idle time and steady workflow [6]. However, excessive workloads can also lead to worker fatigue, reduced efficiency, and increased error rates over time [11].

Conversely, the lower utilization rate of Worker 3 highlights inefficiencies that may result in wasted production time and underperformance. Studies suggest that worker idle time exceeding 20% can lead to a 5-15% reduction in overall assembly line efficiency, as it disrupts workflow continuity and increases lead times [8]. Furthermore, uneven task distribution can create bottlenecks in the production line, leading to delays in subsequent processes [15].

3.3 Line Balancing Efficiency

Table IV presents the line balancing efficiency (LBE) for selected workstations, highlighting the relationship between work time, cycle time, and efficiency percentage. This analysis helps identify inefficiencies in task distribution and provides insights into optimizing workstation performance to achieve a more balanced and efficient assembly line.

Table IV: Line Balancing Efficiency

Workstation	Work Time (mins)	Cycle Time (mins)	LBE (%)
WS1	45	50	90.0
WS2	50	50	100.0
WS3	30	50	60.0
WS4	40	50	80.0
WS5	45	50	90.0

Table IV presents the Line Balancing Efficiency (LBE) for selected workstations, showing the relationship between work time, cycle time, and efficiency percentage. Line balancing is a crucial factor in optimizing assembly line performance, as an imbalance can lead to bottlenecks, idle time, and productivity losses [6]. The data in Table III reveals variations in efficiency across different workstations, indicating areas that require improvement to enhance overall production flow.

The results indicate that Workstation 1 had a work time of 45 minutes and a cycle time of 50 minutes, yielding a line balancing efficiency of 90.0%. This suggests an effectively utilized workstation with minimal idle time. Workstation 2 exhibited the highest efficiency at 100.0%, meaning its task allocation perfectly matched the cycle time, ensuring continuous workflow without delays. However, Workstation 3 recorded the lowest efficiency at 60.0%, with a work time of 30 minutes against a cycle time of 50 minutes, highlighting a significant imbalance that may contribute to production inefficiencies.

The results further shows that Workstation 4 had a work time of 40 minutes and a cycle time of 50 minutes, yielding a line balancing efficiency of 80.0%. This suggests there is an effective utilization of workstation with minimal idle time. Workstation 5 also exhibited the high efficiency at 90.0%, meaning that the task allocation of 45 minutes and the cycle time of 50 minutes, yielding a line balancing efficiency, ensuring continuous workflow without delays.

The disparities in line balancing efficiency across workstations have direct consequences on assembly line performance and worker utilization. A workstation with high efficiency, like Workstation 2, ensures a smooth production flow, reducing delays and optimizing resource utilization [15]. However, low efficiency, as seen in Workstation 3, suggests under-utilization, which can cause bottlenecks at subsequent workstations, leading

to an uneven workload distribution and reduced overall system efficiency [8]. Studies show that an LBE below 70% can reduce production output by up to 15%, as unbalanced workloads increase cycle time variations and disrupt workflow synchronization [13].

Furthermore, inefficiencies in line balancing can lead to worker fatigue and increased operational costs. Overloaded workstations force workers to rush tasks, increasing error rates, while under-loaded stations cause unnecessary downtime and productivity losses [8]. To achieve an optimal balance, task redistribution and line balancing techniques, such as the Ranked Positional Weight (RPW) method and heuristic algorithms, should be employed to distribute workloads more evenly [15].

3.4 Ergonomic Risk Assessment

Table V presents the Rapid Upper Limb Assessment (RULA) scores for selected workstations, indicating the level of ergonomic risk associated with each workstation setup. Analyzing these scores, potential ergonomic hazards can be identified, and appropriate interventions can be recommended to improve worker well-being and optimize workstation design.

Table V: Ergonomic Risk Assessment Results

Workstation	RULA Score	Risk Level
WS1	4	Medium
WS2	5	High
WS3	3	Low
WS4	3	Low
WS5	4	Medium

Table V presents the Rapid Upper Limb Assessment (RULA) scores for selected workstations, highlighting the ergonomic risks associated with each workstation setup. Ergonomic assessments are crucial in identifying postural risks, worker discomfort, and potential musculoskeletal disorders (MSDs), which can negatively impact worker productivity and well-being [10]. Table IV reveals varying levels of ergonomic risk, emphasizing the need for workstation adjustments to enhance comfort and efficiency. The results show that Workstation 1 received a RULA score of 4, indicating a medium risk level that requires further investigation and possible ergonomic interventions. Workstation 2 recorded the highest risk, with a RULA score of 5, categorizing it as a high-risk workstation that demands immediate ergonomic improvements. This score suggests that workers at this station may be experiencing poor posture, excessive force exertion, or repetitive motion stress, which could lead to musculoskeletal strain and long-term injuries if not addressed [9]. Conversely, Workstation 3 had the lowest RULA score of 3, indicating a low-risk level where ergonomic conditions are relatively acceptable, though minor improvements could still be beneficial. The results further reveals that Workstation 4 received a RULA score of 3, indicating a low risk level that requires further investigation and possible ergonomic interventions. Workstation 5 recorded the medium risk, with a RULA score of 4, categorizing it as a medium-risk workstation that demands immediate ergonomic improvements. This score suggests that workers at this station may be experiencing poor posture, excessive force exertion, or repetitive motion stress, which could lead to musculoskeletal strain and long-term injuries if not addressed [9].

The presence of high ergonomic risk in Table IV suggests that certain workstations may contribute to worker discomfort, reduced efficiency, and increased injury rates. Studies have shown that workstations with poor ergonomic design can lead to a 20-30% reduction in productivity, as workers experience fatigue, discomfort, and potential health issues that affect their ability to perform tasks effectively [11]. Additionally, prolonged exposure to awkward postures and repetitive movements has been linked to increased cases of lower back pain, wrist injuries, and shoulder strain, which are common in assembly line operations [16]. Workstation 2's high RULA score is particularly concerning, as it may indicate poor seating posture, excessive reaching distances, or improper tool placement. Research suggests that workers exposed to high ergonomic risks are more likely to suffer from work-related MSDs, which not only affect individual performance but also contribute to higher absenteeism rates and increased healthcare costs for employers [17].

4. DISCUSSION

Table II presents the workstation space utilization analysis, which examines the relationship between available space, utilized space, and utilization percentage. Workstation efficiency plays a crucial role in manufacturing operations, as poor space management can lead to excessive worker movement, workflow inefficiencies, and increased fatigue [6]. Underutilized workstations can result in unnecessary worker movements, workflow disruptions, and inefficiencies in production, while overcrowded workstations may lead to ergonomic strain and restricted movement [7]. Studies indicate that optimizing workstation layout and tool placement can improve productivity by up to 15% by minimizing physical exertion and enhancing

workflow organization [3]. To address these inefficiencies, adjustments should be made to workstation layouts, tool positioning, and material placement. Implementing ergonomic interventions, such as adjustable workstation heights and anti-fatigue flooring, can further enhance worker comfort and overall productivity [9].

Table III presents an analysis of worker utilization, which highlights how task allocation impacts worker efficiency. Worker utilization is a critical factor in assembly line performance, as imbalanced workloads can lead to bottlenecks, increased idle time, and worker fatigue [10]. Studies suggest that workers with utilization rates below 70% often contribute to production delays and reduced efficiency, as idle time disrupts workflow synchronization and increases cycle time variability [11]. Task allocation imbalances can also lead to worker fatigue, increased error rates, and reduced product quality, all of which negatively impact operational efficiency [12]. To enhance worker utilization, the study recommends task redistribution strategies that ensure even workload distribution across workstations. Additionally, process optimization techniques, such as eliminating redundant steps and improving task sequencing, can streamline workflows [13]. The integration of semi-automated systems can also help reduce worker strain, improve efficiency, and minimize task completion times [14].

Table IV presents the Line Balancing Efficiency (LBE) calculations, which measure the effectiveness of task distribution across workstations. A well-balanced assembly line minimizes idle time, reduces bottlenecks, and ensures continuous workflow [13]. An unbalanced assembly line contributes to worker fatigue, bottlenecks, and longer cycle times, which ultimately reduces production efficiency [16]. Research suggests that LBE values below 70% correlate with a 10 to 20% decrease in overall production output due to workflow disruptions and excessive idle time [18]. To improve line balancing efficiency, tasks should be reallocated evenly across workstations to minimize idle time [19]. Standardizing cycle times across workstations and integrating real-time monitoring systems can also help track inefficiencies and optimize workload distribution [20].

Table V presents the RULA scores for ergonomic risk assessment, which highlights postural risks and ergonomic deficiencies across workstations. Poor ergonomic conditions can lead to musculoskeletal disorders (MSDs), worker discomfort, and decreased productivity [8]. Studies show that ergonomic improvements can enhance worker comfort, reduce injury risks, and increase productivity by up to 20% [18]. To address ergonomic risks, workstations should be adjustable in height to accommodate different worker postures [18]. Providing anti-fatigue mats, wrist supports, and adjustable chairs can also help reduce strain on workers [19]. Additionally, structured break intervals should be introduced to prevent repetitive strain injuries and allow workers time to recover from physically demanding tasks [20].

The study highlights inefficiencies in workstation design, task allocation, line balancing, and ergonomic conditions in an assembly line. The findings emphasize the importance of optimizing space utilization, balancing workloads, and improving ergonomic conditions to enhance overall productivity. Implementing task redistribution strategies, ergonomic interventions, and automation can significantly reduce idle time, enhance efficiency, and improve worker well-being [20].

5. CONCLUSION

The study examined the impact of workstation design, task allocation, line balancing, and ergonomic factors on assembly line efficiency. The findings revealed that inefficient workstation layouts, unbalanced task distribution, and poor ergonomic conditions contribute to reduced productivity, increased worker fatigue, and operational inefficiencies. The analysis of workstation space utilization showed that some workstations were underutilized, leading to unnecessary worker movements and workflow disruptions, while others were overcrowded, restricting worker comfort and efficiency [21]. The worker utilization analysis highlighted imbalances in task assignments, with some workers experiencing excessive idle time while others were overburdened, resulting in decreased overall productivity. The line balancing efficiency assessment indicated significant disparities among workstations, with some achieving optimal efficiency while others exhibited severe inefficiencies that disrupted the production flow [22]. The ergonomic risk assessment further identified workstation setups that posed significant health risks to workers, increasing the likelihood of musculoskeletal disorders and reducing efficiency.

To address these inefficiencies and improve overall assembly line performance, several recommendations should be implemented. Workstation layouts should be optimized to ensure efficient space utilization, reduce unnecessary worker movements, and enhance accessibility to tools and materials. Task redistribution strategies should be employed to balance workloads effectively, minimizing idle time and preventing overburdening of

workers [23]. Line balancing techniques, such as the Ranked Positional Weight (RPW) method and heuristic optimization algorithms, should be utilized to ensure an even distribution of tasks across all workstations. Ergonomic interventions, including the introduction of adjustable workstations, proper seating, and anti-fatigue flooring, should be implemented to reduce physical strain and enhance worker comfort. Additionally, automation and digital monitoring tools should be incorporated into the production process to improve task efficiency, minimize human errors, and maintain consistent cycle times [24].

The study underscores the importance of integrating efficient workstation design, balanced task allocation, optimized line balancing, and ergonomic best practices to enhance productivity and worker well-being in assembly line operations. Adoption of these recommendations, manufacturing firms will improve efficiency, reduce operational costs, and create a safer and more productive working environment for employees.

REFERENCES

[1] G. Boothroyd, P. Dewhurst, and W. Knight, Product Design for Manufacture and Assembly, 3rd ed. Boca Raton, FL, USA: CRC Press, 2010.

[2] S. P. Choi and Y. K. Chan, "Workstation layout optimization in lean manufacturing systems," International Journal of Production Research, Vol. 56, No. 3, pp. 876–891, 2018.

[3] R. H. Brown, Design of Workplaces and Workspaces in Manufacturing, London, U.K., Springer, 2017.

[4] A. Goydziewska-Nowicka, "Ergonomic study and analysis of workstation in a manufacturing enterprise," Scientific Papers of Silesian University of Technology. Organization & Management, Vol. 1, No. 199, 2024.

[5] M. Eswaran, A. K. Inkulu, K. Tamilarasan, M. R. Bahubalendruni, R. Jaideep, M. S. Faris and N. Jacob, "Optimal layout planning for human robot collaborative assembly systems and visualization through immersive technologies," Expert Systems with Applications, Vol. 241, p. 122465, 2024.

[6] J. H. Black and R. L. Hunter, "Task allocation strategies for improved assembly line productivity," Journal of Manufacturing Systems, Vol. 45, pp. 135–145, 2019.

[7] M. L. Pinedo, Scheduling: Theory, Algorithms, and Systems, 6th ed. Cham, Switzerland: Springer, 2020.

[8] S. Vijay and M. G. Prabha, "Work standardization and line balancing in a windmill gearbox manufacturing cell: A case study," Materials Today: Proceedings, Vol. 46, Part 19, pp. 9721-9729, 2021.

[9] M. Faccio, I. Granata and R. Minto, "Task allocation model for human-robot collaboration with variable cobot speed," Journal of Intelligent Manufacturing, Vol. 35, pp. 793-806, 2024.

[10] A. K. Gupta and M. S. Sinha, "Effect of unbalanced workloads on assembly line efficiency," Manufacturing Science and Engineering, Vol. 58, No. 2, pp. 239–250, 2019.

[11] C. L. Smith and J. M. Johnson, "Ergonomic considerations in workstation design: A case study," Applied Ergonomics, Vol. 72, pp. 168–175, 2018.

[12] P. Hignett and L. McAtamney, "Rapid Upper Limb Assessment (RULA)," Applied Ergonomics, Vol. 31, No. 2, pp. 201–205, 2000.

[13] R. M. Besharati, "The impact of ergonomic workstation design on worker productivity," Human Factors and Ergonomics in Manufacturing, Vol. 30, No. 4, pp. 479–491, 2020.

[14] M. Iqbal and K. Alam, "Challenges in workstation optimization in developing economies," International Journal of Industrial Engineering, Vol. 60, No. 3, pp. 345–359, 2021.

[15] S. T. Mukhopadhyay and D. Roy, "A review of line balancing methodologies in modern manufacturing," Production Planning & Control, Vol. 32, No. 5, pp. 721–734, 2021.

[16] K. N. Park and J. S. Lee, "Analysis of workstation bottlenecks using discrete event simulation," Journal of Manufacturing Processes, Vol. 42, pp. 387–398, 2019.

[17] Y. R. Tan and P. K. Wong, "Task allocation using heuristic optimization in manufacturing systems," International Journal of Production Economics, Vol. 235, p. 108095, 2021.

[18] B. A. Heady and T. L. Hammond, "Impact of ergonomic interventions on assembly line efficiency," Occupational Safety and Health Journal, Vol. 51, No. 4, pp. 589–604, 2022.

[19] A. L. Green and M. C. Jones, “Effects of poor workstation design on worker performance in assembly lines,” Occupational Ergonomics, Vol. 22, No. 2, pp. 223–238, 2022.

[20] F. R. Montes and L. A. Jiménez, “Workstation design and its effect on cognitive load in industrial settings,” Ergonomics, Vol. 64, No. 11, pp. 1423–1438, 2021.

[21] R. K. Narang and A. Ghosh, “Assembly line task reassignment and its impact on cycle time efficiency,” Manufacturing Technology Today, Vol. 68, No. 3, pp. 291–305, 2020.

[22] T. J. Williams, “Automation and its influence on human workload in assembly operations,” Journal of Industrial Automation, Vol. 55, No. 6, pp. 980–996, 2019.

[23] P. H. Verma and D. A. Nolan, “The role of human factors in task allocation strategies in modern manufacturing,” Human Factors and Manufacturing Systems, Vol. 32, No. 4, pp. 399–413, 2021.

[24] N. K. Patel and B. W. Sanders, “Digital simulation for workstation optimization in lean environments,” International Journal of Production Research, Vol. 59, No. 12, pp. 3695–3711, 2021.

Dynamic Thresholding based Real Time ECG Signal Processing and Monitoring System using FPGA

Md. Anwarul Abedin*, Jahid Hasan, Akash Modak and Shubro Biswas

Department of Electrical and Electronic Engineering, Dhaka University of Engineering & Technology, Gazipur, Bangladesh

ABSTRACT

This paper presents the design and implementation of a real-time ECG signal processing and monitoring system using dynamic thresholding on an FPGA platform. The proposed system focuses on efficient and accurate detection of the QRS complex, a key feature in the ECG signal, while minimizing computational overhead. The motivation for this research stems from the growing need for reliable, high-speed medical monitoring systems capable of handling noisy ECG signals in real-time. The study demonstrates that the dynamic thresholding method, combined with FIR filters for noise reduction, offers a significant improvement in QRS detection accuracy compared to traditional constant threshold techniques. The implementation of the algorithm on FPGA hardware ensures faster processing, real-time performance, and low power consumption. The system adapts the threshold based on the previous R-peaks and RR intervals, allowing it to accurately detect heartbeats across different ECG signals. The proposed system is built using VHDL by Xilinx ISE14.6 package. Simulation of the algorithm is performed using MATLAB Version 8.3.0.532 (R2021a) System Generator. Experimental validation is conducted using multiple ECG signals from MIT-BIH databases. The results show that the proposed system achieves an error rate of 0.54%, sensitivity of 99.46% and F1 score of 99.73% outperforming similar systems in both detection accuracy and processing speed. The FPGA implementation effectively meets the requirements for real-time medical applications, ensuring high reliability in detecting arrhythmias while maintaining low computational complexity.

1. INTRODUCTION

The heart is just the size of a large fist but it is the most vital organ of human body. Its proper functioning is critical to maintaining human life; without it, life becomes unstable. Cardiovascular diseases have long been, and continue to be, the leading cause of death in the modern world. Sudden cardiac death accounts for about 50 percent of these fatalities, with the majority being caused by acute ventricular arrhythmias. These arrhythmias can sometimes occur sporadically, making them difficult to detect through routine check-ups and monitoring, further complicating the identification of underlying heart conditions [1].

Electrocardiograph (ECG) signal is a compulsive recording of the heart on a graph with help of various electrodes placed at specific points on the body. This recording helps assess the heart's functionality. By analyzing the ECG waveform, valuable insights into the patient's heart condition can be obtained. Among the key features of the ECG is the Q wave, R wave and S wave (QRS), which provides significant information related to arrhythmias. To make the most of this data, the ECG signal can be preprocessed, and advanced signal processing techniques can be employed to extract critical features, such as detecting the QRS complex, for better diagnosis and monitoring of heart health [2].

In most cases, these processes are carried out using software applications, which offer several advantages. Software is often easy to work with and can achieve high accuracy because it operates in a virtual environment where precise computations are possible. However, one of the main drawbacks of software-based QRS complex detection is the inability to provide real-time results. Typically, the ECG signal is collected from the patient, stored, and then processed offline. This method can be slow, as software applications tend to execute multiple tasks sequentially, and they lack the ability to handle tasks in parallel, which is crucial for faster ECG signal processing introduced in [3].

In contrast, signal processing using hardware presents significant advantages, particularly in terms of performance and efficiency. Hardware implementations,

*Corresponding author's email: abedin@duet.ac.bd

such as Field Programmable Gate Array (FPGA) or Application-Specific Integrated Circuit (ASIC), enable real-time processing with minimal delays, as they can perform parallel signal processing, drastically improving execution speed compared to the linear nature of software. Moreover, hardware systems are generally more power-efficient, as they are custom-built to perform only the necessary function, which eliminates unnecessary computations and overhead. They also tend to be more reliable because, once deployed, hardware is less prone to errors like software bugs or system crashes [4].

FPGA is considered one of the best hardware options for signal processing due to its nature as a dedicated hardware platform. It is increasingly being utilized for various computationally intensive tasks, particularly in the fields of Digital Signal Processing (DSP) and communications. Advances in technology have led to modern FPGAs containing a large number of Configurable Logic Blocks (CLBs), making them more practical for a wider range of applications. The high Nonrecurring Engineering (NRE) costs and extended development times associated with ASICs have also made FPGAs a more appealing choice for application-specific DSP tasks. In the context of ECG signal processing, FPGAs offer a faster, more efficient and reliable solution, particularly in scenarios that demand high throughput and real-time performance [4].

In [5] the authors have proposed an efficient method for detecting the QRS complex using dynamic thresholding, designed to minimize computational overhead. The method begins by employing a series of window-based Finite Impulse Response (FIR) filters to remove baseline wander noise and high-frequency interference from the ECG signal. Once the signal is filtered, it is passed to the QRS complex detection stage. At this stage, the initial threshold for detecting the QRS complex is determined using the baseline and Root Mean Square (RMS) values of the ECG signal over the first three seconds. A dynamic thresholding process is then employed to continuously update the threshold after each *R-peak* detection. This adaptive process adjusts the threshold based on the amplitude of the previously detected *R-peak* and the RR intervals, ensuring that the detection remains accurate even as the ECG signal varies over time. The *R-peak* is detected using the updated threshold value, and subsequently, the Q-wave and S-wave are identified by searching for local minima and maxima in relation to the detected *R-peak*. After detecting the QRS complex, the heart rate is calculated based on the detected beats, and this information is passed to the decision-making stage, where the arrhythmia condition is evaluated. The proposed method has been validated by applying it to several ECG signals from various databases, demonstrating its effectiveness in detecting arrhythmias with minimal computational demands.

In [6], the authors have introduced implementation of LPF, HPF and FIR filters using FPGA. The work highlights the advantages of using FPGA for real-time digital signal processing, including high-speed computation, parallelism, and low latency. These features are essential for applications that require efficient, fast processing of signals, such as ECG signal processing in medical monitoring systems. In relation to our thesis, this paper demonstrates the practical implementation of FIR filters for noise reduction, which is a key element in ECG signal preprocessing. The filtering methods discussed are crucial for cleaning ECG signals, removing baseline wander (low-frequency noise) and high-frequency interference steps that align closely with our work. Additionally, the paper underscores the flexibility of FPGA platforms for handling digital signal processing, supporting our decision to use FPGA for real-time ECG processing.

The implementation of real-time ECG signal processing using FPGA, specifically targeting noise reduction and beat detection has been presented in [4]. The work outlines the design of filters to eliminate noise, such as baseline wander and high-frequency interference, followed by the use of algorithms to detect ECG beats. The FPGA platform's parallel processing capabilities allow for efficient and high-speed ECG signal processing, making it well-suited for real-time medical applications.

The effectiveness of FPGA for real-time ECG processing, emphasizing the need to reduce computational complexity for faster results has been proposed in [7]. The use of FPGA for parallel processing in beat detection is directly applicable to the present work in improving the performance of dynamic thresholding algorithms. However, the work does not delve into dynamic thresholding techniques or adaptive algorithms for *QRS*-complex detection, which are central to our proposed method. While it provides a solid foundation for FPGA-based ECG processing, it lacks the adaptive capability that our dynamic thresholding method introduces, thus showcasing a gap that our research aims to fill in improving accuracy and real-time performance in ECG beat detection.

In [8], an efficient algorithm for real-time *QRS* complex detection in ECG signals has been presented, with

a focus on low computational complexity and adaptability to resource-constrained platforms. The combination of a pre-processing stage (which reduces noise) with a dynamic thresholding mechanism (adjusted by a finite-state machine) ensures robust detection of R peaks even in noisy environments, with reported sensitivities and positive predictivities exceeding 99%. The proposed methodology of this paper presented in Fig. 1, begins with real-time ECG data being passed through a preprocessing stage, where the signal is filtered to eliminate noise and artifacts. Once the signal is filtered, it is sent to the *QRS* complex detection unit for further analysis. This unit accurately identifies and detects the R peaks, which are critical components of the ECG waveform. The detection process involves sophisticated algorithms that ensure precise identification of the *QRS* complexes, even in noisy environments. This system provides real-time feedback, allowing for continuous monitoring of heart activity, and is particularly effective for identifying cardiac abnormalities. The combination of preprocessing and detection stages ensures both accuracy and reliability in detecting *R-peaks*.

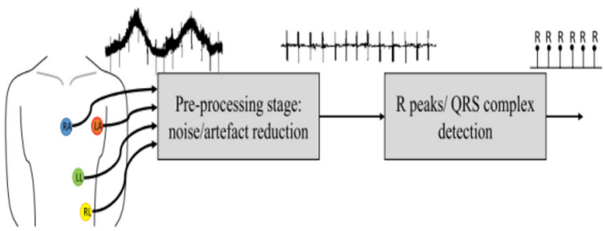

Fig. 1: Typical Structure of a QRS Complex Detection Algorithm

The study fills a crucial gap in ECG signal processing by addressing the challenge of real-time detection on devices with limited computational resources, making it suitable for portable medical applications. The outcomes show a 50% reduction in processing time and a 75% decrease in resource usage compared to the well-known Pan and Tompkins algorithm.

However, hardware implementations do not explore here such as FPGA, which could further enhance performance. This gap is relevant to our work, as we focus on FPGA based dynamic thresholding for ECG processing, which would offer real-time processing advantages that complement the algorithm's low complexity and high accuracy.

There are numerous methods for detecting the QRS complex, with thresholding being one of the more effective approaches. However, a key limitation of traditional thresholding is its inability to consistently detect peaks across varying ECG signals, as it relies on a constant threshold value. This approach fails to account for the fact that the magnitude of different ECG signals can vary significantly. Moreover, the conventional thresholding method is unsuitable for real-time signal processing since it requires an initial calculation of the signal's average to establish the threshold. To address these issues, we propose a dynamic thresholding method, which adapts the threshold value in real time, ensuring more accurate peak detection and making the system more suitable for real-time ECG signal processing.

This study aims to implement a real-time ECG signal processing and monitoring system based on dynamic thresholding using FPGA technology. The primary objective of the dynamic thresholding technique is to provide an effective and adaptive method for detecting heartbeats across various types of ECG signals. By utilizing dedicated hardware, the design is intended to ensure faster and more efficient signal processing. Once the ECG beats are detected, the system will perform an analysis to assess the heart rate and identify potential arrhythmias, enabling real-time monitoring of the patient's cardiac condition.

2. IMPLEMENTATION OF ECG SIGNAL PROCESSING SYSTEM

The complete methodology of QRS-complex detection is represented by a process flow diagram shown in Fig. 2. Although the model is designed to work with real-time signals, for simplicity, we have used a sample signal in this instance. Our proposed technique is subdivided into four stages. Since the signal may contain some noise, we first preprocess it before moving to the actual analysis. Once preprocessed, the signal is passed through the primary detection process to identify the QRS complexes. Based on the QRS complexes, arrhythmia is calculated and subsequently evaluated using a decision-making device to determine its classification.

Fig. 2: Process Flow Diagram of the Proposed System

2.1 Sample Signal

For data collection, we utilize the widely recognized Physionet Massachusetts Institute of Technology- Beth Israel Hospital (MIT-BIH) Arrhythmia Database, a crucial resource in ECG signal research renowned for its precise annotations and wide-ranging diversity. This freely accessible database plays a pivotal role in facilitating

research and educational initiatives globally, offering access to various types of ECG records from several patients. Each record includes two signals spanning two hours, sampled at 1000 samples per second, with a resolution of 12 bits within a 20 mV interval. Since all the 12 signals from various electrodes are stored in a single ".mat" file, we have used the MATLAB coding to separate the individual signals and separated individuals signal has been shown in Fig. 3.

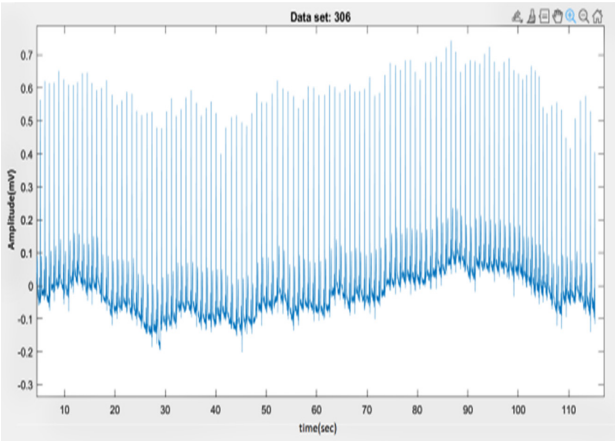

Fig. 3: Sample ECG Signal

2.2 Preprocessing

The sample ECG signal contains various types of noise, such as baseline wander, power line interference, and high-frequency noise. To ensure accurate signal analysis, the ECG signal must undergo a preprocessing stage to adjust certain parameters and remove noise. Initially, the signal is passed through a high-pass filter to eliminate baseline wander and low-frequency noise. Following this, it is processed through a low-pass filter to reduce power line interference and remove high-frequency noise, making the signal suitable for further analysis.

2.3 Peak Detection

The detection of the QRS complex is the most vital part of the ECG signal processing scheme. There are several methods for QRS complex detection, but the proposed method stands out by offering a dynamic threshold value. This allows the detection of peaks even in noisy signals, as the threshold is continuously updated every second, ensuring more accurate and reliable detection in varying signal conditions. Additionally, the signal is transmitted to a real-time monitor, allowing continuous observation and analysis of the signal. The inner functional diagram of the arrhythmia detection is shown in Fig. 4.

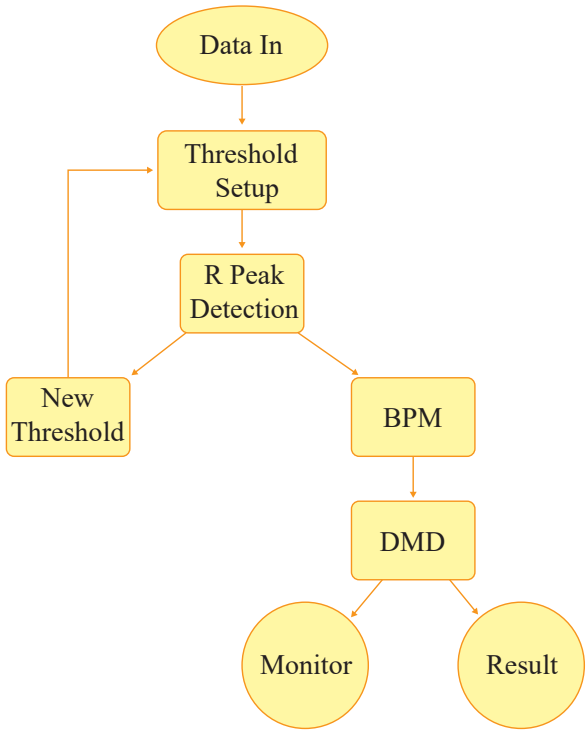

Fig. 4: Inner Functional Diagram of the Arrhythmia Detection Algorithm

2.3.1 Input Signal

The enhanced ECG signal, after passing through the filter, is stored in a Xilinx state array variable. This array is essential for comparing the previous values of the ECG signal with the new values, allowing for the accurate detection of peaks.

2.3.2 Dynamic Threshold

The threshold is a reference value used to detect the R-peak in an ECG signal. If the threshold is set as a constant, peak detection may be inaccurate, as ECG signals vary in magnitude across individuals. Additionally, the magnitude of a noisy ECG signal can fluctuate over time. In such scenarios, a constant threshold method may fail to accurately detect all peaks. This highlights the necessity of a dynamic threshold method, which adapts to changing signal conditions, ensuring more reliable and accurate peak detection. Initially, a constant value is set as the threshold. A counter is then started to measure a one-second interval, during which the maximum value of the ECG signal is determined. If this maximum value is greater than 0.1, the threshold is updated to half of the maximum value detected within that second. This condition is necessary because, in some cases, no R-peak may occur within a one-second interval. Without this safeguard, the

algorithm might mistakenly select the highest value from background noise, which typically hovers near zero, as the R-peak. This would result in an incorrect threshold value.

$$TH(n) = \frac{R_{peak}(n-1)}{2} + \frac{R_{peak}(n-1)}{4} \quad \text{..... (1)}$$

Eqn. (1) outlines the threshold calculation. In the n-th iteration, the threshold is set as half of the R-peak value from the previous iteration. This adaptive approach ensures that if the *R-peak* level decreases; the corresponding threshold value will also decrease, allowing the algorithm to adjust dynamically to changes in signal amplitude. This process ensures that the threshold is dynamically adjusted and is updated continuously at one second intervals for more precise peak detection.

2.3.3 *R-peak* Detection

The *R-peak* in the QRS complex for each beat is an important aspect to be identified. The *R-peak* acts as a reference point for the identification of other aspects of the signal. Thus, to detect the *R-peak* accurately is an important part of this algorithm. As previously explained, the algorithm designed here serves as a foundation for applications that require real-time detection of *R-peak* positions. Additionally, it is optimized for implementation on platforms with limited resources, ensuring efficient processing and performance even in constrained hardware environments. In this real-time signal processing system, it's impossible to store all the data at once for processing. Instead, the algorithm works with individual data points sequentially. The key idea of the proposed algorithm is that, we know, the value next to the peak value in any signal will be lower than the peak itself. While ECG signals have many fluctuations, this condition alone does not make any sense. But this becomes meaningful when combined with two other conditions described in (2). Together, these three conditions form an effective method for detecting the *R-peak*, which is then used to detect other peaks.

If(*data*(*n*) > *TH* && *data*(*n*) >*data*(*n* - 1) && *Flagtimer* = 1) *Then R-peak* = *data*(*n*) .....(2)

The first condition ensures that the current data point *data*(*n*) is greater than the threshold, eliminating the chance of falsely detecting other peaks as *R-peak*. If this condition holds, the algorithm checks whether the current data point *data*(*n*) is higher than the previous one *data*(*n* - 1). If both the conditions are true, which ensures that the data is a peak value laying above the threshold. So, the data is obviously denoting an *R-peak* as shown in Fig. 5(a). The problem arises with the with the falling edge of the *QRS* complex of an ECG signal. The previous both conditions are true for this edge. So, it will detect all the points on the falling edge as *R-peak*. Here comes the necessity of the third condition. We used a timer that counts 300 ms after an R-peak is detected which holds the algorithm for further detection of peak during the time interval. Initially, the timer flag is set to 1(High). When a peak is detected, the timer set the timer flag to 0(Low) and it starts then counting again. After 300 ms interval, it set the timer flag to 1 (High) again as described in eqn. (2). The 300 ms interval is chosen because the falling edge duration of *QRS* complex is typically less than that, ensuring no additional R-peak appears within that period. The process continues and the detected R-peaks will immediately be passed to the output.

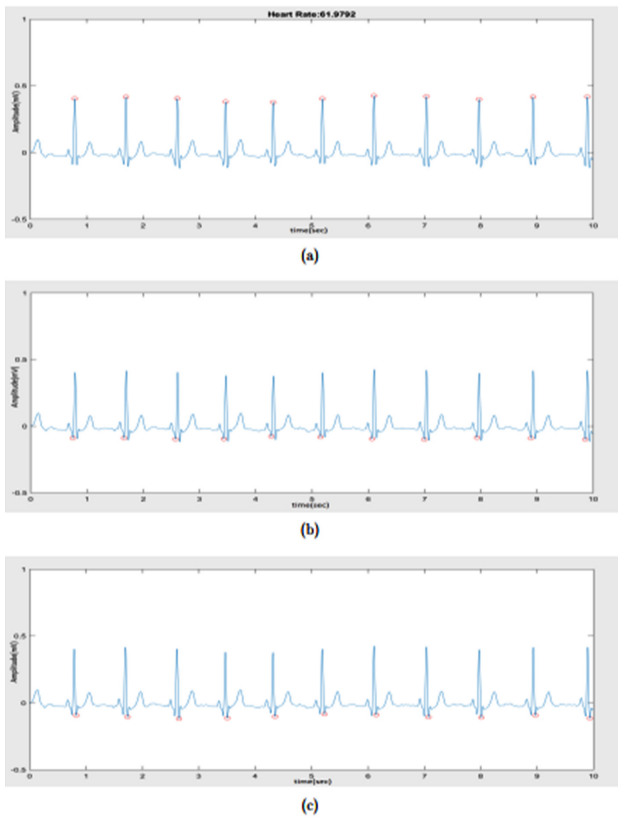

Fig. 5: Detected QRS complex in MATLAB (a) *R-peak* (b) *Q-peak* and (c) *S-peak*

2.3.4 QRS Complex Detection

The *R-peak* detected in the previous stage will be used as reference to find the remaining *Q* wave and *S* wave. The *R-peak* location plays a very important role in detecting the *QRS* complex as these tow peaks remain near the *R-peak*, we can easily detect these waves finding the

minimum value near the *R-peak*. The *Q* wave represents the minimum value that occurs just before each *R-peak* within a specific time interval. We identified the *Q* wave by locating the minimum value within a 300 ms interval preceding each *R-peak*. Similarly, the *S* wave is the minimum value that follows each *R-peak* as shown in Fig. 5(b). We determined the *S* wave by finding the minimum value in the 300 ms interval following each *R-peak* as illustrated in Fig. 5(c). Once detected, the *Q* and *S* waves were stored in a file for further analysis. By combining the corresponding *Q* wave, *R* wave and *S* wave, we identified the *QRS* complex, which is then used for heart rate detection in the next stage.

2.3.5 Determination of Heart Rate

There are several ways of calculating the heart rate (HR). We used the following technique to calculate Beats Per Minute (BPM) of an ECG signal. we first identify the number of heartbeats detected within a specific time frame. The ECG records electrical activity of the heart over time and each *R-peak* corresponds to a single heartbeat. The formula we used for calculating the heart rate is:

$$HR = \frac{No_{beat} * 60}{Time}(bpm) \qquad \text{..... (3)}$$
$$Time = \frac{No_{sample}}{f_s}(sec)$$

Here, No_{beat} refers to the number of *QRS* complex detected within the given time (in seconds), and "time" refers to the duration over which the beats are measured. The result is then multiplied by 60 to convert it from beats per second to beats per minute. This method provides an accurate estimation of heart rate based on the detected *QRS* complexes in the ECG signal.

2.3.6 Decision Making Device

Decision making device (DMD) is a crucial component. The primary function of the DMD is to assess the HR derived from the previous signal processing stage and determine the corresponding heart condition. We have used tow relational operator blocks to design this DMD. The DMD evaluates the HR by comparing it against predefined thresholds specifically, 60 BPM and 100 BPM. If the HR exceeds 100 BPM, the DMD classifies the condition as tachycardia, indicating an abnormally fast heart rate. Conversely, if the HR is below 60 BPM, it identifies the condition as bradycardia, signifying an unusually slow HR mentioned in [9]. For HR values within the range of 60 to 100 BPM, the DMD categorizes the heart condition as normal described in eqn. (4). This simple yet effective classification method enables real-time monitoring of cardiac health, providing essential information for detecting and responding to abnormal heart rhythms in a timely manner.

$$\begin{cases} \text{if} & HR > 100 & \text{Result} = \text{“Tachycardia”} \\ \text{else if} & HR < 60 & \text{Result} = \text{“Bradycardia”} \\ \text{else} & & \text{Normal} \end{cases} \qquad \text{..... (4)}$$

2.3.7 Monitor

The monitoring section of the system plays a vital role in this real-time ECG signal observation and interpretation. This part of the design continuously monitors the ECG signal, displaying crucial information such as the HR and the heart's condition. Once the heart rate is determined, it is sent to the DMD, which classifies the heart condition into one of three categories: tachycardia, bradycardia, or normal, based on predefined thresholds. Both the HR and the classified heart condition are displayed on the monitoring system interface, providing immediate feedback. This real-time display allows for continuous tracking of cardiac health, enabling quick diagnosis and response to abnormal heart conditions. The integration of dynamic thresholding ensures that the system adapts to signal variations, ensuring accurate monitoring and timely detection of any peak.

3. FPGA IMPLEMENTATION

In the FPGA implementation phase, we began by executing the proposed algorithm and simulating the design in MATLAB Simulink to verify its functionality before moving on to hardware implementation. The simulation results, which will be included in this section, provided a crucial preliminary validation of the design. After successfully simulating the design in Simulink, we transitioned to the Xilinx System Generator for hardware implementation.

3.1 Simulation Using MATLAB Simulink

Figure 6 show the simulation of the proposed ECG signal processing system was conducted using MATLAB Simulink to validate the algorithm's functionality before hardware implementation. Simulink provides a graphical environment to model and simulate dynamic systems, making it ideal for testing complex signal processing designs. By using Simulink, we were able to simulate

various stages of the ECG processing system, including signal acquisition, filtering, and HR detection. The results from these simulations will be presented in the following sections, demonstrating the system's performance and accuracy prior to hardware integration.

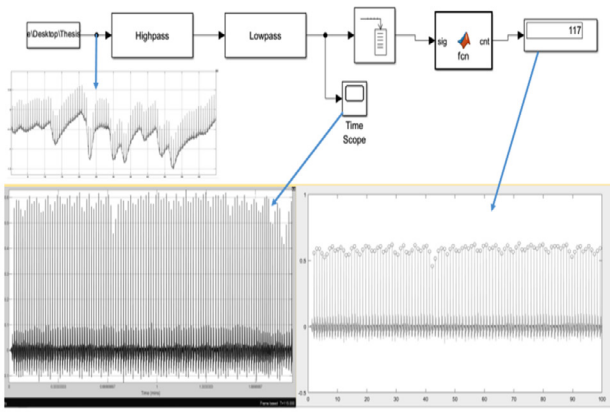

Fig. 6: Simulation Model of the Proposed System with Output Wave Shapes

3.2 Implementation Using System Generator Blocks

It is important to note that standard Simulink blocks are not directly supported by hardware, meaning they are more suited for algorithm testing and simulation rather than real-world execution on FPGA devices. In contrast, Xilinx System Generator blocks are specifically designed for FPGA-based systems, allowing for direct implementation on hardware. System Generator is a powerful tool that integrates seamlessly with Simulink, enabling FPGA code generation and ensuring the design is optimized for real-time hardware execution. By using System Generator blocks, the design is effectively translated into hardware-level operations, providing a path from simulation to physical implementation. The results from the System Generator simulations will also be included to illustrate the successful transition from software to hardware. This methodology ensures the reliability and accuracy of the FPGA-based real-time ECG signal processing and monitoring system.

Figure 7 illustrates the overall architecture of the proposed system, implemented using System Generator blocks. The filters are designed using the FDA Tool in MATLAB Simulink, with the filter coefficients saved in a MATLAB file and subsequently uploaded into the filters. The results for each segment are presented in the Fig. 8.

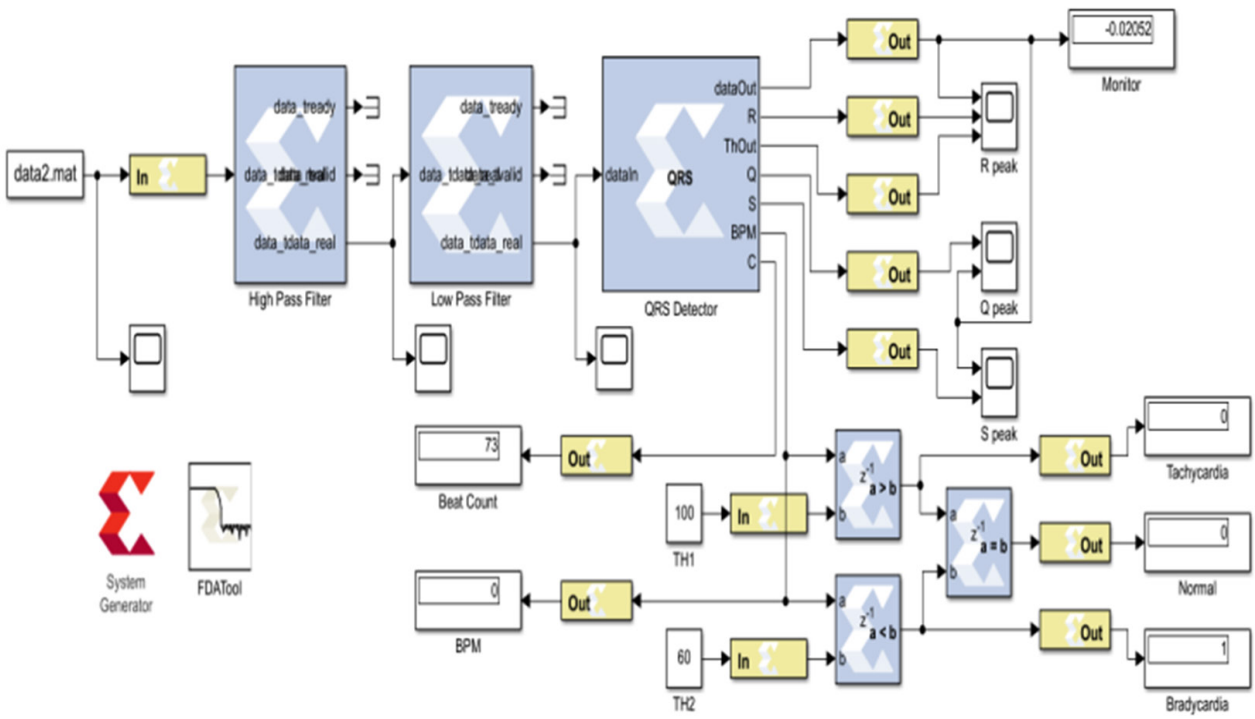

Fig. 7: Architecture of the *QRS* Complex Detection and Monitoring System Using System Generator Blocks

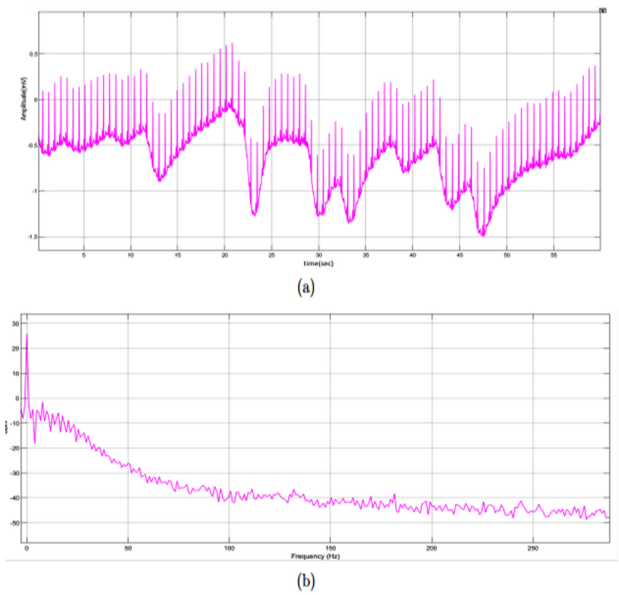

Fig. 8: Raw Ecg Signal for System Generator (a) Signal in Time Domain and (b) Signal in Frequency Domain

4. RESULTS AND DISCUSSION

The proposed method was applied to ECG signals from 10 different subjects from the MIT-BIH database to evaluate its performance. After detecting the heartbeats, a comparative analysis was conducted between the actual beats and the beats detected by the system. The results, summarized in Table I, include the percentage error between the actual and detected beats, highlighting the accuracy of the system.

Table I: Performance Evaluation of Proposed Methodology of Beat Detection

Data set	Actual Beats	Detected Beats	% error
101	122	119	2.46
113	123	123	0.00
118	176	176	0.00
122	162	161	0.61
124	180	180	0.00
136	163	162	0.61
145	169	169	0.00
162	116	116	0.00
174	152	150	1.31
187	107	106	0.93
Total	1470	1462	0.54

The results of our proposed ECG signal processing system demonstrate its high accuracy and reliability in real-time beat detection. As shown in Table I, the overall error rate of the system is just 0.54%, highlighting its efficiency in detecting heartbeats. Out of a total of 1,470 beats, only 8 beats were undetected, which is a low error margin compared to similar systems. From this result we have calculated the sensitivity and F1 score and the values are found 99.46% and 99.73% respectively. Compared to ref [5] though the sensitivity is little low but the F1 score was found better. This showcases the effectiveness of the dynamic thresholding algorithm implemented in FPGA, which adapts varying ECG signal amplitudes and noise levels, ensuring accurate detection of the *QRS* complex. Furthermore, Table II evaluates the performance of the DMD, which uses the detected beats to analyze the heart rate and assess potential arrhythmia conditions.

Table II: Performance Evaluation of the DMD

Data set	Actual BPM	Detected BPM	DMD Output
096	110.0	109.2	Tachycardia
113	64.00	64.00	Normal
162	58.56	58.00	Bradycardia
174	79.10	78.12	Normal
181	105.3	104.5	Tachycardia
187	55.00	55.00	Bradycardia
193	89.82	89.34	Normal
207	44.64	43.00	Bradycardia
399	108.00	107.3	Tachycardia
412	103.00	102.0	Tachycardia

Although there are minor discrepancies in the detected BPM compared to the actual BPM values, the overall output of the DMD is 100% accurate in terms of identifying arrhythmias. This demonstrates that, despite small errors in BPM detection, the system is highly reliable in diagnosing cardiac conditions. The integration of real-time signal processing with FPGA and the dynamic thresholding method has significantly improved the system's performance, making it a robust solution for medical applications. Additionally, the real-time monitoring system continuously updates the BPM on the display every minute, providing ongoing feedback on the heart's condition. The arrhythmia status, as determined by the DMD, is also displayed, offering immediate identification of tachycardia, bradycardia, or normal heart rhythms. Alongside these results, the enhanced real-time ECG signal is monitored on the system interface, allowing for continuous observation and analysis of the cardiac activity. This comprehensive monitoring and analysis showcase the system's effectiveness in real-time heart rate detection and condition monitoring.

5. CONCLUSION

The paper focuses on designing and implementing an ECG signal processing and monitoring system that sacrifice memory utilization for improved performance, accuracy, speed, and real time operation. It also explores various strategies in signal processing system design, including window filtering, adaptive method and thresholding method. The dynamic thresholding technique updates the threshold value continuously after each *R-peak* detection. The advantage of this method over traditional ECG signal processing systems is a real time processing system with dynamic detection technique. The proposed system can be applied for different types of signals and also it can detect the peaks form noisy signals. The system is suitable for applications where different types of ECG signal are needed to be processed and high speed is required. The work also focuses on designing and analyzing a high-performance system using FPGA hardware. The implemented system detected 1462 beats among 1470 beats from several ECG signals. The overall percentage of error of the system was 0.54%, sensitivity of 99.46% and the F1 score was 99.73%. The FDA tool is used to design the filters to preprocess the raw signal and the system generator block sets are used for hardware implementation. The analysis includes beat detection error and evaluation of DMD to classify the signal condition. The findings of this work provide that the system cannot detect a peak if the magnitude difference between that peak and the previous peak is greater than the threshold value. Additionally, the system may miss a peak at the very beginning when the threshold has not yet been established.

REFERENCES

[1] J. F. Pascual, P. J. Marchite, J. R. Silva and N. R. Gándara, "Arrhythmic syncope: From diagnosis to management," World Journal of Cardiology, Vol. 15, Issue 4, pp. 119-141, 2023.

[2] M. F. Safdar, R. M. Nowakand P. Palka, "Pre-Processing techniques and artificial intelligence algorithms for electrocardiogram (ECG) signals analysis: A comprehensive review," Computers in Biology and Medicine, Vol. 170, 107908, 2024.

[3] R. Popa, "ECG signal filtering in FPGA," 6th International Symposium on Electrical and Electronics Engineering (ISEEE), pp. 1–6, 2019.

[4] M. B. Altman, W. Wan, A. S. Hosseini, S. A. Nowdeh and M. Alizadeh, "Machine learning algorithms for FPGA Implementation in biomedical engineering applications: A review," Heliyon, Vol. 10, Issue 4, e26652, 2024.

[5] Z. Habibi, K. Karimizadeh, A. Nosratpour and I. Alipourfard, "Enhanced QRS detection and ECG compression using adaptive thresholding: A real-time approach for improved monitoring and diagnosis," Computers and Electrical Engineering, Vol. 119, Part A, 109528, 2024.

[6] E. S. Kolawole, W. H. Ali, P. Cofie, J. Fuller, C. Tolliver and P. Obiomon, "Design and implementation of low-pass, high-pass and band-pass finite impulse response (FIR) filters using FPGA," Circuits and Systems, Vol. 6, pp. 30-48, 2015.

[7] J. Rahul, M. Sora and L. D. Sharma, "Dynamic thresholding based efficient *QRS* complex detection with low computational overhead," Biomedical Signal Processing and Control, Vol. 67, p. 102519, 2021.

[8] V. K. Sinha and S. K. Kar, "An efficient real-time ECG QRS-complex identification by A-CLT and digital fractional order differentiation," Biomedical Signal Processing and Control, Vol. 92, 106055, 2024.

[9] Y. Chou, J. Gu, J. Liu, Y. Gu and J. Lin, "Bradycardia and tachycardia detection using a synthesis-by-analysis modeling approach of pulsatile signal," IEEE Access, Vol. 7, pp. 131256–131269, 2019.

Configuring Windows and Clerestories of Bedrooms for Optimum Daylighting in Dining Spaces of Contemporary Apartment Buildings in Dhaka

Fariha Seraj[1*] and Md Ashikur Rahman Joarder[2]

[1]Department of Architecture, Dhaka University of Engineering & Technology, Gazipur, Bangladesh
[2]Department of Architecture, Bangladesh University of Engineering and Technology, Dhaka, Bangladesh

ABSTRACT

The majority of Dhaka's residential apartments contain dining spaces without windows due to their spatial organization. While large bedroom windows could improve dining space daylighting through doors and clearstories, if the bedroom is connected to the dining spaces; however, they risk glare and overheating in the bedrooms. This research explores optimal bedroom window position, shape and size, along with clerestories of varying widths in partition walls shared with dining spaces, to enhance dining space daylighting without causing glare to bedrooms. Using daylight simulations based on Leadership in Energy and Environmental Design (LEED v4.1) metrics and the daylight glare probability (DGP) index, various options were tested with ClimateStudio in Rhinoceros 7 and Grasshopper. Results show that strategically placing doors, windows and clerestories in adjacent bedrooms can significantly improve dining space daylighting. Optimally positioned rectangular windows (aspect ratio 0.3) and clerestories increased spatial daylight autonomy ($sDA_{300/50\%}$) by 2.8% and illuminance by 57% without creating glare.

1. INTRODUCTION

Buildings, particularly residences, support various human needs by serving as a place of convergence for people and societal identities. Optimal use of daylight is essential for visual comfort and well-being. Windows enhance spaces by providing daylight and views, supporting physiological and psychological health. Studies show daylight exposure reduces risks linked to vitamin D deficiency [1], boosts immunity [2], improves visual perception and mood [3], and increases occupant satisfaction [4].

The urban house form in Dhaka evolved through various phases. Initially, during the pre-Mughal period, resembling traditional rural designs (Fig. 1[a]) [5], houses were featured with rooms around courtyards for light and ventilation (Fig. 1[b]) [6]. In the Colonial period, this style merged with European bungalow designs, converting central courtyards into indoor spaces (Fig. 1[c]). Post-colonial houses became compartmentalized multistory blocks, with dining areas acting as central transition spaces to connect other rooms and balconies attached to peripheral rooms (Fig. 1[d]). The central living-dining areas, inspired by traditional courtyards, often lack adequate daylight and thermal comfort [7]. Large full-height apertures in surrounding rooms of the dining spaces may be used to improve daylight in the central dining space (Fig. 1[e]); however, it can cause indoor heat gain and glare, particularly in the rooms with south-facing facades.

Dhaka's rapid urbanization has led to severe housing challenges, prompting private developers to construct multistory apartment buildings with several units per floor. These deep-plan buildings (Fig. 1[e]), with large interior-to-external wall ratios [8], hinder natural ventilation and daylight, making them unsuitable for Dhaka's hot, humid climate [9]. An appropriate combination of window and shading systems can help extend non-cooling periods and save energy. The Bangladesh National Building Code (BNBC, 2020) [10] provides only general guidelines, lacking specificity for building function or performance targets. Dynamic daylight simulation can be used to enhance daylighting through passive features such as windows and clerestories.

Optimum window system design is essential to achieve standard illumination levels and minimize glare and even daylight distribution in interior spaces. According to Maleki [11], square and horizontal window shapes with a 30% window-to-wall ratio (WWR) in central and upper positions were optimum for south orientation in the context of Iran. The same configuration of windows with a WWR of 40% was found as optimum for the north orientation. Another study found that, a WWR of 39% in the middle position can enhance daylight and energy

*Corresponding author's email: fariha.seraj@duet.ac.bd

performance up to 12% [12] for an office space. Another study reported a 68% reduction in glare and a 70% increase in daylighting performance by adjusting WWR and shading in the educational space of Iran [13]. Most of these experiments are related to non-residential buildings.

A study related to residential daylight performance in warm-humid climates reported that a change in the window position could be beneficial in maintaining spatial daylight autonomy ($sDA_{300/50\%}$) and annual sunlight exposure ($ASE_{1000,250h}$) within the prescribed limit of 75% and 20% respectively [14]. Another study reported that 61% of the variability in energy consumption can be defined by changes in the WWR of residential buildings in hot-arid climatic zones [15]. These studies are limited to a specific climatic context. Little or no guideline is found on window location and WWR of bedrooms and clerestories of the peripheral walls of dining spaces to improve the overall luminous environment of the apartments by illuminating dining spaces. Multiple apertures, such as windows on two sides of a space or clerestories, can increase the distribution of daylight in a space. Against this backdrop, this research aims to find the optimum position, shape and size of windows on the bedrooms' facades and optimum clerestory configuration in the partition walls around the adjacent dining space to enhance daylight illumination of the dining space without creating glare in the bedrooms.

Fig. 1: Transformation of Courtyards and Balconies in Urban Houses Through Different Periods (After [16])

2. METHODOLOGY

This research followed a five-step methodology. First, the case space and climatic context were defined. Second, key design variables were selected, and a parametric model was developed using Rhinoceros 7 and Grasshopper. Third, dynamic daylight metrics were chosen to optimize daylight in the dining space through bedroom windows while minimizing glare in the bedrooms, with performance benchmarks set to ensure balanced lighting. In the fourth step, the impact of each variable on daylight quantity and glare probability was evaluated. Finally, a sensitivity analysis was conducted to assess the effects of window configurations, leading to the development of design guidelines.

2.1 The Case Space

Nearly 57% of Dhaka residents were classified as a mid-middle income group (monthly income 370 USD to 555 USD) and preferred two-bedroom apartments due to their financial capacity [17]. Three distinct types of living-dining layouts were identified in these middle-income group apartments: attached, continuous and separate (Fig. 2[a]. The attached type was significantly prominent in numbers [18]. Taking into account those mentioned above, a case residential apartment of 88m2 area [16,18] was selected as the case space for the simulation study (Fig. 2[b]). It had two bedrooms, one attached type living-dining space, a kitchen, two toilets and one verandah. The dining space area was 12.7 m2 without any window for direct penetration of daylighting. The average area and WWR of bedrooms were 14.4 m2 and 19%, respectively. The floor-to-ceiling height was 3.0 m, and the width of the shading device was 0.5 m [10]. To investigate the effect of the selected variables on the daylighting condition of the dining space, the interior of the case apartment and the surroundings were considered vacant. The case space was considered on the ground floor of a six-story building as the daylighting condition is expected to be the worst on ground floor. The 3D model of the case apartment was validated for daylighting in a previous study [7].

2.2 Climatic Context and Weather Data

Dhaka is located between the latitudes of 23°40' N and 23°55' N and the longitudes of 90°20' E and 90°30' E. According to the Koppen Climate Classification, it falls under Category-A, that is, Tropical Savanna. Primarily, three distinct seasons can be observed here– the hot dry (March-May), the warm humid (June-November) and the cool dry (December-February) seasons. Both clear

Fig. 2: [a] Types of Living-Dining Layout in Dhaka's Residential Apartment; and [b] Plan of the Case Apartment

and overcast sky conditions are observed in different parts of various seasons. The sky remains clear with the sun and overcast in the hot dry season. The sky remains significantly overcast during the warm humid period, including the monsoon. Only in the cool dry season, the sky remains mostly clear.

Hourly weather data BGD_Dhaka.419230_SWERA, downloaded from the website of EnergyPlus™, was used in this research. It is based on high quality solar and wind energy information developed by the Solar and Wind Energy Resource Assessment (SWERA) project, financed by the United Nations Environment Program (UNEP) [19].

2.3 Design Variables for Residential Daylighting

Daylight availability in spaces depends on different features, such as window location, placement or position, width, window head height and size [20, 21]. WWR is one of the factors that determine how much daylight enters a building's interior. Increasing the WWR to maximize daylight quantity will not always ensure an effective visual environment but may also cause glare and overheating [22]. Clerestories or combined side lighting systems permit deeper penetration of daylight while little glare and discomfort, depending on the mounting height and width [7, 26]. In this study, three independent design variables for window design: window shape, position and window size were selected for simulation study. In the case of clerestory window design, only the width of the clerestory was considered here as the mounting height (2.1 m) for clerestories in residential apartment's partition walls were fixed above the lintel and maximum window height (i.e., up to the ceiling) will not cause overheating and glare.

2.4 Benchmark of Daylighting Performance Metrics

Leadership in Energy and Environmental Design (LEED) Version 4.1 introduced a rating system to evaluate the daylight performance of buildings using the IES-LM-83-12 Standard [24]. In this standard, two dynamic metrics are used: $sDA_{300/50\%}$ and $ASE_{1000,250h}$. These two metrics are evaluated in a grid analysis on a horizontal work plane. In the $sDA_{300/50\%}$ metrics, daylight sufficiency of a specific area is measured as a percentage of the area that exceeds a target illuminance value (300 lux) for a specified amount of time of a year (50% of the annual hours). The target value of $sDA_{300/50\%}$ was considered as 75% for this study [24].

$ASE_{1000,250h}$ refers to the percentage or fraction of area that exceeds the direct sunlight level of 1000 lux more than 250 hours per year, which can cause glare over a specified daily schedule with the operable shading devices retracted. As residential tasks are less desk and screen-oriented, glare is usually less concern and the use of blinds is determined by several factors, including privacy and thermal comfort. Consequently, the target value of $ASE_{1000/250h}$ was considered as 20% for this study [25].

Besides these two metrics, a complementary approach of glare prediction assesses the probability of glare in the perceptual field of view, termed daylight glare probability (DGP). DGP is an index indicating the probability of an occupant's dissatisfaction with the difference between bright and dark areas within the visual environment caused by direct sunlight or high light source luminance [26]. It is presented as a percentage of time or space an occupant may be disturbed by glare on a four-point scale: imperceptible (DGP<35%); perceptible (35%≤DGP<40%); disturbing (40%≤DGP<45%); intolerable (DGP≥45%) on a scale between 20% to 80%. Daylight standard of the European Committee for Standardization (CEN) [27] proposed different levels for glare protection in interior spaces: minimum 45%, medium 40% and high 35%, not more than 5% of the occupied time of a space. So, the minimum accepted level of DGP for glare protection was considered 45%.

2.5 Daylight Simulation Method

The parametric model of the case space was constructed using Rhinoceros and Grasshopper (Fig. 3[a]). Then, the weather data and surface materials were assigned in the ClimateStudio (CS) plugin, regarded as the fastest and most accurate simulation tool based on EnergyPlusTM and a novel RADIANCE-based path tracing technology. Reflectance values for the ceiling, walls, floor and shading devices were 88.4%, 83.9%, 64.9% and 82.4%, respectively. The window construction was 6mm single clear glass with a solar heat gain coefficient (SHGC) value of 0.64. The sensor grid was set at 0.75m high from the finish floor level. The grid spacing was considered as 0.6 m (36 sensors in the dining space and 80 sensors in the bedrooms) (Fig. 3b). For the calculation of the DGP index simulation, ClimateStudio software considered the height of the subject's field of view in the seated position at 1.2m from the finished floor level. The daylight simulation schedule was considered from 8:00 AM to 6:00 PM. The simulation outputs of each design variable were measured to achieve a maximum amount of $sDA_{300/50\%}$ for the dining space by placing the optimum window size on the bedrooms' facades to reduce the risk of glare in the bedrooms.

The daylight performance of each selected variable was assessed based on the chosen daylight performance metrics (Section 2.4). There were three steps in the assessment process (Fig. 4). In the first step, window shapes and positions were assessed. In the second step, the variable of clerestory configuration was assessed along with the window shape and position found best in the first step. The impact of several WWRs of the ideal window shape and position, along with the best clerestory configuration, was then evaluated for the dining area and the bedrooms.

3. DAYLIGHT SIMULATION ANALYSIS AND RESULTS

3.1 Assessment of Window Shapes and Positions

The first two variables were window shape and position (Table I). Two types of window shapes- square and rectangular, were used for each of the four window positions: low, high, middle and corner. The low window begins at the bottom of the facade and the middle window is located precisely on the central axis of the facade [11, 20]. In the case of the corner window, two design options were evaluated. In the first option, windows were placed at one end of the facades just opposite the bedroom doors to provide daylight in the dining through the doors. In the second option, windows were placed away from the door. Multiple design options were created by changing these two design variables and keeping the WWR at 14% according to BNBC 2020 [10] (Table I). Aspect ratio (AR) width to height ratio (W/H) was used to define the window shapes in this study. Rectangular vertical windows with an AR value of 0.3 were the same in the case of low, middle and high positions as in this specific facade, AR 0.3 comprised the full length of the facade. These window configurations were placed on the facades (Fig. 3) to investigate their effect on the daylight illuminance of the dining space (Fig. 3[b]).

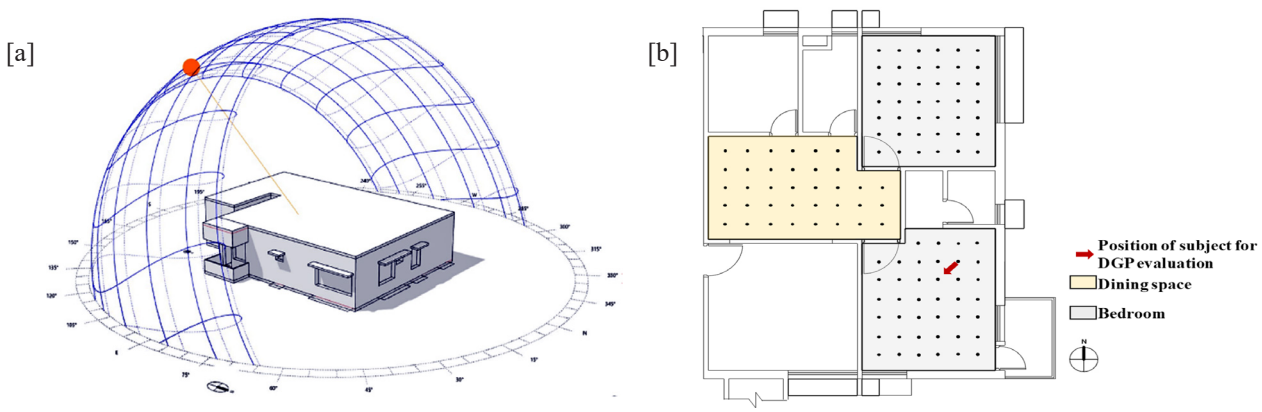

Fig. 3: [a] Three-Dimensional Model of the Case Residential Apartment in Rhinoceros; and [b] Sensor Grid Setup of Dining Space and Two Bedrooms

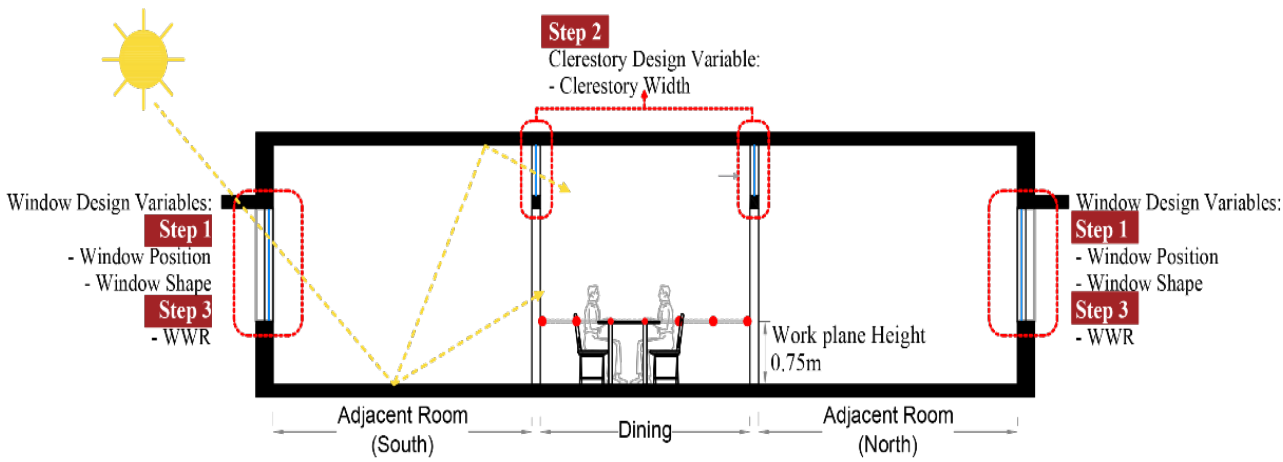

Fig. 4: Conceptual Section Showing Different Window Design Variables (Position, Shape and WWR) and Clerestory Configurations for Performance Evaluation

The results of daylight simulations for different window positions and shapes with a constant WWR of 14%, along with rating points (RPs) and ranking, are presented in Table III. The studied design options produce zero $ASE_{1000,250h}$ values in the dining space, $sDA_{300/50\%}$ values range from 0.0-1.8% and annual average illumination values from 62.5-84.8 lux. As the $ASE_{1000,250h}$ values were zero, and the $sDA_{300/50\%}$ and illumination

values were below the acceptable and standard level, a rating system [25] was developed to analyze the simulation results. The rating was done considering 0 to 24 points to recommend the configurations from 1st to 25th rank. Rectangular vertical window with AR value 0.3 ranked 1st. Rectangular vertical window with an AR value of 0.5 in the low window position and a square window in the middle position of the facade, ranked 2nd and 3rd positions, respectively.

Considering the rating point distribution, rectangular vertical windows performed better than rectangular horizontal windows. In addition, the middle windows performed better than the other three window positions (Table III). This is because it can transmit more daylight by creating better reflections from the walls of bedrooms due to its central position in the facade. This indicates that vertical windows with greater height perform better than horizontal windows, and window head height has a more significant impact on the $sDA_{300/50\%}$ and illuminance values than the window width. In contrast, horizontal windows performed better in corner positions with a greater AR value.

3.2 Assessment of Clerestory Configuration

Clerestories with two different widths (Table I and Fig. 4) were inserted alternatively in the partition walls around the dining space after placing the optimum window position and shape (rectangular middle window with AR=0.3) in the bedrooms' facades. The effectiveness of the width of the clerestory was investigated only as the mounting height (above the lintel level, 2.3m) and the height of the clerestories (between lintel and ceiling, 0.6m) was fixed. The results of the simulations revealed that the $sDA_{300/50\%}$ value after inserting a clerestory C1 was not changed, the illuminance value increased by 18.9% from the previous condition. $sDA_{300/50\%}$ and annual average illumination values increased by 1.2% and 18% after inserting the clerestory C2 in the partition wall around the dining space.

3.3 Assessment of Window-to-Wall Ratio (WWR)

Optimum WWR is required in the bedrooms to balance daylight illumination of the dining space and bedrooms. The optimum WWR of the best window shape and position found in Section 3.1, along with the best clerestory configuration (Section 3.2), were investigated in this section. WWR of the base case was selected as 14%, according to BNBC 2020 [10]. The selected range of WWR for the daylighting assessment is 20%- 90% other than the base case (Fig. 5). The impact of each WWR of the test windows on the bedrooms' facades was investigated in two steps. In the first step, the impact of the nine different WWRs of bedrooms on the illumination condition of the dining space (Fig. 3[b] and Fig. 4) was investigated. Then, their effect on the illumination condition of the bedrooms (Fig. 3[b] and Fig. 4) was also assessed to avoid glare.

In the dining space, the preferred or accepted levels of $sDA_{300/50\%}$ were not achieved, even with a WWR of 90% on the bedrooms' facades. The $ASE_{1000,250h}$ and DGP values remained 0% (Fig. 5). In the case of bedrooms, $sDA_{300/50\%}$ values were increasing slowly with an increase in WWR and were in the preferred limit; however, the $ASE_{1000,250h}$ increased to 44.7% from the lowest to the highest value of WWR. WWRs from 40% and above exceeded the acceptable limit (<20%) of $ASE_{1000,250h}$, though it can provide a preferable daylight level. Considering the benchmark values of the daylight performance metrics, 30% is the optimum WWR among the studied WWR that can provide useful daylight both in dining space and bedrooms without risk of glare (Fig. 6). Although the greater value of WWRs provided the preferred $sDA_{300/50\%}$, it has the possibility of glare in the bedrooms.

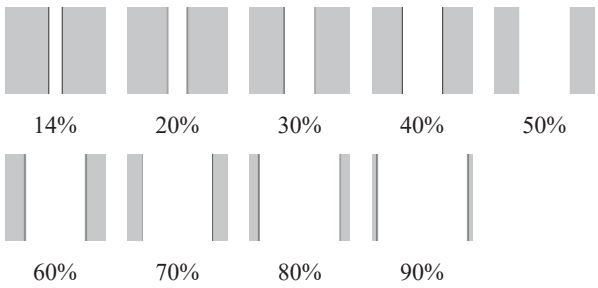

Fig. 5: Selected Range of WWR of the Test Windows on the Bedrooms' Facades for the Simulation Assessment

3.4 DGP Evaluation of Bedrooms

To determine whether discomfort glare is present in the visual field of bedrooms and to confirm the accuracy of the results computed in the preceding section, the glaring probability of the bedrooms was estimated through targeted glare analysis. The subject's location was considered in such a position that the maximum bedroom area can be visible (3[b]). It was carried out on a point-in-time basis in the critical periods of the year with the optimum WWR. Glare analysis was done on the summer solstice (21st June), autumnal equinox (22nd September), the winter solstice (22nd December) and the vernal equinox (20th March) at 9.00h, 12.00h and 15.00h, to visualize the risks of glare in a visual field. Results of the point-in-time glare analysis with the position of the subject are summarized in Fig. 7. The annual DGP value of the bedrooms with optimum WWR of 30% (opposite wall of the bedrooms' door) was 34.9%, which indicates the occurrence of

Table I: Window Position and Shape with Different Aspect Ratios for the Simulation Study

Window Shape and position	Shape and AR	Position: Low	High	Middle	Corner (opposite to door)	Corner (away from the door)
	Rectangular (vertical) 0.3					
	Rectangular (vertical) 0.5					
	Square 1.0					
	Rectangular (horizontal) 2.0					
	Rectangular (horizontal) 3.0					
Clerestory Width		Door (Open)	Door (Open)			
		Only over the Door (C1)	Over the Entire Length of the Partition Walls (C2)			

perceptible glare within the preferred range for this study (Section 2.4). From the point-in-time glare analysis for the south-east bedroom, imperceptible glare (DGP<35%) was found on the critical dates.

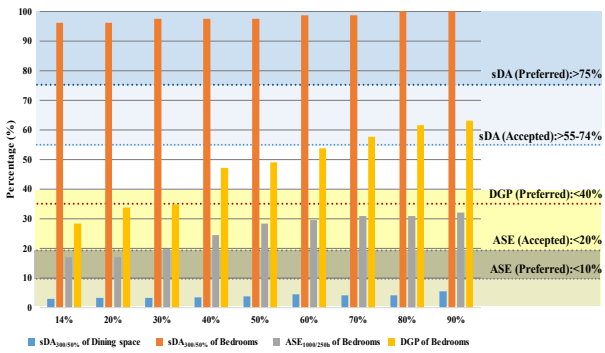

Fig. 6: Performance of Different WWRs of Bedrooms' Facades on Daylight Condition of the Dining and Bedrooms Based on SDA, ASE and DGP Metrics

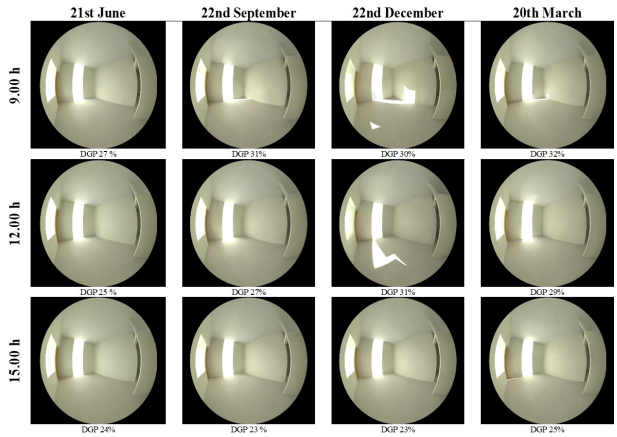

Fig. 7: Daylight Glare Probability of the Bedroom (South-East) with Optimum WWR of 30%

WWR of 30% on the bedrooms' facades opposite the doors increased the $sDA_{300/50\%}$ and annual average

Table II: Summary of Daylight Simulation Results for Different Window Positions and Shapes with a Window Area of 14% of the Bedrooms, Along with the Rating Points and Ranking

Window position	Window shape	Aspect ratio (W/H)	Value and rating points (RP)	$sDA_{300/50\%}$ (%)	Annual average illumination (Lux)	Total RPs		Rank
Low window	Rectangular (vertical)	0.3	Value	1.8	84.8	48	155	1st
			RP	*24*	*24*			
		0.5	Value	1.5	80.2	45		2nd
			RP	*23*	*22*			
	Square	1.0	Value	0.0	62.0	4		20th
			RP	*0*	*4*			
	Rectangular (horizontal)	2.0	Value	0.5	72.0	31		10th
			RP	*17*	*14*			
		3.0	Value	0.3	71.2	27		14th
			RP	*16*	*11*			
High Window	Rectangular (vertical)	0.3	Value	1.8	84.8	48	189	1st
			RP	*24*	*24*			
		0.5	Value	1.0	71.3	32		5th
			RP	*20*	*12*			
	Square	1.0	Value	1.3	79.8	43		8th
			RP	*22*	*21*			
	Rectangular (horizontal)	2.0	Value	1.3	74.7	38		4th
			RP	*22*	*16*			
		3.0	Value	1.0	67.0	28		12th
			RP	*20*	*8*			
Middle Window	Rectangular (vertical)	0.3	Value	1.8	84.8	48	191	1st
			RP	*24*	*24*			
		0.5	Value	1.2	74.8	38		9th
			RP	21	*17*			
	Square	1.0	Value	0.8	73.3	34		3rd
			RP	*19*	*15*			
	Rectangular (horizontal)	2.0	Value	0.8	81.0	42		5th
			RP	*19*	*23*			
		3.0	Value	0.7	70.2	29		13th
			RP	*18*	*11*			
Corner Window (Opposite to door)	Rectangular (vertical)	0.3	Value	0.5	62.5	22	124	18th
			RP	*17*	*5*			
		0.5	Value	0.2	46.8	15		19th
			RP	*15*	*0*			
	Square	1.0	Value	0.5	69.5	27		14th
			RP	*17*	*10*			
	Rectangular (horizontal)	2.0	Value	0.5	63.8	23		17th
			RP	*17*	*6*			
		3.0	Value	0.7	76.8	37		6th
			RP	*18*	*19*			

Window position	Window shape	Aspect ratio (W/H)	Value and rating points (RP)	$sDA_{300/50\%}$ (%)	Annual average illumination (Lux)	Total RPs		Rank
Corner Window (away from the door)	Rectangular (vertical)	0.3	Value	0.5	79	37		6th
			RP	*17*	*20*			
		0.5	Value	0.5	66.2	24		16th
			RP	*17*	*7*			
	Square	1.0	Value	0.5	71.5	30	153	11th
			RP	*17*	*13*			
	Rectangular (horizontal)	2.0	Value	0.5	69	26		11th
			RP	*17*	*9*			
		3.0	Value	0.67	75.2	36		7th
			RP	18	18			

illumination values by 0.3% and 8.9%, respectively. The distribution of daylight in the dining space was also improved. Comparison of the daylight condition of the original model and updated model in terms of $sDA_{300/50\%}$ and annual average illumination are shown in Table III.

Table III: Comparison of the Original and Updated Model's $sDA_{300/50\%}$ and Annual Average Illumination Distribution

	Original model	Updated model
$sDA_{300/50\%}$	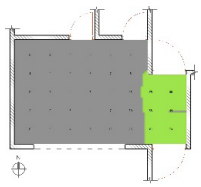	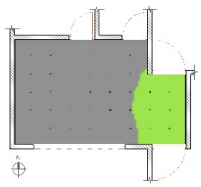
Annual average illumination	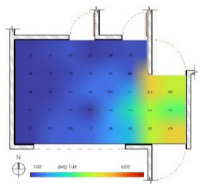	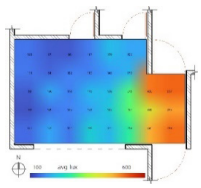

4. SENSITIVITY ANALYSIS

A sensitivity analysis was conducted to evaluate the impact of window size (WWR) on four performance metrics: mean illuminance, $sDA_{300/50\%}$, $ASE_{1000/250h}$ and DGP. The coefficient of determination (R^2) from regression models was calculated and compared for both the dining space and bedrooms, as shown in Fig. 8. An R^2 value close to 1.00 indicates that WWR explains nearly all variability in a given metric. In contrast, lower values suggest the influence of additional factors. For ASE, mean illuminance, and DGP, high R^2 values (0.98–1.00 in the dining space and 0.97–0.99 in the bedrooms) confirm that WWR predominantly governs these metrics. In contrast, $sDA_{300/50\%}$ showed slightly lower R^2 values (0.85–0.87), suggesting that while WWR has a strong influence, it is not the sole determining factor.

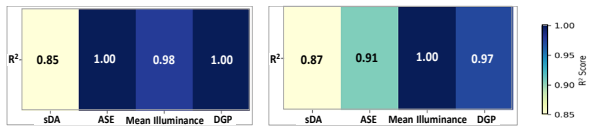

[a] Dining space [b] Bedroom

Fig. 8: Heat Map of the Sensitivity Analysis for Dining Space and Bedroom

5. CONCLUSION

This study demonstrates how reflected or diffused daylight from adjacent bedrooms can enhance dining space illumination by adjusting key design variables-window position, shape, clerestory width and WWR, highlighting the critical role of bedroom window design in improving daylighting in deep urban residences. The optimum window position was found to be the middle of the facade, where a vertical rectangular window (AR 0.3) with increased window head height significantly boosted daylight in the dining space, improving $sDA_{300/50\%}$ by 1.3% and illuminance by 32% from the base case. Adding a full-length clerestory further improved $sDA_{300/50\%}$ by 1.2% and illuminance by 14.7%. A 30% WWR vertical window on the wall opposite the bedroom door enhanced $sDA_{300/50\%}$ and illuminance by 0.3% and 9%, respectively. While 30% WWR proved optimal, larger windows with adjustable shading could further enhance daylight without causing glare in bedrooms.

The optimum results of this study can be directly used in buildings with similar contexts to improve daylight availability. In addition, this methodology of daylight inclusion in the deepest part of the residence can be used as a basis for deriving design solutions for other climatic contexts and building types. Besides the variables presented in this paper, other variables, such as external and internal shading devices, and occupant behavior related to daylight inclusion along with surrounding context, can be investigated in future studies. On the other hand, the benchmark of daylighting metrics may not apply to all types of climates. In that case, threshold values for the daylighting metrics can be investigated for different climatic contexts.

REFERENCES

[1] G. Muscogiuri et al., "The lullaby of the sun: the role of vitamin D in sleep disturbance," Sleep Medicine, Vol. 54, pp. 262–265, 2019.

[2] L. Barrea et al., "Vitamin D: A Role Also in Long COVID-19?" Nutrients, Vol. 14, No. 8, pp. 1–15, 2022.

[3] M. S. Mirdamadi, Z. S. Zomorodian, and M. Tahsildoost, "Evaluation of Occupants' Visual Perception in Day Lit Scenes: A Virtual Reality Experiment," J of Daylighting, Vol. 10, No. 1, pp. 45–59, 2023.

[4] J. A. Veitch and A. D. Galasiu, "The physiological and psychological effects of windows, daylight and view at home," National Research Council of Canada, pp. 60, 2011.

[5] A. H. Imamuddin, "A Study on Urban Housing in the Context of Dhaka, Bangladesh," Catholic University of Leuven, Belgium, 1982.

[6] A. K. M. K. Islam, "Patterns and changes of vernacular architecture in Bangladesh," M.Sc Thesis. The Royal Institute of Technology, Stockholm, 2003.

[7] F. Seraj and M. A. R. Joarder, "Clerestories for Daylighting Deep in Residential Apartments: A search for window to wall ratio for bedrooms for dining illumination", 35th PLEA Conference on Passive and Low Energy Architecture: Planning Post Carbon Cities, pp. 896–901, 2020.

[8] M. Lucchini and G. J. I Urban, "The 'deep plan' as an engine of modernity in Barcelona's residential buildings," Revista De Expresión Gráfica En La Edificación, Vol. 16, pp. 79–92, 2022.

[9] S. I. Ahsanullah and S. Van Zandt, "The impact of zoning regulations on thermal comfort in non-conditioned housing in hot, humid climates: findings from Dhaka, Bangladesh," Journal of Housing and Built Environment, Vol. 29, No. 4, pp. 677–697, 2014.

[10] BNBC, Ministry of Housing and Public Works, Bangladesh National Building Code (BNBC), Vol. 2, Part. iv, Chapter 3, pp. 2770–2773, 2020.

[11] A. Maleki and N. Dehghan, "Optimum characteristics of windows in an office building in Isfahan for save energy and preserve visual comfort," J of Daylighting, Vol. 8, No. 2, pp. 222–238, 2021.

[12] P. Pilechiha et al., "Multi-objective optimization framework for designing office windows: quality of view, daylight and energy efficiency," Applied Energy, Vol. 261, No. March, 2020.

[13] M. Sedaghatnia et al., "Energy and Daylight Optimization of Shading Devices, Window Size, and Orientation for Educational Spaces in Tehran, Iran," Journal of Architectural Engineering, Vol. 27, No. 2, pp. 1–12, 2021.

[14] K. Kalaimathy et al., "Daylight performance analysis of a residential building in a tropical climate," Energy Nexus, Vol. 11, pp. 100226, 2023.

[15] T. M. Kamel et al., "Optimizing the View Percentage, Daylight Autonomy, Sunlight Exposure, and Energy Use: Data-Driven-Based Approach for Maximum Space Utilization in Residential Building Stock in Hot Climates," Energies, Vol. 17, No. 3, pp. 684, 2024.

[16] F. Seraj, "Configuration of windows and partition walls of residential apartments to improve daylight condition in dining spaces," M. Arch Thesis, Bangladesh University of Engineering and Technology, 2018.

[17] S. S. Sonia, "Factors Affecting Apartment Buying Decision of Middle-Income People in Dhaka, Bangladesh. From the perspective of COVID-19-led economic situation," Centria University of Applied Sciences, 2020.

[18] C. D. Gomes, "Visibility effecting gender aspects in middle income group apartments in Dhaka," 10th International Space Syntax Symposium, pp. 104:1-104:15, 2015.

[19] EnergyPlus, Energy Simulation Software for Buildings, 2024.

[20] R. M. J. Bokel, The effect of window position and window size on the energy demand for heating, cooling and electric lighting, Build. Simul., pp. 117–121, 2007.

[21] J. Lee, M. Boubekri, and F. Liang, "Impact of building design parameters on daylighting metrics using an analysis, prediction, and optimization approach based on statistical learning technique," Sustainability, Vol. 11, No. 5, pp. 1474, 2019.

[22] A. M. AL-Dossary and D. D. Kim, "A study of design variables in daylight and energy performance in residential buildings under hot climates," Energies, Vol. 13, No. 21, 2020.

[23] A. Razmi, M. Rahbar, and M. Bemanian, "PCA-ANN integrated NSGA-III framework for dormitory building design optimization: Energy efficiency, daylight, and thermal comfort," Applied Energy, Vol. 305, 2022.

[24] IESNA, Approved Method: IES Spatial Daylight Autonomy (sDA) and Annual Sunlight Exposure (ASE), New York, 2012.

[25] C. F. Reinhart, J. Mardaljevic and Z. Rogers, "Dynamic daylight performance metrics for sustainable building design," LEUKOS- Journal of Illuminating Engineering Society of North America, Vol. 3, No. 1, pp. 7–31, 2006.

[26] J. Wienold and J. Christoffersen, "Evaluation methods and development of a new glare prediction model for daylight environments with the use of CCD cameras," Energy and Buildings, Vol. 38, No. 7, pp. 743–757, 2006.

[27] BS/EN 17037:2018 Daylight in buildings, BSI Standards Publication, 2019.

A Comprehensive Study on the Existing Techniques of SOC Estimation of the EVs Battery

Anik Kumar Saha[1*], Md. Anwarul Abedin[2] and Kawshik Das[3]

[1]Department of Electrical and Electronic Engineering, Islamic University, Bangladesh
[2]Department of Electrical and Electronic Engineering, Dhaka University of Engineering & Technology, Gazipur, Bangladesh
[3]Department of Electrical and Electronic Engineering, Jashore University of Science & Technology, Bangladesh

ABSTRACT

Due to the rapid development of Electric vehicles (EVs) day by day as well as the global focus on mitigating the environmental pollution, a large portion of the world is growing interest on EVs. To ensure efficient driving performance, an advanced battery management system is required, incorporating State of Charge (SOC) techniques with high accuracy. SOC is similar to fuel gauge for EVs, which indicates the remaining capacity of battery. Researchers are actively working to develop more advanced method for stable and nearly 100% SOC estimation. Although many SOC estimation techniques have been developed, a significant research gap remains in addressing the limitations related to handling non-linear behaviors, sensor errors, data dependency, and the lack of physical feedback in practical scenarios. The main aim of this article is to review the literature of existing categories and mathematical model of SOC estimation. This paper also describes each method of SOC estimation in details with present drawbacks and positive aspects as well as provides an opinion which methods are best in various conditions.

Keywords: State of Charge (SOC), Electric Vehicles, Battery Management System (BMS), Coulomb Counting Method, Kalman Filter, Deep Learning Model.

1. INTRODUCTION

Currently whole world is concerned due to the use of high number of diesels, gasoline in vehicles which produces tremendous amount of carbon dioxide, sulfur dioxide, nitrogen oxide results in global pollution and fast change of climates. The transportation industry, which is largely concentrated in urban areas, emits more than 20% of total greenhouse gas emissions [1]. Another concerning portion is that, due to the use of high amount of fossil fuels which may lack in recent future [2]. To mitigate these issues, most of the countries are focusing on Electric vehicles (EVs) which is comparatively more environment friendly, and emits very lower amount of greenhouse gas [3]. To power up EVs, generally rechargeable lithium-ion, lead acid and metal-nickel-hydride batteries are so much popular. But these batteries have few drawbacks with several advantages. One of the disadvantages is over charging and over discharging reduce battery life sometimes may damage completely [4]. To solve this problem Battery Management System (BMS) as shown in Fig. 1 is introduced, which enhances battery life. The main function of BMS is to collect raw data of voltage, current, temperature, State of Charge (SOC), State of Health (SOH), State of Power (SOP), protects from over charging, over discharging, overheating and short circuit, cell balancing, and communication with External Control Unit (ECU) [5-8].

In this study, we will only focus on SOC estimation of battery. SOC is mainly responsible to protect the battery from over charging and over discharging. It defines as the ratio of remaining charge to the nominal capacity of the battery. It generally expresses as percentage [9].

$$\text{SOC} = \frac{\text{Current Capacity (Ah)}}{\text{Total Capacity (Ah)}} \times 100\% \quad (1)$$

For Example, considering a half charged 12V 100 Ah battery,

$$\text{SOC} = \frac{50}{100} \times 100\% = 50\% \quad (2)$$

Accurate SOC estimation directly affects electric vehicles performance. Due to the parameter uncertainties, SOC estimation is not easy [10, 11]. A lot of research was already done for effectively SOC estimation. Researchers

*Corresponding author's email: anikjoy1997@gmail.com

estimated SOC through following categories: Direct measurement, Book keeping, Filter based and Data driven. Direct measurement method utilizes physical properties such as voltage and impedance [12]. But it is more applicable during stable state condition of battery as well as is not an effective method. Book keeping method [13] is far better than direct measurement method. But due to the error of initial SOC estimation, Kalman filter family [14-16] is over popular. Few researchers estimated SOC through data driven category such as Neural Network [17], Fuzzy Logic [18], Random Forest [19] etc. But in this case for higher efficiency, enormous data collection is required. This article presents every existing method of SOC estimation. Lastly, the best method for SOC estimation is determined.

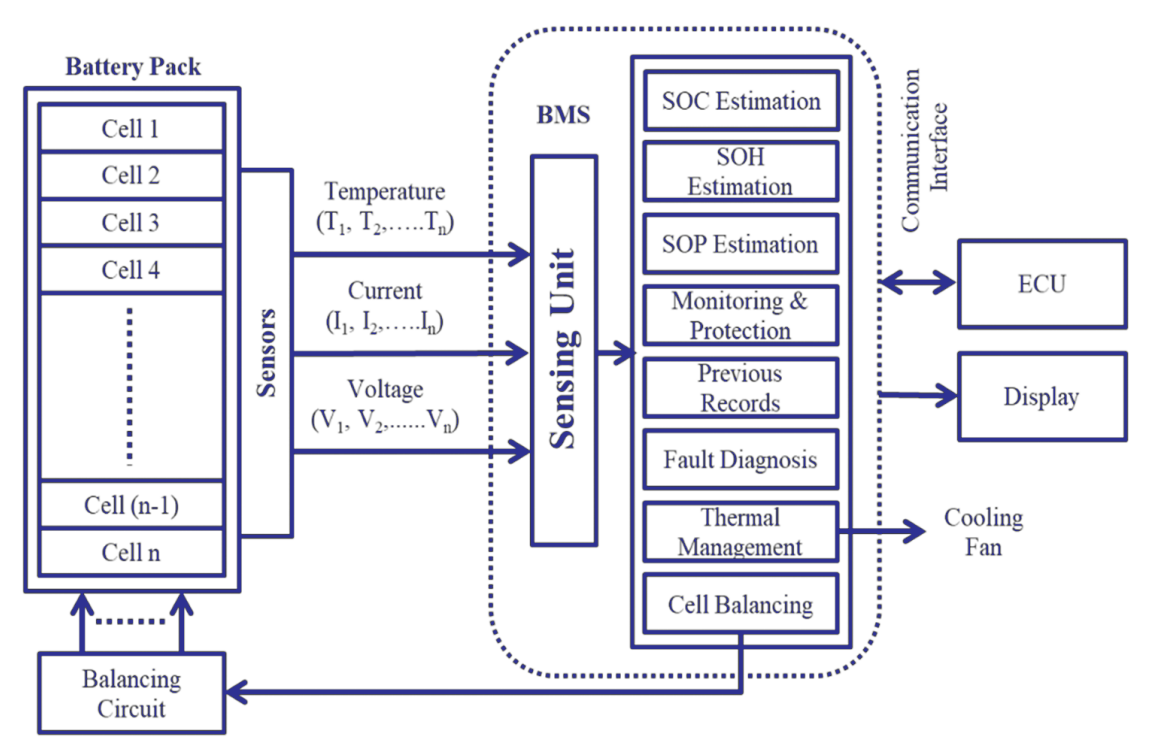

Fig. 1: Simple Block Diagram of Battery Management System

2. BATTERY MODEL

Modeling helps us to understand the battery behavior that will help to improve the system performance and increase the system efficiency. Battery can be modeled to describe the V-I Characteristics, charging status and battery's capacity. It is therefore necessary to create an exact electrical equivalent model that will help to determine the battery efficiency. There are different electrical models which will be discussed and examined along with the benefits and demerits. The mathematical relationship between the elements of Lithium-ion batteries and their V-I characteristics, state of charge (SOC), internal resistance, operating cycles, and self-discharge is depicted in a Lithium-ion battery model. The equivalent circuit model of a Lithium-ion battery is a performance model that uses one or more parallel combinations of resistance, capacitance, and other circuit components to construct an electric circuit to replicate the dynamic properties of Lithium-ion batteries. Time domain analysis is used to produce the most often utilized electrical equivalent models.

The battery model must reflect proper static and dynamic characteristics of the battery for the accurate estimation of SOC.

(a) Rint Battery Model: Rint model (Internal Resistance Model) is a basic equivalent circuit, consists of internal resistance and ideal voltage source. It is also known as 'resistance in series' model. This model design is simple and easy to implement. But it is able to capture some aspects of dynamic behavior of batteries in a limited sense and ignores hysteresis because of the absence of capacitance, which leads an inaccurate SOC estimation [20, 21].

(b) Thevenin Battery Model: Thevenin model which is the combination of a parallel R_pC_p network with Rint model in series. It is also known as Single RC model. It is able to describe the polarization effect of the battery. It has a good controlling capability of dynamic behavior [21]. This model exhibits the abrupt and gradual changes of voltage during charging and discharging.

Polarization Behavior:

$$V_{RC}(t) = V_{RC}(0)e^{\frac{-t}{R_PC_P}} + 1R_P\left(1 - e^{\frac{-t}{R_PC_P}}\right) \quad (3)$$

Dynamic Behavior:

$$V(t) = V_{OC}(SOC) - IR_0 - V_{RC}(t) \quad (4)$$

Here, the series resistance R_0 represents sudden change of resistance and parallel R_pC_p network is used to gradual voltage changes [22]. The C_p partially corrects the hysteresis behavior. Higher the value of C_p, lower the hysteresis behavior.

(c) PNGV Battery Model: It is a nonlinear equivalent circuit model, which is preferred over Thevenin model

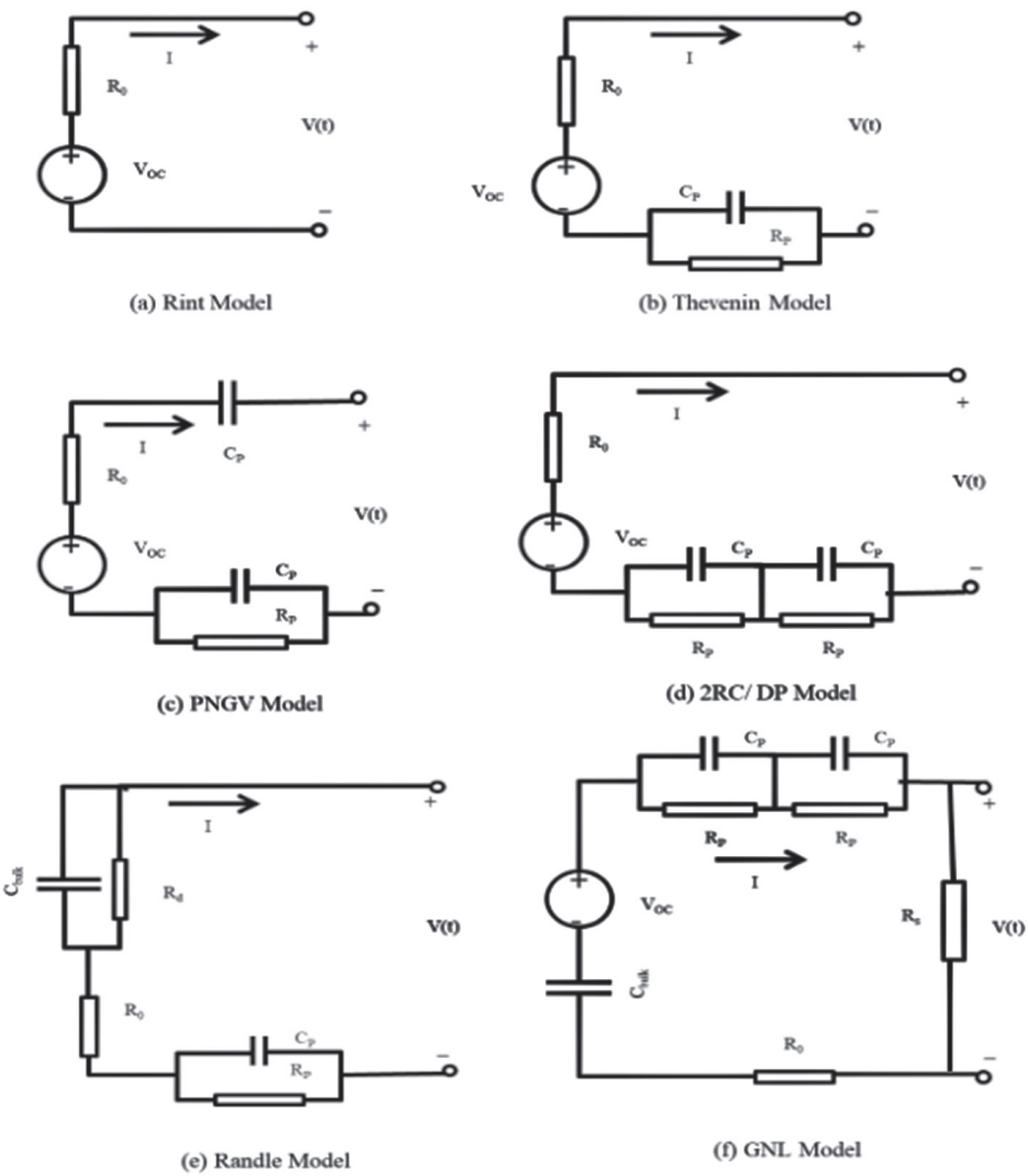

Fig. 2: Battery Model

because it represents the complex battery dynamic behavior more accurately [20, 23]. PNGV model is the combination of Thevenin model and a bulk capacitor which is shown in Fig. 4. The bulk capacitor provides long-term charge storage effects, improving SOC estimation [21]. During transient phase, PNGV model can determine voltage at various SOC. This model is also able to capture both slow and fast dynamic response, which make it more applicable for hybrid electric vehicles. Another improved version of PNGV battery model is proposed, in which an extra parallel R_PC_P network is added in series with conventional PNGV model, to describe the cell polarization more accurately. Also, this improved version of PNGV model provides more accuracy than other models [24].

(d) Dual-polarization Battery Model: Dual-polarization (DP) model is more preferred for online SOC estimation [25]. This model is the improve version of Thevenin model. An extra parallel R_PC_P network is connected in series with the first R_PC_P network as shown in Fig. 5. To capture electrochemical polarization and slow diffusion and relaxation effects as well as higher accuracy 2RC is generally used over Thevenin model [21, 26]. Because of the higher-order RC model (3RC, 4RC etc.) calculation is comparatively complex, 2RC model is used more for battery SOC estimation, despite the slightly lower precision.

(e) Randle Battery Model: The Randle battery model is a mathematical representation which primarily focuses on battery impedance and electrochemical behavior. The battery or power source isn't directly included with this equivalent circuit unlike previously mentioned battery models. The Randle model is shown in Fig. 2(e), where capacitive charge storage C_{bulk} represents SOC indicator, a high valued self-discharge resistance R_d is connected with C_{bulk} in parallel, parallel R_PC_P network indicates small time-constant electrochemical transitions, and R_0 is the internal resistance. The impedance of the battery is obtained through the Electrochemical Impedance Spectroscopy and based on the impedance value; all components of this equivalent circuit are chosen. This model was developed by targeting lead acid batteries [27]. The design of this model is pretty similar to Thevenin model but its accuracy to estimate SOC is comparatively lower. To analyze multiple transient responses, a large number of parallel R_PC_P networks can be added in series with the model [20, 28].

(f) GNL Battery Model: The GNL model contains the characteristics of Rint model, Thevenin model and PNGV model. Comparing other models, the battery SOC estimation accuracy, performance of charging and discharging process are higher of this model. But due to the high complexity in calculation and parameter selection, this model is not popular for real time SOC estimation [20, 29, 30].

3. SOC MEASUREMENT METHODS

3.1 Direct Measurement Methods

Based on the physical attributes of batteries, Direct Measurement Methods are classified as following categories-

(a) Open Circuit Voltage Method: Open Circuit Voltage (OCV) method refers to measure the potential difference across the two terminals of power source or circuit when no current flows. This method is more applicable when there is a direct relationship between open circuit voltage and SOC.

Mathematically, open circuit voltage,

$$V_{OC}(t) = a \times SOC(t) + V_0 \quad (5)$$

Where, V_0 is the lowest possible OCV, when SOC is 0% and is the slop, which represents the change of OCV with respect to SOC. This linearity is generally observed in lead acid battery [31]. But all batteries don't follow linearity such as lithium-ion batteries [32]. Also, this method gives reliable output when the battery is in stable state. To reach in equilibrium state, sometimes battery takes long time around two hours. It is impossible to wait for this long duration practically to SOC estimation [13]. Another demerit is the OCV method is heavily influence by the cell ambient temperature [33].

(b) Terminal Voltage Method: Terminal voltage method which considers internal resistance (R_{int}) during discharging. Due to the internal resistance, it differs from the OCV method [31].

Mathematically, terminal voltage,

$$V_t = V_{OC}(t) + IR_{int} \quad (6)$$

According to equation 5, OCV is proportional to SOC, similarly terminal voltage is approximately proportional to SOC. The main disadvantage is that due to sudden drop of battery voltage at the end of discharge the inaccuracy of terminal voltage is higher [34]. The output terminal voltage is also affected by temperature and to get the proper output, the system must be in equilibrium state.

(c) Impedance Method: The impedance is measured through the ratio of voltage and current, which represents the capacity of battery. This method has high accuracy to estimate SOC at the end of discharging. But it is difficult to get correct internal impedance due to its milliohm range value. The impedance parameters are not identical, this is why this method is preferred for SOC estimation [13].

(d) Electrochemical Impedance Spectroscopy Method: According to the authors [35], the main principle of this method is to excite the steady state electrochemical system by using a small amplitude AC signal and measures the impedance spectroscopy through the ratio of fluctuating voltage and current. This impedance is generally used to estimate SOC indirectly [31].

3.2 Book-Keeping Method

Book-keeping is known as coulomb counting method. Coulomb counting is one of the easiest ways to estimate SOC which is shown in Fig. 3. In this case SOC is determined through the combination of initial value of SOC and the integration of current which flows in or out of the battery [36]. The charging and discharging state of battery is defined through the direction of the current.

During charging,

$$SOC_t = SOC_0 + \left(\int_0^t \frac{\eta I_{bc}}{C_b} dt \times 100\% \right) \quad (7)$$

During discharging,

$$SOC_t = SOC_0 - \left(\int_0^t \frac{\eta I_{bd}}{C_b} dt \times 100\% \right) \quad (8)$$

To set the value of SOC_0, generally the battery should be full charged, if possible, otherwise based on starting condition SOC_0 is estimated through the test either open circuit or loaded voltage. The SOC is estimated correctly through this method for short term. In the case of long term, due to the lack of self-correction ability, this method is failed to provide proper estimation. With the number of charging and discharging cycle the error of SOC is increased. The researchers Ng et al exhibited that during 5th cycle the error is around 2.2% and this error reaches to 9% after 25th cycle [37]. This is why periodic recalibration is requires for reliable estimation of SOC. Another disadvantage is that this method isn't count the issue of battery capacity due to aging by repeated charging and discharging, internal impedance as well as self-discharge of the battery, which lead an inaccurate SOC. Some groups of researchers already tried to enhance the coulomb counting efficiency. Two groups of researchers [38, 39] considered recalibration and self-discharge correction to enhance coulomb counting which depicts through the flowchart in Fig. 4. When the battery is at open circuit ($I_b = 0$), self-discharging is occurred. Also, due to the over discharge and over charge, internal resistance is varied, which can affect correct SOC estimation. To remove this issue and for the safety of battery recalibration are introduced by them. Another researcher focused on internal resistance of battery and battery aging. To reduce the error of initial value of SOC, they combined open circuit voltage and the potential drop across the internal resistance as shown in equation 9. They also monitor battery capacity that is decreased with charging and discharging cycle.

At k-1 cycle,

$$SOC_{t\text{-}1,k} = V_{OC} \pm (I_b \times R_{b,\,k\text{-}1}) \times 100\% \quad (9)$$

During Charging,

$$SOC_{tcc,k} = \left(\left(V_{OC} - (I_{bc} \times R_{b,k-1}) \right) \times 100\% \right) + \left(\int_0^{t_{cc}} \frac{\eta_{k-1} I_{bc}}{C_{b,k-1}} dt \times 100\% \right)$$
$$= \left(\left(V_{OC} - (I_{bc} \times R_{b,k-1}) \right) \times 100\% \right) + \left(\frac{t_{cc} \eta_{k-1} I_{bc}}{C_{b,k-1}} \times 100\% \right) \quad (10)$$

Similarly at cut-off voltage during discharging,

$$SOC_{tcut\_off,k} = ((V_{OC} + (I_{bd} \times R_{b,k-1})) \times 100\%) - \left(\frac{t_{cut\_off} \eta_{k-1} I_{bd}}{C_{b,k-1}} \times 100\% \right) \quad (11)$$

At the K cycle,

Coulombic efficiency,

$$\eta_k = \frac{t_{cut\_off}\, I_{bd}}{t_{cc}\, I_{bc}} \quad (12)$$

The battery capacity for charging,

$$C_{b,k} = \frac{t_{cut\_off}\, I_{bd}}{SOC_{tcc,k}} \quad (13)$$

The battery capacity for discharging,

$$C_{b,k} = \frac{\left(t_{cut_{off}}\, I_{bd} \right)^2}{t_{cc}\, I_{bc} \times SOC_{tcut\_off,k}} = \frac{t_{cut\_off}\, I_{bd}}{SOC_{tcut\_off,k}} \quad (14)$$

The enhance coulomb counting methods are not completely capable for estimating SOC despite by removing issues of conventional coulomb counting method. These methods are unable to eliminate the sensors errors, which is one of the obstacles to correctly estimate SOC. For this reason, most of the researchers, battery management companies are currently shifting to Kalman filter family or Data driven methods.

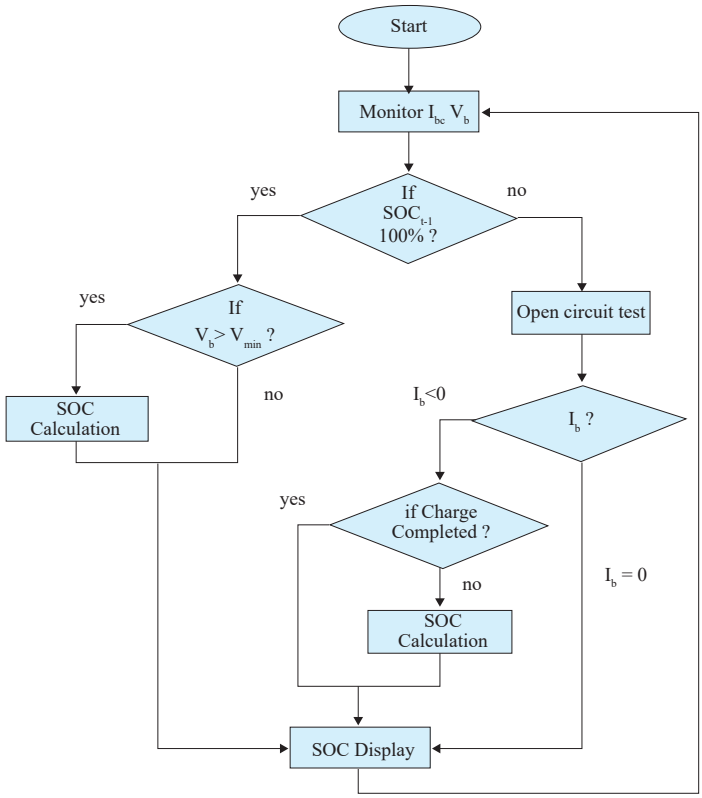

Fig. 3: Flowchart of Conventional Coulomb Counting Method

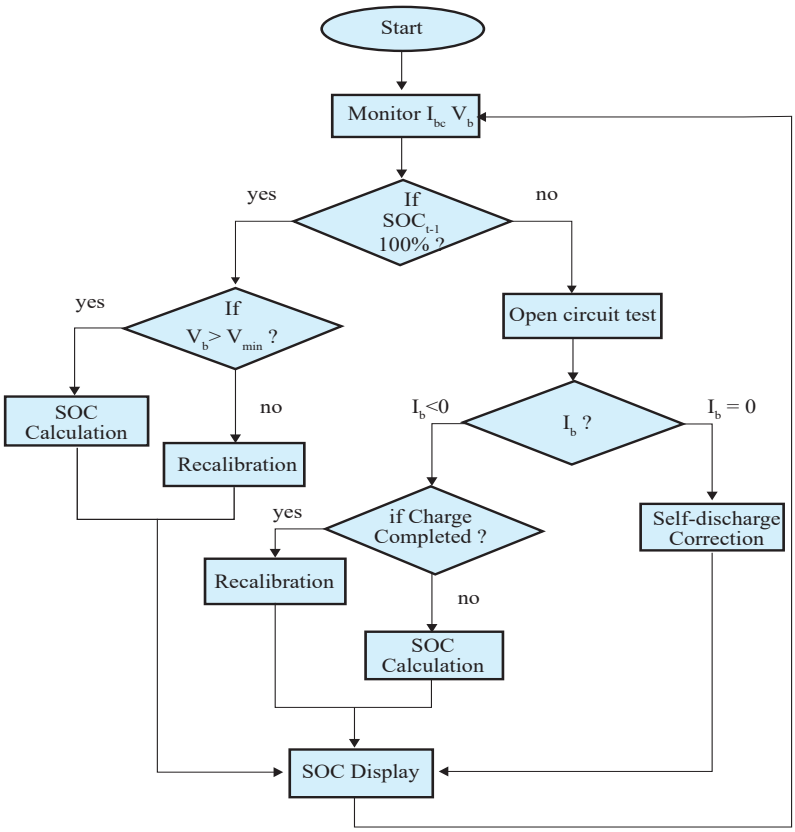

Fig. 4: Flowchart of Enhanced Coulomb Counting Method

3.3 Filter Based Methods

Filter-based methods estimate the state of the system from the perspective of noise elimination. The filter-based approach, which combines a battery model with an iterative process of closed-loop SOC estimation, has been proven to be accurate and real-time achievable due to its low complexity. Compared with the state observer method, the filter-based method the filter-based method has lower computational complexity and is easy to implement online SOC estimation. Moreover, compared to the state observer method, the filter-based method avoids the complicated proof process of the convergence performance. Therefore, the filter-based method is more suitable for the battery SOC estimation.

(a) Kalman Filter: Kalman filter is a recursive estimation technique, which was developed by Rudolf. E Kalman in the 1950s. This method offers real time correction and also has excellent capability to handle noise and work in dynamic conditions capability that makes it more suitable for SOC estimation over coulomb counting method [40]. The summary of Kalman filter algorithm for SOC estimation is given in table I.

Fig. 5 describes the SOC estimation using Kalman filter, where the temperature, current and voltage of battery pack are measured through the sensor. The estimated voltage obtained from the battery model and the difference between estimated voltage and measure voltage are the input of update step where Kalman gain is calculated [41]. As well as in this step, the SOC state is updated using state update equation.

Table I: Summary of Kalman Filter Algorithm for SOC Estimation [42, 43]

Initialization Step	$\hat{x}_0$, P_0
Measurement Step	$z_k - H\hat{x}_k^-$, $H\hat{x}_k^-$
Update Step	$K_k = P_k^- H^T (HP_k^- H^T + R)^{-1}$ $\hat{x}_k = \hat{x}_k^- + K_k(z_k - H\hat{x}_k^-)$ $P_k = P_k^-(I - HK_k)$
Prediction Step	$\hat{x}_k^- = A\hat{x}_{k-1} + Bu_{k-1} + w_k$ $P_k^- = AP_{k-1}A^T + Q$

Here, $\hat{x}_0$ = initial estimated SOC, P_0 = initial error covariance, z_k = measured voltage (Sensor Output), $H\hat{x}_k^-$ = estimated Voltage, $(z_k - H\hat{x}_k^-)$ = residual, K_k = Kalman gain, P_k^- = predicted error covariance, H = measurement matrix, R = measurement noise covariance, $\hat{x}_k^-$ = predicted SOC, P_k = updated error covariance, I = identity matrix, A = state transition matrix, $\hat{x}_{k-1}$ = previous estimated SOC, B = control matrix, u_{k-1} = previous control input (typically indicates battery current), w_k = process noise, P_{k-1} = previous error covariance, Q = process noise covariance.

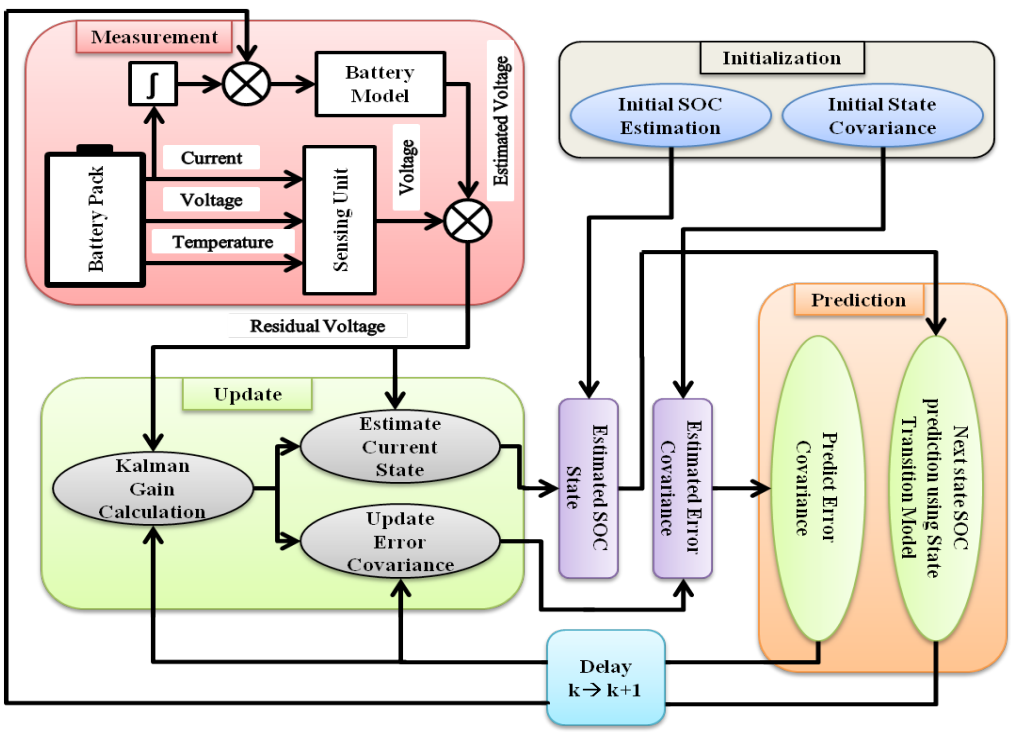

Fig. 5: Flowchart of Kalman Filter

Kalman gain is high when the measurement is more reliable otherwise the value of Kalman gain is poor. If the gain is high, SOC estimation follows the sensor value as shown in equ. 17. On the other hand, if the gain is low, SOC estimation follows the predicted value as shown in equ. 18 [44].

$$\lim_{R\to 0} K_k = \lim_{R\to 0} P_k^- H^T (HP_k^- H^T + R)^{-1} = H^{-1} \quad (15)$$

$$\lim_{P_k^-\to 0} K_k = \lim_{R\to 0} P_k^- H^T (HP_k^- H^T + R)^{-1} = 0 \quad (16)$$

$$\lim_{R\to 0} \hat{x}_k = \lim_{R\to 0} \hat{x}_k^- + K_k(z_k - H\hat{x}_k^-) = H^{-1} z_k \quad (17)$$

$$\lim_{P_k^-\to 0} \hat{x}_k = \lim_{P_k^-\to 0} \hat{x}_k^- + K_k(z_k - H\hat{x}_k^-) = \hat{x}_k^- \quad (18)$$

The last step is the prediction step, where the SOC is estimated based on the previous SOC using State Transition Model with Gaussian noise and also predicts the error covariance.

But the Kalman filter is applicable for the linear systems [45] in which all noises and errors are strictly Gaussian. In reality, the battery is a non-linear dynamic system. During the driving on high hill, downhill, the SOC of battery wouldn't be linearly changed. Even the noise of battery SOC estimation is non-Gaussian due to the temperature variation, aging effect, sensor inaccuracy etc. As a result, Kalman filter produces an inaccurate Kalman gain which generates wrong estimation of SOC [46].

(b) Extended Kalman Filter (EKF): This filter is introduced to handle the non-linearity of the system. It is the modified version of Kalman filter. Since the battery charging and discharging don't follow the linear behavior, this extended Kalman filter is required to convert into linear behavior through state space model. Then Kalman filter is applied to obtain optimal estimation.

Considering, a state space equation for SOC estimation [47],

$$x_{k+1} = f(x_k, u_k) + w_k \quad (19)$$

Measurement equation,

$$z_k = h(x_k, u_k) + v_k \quad 20)$$

To generate a linear approximation of non-linear function ($f(x_k, u_k)$), first term of Taylor series expansion is utilized [48].

$$f(x_k, u_k) \approx f(\hat{x}_k, \hat{u}_k) + \left.\frac{\partial f}{\partial x_k}\right|_{(\hat{x}k,\, \hat{u}k)} (x_k - \hat{x}_k) + \left.\frac{\partial f}{\partial u_k}\right|_{(\hat{x}k,\, \hat{u}k)} (u_k - \hat{u}_k) \quad (21)$$

where, $\left.\frac{\partial f}{\partial x_k}\right|_{(\hat{x}k,\, \hat{u}k)} = A_k =$ Jacobian of f with respect to x_k

$\left.\frac{\partial f}{\partial u_k}\right|_{(\hat{x}k,\, \hat{u}k)} = B_k =$ Jacobian of f with respect to u_k

$$h(x_k, u_k) \approx h(\hat{x}_k, \hat{u}_k) + \left.\frac{\partial h}{\partial x_k}\right|_{(\hat{x}k,\, \hat{u}k)} (x_k - \hat{x}_k) + \left.\frac{\partial h}{\partial u_k}\right|_{(\hat{x}k,\, \hat{u}k)} (u_k - \hat{u}_k) \quad (22)$$

where, $\left.\frac{\partial h}{\partial x_k}\right|_{(\hat{x}k,\, \hat{u}k)} = C_k =$ Jacobian of h with respect to x_k

$\left.\frac{\partial h}{\partial u_k}\right|_{(\hat{x}k,\, \hat{u}k)} = D_k =$ Jacobian of h with respect to u

Simplifying equation 21 and 22, we get the linear system,

$$x_{k+1} \approx f(\hat{x}_k, \hat{u}_k) + A_k(x_k - \hat{x}_k) + B_k(u_k - \hat{u}_k) + w_k \quad (23)$$

$$z_k \approx h(\hat{x}_k, \hat{u}_k) + C_k(x_k - \hat{x}_k) + D_k(u_k - \hat{u}_k) + v_k \quad (24)$$

Here, x_k = SOC value at time k, u_k = charging and discharging current, w_k = process noise, z_k = battery voltage, v_k = measurement noise, x_{k+1} = predicted SOC.

Now, through the Kalman filtering process more corrected SOC is estimated. But this extended Kalman filter sometimes fails to estimate correct SOC, when the battery plays highly nonlinear behavior.

(c) Unscented Kalman Filter (UKF): Unscented Kalman filter is considered as more advanced in Kalman filter family, which was introduced by Julier and Uhlman in 1997. Like EKF, the UKF doesn't need to consider Jacobian matrix, convert into linearized from non-linear equation, which improves the accuracy of SOC estimation. Previously, researchers used this filter to estimate SOC [30, 42]. According to their research, a small set of sigma points is denoted by x_i, which passes through the non-linear functions and a new mean and covariance are generated. These sigma points actually indicate the uncertain SOC. For example, the actual SOC is 60%, but sigma points will represent variables such as 63%, 59%, 58%, 61%, 60% etc. These points are calculated as-

$$x_i = \hat{x}_{k-1} \pm \sqrt{(n + \lambda) P_{k-1}}, \quad (25)$$

Where, i = 1, 2, ….., 2n

Predicted mean,

$$x_{k|k-1} = \sum_{i=0}^{2n} W_i^m x_i \quad (26)$$

Predicted covariance,

$$P_{k|k-1} = \sum_{i=0}^{2n} W_c^i \left(x_i - \hat{x}_{k|k-1}\right)\left(x_i - \hat{x}_{k|k-1}\right)^T + Q \quad (27)$$

Kalman gain, $K_k = P_{xy} P_y^{-1} = (\sum_{i=0}^{2n} W_c^i (x_i - x)(y_i - \hat{y}))$ $(\sum_{i=0}^{2n} W_c^i (y_i - \hat{y})(y_i - \hat{y})^T) + R)^{-1}$ (28)

Estimated SOC update,

$$\hat{x}_k = \hat{x}_{k|k-1} + K_k(y - \hat{y}_k) \quad (29)$$

Error covariance update,

$$P_k = P_{k|k-1} - K_k P_y K_k^T \quad (30)$$

Here, = previous estimated SOC, = dimension of state, = scaling parameter, = weight for the i^{th} sigma points = cross-covariance matrix, = innovation covariance matrix, = weight for covariance, Q = process noise covariance, R = measurement noise covariance.

But, the accuracy of SOC estimation through this method sometimes affected by initial values and system noise. This is why, Zhou *et. al.* [49] introduced a fading factor and an adaptive adjustment factor to minimize those issues. The modified version of covariance equations is shown below-

$$\text{Modified } P_{k|k-1} = S\sum_{i=0}^{2n} W_c^i \left(x_i - \hat{x}_{k|k-1}\right)\left(x_i - \hat{x}_{k|k-1}\right)^T + Q \quad (31)$$

$$\text{Modified } P_y^{-1} = \frac{1}{\alpha_k}\sum_{i=0}^{2n} W_c^i \,(y_i - \hat{y})(y_i - \hat{y})^T) + R \quad (32)$$

$$\text{Modified } P_{xy} = \frac{1}{\alpha_k}\sum_{i=0}^{2n} W_c^i \,(x_i - x)(y_i - \hat{y})) \quad (33)$$

$$\text{Modified } P_k = \frac{1}{\alpha_k} P_{k|k-1} - K_k P_y K_k^T \quad (34)$$

Here, S is fading factor and is adaptive adjustment factor

3.4 Data Driven Methods

(a) Neural Network: Neural network is a very popular data driven approach for its higher accuracy, capability to handle non-linearity and real time SOC estimation. It consists of three layers- Input layer, Hidden layer, and output layer. Input layer receives real time data from sensors such as voltage (v), current (I), temperature (T) that are obtained from battery. Hidden layer builds a complex relation between input data and estimated SOC. It typically contains 1 to 3 layers. The last one is output layers which represents the estimated SOC. The input layer transmits the input variables with weights and without any computational complexity. On the other hand, the other two layers are responsible for processing the data through activation function [50, 51, 52].

Researchers already used various version of neural network such Back propagation neural network (BPNN), Recurrent neural network (RNN), Convolutional neural network (CNN) to estimate SOC. For example, Shuo Li, S. L. researchers [53] were estimated SOC by using BPNN with input of voltage, current and temperature of battery. BPNN consists of two phases: forward propagation and back propagation. After generating output of SOC through forward propagation and the difference between the output value and actual SOC value, the error is used as feedback to modify the weights and biases between neurons till to get proper SOC output value. Since BPNN has the excellent capability to handle the high non-linearity, this is why another research group [54] used BPNN with duel EKF. Here they used duel EKF to get real time SOC which is justified by the BPNN. And the predicted error by BPNN is combines with the output of dual EFF to estimate correct SOC.

Another version of NN is RNN which is also used to estimate SOC. But RNN is able to remember most recent data due to the vanishing gradient issue. So, the advanced architecture of RNN, LSTM is preferred over traditional RNN, which mitigates the existing problem of RNN [55]. The architecture of LSTM consists of memory cell, and three gates- input gate, output gate, and forget gate. Input gate decides which new input variables such as voltage, current, temperature would be stored in memory cell through sigmoid and tanh activation function. Forget gate uses sigmoid activation function to erase irrelevant old data from memory cell that have less affect to estimate SOC. Based on output forget gate and input gate, memory cell is updated. Finally, the output gate determines output SOC from the memory cell [56]. S. Bockrath, A. R. researchers [57] used LSTM to estimate SOC and compare the accuracy EKF method. In their experiment, they used voltage, current and temperature of lithium-ion battery as input for LSTM NN model and the equivalent circuit model voltage is used as input for EKF model. And during dynamic operation LSTM performs better then EKF to estimate SOC. Another research team [58] used LSTM with extended input and constrained output (EI-LSTM-CO model) during SOC estimation. Due to the highly non-linear behavior of the battery, most machine learning models are failed to figure out the relationship between input variables such as voltage, current, temperature with output SOC during real time operation. This is why, these models are unable to predict SOC properly with new input data. To increase the accuracy, they also used another input, average voltage, which alters more slowly compare to real time variables. Due to use to the extension of input of LSTM, they got less SOC error compare to LSTM-RNN method with various datasets.

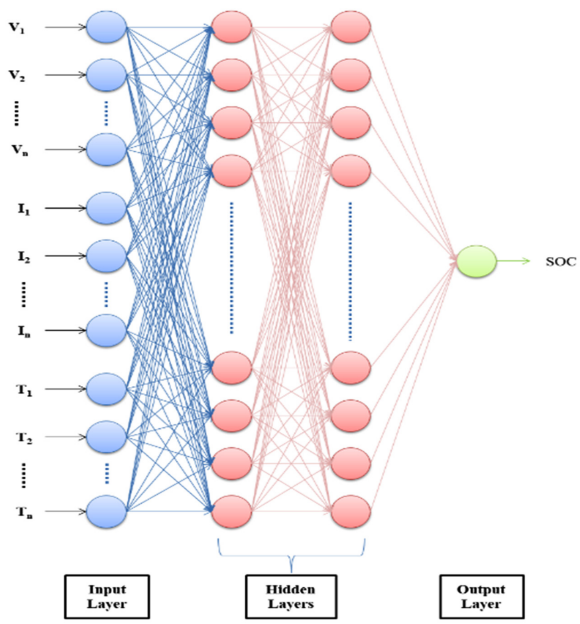

Fig. 6: The structure of Neural Network

Convolutional neural network (CNN) is also is a well-known deep learning method for SOC estimation. The architecture of a CNN consists of several layers, including image input, convolutional, activation, pooling, flatten, dense, and output layers. The image input layer takes the input and passes it into the network. In this case, the inputs are the voltage, current, and temperature of the battery. The conventional layer was used to extract low-level features (trends or sudden changes) from the input data, followed by an activation layer (ReLU) which applies non-linear function to learn complex pattern. The output of activation layer goes to pooling layer to reduce the dimensionality of the data. Then flatten layer converts the feature maps into 1D which used as input of dense layer. In dense layer, the input is multiplied with weight matrix and a bias vector is also added. Finally, the output layer which is a single neuron predicts the SOC value [59]. For checking accuracy, an author group [60] also used loss function layer to calculate the error between actual SOC and predicted SOC. In their experiment, they got a little deviation between true SOC and predicted SOC. XIANGBAO SONG, F. Y.-L. [61] combined CNN with LSTM with the voltage, current, temperature, average voltage and average current of battery as input for increasing accuracy of SOC estimation. The output SOC is fluctuated and has a deviation from the true value of SOC while using only CNN method. But combination of CNN and LSTM, the output SOC is more stable and a very low deviation (2%) from the actual SOC of battery.

(b) Support Vector Machine (SVM): SVM is preferred to estimate state of charge for solving the high non-linearity of the batteries through kernel function as well as its higher accuracy around 98%. SVM is generally used to handle vector problems and vector regression problems. Since, SOC estimation is a regression problem, this is why SVM for regression (SVR) algorithm is used. To estimates SOC through SVR a researcher group used a dataset where battery voltage, current and temperature are used as input to train the SVR model and SOC is used as ground truth to the model. The dataset is randomly divided into 10 equal-sized subsets to efficiently use of data. The basic SVR function to predict SOC is [62]-

$$f(x) = \omega^T \varphi\,(x_i) + b \tag{35}$$

where, function maps the input feature (terminal voltage, current, temperature) into a higher dimensional space to capture the batteries dynamic behavior.

To minimize the prediction error following objective function [63]-

$$\varphi[\omega, b, \varepsilon] = \frac{\|\omega\|^2}{2} + C\sum_{i=1}^{L}(\varepsilon_i^+ + \varepsilon_i^-) \tag{36}$$

The constraints are-

$$\left.\begin{aligned} & y_i - \langle \omega, \varphi\,(x_i)\rangle - b \le \epsilon + \varepsilon_i^+ \text{ (upper bound)} \\ & \langle \omega, \varphi\,(x_i)\rangle + b - y_i \le \epsilon + \varepsilon_i^- \text{(lower bound)} \\ & \varepsilon_i^+, \varepsilon_i^- \ge 0 \end{aligned}\right\} \tag{37}$$

In equation 36, first term reduces overfitting to noisy voltage, current and temperature values and second term ensures the noises or errors are minimized in SOC prediction. The constraint equations 37 represent the estimated SOC stays in an acceptable deviation () from the actual SOC reading. To handle these constraints, Lagrange multipliers are introduced.

$$\varphi[\omega, b, \varepsilon, \alpha_i] = \frac{\|\omega\|^2}{2} + C\sum_{i=1}^{L}(\varepsilon_i^+ + \varepsilon_i^-) - \sum_{i=1}^{N}\alpha_i^+ (y_i - f(x_i) - \epsilon - \varepsilon_i^+) - \sum_{i=1}^{N}\alpha\alpha_i^- (y_i - f(x_i) - \epsilon - \varepsilon_i^-) \tag{38}$$

To handle the non-linearity and establish a linear relationship, RBF kernel comes into play,

$$k(x_i, x_j) = e^{-\frac{\|x_i, x_j\|^2}{2\varphi^2}} \tag{39}$$

For computational efficiency, the dual formulation is introduced instead of primal form. In equ. 36, where the weight , bias , slack variables becomes ineffective for highly non-linear battery variables. This is why, the primal problem is transformed into dual form by applying

Lagrange multipliers which allows kernel function to replace the dot product . The final predicted SOC through SVR function is-

$$f(x) = \sum_{i=1}^{L}(\alpha_i^+ - \alpha_i^-)\, K(x_i, x) + b \qquad (40)$$

Here, x is the new input data such as voltage, current, temperature.

(c) Fuzzy Logic: Fuzzy logic was developed by Lotfi A. Zadeh in the mid-1960s. It is preferred for SOC estimation because of less mathematical difficulties, well suited for dealing with uncertainties, and provides continuity in SOC values. A simple block diagram of Fuzzy Logic Controller is shown in Fig. 07, which consists of Fuzzification, Decision Rules, Fuzzy Inference, and Defuzzification [64]. Fuzzification block takes voltage, current, temperature, required power etc. as inputs and converts into fuzzy sets (Ex: For voltage fuzzy set would be: "Low," "Medium," "High"). Every fuzzy set is connected with membership function. Decision Rules block considers as heart of the controller which consists of if-then rules that represent the relationship between crisp input and output SOC. The Fuzzy Inference is a computational unit that applies fuzzy rules to the fuzzified inputs and the Defuzzification generates the output SOC.

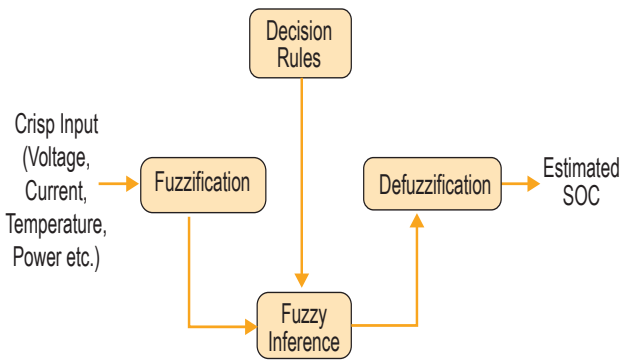

Fig. 7: Block Diagram of Fuzzy Logic Controller

A group of researchers [65] incorporated fuzzy logic into bi-directional equalization circuit to equally charging and discharging of each cell in a battery pack. They used the SOC difference of cells and modules as input of Fuzzification and also set start and stop threshold. Based on the threshold values the SOC equalization process starts and stops. Darsana Saji, P. S. [66] used fuzzy logic with coulomb counting method to enhance the accuracy of SOC estimation. In this case, the input of Fuzzification is SOC which comes from the coulomb counting method. According to their experiment, during charging only using coulomb counting the SOC error is around 13.8% and after incorporating fuzzy logic the SOC estimation error is 3%. Similarly, during discharging, combination of fuzzy logic with coulomb counting method exhibits excellent accuracy.

(d) Random Forest: Random Forest is an ensemble of decision trees. Due to easy implementation and training with small dataset compare to RNN and CNN, first prediction, and lower overfitting risk random forest is preferred for SOC estimation of EVs' batteries. According to Mohd Herwan Sulaiman, Z. M. [67] random forest follows eight steps during SOC estimation. Firstly, the real time data of voltage, current, battery temperature and ambient temperature are recorded in a single dataset with proper alignment. Secondly, around 87% of data of the dataset are used for training and remaining of them is used for testing. Then the model is configured and the training data are divided into 5 subsets. After that various number (25, 50, 75 and 100) of trees are used for trial with 5 subsets. Based on the trial performance, 25 trees random forest architecture provides more balance accuracy and this architecture is used for model training. Finally, the model is evaluated and analyzed the result. According to the Chuanjiang Li, Z. C. research group [68], random forest regression (type of random forest) provides 0.5% less error compares to BPNN to estimate SOC. Similarly, another research team [69] founds small error to estimate SOC through random forest compare to ANN. But this model is unable to exhibit high performance with large dataset.

The advantages and disadvantages of each category are shown in Table II.

4. DISCUSSION

By reviewing each existing method of SOC estimation, we are clear that SOC estimation has shifted significantly toward data-driven and hybrid methods, as conventional techniques face limitations in real-time accuracy and adaptability. Earlier methods such as Open Circuit Voltage (OCV), Coulomb Counting, and even standard Kalman Filters were useful but often struggled with non-linearity, sensor noise, and battery aging effects. This has led to a growing trend of integrating advanced filtering techniques (like EKF, UKF) with machine learning models for improved estimation accuracy.

Among the most prominent trends is the use of deep learning, particularly LSTM and CNN-LSTM hybrid models, which outperform traditional methods due to their ability to model non-linear dynamic behavior and extract time-dependent features from large datasets. The EI-LSTM-CO model, incorporating extended input and constrained output, has also gained attention for its enhanced accuracy in real-time applications.

Table II: Advantages and Disadvantages for Battery SOC Estimation Methods

Category	Method	Advantage	Disadvantage
Direct Measurement	Open Circuit Voltage	• Simple and easy implementation • Good accuracy and low cost	• Requires long time rest before measure • Gives wrong estimation during operation
	Terminal Voltage	• Simple and easy implementation • Can be used in real time operation	• Sensitive current fluctuation • Output can be affected by internal resistance
	Impedance	• Easy to implement • More accurate estimation than terminal voltage method	• Accuracy is varied with temperature and aging • Difficult to find accurate impedance due to its lower value
	Electrochemical Impedance Spectroscopy	• Higher accuracy	• Requires complex equipment and high cost • Not suitable for real time application • Requires expert knowledge
Book Keeping	Coulomb Counting	• Simple and easy for implementation • Real time monitoring is possible	• Decrease the SOC estimation accuracy due to the error of initial SOC • Self-discharge and sensor errors aren't counted
	Enhance Coulomb Counting	• Higher accuracy compared to conventional coulomb counting method	• Doesn't consider sensor errors • Calibration is required
Filter Based	Kalman Filter (KF)	• Higher accuracy due to considering sensor errors • Comparatively more suitable for real-time operation	• Not suitable for non-linear systems • Due to increase of state variable calculation time increases
	Extended Kalman Filter (EKF)	• Suitable for non-linear system • Good balance between accuracy and complexity	• Complex calculation • Due to increase of state variable calculation time increases • Unable to accurate SOC estimation for highly non-linear systems
	Unscented Kalman Filter (UKF)	• Handles highly non-linear battery system • Lower complex calculation compares to EKF	• Sometimes accuracy is affected by initial values and system noise
Data Driven	Neural Network (NN)	• Handles highly non-linear battery system • Higher accuracy and can improve overtime with more training • Doesn't need to consider electrical and physical changes of battery • Able to estimate in both offline and online	• Needs large dataset • During training high amount computational power is required
	Support Vector Machine (SVM)	• Higher accuracy • Able to work well with small to medium dataset	• Inflexible model • Greatly depends on kernel function
	Fuzzy Logic	• Doesn't require complex mathematical model • Capable to handle uncertainty	• Less accuracy • Performance depends on membership function & rule base
	Random Forest (RF)	• Good accuracy with small dataset • Lower prediction time	• Performance is lower with large dataset

Moreover, researchers are increasingly combining filter-based methods with neural networks to create hybrid models, aiming to reduce errors due to battery aging, environmental variation, and sensor inaccuracies.

Furthermore, SVM model and Random Forest model are trending as fast and efficient alternatives for small to medium datasets, especially where computational resources are limited. These models offer high prediction accuracy with less training time and are favored in embedded battery management systems.

Looking ahead, the research is trending toward hybrid approaches that fuse Enhanced Coulomb Counting techniques with neural networks or Kalman filters to adaptively learn from real-time data while correcting for accumulated errors. In our opinion, combining enhanced Coulomb Counting with CNN-LSTM or EI-LSTM-CO models presents a promising future direction. Such hybrid systems can utilize real-time SOC readings as feedback to continuously optimize the machine learning models, resulting in more robust, adaptive, and highly accurate SOC estimation frameworks suitable for commercial EV applications.

4. CONCLUSION

This article analyzed various methods of battery SOC estimation with battery models and identified higher accuracy approaches. Every researcher has tried to increase the accuracy of the SOC estimation by using various methods, both in the past and even today. Previously, SOC monitoring techniques are inefficient because of their limitations. But current techniques of SOC estimation are offering higher precision, which contributes to battery longer life as well as ensures more reliable vehicle performance. In near future, we will try to build a hybrid model that we previously mentioned, for getting more correct and stable SOC of EVs battery.

REFERENCES

[1] M. Bharathidasan, V. Indragandhi, V. Suresh, M. Jasiński and Z. Leonowicz, "A review on electric vehicle: Technologies, energy trading, and cyber security," Energy Reports, Vol. 8, pp. 9662-9685, 2022.

[2] H. Zhang, W. Na and J. Kim, "State-of-Charge Estimation of the Lithium-Ion Battery Using Neural Network Based on an Improved Thevenin Circuit Model," IEEE Transportation Electrification Conference and Expo, pp. 342-346, 2018.

[3] A. F. Challoob, N. A. B. Rahmat, V. K. A/L Ramachandaramurthy and A. J. Humaidi, "Energy and battery management systems for electrical vehicles: A comprehensive review & recommendations," Energy Exploration & Exploitation, Vol. 42, pp. 341-372, 2024.

[4] P. Kumari, A. K. Singh and N. Kumar, "Electric vehicle battery state-of-charge estimation based on optimized deep learning strategy with varying temperature at different C Rate," Journal of Engineering Research, Vol. 11, pp. 158-163, 2023.

[5] L. Lu, X. Han, J. Li, J. Hua and M. Ouyang, "A review on the key issues for lithium-ion battery management in electric vehicles," Journal of Power Sources, Vol. 226, pp. 272-288, 2013.

[6] J. Meng; M. Ricco; G. Luo; M. Swierczynski; D. Stroe and A. Stroe, "An Overview and Comparison of Online Implementable SOC Estimation Methods for Lithium-Ion Battery," IEEE Transactions on Industry Applications, Vol. 54, pp. 1583-1591, 2018.

[7] S. A. Hasib, S. U. Islam, R. K. Chakrabortty, M. Ryan, D. K. Saha, M. H. Ahamed, S. I. Moyeen, S. K. Das, M. F. Ali, M. R. Islam, Z. Tasneem and F. R. Badal, "A Comprehensive Review of Available Battery Datasets, RUL Prediction Approaches, and Advanced Battery Management," IEEE Access, Vol. 9, pp. 86166-86193, 2021.

[8] L. Buccolini; A. Ricci; C. Scavongelli, G. DeMaso-Gentile, S. Orcioni and M. Conti, "Battery Management System (BMS) simulation environment for electric vehicles," International Conference on Environment and Electrical Engineering, 2016.

[9] C. Truchot, M. Dubarry and B. Y. Liaw, "State-of-charge estimation and uncertainty for lithium-ion battery strings," Applied Energy, Vol. 119, pp. 218-227, 2014.

[10] B. D. Soyoye, I. Bhattacharya, M. V. A. Dhason and T. Banik, "State of Charge and State of Health Estimation in Electric Vehicles: Challenges, Approaches and Future Directions," Batteries, Vol. 11, pp. 1-42, 2025.

[11] B. Zine, H. Bia, A. Benmouna, M. Becherif and M. Iqbal, "Experimentally Validated Coulomb Counting Method for Battery State-of-Charge Estimation under Variable Current Profiles," Energies, Vol. 15, pp. 1-15, 2022.

[12] T. Kunatsa, H. C. Myburgh and A. D. Freitas, "A Review on State-of-Charge Estimation Methods, Energy Storage Technologies and State-of-the-Art Simulators: Recent Developments and Challenges," World Electric Vehicle Journal, Vol. 15, pp. 1-44, 2024.

[13] W.-Y. Chang, "The State of Charge Estimating Methods for Battery: A Review," International Scholarly Research Notices, Vol. 2013, pp. 1-7, 2013.

[14] P. Spagnol, S. Rossi and S. M. Savaresi, "Kalman Filter SoC estimation for Li-Ion batteries," International Conference on Control Applications, pp. 587-592, 2011.

[15] D.-W. Chung and S.-H. Yang, "SOC Estimation of Lithium-Ion Battery Based on Kalman Filter," E3S Web of Conferences, pp. 1-6, 2018.

[16] J. Guo, S. Liu and R. Zhu, "An unscented Kalman filtering method for estimation of state-of-charge of lithium-ion battery," Frontiers in Energy Research, Vol. 10, pp. 1-9, 2023.

[17] D. Wang, J. Lee, M. Kim and I. Lee, "Neural Network-Based State of Charge Estimation Method for Lithium-ion Batteries Based on Temperature," Intelligent Automation & Soft Computing, Vol. 36, No. 2, pp. 2025-2040, 2023.

[18] D. Jiani, L. Zhitao, W. Youyi and W. Changyun, "A Fuzzy Logic-based Model for Li-ion Battery with SOC and Temperature Effect," International Conference on Control & Automation, pp. 1333-1338, 2014.

[19] F. A. Tantri, D. Harjunowibowo, E. R. Dyartanti, M. Nizam, M. R. A. Putra, R. R. MP, T. H, Lim and A. Jamaluddin, "Predictive State of Charge (SoC) Modeling using Machine Learning Algorithms in Lithium-Ion NMC Batteries," Engineering Journal, Vol. 28, No. 9, pp. 1-10, 2024.

[20] N. Li, Y. Zhang, F. He, L. Zhu, X. Zhang, Y. Ma and S. Wang , " Review of lithium-ion battery state of charge estimation," Global Energy Interconnection, Vol. 4, pp. 619-630, 2021.

[21] W. Zhou, Y. Zheng, Z. Pan and Q. Lu, "Review on the Battery Model and SOC Estimation Method," Processes, Vol. 9, pp. 1-23, 2021.

[22] H. He, R. Xiong and J. Fan, " Evaluation of Lithium-Ion Battery Equivalent Circuit Models for State of Charge Estimation by an Experimental Approach," Energies, Vol. 4, pp. 582-598, 2011.

[23] C. Liu, W. Liu, L. Wang, G. Hu, L. Ma and B. Ren, " A new method of modeling and state of charge estimation of the battery," Journal of Power Sources, Vol. 320, pp. 1-12, 2016.

[24] H. Zhou, S. Wang, C. Yu, L. Xia and C. Fernandez, "Research on SOC Estimation for Lithium ion batteries Based on Improved PNGV Equivalence Model and AF-UKF Algorithm," International Journal of Electrochemical Science, Vol. 17, pp. 1-13, 2022.

[25] H. Bouchareb, K. Saqli, N.K. M'sirdi, M. O. Bentaie and A. Naamane, "Sliding Mode Observer Design for Battery State of Charge estimation," International Conference on Renewable Energies for Developing Countries, pp. 1-5, 2020.

[26] B. V. Rajanna and M. K. Kumar, "Comparison of one and two time constant models for lithium ion battery," International Journal of Electrical and Computer Engineering, Vol. 10, No. 1, pp. 670-680, 2020.

[27] S. Nejad, D.T. Gladwin and D.A. Stone, "A systematic review of lumped-parameter equivalent circuit models for real-time estimation of lithium-ion battery states," Journal of Power Sources, Vol. 316, pp. 183-196, 2016.

[28] Q. Chen, J. Jiang, H. Ruan and C. Zhang, "A New Double Sliding Mode Observer for EV Lithium Battery SOC Estimation," Mathematical Problems in Engineering, Vol. 2016, pp. 1-9, 2016.

[29] W. Kai, F. Xiao, P. Jinbo, R. Jun, D. Chongxiong and L. Liwei, " State of Charge (SOC) Estimation of Lithium-ion Battery Based on Adaptive Square Root Unscented Kalman Filter," International Journal of Electrochemical Science, Vol. 15, pp. 9499-9516, 2020.

[30] L. Wang, F. Wang, L. Xu, W. Li, J. Tang and Y. Wang, "SOC estimation of lead–carbon battery based on GAMIUKF algorithm," Scientific Reports, pp. 1-14, 2024.

[31] M. Danko, J. Adamec, M. Taraba and P. Drgona, "Overview of batteries State of Charge estimation methods," International Scientific Conference on Sustainable, Modern and Safe Transport, pp. 186-192, 2019.

[32] M. Coleman, C. K. Lee, C. Zhu and W. G. Hurley, "State-of-Charge Determination From EMF Voltage Estimation: Using Impedance, Terminal Voltage, and Current for Lead-Acid and Lithium-Ion Batteries," IEEE Transactions on Industrial Electronics, Vol. 54, No. 5, pp. 2550-2557, 2007.

[33] S. Jeon, J.-J. Yun and S. Bae, "Comparative Study on the Battery State-of-Charge Estimation Method," Indian Journal of Science and Technology, Vol. 8, pp. 1-6, 2015.

[34] S. R. C. Geda and M. Sharam, "An overview of SOC estimation in Li-ion batteries with direct measurement methods and coulomb counting," International Journal of Engineering Applied Sciences and Technology, Vol. 7, pp. 237-242, 2022.

[35] Y. Liu, L. Wang, D. Li and K. Wang, "State-of-health estimation of lithium-ion batteries based on electrochemical impedance spectroscopy: a review," Protection and Control of Modern Power Systems, pp. 1-17, 2023.

[36] K. C. Ndeche and S. O. Ezeonu, "Implementation of Coulomb Counting Method for Estimating the State of Charge of Lithium-Ion Battery," Physical Science International Journal, Vol. 25, pp. 1-8, 2021.

[37] K. S. Ng, C.-S. Moo, Yi-Ping Chen and Y.-C. Hsieh, "Enhanced coulomb counting method for estimating state-of-charge and state-of-health of lithium-ion batteries," Applied Energy, Vol. 86, pp. 1506–1511, 2009.

[38] I. Baccouche, A. Mlayah, S. Jemmali, B. Manai and N. E. B. Amara, "Implementation of a Coulomb counting algorithm for SOC estimation of Li-Ion battery for multimedia applications," International Multi-Conference on Systems, Signals & Devices, pp. 1-6, 2015.

[39] J. LEE and J. Won, "Enhanced Coulomb Counting Method for SoC and SoH Estimation Based on Coulombic Efficiency," IEEE Access, Vol. 11, pp. 15449-15459, 2023.

[40] G. Fathoni, S. A. Widayat, P. A. Topan, A. Jalil, A. I. Cahyadi and O. Wahyunggoro, "Comparison of State-of-Charge (SOC) estimation performance based on three popular methods: Coulomb counting, open circuit voltage, and Kalman filter," International Conference on Automation, Cognitive Science, Optics, Micro Electro-Mechanical System, and Information Technology, pp. 70-74, 2018.

[41] M. U. Ali, A. Zafar, S. H. Nengroo, S. Hussain, M. J. Alvi and H. Kim, "Towards a Smarter Battery Management System for Electric Vehicle Applications: A Critical Review of Lithium-Ion Battery State of Charge Estimation," Energies, Vol. 12, pp. 1-33, 2019.

[42] P. Shrivastava, T. K. Soon, M. Y. I. B. Idris and S. Mekhilef, "Overview of model-based online state-of-charge estimation using Kalman filter family for lithium-ion batteries," Renewable and Sustainable Energy Reviews, Vol. 113, pp. 1-23, 2019.

[43] Z. Zhou and C. Zhang, "An Extended Kalman Filter Design for State-of-Charge Estimation Based on Variational Approach," **Batteries,** Vol. 9, No. 12, 2023.

[44] J. Yun, Y. Choi, J. Lee, S. Choi and C. Shin, "State-of-Charge Estimation Method for Lithium-Ion Batteries using Extended Kalman Filter with Adaptive Battery Parameters," IEEE Access, Vol. 11, pp. 90901-90915, 2023.

[45] A. Khalid, S. A. R. Kashif, N. U. Ain, M. Awais, M. A. Smieee, J. E. M. Carreño, J. C. Vasquez, J. M. Guerrero and B. Khan, "Comparison of Kalman Filters for State Estimation Based on Computational Complexity of Li-Ion Cells," Energies, Vol. 16, pp. 1-20, 2023.

[46] M. A. Akram, P. Liu, M. O. Tahir, W. Ali and Y. Wang, "A State Optimization Model Based on Kalman Filtering and Robust Estimation Theory for Fusion of Multi-Source Information in Highly Non-linear Systems," Sensors, Vol. 19, pp. 1-22, 2019.

[47] R. Zhang and H. Zhang, "Extended Kalman Filter-Based SOC Estimation for Lithium Battery Packs," International Conference on Energy Materials and Environment Engineering, pp. 1-4, 2023.

[48] N. A. Windarko, J. Choi and G.-B. Chung, "SOC Estimation of LiPB Batteries using Extended Kalman Filter based on high accuracy electrical model," International Conference on Power Electronics, pp. 2015-2022, 2011.

[49] H. Zhou, S. Wang, C. Yu, L. Xia and C. Fernandez, "Research on SOC estimation for lithium ion batteries based on improved PNGV equivalence model and AF-UKF algorithm," International Journal of Electrochemical Science, Vol. 17, pp. 1-14, 2022.

[50] W. He, N. Williard, C. Chen and M. Pecht, "State of charge estimation for Li-ion batteries using neural network modeling and unscented Kalman filter-based error cancellation," International Journal of Electrical Power & Energy Systems, Vol. 62, pp. 783-791, 2014.

[51] B.-A. Enache and E. Diaconescu, "Estimating a battery SoC using neural networks," International Symposium on Fundamentals of Electrical Engineering, pp. 1-7, 2014.

[52] M. Ismail, R. Dlyma, A. Elrakaybi, R. Ahmed and S. Habibi, "Battery State of Charge Estimation using Artificial Neural Network," IEEE Transportation Electrification Conference and Expo, pp. 342-349, 2017.

[53] S. Li, S. Li, H. Zhao and Y. An, "Design and implementation of state-of-charge estimation based on back-propagation neural network for smart uninterruptible power system," International Journal of Distributed Sensor Networks, Vol. 15, pp. 1-9, 2019.

[54] L. Xing, L. Ling and X. Wu, "Lithium-ion battery state-of-charge estimation based on a dual extended Kalman filter and BPNN correction," Connection Science, Vol. 34, No. 1, pp. 2332-2363, 2022.

[55] S. Tao, B. Jiang, X. Wei and H. Dai, "A Systematic and Comparative Study of Distinct Recurrent Neural Networks for Lithium-Ion Battery State-of-Charge Estimation in Electric Vehicles," Energies, Vol. 16, pp. 1-17, 2023.

[56] X. Chai, S. Li and F. Liang, "A novel battery SOC estimation method based on random search optimized LSTM neural network," Energy, Vol. 306, pp. 1-13, 2024.

[57] S. Bockrath, A. Rosskopf, S. Koffel, S. Waldhör, K. Srivastava and V.R.H. Lorentz, "State of Charge Estimation using Recurrent Neural Networks with Long Short-Term Memory for Lithium-Ion Batteries," 45th Annual Conference of the IEEE Industrial Electronics Society, pp. 2507-2511, 2019.

[58] J. Chen, Y. Zhang, J. Wu, W. Cheng and Q. Zhu, "SOC estimation for lithium-ion battery using the LSTM-RNN with extended input and constrained output," Energy, pp. 1-14, 2023.

[59] Z. Cui, L. Wang, Q. Li and K. Wang, "A comprehensive review on the state of charge estimation for lithium-ion battery based on neural network," International Journal of Energy Research, Vol. 46, pp. 5423-5440, 2021.

[60] H. S. Bhattacharyya, A. Yadav, A. B. Choudhury and C. K. Chanda, "Convolution Neural Network-Based SOC Estimation of Li-ion Battery in EV Applications," International Conference on Electrical, Electronics, Communication, Computer Technologies and Optimization Techniques, pp. 587-592, 2021.

[61] X. Song, F. Yang, D. Wang and K.-L. Tsui, "Combined CNN-LSTM Network for State-of-Charge Estimation of Lithium-Ion Batteries," IEEE Access, Vol. 7, pp. 88894-88902, 2019.

[62] K. Wei, J. Wu, W. Ma and H. Li, "State of charge prediction for UAVs based on support vector machine," International Symposium on Test Automation and Instrumentation, pp. 9133-9136, 2019.

[63] J. C. Á. Antón, P. J. G. Nieto, F. J. d. C. Juez, F. S. Lasheras, M. G. Vega and M. N. R. Gutiérrez, "Battery state-of-charge estimator using the SVM technique," Applied Mathematical Modelling, Vol. 37, pp. 6244-6253, 2013.

[64] N. Feng, T. Ma and C. Chen, "Fuzzy energy management strategy for hybrid electric vehicles on battery stateofcharge estimation by particle filter," SN Applied Sciences, Vol. 4, No. 256, pp. 1-11, 2022.

[65] Y. Ma, P. Duan, Y. Sun and H. Chen, "Equalization of Lithium-ion Battery Pack based on Fuzzy Logic Control in Electric Vehicle," IEEE Transactions on Industrial Electronics, Vol. 65, pp. 6762-6771, 2018.

[66] D. Saji, P. S. Babu and K Ilango, "SOC Estimation of Lithium Ion Battery using Combined Coulomb Counting and Fuzzy Logic Method," International Conference on Recent Trends on Electronics, Information, Communication & Technology, pp. 948-952, 2019.

[67] M. H. Sulaiman and Z. Mustaffa, "State of charge estimation for electric vehicles using random forest," Green Energy and Intelligent Transportation, Vol. 3, pp. 1-10, 2024.

[68] C. Li, Z. Chen, J. Cui, Y. Wang and F. Zou, "The Lithium-ion Battery State-of-Charge Estimation using Random Forest Regression," Prognostics and System Health Management Conference, pp. 336-339, 2014.

[69] A. Johnson; N. A. Varghese, R. R. Thomas, S. Mathews and R. A. Koshy, "Random Forest Regressor Based SOC Estimation of Li-Ion Battery for Electric Vehicle Applications," International Conference on Power Electronics, Smart Grid, and Renewable Energy, pp. 1-8, 2023.

First-Principles and Numerical Investigation of a High-Efficiency Lead-Free $Rb_2NaGaBr_6$-Based Perovskite Solar Cell

Md. Jahidul Islam[1]*and Mahbub Alam Rabin[2]

[1]Department of Materials and Metallurgical Engineering, Dhaka University of Engineering & Technology, Gazipur, Bangladesh
[2]Department of Materials and Metallurgical Engineering Bangladesh University of Engineering and Technology, Bangladesh

ABSTRACT

Lead-free double perovskites have emerged as promising alternatives to conventional lead-based perovskite solar cells (PSCs), offering improved environmental safety and long-term stability. In this study, we explore the photovoltaic potential of a novel, non-toxic double perovskite material, $Rb_2NaGaBr_6$, using a Density Functional Theory and utilize it to design and simulate a new PCS by using SCAPS-1D simulation approach. DFT analysis reveals a direct bandgap of 1.56 eV, low effective carrier masses, and higher carrier mobility, indicating excellent optoelectronic properties. Based on these DFT explored properties, a planar solar cell architecture—Glass/FTO/TiO_2/$Rb_2NaGaBr_6$/Cu_2O/Au was modeled and simulated in SCAPS-1D. The device showed favorable energy band alignment and charge extraction characteristics. Upon optimizing the thicknesses and absorption layer defect density, the structure achieved a power conversion efficiency (PCE) of 27.004%, with Voc = 1.274 V, Jsc = 25.20 mA/cm², and FF = 88.08%. These findings establish $Rb_2NaGaBr_6$ as a viable and efficient candidate for next-generation lead-free photovoltaic technologies.

1. INTRODUCTION

In recent years, the global energy sector has experienced an increased emphasis on sustainable and renewable energy sources. Among these, solar energy stands out due to its abundant availability and potential to meet the world's energy demands. It has been reported that the sun provides over 1500 exawatt-hours of energy annually, which is more than 200 times the total energy reserve of all fossil fuels combined [1]. Harnessing 0.3% of this energy could significantly reduce reliance on non-renewable resources and lower the environmental footprint of power generation [1]. Traditional solar cells, including silicon-based or gallium arsenide (GaAs) technologies, have achieved considerable efficiency over the years. However, their production involves complex processes, high costs, and in some cases, the use of scarce or toxic materials [2]. To address these limitations, researchers have shifted their focus toward alternative photovoltaic (PV) technologies. Among them, PSCs have emerged as a transformative solution due to their excellent optoelectronic properties and low-cost fabrication potential. These attributes have driven significant progress in PSCs, which have rapidly evolved from an initial 3.8% efficiency to over 26% in single-junction cells and 34% in perovskite-silicon tandem configurations [3][4][5]. This rapid development is largely attributed to the favorable properties of halide perovskite materials, such as high absorption coefficient, long charge carrier diffusion lengths, low exciton binding energy, and tunable bandgap. Different lead-based perovskites like $MAPbI_3$ have a PCE of 22.4% [6], $CsPbI_3$ with a PCE of 21.15% [7], $FAMAPbI_3$ with a PCE of 23.32 % [8] show excellent efficiency. However, most of the high-performing perovskites contain lead (Pb), which poses significant environmental and health hazards. Lead is known to be highly toxic and water-soluble, making its leakage from solar panels a serious concern for both ecosystems and human safety [9].

In the pursuit of sustainable and non-toxic alternatives to lead-based perovskites, researchers have increasingly turned their attention to a new class of materials known as lead-free double perovskites. These compounds, typically represented by the general formula $A_2M^+M^{3+}X_6$, replace lead with a combination of monovalent and trivalent cations, offering a promising pathway toward safer and more stable solar cell technologies. Among them, materials such as Cs_2AgBiI_6 have already demonstrated encouraging results, achieving PCE of up to 21.59% while maintaining thermal and chemical stability [10].

*Corresponding author's email: jahidulislam@duet.ac.bd

Others, like $Cs_2AgGaBr_6$, have shown even greater theoretical promise, with simulated PCEs reaching as high as 32.57% under optimized conditions [11]. Yet, despite these advances, the search continues for a material that not only delivers high efficiency but also leverages abundant, non-toxic elements. It is within this context that we explore $Rb_2NaGaBr_6$, a relatively unstudied double perovskite composed of rubidium (Rb^+), sodium (Na^+), gallium (Ga^{3+}), and bromine (Br^-). Each of these elements is earth-abundant and environmentally benign, making $Rb_2NaGaBr_6$ a strong candidate for future green photovoltaic technologies. Beyond the absorber layer itself, the performance of a perovskite solar cell also hinges on the materials used to transport charge carriers. The electron transport material (ETM) and hole transport material (HTM) play a crucial role in guiding the photogenerated electrons and holes toward their respective electrodes with minimal resistance and recombination. To serve as an effective window layer, the ETM must be an n-type semiconductor with a wide bandgap, allowing most incident light to reach the absorber beneath it. These layers work in tandem with the perovskite to ensure that the flow of charge is as smooth and efficient as possible, forming the backbone of a high-performing solar cell. It is important to note that a recent study investigated a structurally similar perovskite, $Rb_2LiInBr_6$, using DFT and SCAPS-1D simulations, and achieved a notable PCE of 26.90% with TiO_2 and Cu_2O as transport layers, optimizing both defect density and absorber thickness to reach a configuration with Voc = 1.277 V, Jsc = 25.06 mA/cm², and FF = 83.96% [12]. While that work validated the photovoltaic viability of Rb-based double perovskites, the material chemistry and transport layer strategy differed from ours.

Our research utilizes Density Functional Theory (DFT) to explore the electronic structure, bandgap, electron affinity, relative dielectric constant and carrier mobility of $Rb_2NaGaBr_6$. The DFT analysis reveals that the material has a direct bandgap of approximately 1.56 eV, which lies within the optimal range for single-junction solar cells. To evaluate the photovoltaic performance, we employed SCAPS-1D simulations using a typical layered architecture: FTO/TiO_2/$Rb_2NaGaBr_6$/Cu_2O/Au. The selection of TiO_2 as the ETM is based on its high transparency, wide bandgap, and good electron mobility [1]. Cu_2O is chosen as the HTM due to its suitable energy band alignment and strong hole conductivity.

Furthermore, the impact of absorber layer thickness and bulk defect concentration was systematically analyzed to identify the optimal conditions for peak device performance. The simulations revealed that an absorber thickness of 800 nm delivers the most favorable outcome. Under this configuration, the solar cell achieved a maximum PCE of 27.004%, accompanied by a short-circuit current density (Jsc) of 25.20 mA/cm², an open-circuit voltage (Voc) of 1.274 V, and a fill factor (FF) of 84.08%. These findings are consistent with prior studies, where optimizing layer thickness significantly enhanced the device output [5], [6]. The growing interest in lead-free and stable perovskite materials necessitate the discovery of new candidates that can offer better performance without compromising on safety. $Rb_2NaGaBr_6$ shows promise as a sustainable and efficient light absorber in next-generation solar cells. This study contributes to the ongoing efforts to develop viable alternatives to lead-based perovskites by presenting simulation-backed evidence of high efficiency and stable performance in a carefully designed device structure. In summary, this work introduces $Rb_2NaGaBr_6$ as a potential material for efficient and environmentally friendly perovskite solar cells. Through a combination of DFT-based electronic structure calculations and SCAPS-1D numerical simulations, we demonstrate its applicability and advantages in a practical solar cell configuration. The insights gained from this study may guide future experimental efforts in the development and fabrication of high-performance, lead-free perovskite photovoltaics.

2. METHODOLOGY

This research integrates first-principles quantum mechanical modeling and device-level numerical simulation to evaluate the suitability and performance of a novel lead-free double perovskite material, $Rb_2NaGaBr_6$, for photovoltaic applications. The investigation involves optoelectronic calculations using DFT and solar cell modeling using SCAPS-1D.

2.1 Device Structure

Fig. 1 illustrates the schematic structure of the proposed planar solar cell, comprising the following layered configuration: Glass/FTO/TiO_2/$Rb_2NaGaBr_6$/Cu_2O/Au. The glass substrate serves as the mechanical support for the entire device. Fluorine-doped tin oxide (FTO) functions as a transparent conducting front electrode, allowing incident light to reach the active layer while simultaneously acting as the negative contact for electron collection. Titanium dioxide (TiO_2), with its wide bandgap and high electron mobility, serves as the electron transport layer (ETL) and extracts photo-generated electrons from the absorber layer. The active layer, $Rb_2NaGaBr_6$, is a newly explored,

non-toxic double perovskite material with a theoretically predicted direct bandgap of approximately 1.56 eV. This absorber is expected to provide strong visible light absorption and efficient charge carrier transport. Cuprous oxide (Cu_2O) is used as the hole transport layer (HTL) due to its excellent hole mobility, favorable valence band alignment, and chemical stability. Gold (Au) is selected as the back electrode, providing an efficient interface for hole collection and ensuring high conductivity. Fig.2. illustrates the energy band alignment of the proposed photovoltaic system.

2.2 First-Principles DFT Simulation

First-principles calculations based on DFT were performed using the Vienna Ab Initio Simulation Package (VASP). The Projector Augmented-Wave (PAW) method was employed to represent the interaction between the valence electrons and the ionic cores. Exchange-correlation energy was treated within the Generalized Gradient Approximation (GGA), utilizing the revised Perdew–Burke–Ernzerhof (PBEsol) functional, which is specifically optimized for solid-state systems.

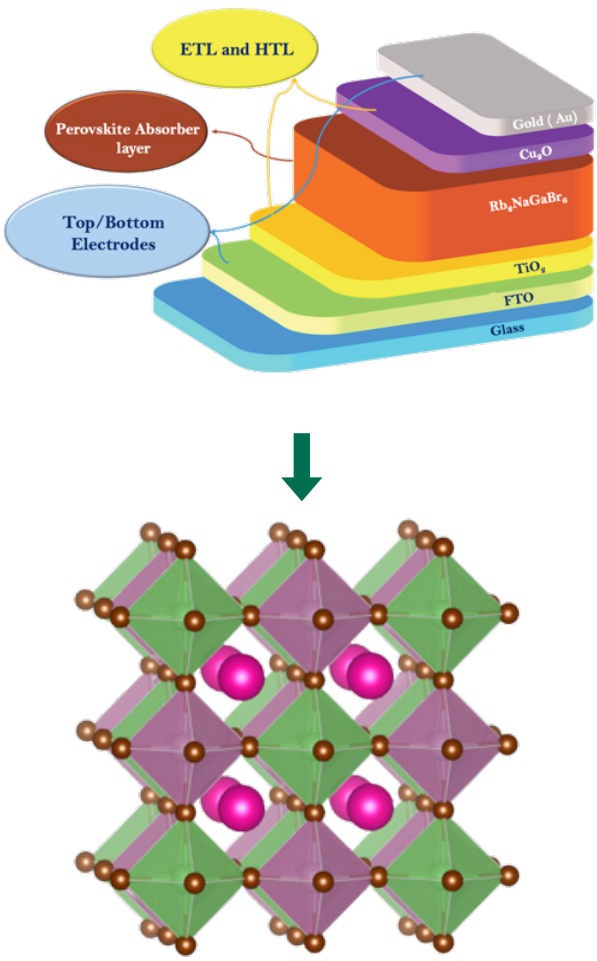

Fig. 1: Structural Architecture of the Proposed Device

The calculations were carried out using a plane-wave energy cutoff of 520 eV. A Monkhorst–Pack k-point mesh of 9×9×9 was used for structural relaxation, which was refined to 11×11×11 for the calculation of the electronic band structure and density of states. Geometry optimization was considered converged when the total energy difference between successive steps was less than 10^{-8} eV and the residual forces on each atom were less than 0.001 eV/Å. In this study, the electronic band structure of $Rb_2NaGaBr_6$ was calculated using the GGA within the PBEsol functional. A line-mode band structure calculation was carried out by sampling the electronic eigenvalues along the standard high-symmetry directions in the first Brillouin zone, specifically following the path Γ → X → W → K → Γ → L. To ensure sufficient resolution of the dispersion features, 30 k-points were interpolated between each pair of high-symmetry points.

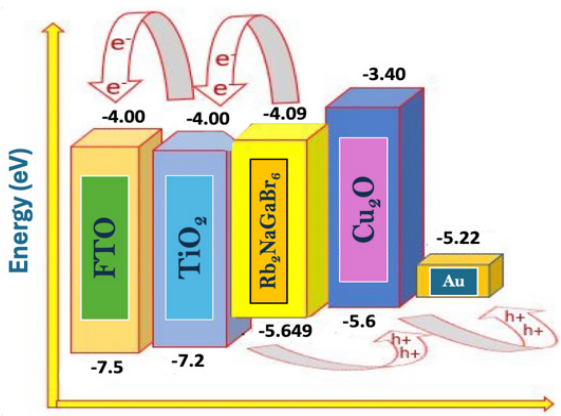

Fig. 2: Energy Band Alignment of the Proposed Device

The effective masses of charge carriers were calculated by performing second-order polynomial fitting to the energy–momentum (E–k) dispersion near the conduction band minimum (CBM) and valence band maximum (VBM), using the expression:

$$m^* = \hbar^2 \left(\frac{d^2E}{dk^2} \right)^{-1} \quad (1)$$

The carrier mobility was estimated from the effective mass using the relaxation time approximation as follows:

$$\mu = \frac{e\tau}{m^*} \quad (2)$$

Where, τ is the scattering time, assumed to be 2×10^{-14} s for semiconductors [13]. Additionally, the effective density of states for the conduction and valence bands were calculated using the relations:

$$N_C = 2 \left(\frac{2\pi m_e^* K_B T}{h^2} \right)^{3/2} \quad (3)$$

$$N_v = 2\left(\frac{2\pi m_h^* K_B T}{h^2}\right)^{3/2} \quad (4)$$

The extracted parameters, such as bandgap, effective masses, mobilities, effective density of states and dielectric permittivity, were incorporated into the SCAPS-1D simulation environment to assess device-level performance.

2.3 Numerical Simulation Using SCAPS-1D

The SCAPS-1D software, developed at the University of Gent, was used to simulate the performance of the full solar cell structure. The program solves the fundamental set of equations governing the operation of a semiconductor device, which include Poisson's equation and the continuity equations for electrons and holes under steady-state illumination conditions. Poisson's equation is expressed as:

$$\frac{d}{dx}\left(\varepsilon\frac{d\phi}{dx}\right) = -q(p - n + N_D^+ - N_A^-) \quad (5)$$

The electron and hole continuity equations are:

$$\frac{dn}{dt} = \frac{1}{q}\frac{dJ_n}{dx} + G_n - R_n \quad (6)$$

$$\frac{dp}{dt} = -\frac{1}{q}\frac{dJ_p}{dx} + G_p - R_p \quad (7)$$

Here, is the electrostatic potential, ε is the dielectric permittivity, q is the elementary charge, n and p are the electron and hole concentrations, are the current densities, and G and R represent generation and recombination rates, respectively. Shockley–Read–Hall recombination was used to model trap-assisted recombination in the absorber.

Table I presents the key physical and electronic parameters of each layer in the Glass/FTO/TiO_2/$Rb_2NaGaBr_6$/Cu_2O/Au device structure. These values, obtained from DFT calculations and validated literature were used in SCAPS-1D to simulate charge transport, recombination and band alignment behavior.

The simulations were conducted under standard AM 1.5G illumination with an incident power of 1000 W/m² and at a temperature of 300 K. The thicknesses of the FTO and metal contact layers were set based on experimentally common values, while the absorber layer thickness was varied between 200 nm and 1300 nm. Similarly, the bulk defect density in the absorber was varied over the range of 10^8 to 10^{19} cm^{-3} to evaluate its impact on photovoltaic parameters such as Voc, Jsc, FF, and PCE.

Table I: Material Parameters Used in SCAPS-1D Simulation

Parameters	FTO [14]	TiO_2 [15]	$Rb_2NaGaBr_6$	Cu_2O [15]
W (nm)	50	100	80	200
E_G (eV)	3.5	3.2	1.559	2.17
X (eV)	4.00	4.20	4.09	3.20
εR	9.00	9.00	10.21	7.11
N_C (cm^{-3})	2.2×10^{18}	1.0×10^{19}	1.768×10^{18}	2.02×10^{19}
N_V (cm^{-3})	1.8×10^{19}	1.0×10^{19}	5.104×10^{18}	1.1×10^{19}
V_{TE} (cm/s)	1×10^7	1×10^7	1×10^7	1×10^7
V_{TP} (cm/s)	1×10^7	1×10^7	1×10^7	1×10^7
μ_n (cm^2/Vs)	20	20	100	200
μ_p (cm^2/Vs)	10	10	45	80
N_D (cm^{-3})	2×10^{19}	2×10^{19}	2×10^{19}	0
N_A (cm^{-3})	1×10^{15}	0	1×10^{19}	2×10^{19}
N_T (cm^{-3})	1×10^{15}	1×10^{15}	1×10^{13}	1×10^{14}

3. RESULTS AND DISCUSSION

3.1 ETL Layer Optimization

To evaluate the impact of ETL thickness on the photovoltaic performance of the proposed solar cell, a systematic simulation was conducted by varying the thickness of the TiO_2 (ETL) in the range of 0.025 µm to 0.3 µm, in increments of 0.025 µm. During this analysis, the thicknesses of the absorber ($Rb_2NaGaBr_6$) and the HTL (Cu_2O) were kept constant at 0.3 µm and 0.2 µm, respectively, to isolate the effect of the ETL. Key photovoltaic parameters—namely Voc, Jsc, FF, and PCE—were extracted for each configuration.

The simulation results reveal that variations in the TiO_2 layer thickness exert a minimal influence on the overall device performance. Specifically, the PCE and FF remain nearly unchanged across the examined range, shown in Fig. 3, indicating that carrier extraction from the conduction band of the absorber to the ETL is not significantly hindered by thinner ETL layers. This is likely due to TiO_2's high electron mobility and wide bandgap, which ensure efficient electron transport even at reduced thicknesses. As a result, a minimal ETL thickness of 0.03 µm was found sufficient to maintain high performance while also benefiting from material and cost savings in practical implementations. Therefore, this value is selected as the optimal ETL thickness for the proposed device configuration.

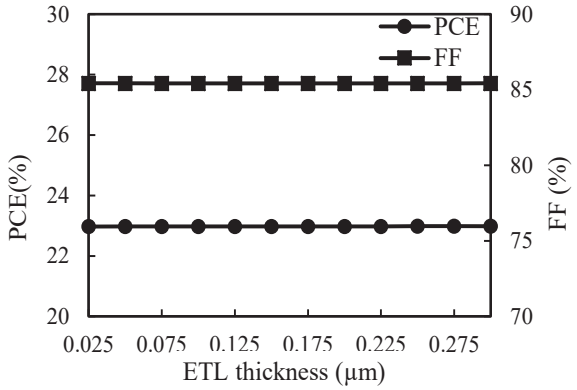

Fig. 3: Effect of ETL Layer Thickness on Power Conversion Efficiency and Fill Factor

3.2 HTL Layer Optimization

Following ETL optimization, the effect of hole transport layer thickness on device performance was investigated using a similar parametric approach. The thickness of the Cu_2O (HTL) was varied from 0.025 μm to 0.3 μm, while maintaining constant thicknesses of the ETL (0.03 μm) and the absorber (0.3 μm). The goal was to determine the optimal Cu_2O thickness that maximizes carrier extraction and minimizes energy losses at the absorber/HTL interface. Fig. 4 and Fig. 5 show that unlike the ETL, the Cu_2O HTL displayed a noticeable influence on photovoltaic performance. An increase in HTL thickness led to a gradual improvement in both PCE and Jsc, while the FF remained relatively stable. The Voc showed little variation, indicating that the increase in efficiency is primarily driven by enhanced current generation rather than changes in the built-in potential. This enhancement can be attributed to the favorable band alignment of Cu_2O with $Rb_2NaGaBr_6$ and its high hole mobility, which allows for effective collection of photo-generated holes. Moreover, Cu_2O's absorption onset in the visible range facilitates the transmission of high-energy photons to the absorber, further boosting carrier generation.

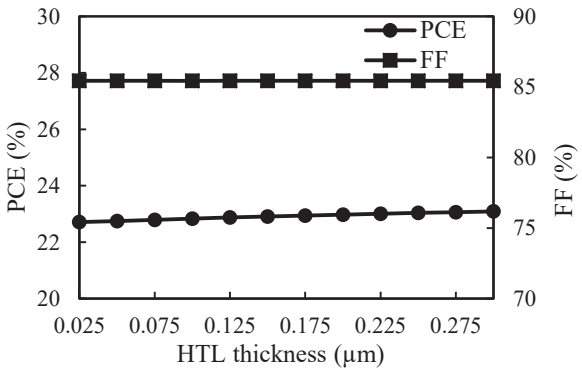

Fig. 4: Effect of HTL Layer Thickness on Power Conversion Efficiency and Fill Factor

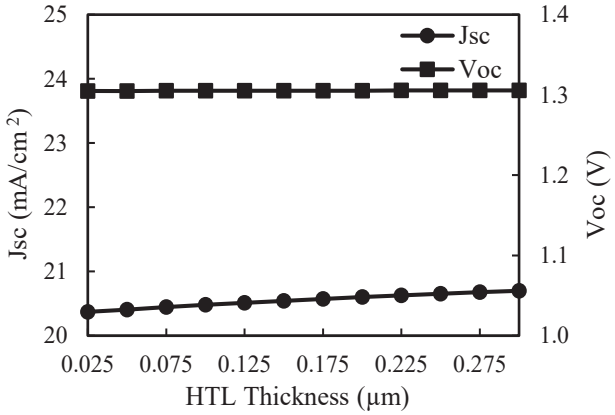

Fig. 5: Effect of HTL Layer Thickness on Short Circuit Current and Open Circuit Voltage

From the observed trend, it is evident that a thicker Cu_2O layer enables more efficient hole extraction and reduces recombination losses at the interface. Consequently, a thickness of 0.3 μm was determined as the optimum value for the HTL, balancing carrier transport, optical transparency, and material usage. This selection contributes to the overall high efficiency of the device and underlines the importance of precise interface engineering in lead-free perovskite solar cells.

3.3 The Effect of Absorber Layer Thickness on Photovoltaic Performance

The thickness of the absorber layer is a key determinant of a solar cell's overall efficiency, as it directly governs light absorption, carrier generation, and transport dynamics. Following the optimization of the ETL and HTL thicknesses, the absorber layer thickness was systematically varied to evaluate its influence on the photovoltaic performance of the $Rb_2NaGaBr_6$-based device. Simulations were carried out by increasing the thickness of the absorber from 0.05 μm to 1.0 μm in increments of 0.05 μm, while maintaining constant thicknesses for the ETL and HTL layers at 0.03 μm and 0.3 μm, respectively. The results reveal that an increase in absorber thickness leads to a sharp and nearly exponential rise in the J_{sc}, shown in Fig. 7, driven by the enhanced absorption of incident photons and the generation of a larger number of electron–hole pairs. This enhancement, however, begins to saturate beyond a certain thickness as optical absorption nears its upper limit. The simulations indicate that J_{sc} begins to plateau around 0.8 μm, marking a point of diminishing returns with further thickness increase.

In contrast, the V_{oc} exhibits a gradual decline with increasing absorber thickness. This is attributed to enhanced bulk recombination, which becomes more prominent in thicker layers due to longer carrier transit paths and limited diffusion lengths. The effect of absorber layer on PCE and FF is shown in Fig. 6, and it is found that when the absorber thickness exceeds the effective carrier diffusion length, recombination losses dominate, leading to a decline in Voc and, in turn, affecting the FF and PCE.

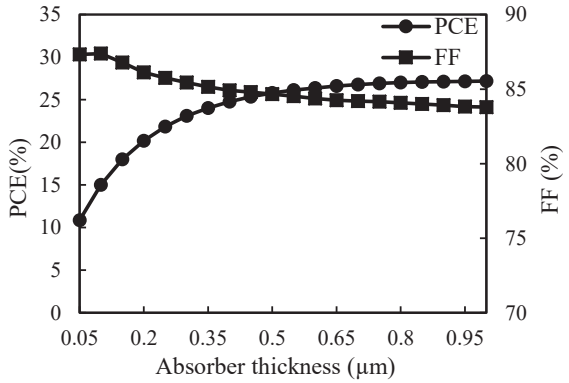

Fig. 6: Effect of Absorber Layer Thickness on Power Conversion Efficiency and Fill Factor

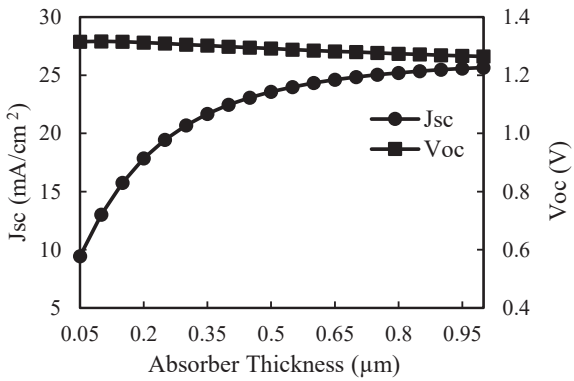

Fig. 7: Effect of Absorber Layer Thickness on Short Circuit Current and Open Circuit Voltage

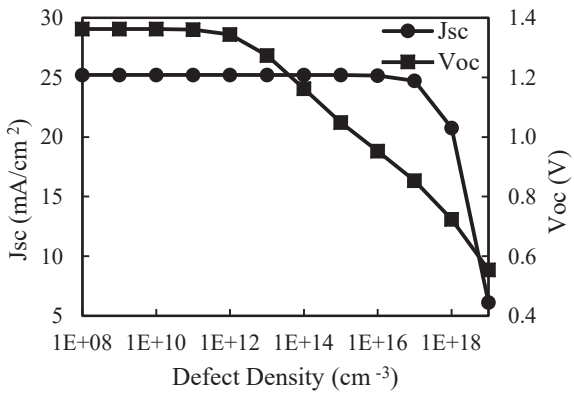

Fig. 8: Effect of Bulk Defect Density on Power Conversion Efficiency and Fill Factor

The trade-off between J_{sc} enhancement and V_{oc} degradation highlights the importance of identifying an optimal absorber thickness that maximizes overall efficiency. In this study, a thickness of 0.8 μm was found to provide the best compromise, leading to a peak PCE of 27.08%. This value corresponds to the point where photon absorption is near-saturated, while recombination losses remain adequately controlled. These findings reinforce the critical role of absorber layer optimization in the performance tuning of lead-free perovskite solar cells.

3.4 Effect of Bulk Defect Density of the Absorber Layer on PV Performance

Bulk defect density plays a critical role in determining the recombination dynamics within the absorber layer, and consequently, the overall performance of a solar cell. These defects—introduced during material processing—can act as non-radiative recombination centers by trapping charge carriers, reducing their lifetime, and increasing Shockley–Read–Hall (SRH) recombination. To assess this effect, the defect density of the $Rb_2NaGaBr_6$ absorber layer was varied from 1×10^8 to $1\times 10^{19}\,cm^{-3}$ while keeping other parameters constant. The effect of bulk defect density on PCE and FF is shown in Fig. 8 and on short circuit current and open circuit voltage is expressed in Fig. 9.

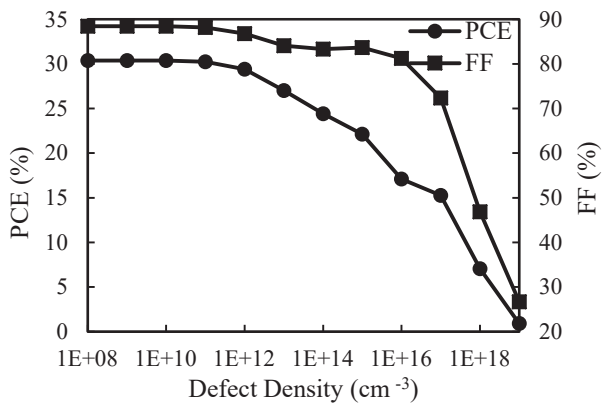

Fig. 9: Effect of Bulk Defect Density on Short Circuit Current and Open Circuit Voltage

Simulation results reveal that device performance remains largely unaffected for defect densities up to $1\times10^{12}\,cm^{-3}$, with minimal changes in V_{oc} and J_{sc}. However, beyond this threshold, particularly between 1×10^{13} and $1\times10^{16}\,cm^{-3}$, performance metrics begin to decline. This decline becomes exponential at higher defect levels due to reduced carrier diffusion length and increased recombination losses. The most severe degradation is observed at a defect density of $1\times10^{19}\,cm^{-3}$, where the PCE drops to a minimum of 0.905%. The FF follows

a similar trend, initially declining gradually and then dropping sharply beyond $1\times10^{16}\,cm^{-3}$. Based on these observations, an optimized defect density of $1\times10^{13}\,cm^{-3}$ is selected for modeling, as it offers a balance between material tolerances and device performance. This result emphasizes the necessity of precise fabrication control to limit defect formation and ensure reliable high-efficiency operation of lead-free perovskite solar cells.

3.5 Effect of Working Temperature on PV Performance

Temperature is a vital environmental factor affecting the operational stability and efficiency of photovoltaic devices. Thermal variations can alter charge carrier mobility, layer interfaces, and bandgap energy, leading to either performance enhancement or degradation depending on the thermal stability of the materials involved. To study this effect, the $Rb_2NaGaBr_6$-based solar cell was simulated across a temperature range of 275 K to 450 K, in increments of 25 K, under standard illumination conditions. Fig. 10 reveals the effect of this on PCE and FF and Fig. 11 reveals the effect on Jsc and Voc. Fig. 10 shows that at the baseline temperature of 275 K, the device exhibits its highest efficiency of 28.1%, along with a fill factor of 85.62%. As the temperature increases, both PCE and FF gradually decline, reaching 20.6% and 76.04%, respectively, at 450 K. This decline is attributed to increased phonon scattering and enhanced non-radiative recombination, which negatively impact carrier lifetimes and reduce charge collection efficiency. Interestingly, the PCE remains above 20.6% throughout the temperature range, suggesting that the device maintains functional stability even at elevated temperatures.

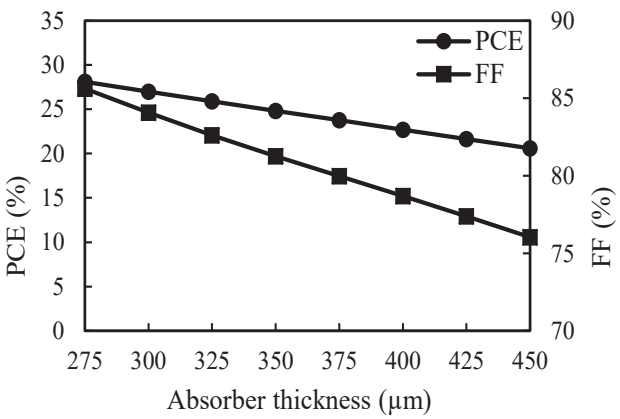

Fig. 10: Effect of Temperature on Power Conversion Efficiency and Fill Factor

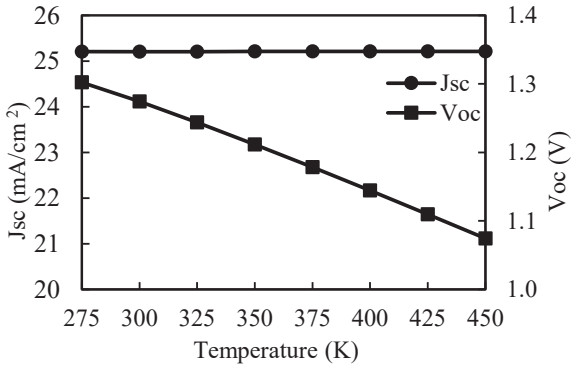

Fig. 11: Effect of Temperature on Short Circuit Current and Open Circuit Voltage

V_{oc} shows a clear inverse correlation with temperature, steadily decreasing as thermal energy disturbs the built-in potential and widens the recombination window. In contrast, Jsc remains relatively stable across the range, with only minor fluctuations. These results indicate that while thermal management is crucial for maximizing output, the proposed $Rb_2NaGaBr_6$ device architecture retains robust photovoltaic characteristics under varying environmental conditions, reinforcing its applicability for real-world deployment.

3.6 Benchmarking SCAPS-1D Results with Previously Reported Data

Table II presents a comparative analysis of the photovoltaic performance of various previously reported devices alongside our proposed structure. The designed configuration-—FTO/TiO_2/$Rb_2NaGaBr_6$/Cu_2O/Au—demonstrates a remarkable power conversion efficiency of 27.004%, highlighting a strong synergy between open-circuit voltage and short-circuit current density. This performance significantly surpasses that of other reported double perovskite-based PSCs, underscoring the superior potential of our device architecture.

Table II: Comparison of PV Parameters of Perovskite Structures with Previously Reported Data.

Device Structure	Voc (V)	Jsc (mA/cn	FF (%)	PCE (%)
FTO/SnO_2/$Rb_2NaGaBr_6$ CuI/W [16]	1.278	25.02	84.01	26.86
FTO/TiO_2/$Rb_2LiInBr_6$ Cu_2O/Ni [17]	1.277	25.06	83.96	26.90
ITO/ZnO_2/Cs_2BiAgI_6 CBTS/Au [18]	1.09	23.76	83.78	21.59
ITO/WS_2/$Cs_2CuBiBr_6$ CBTS/Ni [19]	0.712	35.63	77.57	19.70
FTO/TiO_2/$Rb_2NaGaBr_6$ Cu_2O/Au [This work]	1.274	25.20	88.08	27.004

4. CONCLUSION

This work presents a detailed theoretical and numerical analysis of the photovoltaic potential of $Rb_2NaGaBr_6$, a novel lead-free double perovskite material. Through DFT calculations, the material was shown to possess a direct bandgap and favorable carrier transport properties, making it suitable for solar energy harvesting. The electronic parameters extracted from the DFT simulation were used to model a solar cell device in SCAPS-1D, featuring a layered structure of FTO/TiO_2/$Rb_2NaGaBr_6$/Cu_2O/Au. The device demonstrated outstanding performance under optimized simulation conditions, achieving a power conversion efficiency of 27.004%. The influence of absorber layer thickness and bulk defect density was also investigated, confirming the material's tolerance to minor structural variations. Additionally, energy band alignment analysis showed efficient charge separation and minimal recombination losses due to appropriate ETL and HTL selection. Overall, the results suggest that $Rb_2NaGaBr_6$ is a viable candidate for stable, efficient, and environmentally friendly perovskite solar cells and warrants further experimental validation for real-world deployment.

REFERENCES

[1] W. A. Herrmann, "Quantifying global energy resources," Energy, Vol. 31, No. 12, pp. 1685–1702, 2006.

[2] R. E. H. Sims, H. Rogner and K. Gregory, "Carbon emission and mitigation cost comparisons between fossil fuel, nuclear and renewable energy resources for electricity generation," Energy Policy, Vol. 31, No. 13, pp. 1315–1326, 2003.

[3] M. A. Green, E. D. Dunlop, J. Hohl-Ebinger, M. Yoshita and A. W. Y. Ho-Baillie, "Solar cell efficiency tables (Version 64)," Prog. Photovolt. Res. Appl., Vol. 32, No. 7, pp. 425–441, 2024.

[4] W. S. Yang, B. W. Jung, N. J. Jeon, D. U. Lee, S. S. Shin, J. Kim, K. E. Kim, H. S. Jeong and S. I. Seok, "Iodide management in formamidinium-lead halide-based perovskite layers for efficient solar cells," Science, Vol. 356, No. 6345, pp. 1376–1379, 2017.

[5] Z. Li, B. Wu, X. Sheppard, S. Zhang, S. Gao, D. Long, N. Zhu and J. Zhu, "Organometallic-functionalized interfaces for highly efficient inverted perovskite solar cells," Science, Vol. 376, No. 6591, pp. 416–420, 2022.

[6] J. Wang, Z. Li, J. Li, S. Wei, and S. Suhaily, "α-$CsPbI_3$ perovskite solar cells fabricated via an efficient two-step process," Mater. Today, Vol. 55, No. 12, pp. 2103–2109, 2023.

[7] W. Guo et al., "Low-temperature flexible $MAPbI_3$ perovskite solar cells," Chem. Eng. J., Vol. 448, Art. No. 142366, 2023.

[8] Q. Jiang et al., "Surface passivation of perovskite film for efficient solar cells," Nat. Photonics, Vol. 13, No. 7, pp. 460–466, 2019.

[9] V. Srivastava, R. K. Chauhan, and P. Lohia, "Numerical analysis of $Cs_2AgBiBr_6$ double-perovskite solar cell with optimized performance," Nanomaterials and Energy, Vol. 12, No. 3, pp. 131–138, 2023.

[10] M. K. Hossain et al., "Combined DFT, SCAPS-1D, and wxAMPS frameworks for design optimization of efficient $Cs_2AgBiBr_6$-based solar cells," RSC Adv., Vol. 12, No. 34, pp. 35023–35032, 2022.

[11] M. Kibou, Z. Haman, N. Khosossi, I. Essaoudi, A. Ainane, and R. Ahl Laamara, "Computational insights into the optoelectronic potential of $Cs_2AgGaBr_6$ double halide perovskite solar cells," Mater. Chem. Phys., Vol. 294, Art. No. 126978, Jan. 2023.

[12] M. J. Islam, S. H. Cheragee, M. A. H. Chowdhury, S. Subrina, M. Hossain, and F. Gulshan, "Numerical Study of Higher Efficiency Perovskite Solar Cell Using Density Functional Theory," Int. Conf. on Advances in Computing, Communication, Electrical, and Smart Systems, pp. 1617–1623, 2024.

[13] K. F. Brennan, The Physics of Semiconductors: With Applications to Optoelectronic Devices, Cambridge University Press, 1999.

[14] M. J. Islam et al., "Numerical Study of Higher Efficiency Perovskite Solar Cell Using Density Functional Theory," in Proc. Int. Conf. on Advances in Computing, Communication, Electrical, and Smart Systems, pp. 1–5, 2024.

[15] M. K. Hossain et al., "Effect of Various Electron and Hole Transport Layers on the Performance of CsPbI3-Based Perovskite Solar Cells: A Numerical Investigation in DFT, SCAPS-1D, and wxAMPS Frameworks," ACS Omega, Vol. 7, No. 47, pp. 43210–43230, 2022.

[16] M. J. Islam, M. Tarek, and F. Gulshan, "A numerical analysis of a high-efficiency solar cell using a DFT explored nontoxic perovskite material," Int. Conf. Adv. Appl. Electr. Eng. Energy, pp. 1–5, 2024.

[17] M. J. Islam, S. H. Cheragee, M. A. Haque Chowdhury, S. Subrina, M. Hossain, and F. Gulshan, "Numerical study of higher efficiency perovskite solar cell using density functional theory," Int. Conf. Adv. Comput., Commun., Electr., Smart Syst. pp. 1–5, 2024.

[18] M. K. Hossain et al., "Combined DFT, SCAPS-1D, and wxAMPS frameworks for design optimization of efficient Cs2BiAgI6-based perovskite solar cells with different charge transport layers," RSC Adv., Vol. 12, No. 54, pp. 35002–35025, 2022.

[19] K. I. Ferdous Utsho et al., "Optimizing Cs2CuBiBr6 double halide perovskite for solar applications: the role of electron transport layers in SCAPS-1D simulations," RSC Adv., Vol. 15, No. 3, pp. 2184–2204, 2025.

Exploring the Key Determinants of Language Proficiency in Polytechnic Engineering Students: A Critical Examination Using PSA Framework

Fatema Sultana

Department of Humanities and Social Sciences, Dhaka University of Engineering & Technology, Gazipur, Bangladesh

ABSTRACT

English, as the global *lingua franca*, holds significant academic and professional relevance, particularly in non-native contexts such as Bangladesh. Despite its established role in the national curriculum, polytechnic engineering students frequently struggle to achieve the level of English language proficiency required for academic success and professional advancement. This study aims to identify the key socio-economic, psychological, and pedagogical factors hindering the language competence of these students through the lens of the Present Situation Analysis (PSA), a core component of needs analysis in English for Specific Purposes (ESP). The research further examines how these factors impact students' academic performance and employability, and proposes practical solutions to address the challenges. To achieve this, the researcher employed a mixed-method approach, collecting quantitative data from 511 students across ten polytechnic institutions and complementing these with qualitative insights from teachers, current students, and alumni. Data analysis using Microsoft Excel and SPSS highlighted several critical barriers, including students' low socio-economic and educational backgrounds, insufficient prior exposure to English, ineffective teaching methodologies, limited instructional resources, infrastructural inadequacies, teacher shortages, oversized classes, restricted class hours, lack of extracurricular language practice, the predominance of the mother tongue (L1) as the medium of instruction (MOI), and various learner affective and psychological challenges. Based on these findings, the study proposes strategic recommendations to enhance the quality of English language education in polytechnic institutions. These insights are expected to contribute to informed policy-making and the design of context-sensitive pedagogical interventions to improve language outcomes for engineering students in Bangladesh.

Keywords: ESP, Needs Analysis, PSA, Competence, Lingua Franca, EFL, Language Determinants

1. INTRODUCTION

English as a global *lingua franca* (ELF, a common language) has gained widespread attention among all nationalities worldwide in research and academic activities [1]-[7], higher education, national and international communications, job, and business sectors. A significant consequence of English's recent globalization has been the rise of non-native speakers (NNSs) in various parts of the world, who now comprise the vast majority of English users [8]. Due to the greater availability and number of non-native English speakers from the expanding circle compared to English speakers in either the inner or outer circles, they tend to utilize English in various academic, socio-cultural, professional, and economic contexts [9], [10].

Kachru's Three Circles Model (Inner, Outer, Expanding) provides a valuable framework for understanding the global spread and functional diversity of English, with a particular emphasis on the Expanding Circle, where non-native speakers predominantly use English as a *lingua franca* in international settings. This model contextualizes the sociolinguistic realities of English variation and legitimizes the evolving norms beyond traditional native-speaker benchmarks.

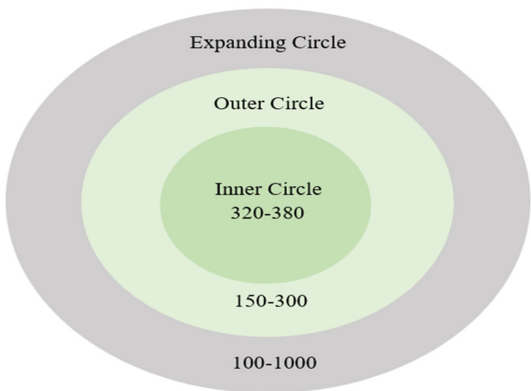

Fig. 1: Kachru's Three Circles Model of English

The very nature of the internationalization of English thus precedes that it is no longer exclusively bound to

*Corresponding author's email: fatemasultana309@duet.ac.bd

the prominence of the native speakers (NESs); instead, it is now a sort of plurilithic language with diversities, varieties, and with extensive purposes.

To build English competence among engineering learners in Bangladesh, academic stakeholders have implemented English for Academic Purposes (EAP) and English for Specific Purposes (ESP) courses within the first two years of study [11]. However, students, especially those in polytechnic engineering, continue to struggle with mastering English language rules and strategies, which negatively affects their academic and professional performance [12]. These challenges are entrenched in systemic issues such as grammar-focused teaching methods, insufficient teacher training, and extensive reliance on Bangla as the medium of instruction, which collectively hinder the acquisition of English communicative competence [13], [14]. The ongoing difficulties underscore an urgent need to identify precise contextual factors that influence English learning and to develop effective, locally informed strategies to address them.

This study examines the intricate interplay of socio-economic, psychological, and pedagogical determinants that influence English language acquisition among diploma-level engineering students in Bangladesh. Grounded in the Present Situation Analysis (PSA) framework, the research examines how these interrelated variables restrict students' ability to develop adequate language proficiency. These constraints have significant implications for their academic achievement and future professional engagement, as inadequate language skills impede their ability to access technical content, communicate effectively, and compete in globalized job markets. The study further aims to identify practical, context-sensitive solutions that address these barriers and support the development of targeted pedagogical strategies to enhance language outcomes in polytechnic education.

1.1 Background of the Research Context

English, recognized as the *global lingua franca [15],* is a primary medium of communication across academic, professional, and technical domains worldwide. Cogo and Pitzl assert that English is now a truly international language for business, education, science, and global interaction [16]. With globalization intensifying cross-border communication, English has become essential in workplace settings [17]. For engineering and science students, English facilitates access to specialized knowledge and professional discourse [18]. As a result, English language proficiency is prioritized in technical and vocational education globally, including in Bangladesh, where it is viewed as a vital tool for economic advancement and integration into the global market. Recognizing this, the Bangladeshi government has mandated English education at all levels, with a particular emphasis on its role in achieving Sustainable Development Goal 4, which aims to ensure inclusive, equitable, and quality education [19].

In Bangladesh, polytechnic students study English as a part of their four-year diploma program. These courses, grounded in English for Specific Purposes (ESP), aim to develop communicative skills relevant to technical disciplines. However, despite curriculum integration, many students struggle due to their socio-economic backgrounds, limited English exposure, and anxiety around language learning.

Diploma engineering students often come from Bengali-medium instruction backgrounds and rural or lower-middle-class families. Although these students acquire significant technical skills, their limited English proficiency obstructs their academic success and employability. Many students hesitate to communicate in English, both in and out of the classroom, due to fear, lack of confidence, and insufficient pedagogical support.

Moreover, while some diploma graduates pursue further education, such as B.Sc. engineering degrees from institutions like Dhaka University of Engineering and Technology, Gazipur, many enter the workforce directly. This bifurcation highlights the need for English skills that are both academically and professionally viable.

It has been found that, under the Directorate of Technical Education (DTE), 205 institutions operate technical education at the certificate, diploma, and degree levels. Among them, 50 government polytechnics offer diploma-level engineering education. These institutes aim to produce skilled mid-level technicians, but the gap in English proficiency continues to hinder the full realization of this goal.

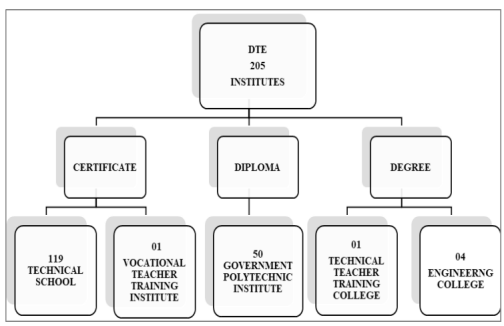

Fig. 2: Technical Institutes Division Under DTE

Note. Adapted from the Directorate of Technical Education (DTE) Webpage, Bangladesh

The research highlights key areas where Bangladeshi polytechnic learners encounter significant challenges related to language proficiency, specifically in curriculum design, materials development, assessment practices, and teacher training, all of which require targeted improvement. While existing literature has examined learners' short-term English needs and challenges [20], [21], few studies have addressed comprehensive second language acquisition (SLA) practices, including learner autonomy, affective filter, needs-based instruction, and socio-economic and socio-cultural factors. The absence of these elements can significantly impede language development [22], [23].

This study adopts a needs analysis approach, examining the PSA framework for Bangladeshi polytechnic students to investigate the socio-economic, psycho-social, and pedagogical factors that pose challenges to their language competency. Hence, it examines their current language competencies and learning conditions that hinder their overall academic and professional achievement. By evaluating these factors, the study seeks to inform policy and curriculum development for more effective ESP implementation in Bangladesh's technical and vocational education system.

1.2 Implications of the Research Paper

Bangladesh is progressing toward achieving a developed country status, marked by advancements in education, technology, and trade. However, persistent unemployment, particularly among graduates, remains a significant challenge. One viable solution lies in strengthening technical and vocational education, which directly contributes to the development of skilled human resources. Enhancing polytechnic education, particularly through improved English language instruction, can play a pivotal role in addressing this issue, as English serves as a crucial gateway to global communication and employment opportunities.

Polytechnic students, as future engineers, have the potential to significantly impact sectors such as transport, construction, electronics, and textiles. However, many come from rural, underprivileged backgrounds and lack adequate educational support, particularly in English proficiency. Addressing this gap through targeted English language learning and needs-based instruction will better equip them for the job market, potentially reducing unemployment and supporting sustainable economic development.

1.3 Problem Statement

Globalization has positioned English as the dominant medium of communication in engineering education and professional practice [24], [25]. Engineering students have to navigate English-based lectures, research materials, and technical documentation during their studies and use the language in professional contexts for collaboration and communication.

Bangladesh hosts 437 polytechnic institutes, comprising 50 public and 387 private institutions, with over 257,000 students enrolled [26]. Many students graduate annually, most continuing their education toward a B.Sc. degree.

Despite the scale of enrollment, English proficiency among these students remains limited. The primary factors include socio-economic disparities, inadequate teaching methodologies, and limited institutional resources [27]. Many students come from rural backgrounds and lack exposure to English in their formative years, which affects their ability to engage with technical content in English.

The curriculum in these institutes typically offers two English for Specific Purposes (ESP) courses, which are often insufficient in terms of content and duration. Furthermore, classrooms often consist of learners with varied proficiency levels, yet the instruction is not differentiated accordingly. Language instruction largely relies on the grammar-translation method, emphasizing rote memorization of grammar rules over functional language use [28], [29]. This results in the neglect of productive skills, such as speaking and listening, which are essential for effective workplace communication.

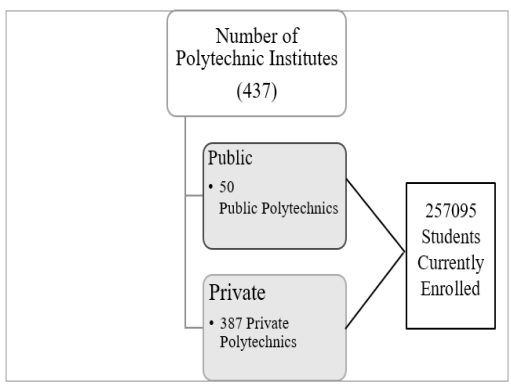

Fig. 3: Number of Polytechnic Institutes and Students in Bangladesh [23]

Institutional challenges, outdated curricula, and the lack of infrastructure hinder the development of comprehensive English language skills [30], [31]. Addressing these

gaps requires a thorough needs analysis framework, specifically the Present Situation Analysis (PSA). This study, employing a mixed-method approach, explores these determinants to inform ESP curriculum reform and enhance the employability of Bangladeshi polytechnic engineering students in national and international contexts.

1.4 Research Questions

To critically investigate the existing realities of language development and learning challenges faced by Bangladeshi polytechnic learners, this paper formulates the following research question as the central focus of its inquiry.

1. What are the socio-economic, psychological, and pedagogical factors that influence the language proficiency levels of diploma engineering students as assessed through the PSA framework?
2. How do they affect their academic and professional competence?
3. What are the probable solutions to address these factors?

2. THEORETICAL OVERVIEW

2.1 Need for Technical Education in Bangladesh

A developing country like Bangladesh's economic and technological development largely depends on its investment in science, technology, and engineering education. Bangladesh needs engineering education more for the certainty of financial stability than developed countries do. Chowdhury and Alam thus advocate that "a nation can move forward and secure a place in global trade if it is adept and developed in technological and engineering education despite being deficient in wealth, power, and natural resources. The global industry and the demand in technical fields heightened the ardent need for engineers in Bangladesh. Accordingly, engineering education is valued highly in Bangladesh because it has immensely influenced and developed the nation's economic growth and sustainability" [32].

Thus, to make the country culturally, socially, and economically advanced in the global village, the prospect of engineering education and engineers can contribute immensely to all sectors of Bangladesh. Besides, the resurgence of technological advancement, industrialization, and globalization advocates the demand for quality education. It helps promote a country's economic, social, cultural, and national development. Quality education can be ascertained through the formation of human resource development. To equip the learners with quality education, they need different skills to determine their human capacity [27].

Educational institutions play a crucial role in providing skills related to technical education and vocational training to designated learners. It is evident that a close relationship exists between a country's technical education system and its socio-economic and cultural development. It is an overriding requirement for Bangladeshi learners to be skilled in technical and vocational education and training to keep pace with the global community and its development force. Inopportunely, Neelim and Siddiqui have noticed that "the majority of students in Bangladesh predominantly enroll in mainstream schools and madrassa education, with a tiny fraction opting for vocational schools. Consequently, there is a limited supply of individuals equipped with vocational skills that align with both domestic and international labour market demands. Hence, Bangladesh primarily participates in the international labour market for unskilled and semi-skilled workers. These circumstances require reformulation of the education system to increase the pool of vocationally skilled human resources that can effectively cater to domestic and international job markets" [33, pp. 30-32].

Bangladesh's Technical and Vocational Education and Training (TVET) is striving to provide learners with specialized, practical knowledge of technologies and skills. Here, TVET runs short-length courses that last 360 hours. It also has a three-level formal technical education. They offer two-year vocational SSC, two-year vocational HSC, and four-year diploma courses in various engineering disciplines, including civil, mechanical, architecture, and electrical. Students can pursue diploma degrees from various public and private polytechnics located in different regions of Bangladesh.

Likewise, language proficiency is essential for polytechnic engineering students to become competent global engineers. It is used as the medium of instruction (MOI) in almost all engineering institutes in Bangladesh. Currently, 257,095 polytechnic students are pursuing their four-year diploma in engineering courses from various polytechnic institutes in Bangladesh, who urgently need English to secure a place in the global market [26]. The requirement of English for engineering students in Bangladesh is evident in the culture of offering English as a compulsory ESP course in their first or second year of academic study. Regrettably, the language proficiency of polytechnic learners is found to be dissatisfactory due to socio-economic, cultural, infrastructural, and institutional logistical factors. Therefore, this paper attempts to examine

the determinants that hinder their language proficiency through the present situation analysis (PSA) framework.

2.2 ESP and PSA Framework as Theoretical Base

English for Specific Purposes (ESP) began its journey nearly fifty years ago because of the demand for English language skills in worldwide occupational pursuits; the transitional phase evolved in theoretical and applied linguistics, and the burgeoning stance in educational institutions for learners' justification for their needs.

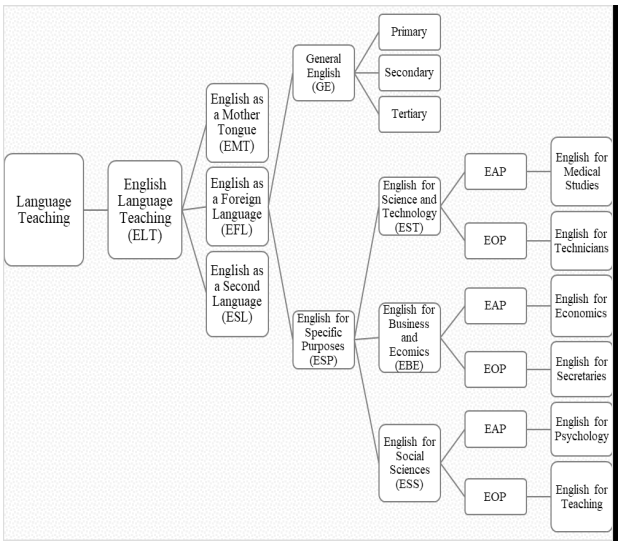

Fig. 4: The Prognoses of ELT and ESP [31]

Hutchinson and Waters demarcated that ESP emerged during the mid-1980s as a part of the learner-centered style of teaching under the brolly term EFL/ESL. It is a subfield of English language teaching (ELT) and learning that focuses on the language needs of learners in specific fields or professions [34]. One of the key components of ESP is the Needs Analysis (NA), a process that determines the language needs of learners. The NA process helps teachers identify what language skills and knowledge learners need to achieve their goals. It is again seen as a pre-course evaluation process and is crucial for the successful implementation of ESP. ESP needs analysis identifies the precise language needs of a particular group of learners to design an appropriate English language curriculum. ESP is notable for its purpose-oriented learning and teaching, which incorporates authentic and contextual materials, prioritizes affective and emotional factors, and emphasizes the nature of self-guided and directed learning.

Earlier, the learners as psycho-social human beings and their affective prospect of emotional behaviour were not emphasized in language-learning theories of English. However, the development found in ESP initiated the learners' prominence by emphasizing their affective factors in learning [35]. Thus, it guides the learners toward communicative tasks and the meaningfulness prospect of the language.

Students' language learning needs and determinants can be identified through present situation analysis (PSA), learning situation analysis (LSA), and target situation analysis (TSA). Robinson demonstrated that "needs analysis is formed of two types of the students' requirements in verbal skills. They are the present situation analysis (PSA) and target situation analysis (TSA)" [36, pp. 8-9]. Dudley-Evan and St. John augment another form of student needs: learning situation analysis (LSA). It focuses on the students' felt needs, subjective opinions, and requirements, as well as their process-oriented needs in the teaching-learning context and language skills [37].

PSA aims to assess and classify the students' current language levels and language skills needs at the beginning of their ESP courses, whereas TSA proposes to identify and categorize the language needs required in the target socio-cultural authentic contexts. Therefore, PSA determines the students' existing language status. It is sought by identifying their language proficiency, whether their level is primary, secondary, or advanced, and through their educational background information. Richterich and Chancerel presented intriguing efforts to consider the learners' PSA while addressing English language learning needs. It helps to emulate the linguistic gap between what the students face before the course starts and what actions need to be accomplished after the course ends [38]. It is the "lack" of students in the language course.

In this study, the author employs the PSA framework as a theoretical base to identify the challenges polytechnic engineering students face in learning English as an ESP course. The key factors essential in identifying PSA include the learners' language level, knowledge of the language and skills, their previous educational and cultural background, their attitude and motivational prospects for the course, and the reason for pursuing this course.

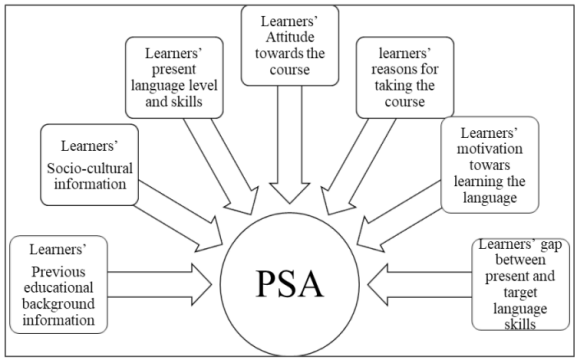

Fig. 5: Present Situation Analysis (PSA) Components (Author's creation)

The learners' gap between their existing language skills and the target language level they aim to develop is also addressed in this section of PSA. McDonough specified that PSA deals with the "fundamental variables" of language learners and language learning contexts that must be considered before conducting TSA [39].

As ESP is specialized in its nature, aims, and objectives, various challenges emerge for both teachers and learners in pedagogical contexts. These challenges include selecting appropriate content, materials, techniques, textbooks, and assessment methods, as well as ensuring adequate logistical and administrative support. Policy and funding limitations often exacerbate these issues, restricting the availability of resources and the implementation of targeted curriculum development [34]. Furthermore, the effectiveness of ESP instruction is influenced by the emotional and psychological states of learners. According to Krashen's Affective Filter Hypothesis, factors such as motivation, self-confidence, and anxiety can significantly impact language acquisition; a high affective filter may hinder input from being processed effectively, while a low affective filter can facilitate learning [40]. Therefore, addressing both institutional constraints and affective factors is crucial in successfully implementing ESP programs tailored to learners' specific needs.

Brown found three constraints that are generally encountered in ESP language learning situations. They are situational, stakeholder, and theoretical, which also comply with the PSA prospects [41].

Patil revealed that 75% of engineering students come from rural socio-economic backgrounds [25]. As they come from regional English language medium schools, they face obstacles in understanding the English language at every step of their life and careers. Thus, problems are noticed in the proficiency levels of students who are from rural and urban areas. The language inadequacy of the majority of the students led to inconsistency in selecting and applying materials, strategies, methodologies, and approaches to teaching English holistically. Similarly, non-local and culturally inconsistent textbooks create problems for students to be intrinsically motivated to learn English, as they are generally removed from local and cultural realities [42].

Constraints		
	Situational	Society
		Policy/Policies
		Resource
		Curriculum
	Stakeholder	Students
		Teachers
		Local Administrators
	Theoretical	Approaches
		Syllabus

Fig. 6: Constraints Found in ESP Context

Besides, some other challenges appear in terms of the lack of trained English teachers and practitioners, inadequate ESP resources and materials, and students' poor socio-economic and educational background, which have greatly influenced the use of local or mother tongue instead of English as MOI in the tertiary level education system. It is directed at using the local language or L1 as MOI in classroom teaching and assessing the students using English [43], [44]. The use of L1 in classrooms introduces "translanguaging," a pedagogical practice where language exposure and input are provided in one language, and students are assessed in another, especially in bilingual classes [45].

It has been found that a handful of studies have been conducted on the analysis of ESP needs and challenges for polytechnic engineering learners. Unswervingly, certain aspects of language determinants in the context of Bangladeshi polytechnic engineering students have still not been advocated so far by any prospective researcher. More specifically, the challenges faced by polytechnic engineering students have not been adequately addressed, as they do not align with learners' preferences in selecting content, materials, techniques, methods, and approaches for learning English. Furthermore, no in-depth research study has been conducted to examine the teaching-learning challenges prevailing in Bangladesh's polytechnic engineering contexts, particularly in learning English as an ESP course. As their needs are not justified in their syllabus, it has been found that most diploma engineering students feel demotivated to learn English, and their affective filter becomes higher.

As a result, in most cases, Bangladeshi polytechnic engineering students remain incompetent in their language

skills and fail to secure the higher academic education and prospective careers they desire. These perspectives on inattention necessitate more significant research implications for identifying the challenges that polytechnic engineering students face in learning English. Therefore, this research work aims to address the gap that prevails in the polytechnic engineering sector in Bangladesh, specifically in identifying language impediments among students.

4. METHODOLOGY OF THE RESEARCH

This section of the research focuses on the method that has been applied in this study. It has considered the research design, including population, sampling, data analysis, and the construction of the instruments used for the study.

4.1 Nature of the Research

The research has employed both qualitative and quantitative methods to collect research data. Hence, it is mixed-methods (Qn-Ql) research. It has used survey questionnaires and interviews as part of the mixed-methods strategy.

4.2 Population

For this study, the target population is drawn from the engineering sector, with Bangladeshi engineering students specifically identified as the target group. The reason for selecting them as the target population is that they are believed to comprise a larger proportion of the population in a country like Bangladesh. Additionally, they have been identified as the most expedient sources of human resources over the last couple of years, who can consistently influence and contribute to the county's sustainable development through their expertise and skills.

4.3 Sampling

The samples that have been used in this research study were selected from polytechnic engineering learners studying at different public polytechnic institutes in Bangladesh. For the students' questionnaire survey data, the researcher took a sample of five hundred eleven (511) polytechnic engineering students who have completed the two English courses [English- I (25712) and English- II (25722)] from ten diverse public polytechnic institutes situated in five divisions of Bangladesh. The participants were randomly selected from the six departments (Civil Technology, Mechanical Technology, Electronics Technology, Computer Technology, Power Technology, and Architecture).

For the students' interview data, the researcher randomly chose fifteen (15) present polytechnic students from the six departments mentioned above, ten (10) English instructors for the teachers' interview data, and six (6) alumni students for the alumni interview data.

4.4 Data Analysis Instrument

For quantitative analysis, the scholar used SPSS software version 20 and MS Excel, and for the qualitative component, she employed descriptive analysis and textual/content analysis procedures. The findings are presented using tables and graphs, displaying data in terms of frequency (F), percentage (P), cumulative percentage (CP), mean (M), standard deviation (St. D), and mode (Mo). Four-point Likert scales are used to present the language skills and the severity of challenges encountered at the research sites while learning English as an ESP course.

Table I: The List of Polytechnic Institutes and the Number of Students

Name of Polytechnic Institutes	Division	Name of the Departments						Frequency	Percentage (%)
		Civil	Mechanical	Architecture	Electronics	Power	Computer		
Dhaka Polytechnic Institute	Dhaka	115	115	114	66	44	22	556	10.96%
Narsingdi Polytechnic Institute	Dhaka	113	110	N/A	99	NN/A	113	445	8.81%
Munshiganj Polytechnic Institute	Dhaka	221	112	NN/A	99	55	77	554	10.57%
Mymensingh Polytechnic Institute	Mymen-singh	115	88	NN/A	111	77	99	550	9.78%
Sylhet Polytechnic Institute	Sylhet	221	113	NN/A	44	33	66	447	9.20%
Khulna Polytechnic Institute	Khulna	114	44	NN/A	111	112	88	449	9.59%
Kulna Mahila Polytechnic Institute	Khulna	99	NN/A	117	221	N/A	110	557	11.15%
Kustia Polytechnic Institute	Khulna	99	115	NN/A	113	33	117	557	11.15%
Jhenidah Polytechnic Institute	Khulna	226	NN/A	NN/A	222	NN/A	88	556	10.69%
Dinajpur Polytechnic Institute	Rangpur	88	112	110	NN/A	NN/A	110	440	7.83%
N =								511	100%

The four-point Likert scale is employed as a structured and reliable instrument to quantify the self-assessed language proficiency levels of polytechnic learners. It facilitates clear differentiation across performance categories and enables statistically meaningful analysis of their abilities and challenges in ESP course contexts [46].

Table II: Mean Range Value for Likert Four-Point Scale [46]

Numerical Value	Items	Range/ Mean Interval Scale	Descriptive Mean Equivalent / Interpretation
1	Very Poor	1.00 - 1.75	Poor Language Skill
2	Below Average	1.76 - 2.49	Below-average Language Skill
3	Average	2.50 - 3.24	Average Language Skill
4	Excellent	3.25 - 4.00	Excellent Language Skill

4.5 Conceptual Theories Applied in this Study

The study employs multiple theoretical approaches to systematically identify and analyze critical variables in language learning, with a focus on the specific features and challenges associated with the PSA framework.

The researcher used Brown's framework when choosing the interview questions for the study's concerned stakeholders [37].

Table III: Theories Applied in this Research

SL.	Name of the Theorist/s	ESP Needs/Determinants Identifying Theories
1.	Richterich and Chancerel (1977)	Present Situation Analysis (PSA)
2.	Jordan (1997)	"Means Analysis" for identifying the existing challenges

Table IV: Interview Scheme Used in this Research [37]

SL.	Areas Addressed	What to Ask About
1.	Abilities	• General language aptitudes, proficiencies of students, especially with regard to reading, writing, speaking, listening, pragmatics, but also their abilities in the same aspects of the ESP involved
2.	Problems	• Difficulties and problems participants perceive in a particular ESP learning and teaching context
3.	Attitudes	• Wants, desires, and attitudes (for example, toward the language being studied, toward existing course objectives, and toward the ESP involved)
4.	Priorities	• Topics, activities, functions, skills, grammar points, vocabulary, and so on that stakeholders' feel are most important, second most important, third most important, and so on
5.	Solutions	• Answers or solutions to whatever problems or issues are uncovered in the process of gathering NA data

5. FINDINGS OF THE STUDY

This section of the research presents the interpretation and findings of survey data, with a focus on the insights gathered from student questionnaires. Additionally, the study incorporates results from interviews conducted with current students, teachers, and alumni to identify the key issues affecting language development among polytechnic learners.

Q1. What is your Current Level of English Language Skills?

Table V presents participants' self-assessments of their English language proficiency across various skills, measured on a 4-point scale (1 = very poor, 2 = below average, 3 = average, 4 = excellent). Overall, respondents reported average competence in listening, reading, and writing but below-average ability in speaking, grammar, and vocabulary.

Listening comprehension was rated as average (M = 2.89, SD = 0.764), with 63% of respondents identifying their ability as average, 17% as excellent, and only 20% as below average or very poor. In contrast, speaking fluency and confidence received a below-average rating (M = 2.27, SD = 0.834), with 35% rating it as below average and 21% rating it as very poor, while 40% considered it average.

Similarly, accuracy in speaking was also rated below average (M = 2.27, SD = 0.878), with 34% rating themselves below average, 22% very poor, and only 6% excellent. Reading comprehension was viewed more favorably (M = 2.96, SD = 0.724), with 59% rating it average and 21% excellent.

In writing, participants assessed their academic writing accuracy as average (M = 2.70, SD = 0.775); 55% rated themselves average, while 25% rated below average

Table V: Students' Current Level of English Language Skills

English Language Skills	Excellent (E)		Average (A)		Below Average (BA)		Very Poor (VP)		M	St. D	Mo	Cur-rent Level
	F	P	F	P	F	P	F	P				
Understanding other speakers while listening	85	17%	321	63%	67	13%	38	7%	2.89	.764	3	A
Fluency and confidence in speaking	22	4%	202	40%	178	35%	109	21%	2.27	.834	3	BA
Accuracy in speaking	32	6%	189	37%	176	34%	114	22%	2.27	.878	3	BA
Comprehension when reading any text	106	21%	300	59%	86	17%	19	4%	2.96	.724	3	Av
Accuracy in academic writing	59	12%	283	55%	128	25%	41	8%	2.70	.775	3	A
Accuracy in Grammar	40	8%	237	46%	167	33%	67	13%	2.49	.819	3	BA
Range of vocabulary	52	10%	219	43%	163	32%	77	15%	2.48	.869	3	BA

and 12% excellent. Grammar accuracy was rated below average (M = 2.49, SD = 0.819), with 33% identifying as below average and 13% as very poor. Only 8% considered their grammar excellent. Finally, the vocabulary range was also assessed as below average (M = 2.48, SD = 0.869), with 32% rating it as below average and 43% average. One of the students in an interview session uttered:

> *"I have always been more inclined towards developing my core disciplined courses, focusing more on numbers and equations rather than language skills. Unfortunately, it has left me with a language level that I would describe as below average. I fight with conveying my ideas expressively in reading, writing, and verbal formats."*

Despite acknowledging the critical role of English in polytechnic education, instructors report that students' current proficiency levels fall significantly short of expected standards across multiple domains. According to teacher evaluations, 90% rate students' listening comprehension as poor, and an equal proportion identify a lack of fluency and confidence in speaking. One teacher expressed his concern as:

> *"Out of every 40 to 50 students, there are two to three students who really want to study English and do well in English. As they are concerned about their future career. The rest are poor in language skills and just want to pass the exam. The rest of the weak students are not able to improve their condition even if the teachers put a lot of pressure on them. But this situation will improve if students are more interested in English."*

Additionally, 85% note deficiencies in spoken accuracy, 65% report weak reading comprehension, and 55% highlight inadequacies in academic writing. Furthermore, 70% of instructors observe insufficient grammatical knowledge, while 75% assess students' vocabulary range as inadequate. Likewise, the alumni also stressed that polytechnic learners tend to be weaker in speaking, vocabulary, listening, and grammar skills than in writing and reading skills.

These results suggest that productive language skills (e.g., speaking and vocabulary) were perceived as less developed compared to receptive skills (e.g., listening and reading), and they highlight potential areas for targeted instructional support.

Table VI outlines the frequency and percentage of responses from Bangladeshi polytechnic engineering students regarding perceived causes of their English language weaknesses. Participants were asked to identify factors contributing to their language difficulties across six predefined categories.

The most frequently cited factor was the lack of English learning facilities in academic institutions, reported by 348 respondents. It highlights a perceived inadequacy in institutional support, including limited access to language labs, libraries, and multimedia resources. The second most reported factor was the lack of opportunities to practice English outside the classroom (n = 312), which reflects insufficient exposure to authentic communicative contexts such as language clubs, conversational interactions, or extracurricular language activities.

Q2. What do You Think are the Reasons for Weakness in English?

Table VI: Reasons for Polytechnic Students' Weakness in English

SL.	Reasons for Weakness in English				
	Options	F	P	VP	CP
1.	Lack of English learning facilities in your academic institutions	348	26.1	26.1	26.1
2.	Lack of opportunities to practice outside the classrooms	312	23.4	23.4	49.5
3.	Lack of English teachers' co-operation	203	15.2	15.2	64.8
4.	English phobia as a foreign language	101	7.6	7.6	72.4
5.	Weakness in English since childhood	195	14.6	14.6	87.0
6.	Weak syllabus of English	173	13.0	13.0	100.0
	Total	1332	100.0	100.0	

The third prominent cause was the lack of co-operation from English teachers, as indicated by 203 participants. It suggests perceived deficiencies in instructional support, motivation, and engagement from educators. Additionally, 195 respondents attributed their weakness to a long-standing difficulty in English since childhood. It reflects foundational gaps in early language education.

Another contributing factor, identified by 173 participants, was the ineffectiveness of the English syllabus, suggesting a misalignment between curriculum content and learners' needs. Finally, 101 students reported English language anxiety or phobia as a key issue, implying that psychological barriers such as fear or low self-confidence negatively impact their language acquisition and use.

Both teachers and alumni concur that polytechnic learners face significant challenges in acquiring the English language, mainly due to their disadvantaged socio-economic and cultural backgrounds. These learners have limited exposure to English, insufficient academic resources and learning facilities, and a lack of structured opportunities for language practice. One teacher uttered as:

> *"It is seen that the main reason is that English only remains in two semesters, 1st and 2nd in their first academic year. The credit for each course is only 2. Besides, the result of the first year in their diploma program contributes only 5% to their overall result. As English remains in its first year, the proportion for contribution in English goes to only 2 to 3%, which is very much scanty compared to the overall result of 100%."*

Another teacher outlined the phobia of English since childhood as:

> *"The students somehow pass English with a little study as if they want to be trouble-free. They treat it like a course of antibiotics. A big reason for this is their fear of English. Having a weak background in English, they somehow want to pass engineering subjects well. Besides, English is considered an optional subject required only for the examination to them."*

These findings reveal that students' language difficulties are influenced by a combination of institutional limitations, pedagogical gaps, curriculum inadequacies, and psychological factors.

Q3. How do you Value the Importance of Learning English for Polytechnic Engineering Students?

Table VII illustrates the Bangladeshi polytechnic engineering students' perceptions of the importance of learning the English language. The data reveal a strong consensus on its critical role in academic and professional advancement.

Table VII: Students' Perception Toward the Value of Learning English

SL.	Importance of Learning English				
	Options	F	P	VP	CP
1.	Absolutely essential	341	66.7	66.7	66.7
2.	Important	159	31.1	31.1	97.8
3.	Moderately important	10	2.0	2.0	99.8
4.	Not important at all	1	0.2	0.2	100.0
	Total	511	100.0	100.0	

A substantial majority (n = 341) regarded English as "absolutely essential," while 159 participants rated it as "very important." Only 10 respondents considered it "moderately important," and a single participant deemed it "not important at all."

During the Interview, one Student Said:

> *"In the present world, learning English is very important for all. Because in our daily activities, English is ingrained invisibly, and its existence and significance cannot be undermined. I need to develop my skills for educational achievement in my polytechnic and B.Sc phases and for my career pursuits."*

Similarly, teachers and alumni also recognized its importance for both pedagogical and professional excellence. One of the teachers opined on the importance of English as:

> *"For polytechnic engineering students, English is very important. I think they will need the English language for higher studies and the job sector as well."*

As well, one Alumnus Expressed their Need as:

> *"Some of our senior brothers who joined the Ruppur Power Plant were sent to Russia directly after joining for their first training. As the whole training is conducted in English in a foreign setting, it seems to me that English is, of course, important for both professional development and communication."*

Q4. Why are you taking this course/s?

Table VIII outlines the motivations of Bangladeshi polytechnic engineering students for enrolling in English language courses, categorized into six predefined options.

The most frequently reported reason (n = 362) is the belief that English proficiency enhances social status. It suggests that students perceive the language as a means for achieving upward social mobility and greater life opportunities, particularly in professional contexts. The second most common motivation (n = 308) is the pursuit of higher education, reflecting awareness of English as a key medium of instruction in both national and international academic institutions.

Additionally, 277 students cited improved employment prospects and financial stability as a major reason for studying English. It highlights the language's perceived value in an increasingly competitive job market. A total of 229 participants reported academic purposes, such as enhancing writing, communication, and research skills, as their primary motivation.

Table VIII: Students' Reasons for Taking the English Course/s

SL.	Reasons for Taking English Course/s				
	Options	F	P	VP	CP
1.	The course is compulsory	185	12.2	12.2	12.2
2.	For academic purposes	229	15.1	15.1	27.3
3.	Learning English will enhance your status	362	23.9	23.9	51.2
4.	Help getting a job	277	18.3	18.3	69.5
5.	For higher study	308	20.3	20.3	89.8
6.	Because learning English is interesting to me	154	10.2	10.2	100.0
	Total	1515	100.0	100.0	

A further 185 students noted that English courses were a compulsory part of their academic program, while 154 expressed a genuine interest in the language itself, including its literature and culture. Likewise, teachers and alumni viewed the course as necessary for academic, social, professional, and higher studies.

These results demonstrate the diverse and layered motivations behind English language learning, shaped by practical, academic, and personal factors. They also point to the importance of aligning English curricula with the real-world goals and needs of learners in polytechnic education.

Q5. What is your Polytechnic Background?

Table IX presents the educational backgrounds of Bangladeshi polytechnic engineering students. The majority of respondents (n = 427) reported completing SSC General, which offers a broad academic curriculum without vocational specialization. The second most common background was SSC Vocational (n = 71), indicating prior exposure to industry-specific skills. A small minority reported completing HSC Vocational (n = 11) and HSC General (n = 2), and they likely represent limited representation from higher secondary education streams.

The teachers' and alumni interview data also represent the same scenario. However, some teachers noted that, to some extent, students from madrassas and vocational backgrounds are comparable to those from the general SSC level in certain polytechnics.

Table IX: Students' Polytechnic Background

SL.	Learners' Polytechnic Background				
	Options	F	P	VP	CP
1.	SSC vocational	71	13.9	13.9	13.9
2.	SSC general	427	83.6	83.6	97.5
3.	HSC vocational	11	2.2	2.2	99.6
4.	HSC general	2	0.4	0.4	100.0
	Total	511	100.0	100.0	

Q6. How was the Learning Environment at Your Home?

Figure 7 presents participants' evaluations of the English language learning environment at home. Over half of the respondents (55.2%) reported that their home environment was *not at all helpful*, indicating a substantial lack of familial or material support for language development. A further 20.4% described it as *minimally supportive*. It suggests that while some language-related resources or encouragement may exist, they are insufficient to make a meaningful impact.

Only 14.1% of respondents found their home environment *somewhat helpful*, which reflects inconsistent or limited support. Notably, just 10.4% considered it *very helpful*, revealing that strong home-based reinforcement of English language learning is rare among these learners.

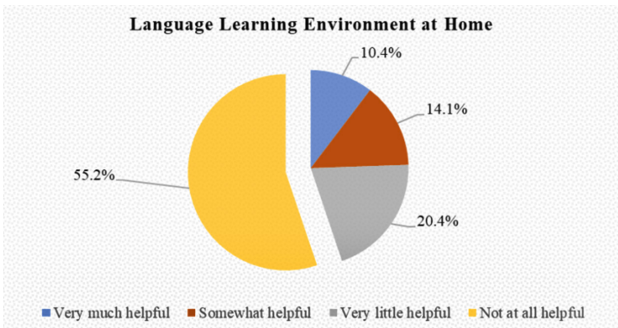

Fig. 7: Students' Perception of the Learning Environment Experienced at Their Homes

The interview data gathered from three-level participants also indicate the same scenario regarding the home atmosphere as a language learning setting. Thus, these findings highlight a critical gap in domestic language support, which likely hinders learners' ability to develop proficiency outside the classroom.

Q7. How was the Learning Environment at Your Pre-Polytechnic Level?

The pie chart illustrates students' perceptions of their language learning experiences before entering polytechnic education. According to the data, 44.2% of respondents rated the environment as "somewhat good," while only 9.8% found it "highly satisfactory." In contrast, a considerable portion expressed dissatisfaction: 31.5% rated the environment as "not good," and 14.5% found it "disappointing," together comprising 46% of the responses. During interview sessions, teachers, alumni, and current students consistently expressed concern about a notable lack of adequate exposure to language development at the school level.

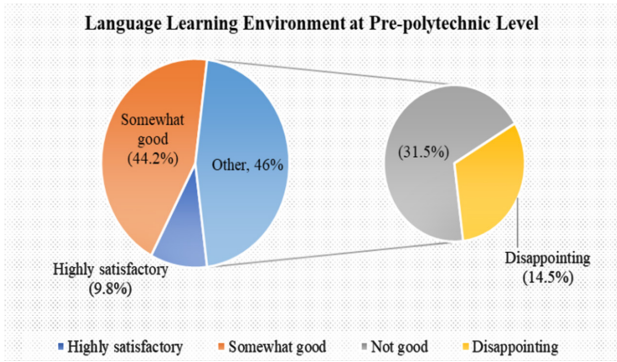

Fig. 8: Students' Perception Regarding the Learning Environment at Pre-polytechnic Level

These findings suggest that nearly half of the students perceived their pre-polytechnic language learning environment as inadequate, which underscores the need for significant improvements in early language education practices and support systems.

Q8. How many students are there in your class?

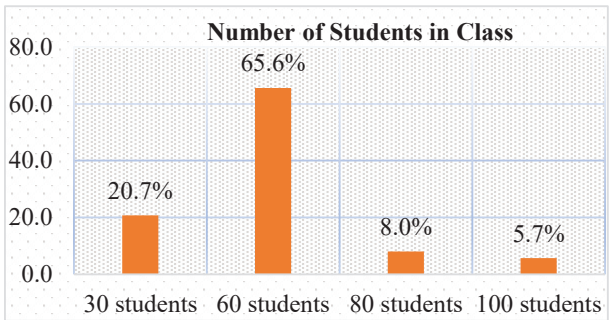

Fig. 9: Present Number of Students in Language Class

The bar chart illustrates the distribution of classroom sizes based on respondents' experiences. A significant majority (65.6%) reported being in classes of around 60 students.

It indicates the most prevalent class size in polytechnic institutes across most departments. In contrast, only 20.7% experienced smaller classes of 30 students, which are generally more conducive to personalized instruction. Larger class sizes were comparatively rare, with 8.0% and 5.7% reporting classes of 80 and 100 students, respectively. These figures suggest a predominant trend of large class sizes, which generally limit opportunities for individual engagement and pose challenges to effective language learning for Polytechnic learners.

Q9. How Frequently does the ESP Course Take Place at Your Polytechnic Institute?

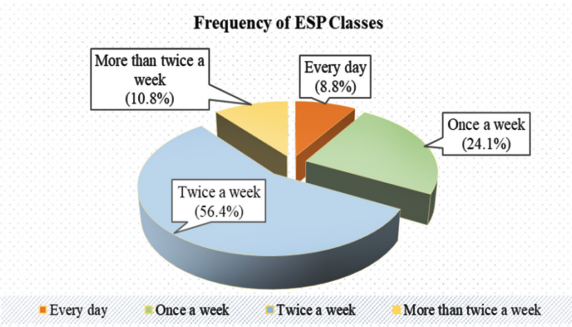

Fig. 10: Frequency of ESP Classes Held at Polytechnic Institutes

The chart presents the distribution of how often English for Specific Purposes (ESP) classes are conducted. The majority of respondents (56.4%) reported attending ESP classes twice a week. It indicates the most common scheduling pattern. A smaller portion (24.1%) noted having classes once a week, while 10.8% reported attending more than twice a week. Only 8.8% of respondents stated that ESP classes were held every day. The findings suggest that the frequency of language classes remains limited for polytechnic students in their academic contexts, potentially hindering learners' consistent language skill development.

Q10. How Many Teachers are there for the Assigned English Courses in Your Polytechnic Institution?

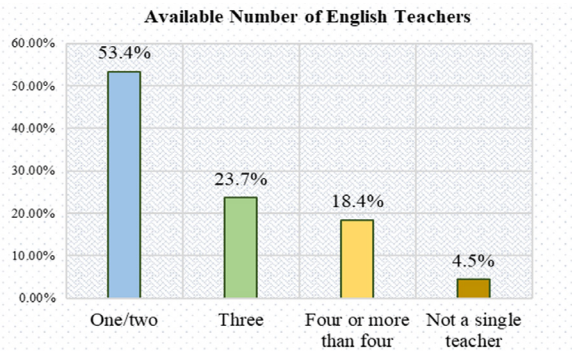

Fig. 11: Students' Perception of the Frequency of English Teachers' Availability at Polytechnic Institutes

Figure 11 illustrates that 53.4% of respondents indicated that only one or two English teachers are available to conduct ESP classes at their polytechnic institutes. Additionally, 23.7% reported access to three teachers, while 18.4% noted the availability of four or more teachers. Notably, 4.5% of respondents stated that no English teacher was available to conduct language classes.

This data reflects a significant disparity in teacher allocation, and it suggests potential challenges in ensuring consistent and effective ESP instruction at the polytechnic institutes.

Q11. Do you Think Language Learning Materials are Available in your Polytechnic Institution?

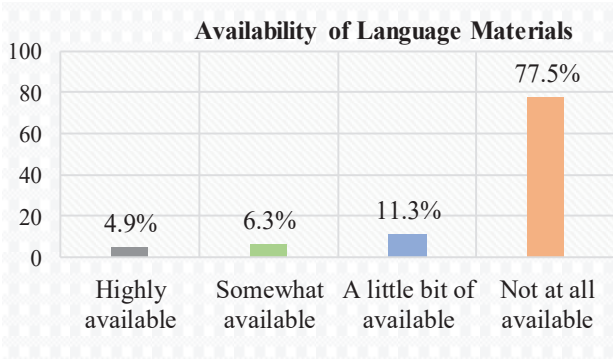

Fig. 12: Students' Perception Regarding the Availability of Language Materials

Figure 12 highlights a severe shortage of language learning materials reported by the participants. Only 4.9% of respondents indicated that such materials are readily available, and 6.3% stated they are somewhat available. An additional 11.3% noted that only a limited number of materials could be accessed. Most notably, 77.5% of participants reported a complete lack of available language learning resources.

These findings highlight a significant gap in instructional support, which can substantially hinder the language development of polytechnic engineering students. Addressing this issue is essential, as it emphasizes the need for targeted efforts to enhance the availability and accessibility of language learning materials across these institutions.

Q12. How are the Teaching Strategies, Like Pair Work, Group Discussion, and Practice, Done in Your Class?

Figure 13 shows that 74.4% of participants reported no use of teaching strategies in language classrooms.

It implies a widespread neglect of contemporary and eclectic instructional methods in polytechnic institutes. An additional 11.2% observed minimal application, while only 8.0% reported a moderate level of strategy use.

These findings indicate a notable shortfall in pedagogical planning and suggest limited implementation of effective teaching strategies, which can negatively impact the overall quality of language instruction.

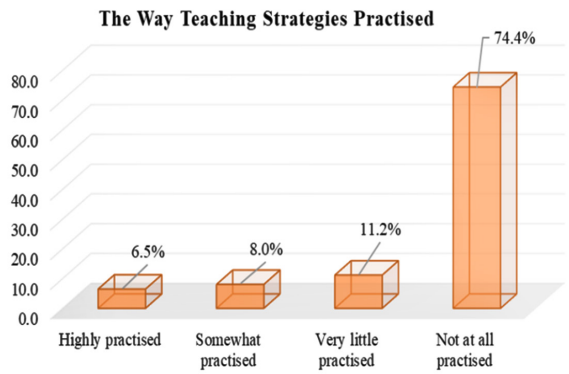

Fig. 13: Students' Perception Regarding the Teaching Strategies Practised in Language Classrooms

6. OVERALL FINDINGS AND DISCUSSIONS

This segment provides an overview of the findings, discussions, and recommendations derived from the questionnaires and interview data.

All respondents who participated in the research study unanimously agreed that the English proficiency needs of Bangladeshi polytechnic engineering students are multifaceted, primarily centered on achieving proficiency for effective academic and professional communication. It aligns with the study by Herve, where the scholar posits that English language proficiency is crucial for engineering learners, particularly for educational and professional purposes [47]. To keep pace with global academic and professional standards, students prioritize developing speaking and communication skills, followed by writing, reading, and listening abilities.

Answer to Research Question 1: What are the socio-economic, psychological, and pedagogical factors that influence the language proficiency levels of diploma engineering students as assessed through the PSA framework?

Regarding the present situation analysis (PSA) based on socio-economic and psycho-social prospects, it has been found that most of the students are from disadvantaged socio-economic, educational, and cultural backgrounds, as reflected in [22], [24], and [39]. Patil noted that a significant proportion of engineering learners are weak in English, as 75% come from rural socio-economic backgrounds [22].

Although the polytechnic learners showed intrinsic interest in the language and a desire to acquire language proficiency, their PSA reveals that most of the learners' grammar, vocabulary, listening, speaking, reading, and writing skills are *"below average"* or *"poor."* The data findings indicate that polytechnic learners rarely receive proper language exposure during their childhood and pre-polytechnic educational phases due to their poor socio-economic backgrounds and limited institutional support. Thus, the reasons for their weakness in English are outlined as the lack of socio-cultural, instructional, and educational support.

Moreover, the polytechnic student population represents a diverse range of educational backgrounds, including SSC General, SSC Vocational, HSC General, and SSC Dakhil (a religious or madrasa stream). This heterogeneity presents challenges in uniformly assessing language proficiency levels. The study indicates that students from SSC General backgrounds generally demonstrate stronger English language skills than those from vocational or religious education. This disparity suggests a poor intake system for polytechnic learners, where both students and teachers face challenges in demonstrating and practicing language skills in classrooms.

Polytechnic learners face several pedagogical challenges that hinder their language development. The key issues identified include inadequate teaching and learning facilities at the research sites, a limited frequency of language classes (typically only one or two sessions per week), and an insufficient number of qualified language instructors. Additional constraints include the absence of pair and group activities, a lack of structured feedback mechanisms, overcrowded classrooms that often accommodate around 60 students, and the scarcity and inaccessibility of language learning materials. Furthermore, limited opportunities for language practice outside the classroom exacerbate these challenges. The interview data also revealed that the frequent use of Bangla during English classes, along with an outdated and poorly structured syllabus and curriculum, further impede effective language acquisition.

Answer to Research Question 2: How do they affect their academic and professional competence?

The study findings indicate that the language competence of polytechnic learners is unsatisfactory, which has an adverse impact on their academic and professional performance. A majority of students report experiencing anxiety when using English in educational and professional contexts. It leads to reduced confidence and hesitation in communication. Consequently, they often exhibit a sense of inertia or reluctance in comparison to their peers. One of the alumni expressed his concern like this:

> *"In my profession, the problem I face is that we are habituated to speaking Bengali. So, when I suddenly start talking in English, I face difficulties, shyness, or nervousness. Sometimes, L1 interference does often happen frequently. This case happens not just with me but mostly with others in my profession. It happens because we did not get any scopes to practice at our earlier institutions and are not habituated to speaking English; rather, we do use Bengali."*

Answer to Research Question 3: What are the probable solutions to address these factors**?**

Recognizing the promising potential of English for academic and career advancement, the surveyed and interviewed participants offer prospective solutions to address the aforementioned issues. They are outlined as:

- The upgradation and modification of the language syllabus and curriculum;
- Increasing the language credit hours and classes;
- Using English as EMI in polytechnic institutes and avoiding teaching English using the L1, Bengali;
- Integrating extensive and advanced English language skills into the polytechnic engineering curriculum;
- Creating interactive, standard, authentic, and easily accessible language learning materials;
- Using multimedia-enhanced language classrooms;
- Providing support and guidance from teachers;
- Increasing interaction and communication between teachers and students;
- Creating opportunities for out-of-class practice sessions;
- Creating opportunities for English sessional or lab classes;
- Altering the language assessment systems and focusing on small-scale assessments like quizzes, language puzzles, language games, presentations, debates, role-playing, mock-viva, story-telling, etc.
- Ensuring more listening and speaking opportunities;
- Recruiting more skilled and proficient language teachers and facilitating teacher training in resource-scarce settings;
- Introducing sessions at regular intervals with the guardians to let them know the sources and resources on how they can assist their children in teaching and supporting language education at home;
- Ensuring remedial support as constructive feedback on learners' errors and mistakes;
- Inclusion of technical registers or jargon;
- Improving the overall communication strategies of polytechnic learners.

7. CONCLUSION

In this study, the researcher aims to identify the key determinants of English language learning among selected polytechnic engineering students in Bangladesh using the PSA framework. Here, she considers the socio-economic, psycho-social, and pedagogical factors to determine the challenges. To address this, she formulated three research questions. The scholar used qualitative interviews and quantitative questionnaire survey data as part of a mixed-methods research. She collected data from the current polytechnic students, language instructors, and alumni students to focus on the respective research questions.

The triangulation of quantitative and qualitative data from the three-level participants (students, teachers, and alumni) shows that polytechnic learners are highly motivated to learn and develop English language proficiency. However, in most cases, they lag behind due to inadequate socio-cultural, economic, educational, instructional, and institutional support during their pre-polytechnic and polytechnic educational phases. As a result, their expertise in grammar, vocabulary, listening, speaking, and reading skills appears dissatisfactory, marking the levels as *"below average"* and *"poor."* The primary challenges they encounter revolve around issues such as an inadequate language curriculum with minimal credit allocation and a scarcity of classroom hours, the use of sub-standard language contents and materials, a deficiency of qualified language instructors, the utilization of Bengali (L1) as the medium of instruction (MOI) in language classrooms, too many students in one class, few language classes, lack of pair and group activities, lack of language lab sessions, and limited opportunities for practical sessions. Finally, some groundbreaking

recommendations; syllabus modification, more credit hour allocation, use of English as EMI, availability of language materials, recruiting more language teachers, providing feedback, focusing on communicative skills, ensuring out-of-class practices, and ensuring more structured assessment systems are proposed for polytechnic engineering learners in Bangladesh. It is expected that this will help the ELT teachers, practitioners, and concerned authorities take the necessary initiatives to determine and remove their specific English language barriers. Consequently, it will result in a significant segment of the Bangladeshi population becoming a proficient and skilled workforce, thereby substantially contributing to the nation's sustainable economic growth and global social standing.

REFERENCES

[1] J. Jenkins, The phonology of English as an international language. Oxford University Press, 2000.

[2] J. Jenkins, English as a Lingua Franca: Attitude and Identity. Oxford: Oxford University Press, 2007.

[3] A. Mauranen, "Academic English as lingua franca—a corpus approach," TESOL Quarterly, Vol. 37, No. 3, pp. 513-527, 2003.

[4] A. Mauranen, "English as lingua Franca: an unknown language?" in Identity, Community, Discourse: English in Intercultural Settings, pp. 269-292, 2005.

[5] A. Mauranen, "A rich domain of ELF-the ELFA corpus of academic discourse," Nordic Journal of English Studies, Vol. 5, No. 2, pp. 145-59, 2006.

[6] B. Seidlhofer, "Closing a conceptual gap: The case for a description of English as a lingua franca," International Journal of Applied Linguistics, Vol. 1, No. 2, pp. 133-158, 2001.

[7] B. Seidlhofer, "Research perspectives on teaching English as a lingua franca," Annual Review of Applied Linguistics, Vol. 24, pp. 209-239, 2004.

[8] B. Seidlhofer, Understanding English as a Lingua Franca: A complete introduction to the theoretical nature and practical implications of English used as a lingua franca. Oxford University Press, 2011.

[9] D. Graddol, Why Global English may Mean the End of "English as a Foreign Language." United Kingdom: British Council, 2006.

[10] D. Crystal, English as a Global Language, 2nd ed. Cambridge: Cambridge University Press, 2003.

[11] T. A. Chowdhury and M. Z. Haider, "A need-based evaluation of the EAP courses for the pharmacy students in the University of Asia Pacific (UAP), Bangladesh," Asian Social Science, Vol. 8, No. 15, pp. 93–104, 2012.

[12] M. Hassan and K. A. Mostafa, "ESP and needs analysis: Teaching English to engineering students in Bangladesh," MIST International Journal of Science and Technology, Vol. 4, No. 1, 2019.

[13] M. Seraj et al., "Students' low proficiency in spoken English in private universities in Bangladesh: reasons and remedies," Language Testing in Asia, Vol. 11, article 1, 2021.

[14] N. S. Eza, "The challenges of teaching ESP in Bangladesh: a critical observation," Master's thesis, Brac University, 2021.

[15] E. Zikmundová, English as a lingua franca: Theory and practical implications, 2016.

[16] A. Cogo and M. Pitzl, "English as a lingua Franca (ELF)," International Journal of Applied Linguistics, Vol. 22, No. 2, pp. 284–285, 2012.

[17] M. Dahbi, "Towards an ESP course for engineering students in vocational schools in Morocco: The case of the National School of Applied Sciences," Arab World English Journal, 2016.

[18] R. Pritchard and A. Nasr, "Improving reading performance among Egyptian engineering students: Principles and practice," English for Specific Purposes, Vol. 23, No. 4, pp. 425–445, 2004.

[19] P. Comyn, "Skills, employability and lifelong learning in the Sustainable Development Goals and the 2030 labour market," International Journal of Training Research, Vol. 16, No. 3, pp. 200–217, 2018.

[20] H. Kassim and F. Ali, "English communicative events and skills needed at the workplace: Feedback from the industry," English for Specific Purposes, Vol. 29, No. 3, pp. 168–182, 2010.

[21] T. Hua and S. Beverton, "General or vocational English courses for Taiwanese students in vocational high schools? Students' perceptions of their English courses and their relevance to their future careers," Educational Research for Policy and Practice, Vol. 12, No. 2, pp. 101–120, 2013.

[22] D. Allison, "Pragmatist discourse and English for academic purposes," English for Specific Purposes, Vol. 15, No. 2, pp. 85–103, 1996.

[23] S. Benesch, Critical English for Academic Purposes: Theory, Policies and Practice. London: Lawrence Erlbaum, 2001.

[24] M. J. Riemer, "English and communication skills for the global engineer," Global Journal of Engineering Education, Vol. 6, No. 1, pp. 91–100, 2002.

[25] M. R. Patil, "Importance of English communication for engineering students from rural areas and its remedies," IOSR Journal of Mechanical and Civil Engineering, pp. 35–38, 2014.

[26] Bangladesh Bureau of Educational Information and Statistics [BANBEIS], Bangladesh Education Statistics 2021, Mar. 23, 2022.

[27] M. A. R. Forhad, G. M. Alam, M. Rashid, A. Haque, and M. S. K. S. Khan, "Sustainable development in higher engineering education: A comparative study between private and public polytechnics," Sustainability, Vol. 14, No. 13, p. 8094, 2022.

[28] R. Chowdhury and S. Farooqui, "Teacher training and teaching practice: The changing landscape of ELT in secondary education in Bangladesh," English Language Education in South Asia: From Policy to Pedagogy, pp. 147–159, 2011.

[29] M. K. Hasan, A linguistic study of English language curriculum at the secondary level in Bangladesh: A comparative approach to curriculum development, Doctoral dissertation, Aligarh Muslim Univ., 2004.

[30] A. G. Clement and T. Murugavel, "English for employability: A case study of the English language training need analysis for engineering students in India," English Language Teaching, Vol. 8, No. 2, pp. 116–125, 2015.

[31] M. C. Midoul, Needs analysis of engineering students at ENSAM, Master's thesis, Moulay Ismail Univ., Morocco, 2013.

[32] H. Chowdhury and F. Alam, "Engineering education in Bangladesh – an indicator of economic development," European Journal of Engineering Education, Vol. 37, No. 2, pp. 217–228, 2012.

[33] A. Neelim and T. Siddiqui, Situation Analysis of Migration Context & Policy Framework in Bangladesh, Dhaka, Bangladesh: International Organization for Migration, 2015.

[34] T. Hutchinson and A. Waters, English for Specific Purposes: A Learning-Centered Approach, Cambridge: Cambridge University Press, 1987.

[35] A. M. Johns and M. A. S. Nodoushan, "English for Specific Purposes: The state of the art (An online interview with Ann M. Johns)," Int. J. Lang. Stud., Vol. 9, No. 2, pp. 113–120, 2015.

[36] P. Robinson, ESP Today: A Practitioner's Guide, Hemel Hempstead: Prentice Hall International, 1991.

[37] T. Dudley-Evans and M. J. St John, Developments in English for Specific Purposes: A Multidisciplinary Approach. Cambridge, U.K.: Cambridge Univ. Press, 1998.

[38] R. Richterich and J. L. Chancerel, Identifying the Needs of Adults Learning a Foreign Language, Strasbourg: Council for Cultural Co-operation of the Council of Europe, 1978.

[39] J. McDonough, ESP in Perspective: A Practical Guide, London and Glasgow: Collins Educational, 1984.

[40] S. D. Krashen, Principles and Practice in Second Language Acquisition, Oxford: Pergamon Press, 1982.

[41] J. D. Brown, Introducing Needs Analysis and English for Specific Purposes, London: Routledge, 2016.

[42] M. Kafle, "EAP in Nepal," in English for Academic Purposes (EAP) in Asia, I. Liyanage and T. Walker, Eds., Rotterdam: SensePublishers, pp. 53–66, 2014.

[43] S. Canagarajah and H. Ashraf, "Multilingualism and Education in South Asia: Resolving Policy/ Practice Dilemmas," Annu. Rev. Appl. Linguist., Vol. 33, pp. 258–285, 2013.

[44] F. Shamim, "English as the language for development in Pakistan: Issues, Challenges and possible solutions," in Dreams and Realities: Developing Countries and the English Language, H. Coleman, Ed., London: British Council, 2011, pp. 291–310.

[45] J. Cenoz and D. Gorter, "A Holistic Approach to Multilingual Education: Introduction," Mod. Lang. J., Vol. 95, No. 3, pp. 339–343, 2011.

[46] S. S. Shukor, "ESL students' perceptions on the use of Facebook as a collaborative writing tool in improving writing performance," Asian Journal of English Language and Pedagogy (AJELP), Vol. 3, pp. 205–227, 2015.

[47] C. Herve, "The importance of English for engineering students," NUS Blog, Jan. 27, 2009.

Impact of Back Surface Layers on the Performance of $Zn_xcd_{1-X}s/Cu_2SnS_3$ (CTS) Solar Cell

Md. Sharafat Hossain[1*], Rosni Roman Wahid[1], Md. Simul Hasan Talukder[1] and Md. Nasim Adnan[2]

[1]Department of Electrical and Electronic Engineering, Dhaka University of Engineering & Technology, Gazipur, Bangladesh
[2]Department of Computer Science and Engineering, Jashore University of Science & Technology, Bangladesh

ABSTRACT

The project focuses on the potentiality of CTS absorber layer in a $Zn_xCd_{1-x}S$/CTS solar cell, incorporating a back surface reflector (BSR), was explored through numerical simulations using the AMPS-1D (Analysis of Microelectronic and Photonic Structures) simulator. CTS has been identified as a favorable candidate among thin-film materials due to its optimal direct bandgap, high absorption coefficient, and suitable electronic properties. The primary objective of this study was to improve the cell output parameters of $Zn_xCd_{1-x}S$/CTS photovoltaic (PV) cell with micro-range absorber layers, aiming to significantly reduce production costs. The targeted $Zn_xCd_{1-x}S$/CTS PV cell shows 21.592% efficiency (V_{oc} = 1.049 V, J_{sc} = 27.841 mA/cm^2, FF = 0.805) with a 1 µm thick CTS absorber and without a back surface reflector (BSR). However, the proposed structures integrating with BSR configurations demonstrated promising results even with ultra-thin absorbers. Arsenic telluride (As_2Te_3) was selected as the BSR material for further investigation. The As_2Te_3-based BSR demonstrated a notable improvement in performance, achieving an efficacy of 23.433% (V_{oc} = 1.06 V, J_{sc} = 29.503 mA/cm^2, FF = 0.819) by an ultra-thin CTS absorber thickness of only 1 µm. It was also observed that increasing operating temperature significantly affects solar cell performance. Among the investigated configurations, the cell with BSR exhibited better thermal stability than the cell without BSR, with thermal tangent of -0.12%/^{0}K and -0.19%/^{0}K respectively. These simulation outcomes provide valuable insights into the feasible fabrication of cost-effective, non-toxic, highly efficient and thermal stable CTS-based cells.

1. INTRODUCTION

The second-generation thin-film material, Cu_2ZnSnS_4 (CZTS), has drawn substantial attention from contemporary researchers due to its favorable properties, making it a strong candidate as an absorber layer in thin-film solar cells. As a p-type quaternary semiconductor, CZTS exhibits excellent photovoltaic characteristics, including a high absorption coefficient exceeding 10^4 cm^{-1} and a direct bandgap ranging from approximately 1.4 to 1.56 eV [1–2], aligning well with the optimal range for single-junction solar cell applications. In recent years, CZTS has been widely explored as an eco-friendly and cost-effective alternative to conventional materials like CIGS and CdTe, as it consists of earth-abundant and non-toxic elements. However, one of the key challenges with CZTS is its narrow thermodynamic stability range, which often results in the formation of undesirable secondary phases such as binary compounds (CuS, SnS, SnS_2, ZnS) and ternary phases like Cu_2SnS_3 during its synthesis [3–6].

To address these limitations, researchers have been investigating other absorber materials that are both non-toxic and abundantly available. Among these, copper tin sulfide (Cu_2SnS_3 or CTS) has emerged as a promising alternative. Notably, CTS shares a similar crystal structure with CZTS and offers a direct bandgap in the range of 0.9 to 1.4 eV—close to the ideal value for photovoltaic applications. Additionally, CTS possesses a high absorption coefficient and p-type conductivity, making it a viable material for solar energy conversion [3, 6]. Interestingly, CTS can exhibit multiple crystal phases, such as cubic, monoclinic, tetragonal, triclinic, and hexagonal structures, where variations in cation and anion ordering influence its bandgap properties [7–12]. Several physical and chemical deposition techniques have been employed to fabricate CTS thin films, enhancing its applicability in photovoltaic technologies [6, 9, 11, 12–15]. Compared to these above-mentioned properties, CTS is one of the best choices of the current researcher as an absorber layer for the next generation thin film solar cells. Currently, the key objective of PV research and

*Corresponding author's email: sharafat@duet.ac.bd

development is to design and fabricate solar cells that are commercially feasible by meeting three central criteria: high efficiency, cost-effectiveness and stable operating capacity. Reducing the thickness of the CTS absorber layer can significantly decrease the amount of material required, thereby lowering fabrication costs. Minimizing the thickness of various layers in the overall solar cell structure not only cuts down on production expenses, energy consumption, and manufacturing time but also reduces the total material usage. These combined benefits contribute to making solar cells more affordable and accessible. In considering window material, conventional cadmium sulfide (CdS) presents several limitations when used as the window layer in CdTe/CTS-based thin-film solar cells. Among numerous limitations, the lattice mismatch between CdS and CdTe/CTS is approximately 10%, which introduces a high density of structural defects at their junction, adversely affecting cell performance. Due to these drawbacks, researchers have turned their attention to alternative window materials that offer higher bandgaps and better lattice compatibility. Some promising candidates include ZnS (bandgap ~3.70 eV), ZnSe (~2.69 eV), and the alloyed compound ZnxCd1-xS, which allows bandgap tuning between 2.42 and 3.70 eV depending on composition. Therefore, investigating the limits of CTS absorber layer thinning will be a central focus of this project. The theoretical and experimental efficiency of CTS thin film solar cell is increasing day by day in recent years [16-18]. Its efficiency remains far below the theoretical limit, and it has not yet been introduced commercially. Considering the potential for future commercialization of CTS technologies, attention has been directed towards developing a new device structure consisting of Glass/TCO/Front contact buffer layer/$Zn_xCd_{1-x}S$/CTS/Back Surface Reflector (BSR)/ suitable metal contact with promising window layer of $Zn_xCd_{1-x}S$. Efforts have been deliberately concentrated on optimizing the various layers of this proposed CTS solar cell to enhance its efficiency. Therefore, the aim of this project is to investigate a novel $Zn_xCd_{1-x}S/Cu_2SnS_3$ thin-film solar cell design, targeting improved conversion efficiency and reduced costs by minimizing the thickness of the material layers. Consequently, a novel device architecture featuring ultra-thin CTS layers with a back surface reflector (BSR) Glass/TCO/$Zn_2SnO_4/Zn_xCd_{1-x}S$/CTS/As_2Te_3/Al has been proposed, with various strategies being explored to enhance efficiency through improved cell designs. This work focuses on the analysis of Glass/TCO/$Zn_2SnO_4/Zn_xCd_{1-x}S$/CTS/As_2Te_3/Al using a computational modeling approach. Numerical simulation serves as a powerful tool for examining how variations in material characteristics impact device performance, enabling researchers to assess design feasibility, fine-tune structural parameters, and predict overall device behavior before physical fabrication. In this investigation, simulations were conducted using the AMPS-1D (Analysis of Microelectronic and Photonic Structures) [19] platform to evaluate how the thickness and charge carrier concentration of the monoclinic CTS absorber layer influence key performance metrics. In addition, the effect of varying the buffer layer thickness was examined to identify the most suitable option for forming an effective interface with the monoclinic CTS absorber and to determine its contribution to cell efficiency. Key output parameters, including open-circuit voltage (V_{oc}), short-circuit current density (J_{sc}), fill factor (FF), and power conversion efficiency (Eff), were systematically recorded and analyzed to assess the overall behavior of the proposed configurations.

2. METHODOLOGY

Before physically fabricating a solar cell, conducting a numerical investigation is a crucial step for evaluating how different design parameters influence device behavior and for identifying optimal configurations in a cost-effective manner. In the present study, simulations of $Zn_xCd_{1-x}S$/CTS thin-film solar cells were performed using the AMPS-1D software (Analysis of Microelectronic and Photonic Structures), a computational tool originally developed by Stephen Fonash and colleagues at Pennsylvania State University in 1999 [19]. This one-dimensional simulator is capable of modeling a wide variety of device structures, including heterojunctions, homojunctions, multijunction systems, and Schottky barrier-based solar cells. Users define the properties of each material layer in the simulated device, allowing for detailed customization of the model. AMPS-1D has been widely recognized and adopted across research groups due to its strong ability to replicate the physics and behavior of crystalline, polycrystalline, and amorphous photovoltaic devices. It utilizes finite difference methods along with the Newton-Raphson iterative approach to solve the coupled one-dimensional continuity and Poisson's equations for charge carriers. By inputting accurate material data, the software can compute essential device metrics such as open-circuit voltage (V_{oc}), short-circuit current density (J_{sc}), fill factor (FF), and efficiency (Eff), along with internal device characteristics including space charge region profiles, charge generation and recombination dynamics, and spectral response.

As shown in Fig. 1, the updated solar cell configuration includes an additional buffer layer—Zn_2SnO_4—inserted between the SnO_2 front contact and the $Zn_xCd_{1-x}S$ window layer. This modification aims to improve the effectiveness of the ultra-thin $Zn_xCd_{1-x}S$ layer. Additionally, although SnO_2 continues to serve as the transparent conductive oxide (TCO) at the front of the device, its thickness has been significantly reduced from the conventional 500 nm to 100 nm to help optimizing the cell's overall performance.

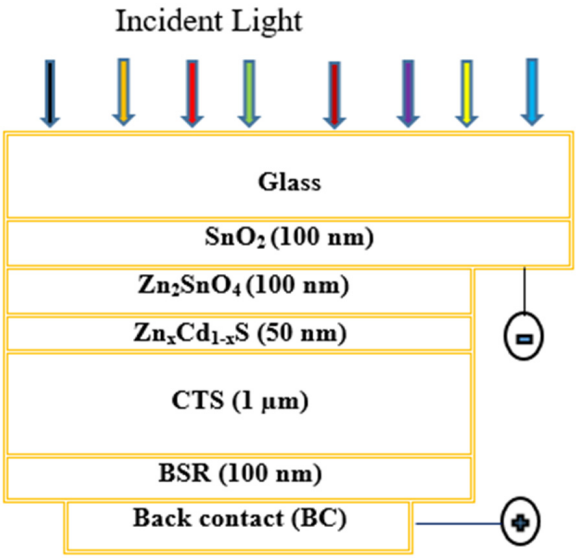

Fig. 1: Structures of the Proposed $Zn_xCd_{1-x}S$/CTS Cell for Enhanced Performance

To construct the front contact of the solar cell, SnO_2 is combined with a buffer layer of Zn_2SnO_4. The traditional CdS window layer has been replaced by $Zn_xCd_{1-x}S$, with the composition 'x' optimized for enhanced cell performance. The absorber layer is based on copper tin sulfide (CTS), selected due to its eco-friendly composition, economic viability, promising efficiency, and wide availability in nature. To mitigate performance limitations such as rollover effects, thermal instability, and minority carrier losses at the rear interface, specially chosen back surface reflector (BSR) layers [20, 21] have been incorporated into the redesigned ultra-thin $Zn_xCd_{1-x}S$/CTS configuration.

Instead of using costly gold (Au) as the rear electrode, aluminum (Al) has been adopted to maintain the necessary barrier height while significantly lowering production costs. Given the complexity of the simulation, which involves tuning over 50 individual parameters [22], many variables were fixed to realistic values to simplify the model. Identifying these constants was challenging because many are sensitive to fabrication techniques and can vary between batches. The values used for simulation inputs—sourced from published literature, theoretical analysis, or practical assumptions—are detailed in Tables I and II.

At this point in the study, it becomes critical to identify the most suitable value of 'x' in the $Zn_xCd_{1-x}S$ window layer using the input parameters provided in Table II. The simulation process involved systematically modifying the thicknesses of different layers: the CTS absorber thickness was explored in the range of 100 nm to 3 µm; the $Zn_xCd_{1-x}S$ window layer varied between 25 nm and 200 nm; the Zn_2SnO_4 buffer layer was adjusted from 25 nm up to 500 nm; and the SnO_2 front contact layer was tuned within the same thickness range. All remaining parameters were kept fixed, as outlined in Table I.

The scope of analysis also extended to the effects of doping concentration in the absorber layer, variations in minority carrier lifetime, bandgap shifts within the absorber, and performance response to changing operational temperatures. There remains strong potential for improving $Zn_xCd_{1-x}S$/CTS solar cell performance by optimizing critical parameters such as open-circuit voltage (Voc), short-circuit current (Jsc), and fill factor (FF). This can be accomplished through refinement of the front contact buffer layers (Zn_2SnO_4) and the back surface reflector (BSR) layer (As_2Te_3). All simulations were carried out using the AMPS-1D modeling platform. Detailed interpretation of these results follows in the next section.

Table I: Different Layers' Properties used for Numerical Modelling

Parameter	n-SnO_2	n-ZnO	p-CTS	BSR (As_2Te_3)	Comments and references
W (µm)	0.025-0.5	0.025-0.5	0.1-3.0	0.1	Theory & estimations
$\varepsilon/\varepsilon_0$	9.0	9.0	10	20	[23], [3], [16], [24]
μ_e (cm^2/Vs)	100	100/32	100	500	[23], [3], [16], [24]
μ_p (cm^2/Vs)	25	25/03	25	210	[23], [3], [16], [24]
n,p (cm^{-3})	1×10^{17}	1×10^{19}	1×10^{14}~1×10^{16}	6.8×10^{19}	[23], [3], [16], [24]
E_g (eV)	3.60	3.0/3.35	0.9-1.4	0.6	[23], [3], [16], [24]
N_c (cm^{-3})	2.2×10^{18}	2.2×10^{18}	2.2×10^{18}	1×10^{16}	[23], [3], [16], [24]
N_v (cm^{-3})	1.8×10^{19}	1.8×10^{19}	1.8×10^{19}	1×10^{17}	[23], [3], [16], [24]
χ (eV)	4.5	4.35/4.50	4.77	4.0	[23], [3], [16], [24]

Table II: Material Properties [24-25] of n-$Zn_xCd_{1-x}S$ used for Simulation

Parameter	x = 0.05	x = 0.08	x = 0.1	x = 0.2	x = 0.3	x = 0.5	x = 0.6	x = 0.8
W (μm)	0.1	0.1	0.1	0.1	0.1	0.1	0.1	0.1
$\varepsilon/\varepsilon_0$	9.3	9.3	9.3	9.3	9.3	9.3	9.3	9.3
$\mu_e(cm^2/Vs)$	100	100	95	85	75	70	65	60
$\mu_p(cm^2/Vs)$	40	40	35	30	25	20	15	10
n,p (cm^{-3})	3.0×10^{16}	2.5×10^{16}	2.5×10^{16}	1.7×10^{16}	1.6×10^{16}	4.1×10^{15}	2.5×10^{15}	1.7×10^{15}
E_g (eV)	2.48	2.50	2.55	2.58	2.64	2.70	3.07	3.33
N_c (cm^{-3})	2.1×10^{18}	2.1×10^{18}	2.1×10^{18}	2.1×10^{18}	2.1×10^{18}	2.1×10^{18}	2.1×10^{18}	2.1×10^{18}
N_v (cm^{-3})	1.7×10^{19}	1.7×10^{19}	1.7×10^{19}	1.7×10^{19}	1.7×10^{19}	1.7×10^{19}	1.7×10^{19}	1.7×10^{19}
χ (eV)	4.47	4.46	4.44	4.38	4.32	4.26	4.14	4.02

3. RESULTS AND DISCUSSIONS

To develop a high-efficiency solar cell, a $Zn_xCd_{1-x}S$ /CTS configuration was adopted using a superstrate design. This approach emphasized the strategic arrangement and optimization of individual layers, including reduced thicknesses and the integration of experimentally validated doping concentrations. Improvements were also made to the front and rear contact interfaces. In this updated structure, commercially available SnO_2 was chosen as the front contact material, with its thickness reduced from 500 nm to 100 nm to enhance overall performance of the solar cell. The window layer consisted of $Zn_xCd_{1-x}S$, while CTS functioned as the primary absorber layer. To limit the forward leakage current often associated with ultra-thin $Zn_xCd_{1-x}S$ layers, the window thickness was constrained to 50 nm. A Zn_2SnO_4 buffer layer was introduced between SnO_2 and $Zn_xCd_{1-x}S$, serving the dual purpose of charge carrier management and acting as a back surface layer (BSR). Further tuning of the window composition revealed that a 30% zinc concentration yielded optimal performance improvements.

3.1 Front Contact's Buffer Layer Selection

To enhance the efficiency of $Zn_xCd_{1-x}S$ /CTS thin-film solar cells, the window layer thickness was reduced to minimize parasitic absorption. However, excessive thinning can cause forward leakage due to pinhole formation—though less severe than in CdS-based layers. To counter this, a high-resistivity Zn_2SnO_4 buffer was added between SnO_2 and $Zn_xCd_{1-x}S$. This design improves structural quality by promoting larger grain growth and maintains good lateral current collection via the SnO_2 front contact. Simulations using AMPS-1D, with a 1 μm CTS absorber, 50 nm $Zn_xCd_{1-x}S$ window, and 100 nm SnO_2 front layer, showed that both doped and undoped Zn_2SnO_4 buffers yield comparable performance. The resulting J–V characteristics are shown in Fig. 2.

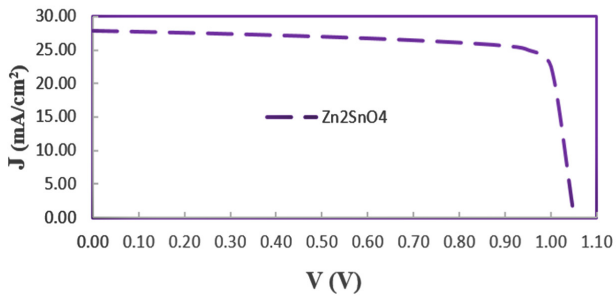

Fig. 2: Influence of Zn_2SnO_4 on J-V Curve of $Zn_xCd_{1-x}S$/CTS Solar Cell

Additional simulations were conducted to investigate the influence of buffer layer thickness on the overall performance of the solar cell. The results indicated that the primary performance indicators remained relatively consistent when the Zn_2SnO_4 buffer thickness varied between 25 nm and 500 nm. Moreover, the spectral response (SR) exhibited minimal variation across this range, suggesting that even a relatively thin buffer layer is sufficient to maintain optimal device operation. Considering practical aspects of fabrication, a buffer thickness of 100 nm was chosen as the standard for all devices in this study, as it offers a favorable compromise between efficiency and ease of manufacturability.

3.2 Optimization of Zn, Cd ratio in $Zn_xCd_{1-x}S$ Window Layer

In the proposed enhanced $Zn_xCd_{1-x}S$/CTS solar cell design, an additional Zn_2SnO_4 layer is introduced between the SnO_2 and $Zn_xCd_{1-x}S$ layers. To analyze the effect of varying zinc concentration (x) on the device's conversion efficiency, numerical simulations were performed for values of x ranging from 0 to 1. The simulations utilized material and device parameters detailed in Table II, based on data reported in references [24-25]. The modeled structure included a 1 μm thick CTS absorber layer, a 100 nm Zn_2SnO_4 buffer layer, and an aluminum (Al) rear metal contact.

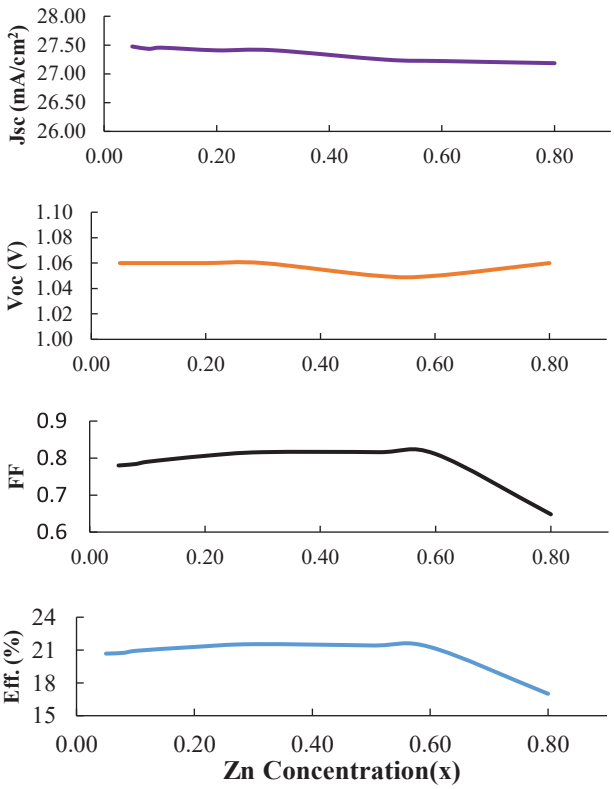

Fig. 3: Impact of Zn Concentration on $Zn_xCd_{1-x}S$/CTS Cell Output Parameters

As illustrated in Fig. 3, the solar cell demonstrated improved performance metrics—namely, higher conversion efficiency, open-circuit voltage (V_{oc}), and fill factor (FF)—at lower zinc concentrations ($x \leq 0.3$). The short-circuit current density (Jsc) remained relatively stable up to x = 0.3 but showed a gradual decline as the zinc content increased beyond this point. Specifically, the simulation yielded efficiencies of 20.672% (V_{oc} = 1.06 V, J_{sc} = 27.475 mA/cm², FF = 0.780) for x = 0.05 and 21.537% (V_{oc} = 1.06 V, J_{sc} = 27.410 mA/cm², FF = 0.816) for x = 0.3. Furthermore, the resistivity of the $Zn_xCd_{1-x}S$ layer was observed to rise substantially, from 1 Ω·cm at x = 0 to approximately 10^{10} Ω·cm at x = 1 [26]. Considering the combined impact of fabrication feasibility, electrical resistivity, and simulation results, a zinc concentration of x = 0.3 was identified as optimal for the window layer. Accordingly, all subsequent device configurations presented in the following section adopt $Zn_xCd_{1-x}S$ with x = 0.3.

3.3 Effect of $Zn_xCd_{1-x}S$ Window Layer's Thickness

This study also examined the impact of the $Zn_xCd_{1-x}S$ (x=0.3) window layer thickness on the overall performance of the solar cell. To assess this, simulations were conducted with the window layer thickness varied between 25 nm and 200 nm. The device architecture for the simulations included a 1 µm CTS absorber layer, a 100 nm Zn_2SnO_4 buffer layer, a 100 nm SnO_2 front contact, and an aluminum (Al) rear electrode. The results of these simulations are presented in Fig. 4. As shown in Fig. 4, increasing the thickness of the $Zn_xCd_{1-x}S$ (x = 0.3) window layer led to a clear decrease in short-circuit current density (Jsc) and overall conversion efficiency, while the fill factor (FF) remained nearly constant. Interestingly, the open-circuit voltage (Voc) initially increased with greater thickness but began to decline after reaching a certain threshold. This trend is attributed to the fact that a thicker window layer absorbs more incident photons before they can reach the CTS absorber, thereby reducing the generated photocurrent. In contrast, thinner $Zn_xCd_{1-x}S$ layers improve efficiency mainly due to enhanced Jsc. However, extremely thin layers can develop pinholes, potentially resulting in forward leakage currents. To counteract this, a high-resistivity Zn_2SnO_4 buffer was included between the SnO_2 and $Zn_xCd_{1-x}S$ layers. Balancing fabrication feasibility with device performance, a window layer thickness of 50 nm for $Zn_xCd_{1-x}S$ (x = 0.3) was determined to be optimal, yielding a conversion efficiency of 21.592%, with V_{oc} = 1.049 V, J_{sc} = 27.841 mA/cm², and FF = 0.805.

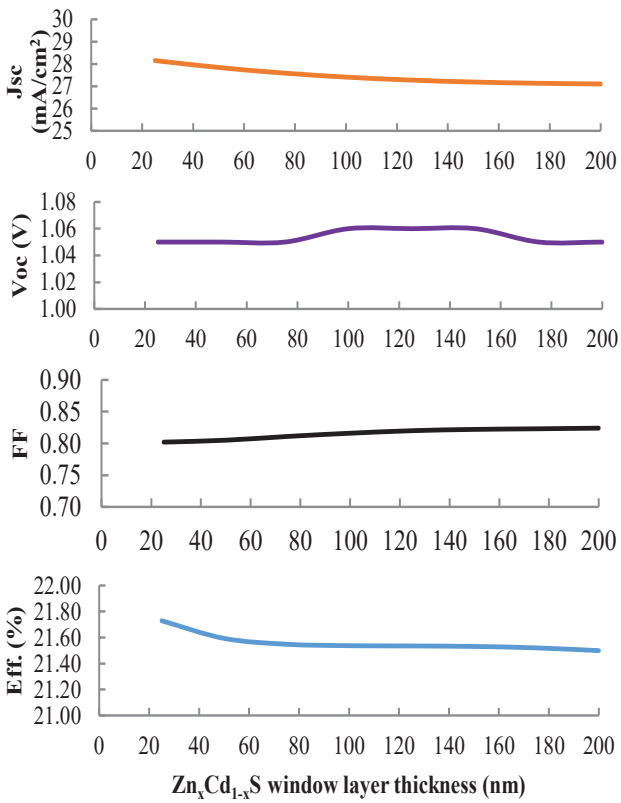

Fig. 4: Effect of Thicknesses Variation of Window Layer on $Zn_xCd_{1-x}S$/CTS Cell Parameter

3.4 Thickness Variation of CTS Absorber Layer

To evaluate material savings and cost efficiency, additional simulations were conducted by varying the CTS absorber thickness from 0.1 µm to 3 µm in the $Zn_xCd_{1-x}S$ /CTS (x = 0.3) solar cell. The configuration included a 50 nm $Zn_xCd_{1-x}S$ window layer, 100 nm Zn_2SnO_4 buffer, 100 nm SnO_2 front contact, and an aluminum (Al) back contact. As shown in Fig. 5, device performance remains stable for CTS thicknesses above 1.5 µm. Reducing the thickness led to a gradual drop in Jsc and efficiency, while V_{oc} and FF were largely unchanged until the thickness fell below 0.5 µm—beyond which all performance metrics sharply declines, likely due to limited minority carrier diffusion. These results indicate that CTS layers thinner than 0.5 µm are unsuitable for this configuration. However, a 1 µm CTS layer achieved a strong performance, with an efficiency of 21.592%, with V_{oc} = 1.049 V, J_{sc} = 27.841 mA/cm², and FF = 0.805, only 0.930% lower than that of the 3 µm design (22.522%), while using significantly less material. Thus, a 1 µm CTS absorber is considered optimal for further simulations, offering a practical balance between efficiency, material usage, and deposition time.

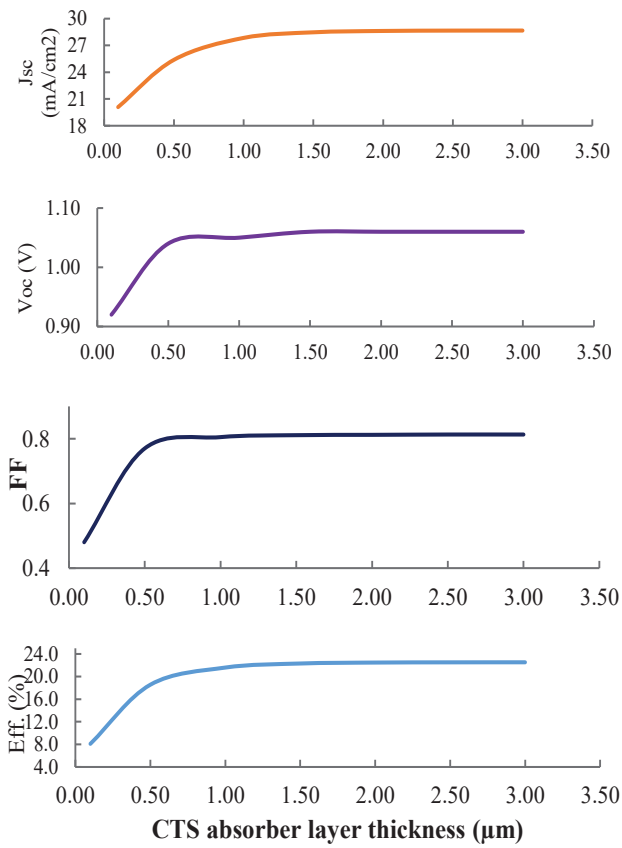

Fig. 5: CTS Thickness Variation Influences the Performance of $Zn_xCd_{1-x}S$/CTS Cell

1.1 Impact of Absorber Layer Doping Concentration

The doping concentration in the absorber layer significantly influences solar cell performance. In this part of the study, simulations were performed using a fixed device structure comprising a 1 µm CTS absorber, 50 nm $Zn_xCd_{1-x}S$ (x = 0.3) window layer, 100 nm Zn_2SnO_4 buffer, 100 nm SnO_2 front contact, and aluminum (Al) back contact.

To explore the effect of doping on device performance, the acceptor concentration in the p-type CTS absorber was varied from 4×10^{10} cm^{-3} to 4×10^{16} cm^{-3}. The resulting performance characteristics of the $Zn_xCd_{1-x}S$ /CTS (x = 0.3) thin-film solar cell are shown in Fig. 6. As depicted in Fig. 6, the solar cell's performance remains stable when the doping concentration ranged from 4×10^{10} cm^{-3} to 4×10^{13} cm^{-3}. However, beyond 4×10^{13} cm^{-3}, most output parameters improved, except for the short-circuit current density (Jsc), which gradually decreased. This reduction in Jsc is attributed to a decreasing depletion width in the p-type CTS absorber with increasing doping levels. In contrast, both the open-circuit voltage (Voc) and fill factor (FF) increased due to a rise in the built-in voltage. The solar cell achieved peak conversion efficiency of 21.592% at a doping concentration of 4×10^{16} cm^{-3}. This concentration is therefore selected as the standard for further simulations and analysis.

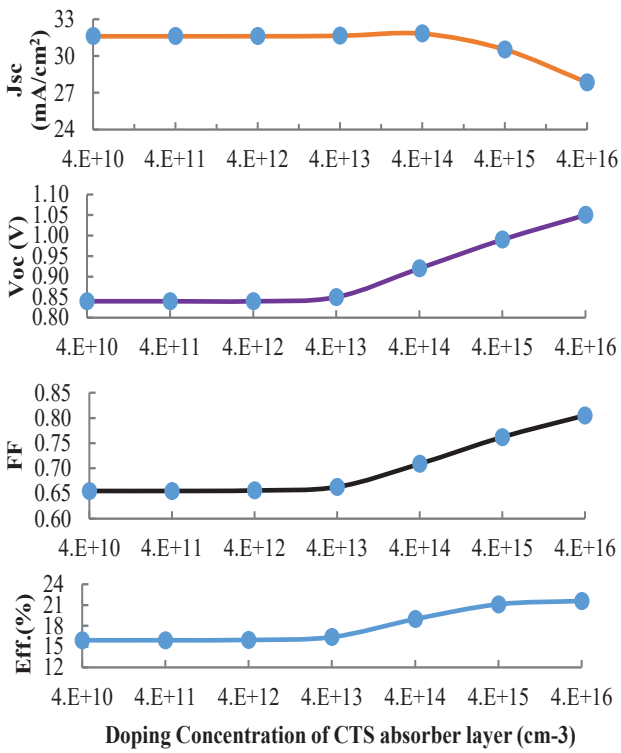

Fig. 6: Effect of the CTS Doping Concentration on Cell Output Parameters

3.6 Effect of Operating Temperature without BSR

Operating temperature plays a crucial role in solar cell performance. While the ideal operating temperature is around 298 K (room temperature), solar panels are often exposed to higher temperatures in outdoor conditions due to direct sunlight. Elevated temperatures can affect key material properties such as the effective density of states, absorption coefficients, carrier mobility, band gaps, and carrier concentrations. To evaluate the thermal stability of the proposed solar cell design (without a back surface reflector, BSR), the impact of increased operating temperatures was examined. In this simulation, the cell temperature was varied between 298 K and 400 K to assess the resulting performance changes. The outcomes are shown in Fig. 7.

As shown in Fig. 7, the normalized efficiency of the solar cell without a back surface reflector (BSR) layer decreases linearly with rising operating temperature, exhibiting thermal tangent of -0.19%/K. This low TC indicates that the cell maintains strong thermal stability and experiences minimal performance degradation under higher temperature conditions.

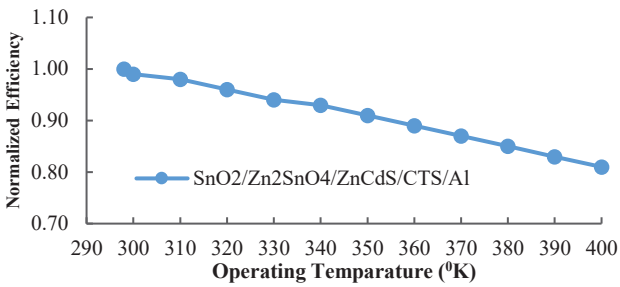

Fig. 7: Effect of Operating Temperature on Normalized Efficiency without BSR

3.7 Effect of Back Surface Reflector (BSR) on the $Zn_xCd_{1-x}S$/CTS Solar Cell Structure

To assess the impact of electron-hole reflectors on ultra-thin cell performance, this study explores a CTS solar cell with a carefully chosen BSR layer. The numerically modeled ultra-thin cell, consisting of a 1 µm CTS absorber layer, 50 nm $Zn_xCd_{1-x}S$ (x = 0.3) window layer, 100 nm Zn_2SnO_4 buffer, 100 nm SnO_2 front contact, and Al back contact, demonstrates strong performance with a conversion efficiency of 21.592%, J_{sc} of 27.841 mA/cm², V_{oc} of 1.049 V, and FF of 0.805%. The carrier lifetime in this model is 1.6 ns, with a hole concentration of 4×10^{16} cm^{-3}. The corresponding J–V curve for this ultra-thin device is shown in Fig. 8.

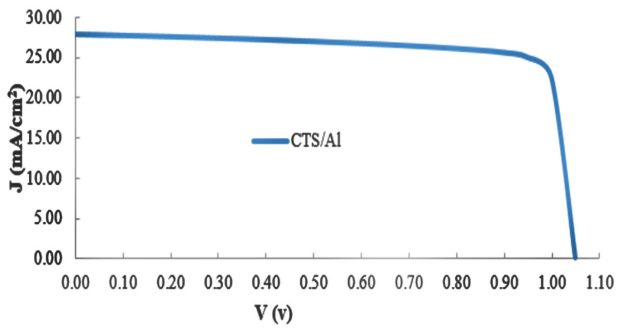

Fig. 8: J-V Curve of the Modified Cell Structure without any BSR Layer

This section investigates the potential of Arsenic Telluride (As_2Te_3) as a back surface reflector (BSR) material to reduce recombination losses in ultra-thin CTS solar cells. As_2Te_3, a p-type semiconductor with a low optical band gap, reflects minority carriers (electrons) back toward the front contact and helps holes move toward the back contact, minimizing rear interface recombination. The feasibility of using As_2Te_3 in thin-film solar cells was first proposed by M. A. A. Noman et al. [20].

A numerical simulation was conducted to evaluate the impact of the As_2Te_3 BSR on the performance of the ultra-thin $Zn_xCd_{1-x}S$ /CTS cell. The cell structure remained unchanged except for the addition of a 100 nm As_2Te_3 BSR layer at the back contact. The full structure includes a 1 µm CTS absorber, 50 nm $Zn_xCd_{1-x}S$ (x = 0.3) window layer, 100 nm Zn_2SnO_4 buffer layer, 100 nm SnO_2 front contact, and a 100 nm As_2Te_3 BSR layer. The results, presented in Table III, show that integrating the BSR layer significantly improves the efficiency of the solar cell. Without the BSR, the proposed ultra-thin $Zn_xCd_{1-x}S$/ CTS cell achieves a conversion efficiency of 21.592%. With the addition of the 100 nm As_2Te_3 BSR layer, the efficiency increases to 23.433%. This performance gain is attributed to improvements in short-circuit current density (J_{sc}), open-circuit voltage (V_{oc}), and fill factor (FF), highlighting the positive effect of the BSR. The J–V characteristics for both versions of the solar cell are shown in Fig. 9, confirming the enhancement in performance.

As shown in Fig. 9, the solar cell with the As_2Te_3 BSR layer exhibits improved open-circuit voltage (V_{oc}), short-circuit current density (J_{sc}), and fill factor (FF) compared to the cell without a BSR. These improvements are attributed to reduced back surface recombination and enhanced back contact quality with the p-type CTS absorber layer. As a result, the conversion efficiency of the cell with the As_2Te_3 BSR is significantly higher than that of the cell without the BSR layer.

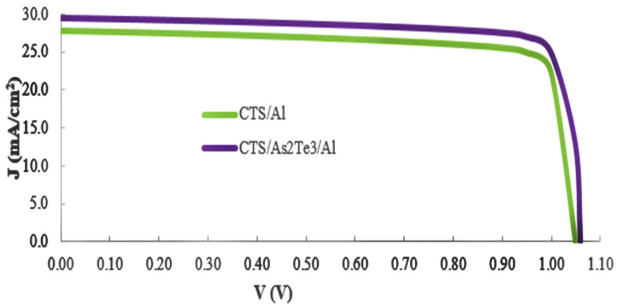

Fig. 9: Effect of BSR on the J-V Curves of the $Zn_xCd_{1-x}S$/CTS Solar Cell

3.8 Effect of Operating Temperature with BSR

Before drawing final conclusions regarding the performance of the As_2Te_3 BSR, it is essential to evaluate the thermal stability of the proposed structure under elevated operating temperatures.

As shown in Fig. 10, the efficiency of the cell without a BSR layer decreases linearly with rising temperature, exhibiting a thermal tangent of –0.19%/K. In contrast, the cell with the As_2Te_3 BSR layer shows significantly improved thermal stability, with efficiency remaining stable from 298 K to 330 K and a reduced thermal tangent of –0.12%/K beyond 330 K. The thermal tangent of |–0.19| %/K is significantly greater than the thermal tangent of |–0.12| %/K. This indicates better performance retention at higher temperatures, highlighting the effectiveness of As_2Te_3 as a BSR in ultra-thin CTS solar cells.

Table III: The Output Parameters of Modified Cells without and with As2Te3 BSR

Cells Structures	Output parameters			
	V_{oc} (V)	J_{sc} (mA/cm²)	FF	Eff. (%)
Glass/SnO_2/Zn_2SnO_4/$Zn_xCd_{1-x}S$/CTS/Al (x = 0.3)	1.05	27.841	0.805	21.592
Glass/SnO_2/Zn_2SnO_4/$Zn_xCd_{1-x}S$ /CTS/ As_2Te_3/Al (x = 0.3)	1.06	29.503	0.819	23.433

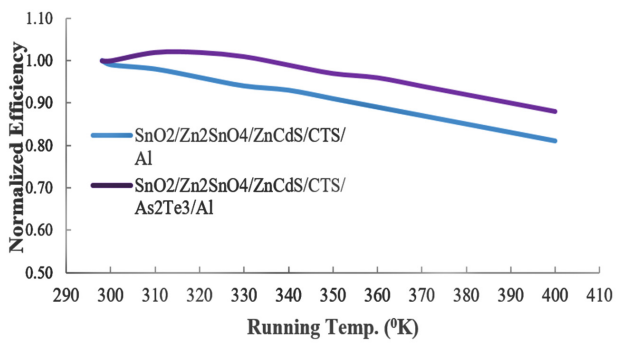

Fig. 10: Effect of Operating Temperature on Normalized Efficiency without and with As_2Te_3 BSR

3.9 Comparative Analysis with Other Published Works

This study aimed to evaluate the simulation results against previously published works. The proposed cell structure—glass/SnO_2/Zn_2SnO_4/$Zn_xCd_{1-x}S$/CTS/As_2Te_3/Al achieved a peak efficiency of 23.433%, with V_{oc} = 1.06 v, J_{sc} = 29.503 mA/cm², and FF = 0.819 for x=0.3. These results show significantly higher V_{oc} and J_{sc}, though the ff is slightly lower compared to other studies (table IV). The higher V_{oc} is likely due to improved lattice matching and reduced defect states at the p-CTS/n-$Zn_xCd_{1-x}S$ (x = 0.3) junction. Based on these findings, doping the window layer with indium (in) could further reduce resistivity and enhance performance. This structure represents a promising candidate for high-efficiency $Zn_xCd_{1-x}S$/CTS solar cells.

Table IV: Comparison between Proposed and other Published Works

Structures	Output parameters				Ref.
	V_{oc}(V)	FF	J_{sc} (mA/cm²)	Eff. (%)	
Mo/$CuSbS_2$/ CdS/ZnO/ ZnO:Al/Contact	0.65	0.6652	24.46	10.71	[21]
FTO/CTS/ZnS/ Ag	0.4252	0.7818	24.82	8.25	[3]
p-CTS/Zn(O, S)/n-ZnO/Al	0.3802	0.7445	48.33	13.65	[16]
Glass/SnO_2/ Zn_2SnO_4/ $Zn_xCd_{1x}S$/CTS/ As_2Te_3/Al (x=0.3)	23.433	0.819	29.503	1.06	Proposed

4. CONCLUSION

This research aimed to design and simulated an ultra-thin CTS solar cell using a Zn_xCd_{1-x}Swindow layer, replacing the conventional CdS/CTS setup, to enhance conversion efficiency via a suitable back surface reflector (BSR). Simulations were conducted using the AMPS-1D tool, with a proposed structure of Glass/SnO_2/Zn_2SnO_4/$Zn_xCd_{1-x}S$/CTS/AS_2Te_3/Al.

Efficiency enhancement was achieved by optimizing the window layer thickness to 50 nm and adding a 100 nm Zn_2SnO_4 buffer layer, improving spectral response—especially in the blue range, Zn_2SnO_4 delivered comparable performance. The optimal window composition was found at x = 0.3 in $Zn_xCd_{1-x}S$. Additionally, CTS absorber

thickness was minimized to 1 μm without significant loss in efficiency. Arsenic telluride (As_2Te_3) was introduced as a BSR due to its carrier reflection capabilities. While it had little effect on thicker absorbers, it significantly improved performance in thin-cell configurations. Incorporating a 100 nm As_2Te_3 BSR with a 1 μm CTS layer resulted in a peak efficiency of 23.433% (V_{oc} = 1.06 V, J_{sc} = 29.503 mA/cm², FF = 0.819).

The thermal performance of the optimized structure ($SnO_2/Zn_2SnO_4/Zn_xCd_{1-x}S$/CTS/$As_2Te_3$/Al, x = 0.3) was also assessed, showing a low thermal tangent of –0.12%/K, indicating good thermal stability. Overall, the proposed structure is suitable for practical fabrication, offering a non-toxic, efficient, and cost-effective alternative for CTS-based solar cells.

ACKNOWLEDGEMENT

The authors would like to acknowledge and appreciate UGC and DUET for the financial support to run the project work.

REFERENCES

[1] K. Devendra, D. Shah, S. Kumar, N. Bhattarai, D. Adhikari, K. B. Khattri, M. S. Akhtar, A. Umar, A. Ibrahim, M. A. M. Alhamami, S. Baskoutas, O. Yang Less, "Enhanced solar cell efficiency: Copper zinc tin sulfide absorber thickness and defect density analysis," Journal of Materials Science, Vol. 34, No. 24, p. 11125, 2023.

[2] H. Wei, W. Guo, Y. Sun, Z. Yang, Y. Zhang, "Hot-injection synthesis and characterization of quaternary $Cu_2ZnSnSe_4$ nanocrystals," Materials Letters, Vol. 64, pp. 1424–1426, 2010.

[3] S. Rahaman, M. K. Singha, P. Sarkar, M. A. Sunil, K. Ghosh, "Optimization of CTS thin film solar cell: A numerical investigation based on USP deposited thin films," Physica B: Condensed Matter, Vol. 698, p. 416751, 2025.

[4] S. Chen, X. G. Gong, A. Walsh, and S. H. Wei, "Defect physics of the kesterite thin-film solar cell absorber Cu_2ZnSnS_4," Applied Physics Letters, Vol. 96, No. 2, p. 021902, 2010.

[5] A. Nagoya, R. Asahi, R. Wahl, and G. Kresse, "Defect formation and phase stability of Cu_2ZnSnS_4 photovoltaic material," Physical Review B, Vol. 81, p. 113202, 2010.

[6] S. Rahaman, M. A. Sunil, M. K. Singha, K. Ghosh, "Optimization and fabrication of low cost Cu_2SnS_3/ZnS thin film heterojunction solar cell using ultrasonic spray pyrolysis," Optical Materials, Vol. 124, p. 111838, 2022.

[7] D. Tiwari, T. K. Chaudhuri, T. Shripathi, U. Deshpande, R. Rawat, "Non-toxic, earth-abundant 2% efficient Cu_2SnS_3 solar cell based on tetragonal films direct-coated from single metal-organic precursor solution," Solar Energy Materials and Solar Cells, Vol. 113, pp. 165–170, 2013.

[8] M. Y. Alia, M. A. Abedin, M. S. Hossain, and E. S. Hossain, "Optimization of monoclinic Cu_2SnS_3 (CTS) thin film solar cell performances through numerical analysis," Chalcogenide Letters, Vol. 17, No. 2, pp. 85–98, 2020.

[9] J. Han, Y. Zhou, Y. Tian, Z. Huang, X. Wang, J. Zhong, Z. Xia, B. Yang, H. Song, and J. Tang, "Hydrazine processed Cu_2SnS_3 thin film and their application for photovoltaic devices," Frontiers in Optoelectronics, Vol. 7, pp. 37–45, 2014.

[10] D. M. Berg, R. Djemour, L. Gütay, G. Zoppi, S. Siebentritt, P. J. Dale, "Thin film solar cells based on the ternary compound Cu_2SnS_3," Thin Solid Films, Vol. 520, No. 19, pp. 6291–6294, 2012.

[11] J. Chantana, K. Tai, H. Hayashi, T. Nishimura, Y. Kawano, and T. Minemoto, "Investigation of carrier recombination of Na-doped Cu_2SnS_3 solar cell for its improved conversion efficiency of 5.1%," Solar Energy Materials and Solar Cells, Vol. 206, p. 110261, 2020.

[12] A. C. Lokhande, R. B. V. Chalapathy, M. He, E. Jo, M. Gang, S. A. Pawar, C. D. Lokhande, and J. H. Kim, "Development of Cu_2SnS_3(CTS) thin film solar cells by physical techniques: a status review," Solar Energy Materials and Solar Cells, Vol. 153, pp. 84–107, 2016.

[13] M. Bouaziz, M. Amlouk, and S. Belgacem, "Structural and optical properties of Cu_2SnS_3 sprayed thin films," Thin Solid Films, Vol. 517, No. 7, pp. 2527–2530, 2009.

[14] S. Rahaman, M. A. Sunil, M. K. Singha, K. Ghosh, "Studies of ultrasonically sprayed Cu_2SnS_3 thin Films by varying Sn concentration," Materials Today Proceedings, Vol. 43, part 6, pp. 3938–3941, 2021.

[15] N. Akcay, V. F. Gremenok, Y. Ozen, K. P. Buskis, E. P. Zaretskaya, S. Ozcelik, "Investigation on photovoltaic performance of Cu_2SnS_3 thin film solar cells fabricated by RF-sputtered In_2S_3 buffer layer," Journal of Alloys and Compounds, Vol. 949, p. 169874, 2023.

[16] V. V. Kutwade, K. P. Gattu, M. E. Sonawane, D. A. Tonpe, I. M. S. Mohammed, R. Sharma, "Theoretical modeling and optimization: Cd-free CTS/Zn(O,S)/ZnO thin film solar cell," Materials Today Communications, Vol. 29, p. 102972, 2021.

[17] M. Y. Zaki, F. Sava, I. D. Simandan, A. T. Buruiana, C. Mihai, A. Velea, and A. C. Galca, "Effect of the stacking order, annealing temperature and atmosphere on crystal phase and optical properties of Cu_2SnS_3," Scientific Reports, Vol. 12, p. 7958, 2022.

[18] M. T. Islam, A. Kumar, and A. K. Thakur, "Defect density control using an intrinsic layer to enhance conversion efficiency in an optimized SnS solar cell," Journal of Electronic Materials, Vol. 50, pp. 3603–3613, 2021.

[19] AMPS Manual, The Electronic Materials and Processing Research Laboratory, Pennsylvania State University, 2007.

[20] M. A. A. Noman, S. Siraj, M. J. Abden, N. Amin, and M. A. Islam, "A numerical analysis of BSF layers for ultra-thin high efficiency CdTe thin film solar cell," Chalcogenide Letters, Vol. 16, No. 4, pp. 185–193, 2019.

[21] E. Puente-López and M. Pal, "Numerical simulation and optimization of physical properties for high efficiency $CuSbS_2$ thin film solar cells," Optik - International Journal for Light and Electron Optics, Vol. 272, 170233, 2023.

[22] M. Burgelman, J. Verschraegen, S. Degrave, and P. Nollet, "Modeling thin film PV devices," Progress in Photovoltaics: Research and Applications, Vol. 12, pp. 143–153, 2004.

[23] Y. Wei, Z. Ma, X. Zhao, J. Yin, Y. Wu, L. Zhang, and M. Zhao, "Improving the performance of $Cu_2ZnSn(S,Se)_4$ thin film solar cells by SCAPS simulation," Materials Science and Engineering: B, Vol. 303, p. 117296, 2024.

[24] M. S. Hossain, N. Amin, and T. Razykov, "Prospects of back contacts with back surface fields in high efficiency ZnxCd1−xS/CdTe solar cells from numerical modeling," Chalcogenide Letters, Vol. 8, No. 3, pp. 187–198, 2011.

[25] O. M. Hussain, P. S. Reddy, B. S. Naidu, S. Uthanna, and P. J. Reddy, "Characterization of thin film ZnCdS/CdTe solar cells," Semiconductor Science and Technology, Vol. 6, pp. 690–694, 1991.

[26] M. S. Hossain, N. Amin, M. A. Matin, M. M. Aliyu, T. Razykov, and K. Sopian, "A numerical study on the prospects of high efficiency ultra-thin $Zn_xCd_{1-x}S$/CdTe solar cell," Chalcogenide Letters, Vol. 8, No. 3, pp. 263–272, 2011.

Socioeconomic Development of Bangladesh through Women's Involvement in Sustainable Social Enterprises (Case Studies)

Mohammad Faizul Haque

Department of Humanities and Social Sciences, Dhaka University of Engineering & Technology, Gazipur, Bangladesh

ABSTRACT

Bangladesh is a developing country where more than half of its population is women (i.e., male/female = 96.3/100 in 2023) [1]. Meanwhile, the participation of women was only 36.4 per cent compared to 84 per cent of men in 2020 [2]. Later, in 2022 and 2023, women's labor participation in the economy remained static, i.e., 37 per cent [3]. Therefore, for economic prosperity, we have to utilize this huge portion of the population. In this study, the focus was on women entrepreneurs in Bangladesh to figure out their accessibility to financial resources. The research was qualitative in nature (interviewed three case studies - two independent women entrepreneurs and one non-governmental organization) and found that women entrepreneurs in Bangladesh face hindrances to accessing financial resources.

1. INTRODUCTION

Bangladesh is a least developed country and is hoping to graduate from least developed country to a developing country in 2026 as recommended by the United Nations committee [4, 5]. The General Economic Division of the Bangladesh Planning Commission is almost at the end of the 8th Five-Year Plan, which is dated from July 2020 to June 2025. This Five-Year Plan has six core themes, and one of the themes is acceleration in gross domestic product (GDP) growth, rapid reduction of poverty, and employment creation [6]. Hence, entrepreneurship can work as an employment generator and can contribute to the country's economy [7].

Entrepreneurship is key to increasing productivity. The phenomenal growth of the garment industry has shown that Bangladesh has significant entrepreneurial potential [8]. The ready-made garment (RMG) industry of Bangladesh begun its journey at the end of 1970 and became a principal leader in the economy [9] (contributes 82.15 per cent of total export earnings of Bangladesh) and from foreign currency earnings point of view Bangladesh is the second largest garment exporter after china earning USD 38.1421 billion in the fiscal year 2022-23 [10, 11]. In 2013-2014, about 4 million people were working in around 4222 garment factories [9]. Presently, around 3555 export-oriented garment factories are employing 3.04 million people [12]. Not only that, the participation of the women workforce in the garment industry has decreased significantly from 80 per cent in 1980 to 53.65 per cent in 2021 [13].

Bangladesh is a country where labor costs are cheap, especially due to female labor. Low-cost female labor is the reason why the RMG industry has become prosperous here [9]. Most of these women (RMG industry workers) come from villages and are economically underprivileged or are a marginalized segment of society. They lack knowledge and awareness, which ultimately increases their migration risk to cities [14]. Female garment workers suffer from stress, suicidal ideation, and anxiety due to stressful garment working conditions and isolation from families and relatives due to their migration to the cities [13]. Female garment workers often quit their factory-based jobs due to stressful working conditions, which impact their mental and physical health. In addition, underpaid wages and unable to fulfil their childcare responsibilities eventually "run them down" [15].

In the RMG industry, the employers prefer young female workers because they are more productive than older female workers. Therefore, female workers cannot work in the RMG industry for a long period of time because of occupational dangers [16]. Another, reason for job loss or job stagnation in the RMG industry of Bangladesh despite its robust growth is the induction of labor saving technology (that is, automation) [17].

The reason for considering Bangladesh's RMG industry is that it has played an important and pivotal role in empowering the country's women's population and improving the socioeconomic scenario [18]. In addition, Bangladesh has already introduced the sustainable development goals (SDGs), as proposed by the UN Open

*Corresponding author's email: mdfaizulhaque@duet.ac.bd

Working Groups, to its national development agenda [19]. One of the SDGs (that is, goal No. 05) (Figure 1) is to ensure gender equality through women's empowerment and bringing women into the mainstream economic and commercial activities [20]. However, as discussed earlier, women's workforce participation in the RMG industry is declining.

In 2023, the female population of Bangladesh comprise more than half of the entire population according to Bangladesh Sample Vital Statistics (i.e., male/female = 96.3/100) [1]. Furthermore, the participation of the women in mainstream economic activities is only 36.4 per cent compared to 84 per cent of men in 2020 [2]. According to the World Bank President Jim Yong Kim, if Bangladesh can ensure its 82 per cent women workforce participation in its economy over the next decade, then it may add 1.8 per cent points to its GDP [22]. Therefore, the increase of women's workforce participation in mainstream economic activities is crucial for Bangladesh's economic prosperity, whereas the extant literature, as discussed earlier, reflects differently, i.e., it is decreasing. Besides, previous scholars identified that women's entrepreneurship has a significant impact in terms of employment generation and can contribute to the country's economy. Women adopting entrepreneurial occupations can balance their personal lives and improve their personal and family economic condition, as well as participate in Bangladesh's socioeconomic growth and overall economic prosperity [7].

Fig. 1: The United Nations Sustainable Development Goals (SDGs) [21]

The growth of entrepreneurial potential is not restricted to the higher-income group of urban settings, but through liberalization policies, the prospect can be observed in the rural areas. The major challenge for Bangladesh is to open up the entrepreneurial talents and increase productivity all over the economy, both in rural (farming along with non-farm activities) and also in urban regions (in both small and medium industries along with the service businesses) [8].

In this scenario, for the economic growth of Bangladesh, we have to occupy the majority of the population, i.e., "Women". We have already seen the positive side of women's participation in the economic sector, such as the RMG industry. Hence, we have to promote entrepreneurship, and it should be home-based, so that women do not need to leave their households and take part in the economic activities.

2. OBJECTIVE OF THE STUDY

The objective of this empirical study is to analyze the current conditions of women's entrepreneurship in Bangladesh. Furthermore, the study aims to identify and understand the key obstacles and impediments hampering the development of women's entrepreneurship in Bangladesh. Eventually, the insights acquired from this study will help address these obstacles to some degree, which will help to promote better women entrepreneurship throughout our country and expedite women's participation in our national economy.

3. LITERATURE REVIEW

Globalization and free market economy are two features of capitalism, where businesses can be done beyond national borders, and capital can flow without restriction. In a free market economy, the host government is always in pursuit of international companies to do business or invest, and for that, the government offers tax or regulatory advantages, operating conveniences, business facilities or infrastructures. With proper guidance and regulations, globalization can be more beneficial in alleviating poverty than any other alternative. But other than that, if there is a lack of guidelines, then it may end up being destructive. China has experienced rapid economic growth after the introduction of economic reform in the late 1970s. After this, the World Bank figured out that more than 400 million Chinese have escaped the vicious cycle of poverty. In the process of development, some matters have been overlooked, such as social problems or environmental issues (i.e., air or water pollution). China has been affected by immense environmental pollution and socioeconomic differences, such as income inequality. Though people have escaped from poverty, the income distribution becomes exceedingly uneven [23].

The income gap problem is growing worse day by day. In 2010, a report by Oxfam indicates that the world's richest 388 people possessed more wealth than the entire bottom half of the world population, i.e., approximately

3.3 billion people. After seven years, this situation has deteriorated further. In January 2017, another report from Oxfam indicates that the super-rich 388 people downsize to only 8 super-rich people who own more wealth than the bottom half of about 3.6 billion people [24, 25].

Capitalism has a tendency to accumulate wealth. In economics, it is taught that human wants are unlimited and there are limited resources to satisfy them. So, in a capitalist system, people try to gather as much wealth as possible to meet their unlimited wants, and that is why the distribution of income becomes unequal [25]. Hence, what we can do is regulate the rules of the game, which ultimately benefits society and brings down this inequality to a reasonable level.

According to Austrian economist Joseph A. Schumpeter, to produce something new, one element needs to be introduced, that is, innovation [26]. Innovation is involved in the process of creating and adopting something new, which eventually generates value [27]. Therefore, scholars like Drucker [28] pointed out that entrepreneurship is an innovative economic instrument that acts as a new way of generating wealth.

Sustainable entrepreneurship signifies an exceptional concept in terms of strategies for sustainable and entrepreneurial businesses, focusing on enhancing social and business value simultaneously. Sustainable innovations focus on the mass market and ensure benefits to the larger portion of society. We can use Sustainable Entrepreneurship and its entrepreneurial approach to come up with business solutions to solve the most vital social and ecological challenges. It is a part of the business commitment towards society to increase economic development as well as improve the quality of social life and the environment [29, 30]. On the other hand, social entrepreneurship plays a role in taking care of societal problems and generating value for society [30].

In the present time, mostly the large companies or industries are the main users of the sustainable entrepreneurship approach, whereas it is a completely opposite scenario in the case of small and medium enterprises (SMEs), they have not adopted this concept widely due to a lack of knowledge, financial, and human resources. However, a large percentage of the majority of nations' businesses are comprised of SMEs [31].

In the transformation of a country's economic and social development, one cannot rely solely on large companies or industries; one needs to rely on SMEs or household or community-based small enterprises as well [7]. In the case of population participation in a country's economic and social development, women are also equally essential as men [32].

The number of women-owned new small and large businesses is increasing, which leads to economic development [7, 33]. In fact, the women entrepreneurship startups increased from 6.1 per cent to 10.4 per cent on average across thirty Global Entrepreneurship Monitor (GEM) participating countries based on 2001-05 and 2021-23 surveys. The incremental trend can be seen regarding women-owned established businesses, which is 4.2 per cent to 5.9 per cent on average in the thirty countries participating in the 2001-05 and 2021-23 surveys [34].

According to Hafiz and Abdul Latiff (2020), the gender gap in business ownership (i.e., micro and SMEs) in Bangladesh is 92.6 per cent men versus 7.4 per cent women [35, 36]. This situation gets slightly worse based on the 2022 Labour Force Survey, where 92.8 per cent of businesses (i.e., micro and SMEs) are owned by men compared to 7.2 per cent owned by women. Women own 0.69 million out of 2.8 million SMEs, according to the Bangladesh Bureau of Statistics (BBS). These women-owned SMEs employed approximately 8.4 million individuals all over the country and played a significant role in economic empowerment and job creation [37].

Previous studies showed proactive personality as entrepreneurial awareness [38]. An individual with creativity possesses a proactive personality and cognitive capabilities to navigate through and overcome difficulties that may arise within their work environment [39-42].

Previous research emphasized that women entrepreneurs in developing countries play a significant role in the economy and overall country's development process [43]. Other researchers also supported this fact and added the urge to understand women's entrepreneurship properly [44-48].

Several researchers also pointed out that in developed countries, women entrepreneurs always remain highlighted and the centre of discussion [48-51]. Hossain, et al. [52] stated in their research that in developed nations, women's entrepreneurship has been the centre of scholarly attention, whereas developing nations have ignored such attention. Isaga [51] also supported this fact and said that research on women entrepreneurs was more extensive in developed nations than in developing nations. There is a research gap in the literature regarding women's accessibility to financial opportunities in a developing country context (such as Bangladesh). Therefore, this research study will make an effort to bridge this research gap and try to find out whether women entrepreneurs in a

developing country like Bangladesh have equal chance to access financial opportunities as their male counterparts [7]. Hence, based on these literature reviews, this research study hypothesised that "*Women entrepreneurs in Bangladesh face hindrances to accessing financial opportunities".*

3.1 Meaning of Entrepreneurship

"The entrepreneur," said the French economist J. B. Say around 1800, "shifts economic resources out of an area of lower and into an area of higher productivity and greater yield." But this definition of Say's does not clarify to us who this "entrepreneur" is. Furthermore, since Say authored the term right around two hundred years ago, there has been a wrong perception about the meanings of "entrepreneur" and "entrepreneurship". In the United States, for example, the entrepreneur is regularly characterized as one who begins their own, new and small business. Undoubtedly, there are numerous similar elements in every newly started small business. Nevertheless, an enterprise needs to have exceptional attributes well beyond being new and small to become entrepreneurial. Surely, among new organizations, entrepreneurs are a minority group. They make something new, something other than what is expected; they change or transform values. Entrepreneurship is commonly trusted, and it is immensely risky [28].

Nobel Laureate Dr. Yunus theorizes entrepreneurs must have two elements: a) profit and b) social returns. He posits that in future the enterprise should be more social and environmentally friendly and side by side it will be financially viable. There are various types of entrepreneurial business where women can involve, such as – handicrafts, farming (cattle, poultry, fishery, etc.), agriculture (growing crops, vegetables, etc.) [53].

3.2 Meaning of Sustainability

In 1987, the Brundtland Commission defined sustainable development as the "ability to make development sustainable—to ensure that it meets the needs of the present without compromising the ability of future generations to meet their own needs" [54].

The Brundtland Report also provides a second politically demanding definition, which is cited less frequently. It reads: "In essence, sustainable development is a process of change in which the exploitation of resources, the direction of investments, the orientation of technological development, and institutional change are all in harmony and enhance both current and future potential to meet human needs and aspirations." [55].

Nowadays, we can find the word "Sustainability" or "Sustainable Development" everywhere. This term emphasizes long-lasting benefits and also ensures the future generation's survivability. Sustainable development is not only considering the future generation and the future of the environment. It is broader than that – it considers the present and future state of the environment, its wellbeing, the development of people, institutional development of the society and inclusive economic development [56].

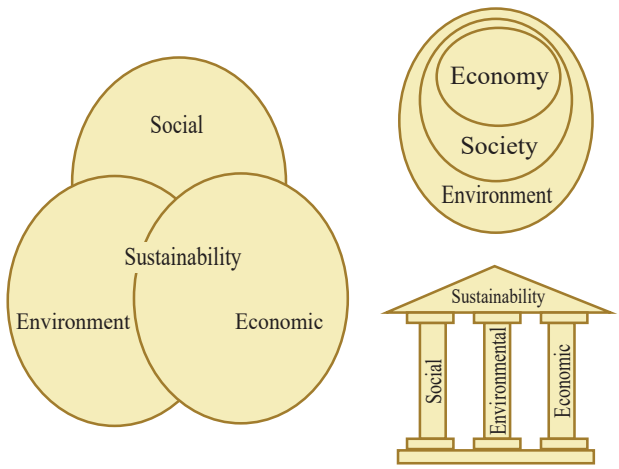

Fig. 2: Left, Sustainability a Typical Representation as three "Intersecting Circles" Approach. Right, Alternative Description: Top as "Concentric Circles" and Below as "Pillars" Approach [56]

Sustainable development tackles the multidimensional poverty from different angles, such as eliminating inequality and exclusion among people within the society, enhancing the capacity and knowledge of people, reducing the risks and maintaining smooth thriving development. It undertakes sustainable utilization of natural resources through proper management and confirming its use in improving people's lives in terms of individual wellbeing, social unity and cohesion, and generating equal opportunity. In addition, developing policies which are appropriate, ensuring social protection for those in need and supporting livelihoods and economic recovery. Overall sustainability works from three dimensions – society, economy and environmental point of view [56].

3.3 Meaning of Social Business

In this contemporary business world, there are lots of business concepts, and social business is one of them. And figuring out the differences between social business and conventional business is very complicated. Social business is more about the social benefits rather than the personal benefits of the entrepreneur or the owner. The owner will not get extra benefits from the social business

if it makes a lot of profit. In spite of that, the extra profit will be reinvested in the business, and the owner will receive a specific salary or benefit for the time he or she is spending in the organization [57].

Social Business is not bound to make a profit due to its unique nature. As it works for social causes and its development, social business investors do not get panicked due to the downfall of the business sector or share prices [57].

The concept of "social entrepreneurship", defined by Mair and Marti as "a process involving the innovative use and combination of resources to pursue opportunities to catalyze social change and/or address social needs" [58].

4. METHODOLOGY

The study is mainly qualitative in nature. It is based on primary and secondary sources of data. The primary sources of data are based on field visits and interviews, which are based on open-ended questions to collect qualitative data, which are mainly test cases opinions and comments in descriptive forms. This study also depends on secondary data sources, such as journals, articles, newspapers, books, etc. In this research study, three test case studies were conducted. Here, I have interviewed two independent women entrepreneurs who are working on their own and one NGO, which basically works with individual women as their development partner. A careful and honest attempt has been made to apprehend these interviews (three case studies), these primary sources of qualitative data, to identify the hindrances that are interrupting the prosperity and development of women entrepreneurship and how sustainable these ventures are from the economic, social and environmental points of view. Based on these observations, a few future research directions have been suggested.

5. CASE DESCRIPTIONS RELATING TO SUSTAINABLE WOMEN ENTREPRENEURSHIPS

First case study starts with a small-scale women entrepreneur, Ms. Shima Shaha (Case-1), who has a sewing teaching centre (Shima Shaha Karchupi Training Centre) for women and also does business of embroidery (Karchupi/Zardozi – embroidery worked with gold and silver thread type and done with regular needle). She belongs to the marginalized Muslim Bihari minority community in Bangladesh (also known as Stranded Pakistanis) living in Kalshi, East Kurmitola Camp, Mirpur. She started her training center back in 2007 and has been doing business since 2008. She also trained women at Mirpur camp and at Baniachong Upazila of Habiganj District in the Division of Sylhet, Bangladesh. She has trained women who have become specialized in Karchupi/Zardozi work, and they work for her from their household. She gets the orders from the traders and distributes the orders among her associates. She gets the job done in due time and coordinates all the activities. So far, she has completed around 350 design frame orders from Baniachong and around 70 design frame orders from Mirpur. And each frame can be done by one to four women, and they can earn from BDT 200 to BDT 1,500, depending on the design work.

"Shongroho" (Case-2) is a Bengali word, which means "collection". It is a bit of a high-end shop for the upper social class people at Mirpur 10, Dhaka. The owner of the business is Ms. Farhana Binte Abbas. She started her business back in 2013. The commencement of her business is quite intriguing. Before entering the business, she was a legal advisor for a company (she has a master's degree in Law). She quit her attractive corporate job to give time to her only child and family. During that time when she was a complete homemaker, she came up with the idea of doing a business that could be operated from her home. So, she started her clothing business from her home and conducted it from there for a while. After that, she rented a place adjacent to her residence and converted it into a boutique shop. Now she operates her business both from the shop and at home. She procures all her materials, such as clothes, threads, etc., from selected suppliers with whom she has written contracts. Subsequently, she introduces her own designs on the clothes and gets the clothes hand embroidered from the Jamalpur District. She markets her products all over Bangladesh. She also uses online platforms (i.e., Facebook, Daraz.com, etc.) to market her product. Within Dhaka, the payment mechanism for online sales is cash on delivery, and outside Dhaka, the payment should be made first through "bKash" (mobile financial services), then the product will be sent through courier services because she cannot use her own delivery system.

"TARANGO" (Case-3) is a women's development organization. The abbreviation stands for "Training Assistance and Rural Advancement Non-Government Organization". It was founded in 1989 with the objective of empowering underprivileged women of society. During my conversation with Ms. Nazlee Jamal, Project Coordinator of TARANGO, I came across the different aspects of the organization. This NGO works on a

voluntary basis and tries to eradicate poverty in society by training society's destitute and handicapped women through its training program. It tries to establish a gender-balance society and makes women self-reliant by nurturing and enhancing their talents and human potential to become productive and skillful entrepreneurs and leaders, so that they can engage in sustainable occupations. In Bangladesh, women are less involved in economic activities. TARANGO aims to reduce the gender gap in relation to participation in economic activities within the society. It has supported 18,800 women in ten districts: Barisal, Bandarban, Cox's Bazar, Dhaka, Dinajpur, Faridpur, Gazipur, Gopalgonj, Lalmonirhat, and Tangail. At present, over 1,800 marginalized women from these ten districts are working for TARANGO [59, 60].

In addition, TARANGO works on gender violence and discrimination issues, especially against women, the deterioration of the environment and forests, and so forth. TARANGO also runs a community enhancement project, like entrepreneurship training (an 11-day program) for those community members who are willing to work on their own. These trainees will not work along with TARANGO but have their own business [59].

TARANGO's motto is to produce high-quality products made from traditional and natural materials, and all products are colored with all-natural vegetable and plant dyes. It works in the field of diversified jute handicraft products, recycled products and artifacts made from straw, clay, leaf, grass, palm, handmade paper, coconut shell, etc. It promotes environmentally sustainable practices and the production and consumption of eco-friendly products. TARANGO follows the fair trade principles (ten principles) [61]. It exports its products to Australia, Canada, China, Finland, Germany, Greenland, Italy, Japan, the Netherlands, New Zealand, Spain, Singapore, the United Kingdom and the USA [60, 62].

6. DISCUSSION AND SOME FINDINGS

The nature of this research study is qualitative, where face-to-face interviews were undertaken. Here, subsections represent questions that were asked to the respondents, and the answers were received in these regards.

6.1 Economic Solvency

One of the major findings of this study was that women have economic solvency due to their entrepreneurial activities. The question asked to respondents – *Whether you have achieved economic solvency through your entrepreneurial venture?* The answers were positive, and they had economic solvency and were able to enrich the socioeconomic strata of their families. For example, women (Case-1) who were doing Karchupi/Zardozi work at Sylhet or Dhaka were poor before and could not do much for themselves or their families. But when they started earning from their sewing works, they reinvested their earnings into the existing and as well as other businesses, i.e., they buy food grains (rice) at regular season and sell them off-season when the price is high or owned small grocery or tea shops adjacent to their homes, etc. For example, Ms. Shima Shaha (Case-1) has a grocery shop other than her usual business, which is another source of income for her. So, they diversified their income from one source to multiple sources.

6.2 Effect of Economic Solvency

Another question was – *How does this economic solvency affect your life?* This economic solvency also helped women participate in their families' decision-making process, which was very apparent in Case-1. Because Case-1 was from a Muslim Bihari minority community, and it is based on a patriarchal family structure. For Case-2, who belonged to the upper social class strata, family decision-making freedom was already there.

Their families' conditions were improved because these working women spent much of their earnings on the betterment of their children and for the greater well-being of their families as well. Women provided nutritious food for their children and sent them to school. Even in some situations, female partners not only morally supported their life partners to get a job when they were unemployed but also financially supported them, i.e., they financed their husbands to start a business or helped them to go abroad for job purposes. For example, Ms. Shima Shaha (Case-1) helped her husband go abroad through the process of workforce export to developed countries.

Women who are economically solvent can also work side by side with men at the community level. Women who are in well-off economic conditions also like to help other women in their community who are backward in terms of economic and social conditions. Sometimes, a family may face difficulties when the male partner becomes low-paid or unemployed or unable to go to work due to illness, and in that case, a household may be unable to run their day-to-day basic livelihoods, e.g., buying foodstuffs etc., and this circumstance may take place when that family has a single wage earner. During my conversation with Ms. Shima Shaha (Case-1), she said that sometimes she supports her neighboring households by giving away a

small amount of money or foodstuffs when they face such difficulties.

6.3 Challenges and Difficulties

Cases were asked – *What type of challenges do you usually face as an entrepreneur?* Marginalized women (Case-1) faced the problem of acquiring financial support from banks. Banks need some forms of collateral, references, or recommendations from other clients of that very bank, which may turn out to be difficult for a marginalized woman to arrange (Case-1). Case-1 relied on her mother's savings and used them as collateral to acquire a loan from the bank. For banking reference, Case-1 belong to the low-income strata of society (minority community); therefore, she and her family members did not have well-known connections in the bank to recommend her. Case-1 requested her landlord to recommend her to the bank so that she could open an account, which was not easy for her to arrange.

Another challenge for women who work from their households is finding it difficult to work in the external business environment or deal with their clients. Case-1 and 2 found it difficult to deal with their business associates and clients. They found it tricky, and sometimes dishonest associates and clients caused losses to them. Further, working with different private and government organizations for business and legal documentation purposes was difficult. For example, getting a trade license from the government office is challenging, where corruption and bribes are common phenomena.

Another challenge women face was pointed out by Case-3, that sometimes women face setbacks from their husbands or families. For that reason, TARANGO (Case-3) uses a unique method and requests their women associates to bring their husbands to TARANGO's regional local offices to communicate about the work of their wives and how their wives can become more supportive of their families' financial conditions. It is a common issue for the majority of women in our society that they must have support from their family, or especially from their husbands, to get involved in any kind of economic activity, that is, a job or start a business.

Another challenge was that any women's enterprise or organization that is working with their partners or development partners have some obligations, such as women are persuaded to sell their products at a lower price or sell their entire production only to them, or cannot work for or with others except them. Case-1 and 2 faced such type of challenge, whereas TARANGO (Case-3) followed the fair-trade principles (ten principles) to ensure fair price payment to their producers or development partners.

There was a challenge for women entrepreneurs to balance their work-life balance. Because women have to maintain their family life (looking after their children and carrying out their household chores) and also manage their businesses. All cases in this research study faced this challenge. For Case-2, she belonged to the upper social class strata, and there was some financial solvency. Therefore, Case-2 hired a helping hand to help her with family responsibilities. On the other hand, for Case-1 and 3, their family members, especially their husbands, did not support them in this regard.

6.4 Lack of Training

During the interview cases were asked – *Do you require training to run your business?* Case-1 answered that she used to work as an apprentice to learn the Karchupi/ Zardozi work before she started to work independently on her own. Case-1 pointed out that she does not know about any managerial and entrepreneurial training program provided by government bodies targeting marginalized women. The same was hinted by Case-2, despite being a member of a privileged social stratum. However, in Bangladesh, there are seven specialized government technical training centers for women located in Dhaka, Barisal, Chittagong, Gazipur, Khulna, Rajshahi, and Sylhet [63]. So, when I told them about these training centers, Case-1 and 2 stated that they do not know about these centers. On the other hand, TARANGO (Case-3) mentioned that they provide a "Women Entrepreneurship Development Program", which is particularly targeted at building capabilities among rural disadvantaged women.

6.5 Sustainability

Another question was - *Do you follow any environmental sustainability practices?* Another finding was that not all women's enterprises in Bangladesh are sustainable in nature. During this research study, it was found that only Case-3 comply with sustainable practices. TARANGO's (Case-3) motto is to produce high-quality products made from traditional and natural materials, and all products are colored with all-natural vegetable and plant dyes. Others (i.e., Case-1 and 2) did not comply with such practices due to financial constraints, as these practices are expensive. Mendes, et al. [31] already mentioned in their literature that SMEs cannot comply with sustainable practices, and one of the reasons is a lack of financial resources.

7. EVALUATION AND SOME THOUGHTFUL IMPLICATION TO OVERCOME OBSTACLES

There should be reform in the financial institutional sector so that proper scopes can be accommodated for the women who can access financial loans easily with less collateral or security. In addition, the loan should be offered at a lower interest rate than the conventional banking sector, with flexible terms and conditions to make it more accessible for women. Some banks have already opened female sections or branches, which are operated by their female employees and are targeted at serving female clients. However, their purpose is to collect deposits from women clients [53]. We need to change this viewpoint from the collection of deposits to the disbursement of loans to women clients. Microcredit is already popular in our country, but sometimes, women need to have a bigger loan amount to start a venture. In this type of scenario, microcredit may not be able to serve the purpose. Therefore, we need to transform our financial sector to provide better accessibility for women entrepreneurs. Financial institutions can provide a loan step by step, starting from a small amount, and after monitoring the client's performance, they can offer a larger loan amount. By this time, that particular woman entrepreneur will be able to come up with some sort of collateral by herself.

These findings also agree with previous literature, where the researchers exposed that women's entrepreneurship is hampered due to a lack of access to loans, higher collateral requirements, complicated banking procedures, lack of inclusiveness or accessibility for women, and high interest rates [37, 64]. Bangladesh Bank loan disbursement data for the time of October-December, 2023 also reflect disparity between male and female SMEs (Table I). Only the manufacturing cottage industry women entrepreneurs dominated by 19.83 per cent [65].

Shoma [66], who mainly based her research on data from banks and financial institutions, found that there is a gap in the loan disbursement between male and female entrepreneurs (Table II, Fig. 3). The reasons found by the researcher [66] match with this research findings as well. For example, women entrepreneurs should have a guarantee or reference in case of getting a loan or opening a bank account, and for this reason, sometimes a woman entrepreneur may need to rely on her husband or family to support her. In this research, it was found that Case-1 relied on her landlord to open a bank account and relied on her mother to avail of a bank loan.

There should be easy procedures for women entrepreneurs to perform official formalities, such as getting a trade license or other permissions from the government or authorities. Besides, the government or NGOs may provide support to women entrepreneurs in market research or train them in how to study the market so that they can conduct business professionally and successfully.

Table I: Bangladesh Bank Quarterly SME Loan Disbursement (October-December, 2023) [65]

Sub-Sector	SME Category	Male	Female	Difference (%)
Service	Cottage	2,565	1,872	15.62
	Micro	11,397	4,749	41.17
	Small	24,707	1,699	87.13
	Medium	2,749	133	90.77
Trade	Micro	83,657	35,021	40.98
	Small	104,258	7,547	86.50
Manu-facturing	Cottage	17,667	26,405	19.83
	Micro	11,585	5,394	36.46
	Small	17,666	1,501	84.34
	Medium	7,907	537	87.28

(Amount in Crore BDT)

Table II: Loan Disbursement in Cottage, Micro, Small and Medium Enterprises, Bangladesh, Year 2010-18 [66]

Year	Loan Receipt			Difference (%)
	Total	Male	Female	
2010	308.726	295.003	13.72	91.10
2011	319.341	302.644	16.70	89.54
2012	462.513	445.151	17.36	92.50
2013	744.252	702.533	41.72	88.79
2014	541.656	498.926	42.73	84.22
2015	567.912	536.670	31.24	89.00
2016	634.574	592.899	41.68	86.86
2017	744.544	690.670	53.87	85.52
2018	687.522	629.951	57.57	83.26

(Amount in Million BDT)

Additionally, proper training scope (managerial and entrepreneurial) should be provided with easy accessibility by government bodies and NGOs all over the country. These findings also comply with Tuhin [37] findings, where the author showed that there is a lack of training programs focusing on marketing, financial management, and regulatory compliance all over the country, especially

in rural areas. The Daily Star conducted a RoundTable session on the 02nd January 2025, where the experts came up with recommendations for the enhancement of training and mentorship programs for Bangladeshi women entrepreneurs [64].

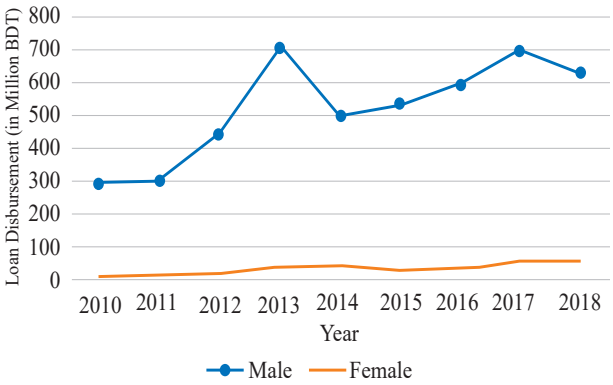

Fig. 3: Loan Disbursement in Cottage, Micro, SME, Bangladesh, Year 2010-18

Women entrepreneurs who work with a development partner or have contracts with business partners or associates should have flexible terms and conditions so that they do not have any obligation to sell products at a lower price than the ongoing market price and can earn better profits. Government regulatory bodies may intervene in this type of situation as a monitoring mechanism.

Government and NGOs should provide adequate knowledge about sustainable practices so that women entrepreneurs become aware of them. Further, there should be government incentives or financial support to promote such SMEs. Nevertheless, the World Bank and Palli Karma-Sahayak Foundation (PKSF) have a Sustainable Enterprise Project (SEP) through which they finance microenterprises to adopt environmentally friendly businesses. So far, under SEP, PKSF has disbursed loans amounting to US dollars 84.65 million and provided training on technical skill development, market linkage, environmental awareness to 45,486 micro-entrepreneurs (male 24,802; female 20,684) [67].

8. FUTURE RESEARCH DIRECTIONS

This research study is not above limitations. Based on these limitations and research findings, this research study comes up with some propositions and future research directions depending on which future research hypotheses can be developed and further research can be conducted. These are:

First, this research was conducted on women entrepreneurs from a limited perspective. In future, extensive research on a particular ethnic group can be performed, or other marginal ethnic groups can be brought under research scope.

Second, future research can focus on the financial accessibility of marginal ethnic communities and other prospects, such as – how to spread and integrate sustainable practices in women entrepreneurs to a greater extent and what initiatives should be undertaken.

Third, this research was qualitative in nature. Therefore, in the future, quantitative research can be pursued in this context for more comprehensive insight.

9. CONCLUSION

Women's entrepreneurship is needed for Bangladesh's economic prosperity. Women occupy more than half of Bangladesh's population [1], and we have to utilise this huge portion of the population. Women can work from their households if they establish their own home-based enterprises. It will be secure and convenient for them and also for their families, such as minor children who are very much dependent on their mothers, so it will be beneficial for both mothers and children. Therefore, the impact of this development is multifaceted, such as creating employment, economic growth of a developing economy, economic betterment of their households, and ensuring welfare for their families, especially for their children [68]. In general, we need to absorb our women population into our economic activities for comprehensive economic advancement, and the government need to think outside the box to employ this huge population in case of a developing economy like Bangladesh because the women workforce participation rate is 36.4 per cent in comparison to 84 per cent male workforce participation in 2020 [2]. The research tried to minimize a literature gap about women's accessibility to financial opportunities in a developing country context. The research was limited due to its nature (i.e., qualitative research study) and found that women entrepreneurs in Bangladesh do face hindrances regarding access to financial opportunities. Therefore, the government needs to think hard and take the necessary initiatives to ensure greater accessibility and inclusiveness of women entrepreneurs in the financial systems so that the development of women entrepreneurs can be ensured.

REFERENCES

[1] Bangladesh Bureau of Statistics, "Bangladesh Sample Vital Statistics 2023: Key Findings," Bangladesh Bureau of Statistics (BBS), Dhaka, Bangladesh, March 2024.

[2] M. K. Mujeri. "Women's economic empowerment and future development of Bangladesh." The Financial Express. https://thefinancialexpress.com.bd/views/views/womens-economic-empowerment-and-future-development-of-bangladesh-1609856560 (accessed 03 April 2025).

[3] R. K. Byron and A. Habib. "Economic output may expand 29% if more women employed: WB." The Daily Star. https://www.thedailystar.net/business/economy/news/economic-output-may-expand-29-if-more-women-employed-wb-3726196 (accessed 02 June, 2025).

[4] R. K. Byron and R. U. Mirdha. "Becoming A Developing Nation: Bangladesh reaches A Milestone." The Daily Star. https://www.thedailystar.net/frontpage/news/becoming-developing-nation-bangladesh-reaches-milestone-2052161 (accessed 04 May, 2025).

[5] United Nations. "Bangladesh graduation status." https://www.un.org/ldcportal/content/bangladesh-graduation-status (accessed 04 May, 2025).

[6] General Economics Division, 8th Five Year Plan July 2020 - June 2025: Promoting Prosperity and Fostering Inclusiveness, 1st ed. Dhaka, Bangladesh General Economics Division (GED), Bangladesh Planning Commission, Government of the People's Republic of Bangladesh, 2020.

[7] I. H. Moral, M. M. Rahman, M. S. Rahman, M. S. Chowdhury, and M. S. Rahaman, "Breaking barriers and empowering marginal women entrepreneurs in Bangladesh for sustainable economic growth: a narrative inquiry," Social Enterprise Journal, Vol. 20, No. 4, pp. 585-610, 2024.

[8] S. A. Mahmood, "Entrepreneurship, Productivity and Investment Climate: Issues of Bangladesh," in Growth and Poverty: The Development Experience of Bangladesh, S. Ahmed and W. Mahmud Eds. Dhaka, Bangladesh The University Press Limited, pp. 149-166, 2009.

[9] D. M. H. Rahman and S. A. Siddiqui, "Female RMG Worker: Economic Contribution in Bangladesh," International Journal of Scientific and Research Publications, Vol. 5, No. 9, pp. 496-504, 2015.

[10] A. U. Zaman. "Bangladesh retains the 2nd position in RMG export." Textile Today. https://www.textiletoday.com.bd/bangladesh-retains-the-2nd-position-in-rmg-export (accessed 05 May, 2025).

[11] BGMEA. "Export Performance " The Bangladesh Garment Manufacturers and Exporters Association. https://www.bgmea.com.bd/page/Export_Performance (accessed 05 May, 2025).

[12] M. Munni. "RMG industry lacks full database of workers." The Financial Express. https://today.thefinancialexpress.com.bd/last-page/rmg-industry-lacks-full-database-of-workers-1739643277 (accessed 05 May, 2025).

[13] S. Akter et al., "The impact of the Fourth Industrial Revolution on female workers in the Ready-made Garments and textile industry, Bangladesh," The International Journal of Community and Social Development, Vol. 6, No. 3, pp. 317-338, 2024, doi: 10.1177/25166026241261187.

[14] K. Farhana, M. Syduzzaman, and M. S. Munir, "Present Status of Workers in Readymade Garments Industries in Bangladesh," European Scientific Journal, Vol. 11, No. 7, pp. 564-574, 2015.

[15] A. Kashyap, "Paid Work, Care Work, and Workers' Health in South Asia: Perspectives from the Garment Industry," in Sex, Gender and Health: Perspectives from South Asia, T. K. S. Ravindran Ed. Singapore: Springer Nature Singapore Pte Ltd., pp. 401-419, 2024.

[16] N. T. Zaman et al., "Factors shaping female migrants to informal sector in Bangladesh," SN Social Sciences, Vol. 4, No. 178, 2024.

[17] Star Business Report. "Robust growth in RMG not reflected in job creation." The Daily Star. https://www.thedailystar.net/business/economy/news/robust-growth-rmg-not-reflected-job-creation-3353631 (accessed 09 May, 2025).

[18] M. Uddin. "How our RMG industry empowered women." The Daily Star. https://www.thedailystar.net/opinion/views/rmg-notes/news/how-our-rmg-industry-empowered-women-3657121 (accessed 08 May, 2025).

[19] M. A. Islam, A. Hunt, A. H. Jantan, H. Hashim, and C. W. Chong, "Exploring challenges and solutions in applying green human resource management practices for the sustainable workplace in the ready-made garment industry in Bangladesh," Business Strategy & Development, Vol. 3, No. 3, pp. 332-343, 2020.

[20] S. Gupta, M. Wei, N. Tzempelikos, and M. M. Shin, "Women empowerment: challenges and opportunities for sustainable development goals," Qualitative Market Research: An International Journal, Vol. 27, No. 4, pp. 608-630, 2024.

[21] United Nations Development Programme. "The SDGs in Action." United Nations. https://www.undp.org/sustainable-development-goals (accessed 09 May, 2025).

[22] R. K. Byron and M. F. Rahman. "Women workforce growing fast." The Daily Star. https://www.thedailystar.net/frontpage/news/women-workforce-growing-fast-155149 (accessed 09 May, 2025).

[23] M. Yunus, Creating a World Without Poverty: Social Business and the Future of Capitalism, 1st ed. New York: PublicAffairs, 2007.

[24] A. Ratcliff. "Just 8 men own same wealth as half the world." Oxfam International. https://www.oxfam.org/en/press-releases/just-8-men-own-same-wealth-half-world (accessed 10 May, 2025).

[25] M. Yunus, A World of Three Zeros: The New Economics of Zero Poverty, Zero Unemployment, and Zero Net Carbon Emissions, 1st ed. New York: PublicAffairs, 2017.

[26] J. A. Schumpeter, The theory of economic development: An inquiry into profits, capital, credit, interest, and the business cycle. New Brunswick: Transaction Publishers, 1982.

[27] E. Baldwin and M. Curley, Managing IT Innovation for Business Value: Practical Strategies for IT and Business Managers. Santa Clara: Intel Press, 2007.

[28] P. F. Drucker, Innovation and Entrepreneurship. New York: Harper Trade, 1985.

[29] World Business Council for Sustainable Development. https://www.wbcsd.org/ (accessed 10 May, 2025).

[30] S. Schaltegger and M. Wagner, "Sustainable Entrepreneurship and Sustainability Innovation: Categories and Interactions," Business Strategy and the Environment, Vol. 22, No. 4, pp. 222–237, 2011.

[31] A. C. S. Mendes, F. A. F. Ferreira, D. Kannan, N. C. M. Q. F. Ferreira, and R. J. C. Correia, "A BWM approach to determinants of sustainable entrepreneurship in small and medium-sized enterprises," Journal of Cleaner Production, Vol. 371, p. 133300, 2022.

[32] J. A. Forson, T. Y. Baah-Ennumh, and S. O. Mensah, "Women's contribution to local economic development: a study of women in cassava production and processing in Central Tongu district of Ghana," Global Social Welfare, Vol. 5, pp. 189-198, 2018.

[33] C. Nassar, C. C. Nastacă, and A. Nastaseanu, "Women's contribution to economic development and the effects of the gender pay gap," Management Research and Practice, Vol. 13, No. 2, pp. 60-68, 2021.

[34] Global Entrepreneurship Monitor, "2023/24 Women's Entrepreneurship Report: Reshaping Economies and Communities," London Business School, London, UK, 2024.

[35] N. Sobhan and A. Hassan, "The effect of institutional environment on entrepreneurship in emerging economies: Female entrepreneurs in Bangladesh," Journal of Entrepreneurship in Emerging Economies, Vol. 16, No. 1, pp. 12-32, 2024.

[36] N. Hafiz and A. S. Abdul Latiff, "Entrepreneurship as a sustainable solution for the female graduates in the SME sector of Bangladesh," Journal of Business and Social Review in Emerging Economies, Vol. 6, No. 2, pp. 483-492, 2020.

[37] A. K. Tuhin. "Leveraging women entrepreneurship." The Financial Express. https://today.thefinancialexpress.com.bd/editorial/leveraging-women-entrepreneurship-1730910215 (accessed 03 June, 2025).

[38] R. Hu, L. Wang, W. Zhang, and P. Bin, "Creativity, proactive personality, and entrepreneurial intention: the role of entrepreneurial alertness," Frontiers in psychology, Vol. 9, p. 951, 2018.

[39] X. Zhang and K. M. Bartol, "Linking empowering leadership and employee creativity: The influence of psychological empowerment, intrinsic motivation, and creative process engagement," Academy of Management Journal, Vol. 53, No. 1, pp. 107-128, 2010.

[40] T. A. Poli, "Mediating role of entrepreneurship capability in sustainable performance and women entrepreneurship: an evidence from a developing country," Journal of Ecohumanism, Vol. 3, No. 3, pp. 2006-2019, 2024.

[41] R. Kunwar and S. Adhikari, "An exploration of the conceptualization, guiding principles, and theoretical perspectives of inclusive curriculum," Journal of Contemporary Research in Social Sciences, Vol. 5, No. 1, pp. 1-13, 2023.

[42] K. H. Larwin, A. Budnik, and S. E. Horne, "Ohio community pathway HUB: The cost benefit of supporting minority mothers," Journal of Contemporary Research in Social Sciences, Vol. 5, No. 2, pp. 27-37, 2023.

[43] L. De Vita, M. Mari, and S. Poggesi, "Women entrepreneurs in and from developing countries: Evidences from the literature," European Management Journal, Vol. 32, No. 3, pp. 451-460, 2014.

[44] G. M. Cardella, B. R. Hernández-Sánchez, and J. C. Sánchez-García, "Women entrepreneurship: A systematic review to outline the boundaries of scientific literature," Frontiers in psychology, Vol. 11, No. 1557, p. 536630, 2020.

[45] V. S. Corrêa, F. R. D. S. Brito, R. M. D. Lima, and M. M. Queiroz, "Female entrepreneurship in emerging and developing countries: a systematic literature review," International Journal of Gender and Entrepreneurship, Vol. 14, No. 3, pp. 300-322, 2022.

[46] S. M. Ghouse, G. McElwee, and O. Durrah, "Entrepreneurial success of cottage-based women entrepreneurs in Oman," International Journal of Entrepreneurial Behavior & Research, Vol. 25, No. 3, pp. 480-498, 2019.

[47] C. S. Marques, C. T. Leal, G. Santos, C. P. Marques, and R. Alves, "Why do some women micro-entrepreneurs decide to formalise their businesses?," International Journal of Entrepreneurship and Small Business, Vol. 30, No. 2, pp. 241-258, 2017.

[48] J. Moreira, C. S. Marques, A. Braga, and V. Ratten, "A systematic review of women's entrepreneurship and internationalization literature," Thunderbird International Business Review, Vol. 61, No. 4, pp. 635-648, 2019.

[49] H. Al-Dajani, H. Akbar, S. Carter, and E. Shaw, "Defying contextual embeddedness: Evidence from displaced women entrepreneurs in Jordan," in Understanding Women's Entrepreneurship in a Gendered Context: Taylor & Francis Group, pp. 32-46, 2021.

[50] E. M. Cabrera and D. Mauricio, "Factors affecting the success of women's entrepreneurship: a review of literature," Journal of Gender and Entrepreneurship, Vol. 9, No. 1, pp. 31-65, 2017.

[51] N. Isaga, "Start-up motives and challenges facing female entrepreneurs in Tanzania," International Journal of Gender and Entrepreneurship, Vol. 11, No. 2, pp. 102-119, 2019.

[52] S. F. A. Hossain, M. Nurunnabi, K. Hussain, and X. Shan, "Smartphone-based m-shopping behavior and innovative entrepreneurial tendency among women in emerging Asia," International Journal of Gender and Entrepreneurship, Vol. 12, No. 2, pp. 173-189, 2020.

[53] M. Yunus, Banker to the Poor – The Autobiography of Muhammad Yunus, Founder of the Grameen Bank, Reprint Edition ed. Bangladesh: The University Press Limited, 2001.

[54] World Commission on Environment and Development, Our Common Future. New York: Oxford University Press, 1987.

[55] "Unsere gemeinsame Zukunft. Der Brundtland-Bericht der Weltkommission für Umwelt und Entwicklung (Our common future. The Brundtland report from the world commission on environment and development)," V. Hauff Ed. Greven: Eggenkamp Verlag, 1987.

[56] B. Purvis, Y. Mao, and D. Robinson, "Three pillars of sustainability: in search of conceptual origins," Sustainability Science Vol. 14, pp. 681-695, 2019.

[57] M. Yunus, Building Social Business, 2nd ed. Bangladesh: The University Press Limited, 2010.

[58] J. Mair and I. Marti, "Social Entrepreneurship Research: A Source of Explanation Prediction and Delight," Journal of World Business, Vol. 41, No. 1, pp. 36-44, 2006.

[59] TARANGO. "About TARANGO." https://www.tarango.org/about.php?page=About%20TARANGO (accessed 03 May, 2025).

[60] World Fair Trade Organization. "Training, Assistance And Rural Advancement NGO (TARANGO) – Handicraft Programme." https://wfto.com/members/training-assistance-and-rural-advancement-ngo-tarango-handicraft-programme/ (accessed 03 May, 2025).

[61] TARANGO. "10 Standards of Fair Trade " https://www.tarango.org/about.php?page=Fair%20Trade%20Standards (accessed 03 May, 2025).

[62] TARANGO. "Fair Trade handicraft." https://www.tarango.org/about.php?page=Fair%20Handicrafts (accessed 03 May, 2025).

[63] Dhamrai Upazila. "Training (Manpower): Name of the Technical Training Centre " Bangladesh National Portal. https://dhamrai.dhaka.gov.bd/en/site/page/azzi-%E0%A6%AA%E0%A7%8D%E0%A6%B0%E0%A6%B6%E0%A6%BF%E0%A6%95%E0%A7%8D%E0%A6%B7%E0%A6%A3-%E0%A6%AE%E0%A6%BE%E0%A6%A8%E0%A6%AC-%E0%A6%B8%E0%A6%AE%E0-%A7%8D%E0%A6%AA%E0%A6%A6 (accessed 05 June, 2025).

[64] The Daily Star. "Creating equal opportunities for women entrepreneurs." The Daily Star. https://www.thedailystar.net/roundtables/news/creating-equal-opportunities-women-entrepreneurs-3789841 (accessed 05 June, 2025).

[65] SME & Special Programmes Department. "Quarterly Statement of SME Loan Disbursement: October-December, 2023." Bangladesh Bank. https://www.bb.org.bd/smespd_portal/cmsme.html (accessed 05 June, 2025).

[66] C. D. Shoma, "Financing female entrepreneurs in cottage, micro, small, and medium enterprises: Evidence from the financial sector in Bangladesh 2010–2018," Asia & the Pacific Policy Studies, Vol. 6, No. 3, pp. 397-416, 2019.

[67] Palli Karma-Sahayak Foundation (PKSF). "Sustainable Enterprise Project (SEP) " Palli Karma-Sahayak Foundation (PKSF). https://pksf.org.bd/sustainable-enterprise-project-sep/ (accessed 06 June, 2025).

[68] S. Muhammad, K. Ximei, S. E. Saqib, and N. J. Beutell, "Women's Home-Based Entrepreneurship and Family Financial Position in Pakistan," Sustainability, Vol. 13, No. 22, p. 12542, 2021.

A Comparative Review of American and British English Variations and Their Pedagogical Relevance for EFL Learners

Mohammad Rukanuddin[1], Nur Mohammad Khan[2*], AKM Zakaria[2] and Sanzida Rahman[2]

[1]Department of Arts and Sciences, Ahsanullah University of Science and Technology, Bangladesh
[2]Department of Humanities and Social Sciences, Dhaka University of Engineering & Technology, Gazipur, Bangladesh

ABSTRACT

This article investigates the differences between American English (AmE) and British English (BrE). For carrying out the specific objective, the authors have selected the qualitative approach based on the secondary data, namely the sample of published documents in both AmE and BrE. For collecting the specific data, the researchers have considered vocabulary, pronunciation, syntax, punctuation usage, and their influences across different communication domains as the study's key variables. Though these variables share a linguistic core, historical and social factors have shaped their differences. Employing a qualitative methodology, the collected secondary data have been analyzed and presented primarily based on thematic analysis, discourse analysis, and narrative construction to identify key insights and differences between the variants. The findings suggest significant differences across the various domains between the two varieties that are significantly relevant to the EFL students. For EFL learners, understanding these differences is crucial for academic, professional, and global interaction. Mastery of both varieties enhances communicative flexibility and supports strategic use of English as a global lingua franca.

Keywords: Linguistic variance, American and British English, EFL learners

1. INTRODUCTION

The distinctions between American English (AmE) and British English (BrE) have their roots in the United States' colonial past. English was introduced to North America by British invaders at the beginning of the 1600s. However, due to cultural, political, and geographic factors, the language evolved naturally over time [1], [2]. American lexicographer Noah Webster played a significant role in the formation of American English as a distinct dialect of the language. He accomplished this by using standardized terminology and simplified spellings in his dictionaries, such as *An American Dictionary of the English Language* (1828). His work was a component of a broader endeavor to forge an American identity separate from British influence [3], [4]. The social, industrial, and cultural shifts taking place in the UK at the same time led to the further development of British English [5]. Additionally, regional language differences on both sides of the Atlantic Ocean developed more quickly in the 19th and 20th centuries due to advancements in communication and transportation [6], [7].

Understanding the distinctions between American English (AmE) and British English (BrE) is crucial for those learning English as a Foreign Language (EFL) in an increasingly globalized world where English is the most widely spoken language. Misunderstandings resulting from variations in language, pronunciation, grammar, and spelling can hinder effective communication [8], [9]. Pronunciation differences, such as the non-rhoticity of BrE versus the rhoticity of AmE, can also lead to further misunderstandings. For instance, a British person may say "*flat*," but an American may not understand because they expect the word "*apartment*" [10], [11]. Additionally, the media, schools, and workplaces regularly expose students to a range of English dialects. This implies that it's critical to recognize these variations and adjust as needed. Research has highlighted the value of media, particularly television and internet streaming services, in giving students the chance to hear various English dialects [12], [13].

This study seeks to give an analysis of the main differences between British and American English in terms of those various elements in the hope that such

*Corresponding author's email: nurkhan@duet.ac.bd

comparison between English varieties will help learners of English as a foreign language (EFL) be more aware of the most important features they will encounter in the two varieties of English language, including vocabulary, pronunciation, grammar, punctuation, and cultural content. It also emphasizes the importance of being given access to a varied mix of English accents so that we can improve our language skills and cross-cultural understanding. Exposure to both types fosters flexibility and improves understanding, both of which are pivotal for international relationships [14], [15].

1.1 Research Questions

This study focuses on the following research questions:

a) What are the significant variations between American English (AmE) and British English (BrE) as evidenced in published documents?
b) What are the specific pedagogical implications of AmE and BrE variations for English as a Foreign Language (EFL) learners?
c) How does mastery of both AmE and BrE varieties enhance communicative flexibility and support the strategic use of English for EFL learners?

1.2 Research Objectives:

a) To identify and compare the key distinctions between American English (AmE) and British English (BrE) across various linguistic domains.
b) To highlight the importance for EFL learners to understand these differences for effective academic, professional, and global interaction.
c) To emphasize how exposure to and mastery of both AmE and BrE varieties can enhance EFL learners' communicative flexibility and proficiency in English.

1.3 Scope of the Study

Scope of the study defines differences between vocabulary, pronunciation, structure, punctuation usage and their communicative domains of application. All analyses are based on published documents and make use of thematic, discourse and narrative-analytical framings. The primary aim will be to recognize these linguistic differences and to consider their pedagogical implications for EFL learners, specifically how knowledge of them fosters communicative flexibility in academic, professional, and international settings. The study's focused examination of American English (AmE) and British English (BrE) is justified by their overwhelming global prominence as the two most influential and widely taught English varieties in EFL contexts worldwide. Historically and pedagogically, AmE and BrE have served as the primary linguistic models for English language education, dominating textbook content, standardized tests (e.g., TOEFL, IELTS), media exposure, and teacher training.

1.4 Research Gap

Existing research on English variants disproportionately focuses on American and British English, creating a significant gap in understanding the distinct linguistic features of other World Englishes due to practical constraints like time and secondary data accessibility. While acknowledging the existence and importance of other significant English variants like Australian, Canadian, and various New Englishes, their inclusion would drastically broaden the study's scope beyond a manageable qualitative review of secondary data. Therefore, to maintain precision and depth in analyzing pedagogical implications for a large segment of EFL learners, this research strategically concentrates on the foundational and most pedagogically prevalent distinctions between AmE and BrE, as a comprehensive exploration of all English variants would necessitate a separate, more extensive study.

2. ANALYTICAL FRAMEWORK

The study presented in this article is based on a review of secondary data. Peer-reviewed publications that concentrate on the linguistic features of both American English (AmE) and British English (BrE) are critically examined and researched in this article; most of the papers were published within the last 20 years. Numerous databases, including ERIC, Psyc INFO, Google Scholar, Science Direct, Research Gate, and peer-reviewed journals, were used to compile these peer-reviewed articles. Keywords like 'American English', 'British English', 'Differences between AmE and BrE', 'linguistic features of American English and British English' among others, were used to choose the papers. Accurate acknowledgement is given to all data gathered from various secondary sources.

The researchers meticulously selected secondary data, primarily published documents on American English (AmE) and British English (BrE), guided by established academic criteria. The focus was on peer-reviewed academic literature, authoritative linguistic reference works, and seminal texts that extensively illustrate AmE-

BrE variations. Key criteria included topical alignment (documents addressing vocabulary, pronunciation, syntax, and punctuation usage), authoritative provenance (prioritizing works by leading linguists and scholars [1], [2], [4], [7], [10], [11], [24]), scope and depth (preferring comprehensive comparative analyses), temporal relevance (including both historical and contemporary publications), and academic verifiability (selecting widely accessible and verifiable sources for transparency and reproducibility).

The qualitative methodology involved a comprehensive review of 26 foundational academic books and peer-reviewed journal articles [1]–[27], covering encyclopedias, historical linguistics, English varieties, grammar, and World Englishes/English as a Lingua Franca. These sources informed the understanding of linguistic variations and their pedagogical implications for EFL learners. The researchers systematically analyzed the collected secondary data using a multi-pronged approach: thematic analysis identified recurring patterns and themes in AmE-BrE differences across variables (e.g., vocabulary like boot/trunk); discourse analysis examined how these variations were articulated and exemplified, including specific linguistic examples and contextual nuances (e.g., punctuation rules [7], [15]); and narrative construction synthesized these insights into a cohesive explanation of the historical, socio-cultural, and pedagogical relevance of these linguistic divergences for EFL learners.

To thoroughly investigate the identified linguistic challenges, an analytical framework has been constructed, detailing how disparities in vocabulary, pronunciation, grammar, and punctuation are assessed. This framework, derived from the analysis of secondary data, provides the structured approach necessary to understand these distinct linguistic elements. For instance, the followings disparities have been furnished in support of the thesis.

2.1 Disparities in Vocabulary

The vocabulary used in American English (AmE) and British English (BrE) is one of the most obvious distinctions between the two languages. It demonstrates how the two languages have changed over time and culturally in different ways. Due to significant differences in common vocabulary, spelling conventions, and colloquial expressions between the two categories, EFL learners may occasionally feel perplexed.

Table I: Differences in Vocabulary

Category	American English (AmE) Examples	British English (BrE) Examples	Pedagogical Relevance for EFL Learners
High-Frequency Words	elevator, truck, cookie, apartment	lift, lorry, biscuit, flat [1]	Avoids miscommunication; expands receptive/productive lexicon for diverse contexts.
Spelling	-or (e.g., color), -er (e.g., center), traveler, -ize (e.g., realize)	-our (e.g., colour), -re (e.g., centre), traveller, -ise (e.g., realise) [3], [20]	Ensures conformity in academic/professional writing; addresses digital communication challenges [12].
Idioms & Phrases	drop by someone's house, throw a wrench in the works, hit a home run	pop round to someone's house, throw a spanner in the works, sticky wicket [8], [1]	Crucial for cultural fluency, understanding non-literal meanings; interpreting media [17], [21].

2.1.1 High Frequency Words

The use of common terminologies, which may differ significantly between BrE and AmE, is a significant difference. For instance, the American word "*elevator*" is equivalent to the British word "*lift*," while the American word "*truck*" is equivalent to the British word "*lorry*" [1]. Other frequent examples are "*biscuit*" (BrE) versus "*cookie*" (AmE) and "*flat*" (BrE) versus "*apartment*" (AmE). The cultural settings in which they were created and the modifications they have experienced over time set the two varieties apart from one another. For example, due to geographical and historical ties, American English frequently borrows Spanish words like "*ranch*" and "*canyon*." In contrast, British English uses more French-based words like "*ballet*" and "*ensemble*" [18]. Furthermore, common words like "*holiday*" (BrE) and "*vacation*" (AmE) demonstrate how cultural influences alter linguistic preferences [19]. To effectively communicate in both contexts, students learning English as a foreign language (EFL) must comprehend the distinctions between British and American English.

2.1.2 Spelling Variations

The main cause of the spelling differences between American and British English is Noah Webster's 19th-century attempts to standardize and simplify American English spelling [3]. British English nouns ending in *"-re*," like "*centre*" and "*metre*," change to "*center*" and "*meter*" in American English, and British English words ending in "-*our*," like "*colour*" and "*flavour*," are spelled with "-*or*" in American English, as in "*color*" and "*flavor*." Notable changes include the removal of unnecessary letters in American English, such as "*traveler*" (American English) as opposed to "*traveller*" (British English), and the preference for "*ize*" over "*ise*" in verbs (for example, "*realize*" in American English versus "*realise*" in British English). According to academic studies on orthographic reform, spelling variations also reflect broader patterns in language standardization efforts [20]. Due to the prevalence of diverse spelling conventions in digital and international communication, EFL learners may encounter challenges with these distinctions [12]. These distinctions can be challenging for EFL learners, particularly in academic and professional writing contexts where conformity to a single standard is typically required.

2.1.3 Variations Across Idioms & Phrases

Since idiomatic expressions capture the subtleties of different civilizations, they also vary greatly. For instance, "pop round to someone's house" in BrE becomes "drop by someone's house" in AmE, and the British expression "throw a spanner in the works" is translated into "throw a wrench in the works" in AmE. Since EFL learners may struggle to understand idiomatic meanings if they are not exposed to enough context, these differences could be confusing to them [8]. Additionally, studies reveal that idiomatic terms often reflect historical events and local norms, contributing to their unique cultural flavor [21].

Since metaphors in American and British idioms can differ significantly, there is also a difference in the significance of metaphor in colloquial expressions. For example, British English uses cricket-related terms like "sticky wicket," whereas American English frequently uses sports metaphors like "hit a home run" [1]. Understanding the sociolinguistic context in which idioms are used is also crucial because cultural norms influence their appropriateness and usage [10].

How well students comprehend idioms is also significantly influenced by literature and the media, including American and British films [17]. Due to exposure to modern platforms like streaming services, learners now possess a greater understanding of idiomatic expressions. But this exposure has also led to the blending of various linguistic varieties [12]. Academic research indicates that because idioms don't have literal meanings, learners typically struggle to understand them. This implies that in order for students to comprehend idioms, they must be exposed to them regularly and practice using them [13].

It has been demonstrated that teaching strategies that incorporate colloquial language into everyday contexts help students gain comprehension and cultural fluency [22]. Additionally, learners are increasingly using digital tools such as online games and language apps to interact with idioms [18]. Learners must practice using idioms in context in addition to understanding them independently in order to become fluent. Students' language and cultural proficiency is enhanced as a result [23].

Understanding and using these idioms in context is crucial to becoming fluent and culturally competent in both forms of English. Over time, EFL learners' confidence and proficiency are enhanced when they are exposed to authentic materials like books, videos, and podcasts from both linguistic varieties [3].

2.2 Differences in Pronunciation

Spoken English can clearly differ due to differences in pronunciation between BrE and AmE. These traits, which pose unique difficulties for English as a foreign language (EFL) learners, include variances in accents, stress and intonation patterns, and vowel and consonant variations.

Table II: Variances in Pronunciation

Category	American English (AmE) Examples	British English (BrE) Examples	Pedagogical Relevance for EFL Learners
Vowel/ Consonant	Rhotic 'r' (e.g., car, hard), short 'a' (/æ/ in bath), flap 't' (butter)	Non-rhotic 'r' (e.g., car, hard), long 'a' (/ɑː/ in bath), clear 't' (butter) [1]	Improves listening comprehension; awareness of accent variations for intelligibility
Stress/ Intonation	Stress on third syllable (advertisement), neutral/falling tag questions	Stress on second syllable (advertisement), rising tag questions (aren't you?) [8]	Enhances naturalness of spoken English; helps distinguish meaning conveyed by tone.
Accents	General American (GA) [3]	Received Pronunciation (RP), regional accents [3]	Fosters adaptability in various English-speaking contexts.

2.2.1 Various Vowel and Consonant Forms

Phonetic differences are also predominant in AmE and BrE. Hence, vowel sounds are also pronounced differently. For example, in American English, the word "*bath*" is pronounced with a short "a" (/æ/), but in British English, it is pronounced with a long "a" (/ɑː/). The following phonemic chart is given here to show IPA notations of both AmE and BrE :

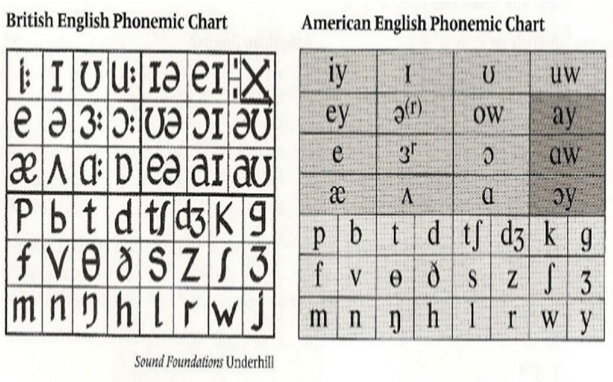

Fig. 1: Phonemic Charts of British English and American English [27]

Disparities are also noticed in consonant sounds. One of the most obvious changes is how the letter "r" is pronounced. The "r" sound in British English is non-rhotic in Received Pronunciation (RP). This implies that it is often not pronounced before consonants or at the end of syllables. Examples of this are the terms "*car*" and "*hard*." On the other hand, AmE is rhotic, meaning that the "r" in these words is pronounced [1].

2.2.2 Variations in Stress and Intonation

Stress and intonation patterns of the two language varieties differ expressively. Words like *"advertisement*" are stressed on the second syllable in BrE, while the third syllable is stressed in AmE. Phrases can also be uttered differently. "*You're coming, aren't you?*" is an example of a tag question in British English (BrE) that often has a rising tone. In similar contexts, American English (AmE) typically has a more neutral or falling tone [8]. These distinctions may affect how natural EFL learners' speech sounds if they are unfamiliar with the conventions of each type.

2.2.3 Difference in Accents across both varieties

One well-known accent associated with British English (BrE) is Received Pronunciation (RP). RP is renowned for its unambiguous pronunciation and lack of regional nuances. Received Pronunciation (RP) is not widely used in modern-day Britain, despite being perceived as a speech pattern associated with the upper class. Rather, regional accents like Geordie, Scouse, and Cockney are more common. In contrast, AmE is usually represented by General American (GA), which is neutral and well-known throughout the US. In contrast to many BrE accents, GA is distinguished by its rhoticity, clear vowel enunciation, and low geographic variability [3]. Exposure to RP, GA, and regional accents can help EFL learners become more adaptive in various English-speaking contexts and enhance their listening comprehension.

2.3 Variations in Grammar

Beyond lexical and phonetic distinctions, American English (AmE) and British English (BrE) exhibit notable grammatical variations, reflecting their divergent evolutionary paths. These differences are evident in areas such as verb conjugation, prepositional usage, and the treatment of collective nouns. For English as a Foreign Language (EFL) learners, recognizing and adapting to these grammatical nuances is crucial for achieving high proficiency and communicative competence across diverse contexts. A comprehensive table illustrating these grammatical disparities between AmE and BrE is presented to further clarify these variations:

Table III: Disparity in Grammar

Category	American English (AmE) Examples	British English (BrE) Examples	Pedagogical Relevance for EFL Learners
Verb Usage	has gotten (acquisition), got (possession)	has got (acquisition/ possession) [1]	Ensures correct verb forms based on regional conventions and intended meaning.
Prepositions	on a team, on the weekend, in the hospital, different than	in a team, at the weekend, in hospital, different from [3]	Improves accuracy in idiomatic expressions and common phrases; highlights contextual usage.
Collective Nouns	Treated as singular (The team is playing well.)	Treated as plural (The team are playing well.) [8]	Facilitates accurate subject-verb agreement according to the target variety's norms.

2.3.1 Disparities Across Verb Usage

The usage of "*got*" and "*gotten*" is one of the most significant differences. In British English, "*got*" can be used as both the past tense and the past participle of the verb "*get*." For instance, the sentence "*He has got a new car*" suggests that he owns a new vehicle [1]. The word "*got*" is usually used to indicate possession in American English, whereas the past participle "*gotten*" is used to indicate acquisition or change. For example, "*He has gotten a new job*" (AmE) is different from "*He has got a new job*" (BrE). These minor variations in verb usage could be confusing to EFL learners because they may need to select the appropriate form depending on the target audience.

2.3.2 Variation Across Prepositions

Additionally, there are notable variations in the usage of prepositions. For instance, BrE speakers typically use "*in a team*," whereas AmE speakers prefer "*on a team*." Similarly, BrE speakers frequently say "*at the weekend*," whereas AmE speakers prefer "*on the weekend*" [3]. Other expressions also differ, such as "*in hospital*" in British English versus "*in the hospital*" in American English, and "*different from*" in British English versus "*different than*" in American English. These changes can affect how well English as a Foreign Language (EFL) learners understand and speak the language, even though they might not be noticeable right away. This highlights how crucial it is to comprehend the context in which each form is employed.

2.3.3 Variation Across Group Nouns

The treatment of collective nouns, or nouns that refer to a group of people, is another significant distinction. Plural verbs are commonly used with collective nouns in BrE to highlight the individual members of the group. As an illustration, "*The team are playing well today*" (BrE) [8]. To master this distinction, English as a Foreign Language (EFL) learners must understand the underlying reasoning and adjust to the conventions of the variety they are using. In contrast, AmE views collective nouns as singular, using singular verbs: "*The team is playing well today*."

2.4 Variations in Punctuation

When it comes to punctuation, there are several differences between British and American English. These differences are most noticeable in the usage of quotation marks and the positioning of punctuation marks in relation to quotation marks. These differences might seem minor, but they matter in professional and academic writing.

The choices made by BrE and AmE for single and double quote marks are different. Double quotation marks (“ ”) are used for quotations that are incorporated within other quotations, while single quotation marks (‘ ’) are typically used for the first quotation in British English. BrE would write, for example: "*He said, “I am leaving now*." In contrast, American English uses single quotation marks (‘ ‘) for quotations that appear inside other quotations and double quotation marks (“ ”) for main quotations. For instance: "*He said, ‘I am leaving now*.’" EFL students may find this standard particularly difficult to meet when they are reading texts that were prepared in a variety of styles [1].

Another notable variation is where punctuation marks are placed in relation to quote marks. Even if they are not included in the quoted text, punctuation such as commas and periods are inserted inside the closing quote marks in AmE. In British English, punctuation is placed outside of quotation marks unless it is a part of the cited text. For instance, AmE would write: "*She said it was ‘amazing*.’" Whereas the example in BrE as follow: *‘She said it was “amazing”.’*. EFL learners may find it challenging to meet this criterion, especially when they are expected to maintain consistency in formal writing.

3. CULTURAL DIMENSIONS OF BRITISH AND AMERICAN ENGLISH

Cultural distinctions, which reflect the distinct historical and social settings of each language, have a considerable impact on the phrases, idioms, and everyday usage of American English (AmE) and British English (BrE). Media, literature, and film all have an impact and are necessary to propagate these kinds of items and broaden their worldwide reach. EFL students must so be able to understand the nuances of other cultures.

British and American English have developed a number of unique words and expressions that are not found in the other version of English due to cultural factors. These expressions and idioms typically reflect the values and customs of a particular culture. For example, the British proverb "*keep a stiff upper lip*" illustrates how important emotional control and resolve are in British culture. In contrast, the American expression "*cut to the chase*" conveys a pragmatic and action-oriented mindset. Hollywood's fast-paced storytelling often influences this way of thinking [1], [3]. Similarly, British English idioms like "*a storm in a teacup*" and their American English counterparts like "*a tempest in a teapot*" show some of the more subtle cultural similarities as well as the differences between the two languages [4].

The ways that people interact with each other in their daily lives also show these differences. British speakers, for instance, would use the word "*queueing*" because it reflects their culture's emphasis on patience and order. However, the phrase "*lining up*" could be used by Americans [24]. Furthermore, regional idioms such as "*it's not rocket science*" in American English and "*Bob's your uncle*" in British English illustrate the practical approach to communication and culturally specific humor in their respective regions [22], [19]. Students learning English as a foreign language (EFL) risk misinterpreting the language if they lack a solid grasp of the cultural contexts that shape it. By understanding these distinctions, learners can improve their communication skills and recognize the diversity that is a natural part of English as a global language. By being exposed to both types through media, literature, and face-to-face interactions with native speakers, learners can enhance their language adaptation and cultural competency [14].

The global expansion of British and American English is greatly influenced by media, literature, and film. They also have an impact on how these two distinct forms of English are perceived and accepted. American English expressions, idioms, and slang have spread throughout the world thanks in part to American films, television series, and music. This is a result of Hollywood's global influence. Many people are familiar with phrases like "*take a rain check*" and "*break a leg*" which are often used by American media [3], [4].

However, British literature, which comprises writings by authors like Shakespeare as well as contemporary authors like J.K. Rowling, has played a significant role in showcasing the diversity of British English. In addition to increasing their fame, British television series like Doctor Who and Downton Abbey have contributed to the globalization of British English dialects and idioms [1], [19]. Both types of programming are now more widely available to viewers thanks to streaming services like Netflix and BBC iPlayer, which enable them to enjoy the distinctive linguistic and cultural elements of each. The distinction between BrE and AmE has also become hazier due to the internet and social media. Two platforms that showcase content producers from both areas are YouTube and TikTok, which contribute to the diversity of languages [22]. For EFL learners, this exposure is crucial because it emphasizes how crucial it is to comprehend a range of linguistic forms in order to successfully negotiate a range of linguistic contexts [14].

In the end, the way that culture shapes language shows that English is constantly changing and that it can adapt to changes in society. Immersion in the cultural contexts of British English (BrE) and American English (AmE) through media, literature, and films can help EFL students better understand the language and interact with people from different cultures [12].

4. ADDRESSING BRE–AME DIFFERENCES IN EFL CLASSROOMS

Understanding both British English (BrE) and American English (AmE) presents unique difficulties for students learning English as a foreign language (EFL). Vocabulary, grammar, pronunciation, and cultural nuances are the areas where these difficulties are most noticeable. Vocabulary differences, such as the use of the word "*truck*" in American English and the word "*lorry*" in British English, can cause confusion for learners who are unfamiliar with both languages [1]. Similarly, grammatical differences can complicate communication in professional and academic contexts. For instance, you might say "*I have just eaten*" in British English, but "*I just ate*" in American English [24]. Disparities in pronunciation can make it even harder for learners of English as a foreign language (EFL) to comprehend and use the language. For instance, many British English (BrE) accents frequently omit the rhotic "r," which is pronounced in American English (AmE) [3].

Understanding the two types also requires an understanding of cultural quirks. For example, students must go beyond literal translations and comprehend the meanings in context when using idiomatic expressions like "*Bob's your uncle*" (British English) and "*spill the beans*" (American English) [22]. Overcoming these challenges requires exposure to academic materials, literature, and media from both BrE and AmE sources. Reading American Newspapers like The New York Times and British newspapers like The Times can provide learners with valuable information about cultural perspectives and spelling conventions (e.g., "*favour*" versus "*favor*") [4].

To effectively communicate on a global level, it is crucial to be familiar with both forms, even though it is typically possible to select one standard for academic or professional purposes. Flexibility is a crucial ability for English as a foreign language (EFL) learners since, as a lingua franca, it is influenced by a wide range of cultural and geographic differences [25]. Learners can manage complex social and professional situations in a globalized society by being fluent in both British and American English, which enhances language proficiency and fosters cross-cultural understanding [23].

Understanding British and American English can be challenging for EFL learners due to differences in vocabulary, grammar, and pronunciation. To address this, contrastive analysis activities can help students directly compare forms, such as spelling (*colour* vs. *color*) or grammar (*have got* vs. *have*). For pronunciation, accent training apps like ELSA Speak and YouGlish allow learners to hear and practice both BrE and AmE accents, improving clarity and comprehension. These tools make learners more adaptable in global communication.

4.1 Challenges in Mastering both Areas

The main challenge for EFL students is the stark differences between BrE and AmE, which can cause miscommunication and confrontations. Students are often expected to memorise multiple different variations of the same term [1]. This can be attributed to variations in spelling, such as "*colour*" in British English and "*colour*" in American English, as well as variations in terminology, such as the usage of "*lift*" in British English and "*elevator*" in American English. Inconsistencies in pronunciation, like the rhotic "r" in AmE versus its absence in BrE, can make spoken communication even more difficult [3]. Additionally, differences in prepositional usage and idiomatic expressions can lead to misunderstandings, especially when learners are exposed to both. These issues are particularly apparent in academic and professional settings, where it is frequently necessary to maintain consistency and conform to a certain standard. For example, people in British English say "*at the weekend*," but in American English, they say "*on the weekend*." Further impeding EFL learners' comprehension are syntactic inconsistencies, such as the past participle "*gotten*" being used in AmE but changed to "*got*" in BrE [24]. Mixed exposure to both types may cause learners to inadvertently combine BrE and AmE traits, leading to "*interlanguage*" forms [26]. Additionally, students' ability to understand context can be impacted if they are unable to identify the subtle cultural context differences that exist in language [23]. AmE's preference for "*apartment*" over BrE's "*flat*" demonstrates lexical ambiguity, which could lead to needless uncertainty [4]. Last but not least, teaching strategies usually fail to systematically consider the subtle differences, leaving students uncertain about which norm to adhere to [22].

4.2 Avoid Mixing the Two Varieties

EFL students should prioritize adopting a single standard, such as American English (AmE) or British English (BrE), based on their academic, professional, or geographic needs in order to overcome these difficulties. While students in the United States or those interacting with American corporations should use American English (AmE), students in the United Kingdom or those interacting with British businesses might benefit from using British English (BrE). Uniformity in vocabulary, spelling, grammar, and punctuation is ensured by using a single standard. For formal writing and communication, this is essential [8]. As a result, students need to be flexible and adaptive, understanding that the standard they have chosen might not always suit the tastes of their target audience. Exposure to the alternate form may help learners identify and adjust to differences in real-time conversations, even though it is rarely used.

4.3 Value of Exposure Across both Varieties

A comprehensive command of the language requires exposure to both British and American English, even though choosing just one standard is practical. Because English is used so widely around the world, learners are likely to come across both forms of the language in contexts such as media, academic research, and business communication. Learners can improve their listening comprehension, cultural awareness, and capacity to engage in meaningful conversations with speakers of various English dialects when they understand both criteria [1], [3].

Learners have many opportunities to familiarize themselves with both British and American English through media, literature, and online content. Watching American television shows like Friends and British shows like Sherlock could help students identify cultural references, idiomatic idioms, and pronunciation differences [22], [19]. Similarly, learners are exposed to real-world language applications through online platforms like YouTube and streaming services, which usually offer a variety of content in both British English and American English [12]. Furthermore, reading materials from American scholarly journals as well as British newspapers like The Guardian may improve students' understanding of vocabulary, grammar, and spelling [24].

It is crucial to understand how American and British English are used in real-world situations. For instance, learners of British English might come across formal terms that are frequently used in Commonwealth nations, while American English's more straightforward communication style is more prevalent in global business contexts [25], [8]. Additionally, incorporating other dictionaries into teaching strategies—such as Merriam-Webster for American English and Oxford English Dictionary for

British English—helps clarify distinctions and improve linguistic flexibility [4], [16].

In the end, EFL students should try to be flexible and adaptive. Learners can effectively navigate linguistic diversity, communicate effectively in a globalized setting, and gain a deeper understanding of the social and cultural dynamics inherent in language use by becoming proficient in one standard language and being exposed to another [23], [14].

6. CONCLUSION

American English (AmE) and British English (BrE) differ in several ways, such as syntax, pronunciation, spelling, and vocabulary. These differences show how language has changed over time as well as the cultural and historical backgrounds of the US and the UK. Understanding these differences is essential for students learning English as a foreign language (EFL) because they affect communication, comprehension, and professional interactions.

By recognizing the importance of the distinctions between the two and choosing one standard for particular contexts, such as academic, professional, or regional ones, EFL learners can succeed in both forms. Depending on their academic and professional objectives or geographic context, learners are advised to focus on either American English (AmE) or British English (BrE). On the other hand, exposure to both kinds is necessary to improve listening comprehension, increase language proficiency, and adjust to different communication situations [8].

Understanding BrE and AmE variations is crucial for EFL learners. Educators and learners must balance focusing on one standard (AmE or BrE), based on goals and context, with broad exposure to both for comprehensive proficiency and adaptability. Future research should investigate pedagogical interventions like corpus tools or AI-driven accent apps, and conduct longitudinal studies on balanced exposure's impact. To overcome challenges, explicit teaching of lexical, grammatical, and pronunciation differences is key. Curriculum designers should implement modular units for focused study alongside comparative activities and integrate authentic materials to convey linguistic and cultural nuances. The aim is to cultivate agile, culturally aware English users for a globalized world.

American English and British English are the two most common forms of communication in English, which has become a universal language. Although the learner's goals frequently dictate which option is best, knowing the cultural and regional factors that influence each variation improves the student's capacity to participate in international discussions. Ultimately, being proficient in English requires more than just knowing a single set of rules; it also requires flexibility, knowledge, and an understanding of other cultures in a world that is complex and interconnected.

REFERENCES

[1] D. Crystal, The Cambridge Encyclopedia of the English Language, 2nd ed. Cambridge: Cambridge University Press, 2003.

[2] A. C. Baugh and T. Cable, A History of the English Language, 6th ed. London: Routledge, 2012.

[3] R. McCrum, R. MacNeil, and W. Cran, The Story of English, 3rd ed. New York: Penguin, 1992.

[4] J. Algeo, British or American English? A Handbook of Word and Grammar Patterns, Cambridge: Cambridge University Press, 2006.

[5] B. Kortmann and E. W. Schneider, A Handbook of Varieties of English: A multimedia reference tool Volume 1: Phonology, Berlin: Mouton de Gruyter, 2004.

[6] Trudgill, The Dialects of England, 2nd ed. Oxford: Blackwell, 1999.

[7] R. Quirk, S. Greenbaum, G. Leech, and J. Svartvik, A Comprehensive Grammar of the English Language, London: Longman, 1985.

[8] A. Kirkpatrick, World Englishes: Implications for International Communication and English Language Teaching, Cambridge: Cambridge University Press, 2007.

[9] G. Leech, M. Hundt, C. Mair, and N. Smith, Change in Contemporary English: A Grammatical Study, Cambridge: Cambridge University Press, 2009.

[10] J. C. Wells, Accents of English, Vol. 1, Cambridge: Cambridge University Press, 1982.

[11] M. Swan, Practical English Usage, 3rd ed. Oxford: Oxford University Press, 2005.

[12] D. Graddol, English Next, London: British Council, 2006.

[13] A. Peters, The Language of Primary School Children, London: Routledge, 2004.

[14] B. Seidlhofer, Understanding English as a Lingua Franca, Oxford: Oxford University Press, 2011.

[15] R. L. Trask, The Penguin Guide to Punctuation, London: Penguin Books, 1999.

[16] R. Ellis, Second Language Acquisition, Oxford: Oxford University Press, 1997.

[17] G. Yule, The Study of Language, 6th ed. Cambridge: Cambridge University Press, 2016.

[18] P. Durkin, Borrowed Words: A History of Loanwords in English, Oxford: Oxford University Press, 2014.

[19] M. Görlach, A Dictionary of European Anglicisms: A Usage Dictionary of Anglicisms in Sixteen European Languages, Oxford: Oxford University Press, 2002.

[20] C. Barber, J. Beal, and P. Shaw, The English Language: A Historical Introduction, 2nd ed. Cambridge: Cambridge University Press, 2009.

[21] C. Fernando, Idioms and Idiomaticity, Oxford: Oxford University Press, 1996.

[22] J. Jenkins, World Englishes: A Resource Book for Students, 2nd ed. London: Routledge, 2009.

[23] M.A.K. Halliday and R. Hasan, Language, Context, and Text: Aspects of Language in a Social-Semiotic Perspective, Oxford: Oxford University Press, 1989.

[24] P. Trudgill and J. Hannah, International English: A Guide to Varieties of Standard English, 5th ed., London: Routledge, 2013.

[25] B. Seidlhofer, “English as a lingua franca,” ELT Journal, Vol. 59, No. 4, pp. 339–341, 2005.

[26] L. Selinker, “Interlanguage,” International Review of Applied Linguistics in Language Teaching, Vol. 10, No. 1–4, pp. 209–232, 1972.

[27] A. Underhill, Sound Foundations: Learning and Teaching Pronunciation, Macmillan Education, 2005.

Effect of Spatial Planning on the Noise Level of Teacher's Chamber in University

Farhana Ahsan* **and Farha Tanzin**

Department of Architecture, Dhaka University of Engineering & Technology, Gazipur, Bangladesh

ABSTRACT

The impact of noise on productivity in institutional buildings can be significant. Excessive noise levels distract individuals, impairing their ability to focus, think clearly, and perform tasks efficiently. In educational settings, students and teachers may struggle to concentrate, leading to reduced learning outcomes. Addressing these issues often requires thoughtful architectural design, soundproofing materials, and strategic noise control measures to create a conducive environment for occupants. This study aims to asses the noise level in teachers chambers for two different spatial planning layout of university buildings. A combination of quantitative research methodology have applied in this study through experiment, computational, and analytic methods. For this study two universities are selected, one is Dhaka University of Engineering and Technology (DUET), Gazipur and the other one is Gazipur Agricultural University (GAU), Gazipur for data collection. Data has measured with a portable digital sound level meter (TES-1353S). A regular class day has been chosen and data was collected for 12 times for that day. The timing of data collection is chosen in accordance with the university's class schedule. In teacher's chamber, noise level measured in the both surveyed space was lower during class time ranging from 53.1 dBA to 41.1 dBA at DUET and from 43.6 dBA to 41.3 dBA at GAU. But during break time noise level was relatively higher, ranging from 68.7 dBA to 52.6 dBA at DUET and from 53.4 dBA to 47.6 dBA at GAU. During class time mean noise level was 46.5 dBA at DUET and 42.3 dBA at GAU whereas during break time mean noise level was 59.8 dBA at DUET and 50.0 dBA at GAU. Moreover, ANOVA test results show that different spatial planning of teachers' chambers had a statistically significant effect on mean noise level. So it could be concluded that the level of background noise in teachers' chamber is considerably affected by the spatial planning of the chambers.

Keywords: Noise level, Teacher's chamber, Spatial planning, University

1. INTRODUCTION

Universities offer a wide range of facilities to support academic, recreational, and social activities for students, faculty, and staff. Facilities range from academic facilities (such as classroom, lecture hall, library, teacher's room, laboratory, etc.) to recreational facilities (such as sports centers, outdoor fields, recreational clubs, etc.). These facilities are designed to enhance the overall university experience, providing support for academic success, and personal growth, especially for teachers and students [1]. By offering a supportive environment, these facilities contribute to various aspects of university life. Among those facilities, a teacher's chamber is a designated space where faculty members conduct their academic and administrative duties [2]. This private area is used for lecture preparation, study, research activities, meetings with students, and administrative and professional work.

Similar to any other study area, this teacher's chamber requires a quiet environment [3]. Noise in university buildings is a common phenomenon that varies based on the type of space, time of day, and the activities occurring within those spaces [4]. Noise can impact the academic environment, particularly in areas designed for studying, teaching, or research. The noise level in a learning space i.e. teacher's chamber, is a crucial factor that can significantly impact concentration, productivity, and overall study effectiveness [5]. Noise can stem from a variety of sources, and it often disrupts concentration and productivity for both students and faculty [6],[7]. Common sources of noise in university are foot traffic and conversations, construction and maintenance work, classroom overflows, noise from adjacent classrooms, lectures, or group discussions that can carry into nearby spaces, HVAC systems, and equipment, social areas near study spaces, events and gatherings etc. [8].

*Corresponding author's email: ar.farhana@duet.ac.bd

Difficulties caused by noise in learning environments have been recognized and understood for over 100 years [9]. The learning process becomes slower in learning environments, which have high background noise levels [10]. Non-optimal acoustical conditions result in decreased learning effectiveness as well as fatigue, tension, health problems, and headaches [11]. High noise levels can significantly hinder the learning process by creating distractions that divert attention from tasks, making it challenging for learners to absorb information or complete assignments effectively [12]. Additionally, background noise contributes to an increased cognitive load, which can reduce both efficiency and retention of information. Over time, constant exposure to elevated noise levels may also lead to heightened stress and mental fatigue, further impacting learners' ability to concentrate and perform academically [13]. Creating a quieter study environment is therefore essential for optimizing focus, learning, and overall well-being [14].

The teacher's chamber is a type of educational setting. So, learning space requirements will be relevant for the teacher's chamber. Table 1 shows the allowable upper limit of indoor background noise for classrooms, libraries, small offices, and conference rooms is 38-48 decibels (dBA) according to BNBC 2020 [15]. ANSI standard for classroom acoustics addresses the issue of background noise. The maximum level of background noise allowed in the same learning space is 35 dBA [16]. In the UK, the allowable upper limit of indoor background noise for learning space is set by Building Bulletin 93 (BB93): Acoustic Design of Schools. For a typical learning space, the allowable upper limit of background noise is also 35 dBA [17].

Numerous studies have been done in the past to evaluate the noise level in educational settings like schools and universities. Most of them focused on subjects like the university or school's classroom. Augustyńska et al., 2010 carried out an assessment of teachers' exposure to noise in primary schools[18]. Noise was measured at the teachers' workplaces. Studies have shown that noise is the main factor of annoyance in the school environment. Almost 50% of teachers surveyed said that noise irritates them, and close to 40% said that noise is excruciating or intolerable. But based on published documents no research was found about the study of the noise level in teacher's chambers at the university. So, this study aims to achieve this research gap. This study aims to evaluate the prevailing noise level in teacher's chambers at the university.

2. METHODOLOGY

The survey was done in three steps. Firstly, a physical survey was conducted. In the second step, ambient noise was measured in the case space. Lastly, the data was analysed.

2.1 Selection of Case Space

In university building plans, different types of spatial planning layouts have been seen. Generally, three types of arrangement are very common. The first one is the classrooms and teachers' rooms in the same block, the second one is classrooms and teachers' rooms in a separate block, and the third is on different floors. Two universities are selected to study noise levels in teachers' chambers. One is Dhaka University of Engineering and Technology (DUET), Gazipur and the other one is GazipurAgricultural University (GAU), Gazipur. The Planning layouts of the universities are different. In DUET the classrooms and teachers' rooms are in the same block, separated by a common corridor (Fig.1). On the other hand the planning layout of GAU is different, these two blocks are separated (Fig. 2).

The teachers' block and the office exist just opposite the classrooms in the corridor of the floor in Architecture Department of New Academic Building, DUET. The noise comes during the interval time of the classes when students enter or exit from the classrooms and chat with each other in the corridor. The primary corridor is 10 feet wide, twelve feet high, and two hundred and twenty feet long. The wall of the corridor is a 5″brick plastered wall with wooden doors at several distances and a high window over 10′ height. The secondary corridor is 6′ wide with the same configuration as well as an additional operable window at 2′-6″ level. The chamber area is varying from144 to 165sft and each studio is 1867sft with 30No.s student capacity. Total floor area is 17851sft with 136 (120 students, 9 teachers and 7 staffs) users.

In GAU, faculty of fisheries building, the classroom and laboratory block is separated from teachers' block by staircase (Fig.2). These two blocks are connected with a 7′ wide corridor. The length of the corridor is 174′, and height is 13′. The wall of the corridor is a 5″-brick plastered wall with wooden doors at several distances and a high window over 10′ height. The chamber area varies from 487 to 681sft. The Lab areas are varying from 487 to 681sft with 30No.s student capacity and the classroom area is 838sft with 60 student capacity. Total floor area is 9078sft with 147 (130 students, 8 teachers and 9 staffs) users.

Table I: Allowable upper Limit of Indoor Background Noise [15], [21]

Type of space	dBA
Broadcast and recording studios (distant microphone used)	18
Large theatres and auditoriums, mosques, churches, temples and prayer space	<28
Small theatres, auditoriums, churches, music rehearsal rooms, large meeting and conference rooms	<38
Classrooms, libraries, small offices and conference rooms	33-48
Living rooms and drawing rooms in dwellings	38-48
Large offices, receptions, retail shops and stores, cafeterias, restaurants, etc.	43-53
Lobbies, laboratories, drafting rooms and general offices	48-58

Fig. 1: Case Study Floor Plan of New Academic Building, DUET

Fig. 2: Case Study Floor Plan of Faculty of Fisheries, GAU

2.2 Data Collection

A portable digital sound level meter (TES-1353S) was used to measure the noise level at the case spaces. The noise level is detected in decibels (dB).

The measurement points is selected in both the adjacent corridor and the teachers' chamber at each university. This selection is based on the objective of the study, which is to assess the noise levels within the teachers' chambers. As these chambers are situated adjacent to the corridors, and noise is primarily transmitted into the chambers through these corridors, it is essential to include the corridor as a measurement location. Within the teachers' chambers, noise measurements are taken at the reading position, approximately at ear level, to reflect the typical exposure experienced by occupants.

For measuring data 8 points are selected on the Architecture Department of NAB building in DUET (Fig. 3). On corridor for the points 1,2 and 3 data are collected at ear level at a standing height of 1.5m. In chambers for points 4,5,6,7 and 8, the data are collected at ear level at sitting position 1.2m [19], [20]. The data was collected 12 times on a regular class day. The time of data collection is selected according to the class routine of the university (Table I). Two different phases of time have been chosen that is class time and break time.

For the other case space GAU floor plan, 9 points have been selected for sound level measuring (Fig. 4). There are three points in the corridor and six points in the chambers. The routine of the university is more or less the same as DUET (Table II). Here also two different phases of time have been chosen that is class time and break time.

2.3 Data Analysis

This study aimed to analyze the collected data according to various zones and times. First, the data was analysed by two different zones, that were the teacher's chamber and the adjacent corridor. Secondly, it was analyzed by class time and break time. Thirdly the data was analysed by different spatial plans of two universities.

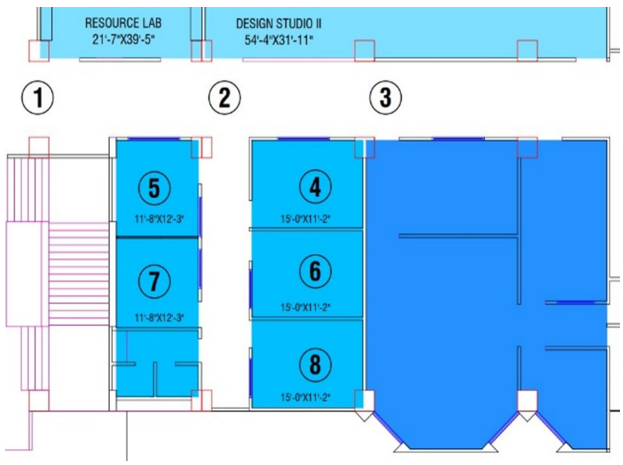

Fig. 3: Noise Level Measuring Points on Case Study Floor for DUET

Table II: Class Routine of DUET

Class Routine of DUET								
	Period 1	Period 2	Tea Break	Period 3	Period 4	Lunch break	Period 5	Period 6
Time	8:30-9:30	9:30-10:30	10:30-10:55	10:55-11:55	11:55-12:55	12:55-13:55	13:55-14:55	14:55-15:55

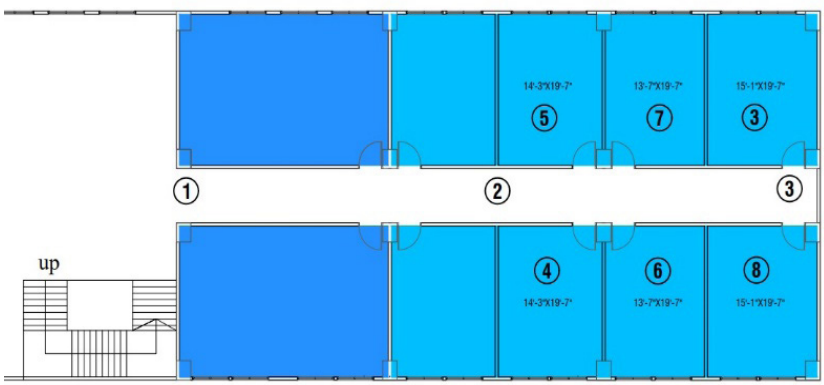

Fig. 4: Noise Level Measuring Points on Case Study Floor for GAU

Table III: Class Routine of GAU

Class Routine of GAU							
	Period 1	Period 2	Period 3	Period 4	Lunch break	Period 5	Period 6
Time	9:30-10:20	10:25-11:15	11:20-12:10	12:15-13:05	13:05-14:10	14:10-15:05	15:05-15:55

This study also tried to check whether there was any statistically significant effect of noise level due to different spatial planning. For this purpose, a one-way Analysis of Variance (ANOVA) is performed using the Analysis ToolPak extension of Microsoft Excel 2010 software. The significance level (α) for the ANOVA test was chosen at 0.05 in accordance with earlier research on this topic [20]. In the ANOVA test, the F_0 value is a ratio of two independent measures of variance for the provided data. The F_{crit} value is a specific value to which the resulting F_0 value is compared. If the F_0 value in the ANOVA test is greater than the F_{crit} value, the null hypothesis is rejected and the alternative hypothesis is accepted. If F_0 value is less than F_{crit} value, it indicates that there is insufficient evidence to reject the null hypothesis.

3. RESULTS AND DISCUSSIONS

3.1 Noise Levels in Teachers' Chamber

Background noise levels of the adjacent corridor and teacher's chamber at DUET are presented in Fig. 5. Data depicts noise levels from the beginning of the class to the end of the class for one day. In the adjacent corridor, the noise level varies from 81.7 dBA to 51.5 dBA. In teachers' chamber noise level varies from 78.8 dBA to 40.6 dBA. Data also shows that the noise level was highest at 15:55 which was the end of class. At 15:55 in the adjacent corridor, the noise level varies from 81.7 dBA to 75.4 dBA, and in the teachers' chamber from 78.8 dBA to 62.5 dBA. The noise level was also greater at 10:30 and 12:55. 10:30 was tea break and 12:55 was lunch break. During all class times such as 9:00, 10:00, 11:30, 12:30, 14:30, and 15:30 noise level was relatively lower.

Figure 6 illustrates the background noise levels of the adjacent corridor and teacher's chamber at GAU for one day. In the adjacent corridor, the noise level varies from 81.4 dBA to 47.2 dBA. In teachers' chamber noise level varies from 65.8 dBA to 40.2 dBA. Data also shows that the noise level was highest at 15:55 which was the end of class. At 15:55 in the adjacent corridor, the noise level varies from 81.4 dBA to 63.9 dBA, and in the teachers' chamber from 65.8 dBA to 58.6 dBA. The noise level was also greater at 13:05. That was lunch break. During all class time noise level was relatively lower.

During class time background noise levels of DUET are presented in Table IV. In the adjacent corridor, the noise level varies from 61.5 dBA to 51.5 dBA. The mean noise level was 56.4 dBA. In teachers' chambers mean noise level varies from 53.1 dBA to 41.1 dBA. The noise level was highest at locations 4 and 5 because these two were located just opposite of classroom and was lowest at location 8 which was located far away from the classroom. The mean value of noise levels of all the teachers' chambers is 46.5 dBA during class time.

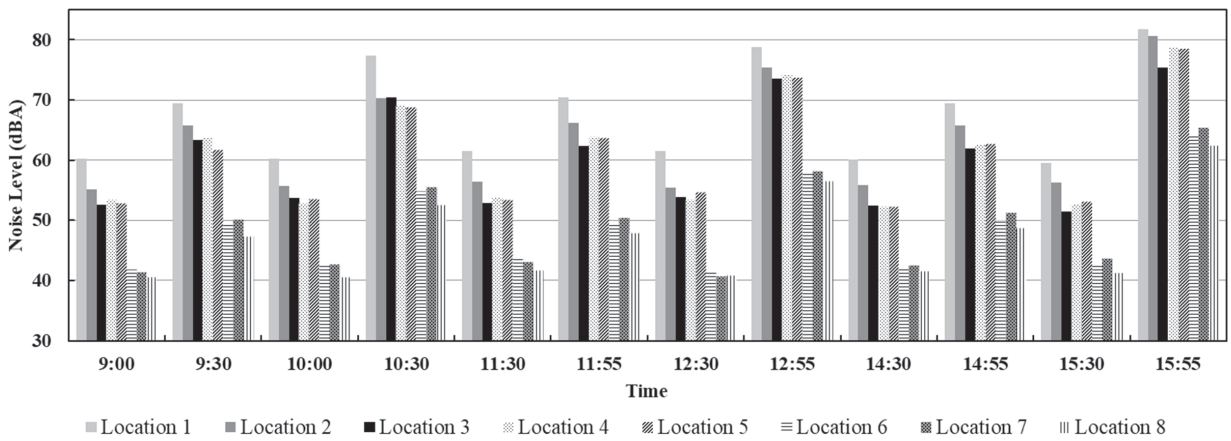

Fig. 5: Background Noise Levels of Adjacent Corridor and Teacher's Chamber at DUET

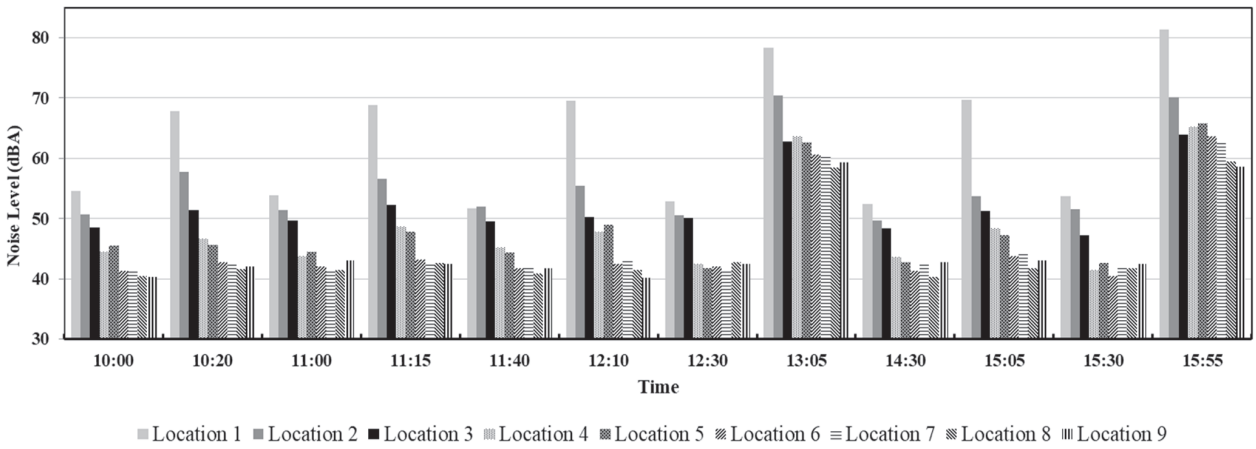

Fig. 6: Background Noise Levels of Adjacent Corridor and Teacher's Chamber at GAU

Table V illustrates data of background noise levels of DUET during break time. In the adjacent corridor, the noise level varies from 81.7 dBA to 61.9 dBA. The mean noise level was 71.0 dBA. In teachers' chambers mean noise level varies from 68.7 dBA to 52.6 dBA. The mean value of noise levels of all the teachers' chambers is 59.8 dBA during break time.

During class time background noise levels of GAU are presented in Table VI. In the adjacent corridor, the noise level varies from 54.5 dBA to 47.2 dBA. The mean noise level was 51.0 dBA. In teachers' chambers mean noise level varies from 43.6 dBA to 41.3 dBA. The noise level was relatively lower in all the teachers' rooms because all of these were located far away from the classroom zone. The mean value of noise levels of all the teachers' chambers is 42.3 dBA during class time.

Table VII illustrates data of background noise levels of GAU during break time. In the adjacent corridor, the noise level varies from 81.4 dBA to 50.3 dBA. The mean noise level was 62.9 dBA. In teachers' chambers mean noise level varies from 53.4 dBA to 47.6 dBA. The mean value of noise levels of all the teachers' chambers is 50.0 dBA during break time.

Figure 7 demonstrates the mean background noise level during class time and break time at DUET and GAU in the teachers' chamber. During class time mean noise level was 46.5 dBA at DUET and 42.3 dBA at GAU whereas during break time mean noise level was 59.8 dBA at DUET and 50.0 dBA at GAU.

Table IV: Background Noise Levels (dBA) of DUET During Class Time

Class time at DUET								
Adjacent Corridor				Teacher's Chamber				
Location				Location				
Time	1	2	3	4	5	6	7	8
9:00	60.2	55.1	52.6	53.5	52.8	41.8	41.4	40.6
10:00	60.3	55.7	53.7	52.9	53.6	42.7	42.6	40.6
11:30	61.5	56.4	52.9	53.8	53.4	43.8	43.1	41.7
12:30	61.5	55.4	53.9	53.5	54.7	41.4	40.7	40.8
14:30	60.1	55.8	52.5	52.3	52.3	42.3	42.5	41.5
15:30	59.6	56.3	51.5	52.7	53.1	42.6	43.7	41.2
Mean	60.5	55.8	52.9	53.1	53.3	42.4	42.3	41.1
Mean		56.4				46.5		

Table V: Background Noise Levels (dBA) of DUET During Break Time

Break Time at DUET								
Adjacent Corridor				Teacher's Chamber				
Location				Location				
Time	1	2	3	4	5	6	7	8
9:30	69.4	65.7	63.4	63.7	61.8	49.6	50.2	47.3
10:30	77.4	70.3	70.4	69.2	68.8	54.8	55.6	52.6
11:55	70.5	66.2	62.4	63.9	63.7	49.4	50.5	47.9
12:55	78.8	75.4	73.6	74.2	73.8	57.9	58.3	56.6
14:55	69.5	65.7	61.9	62.6	62.8	50.1	51.3	48.8
15:55	81.7	80.6	75.4	78.8	78.6	64.0	65.4	62.5
Mean	74.6	70.7	67.9	68.7	68.3	54.3	55.2	52.6
Mean		71.0				59.8		

Table VI: Background Noise Levels (dBA) of GAU During Class Time

Class Time at GAU									
Adjacent Corridor				Teacher's Chamber					
Location				Location					
Time	1	2	3	4	5	6	7	8	9
10:00	54.5	50.6	48.5	44.5	45.5	41.3	41.5	40.5	40.3
11:00	53.9	51.4	49.6	43.7	44.5	42.1	41.6	41.4	43.1
11:40	51.7	51.9	49.5	45.2	44.3	41.8	42.1	40.9	41.7
12:30	52.8	50.5	50.1	42.4	41.8	42.1	41.4	42.7	42.5
14:30	52.4	49.7	48.3	43.6	42.7	41.3	42.7	40.3	42.7
15:30	53.7	51.6	47.2	41.5	42.6	40.5	41.8	41.8	42.5
Mean	53.2	51.0	48.9	43.5	43.6	41.5	41.9	41.3	42.1
Mean		51.0				42.3			

Table VII: Background Noise Levels (dBA) of GAU During Break Time

Break Time at GAU									
Adjacent Corridor				Teacher's Chamber					
Location				Location					
Time	1	2	3	4	5	6	7	8	9
10:20	67.8	57.7	51.4	46.7	45.7	42.7	42.3	41.6	42.1
11:15	68.9	56.6	52.3	48.7	47.8	43.2	42.6	42.6	42.5
12:10	69.5	55.4	50.3	47.8	48.9	42.5	43.2	41.5	40.2
13:05	78.4	70.4	62.8	63.6	62.7	60.6	60.4	58.5	59.4
15:05	69.7	53.7	51.3	48.4	47.2	43.7	44.1	41.7	43.1
15:55	81.4	70.2	63.9	65.3	65.8	63.6	62.6	59.5	58.6
Mean	72.6	60.7	55.3	53.4	53.0	49.4	49.2	47.6	47.7
Mean		62.9				50.0			

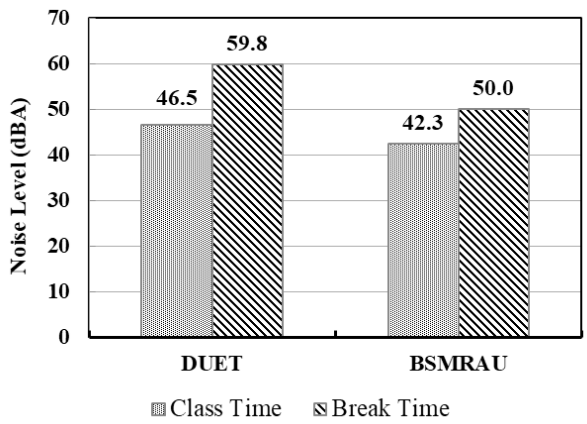

Fig. 7: Mean Noise Level During Class Time and Break Time at DUET and GAU in Teachers' Chamber

3.2 Statistical Analysis

DUET and GAU had two different spatial planning of the teacher's chamber. It was initiated to check whether there was any statistically significant effect of noise level due to different spatial planning of teachers' chambers. The results of ANOVA for the mean noise level in teachers' chambers due to different spatial planning are summarized in Table VIII. Here F_0 value is greater than F_{crit} value, so it can be stated that there are statistically significant effects of mean noise level due to different spatial planning of teachers' chambers in DUET and GAU. Results of ANOVA testing conclude that the level of background noise in teachers' chambers is considerably affected by the spatial planning of the chambers.

Table VIII: ANOVA for Mean Noise Level in Teachers' Chamber Due to Different Spatial Planning

Source of Variation	SS	df	MS	F_0	P-value	F_{crit}
Between Groups	1588.78	1	1588.78	20.76676	1.18×10^{-5}	3.913989
Within Groups	9945.771	130	76.50593	--	--	--
Total	11534.55	131	--	--	--	--

3.3 Summary

A summary result is shown in Table IX.

Table IX: Summary Chart

Case Study	Planning Layout	Noise Level	Conclusion
DUET	Classrooms and teachers' rooms in the same block	The mean noise level is 46.5 dBA during class time and 59.8 dBA during break time	The level of background noise in teachers' chambers is significantly influenced by the way the spaces are planned though it is still higher than the allowable upper limit (48 dBA) [15].
GAU	Classrooms and teachers' rooms in a separate block	The mean noise level is 42.3 dBA during class time and 50.0 dBA during break time	

4. CONCLUSION

This research was initiated to investigate the effect of noise levels on the spatial planning of teacher's chambers in the university. Selected case space DUET and GAU had two different spatial planning of the teacher's chamber. In the teacher's chamber, the noise level measured in both surveyed spaces was lower during class time ranging from 53.1 dBA to 41.1 dBA at DUET and from 43.6 dBA to 41.3 dBA at GAU. But during break time noise level was relatively higher, ranging from 68.7 dBA to 52.6 dBA at DUET and from 53.4 dBA to 47.6 dBA at GAU. During class time mean noise level was 46.5 dBA at DUET and 42.3 dBA at GAU whereas during break time mean noise level was 59.8 dBA at DUET and 50.0 dBA at GAU.

Moreover, ANOVA test results show that different spatial planning of teachers' chambers had a statistically significant effect on mean noise level. So, it could be concluded that the level of background noise in teachers' chambers is considerably affected by the spatial planning of the chambers.

In this study, although the two case spaces exhibit minimal variation in the number of users, there is a significant disparity in floor area. Consequently, the findings may not be entirely conclusive. Further investigation, incorporating additional case spaces with similar floor area, may yield more accurate and reliable results.

Further research would be carried out in other universities with the same spatial plan like DUET and GAU. Again, another case where teachers' block and classroom block located on different floors would be investigated. The findings of this research are expected to provide valuable insights for architects and designers in creating more comfortable and productive workspaces when planning educational facilities.

ACKNOWLEDGMENT

The authors would like to express their heartfelt appreciation to Head, Department of Architecture, DUET as well as Dean, Faculty of Fisheries, GAU. We also appreciate the participation of faculty members, students, and staff that helped to collect data during the long noise measuring session. We acknowledge Dept. of Architecture, DUET for conducting the physical survey in their studio, the drawings and technical support.

REFERENCES

[1] S. Likoko, S. Mutsotso, and J. Nasongo, "The adequacy of instructional materials and physical facilities and their effects on quality of teacher preparation in emerging private primary teacher training colleges in Bungoma County, Kenya," International Journal of Education Research, Vol. 2, No. 1, 2013.

[2] T. Byers, W. Imms, and E. Hartnell-Young, "Making the case for space: The effect of learning spaces on teaching and learning," Curriculum and Teaching, Vol. 29, No. 1, pp. 5–19, 2014.

[3] E. A. Akintunde, J. Y. Bayei, and J. A. Akintunde, "Noise level mapping in University of Jos, Nigeria," GeoJournal, Vol. 87, No. 4, pp. 2441–2453, 2022.

[4] P. H. T. Zannin, M. S. Engel, P. E. K. Fiedler, and F. Bunn, "Characterization of environmental noise based on noise measurements, noise mapping and interviews: A case study at a university campus in Brazil," Cities, Vol. 31, pp. 317–327, 2013.

[5] R. A. Fernandes, D. C. G. M. Vidor, and A. A. D. Oliveira, "The effect of noise on attention and performance in reading and writing tasks," CoDAS, Vol. 31, No. 4, Art. No. e20170241, 2019.

[6] Z. Haron et al., "A preliminary study of environmental noise in public university," Jurnal Teknologi, Vol. 77, No. 16, 2015.

[7] S. Mancini, A. Mascolo, G. Graziuso, and C. Guarnaccia, "Soundwalk, questionnaires and noise measurements in a university campus: A soundscape study," Sustainability, Vol. 13, No. 2, Art. No. 841, 2021.

[8] D. Çolakkadıoğlu, M. Yücel, B. Kahveci, and Ö. Aydınol, "Determination of noise pollution on university campuses: A case study at Çukurova University campus in Turkey," Environmental Monitoring and Assessment, Vol. 190, pp. 1–14, 2018.

[9] B. Shield, R. Conetta, J. Dockrell, D. Connolly, T. Cox, and C. Mydlarz, "A survey of acoustic conditions and noise levels in secondary school classrooms in England," The Journal of the Acoustical Society of America, Vol. 137, No. 1, pp. 177–188, 2015.

[10] K. M. K. Chan, C. Li, E. P. M. Ma, E. M. L. Yiu, and B. McPherson, "Noise levels in an urban Asian school environment," Noise and Health, Vol. 17, No. 74, p. 48, 2015.

[11] L. Scannell, M. Hodgson, J. García Moreno Villarreal, and R. Gifford, "The role of acoustics in the perceived suitability of, and well-being in, informal learning spaces," Environment and Behavior, Vol. 48, No. 6, pp. 769–795, 2016.

[12] T. Liu, C.-C. Lin, K.-C. Huang, and Y.-C. Chen, "Effects of noise type, noise intensity, and illumination intensity on reading performance," Applied Acoustics, Vol. 120, pp. 70–74, 2017.

[13] D. Connolly, J. Dockrell, B. Shield, R. Conetta, C. Mydlarz, and T. Cox, "The effects of classroom noise on the reading comprehension of adolescents," The Journal of the Acoustical Society of America, Vol. 145, No. 1, pp. 372–381, 2019.

[14] C. Lavandier, M. Regragui, R. Dedieu, C. Royer, and A. Can, "Corrigendum to: Influence of road traffic noise peaks on reading task performance and disturbance in a laboratory context," Acta Acustica, Vol. 6, Art. No. 7, 2022.

[15] BNBC, Bangladesh National Building Code-2015, Vol_3_3 (Draft), Part 8, Chapter 3, 2020.

[16] R. T. Muehleisen, "A description of the acoustic requirements in LEED for Schools and a comparison to the ANSI S12.60 Classroom Acoustics Standard," Noise Control Engineering Journal, Vol. 56, No. 5, pp. 365–373, 2008.

[17] B. Shield, "Regulation of school acoustic design in the UK: Recent revision of Building and School Premises Regulations and their application," Euronoise, 2018.

[18] D. Augustyńska, A. Kaczmarska, W. Mikulski, and J. Radosz, "Assessment of teachers' exposure to noise in selected primary schools," Archives of Acoustics, Vol. 35, No. 4, 2010.

[19] Y.-J. Choi, "The intelligibility of speech in university classrooms during lectures," Applied Acoustics, Vol. 162, Art. No. 107211, 2020.

[20] S. M. N. Imam, N. Ahmed, and D. Takahashi, "Effects of reverberation time on percentage syllable articulation for Bangla language," Journal of Asiatic Society of Bangladesh (Science), Vol. 35, No. 1, pp. 37–48, 2009.

[21] Z. Maekawa, J. H. Rindel, and P. Lord, Environmental and Architectural Acoustics, 2nd ed. London, U.K.: Spon Press, 2011.

Spatiotemporal Changes of Wetlands over Gazipur District Bangladesh: A GIS-Based Analysis

Md. Riajul Islam*, Md. Rashel Morshed, Minhajul Islam and Mohammed Alauddin

Department of Civil Engineering, Dhaka University of Engineering & Technology, Gazipur, Bangladesh

ABSTRACT

Gazipur District has undergone rapid urbanization, resulting in significant loss of wetlands and natural ecosystems. This study analyzes land use and land cover changes from 1988 to 2024 using remote sensing and GIS. Landsat imagery (TM, ETM+, and OLI) was classified using the maximum likelihood supervised classification method. The analysis showed that built-up areas have increased more than threefold while agricultural land and wetlands declined by 93.5% and 59%, respectively, representing proportional reductions relative to their original areas. The most substantial changes occurred between 1995 and 2015, driven by Dhaka's urban expansion and limited enforcement of land-use regulations. Wetland loss was most severe near industrial zones and major highways, particularly along the Dhaka–Mymensingh road. These transformations have caused notable ecological impacts, reduced flood buffering capacity, diminished groundwater recharge, and loss of biodiversity. The study demonstrates the utility of GIS and remote sensing for monitoring land transformation and provides critical insights to support sustainable urban planning and wetland conservation in rapidly developing regions.

1. INTRODUCTION

Wetlands operate as one of Earth's most intensive habitats, which supply numerous ecological benefits that encompass water filtering and flood management, and groundwater refilling, and serve as ecological habitats for different plant and animal forms [1].Wetland systems around the world endure serious threats from activities created by humans, but rapid urban sprawl remains the primary threat.

Developing nations like Bangladesh experience specific pressure due to population increase and unregulated infrastructure growth that threatens the natural state of wetlands [2]. Gazipur District, located directly north of Dhaka, illustrates these challenges. Covering an area of approximately 1,818 square kilometers, between 1999 and 2023 the built-up zone in Gazipur expanded nearly 300% of its original area by transforming agriculture fields and wetlands into concrete structures [3]. The rapid growth of Gazipur stems from Dhaka urban expansion as well as the establishment of more than 3,000 industrial units including tanneries, garments and dyeing industries. The construction activities along with industrial establishment have caused both major land conversion and severe environmental damage by creating pollution and interfering with natural water flows. When wetlands degrade or disappear from these areas, essential ecosystem services are lost, and the landscape undergoes substantial alteration. Wetlands play a critical role in flood buffering, water storage, filtration, and they provide fish and aquatic plants that are vital to rural livelihoods [4].

This research adopts a remote sensing and GIS-based approach to analyze LULC dynamic in Gazipur district over 36 years, from 1988 to 2024. This period was selected because reliable, clear satellite imagery prior to 1988 was not available, and it aligns with the major phases of urban growth in Gazipur District. The primary objective is to evaluate the rate and pattern of change in four key land categories: wetlands, vegetation, agricultural land, and built-up area. Landsat satellite images from the USGS Earth Explorer platform were used to derive land cover classifications using the supervised Maximum Likelihood Classification method in ArcGIS. The selection of this method ensures a high degree of classification accuracy and is well-suited for heterogeneous landscapes such as Gazipur [5].

Most existing LULC studies in Gazipur utilize satellite imagery over relatively short periods, often under two decades, thereby constraining insights into long-term urban expansion and wetland degradation trends. The findings of this study not only contribute to the

*Corresponding author's email: 201020@student.duet.ac.bd

academic understanding of land transformation in peri-urban Bangladesh but also have practical implications. In the face of climate change, urban heat islands, and water scarcity, the conservation of wetland ecosystems becomes even more urgent. Policymakers, city planners, and environmental regulators must leverage geospatial data to implement sustainable urban planning strategies that prioritize ecological balance. These might include zoning regulations to protect remaining wetlands, the creation of green buffers, and the integration of nature-based solutions in infrastructure development [6].

The primary goal of this study is to:

(1) Account for spatiotemporal variations of wetlands, agricultural, vegetation, area of built-up, from 1988 to 2024 over the region;

(2) Identify spatial patterns of land cover conversion;

(3) Provide geospatial insights towards the environmental conservation and sustainable urban development.

2. STUDY AREA

The research territory consists of Gazipur district which faces the northern border of Dhaka Bangladesh while situated between 23°50′ N to 24°20′ N latitude and 90°10′ E to 90°40′ E longitude (shown in Fig. 1). The bordering regions of this district include Mymensingh and Kishoreganj to the north along with Narsingdi to the east and Tangail to the west followed by Dhaka–Narayanganj to the south [7][8].

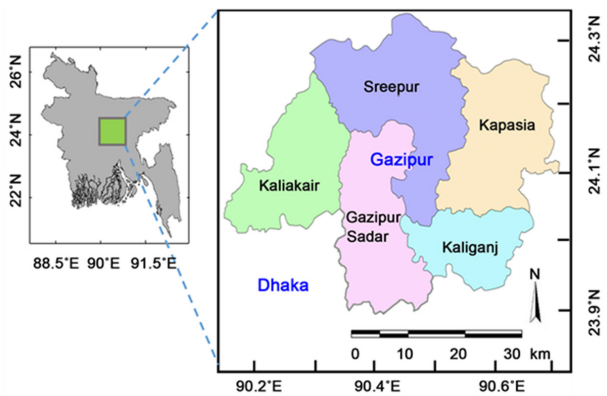

Fig. 1: Study Area [9]

The Shitalakkhya river, Turag river and the Balu river create fundamental geographic limits while the Dhaka–Mymensingh Highway maintains excellent road connections to Dhaka city. The current total population of Gazipur has reached 4.2 million while maintaining a population density of 2.100 inhabitants per square kilometer following its continuous transition to an urbanized industrial city [10]. Population growth in this region continues to rise because its industrial area successfully supports over 3,000 industries that concentrate on textile, garment and dyeing facilities [10]. Gazipur City Corporation operates as the largest metropolitan council in Bangladesh while controlling the urban development process of the city. Urbanization together with industrial development presents substantial pressure on the biodiverse Vawal Pargana forest which used to thrive abundantly. The district climate exhibits wide temperature ranges from 12.7°C to 36°C and receives an average annual rainfall of 2,376 mm according to BBS (2024). The current climate allows multiple diverse wetlands to exist throughout history. The district possessed numerous lowland wetlands (haors and beels) and agricultural areas that developers transformed through time into urbanized zones.

3. METHODOLOGY

Remote Sensing were employed in combination with GIS to examine extensive Land Use and Land Cover transformations within Gazipur District from 1988 up to 2024. The method retrieves satellite data for analysis through a sequence of procedures that starts with data collection then moves to image formatting and classification operations before executing spatial land transformation assessments.

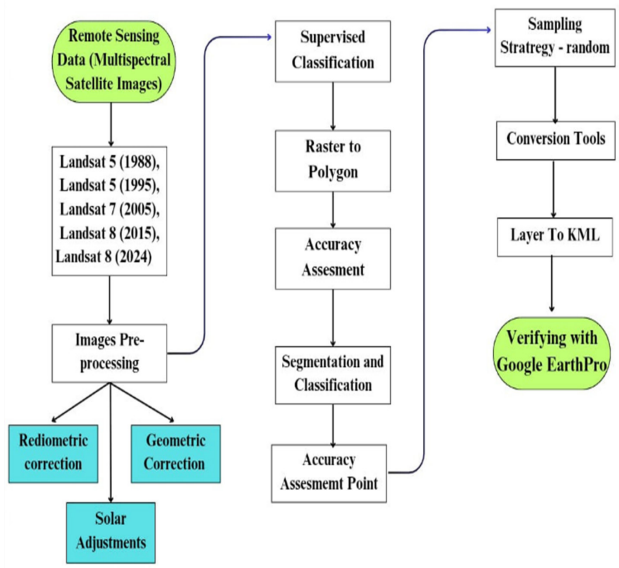

Fig. 2: Methodology Flow Chart

The methodological framework (Fig. 2) operates its steps to guarantee precision while providing consistent results that are strongly connected to the environmental dynamics' analysis across the span of decades.

3.1. Satellite Data Acquisition

Multi-temporal satellite data used to extract Land Use and Land Cover (LULC) information were obtained from the USGS Earth Explorer platform. To maintain spectral and temporal consistency, the study incorporated data from Landsat 5 Thematic Mapper (TM), Landsat 7 Enhanced Thematic Mapper Plus (ETM+), and Landsat 8 Operational Land Imager (OLI), as summarized in Table I. Satellite imagery was selected from the dry season months of December through January for five reference years: 1988, 1995, 2005, 2015, and 2024, ensuring phenological consistency across datasets. All datasets were projected into the Universal Transverse Mercator (UTM) coordinate system (Zone 46N) at a 30-meter spatial resolution to support harmonized spatial and analytical assessments.

3.2 Preprocessing

Satellite imagery preprocessing measures maintained the integrity and multi-temporal consistency of images from 1988 and 1995 up to 2005 and 2015 and 2024. The methods applied to the data increased the precision and steadiness of Land Use/Land Cover classification information for the area of Gazipur.

Table I: Specification of Satellite Image Acquisition

Satellite	Sensor	Date	Band Number	Path/row	Cloud Cover	Spatial Resolution (m)
Landsat 5	TM	2-1-1988	7	137/43	<5	30
Landsat 5	TM	21-11-1995	7	137/43	<3	30
Landsat 7	ETM	10-12-2005	7	137/43	<10	30
Landsat 8	OLI	12-11-2015	11	137/43	<2	30
Landsat 8	OLI	4-11-2024	11	137/43	<2	30

Radiometric correction was applied to convert raw digital numbers (DN) into top-of-atmosphere (TOA) reflectance, minimizing atmospheric and sensor-related effects. Initially, DN values were transformed into TOA radiance using scaling factors provided in the Landsat metadata file, following the USGS standard procedure:

$$L_\lambda = M_L \times Q_{CAL} + A_L$$

where, L_λ represents TOA spectral radiance, M_L and A_L are the band-specific multiplicative and additive rescaling factors, and Q_{cal} is the quantized calibrated pixel value. Subsequently, radiance was converted to TOA reflectance to account for solar irradiance and acquisition geometry:

$$\rho\lambda = \frac{L_\lambda \times d^2 \times \pi}{ESUN_\lambda \times \cos(\theta_s)}$$

where, ρ_λ denotes TOA reflectance, d is the Earth–Sun distance in astronomical units, $ESUN_\lambda$ is the mean solar exoatmospheric irradiance, and θs is the solar zenith angle.

To further reduce atmospheric scattering (haze), the Dark Object Subtraction (DOS) method was employed, wherein the minimum reflectance value identified from dense water bodies was subtracted from all pixels in the corresponding band [11]. This combination of conversion and correction steps ensured radiometric consistency across sensors and acquisition dates. Geometric correction ensures all images are accurately aligned in a common coordinate system, so that each pixel corresponds to the same ground location across years.

Solar angle adjustment was applied to correct for varying illumination conditions, using the cosine of the solar zenith angle recorded in the metadata. The normalized reflectance (ρ corrected) was calculated as [12]:

$$\rho_{corrected} = \frac{\rho\lambda}{\cos(\theta_s)}$$

where, $\rho_{corrected}$ = reflectance normalized to standard illumination.

3.3 Supervised Classification

Land cover was classified into four categories: wetlands, agricultural land, vegetation, and built-up areas as shown in Table II. The Maximum Likelihood Classification (MLC) algorithm operated as part of supervised classification through ArcGIS to classify LULC. A substantial number of training samples for each land cover class were acquired according to field-based expertise and high-resolution imagery checks. Through the use of training sample

spectral signature, the methodology classified land types effectively for precise separation.

Table II: Land Cover Classification

SN	Class	Details
01	Wetlands	Water body like lake, pond, canal, including rivers, water reservoirs, and streams.
02	Vegetation	Trees, natural vegetation, mixed forest, gardens.
03	Built-up	Residential, commercial, industrial area, land covered with concrete.
04	Agricultural	Agricultural lands, crop fields, barren land

3.4 Accuracy Assessment:

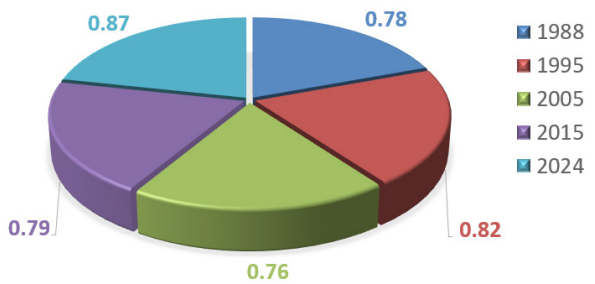

Fig. 3: Kappa value

The LULC classification results underwent validation through accuracy assessment which used random stratified method and confusion matrices processed using 100 reference points generated automatically. The reference data acquisition process involved field validation along with high-definition Google Earth Pro Map. Confidence in the classified outputs increased because the classification accuracy rate across all studied years stayed 0.76-0.87, Fig. 3 shows more details.

4. RESULTS AND DISCUSSION

Landsat images were used to create supervisory classification-driven LULC maps of Gazipur district from (1988-2024). The research examined four main land use and land cover types including wetlands, vegetation, agriculture, and built-up area in 36 years.

4.1 Wetlands Changes

The total wetland area declined from 221.19 sq.km in 1988 to 89.75 sq.km in 2024, marking a 59.4% loss over the study period (shown in Fig. 4). The sharp decline occurred between 2005 and 2015, where wetlands area decreased by 40.87%, largely attributed to rapid peri-urban expansion, land encroachment, and possible sedimentation of natural wetlands. The loss of these areas compromises hydrological stability, increases urban flood vulnerability, and leads potential risk for aquatic and terrestrial species. These findings align with earlier studies on wetland degradation 6.25% between 1989 and 2009 in Mirzapur Union and Dhaka's peripheral zones [13], directing a shared pattern of ecological pressure due to unregulated urbanization.

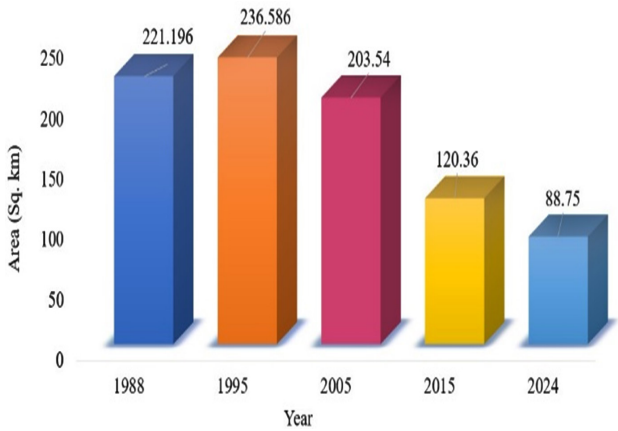

Fig. 4: Degradation of wetlands

4.2 Built-up Area Expansion

As shown in Fig. 5, the built-up areas increased more than threefold, growing from 242.17 sq. km in 1988 to 826.50 sq. km in 2024. The most rapid expansion occurred between 2005 and 2015 (60.86%), coinciding with rapid industrialization, real estate development, and infrastructure in the Gazipur–Tongi corridor and along the Dhaka–Mymensingh Highway. Similar conversion pattern was also noted in earlier articles [14], which reported cropland and forest zones transformed into built-up and homestead areas.

4.3 Agricultural Land Decline

Agricultural land witnessed a reduction of over 93%, from 901.65 sq.km in 1988 to 60.51 sq.km by 2024. The most significant declines were recorded during 1995–2005 (−31.73%) and 2015–2024 (−86.45%), reflecting direct conversion into built-up areas. The similar outcome was also found in previous study on Gazipur [14]. This trend poses serious risks to food security, undermines rural livelihoods.

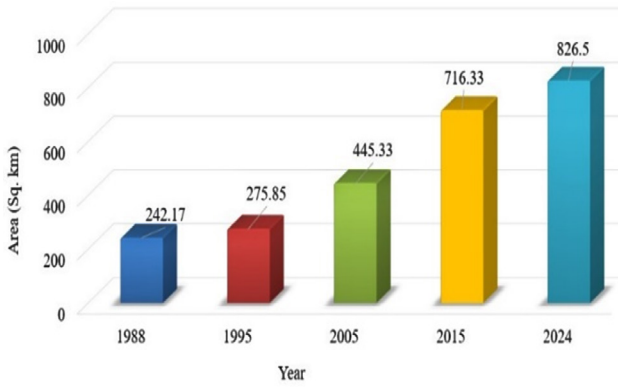

Fig. 5: Urban Expansion in Gazipur District from 1988 to 2024

4.4 Vegetation Cover Changes

Vegetation cover increased from 452.57 sq.km to 841.82 sq.km in terms of between 1988 and 2024, but the most significant increment was in the most recent decade (2015–2024) of 57.24%. The trend is explained by these environmental improvement-oriented projects like the urban greening projects and afforestation initiatives. Land cover reduction due to the destruction of forest and unregulated land use conversions during some periods between 1995 and 2005 led to vegetation cover ceasing to cover 13.31 sq.km of the land area.

The analysis shows how the urban expansion caused a systematic move of agricultural and wetland areas into the urban territories, while uncontrolled urban growth served as the most important factor. Research data aligns with earlier research [2][3][5]. Dhaka fringe area needs urgent sustainable land use planning in combination with wetland conservation especially in fast expanding areas like Gazipur.

5. CONCLUSION

The current research studies the land-use and land-cover change of Gazipur District during the last 36 years, which can be explained by the rapid development of urbanization on the one hand and the excessive growth of industrial enterprises on the other. The discussion shows that there is a more than doubling of built-up areas and a decreasing of wetland and cropland by 59 % and 93.5 respectively. This pattern results in undermining the ecological resilience of the district and weakening flood control abilities, groundwater storage capacity, and biodiversity to maintain native species habitat.

Class	Area (Sq.km)					Change %			
	1988	1995	2005	2015	2024	1988-95	1995-05	2005-15	2015-24
K Value	0.78	0.82	0.76	0.79	0.87				
Wetlands	221.192	236.586	203.54	120.36	89.7546	6.959565	-13.9679	-40.8667	-25.4282
Vegetation	452.573	449.39	548.2	535.36	841.8158	-0.7033	-13.3097	-2.34221	57.24294
Agriculture	901.6451	856.708	621.51	446.51	60.51215	-4.9833	-31.7299	-28.1572	-86.4478
Built-up Area	242.17	275.846	445.33	716.35	826.4975	13.90593	61.44153	60.85824	15.37621

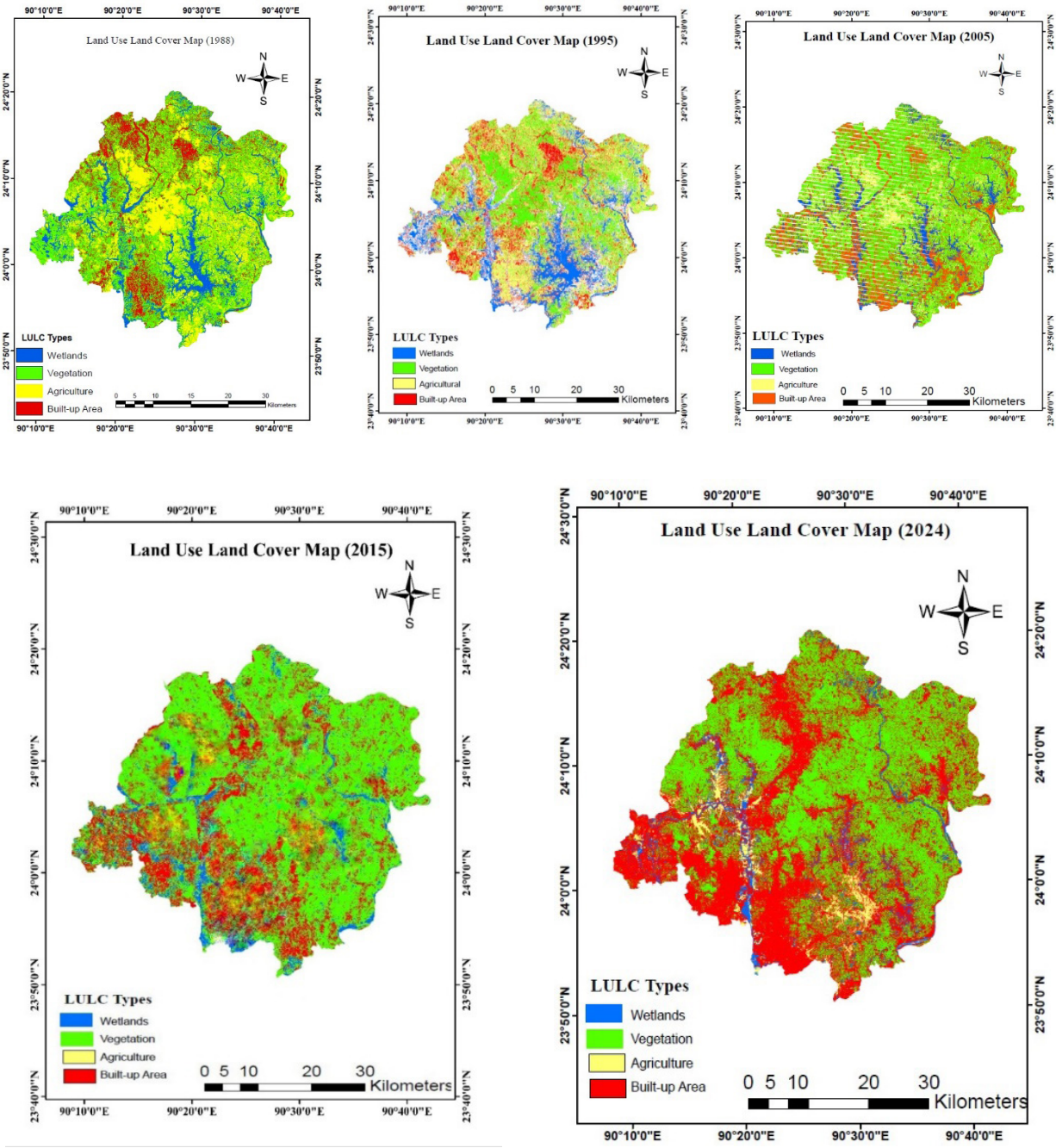

Fig. 6: Land Use Land Cover (LULC) Classify Map in (A) 1988, (B) 1995, (C) 2005, (D) 2015 and (E) 2024

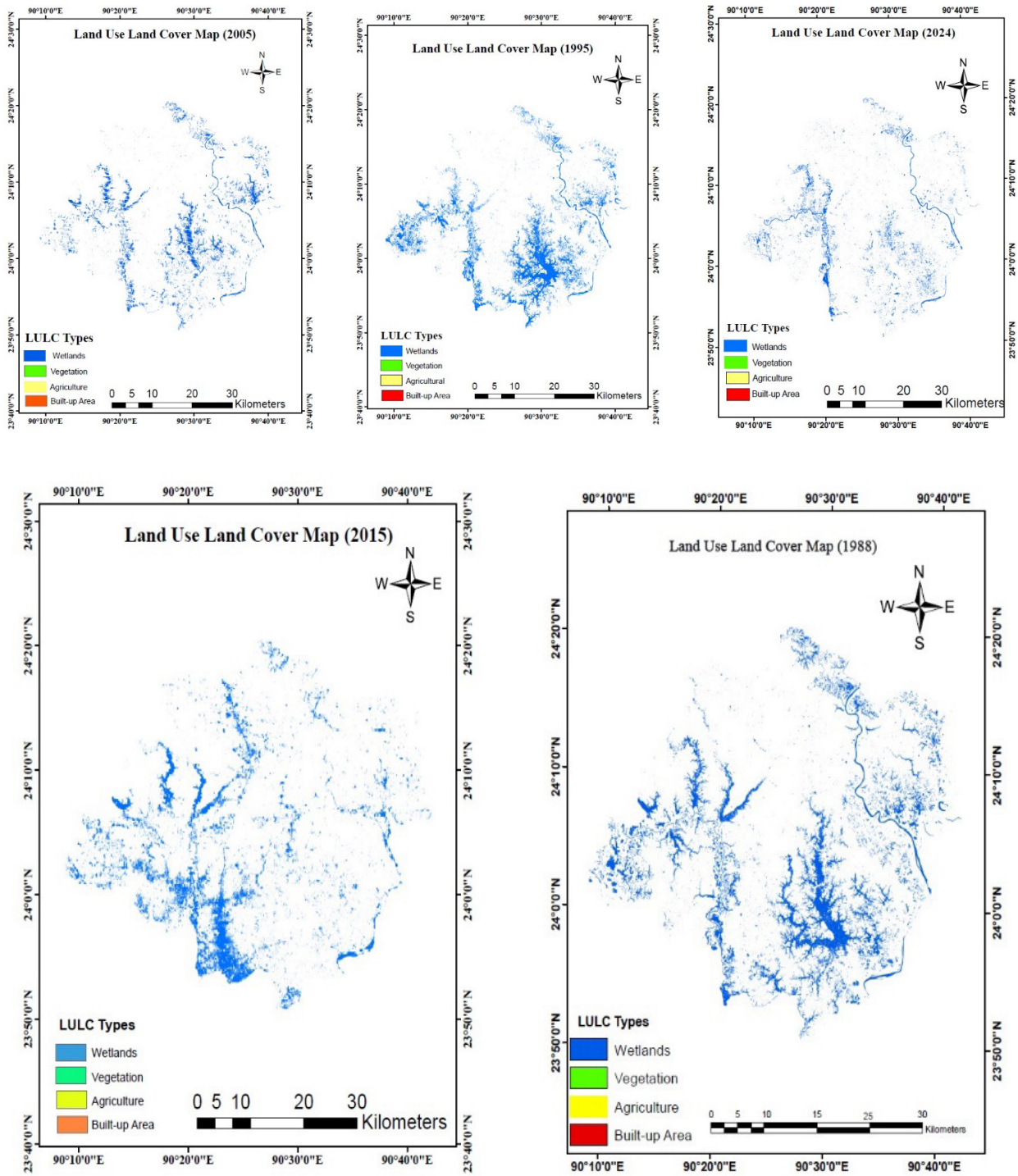

Fig. 7: Land Use Land Cover (LULC) Classify of Wetlands in (F) 1988, (G) 1995, (H) 2005, (I) 2015 and (J) 2024

Ongoing research has established that the use of geospatial monitoring in urban planning and environmental management is inevitable. Especially in the areas of swift peri-urban expansion, it is essential to ensure that the existing wetlands remain intact and that the new development anchors the nature-based solutions, thus maintaining the balance of nature.

The study presents policymakers and city planners with empirical data that they can use in the development of law and spatial plans of protecting wetland systems. In particular, the results indicate the need to use zoning rules, create green buffers, and encourage sustainable land-use patterns. Such proactive actions are pertinent to reduce further the degradation of wetland systems, as livelihoods

and the reduction of the disasters risk rely on such systems in the face of the ongoing urbanization in Bangladesh.

Overall, this research contributes to a deeper understanding of long-term land cover dynamics and provides actionable evidence to inform sustainable urban development and wetland conservation policies

REFERENCES

[1] W. J. Mitsch and J. G. Gosselink, Wetlands, 5th ed. Hoboken, NJ, USA: Wiley, 2015.

[2] H. M. Arifeen et al., "Determine the land-use land-cover changes, urban expansion and their driving factors for sustainable development in Gazipur, Bangladesh," Atmosphere, vol. 12, no. 10, 2021.

[3] A. Al Mahmud, N. Sultana, and M. E. Habib, "Application of GIS for spatio-temporal modeling of land use change and environmental degradation in Dhaka, Narayanganj, and Gazipur: A 24-year study (1999–2023)," Research Square, preprint, Nov. 11, 2024.

[4] R. Sorker, M. W. Khan, A. Kabir, and N. Nawar, "Variations in ecosystem service value in response to land use changes in Dhaka and Gazipur districts of Bangladesh," Environmental Systems Research, vol. 12, no. 1, 2023.

[5] M. A. Hassan, R. Mahjabin, M. R. Islam, and S. Imtiaz, "Land cover classification and change detection analyzing multi-temporal Landsat data: A case study of Gazipur Sadar, Bangladesh between 1973 and 2017," Geography, Environment, Sustainability, vol. 12, no. 1, pp. 104–118, 2019.

[6] S. Bhattacharjee, M. T. Islam, M. E. Kabir, and M. M. Kabir, "Land-use and land-cover change detection in a north-eastern wetland ecosystem of Bangladesh using remote sensing and GIS techniques," Earth Systems and Environment, vol. 5, no. 2, pp. 319–340, 2021.

[7] Banglapedia, "Gazipur District," Banglapedia: National Encyclopedia of Bangladesh, 2025.

[8] Wikipedia, "Gazipur," Wikipedia, 2025.

[9] T. Shapla, J. Park, C. Hongo, and H. Kuze, "Agricultural land cover change in Gazipur, Bangladesh, in relation to local economy studied using Landsat images," Advances in Remote Sensing, vol. 4, no. 3, pp. 214–223, 2015.

[10] Bangladesh Bureau of Statistics and Statistics and Informatics Division, Statistical Yearbook of Bangladesh, 2022.

[11] P. S. Chavez Jr., "An improved dark-object subtraction technique for atmospheric scattering correction of multispectral data," Remote Sensing of Environment, vol. 24, no. 3, pp. 459–473, 1988.

[12] U.S. Geological Survey, "Using USGS Landsat Level-1 Data Products," United States Geological Survey, 2024.

[13] R. Yesmin, A. S. M. Mohiuddin, M. J. Uddin, and M. A. Shahid, "Land use and land cover change detection at Mirzapur Union of Gazipur District of Bangladesh using remote sensing and GIS technology," IOP Conference Series: Earth and Environmental Science, vol. 20, no. 1, 2014.

[14] T. Afroz, M. G. Miah, H. M. Abdullah, M. R. Islam, and M. M. Rahman, "Monitoring of LULC changes and forest loss using geospatial technique: A case study from northern region of Bangladesh," Asian Journal of Geospatial Technology, vol. 1, no. 2, 2023.

Finding the Right Fit: A User-Centric Approach to Master Bedroom Sizing in Compact Dhaka Apartments

Md. Sabbir Hussain[1*] and Lubna Yeasmin[2]

[1]Department of Architecture, Dhaka University of Engineering & Technology, Gazipur, Bangladesh
[2]Freelance Architect, Dhaka, Bangladesh

ABSTRACT

Due to high land prices and rising construction costs, compact apartments have become the most affordable option for Dhaka's middle-income population. Within these smaller living spaces, the master bedroom remains a critical area for comfort and functionality. However, designers often size master bedrooms based solely on the minimum requirements set by building bylaws, overlooking the cultural and personal needs of a diverse range of users. This disconnect frequently leads to post-purchase dissatisfaction among apartment buyers. To address this gap, this study aimed to establish a standard dimension for master bedrooms in compact apartments in Dhaka, one that can accommodate a wide variety of user needs. The research employed a combination of structured and unstructured field surveys to understand the diverse lifestyles and spatial requirements of different middle-income user groups. This data was then used in a user-centric layout study to determine the optimal sizing for master bedrooms. The findings of this study provide valuable insights for architects and interior designers, encouraging them to consider user-specific needs alongside spatial efficiency. This approach challenges the trend of blindly compacting living spaces, offering a more balanced and user-oriented design solution for Dhaka's middle-income population.

1. INTRODUCTION

Due to rising land prices and the gradual increase in construction costs, small-sized flats in multi-story, multi-family residential buildings have become more affordable for the middle-income population in Dhaka [1]. Before the emergence of the apartment culture, middle-income residents typically bought land and built single-family houses. However, after Dhaka became the capital and central business hub of an independent country, a sudden surge in residential demand drastically altered its housing scenario, giving rise to multi-story, multi-family apartment buildings [2, 3].

Initially, when middle-income residents began adapting to apartment living, they preferred spacious units to replicate the openness of a single-family home. Although flats have become increasingly compact over time, cultural norms and family structures have discouraged the popularity of compact studio apartments. Instead, buyers continue to prefer small-sized units that include a master bedroom, a child's bedroom, and a guest bedroom [4, 5].

To meet this demand, architects have continuously worked to reduce spatial dimensions. However, the ideal minimum size of a master bedroom remains under-researched. Most architects design master bedrooms keeping in mind the minimum requirements outlined in building bylaws (a minimum width of 2500 mm and a floor area of 9.5 sqm, as per the Dhaka City Building Construction Act, 2008 [6]), and therefore, often neglect user-centered needs. Consequently, buyers—often unaware of spatial dimensions—may experience dissatisfaction after purchase, attempting to adapt to the limited space and ultimately compromising their quality of life. Nonetheless, spatial compaction is an unavoidable reality in Dhaka's urban context [7, 8].

According to a recent report, bedroom sizes in urban areas like Dhaka have shrunk by approximately 29% between 2020 and 2021 [9]. While some existing studies have attempted to identify apartment size preferences for different income groups in Dhaka [1], literature specifically addressing user-centric master bedroom sizing in the context of Dhaka apartments remains absent. Against this backdrop, this research aims to identify the optimal master bedroom size that can satisfy the needs of middle-income flat buyers in Dhaka.

[*]Corresponding author's email: ar.sabbir@duet.ac.bd

2. METHODOLOGY

The middle-income population of Dhaka constitutes the primary market for the growing trend of compact apartments. Most of these potential buyers currently reside in rental units across the city [10-12]. For this study, Khilkhet—a well-known neighborhood in Dhaka—was selected as the study site. Khilkhet was chosen specifically because it accommodates middle-income tenants from diverse occupational backgrounds, allowing the study to capture a wide range of lifestyles and spatial needs [13, 14]. An unstructured interview and a structured questionnaire survey were conducted among the master bedroom users in 100 apartments in this area.

Table I: User-specific Needs

Occupation (Male)	Occupation (Female)	User Number	Bedroom use	Furniture Requirement	Number Surveyed
Student/ Office worker		Single (1)	1. Sleeping/ Relaxing 2. Working 3. Entertainment 4. Yoga/Exercise	1. Single Bed 2. Desk & Chair 3. Almirah	1
	Student/ Office worker	Single (1)	1. Sleeping/ Relaxing 2. working 3. Entertainment 4. Yoga/Exercise	1. Single Bed 2. Desk & Chair 3. Dressing table 4. Almirah	2
Office worker (private)	Housewife	Couple (2)	1. Sleeping/ Relaxing 2. Working 3. Entertainment 4. Prayer	1. Double Bed 2. Desk & Chair 3. Dressing table 4. Almirah	9
Office worker (private)	Housewife	Couple with infant (3)	1. Sleeping/ Relaxing 2. Entertainment 3. Playing (Baby) 4. Prayer	1. Queen size Bed 2. Desk & Chair 3. Dressing table 4. Almirah 5. Sofa/Easy chair 6. Shelf	48
Office worker (private)	Office worker (private)	Couple (2)	1. Sleeping/ Relaxing 2. Entertainment 3. Prayer	1. King size Bed 2. Desk & Chair 3. Dressing table 4. Almirah	8
Doctor	Housewife	Couple with infant (3)	1. Sleeping/ Relaxing 2. Entertainment 3. Playing (Baby) 4. Prayer	1. Queen size Bed 2. Desk & Chair 3. Dressing table 4. Almirah 5. Sofa/Easy chair 6. Shelf	3
Banker	Housewife	Couple with infant (3)	1. Sleeping/ Relaxing 2. Entertainment 3. Playing (Baby) 4. Prayer	1. Queen size Bed 2. Desk & Chair 3. Dressing table 4. Almirah 5. Sofa/Easy chair 6. Shelf	4
Teacher	Housewife	Couple with infant (3)	1. Sleeping/ Relaxing 2. Studying 3. Entertainment 4. Playing (Baby) 5. Prayer	1. Queen size Bed 2. Desk & Chair 3. Dressing table 4. Almirah 5. Sofa/Easy chair 6. Bookshelf	5
Businessman	Housewife	Couple (2)	1. Sleeping/ Relaxing 2. Entertainment 3. Prayer	1. Double Bed 2. Side table 3. Dressing table 4. Almirah	4
Businessman	Housewife	Couple with infant (3)	1. Sleeping/ Relaxing 2. Studying 3. Entertainment 4. Playing (Baby) 5. Prayer	1. Queen size Bed 2. Desk & Chair 3. Dressing table 4. Almirah 5. Sofa/Easy chair 6. Bookshelf	16

Participants were selected based on two primary criteria:

(1) the participant must be a tenant; and

(2) the participant must belong to the middle-income group. (in 2022-2023 the BBS categorizes individuals earning between Tk 50,000 and Tk 120,000 per month as middle-income [15]).

The interviews (both structured and unstructured) aimed to identify the master bedroom-related needs of user(s) from different occupations. Based on these identified needs, the study outlined the maximum set of furniture requirements necessary to meet them. In the next stage, both desk-based and field research were carried out to determine the standard dimensions of furniture available in Dhaka's furniture market. During the survey, the bedroom configurations of each respondent were meticulously documented, from which eight common room configurations were identified. Using ergonomic principles, several compact bedroom layouts were then designed and evaluated for usability.

Finally, by synthesizing the findings from multiple layout studies, the research proposes an optimal minimum bedroom size that can accommodate the needs of most middle-income buyers of compact Dhaka apartments across various occupational groups.

3. DATA ACCUMULATION AND SYNTHESIS

A total of 100 apartments were surveyed, and the users were asked about the additional uses of their master bedrooms beyond sleeping. Responses varied significantly, revealing diverse usage patterns. Through data synthesis, it was identified that these variations were closely linked to the respondents' occupational backgrounds and the number of users sharing the room. Table I presents the respondents' occupations, number of users, their specific uses of the master bedroom, and the types of furniture required to support those uses. Based on the analysis of Table I, the maximum uses of a master bedroom are as follows: sleeping, working at a desk, storing clothing, playing with children, praying, keeping books and work/entertainment equipment (e.g., laptop/desktop PC, sound system), relaxation, and dressing. These uses may vary depending on the occupant's occupation and user number, with some user(s) requiring only a subset of these uses, while others may need all of them. Therefore, if a master bedroom can effectively accommodate the full range of activities, it is likely to satisfy the needs of most user(s), regardless of their occupational background or user number.

Table I also outlines the furniture required to support each specific use of the master bedroom. Based on this data, accommodating the full range of potential uses necessitates the inclusion of the following essential furniture items: a king-sized bed (the largest amongst standard bed types), a desk and chair for working and keeping PC, a wardrobe for clothing storage, a bookshelf, a sofa or easy chair, and a dressing table. (Note: This study does not consider integrated interior designs that utilize customized, space-saving furniture solutions.) Additionally, to facilitate activities such as prayer, yoga/exercise, and play, a clear and unobstructed area within the room is essential.

In the next phase of the study, the dimensions of the required furniture were determined through a survey of local shops and an analysis of size specifications provided on the websites of several renowned Bangladeshi furniture brands [16-18]. The following Table II presents a comparison of furniture sizes across different branded manufacturers as well as locally produced, non-branded options.

From the analysis of the Table II, the following maximum furniture dimensions were identified as the largest commonly available sizes in the Bangladeshi furniture market:

1. King-sized Bed – 2280 × 2000 mm
2. Almirah (3 part) – 1500 × 600 mm
3. Dressing Table – 800 × 430 mm
4. Work Desk – 1000 × 550 mm
5. Single Sofa – 850 × 750 mm
6. Bookshelf – 600 × 400 mm
7. Wardrobe – 1330 × 550 mm
8. Easy Chair– 1300 × 700 mm

Calculation of Required Open Space for Prayer, Play, and Yoga/Exercise: In this study, "prayer" specifically refers to Salat (Islamic worship), which requires orientation toward the Qibla—westward in the context of Dhaka. A standard prayer mat typically measures 1200mm by 750 mm. Since room orientation may vary, a clear space of at least 1200mm by 1200mm is considered sufficient to accommodate prayer regardless of layout. For yoga, a space of approximately 1800 mm by 900 mm is generally required. Therefore, to accommodate prayer, yoga, and activities such as playing with an infant, a clear, unobstructed area of 1800 mm by 1200 mm within the master bedroom is deemed adequate.

In the next phase, several furniture layout options were analyzed using the maximum dimensions identified in the previous step. These dimensions represent the largest commonly available sizes in the Bangladeshi market, meaning that any smaller-sized furniture would provide additional free space in the room. For instance, if a user chooses a single bed instead of a king-sized bed, the available floor space will increase, offering greater flexibility in the room layout.

Table II: Furniture Size Comparison

Furniture Name		Furniture Size			
		Hatil (mm)	Otobi (mm)	Regal (mm)	Local Shop (mm)
1. Bed	Single	-	2050 × 1080	2075 × 1096	2000 × 1000
	Queen Size	2220 × 1655	2100 × 1750	2100 × 1590	2050 × 1500
	King Size	2220 × 1880	2105 × 1887	2280 × 2000	2100 × 1850
2. Almirah	2 Part	900 × 500	962 × 580	1000 × 595	950 × 500
	3 Part	1470 × 600	1500 × 565	1500 × 600	1450 × 600
3. Dressing table		800 × 400	800 × 430	800 × 400	800 × 400
4. Working Desk		460 × 505	1000 × 550	1000 × 500	950 × 500
5. Sofa (single)		800 × 750	820 × 750	850 × 750	800 × 750
6. Bookshelf		485 × 400	600 × 325	600 × 300	550 × 300
7. Wardrobe		1250 × 585	1330 × 510	1200 × 550	1100 × 550
8. Easy chair		700 × 960	1300 × 660	1025 × 575	700 × 900

4. LAYOUT STUDY & RESULT

At the outset of the layout study, the required clearance for each piece of furniture was determined based on guidelines from Time-Saver Standards for Interior Space Planning [19], a widely recognized reference book used by architects globally. The recommended clearance dimensions are as follows:

Table III: Furniture Clearance

Furniture	Minimum Clearance Required
Bed	560 mm (at least on one side, preferably on two sides)
Wardrobe / Almirah	915 mm (in front)
Dressing Table	1065 (in front)
Working Desk	760 (in front)
Bookshelf	560 mm (in front)
Sofa	560 mm (in front)
Easy Chair / Rocking Chair	560 mm (in front)

Next, eight potential master bedroom plans—along with their mirrored versions (through Y axis, totaling 16 plans)—were identified based on common typologies observed in the survey. For further analysis, only one plan from each mirrored pair was selected and these are shown in Fig. 1 (a) to (h). In each plan, the required furniture was arranged with careful consideration of clearances (listed in Table III) and functional requirements. After finalizing the furniture layouts, the overall dimensions of each room were measured. These measurements represent the primary findings of this study, though slight variations were noted across different room configurations.

Table IV presents the room dimensions for eight different bedroom configurations. It is important to note that the standard clearance of 560 mm on the pillow side of the bed was omitted, considering the practical use of a bed. In some cases, the chair positioned at the work desk slightly overlaps with the designated open space; however, this was deemed acceptable, as chairs are considered movable furniture.

Table IV: Room Size Comparison

Configuration No	Size (mm)
Fig. 2(a)	4170 × 3600
Fig. 2(b)	4320 × 3680
Fig. 2(c)	4320 × 3680
Fig. 2(d)	4060 × 3680
Fig. 2(e)	4070 × 3680
Fig. 2(f)	4070 × 3680
Fig. 2(g)	4070 × 3680
Fig. 2(h)	4190 × 3670

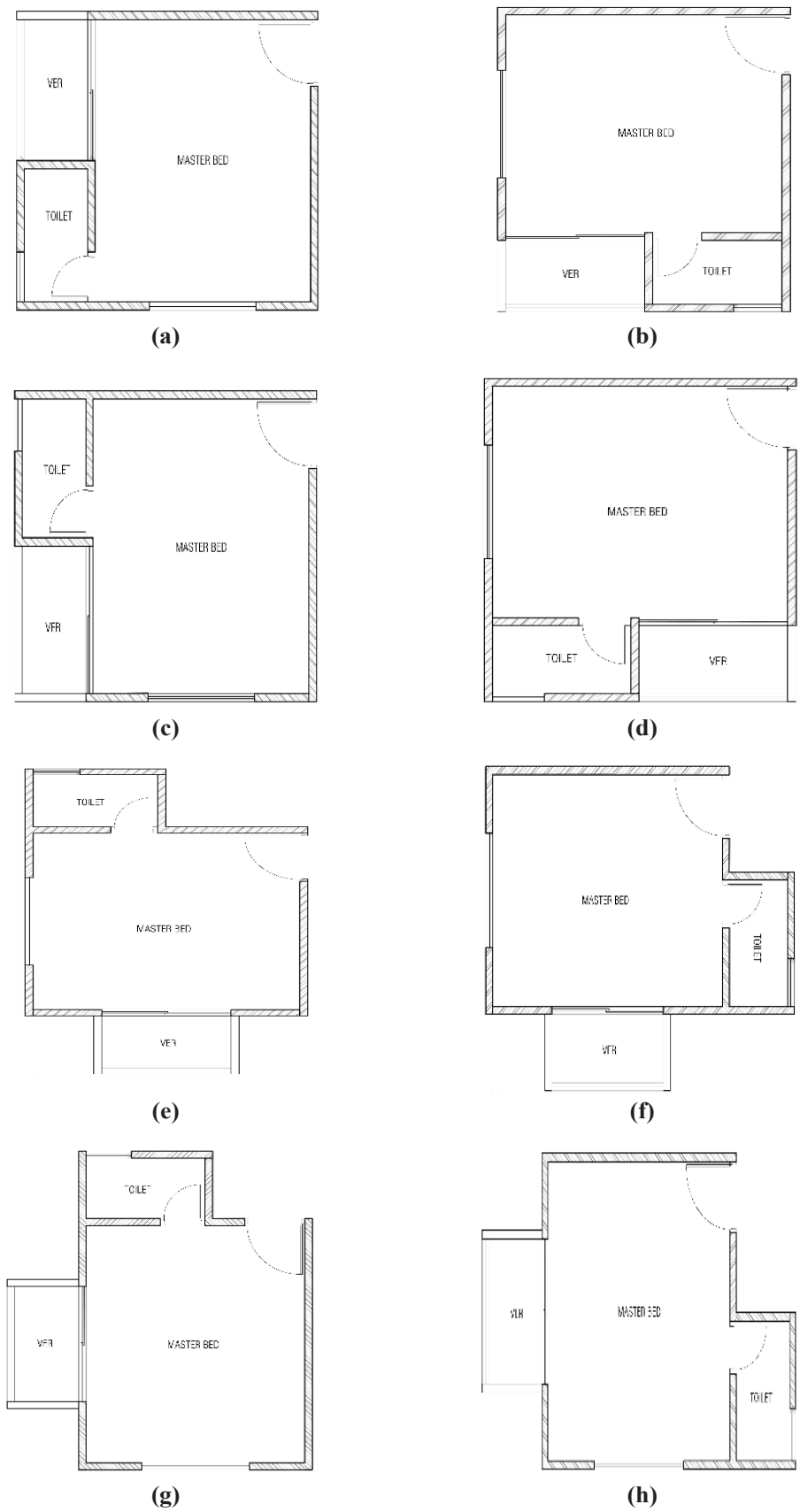

Fig. 1: Master Bedroom Plans

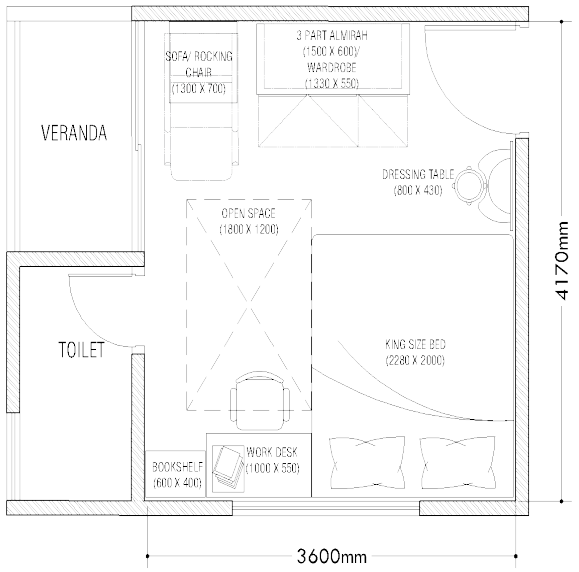
VERANDA
SOFA/ ROCKING CHAIR (1300 X 700)
3 PART ALMIRAH (1500 X 600)/ WARDROBE (1330 X 550)
DRESSING TABLE (800 X 430)
OPEN SPACE (1800 X 1200)
TOILET
KING SIZE BED (2280 X 2000)
BOOKSHELF (600 X 400)
WORK DESK (1000 X 550)
4170mm
3600mm

(a)

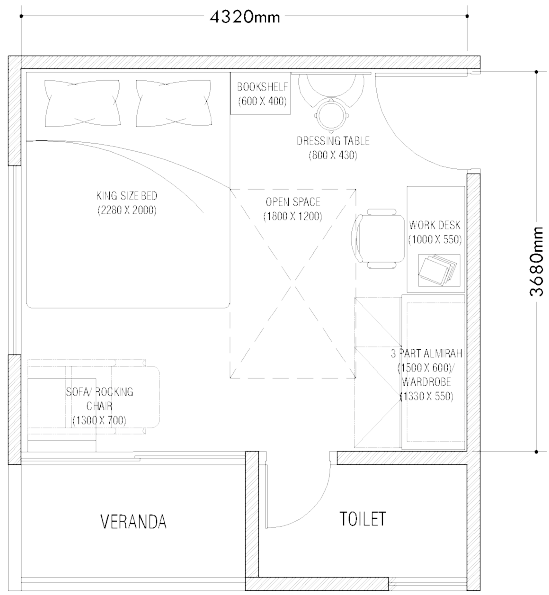
4320mm
BOOKSHELF (600 X 400)
DRESSING TABLE (800 X 430)
KING SIZE BED (2280 X 2000)
OPEN SPACE (1800 X 1200)
WORK DESK (1000 X 550)
3680mm
3 PART ALMIRAH (1500 X 600)/ WARDROBE (1330 X 550)
SOFA/ ROCKING CHAIR (1300 X 700)
VERANDA
TOILET

(b)

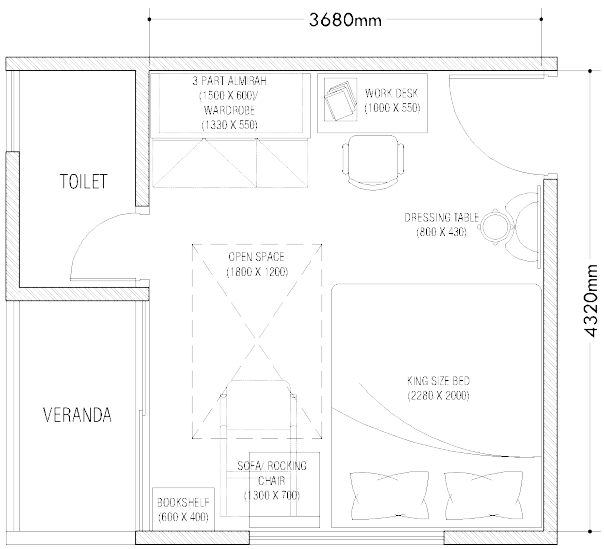
3680mm
3 PART ALMIRAH (1500 X 600)/ WARDROBE (1330 X 550)
WORK DESK (1000 X 550)
TOILET
DRESSING TABLE (800 X 430)
OPEN SPACE (1800 X 1200)
4320mm
KING SIZE BED (2280 X 2000)
VERANDA
SOFA/ ROCKING CHAIR (1300 X 700)
BOOKSHELF (600 X 400)

(c)

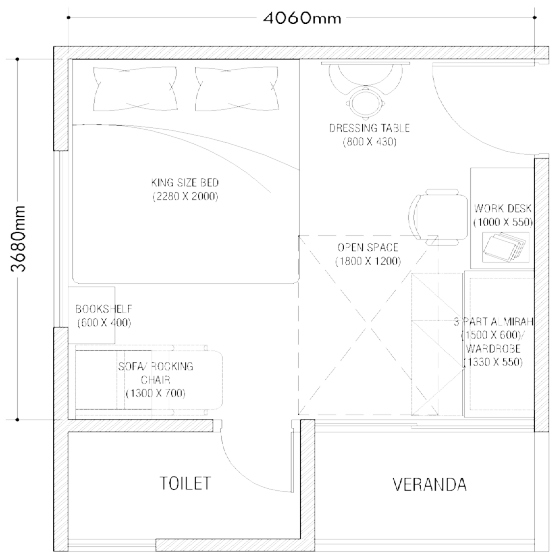
4060mm
DRESSING TABLE (800 X 430)
KING SIZE BED (2280 X 2000)
3680mm
WORK DESK (1000 X 550)
OPEN SPACE (1800 X 1200)
BOOKSHELF (600 X 400)
3 PART ALMIRAH (1500 X 600)/ WARDROBE (1330 X 550)
SOFA/ ROCKING CHAIR (1300 X 700)
TOILET
VERANDA

(d)

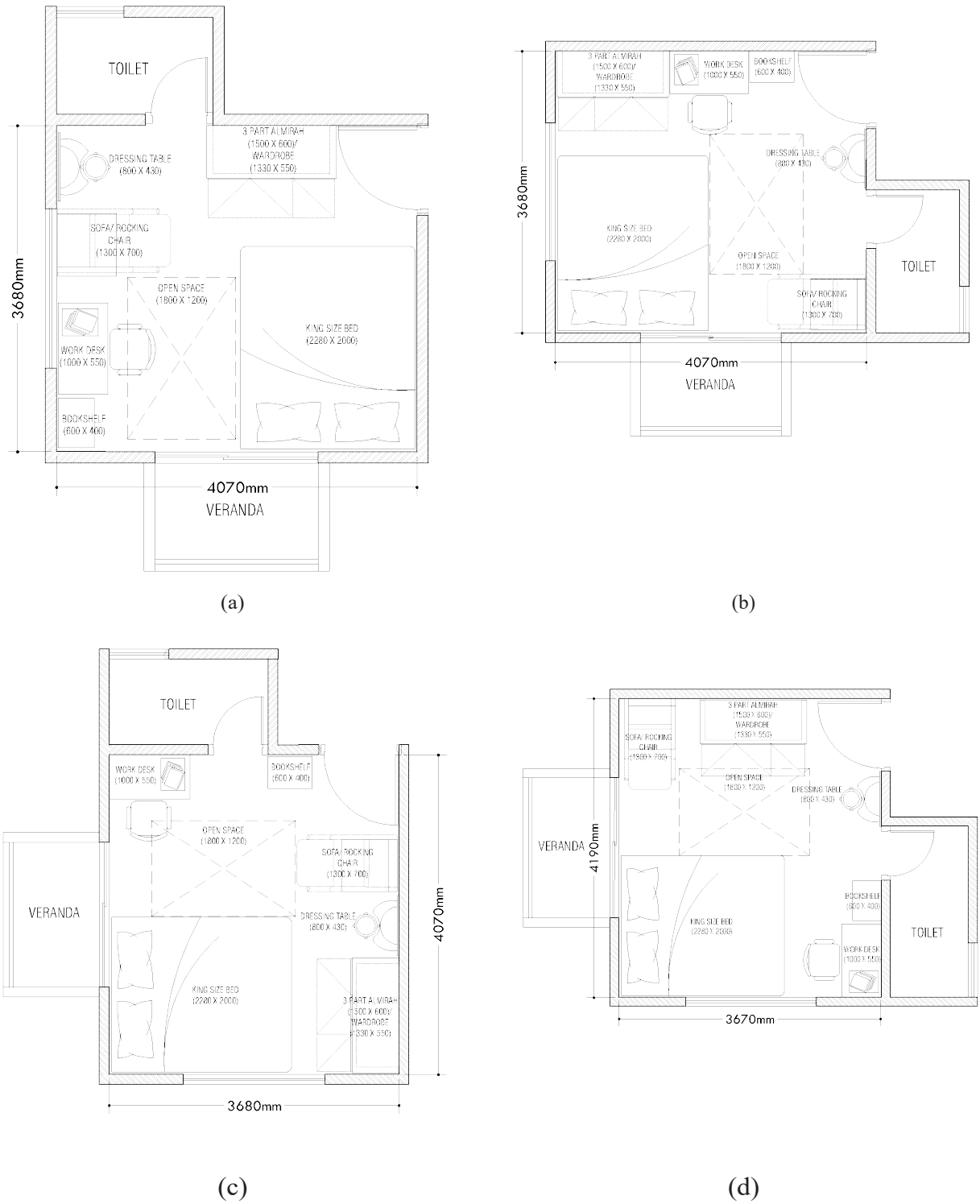

Fig. 2: Master Bedroom Plans with Dimension and Furniture

Based on the maximum dimensions derived from Table IV, it is concluded that a master bedroom measuring 4320 mm × 3680 mm can accommodate the full range of essential furniture identified in the survey. However, room configuration plays a critical role in space usability. The placement of key elements such as doors, windows, verandas, and toilet doors significantly influences the layout possibilities. These spatial constraints were carefully considered during the layout analysis. For instance, in Fig. 2(h), if the veranda door were located at the top-left corner instead of the center, the current furniture arrangement would still be functional. Similarly, here if the toilet door is positioned at the bottom-right, shifting the work desk and bookshelf upward would maintain functionality without altering the room's dimensions. This principle holds true across other configurations as well.

The layout analysis, conducted through rigorous design iterations, established that a room size of 4320 mm × 3680 mm can successfully accommodate the complete set of furniture. For example, in Fig. 2(d), if the toilet door is relocated to the bottom-left corner, increasing the room length from 4060 mm to 4320 mm resolves spatial limitations. This modified arrangement is illustrated in Fig. 3.

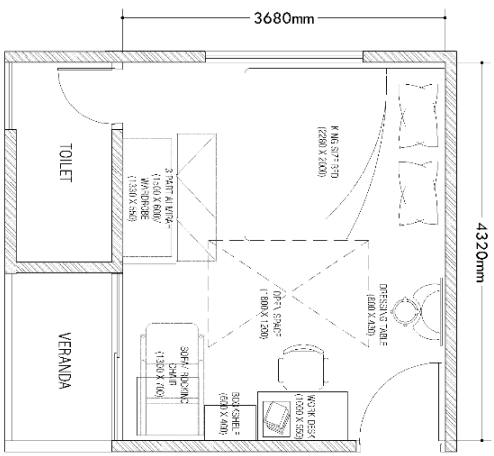

Fig: 3: Modified Arrangement of Bedroom

This holds true for other configurations as well. The study meticulously explored more than four variations in the locations of doors, windows, verandas, and toilet entrances for each bedroom configuration, testing which room dimensions could accommodate the full range of essential furniture. The dimension of 4320 mm × 3680 mm consistently performed well in every scenario. In some cases, slightly smaller dimensions were workable, but the required size never exceeded 4320 mm × 3680 mm.

Therefore, it is recommended that designers do not design master bedrooms smaller than 4320 mm × 3680 mm. However, careful attention must be paid to the room configuration, particularly the placement of the main door, veranda door, toilet entrance, and window(s).

Additionally, the set of maximum uses identified in this research provides valuable insight into the functional requirements a master bedroom in a compact apartment should fulfill—especially when the actual end user is unknown.

5. CONCLUSION

Compact apartments have become an unavoidable reality in Dhaka, where escalating land prices and rising construction costs make smaller living spaces the only affordable option for much of the city's middle-income population. However, maintaining cultural norms and meeting the personal needs of residents remain essential considerations in apartment design—considerations that are often overlooked in developer-led projects where the end user is unknown.

This study addresses that gap by offering a practical resource for architects and designers. It provides insights into optimal master bedroom dimensions and furniture arrangements, enabling designs that accommodate a wide range of family structures and occupational needs—even within compact apartments. While the study's sample size is limited to 100 respondents, they represent a diverse cross-section of Dhaka's middle-income households, offering a reasonable foundation for design guidance.

Future research with larger sample sizes and more comprehensive datasets could further refine these findings, contributing to the development of more precise and user-centric guidelines for master bedroom design in the context of Dhaka's evolving urban housing landscape.

REFERENCES

[1] S. M. Labib, M. Z. Rahaman and M. M. R. Bhuiya, "Location and size preference for apartments in Dhaka and prospect of real estate market," Bangladesh Research Publications Journal, Vol. 9, Issue 2, pp. 87-96, 2013.

[2] M. Masum, The Process of Capital Accumulation through Real-estate Development: The Case of Dhaka City, Master's thesis, Department of Sociology, University of Dhaka, 2015.

[3] M. J. Alam, "Rapid Urbanization and Changing Land Values in Mega Cities: Implications for Housing Development Projects in Dhaka, Bangladesh," Bandung: Journal of the Global South, Vol. 5, No. 2, 2018.

[4] Apartment Sales Down 17pc in FY23, The Daily Star, August 16, 2023.

[5] Mir Real Estate, The Real Estate Sector in Bangladesh, July 3, 2022.

[6] Dhaka City Building Construction Act, Act No. 2 of 2008, Ministry of Housing and Public Works, Government of Bangladesh, pp. 50, 58-ka(1), 2008.

[7] M. S. R. Milan, Real Estate Sector of Bangladesh, Real Estate in Dhaka City Blog, November 23, 2006.

[8] S. Chowdhury, M. Noguchi and H. Doloi, "Domestic Environmental Experience Design," Encyclopedia, Vol. 1, Issue 2, pp. 505-518, 2021.

[9] J. Islam, "Per capita bedroom space shrinks 17% over a year," The Business Standard, Apr. 29, 2023.

[10] Bangladesh Bureau of Statistics (BBS), Urban Housing Demand and Market Trends in Dhaka, 2023.

[11] World Bank, Bangladesh Urbanization Review: Affordable Housing and Middle-Income Growth, 2022.

[12] M. S. Rahman and A. K. M. Hoque, "Migration Patterns and Housing Preferences of Dhaka's Middle-Income Earners," Journal of Urban Development, Vol. 12, No. 3, pp. 45–60, 2021.

[13] N. J. Hossain, "Urban Livability and Environmental Sustainability: A Case of Khilkhet, Dhaka," The Jahangirnagar Review, Part II: Social Science, Vol. 33, pp. 115-121, 2009.

[14] Khilkhet Area Guide: Discover Insights & Price Trends, PropertyGuide, November 2023.

[15] Household Income and Expenditure Survey (HIES) 2022, Bangladesh Bureau of Statistics (BBS), 2023.

[16] https://hatil.com/

[17] https://www.otobi.com/

[18] https://regalfurniturebd.com

[19] J. Panero, M. Zelnik and J. De Chiara, Time-Saver Standards for Interior Space Planning, McGraw-Hill, 1992.

APPENDIX

Questionnaire Used During the Survey

	Question	Response Options
1.	Are you a tenant?	1. Yes 2. No
2.	What is your monthly income?	1. 10,000 – 49,000 BDT 2. 50,000 – 120,000 BDT 3. Over 120,000 BDT
3.	What is your occupation?	Open-ended (recorded as per response)
4.	Are you planning to purchase an apartment in Dhaka in the future?	1. Yes 2. No
5.	What is the size of your current master bedroom?	Documented during field survey
6.	How many people share this bedroom?	1. One 2. Two (Couple) 3. Three (With infant)
7.	What activities do you currently perform in your bedroom?	Open-ended (recorded as per response)
8.	What activities would you like to perform in your future bedroom (in a purchased apartment)?	Open-ended (recorded as per response)
9.	What furniture do you currently use in your bedroom?	Open-ended (recorded as per response)
10.	What additional furniture do you think you need?	Open-ended (recorded as per response)

Numerical Evaluation of Headed Stud Shear Connector in Composite Beam

Md. Khasro Miah*, **Md. Rakibul Hasan and A.K.M. Ruhul Amin**

Department of Civil Engineering, Dhaka University of Engineering & Technology, Gazipur, Bangladesh

ABSTRACT

Steel–concrete composite beams are widely used in modern construction due to their structural efficiency, yet the behavior of shear connectors under varying conditions remains insufficiently explored. This study aims to investigate the mechanical performance of composite beams with a focus on the geometry, diameter, and shape of shear connectors. Finite Element Analysis was conducted using ANSYS software, and the numerical model was validated against experimental test data. A parametric study was performed to evaluate the influence of different connector configurations on load-carrying capacity, stiffness, and slip resistance. The results show that increasing the diameter of shear connectors significantly improves both load capacity and stiffness, while square-shaped connectors offer better slip resistance than circular ones. Additionally, stress distribution at mid-span, shear transfer along the beam length, and failure patterns were analyzed. These findings contribute to optimizing shear connector design for improved composite action in steel–concrete systems.

1. INTRODUCTION

Composite structures are widely used in civil engineering construction throughout the world. A composite structure is defined by the interaction of two or more elements acting together as a single element. In a steel-concrete composite beam, the bonding between the steel and the concrete is established by the headed stud shear connector. It creates composite action by resisting the longitudinal sliding and uplifting between the steel beam and concrete slab. This composite structure provides higher strength and stiffness. In the laboratory, specimens test with varying geometric properties is a time-consuming matter, where numerical analysis can easily verify the effect of any variation. In this perspective, a three-dimensional numerical model of a steel-concrete composite beam is prepared by ANSYS software (version 15.0), based on the Finite Elements Method. The model presented here has been investigated by Chapman and Balakrishnan [1] experimentally. The numerical results had been compared with experimental findings. The length of the shear connector with different diameter and shape have also been analyzed as a parametric study. Three-headed stud shear connectors having a length of 76mm, 88mm, and 102mm with a stud shank diameter of φ16mm, φ19mm, and φ22mm were considered along with the corresponding head diameter of φ25mm, φ32mm, and φ35mm respectively. Square-headed shear connector has also been introduced to observe the effect of composite action. Based on the analytical result it was found that the effect of length of stud shear connector is insignificant. On the other hand, increasing the diameter of the shear connector gives higher load caring capacity and stiffness. It is also found that the square shape shear connector gives better stiffness than the circular shear connector. Besides the parametric study, the first cracking load, cracking pattern, normal stress distribution at mid-span, deformation, and shear distribution of the shear connector along the length, have also been observed. Based on the numerical model and its results obtained using finite element software ANSYS well agree with the experimental results.

Several researchers conducted experimental studies on composite beams. Hafez et al. [2] investigated experimentally the performance of simply supported steel-concrete hybrid beams with corrugated webs under vertical loads. The ultimate load of beams with corrugated webs increased by approximately 63% compared to the beam with flat web. Loqman et al. [3] examined bolted shear connectors, which exhibited 95% shear resistance in comparison to headed stud shear connectors. Zhao and Yuan [4] investigated the influence of high-strength engineering materials on overall flexural responses in their experimental examination of steel-concrete composite beams. Full-scale composite beam specimens used to investigate the flexural response with multiple connector options as blind bolt and welded stud [5]. The behaviour of a composite beam with demountable type shear connectors using push-out tests and composite beam testing done by Rehman [6]. Patil and Shaikh [7]

*Corresponding author's email: mkhasro@duet.ac.bd

investigated numerically the effect of shear connections in composite beams using ANSYS software and discovered that the height of the shear connectors had no influence on the composite beam's deflection. The flexural performance of a hybrid beam with two categories of shear connectors, one being a welded stud and the other being a blind bolt shear connector investigated by Pandilatha and Surumi [8].

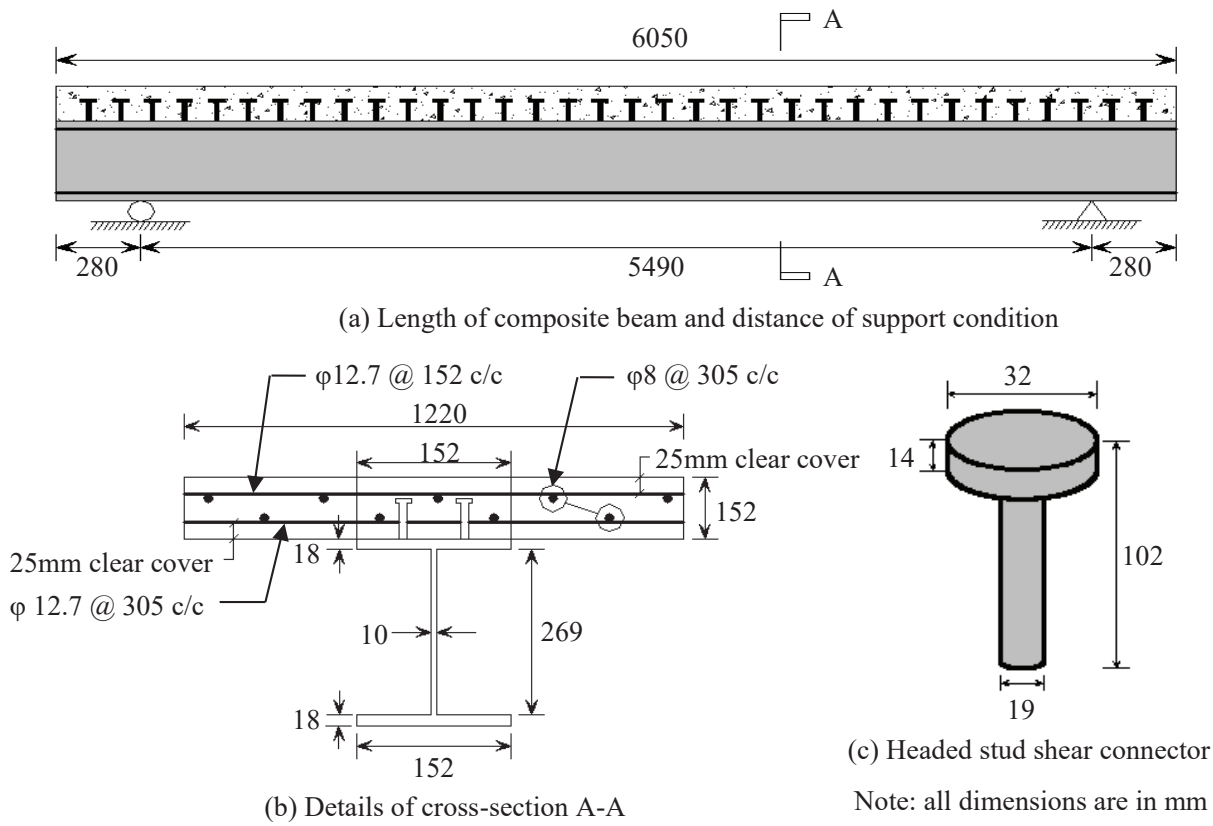

(a) Length of composite beam and distance of support condition

(b) Details of cross-section A-A

(c) Headed stud shear connector

Note: all dimensions are in mm

Fig. 1: Geometry of the Composite Beams

Prakash et al. [9] used numerical simulation to evaluate the performance of stud-connected steel-concrete hybrid girders to experimental work and concluded that the FE model is found to predict a conservative value for the ultimate load. Kotinda [10] modeled the structural performance of steel-concrete hybrid simply supported beams numerically by simulating the contact interaction between the surface of the concrete block and the steel joist. Compressive strength of concrete raised from 20MPa to 70MPa enhanced the load bearing capability of a steel-concrete hybrid beam by approximately 20% [11]. Hoffmann *et al.* [12] explores load–slip behavior, shear force distribution along short headed studs, and failure mechanisms including bond and grout degradation in grouted precast joints. Wu *et al.* [13] Focuses on sleeved vs. conventional headed studs using push-out tests and nonlinear Abaqus models. It examines effects of stud height, sleeve geometry, and UHPC filling, reporting a 4–8% capacity increase and 25–35% higher stiffness for sleeved studs.

Even though there have been experiments and computer simulations on shear connectors before, it still does't fully understand how different geometrical factors affect the general performance of composite beams. ANSYS, a finite element program, is used to simulate the test results of composite beams in this study, which fills in the gap. After the numerical results matched well with the previous experimental and numerical results of the steel-concrete hybrid or composite beam, a parametric study was also carried out.

2. FINITE ELEMENT MODELING

The numerical simulation used parts from the ANSYS library that had already been defined. The modeling method and choice of elements came from the computer

analysis that Kotinda [10] set up. The next part goes over the different kinds of things that are important for numerical analysis. This study's numerical models matched the actual analysis for model beam "A3" that was done by Chapman and Balakrishnan [1]. Fig. 1 shows the shape of the "A3" beam model.

There are 6050mm of length on the beam and 1220mm of width on the slab. The slab is 152mm thick. The slab is twice as strong because it has 152mm wide flanges on both the top and bottom and steel joists that are 305mm deep. The ring is 18mm thick and the web is 10mm thick. There are two rows of a headed stud shear connection that has a diameter of 19mm. There were 68 shear connections in all. The beam is only held up by a heavy load in the middle of its span.

The concrete slab as shown in Fig. 1 was modeled using SOLID65 element. The element has eight nodes, and each node has three degrees of freedom, which means it can move in x, y, and z directions. A 4-node shell element (SHELL43) is used to represent the steel I-beam. Each node has six degrees of motion. The element can move and rotate around the x, y, and z directions that are attached to it. The three-node beam element BEAM189, which has six degrees of freedom at each node, was used to model the stud shear connection. It can rotate and translate the element along the x, y, and z directions. A two-linear model based on the von Mises criterion that includes isotropic hardening for shear joints. The layer of reinforcement has been added to the SOLID65 element as a real constant. The von Mises criterion says that the best elasto-plastic model for the strengthening steel meets its requirements. The properties of the material and the volume ratio are given as real numbers. Divide the rebar's volume by the total volume of the reinforcement layer to get the volume ratio.

It is easier to connect the slab and steel beam interface with the help of the TARGE170 and CONTA173 elements. When two surfaces touch, pressure is created, but it goes away as soon as the surfaces move apart. This part may also show the friction and cohesion at the point where the concrete slab and steel beam meet, in addition to the pressure characteristics. To keep the number of parts and processing time as low as possible, this study only models the symmetric half of the beam. The load was put on in two stages. At first, the weight of the building was thought to be the gravitational load. In the second step, an outside force is put on the composite beam, focusing it in the middle of its span between two supports.

2.1 Concrete Materials Modeling

The stress-strain curve of concrete, which is shown in Fig. 2, is found using the Mander [14] formulae. Concrete is thought to be a uniform isotropic material. The Mander stress-strain curve for unconfined concrete is shown by Equations (1) and (2).

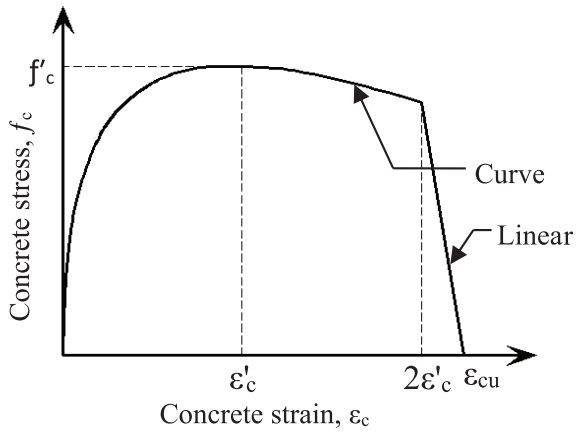

Fig. 2: Mander Stress-strain Curve for Concrete [14]

For $\varepsilon_c \le 2\acute{\varepsilon}_c$ (curve portion)

$$f_c = \frac{f_c' \; xr}{r - 1 + x^r} \tag{1}$$

where

$$x = \frac{\varepsilon_c}{\varepsilon_c'} \text{ and } r = \frac{E_c}{E_c - \left(\frac{f_c'}{\varepsilon_c'}\right)}$$

For $2\acute{\varepsilon}_c < \varepsilon_c \le \varepsilon_{cu}$ (linear portion)

$$f_c = \left(\frac{2 f_c' \; r}{r - 1 + 2^r}\right)\left(\frac{\varepsilon_{cu} - \varepsilon_c}{\varepsilon_{cu} - 2\varepsilon_c'}\right) \tag{2}$$

where r is as defined previously for the curved portion of the curve. f_c= Concrete stress (MPa), ε_c= Concrete strain, E_c= Modulus of elasticity of concrete (MPa), f'_c= Concrete compressive strength (MPa), ε'_c= Concrete strain at f'_c, and ε_{cu}= Ultimate concrete strain capacity.

2.2 Steel Materials Modeling

The steel yield strain, ε_{sy} is determined from $\varepsilon_{sy} = f_{sy} / E_s$, where, ε_s = Steel strain, f_s = Steel stress (MPa), E_s = Modulus of elasticity of steel (MPa), f_{sy} = Steel yield stress (MPa), f_{su}= Steel maximum stress (MPa), ε_{sh}= Strain at onset of strain hardening, ε_{su}= Strain corresponding to steel maximum stress, ε_r = Strain at steel rupture. The following equations define the simple parametric stress-strain curve for the structural steel as shown in Fig. 3.

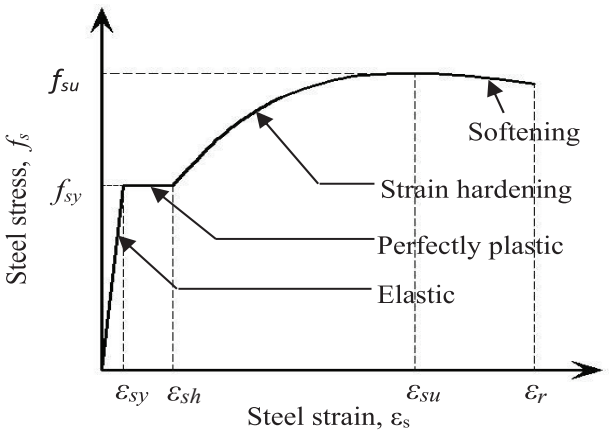

Fig. 3: Structural Steel Parametric Stress-strain Curve [15]

For $\varepsilon_s \le \varepsilon_{sy}$ (elastic region),

$$f_s = E_s \varepsilon_s$$

For $\varepsilon_{sy} < \varepsilon_s \le \varepsilon_{sh}$ (perfectly plastic region),

$$f_s = f_{sy}$$

For $\varepsilon_{sh} < \varepsilon_s \le \varepsilon_r$ (strain hardening and softening regions),

$$f_s = f_{sy}\left[1 + r\left(\frac{f_{su}}{f_{sy}} - 1\right)e^{(1-r)}\right] \quad (3)$$

where,

$$r = \frac{\varepsilon_s - \varepsilon_{sh}}{\varepsilon_{su} - \varepsilon_{sh}}$$

2.3 Finite Element Meshing and Boundary Conditions

In numerical analysis, the mesh size must have fine and consistent in order to have great detail where information is necessary; nevertheless, very fine mesh may require a long time to analyze. In this investigation symmetric half portion of the beam has been considered for modeling because of reducing the elements and computational time. The load was applied in two steps. At the first step, it was considered the weight of the structure itself as the gravitational load. In the second step, applying the external load, concentrated in mid-span between two supports of composite beam as shown in Fig. 4.

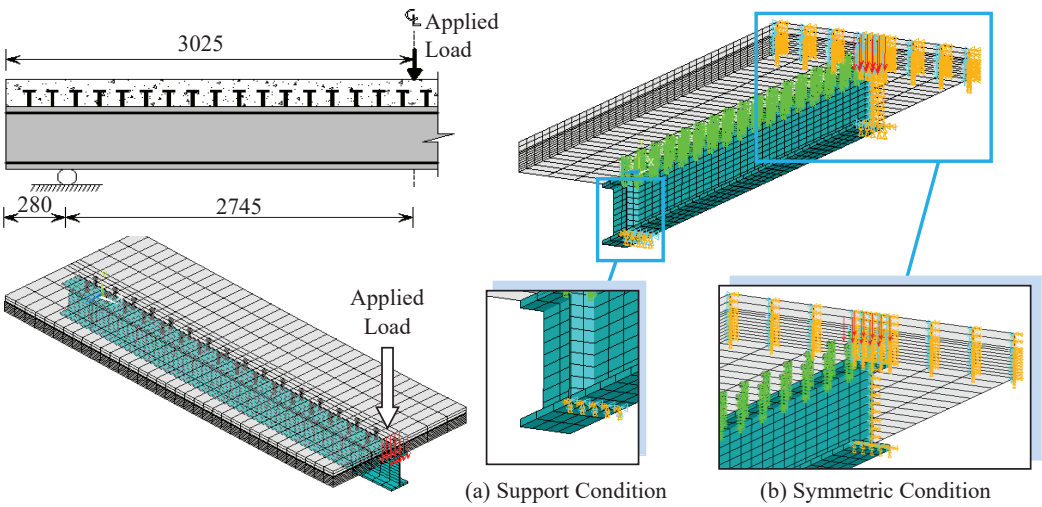

Fig. 4: Symmetric half of the Composite Beam with Single Point Concentrated Load

3. NUMERICAL RESULT

The main thing that was used to check the accuracy of the computer model was the vertical deflection at mid-span under concentrated load. The relative end slip of the composite beam was also looked at.

3.1 Comparison of Numerical Model with Experimental Test Results

Kotinda [10] and Ibrahim et al. [11] conducted numerical analyses on the same model, and their results align closely with those reported in this study, as illustrated in Fig.5. The experimental applied load and mid span deflection investigated by Chapman and Balakrishnan [1] also shown along with the numerical results in Fig.5. The numerical relationships between load and deflection agree well with both the actual and numerical relationships. The numerical model that was made here is used in the subsequent sections to conduct additional parametric research.

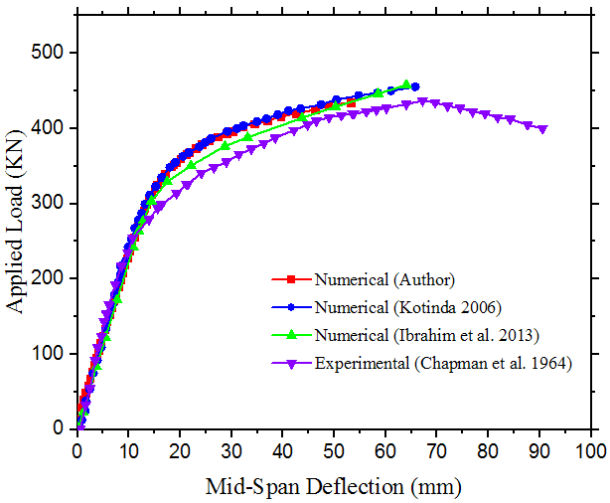

Fig. 5: Load-deflection Curves (Numerical and Experimental)

3.2 Parametric Study

To find out how shear connections affect the performance of composite beams, different shear connector shapes are looked at, and the same model is looked at on its own, as explained in the next parametric study.

3.2.1 Effect of Diameter of Shear Connector

It was looked at how the diameter of the shear connection affects the load-deflection behavior of steel-concrete composite beams by looking at the beams with different diameters of shear connectors. The sizes were φ16mm, φ19mm, and φ22mm, and the stud head widths that went with them were φ25mm, φ32mm, and φ35mm. Table I shows how the diameter of the shear connection affects the behavior of composite beams. The final load capacity goes up by 5.46 percent when the diameter goes from φ16mm to φ22mm.

The findings demonstrate that maximum loading is achieved for connections with a diameter of φ22mm, exhibiting reduced vertical deflection. The load-deflection curve for various diameters of the shear connector exhibits nearly identical results across both the linear and non-linear ranges, as illustrated in Fig. 6.

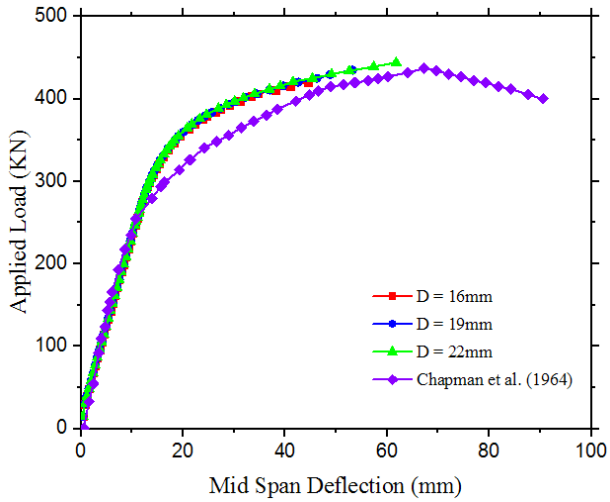

Fig. 6: Load-deflection curves with different diameters of shear connectors

Three different sizes of the shear connection, shown in Table II, were used to test the relative end slip of the composite beam. Increasing the shear connector's diameter makes it much less likely that the concrete block and steel joist will slide along the longitudinal axis. As a result of its lower ultimate load capacity, the φ16mm diameter circular shaped connector shows lower numbers in this study than the φ19mm. The slip resistance goes up by 26.17% when the width is raised from φ19mm to φ22mm. The load versus slip relation of a composite beam with shear connections of different diameters is shown in Fig. 7.

Table I: Ultimate Load Variation Considering Different Diameter of Shear Connectors

Diameter of stud shank (mm)	Connectors Height (mm)	Ultimate Load (kN)	Max. Deflection at Ultimate Load (mm)	Load Capacity Variation (%)
D	H	P_u	Δ_u	$(Pu/P_{D19}) \times 100$
16	102	420.40	44.53	96.66%
19	102	434.90	53.19	100%
22	102	444.12	61.76	102.12%

Table II: End Slip Considering Different Diameter of Shear Connectors

Diameter of stud shank (mm)	Connectors Height (mm)	Ultimate Load (kN)	End Slip at Ultimate Load (mm)	End Slip Variation (%)
D	H	P_u	U_x	$(U_x/U_{D19}) \times 100$
16	102	420.40	0.1334	99.18%
19	102	434.90	0.1345	100%
22	102	444.12	0.0993	73.83%

It is clear from Fig. 7 that as the diameter of a shear connection increases, the relative end slip decreases. In this case, connectors with a diameter of φ22mm do a better job of resisting end slip. Based on our study of how the composite beam behaved, we can say that making the shear connector larger will increase its final load-carrying capacity and make it better at stopping longitudinal sliding.

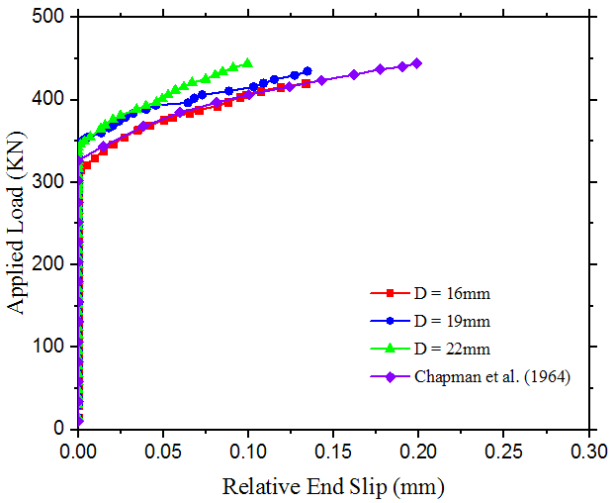

Fig. 7: Load-Slip Curves with Different Diameters of Shear Connectors

3.2.2 Effect of Shape of Shear Connector

The same model was looked at with a square shear connection to see how the shape of the shear connector affected how the load deflected in composite beams. By keeping the same steel area, circular connections with a diameter of φ19mm can be turned into square ones. The body of a square connection is 16.83 mm in size, and the head of that connector is 28.35 mm in size. As shown in Fig. 8, all of the other details about shear connections stay the same.

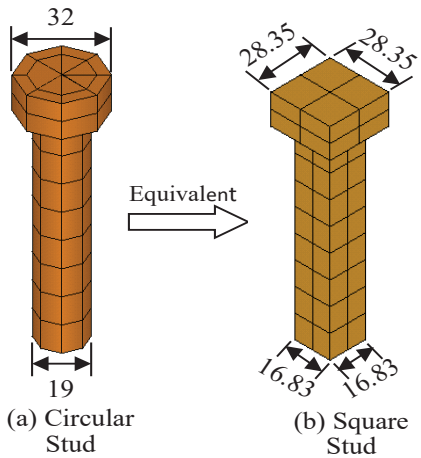

Note: all dimensions are in mm

Fig. 8: Dimensions of Circular and Equivalent Square Headed Shear Connector

The data in Table III show that square shear connections can hold a little more weight than circular shear connections. A square connection measuring 16.83mm × 16.83mm is the same as a circular connector with a diameter of 19mm, but it can hold 0.92% more weight. As shown in Fig. 9, the load-deflection curve shows that changing the shape of the shear connection doesn't have a big effect on how the composite beam behaves.

Table III: Load Capacity Variation Considering the Different Shape of Shear Connectors

Connectors Shape and size	Connectors Height (mm)	Ultimate Load (kN)	Max. Deflection at Ultimate Load (mm)	Load Capacity Variation (%)
	H	P_u	Δ_u	$(P_u/P_{cir}) \times 100$
Circular φ19	102	434.90	53.19	100%
Square 16.83 × 16.83	102	438.92	58.75	100.92%

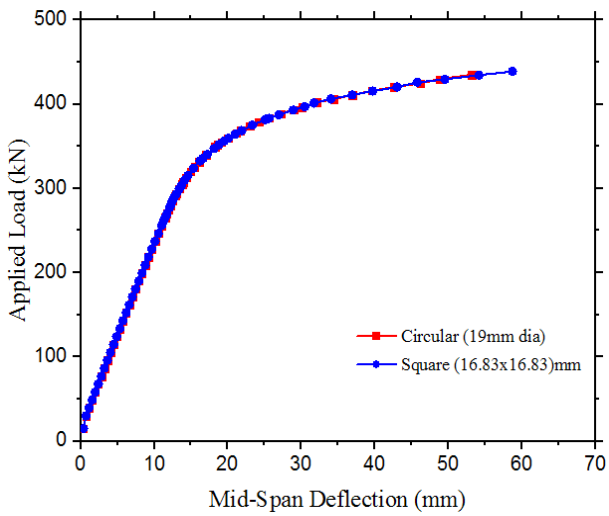

Fig. 9: Load-Deflection Relations with Different Shape of Shear Connectors

The change from a circular to a square shear connection has a small effect on how the load deflects, but the difference in load-relative end slip that happens because of these shape changes is important. Table IV shows that for the 16.83mm×16.83mm square shear connector, the slip drops by 3.50 percent as the ultimate load rises, while

it stays the same for the φ19mm circular connector. Fig. 10 shows a load versus slip curve that shows that square connections work slightly better against resistance. This is shown by the end slip in the curve.

3.2.3 Mid Span Stress Distribution along the Depth of Composite Beam Section

Fig. 11 shows how the normal stress is spread along the beam cross-section at the middle of the combined beams (A3). Stress distribution along the ordinate and the concrete slab is under compressive stress above the neutral axis, and the steel joist is under tensile stress below the neutral axis. Because of the composite action, the force distribution in a composite beam is different from that of a normal concrete beam. Fig. 11 shows how the stress is spread out based on the loads.

Table IV: End Slip Variation Considering Different Shape of Shear Connectors

Connectors Shape and size	Connectors Height (mm)	Ultimate Load (kN)	End Slip at Ultimate Load (mm)	End Slip Variation (%)
	H	**P_u**	**U_x**	**$(U_x/U_{cir}) \times 100$**
Circular φ19	102	434.90	0.1345	100%
Square 16.83 × 16.83	102	438.92	0.1298	96.50%

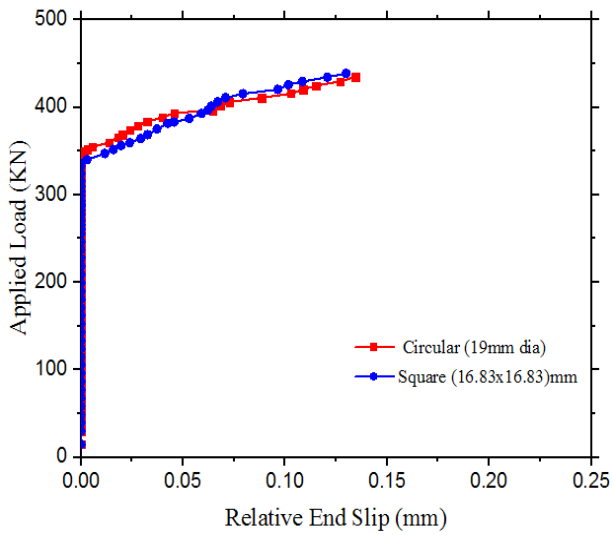

Fig. 10: Load-slip Curve with Different Shape of Shear Connectors

3.2.4 Variation of Shear Force along the Length of Stud Shear Connector

The shear force on the composite system is transferred to the concrete around the shear connection by the bearing forces between them as well. A stud shear connector is put 1458.3 mm from the middle of the span in Fig. 12, which shows how the shear force is transmitted through it. The shear force is zero around the middle of the shear connection shank. Fig. 12 shows that when a certain load of 209.kN is applied, the lower half of the connector's stem resists almost negative shear force, while the upper half resists positive shear force. The connector's head, on the other hand, experiences negative shear and resists vertical separation. In the same way, the shear force distribution along the stud stem follows the same pattern for three different loads viz. 305.02kN, 402.12kN, and 434.90kN with zero shear force at the same location.

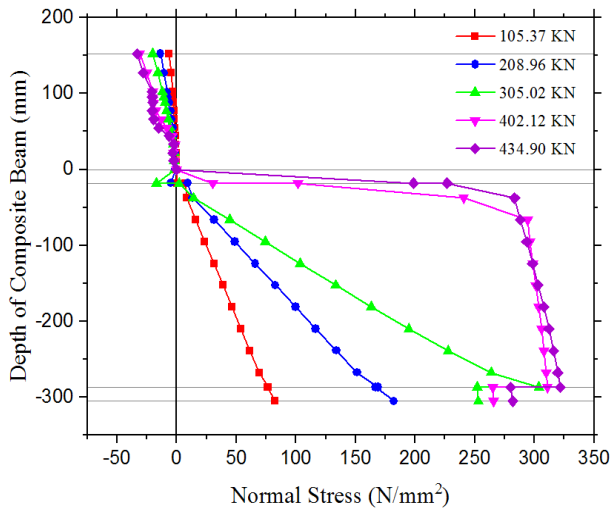

Fig. 11: Mid Span Stress Distribution along the Depth of Composite Beam Section

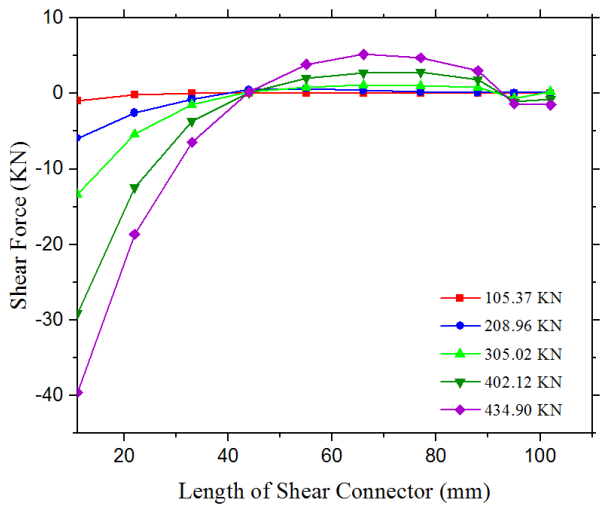

Fig. 12: Shear Force Distribution along the Length of the Shear Connector

3.2.5 Failure of the Composite Beam

According to Chapman and Balakrishnan [1], the failure mode of the composite beam observed in laboratory tests was due to the crushing of the concrete slab at mid-span. In the present numerical analysis, the Von Mises stress distribution shows that the compressive stress at the top surface of the concrete slab exceeds the material's average compressive strength (fc = 18.4 MPa) at a load of 434.90 kN, as illustrated in Fig. 13. This indicates that the concrete reached its ultimate capacity, leading to localized crushing. The stress concentration occurred primarily at mid-span, where maximum compressive forces develop under bending. This corresponds well with the experimental failure pattern. Therefore, the nonlinear finite element model accurately replicates the physical failure mechanism, confirming that the dominant mode of failure in the composite beam is compressive crushing of the concrete slab at mid-span. The convex downward shape in the regions of high stress concentration indicates that compressive stress is dominant in those areas, typically due to load transfer from the slab to the steel beam through the headed studs. In contrast, the concave downward curvature in the low-stress regions represents zones of relatively reduced stress, often due to unloading or redistribution of internal forces.

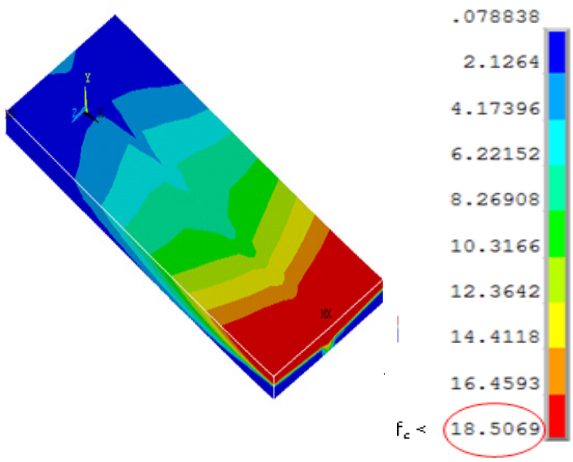

Fig. 13: Von Mess Stress of 434.90 kN

4. CONCLUSIONS

The results of finite element analysis led to the following conclusions:

- The relationship between load and displacement was found to be in good agreement with the numerical results found by Kotinda [10] and Ibrahim et al. [11]. These results showed that the numerical model that was made was accurate in all respect;
- The numerical model well agreed with experimental results [1] in all respect. The load carrying capacity increase by 5.46% and slip decrease by 26.17% with increasing the stud diameter from 16mm to 22mm.
- When a similar square shear connection (16.83mm x 16.83mm) is used instead of the standard stud shear connector (φ19mm), the load-carrying capacity is almost the same, but it is 0.92% higher, and there is 3.50 percent less relative end slip.
- Therefore, a square-shaped shear connector can be used instead of a normal circular shear connector, as long as all the factors are taken into account, such as the ability to hold a load and the resistance to relative end slip.
- Using the model developed here similar research may be performed with different types of shear connectors like; U-type sear connectors, inverted L-type shear connectors, etc. The effect of the variation in concrete strength and steel yield strength on the behaviour of composite beams may also be analysed.

ACKNOWLEDGMENTS

The authors express their profound appreciation to the Department of Civil Engineering, DUET, Gazipur, for their support and collaboration in completing the research effort. This task would not have been accomplished without this unwavering support.

REFERENCES

[1] J. C. Chapman and S. Balakrishnan, "Experiments on composite beams," The Structural Engineer, Vol. 42, pp. 369–383, 1964.

[2] A. M. A. Hafez, M. M. Ahmed, A. S. Alamary, and A. M. Mahmoud, "Behaviour of simply supported composite concrete-steel beam with corrugated web under vertical loads," Journal of Engineering Sciences, Vol. 40, No. 1, 2012.

[3] N. Loqman, N. A. Safiee, N. A. Bakar, and N. A. M. Nasir, "Structural behaviour of steel-concrete composite beam using bolted shear connectors: A review," MATEC Web of Conferences, Vol. 203, 2018.

[4] H. Zhao and Y. Yuan, "Experimental studies on composite beams with high-strength steel and concrete," Steel and Composite Structures, Vol. 10, No. 5, pp. 373–383, 2010.

[5] W. P. Sameera, B. Uy, O. Mirza, and X. Zhu, "Flexural behavior of composite steel-concrete beams utilizing blind bolt shear connectors," Engineering Structures, Vol. 114, pp. 181–194, 2016.

[6] N. U. Rehman, Behaviour of Demountable Shear Connectors in Composite Structures. Bradford, UK: University of Bradford, 2017.

[7] P. S. Patil and M. G. Shaikh, "A study of effect of shear connector in composite beam in combined bending and shear by ANSYS," International Journal of Innovative Technology and Exploring Engineering, No. 3, 2013.

[8] P. Pandilatha and R. S. Surumi, "Comparative study on flexural behavior of steel concrete composite beam using welded and bolted shear connector," International Journal of Civil Engineering and Technology, Vol. 8, No. 5, pp. 1016–1024, May 2017.

[9] A. Prakash, N. Anandavalli, C. K. Madheswaran, J. Rajasankar, and N. Lakshmanan, "Three-dimensional FE model of stud connected steel-concrete composite girders subjected to monotonic loading," International Journal of Mechanics and Applications, Vol. 1, No. 1, 2011.

[10] T. I. Kotinda, Numerical Modeling of Steel-Concrete Composite Beams Simply Supported: Emphasis to the Study of the Slab-Beam Interface. São Carlos, Brazil: University of São Paulo, 2006.

[11] A. M. Ibrahim and Q. W. Ahmed, "Nonlinear analysis of simply supported composite steel-concrete beam," Diyala Journal of Engineering Sciences, Vol. 6, No. 3, pp. 107–126, 2013.

[12] D. Hoffmann, U. Kuhlmann, J. Schorr, M. Kantar, and J. Völlner, "Composite girders with short headed studs in grouted joints of precast concrete elements—Numerical investigations and design recommendations," Steel Construction, Vol. 17, No. 2, pp. 70–80, 2024.

[13] F. Wu, H. Su, Q. Su, and B. Yuan, "Shear performance study of sleeved stud connectors in continuous composite girder," Materials, Vol. 17, No. 13, p. 3326, 2024.

[14] J. B. Mander, M. J. N. Priestley, and R. Park, "Theoretical stress-strain model for confined concrete," Journal of Structural Engineering, Vol. 114, No. 3, pp. 1804–1826, 1988.

[15] S. Holzer, R. Melosh, and A. E. Somers, SINDER: A Computer Code for General Analysis of Two-Dimensional Reinforced Concrete Structures, Report AFWL-TR-74-228, Vol. 1. Kirtland AFB, NM, USA: Air Force Weapons Laboratory, 1975.

Parametric Optimization of Window-to-Wall Ratio to Reduce Thermal Discomfort in Naturally Ventilated Multi-Storied Residential Building in Dhaka

Maria Jebin[1*], Humayra Anan[1] and Md. Mashuk-Ul-Alam[2]

[1]Department of Architecture, Dhaka University of Engineering & Technology, Gazipur, Bangladesh
[2]Department of Architecture, Ministry of Housing and Public Works, Bangladesh

ABSTRACT

Rapid urban population growth in Dhaka has led to dense high-rise housing, often characterized by poor window design, which causes indoor overheating and a greater reliance on air conditioning, thereby escalating energy consumption. This study addresses thermal discomfort in multi-unit residential buildings by optimizing Window-to-Wall Ratios (WWR) using a performance-based, single-objective optimization approach. A case study of a typical Dhaka apartment with four rooms of different orientations was analyzed using parametric modeling in Rhinoceros 3D and Grasshopper, with Galapagos optimizer, using Predicted Percentage of Dissatisfied (PPD) as the primary thermal comfort metric. The results indicate that a WWR between 69% and 70% minimizes PPD across all orientations, improving comfort by 9–13%. The findings highlight the importance of early-stage design optimization for thermal performance and recommend considering window placement, shading, and other metrics for comprehensive building improvements.

1. INTRODUCTION

The ongoing rapid urbanization of Dhaka, the capital city of Bangladesh, is attracting approximately 2000 migrants daily, resulting in a substantial rise in population density [1]. Facing the challenges of land scarcity, soaring land prices, and rising construction costs, high-rise multi-unit residential buildings have gained popularity to meet the ever-increasing housing demand of the growing population [2]. Vertical expansion is a viable solution for an urban area as densely packed as Dhaka. However, the design of these tall structures tends to focus on increasing density, resulting in inadequate provision for natural ventilation. Consequently, high-density buildings trap heat and moisture indoors, causing the internal temperature to rise to intolerable levels [3].

In recent years, Dhaka has experienced unprecedented heat waves, frequently causing overheating in buildings [4]. This rising temperature, driven by climate change, can have adverse effects on residents' health and productivity due to extended exposure to heat [5]. As temperatures continue to rise, air conditioners are being perceived as daily necessities to maintain a comfortable living environment in residential buildings. Market reports show that AC sales in Bangladesh have increased by 25% annually since 2015, with Dhaka accounting for 70% of the national demand [6]. The residential sector accounts for more than one-third of global energy use [7, 8], much of which is dedicated to maintaining suitable thermal conditions within buildings [9, 10].

One of the critical parameters affecting the thermal comfort of the indoor environment is the Window-to-Wall Ratio (WWR) of the building [11-12]. The WWR indicates the percentage of the building's exterior surface occupied by windows or openings compared to solid wall surfaces [13]. Typically, increasing the WWR enhances the thermal exchange between the interior and exterior, which can affect the indoor comfort levels and result in higher energy consumption for cooling or heating [9]. Passive design strategies aim to maximize views while minimizing heat gain and energy loss through the proper sizing and placement of windows and openings [14]. Simulation tools and performance analysis are crucial in aiding architects to assess the impact of various WWR values on energy usage, indoor environmental quality, and overall building performance [15-16]. The size, position, and orientation of a window play a crucial role in determining a building's ability to maintain comfortable indoor temperatures through natural ventilation. Addressing these design elements early in the design development process can reduce reliance on mechanical cooling systems, and the required thermal comfort can be achieved. Early studies have underscored the potential of courtyards and natural ventilation in Dhaka's context, citing improved daylight and airflow through the introduction of courtyard typologies [17].

*Corresponding author's email: mariajebin2013@duet.ac.bd

In recent studies, the focus has shifted towards optimal plan layout, WWR, window design, and shading design to maintain thermal comfort through natural ventilation in apartments in Dhaka [18-20]. It was noted that most existing research on the thermal comfort of residential buildings in Dhaka remains descriptive, adopting manual optimization methods.

In recent literature, several studies have attempted to determine the suitable window-to-wall ratios for different climates and building types [8-10, 13, 16]. Comparative examinations in similar climates such as Butwal in Nepal [21], Guwahati in India [22], Katuanyake in Sri Lanka [23] show strong links between WWR, orientation, and thermal comfort under natural ventilation. However, these studies often target single-unit houses or courtyard typologies and don't utilize parametric optimization frameworks to establish optimal WWR values.

Through literature review, a research gap emerged concerning natural ventilation and thermal comfort using parametric optimization, specifically in multi-unit residential buildings in the context of Dhaka. To address the identified research gap, the study aims to analyze the impact of varying window-to-wall ratios on the thermal performance of multi-unit residential apartment buildings within the climatic context of Dhaka. The primary objective is to optimize the WWR to achieve improved thermal comfort, as measured by the Predicted Percentage of Dissatisfied (PPD), a metric that quantifies occupants' thermal discomfort. Considering recent advancements in building performance optimization techniques [24], this research employs a single-objective optimization algorithm implemented through computer simulations. The simulations are based on prototypical design models representative of typical multi-unit residential buildings in Dhaka. This study aims to provide insights that can help architects and building designers make informed decisions about WWR, ultimately contributing to the development of more energy-efficient and thermally comfortable residential buildings in Dhaka.

2. METHODOLOGY

This study employs a parametric optimization approach to enhance the thermal performance of window designs in residential buildings. In architectural and environmental design, a parametric approach involves the use of computational tools to systematically vary design parameters—here, the WWR—and analyze resulting performance outcomes through iterative simulations. This method enables the identification of optimal design solutions that effectively respond to environmental conditions. A typical residential building located in Dhaka, Bangladesh, was selected as the basis for the study. This building represents standard construction practices commonly found in the region. Four rooms within the building, each facing a different direction, were selected for detailed analysis. These orientations were chosen to represent the varying effects of solar exposure on thermal performance throughout the building envelope. The selected rooms were modeled using Rhinoceros 3D (version 8), a precision modeling tool widely used in architectural workflows. The thermal performance of the base case models was analyzed using ClimateStudio 2.1, an environmental simulation platform that integrates the EnergyPlus engine to evaluate indoor thermal comfort conditions. Input parameters for the simulation included local climate data, material properties, internal heat gains, and occupancy schedules relevant to the climatic context of Dhaka. To explore the performance implications of varying the WWR, the Galapagos evolutionary solver, integrated within the Grasshopper plugin for Rhinoceros, was utilized. Galapagos enables automated parametric optimization by iteratively modifying the WWR and evaluating the performance of each configuration. The fitness function was defined based on thermal comfort metrics, such as PPD, derived from ClimateStudio.

The research process was organized into four primary phases, including (1) field measurements to assess current thermal conditions, (2) development of base case models based on field data and typical construction details to serve as the baseline for performance evaluation, (3) thermal performance analysis of the base case models, and (4) parametric optimization to identify design solutions that improved thermal performance for the studied rooms. This methodology integrates empirical data collection, validated simulation tools, and algorithmic design exploration to ensure a rigorous and reproducible approach to performance-driven design.

2.1 Thermal Performance Metric

The PPD index is used as the primary metric for thermal analysis because it provides a precise estimate of the number of occupants likely to be dissatisfied with thermal conditions. According to recognized standards such as ASHRAE 55 and ISO 7730, keeping PPD below 10% and 15% in occupied spaces is crucial for ensuring thermal comfort. This makes PPD the most effective tool for assessing and optimizing indoor environments.

2.2 Case Study Description

A multistoried government residential apartment building is considered as the case study for the research (Table I). The purposeful selection resembles typical criteria and maximum challenges required for qualitative reflection of housing characteristics and adequate accuracy of expected outcome. It is a 12-storied building with 4 dwelling units in each floor measuring approximately 1250 square feet in area. Each dwelling unit consists of four bedrooms, three bathrooms, two verandas, and combined living-dining space which is the standard Government 'E-Type Apartment' Typology. The layout is also commonly used in multi-unit residential projects for mid to upper middle-income communities in Dhaka. It is situated at the 'Architecture and Public Works Department Officers Quarters, Jigatola', near Dhanmondi-2, Dhaka, established within the urban residential zone and surrounded by one of the most complex and dense built fabric. The location exposes the building and its inhabitants to almost every microclimatic challenge of Dhaka such as elevated ambient temperature, reflected heat and obstructed wind-flow caused by surrounding structures, lack of natural shading elements and cooling agents, compromised air quality and intensive noise pollution. The studying units are located on the fourth floor, standing approximately 45 feet above ground level, representing mid-level environmental condition offering balanced condition of urban exposure and potential for natural ventilation and cooling. All these parameters set an ideal context for studying the impact of WWR on occupants' thermal comfort. Moreover, having built on a government housing complex, within the direct design service, construction supervision, and occupancy opportunities by the authorities responsible for the public building construction sector (Department of Architecture and Department of Public Works under Ministry of Housing and Public Works), the building complies with every construction regulation, codes, and ethics. Besides its institutional importance, the building also exemplifies the concurrent standards and prevailing practices in both public and private residential architecture. The apartment unit size also corresponds to the average dwelling size of the area mentioned in Detailed Area Plan (DAP) 2016-2035. The configuration and orientation reflect the expectation from middle-income urban housing in Dhaka city. Thus, the selection of the building intends to ensure meaningful findings extended to both the public and private sectors of multi-unit high-rise residential.

Table I: Parameters of the Case Studies

Parameters	Case 1 (A4)	Case 2 (B4)	Case 3 (C4)	Case 4 (D4)
Room Dim.	12′×11′			
Window Orientation	South-West, North-West	North-West, North-East	North-East, South-East	South-East South-West
Window Width	SW: 5′0″ NW: 5′5″	NW: 5′5″ NE: 5′0″	NE: 5′0″ SE: 5′5″	SE: 5′5″ SW: 5′0″
Window Height	7′0″			
Sill Level	0′0″			
Lintel Level	7′0″			
Window Type	Sliding glass window with 50% operable area			
Wall	150mm brick plaster wall, off-white color			
Ceiling	Concrete slab, white color			
Floor	Tile floor, beige color			

(a) (b)

Fig. 1: (a) Exterior View of the Case Study. (b) Interior View of the West-Facing Bedroom

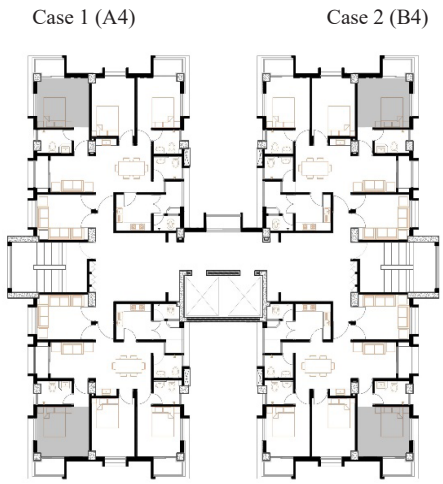

Fig. 2: Floor Plan of the Case Building

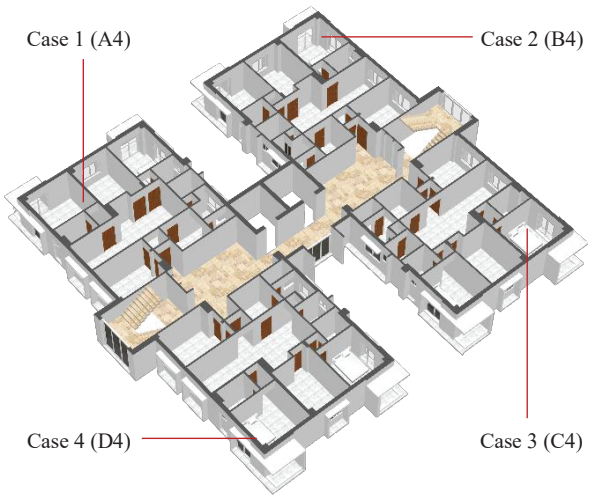

Fig. 3: 3D Model of the Case Building

2.3 Experimental Protocol for Field Measurements

To evaluate the thermal performance of the test room envelope, field measurements were conducted. Air temperature data were recorded over 24 hours from May 9 to May 10, 2025, at the center of the room at a height of 1 meter above the floor, following ASHRAE Standard 55-2010 [25]. Four HOBO MX2202 pendant data loggers shown in Fig. 4(a) were employed for temperature monitoring. This waterproof device, featuring Bluetooth connectivity, allows for direct data transfer to mobile devices or Windows computers via a dedicated application, as shown in Fig. 4(b). It offers temperature measurement accuracy suitable for both air (ranging from -20°C to 70°C) and water (ranging from- 20 °C to 50°C). Table II shows the detailed configuration set for the data logging activity.

Table II: Deployment Information

Configure Date	2025/05/09 14:48:11 Bangladesh Standard Time
Logging Interval	1 hour 0 minutes 0 seconds
Logging Mode	Fixed - Normal
Start Logging	On Date/Time 2025/05/09 16:00:00 Bangladesh Standard Time
Stop Logging	On Date/Time 2025/05/10 15:00:00 Bangladesh Standard Time

(a)

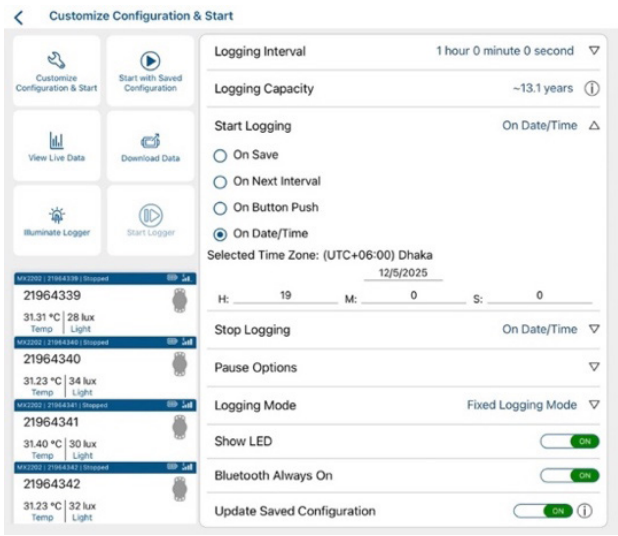

(b)

Fig. 4: (a) Hobo MX2202 Pendant Data Loggers. (b) App Interface and Configuration Settings

2.4 Base Case Model

Building simulation models of the case study rooms were developed based on the existing building design and material characteristics (Table III). Room geometries were created using Rhinoceros 3D (v8), and parametric control was handled via Grasshopper. Thermal simulations were conducted using ClimateStudio (v2.1), which employs the EnergyPlus engine. Each room was modeled as a single thermal zone, using Dhaka's climate data (.epw format). Internal loads assumed an occupancy density of 0.16 persons/m², with 0.1 ACH infiltration and no mechanical heating or cooling systems, reflecting naturally ventilated conditions. Temperature ranges for the natural ventilation are 22° C and 28° C for indoors and 17° C and 28° C for outdoor conditions, based on EN 15251 (Fig. 5).

The base case models were used to evaluate the performance of the base case rooms, considering overall thermal performance over an entire year. The thermal condition was calculated by assessing the PPD.

Table III. Materials used for base Model Simulation

Element	Material								
	Name	Type	Reflectance [%]	Specular [%]	Diffuse [%]	Roughness	U-value [W/m²K]	SHGC*	Tvis*
Ceiling	White painted room ceiling	Glossy	82.20	0.44	81.76	0.200	-	-	-
Floor	Beige floor tile	Glossy	36.83	1.10	35.72	0.200	-	-	-
Wall	Offwhite plaster wall	Glossy	84.07	0.43	83.64	0.200	-	-	-
Window glazing	Solarban 72 on starphire	-	-	-	-	-	3.16	0.31	0.743

*SHGC- Solar Heat Gain Coefficient; Tvis- Visible Light Transmission

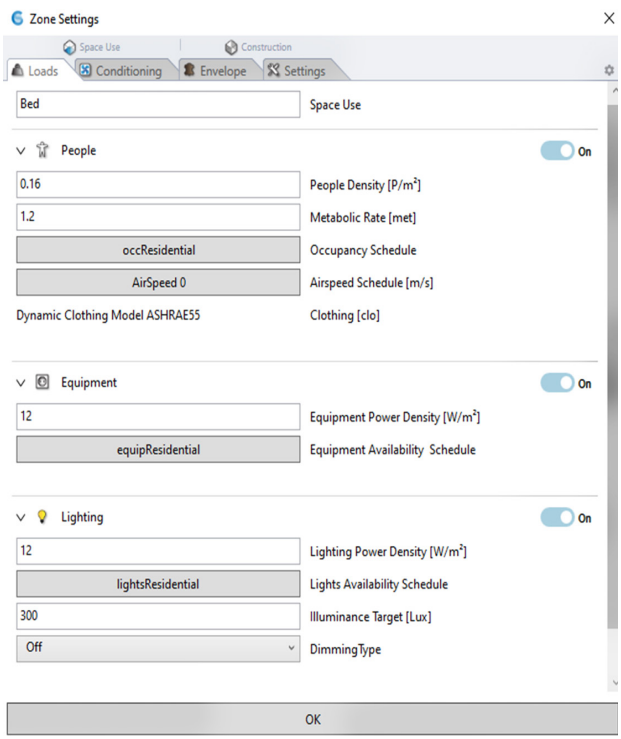

Fig. 5: Zone Settings

2.5 Optimization Approach for Building Performance

Recent developments in building optimization have led to its widespread adoption in architecture, particularly for addressing complex design challenges [24]. Optimization refers to the process of identifying the maximum or minimum value of a function by manipulating certain variables within predefined constraints [26]. Performance-based optimization involves tools such as parametric design, building performance simulations, and Genetic Algorithms [27]. Qingsong and Fukuda state that parametric design involves systematically varying design parameters within a defined space to explore multiple potential solutions. This approach supports informed decision-making by identifying options that satisfy, or closely approach, a set of predefined criteria [28]. Consequently, architects increasingly employ these methods to address complex environmental design issues [24]. Typically, the optimization framework consists of two key components: design variables and objective functions [27]. In the building performance optimization, variables refer to the parameters that define the design's geometry or physical characteristics, while objective functions represent performance indicators that are typically assessed through simulation tools [26]. When optimization targets a single performance criterion, the process is referred to as single-objective optimization, which is the approach adopted in this study.

2.6 Single-Objective Optimization

The main purpose of this step is to use the base case rooms and optimize their window design in terms of WWR for achieving the goal of minimizing PPD, which quantifies thermal discomfort as a percentage. The Grasshopper plugin Galapagos was used to optimize the design parameters for the single-objective optimization approach. Figure 6 shows the grasshopper script developed for single-objective optimization. In the script, there are six parts. The first part is developed for creating the surfaces of the room geometry, including the parametric components of the window, which will be used for the optimization process. The second part comprises selecting the materials for each surface defined in the room geometry from a

wide range of material libraries from the ClimateStudio. The third part is the thermal model, which includes the detailed zone setting for the indoor environment in terms of load, conditioning, envelope, and additional settings. The fourth part is the Galapagos optimization tool, which is the primary basis of this study. It functions by connecting the design variables as the genomes, and performance metrics as the fitness objective. The final part is the data exportation component, which extracts detailed data derived from optimization in a structured Excel format, which is essential for intuitive analysis of the results.

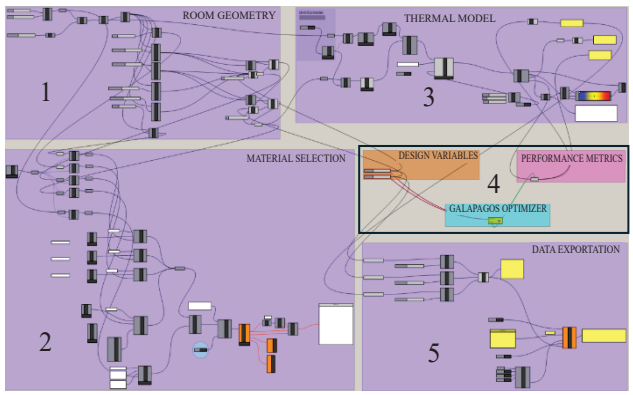

Fig. 6: Grasshopper Script Developed for Single-Objective Optimization

2.7 Optimization Parameters

Windows significantly influence a building's thermal performance and energy use due to their higher heat transfer coefficients compared to opaque envelope components [29]. According to Lee et al. [30], window U-values are typically five times greater than those of walls or doors, accounting for 20–40% of energy loss in buildings. Poor window design can lead to thermal discomfort and increased energy consumption. While prior studies have explored optimal WWR for various climates, they often prioritize energy efficiency over thermal comfort [24]. In this study, WWR is used as a design parameter to evaluate its impact on PPD and identify optimal solutions. As per the Bangladesh National Building Code (BNBC), in mechanically ventilated and air-conditioned buildings across all occupancy types, the allowable WWR must be determined in relation to the glazing performance, specifically the Solar Heat Gain Coefficient (SHGC) or Shading Coefficient (SC) of the installed glass. As the SHGC of the window used in the case building is 0.31, the range of WWR was set to 10% to 70% for the optimization study. Table IV shows the WWR parameters adjusted during the optimization process.

Table IV: Parameters Adjusted During Optimization Process

Window-Wall-Ratio (WWR)	Attributes
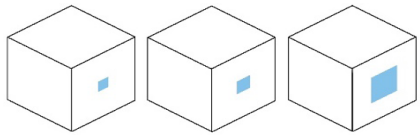 10% 20% 30%	10%-70%
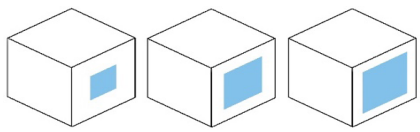 40% 60% 70%	

2.8 Optimization Process

The Galapagos plug-in in Grasshopper was employed for single-objective optimization, generating parameter combinations based on a defined fitness goal. It adjusts one or more genomes to either minimize or maximize a specific performance metric. In this study, the WWRs of individual rooms were used as genomes, with PPD serving as the fitness objective (Fig. 7). The optimization was configured with a maximum of 50 generations, a population size of 20, and an initial boost of 2x (equivalent to 40 individuals).

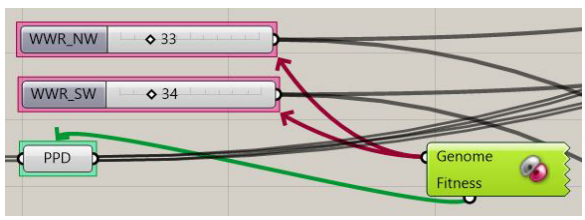

(a)

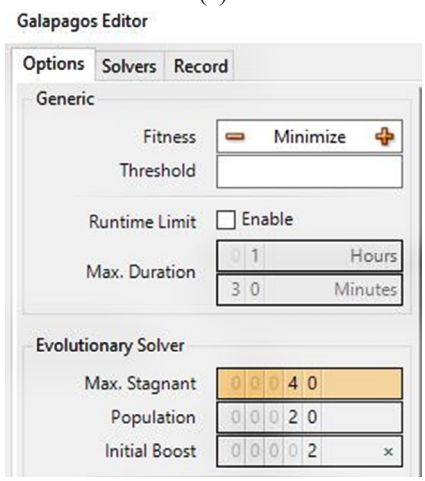

(b)

Fig. 7: (a) Galapagos Genomes and Fitness Objectives; (b) Optimization Settings in Galapagos Editor

3. RESULTS AND DISCUSSION

3.1 Field Measurement

From the field measurement data, it is identified that, case 2 (B4) has the highest average temperature, and case 1 (A4) has the lowest average temperature. However, case 4 (D4) exhibits both the highest maximum temperature and the lowest minimum temperature, indicating the most significant fluctuations in thermal conditions throughout the day among all the rooms studied (Table V).

Table V: Field Measurement Data of Temperature

Case Study (Flat no.)	Max	Min	Average
Case 1 (A4)	33.46	31.01	31.86
Case 2 (B4)	33.03	31.74	32.54
Case 3 (C4)	33.07	31.57	32.15
Case 4 (D4)	33.63	30.59	31.99

Figure 8 shows the 24-hour temperature data for each case study room, derived from field measurements. In nearly all cases, the maximum temperature is observed between 4:00 AM and 6:00 AM. After that, the temperature starts to rise, reaching the peak between 1:00 PM and 2:00 PM.

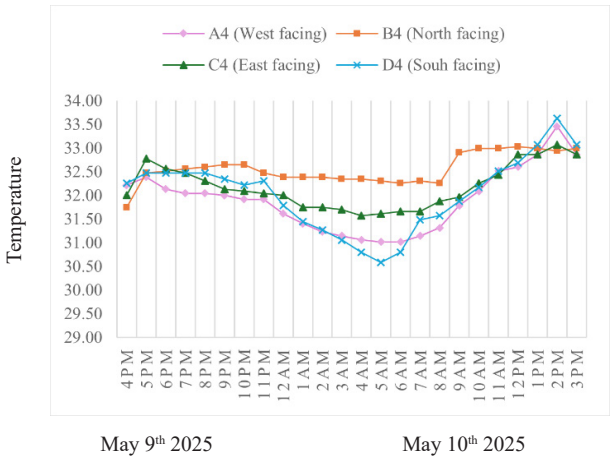

Fig. 8: Temperature data for 24 hours from Field Measurements.

3.2 Base Case Performance

The base case performance was evaluated by setting the WWR the same as the actual studied rooms for each unit of the case building and running the simulation with the EnergyPlus shoebox model. Table VI shows the simulation results of the PPD for the base case in all the different rooms on the same floor level. It is seen that case 2 (B4) has the highest level of PPD, indicating a higher percentage of dissatisfied occupants within that room. Again, case 4 has the lowest level of PPD, meaning better comfort conditions than the other three rooms. The results from the simulation study correlate with the field measurement data, indicating the validity of the simulation model. Table VI also indicates that the Mean Radiant Temperature (MRT) is lower in each optimized case compared to its respective base case, demonstrating improved thermal performance as a result of the optimization.

Table VI: Simulation Results of the PPD and MRT

Case Study	PPD	MRT
Case 1 (A4)	29.97%	27.47 °C
Case 2 (B4)	30.66%	27.53 °C
Case 3 (C4)	29.86%	27.47 °C
Case 4 (D4)	29.02%	27.53 °C

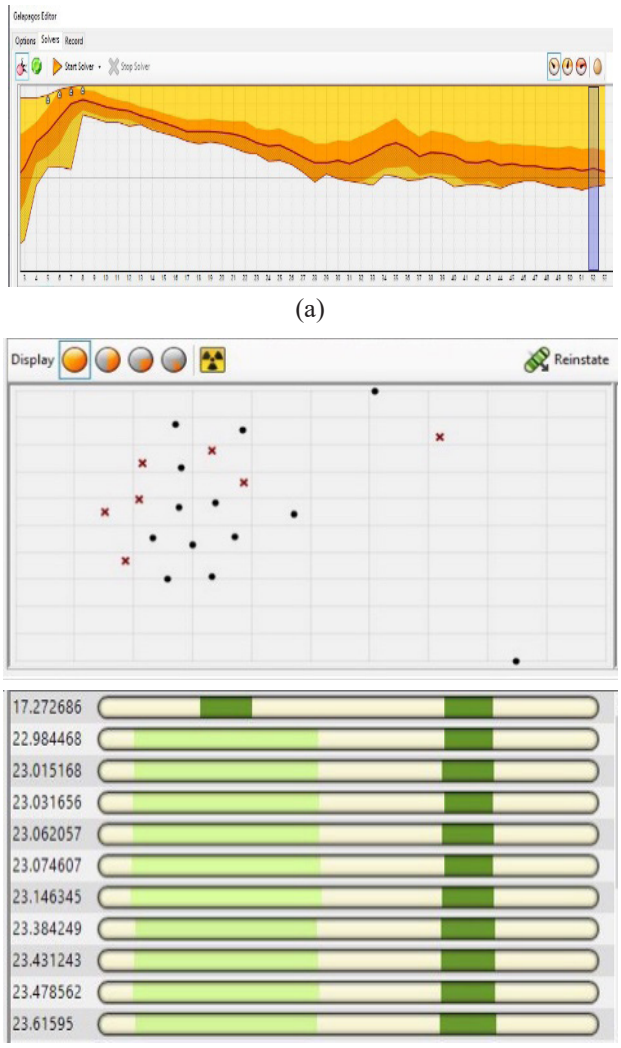

(a)

(b)

Fig. 9: (a) Galapagos Genomes and Fitness Objectives; (b) Optimization Settings in Galapagos Editor

3.3 Optimization Solution for the Case Studies

A single-objective optimization algorithm was utilized to parametrically analyze various combinations of WWR using the PPD as a measure of thermal comfort. The goal of this analysis was to identify design options that offer the best thermal performance by minimizing PPD. Figures 9(a) and 9(b) illustrate how the Galapagos optimizer progressively filters out less effective solutions over successive generations during the simulation process.

Furthermore, all simulation outputs generated by the Galapagos optimizer were exported in .xlsx format for post-processing and cross-checking the identified optimal solutions. A summary of the results, highlighting WWR, PPD, and thermal comfort improvements achieved through optimization, is presented in Table VII. The analysis revealed that a WWR between 69% and 70% consistently yielded the lowest PPD values across all orientations, indicating a notable reduction in thermal discomfort and enhanced indoor environmental quality. Specifically, the optimized PPD values for the case 1, 2, 3 and 4 were 19.75%, 21.07%, 17.27%, and 16.31%, respectively. Compared to the baseline models, these results represent substantial improvements of 10.22% (case 1), 9.59% (case 2), 12.59% (case 3), and 12.71% (case 4) in thermal comfort performance.

Table VII: Summary of the Major Findings

Case	Attributes	Base Model	Test Model
Case 1 (A4)	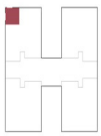 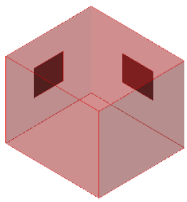 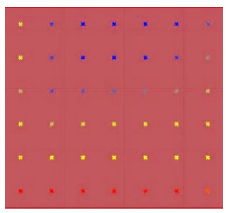 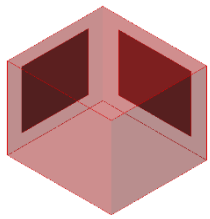 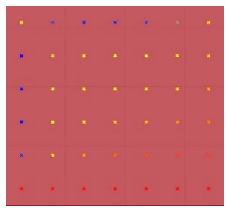		
	WWR	SW: 34%; NW: 33%	SW: 69%; NW: 70%
	MRT	27.47° C	26.36° C
	PPD	29.97%	19.75%
	Remarks	Improved 10.22%	
Case 2 (B4)	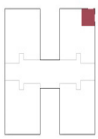 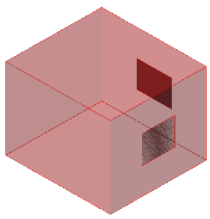 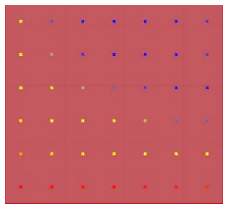 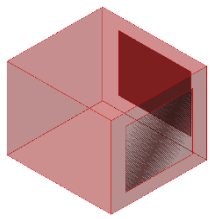 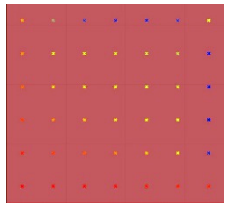		
	WWR	NW: 33%; NE: 34%	NW: 70%; NE: 69%
	MRT	27.53° C	26.49° C
	PPD	30.66%	21.07%
	Remarks	Improved 9.59%	
Case 3 (C4)	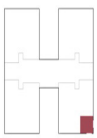 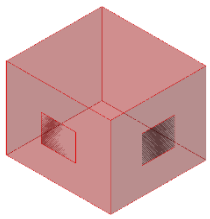 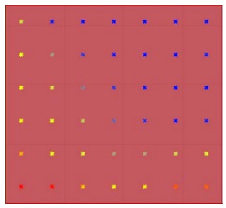 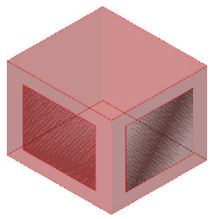 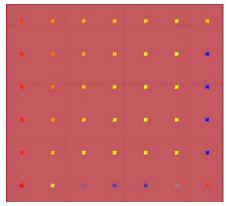		
	WWR	NE: 34%; SE: 33%	NE: 69%; SE: 70%
	MRT	27.47° C	26.12° C
	PPD	29.86%	17.27%
	Remarks	Improved 12.59%	

Case	Attributes	Base Model	Test Model
Case 4 (D4)		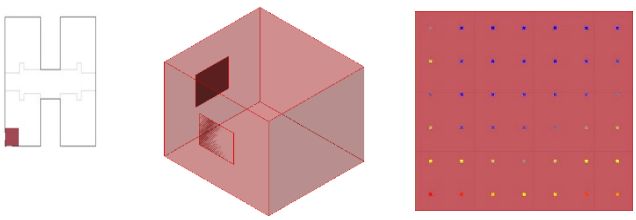	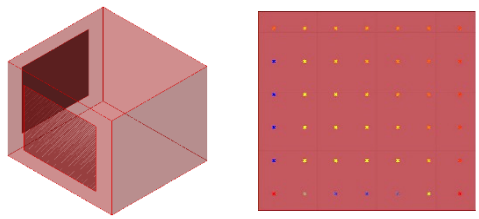
	WWR	SE: 33%; SW: 34%	SE: 70%; SW: 69%
	MRT	27.39° C	26.01° C
	PPD	29.02%	16.31%
	Remarks	Improved 12.71%	

However, it is essential to assess these results in the context of several factors critically. As illustrated in Table VII, among the four rooms oriented in different directions, the southeast-southwest facing corner room (D4) achieved the lowest PPD and the most significant improvement in thermal comfort. In contrast, the northeast-northwest facing corner room (B4) recorded the highest PPD and the least improvement, indicating orientation has a considerable impact on thermal performance outcomes. The improvements observed were more pronounced in the northeast-southeast (C4) and southeast-southwest facing rooms (D4), suggesting that WWR optimization is particularly effective in rooms that experience direct sunlight for extended periods. The northeast-northwest (B4) and northwest-southwest (A4) facing rooms, although showing improvement, exhibited less enhancement compared to the northeast-southeast (C4) and southeast-southwest (D4) orientations, indicating that the design variable had a relatively smaller influence on thermal comfort for these facades. Figure 10 presents a comparative analysis of the PPD values for all four rooms, alongside their corresponding baseline PPD figures.

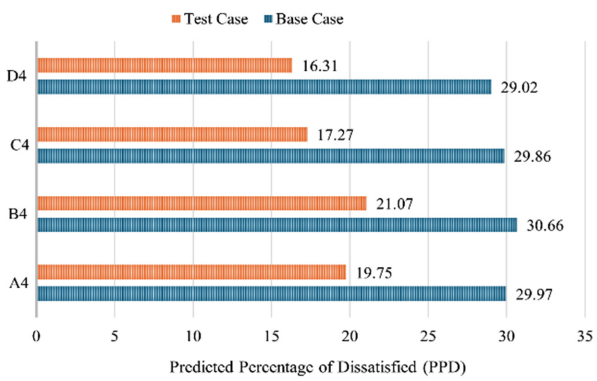

Fig. 10: Comparative Analysis of the Predicted Percentage of Dissatisfied (PPD)

Additionally, while the PPD improvements are notable, the achieved PPD values (ranging from 16.31% to 21.07%) remain above the commonly accepted comfort threshold of 10%. This indicates that while optimizing the WWR contributes to reduced thermal discomfort, it alone may not be sufficient to ensure optimal comfort. Further strategies such as incorporating shading devices or enhancing natural ventilation may be required, particularly for heat-sensitive occupants. Nonetheless, the observed reductions, ranging from 9% to 13%, represent a meaningful enhancement in occupant comfort achieved solely through adjustments to the window-to-wall ratio. It is essential to note that this study did not account for the effects of window placement or shading strategies, which could potentially influence thermal performance and should be explored in future research. Additionally, incorporating other building performance criteria, such as visual comfort and energy efficiency, alongside thermal performance, would provide a more comprehensive evaluation of design effectiveness.

4. CONCLUSION

This study demonstrates the potential of a parametric, single-objective optimization approach to enhance thermal comfort in residential buildings by optimizing the Window-to-Wall Ratio (WWR). Using the Predicted Percentage of Dissatisfied (PPD) as the primary performance metric and employing tools such as Rhinoceros 3D, EnergyPlus, and Galapagos, the research identified that a WWR between 69% and 70% consistently minimizes thermal discomfort across different room orientations. The optimized models showed notable improvements in PPD, ranging from 9% to 13%, compared to baseline scenarios, validating the effectiveness of the method despite PPD values remaining above the ASHRAE-recommended 10% threshold.

The findings underscore the importance of orientation-specific design strategies in warm-humid climates like Dhaka. However, the study acknowledges limitations, particularly the exclusion of window placement and shading strategies. Future research should integrate these factors and extend the optimization to include multi-objective criteria, such as energy efficiency and visual comfort, to support more holistic building performance improvements.

REFERENCES

[1] M. M. Rahman, M. S. Hassan, K. M. Bahauddin, A. K. Ratul and M. A. H. Bhuiyan, "Exploring the Impact of Rural–urban Migration on Urban Land Use and Land Cover: A Case of Dhaka City, Bangladesh," Migration and Development, Vol. 7, No. 2, pp. 222-239, 2018.

[2] K. Ahmed, "Socioeconomic Status and Housing Constraints of Middle-Income Individuals in Rayerbazar, Dhaka: Investigating Effective Multi-Ownership Housing Solutions to Counter Recent Economic Inflation," South East University Journal of Architecture, Vol. 3, No. 2, pp. 49-55, 2023.

[3] Y. Yang, X. Zhang, X. Lu, J. Hu, X. Pan, Q. Zhu and W. Su, "Effects of Building Design Elements on Residential Thermal Environment," Sustainability, Vol. 10, No. 1, pp. 57, 2017.

[4] S. S. Sinthia, "Comparative Analysis of Thermal Comfort in Residential Buildings: A Study of the Impact of Urban Density, Height, and Layout Patterns in The Context of Dhaka," International Journal of Research and Scientific Innovation, pp. 1141-1160, 2024.

[5] N. Aqilah, H. B. Rijal and S. A. Zaki, "A Review of Thermal Comfort in Residential Buildings: Comfort Threads and Energy Saving Potential," Energies, Vol. 15, No. 23, pp. 9012, 2022.

[6] N. Shahriar, "Effects of UHI and increased use of air conditioners in Dhaka," Daily Observer, Apr. 21, 2025.

[7] N. Ruck, Ø. Aschehoug, S. Aydinli, J. Christoffersen, G. Courret, I. Edmonds, R. Jakobiak, M. Kischkoweit-Lopin, M. Klinger, E. Lee, L. Michel, J. Scartezzini, and S. Selkowitz, "Daylight in Buildings: A Source Book on Daylighting Systems and Components," Lawrence Berkeley National Laboratory, California, 2000.

[8] M. M. Adeli, F. Sarhaddi and S. Farahat, "Parametric Study of the Impact of Windows to Wall Ratio on Reduction of Energy Consumption and Environmental Impact of a Zero-Energy Building in Different Orientations," Journal of Computational Applied Mechanics, Vol. 50, No. 2, pp. 295-302, 2019.

[9] H. Tawfeeq and A. M. A. Qaradaghi, "Optimizing Window-to-Wall Ratio for Enhanced Energy Efficiency and Building Intelligence in Hot Summer Mediterranean Climates," Sustainability, Vol. 16, No. 17, pp. 7342, 2024.

[10] S. Bagheri, H. Moradinasab, and M. Yeganeh, "The effect of window proportions in low-rise residential buildings on annual energy consumption in humid temperate climate (case study: Rasht city in Iran)," Frontiers in Energy Research, Vol. 12, pp. 1463678, 2024.

[11] B. Markus, "Simulation of Window-to-Wall Ratio for Thermal Comfort of Fully-Enclosed Courtyard Residential Buildings in Kafanchan," Environmental Technology and Science Journal, Vol. 13, No. 2, pp. 60-66, 2022.

[12] J. Li, B. Zheng, K. B., Bedra, Z. Li, and X. Chen, "Evaluating the effect of window-to-wall ratios on cooling-energy demand on a typical summer day," International Journal of Environmental Research and Public Health, Vol. 18, No. 16, pp. 8411, 2021.

[13] S. Sayadi, A. Hayati, and M. Salmanzadeh, "Optimization of window-to-wall ratio for buildings located in different climates: An IDA-indoor climate and energy simulation study," Energies, Vol. 14, No. 7, pp. 1974, 2021.

[14] J. L. Hensen, and R. Lamberts, "Building Performance Simulation for Design and Operation,"1st ed., Routledge, United Kingdom, 2019.

[15] L. Zhu, B. Wang, and Y. Sun, "Multi-Objective Optimization for Energy Consumption, Daylighting and Thermal Comfort Performance of Rural Tourism Buildings in North China," Building and Environment, Vol. 176, pp. 106841, 2020.

[16] G. Feng, D. Chi, X. Xu, B. Dou, Y. Sun, and Y. Fu, "Study on the Influence of Window-wall Ratio on the Energy Consumption of Nearly Zero Energy Buildings," Procedia Engineering, Vol. 205, pp. 730-737, 2017.

[17] Z. F. Ali, "Comfort with courtyards in Dhaka apartments," BRAC University Journal, Vol. 4, No. 2, pp. 1-6, 2007.

[18] S. H. Tariq, and Z. N. Ahmed, "Effect of Plan Layout on Electricity Consumption to Maintain Thermal Comfort in Apartments of Dhaka," Energy Efficiency, Vol. 13, No. 6, pp. 1119-1133, 2020.

[19] I. Z. H. Mou, "Study on the Impact of Window Size and Proportion on Indoor Air Temperature of Bedrooms in Apartments," M. Arch Thesis, Dept. of Arch., BUET, Dhaka, 2017.

[20] F. Ahmed and S. M. H. Rahman, "Evaluation of thermal comfort in residential buildings: A Case Study of Wari, Dhaka," International Journal of Science and Research Archive, Vol. 13, No. 02, pp. 3213-3222, 2024.

[21] S. Uprety, S. Kafley, and B. Shrestha, (2021). "Window to wall ratio and orientation effects on thermal performance of residential building: A case of Butwal Sub-Metropolis," Journal of Engineering Issues and Solutions, Vol. 1, No. 1, pp. 129-137, 2021.

[22] A. Barman, M. Roy, and A. Dasgupta, "Thermal Requirements of a Residential Apartment Building Through Natural Ventilation in the Warm and Humid Climate of Guwahati," International Journal of Engineering Research & Technology (IJERT), Vol. 9, pp. 1356-1363, 2025.

[23] S. Pathirana, A. Rodrigo, and R. Halwatura, "Effect of building shape, orientation, window to wall ratios and zones on energy efficiency and thermal comfort of naturally ventilated houses in tropical climate," International Journal of Energy and Environmental Engineering, Vol. 10, No. 1, pp. 107-120, 2019.

[24] K. Lakhdari, L. Sriti, and B. Painter, "Parametric Optimization of Daylight, Thermal and Energy Performance of Middle School Classrooms, Case of Hot and Dry Regions," Building and Environment, Vol. 204, pp. 108173, 2021.

[25] Thermal Environmental Conditions for Human Occupancy, A.N.S.I. ASHRAE, Standard 55-2010, American Society of Heating, Refrigerating and Air Conditioning Engineers, Atlanta, USA, 2010.

[26] V. Machairas, A. Tsangrassoulis, and K. Axarli, "Algorithms for Optimization of Building Design: A Review," Renewable and Sustainable Energy Reviews, Vol. 31, pp. 101-112, 2014.

[27] Y. Fang, "Optimization of daylighting and energy performance using parametric design, simulation modeling, and genetic algorithms," PhD Dissertation, North Carolina State University, Raleigh, North Carolina, 2017.

[28] M. Qingsong, and H. Fukuda, "Parametric office building for daylight and energy analysis in the early design stages," Procedia-Social Behavioral Sciences, Vol. 216, pp. 818-828, 2016.

[29] A. R. Amaral, E. Rodrigues, A.R. Gaspar, and A. Gomes, "A Thermal Performance Parametric Study of Window Type, Orientation, Size and Shadowing Effect," Sustainable Cities and Societies, Vol. 26, pp. 456–465, 2016.

[30] J.W. Lee, H.J. Jung, J.Y. Park, J.B. Lee, and Y. Yoon, "Optimization of building window system in Asian regions by analyzing solar heat gain and daylighting elements," Renewable Energy, Vol. 50, pp. 522–531, 2013.

Green-Synthesized Silver Nanoparticles as a Sustainable Seed Priming Agent for Improved Rice Cultivation

Md. Rashedul Islam*, Sourav Kumar Biswas and Jakia Mustary

Department of Electrical and Electronic Engineering, Dhaka University of Engineering & Technology, Gazipur, Bangladesh

ABSTRACT

This research investigates the effects of silver nanoparticle (AgNP) priming, achieved through both green and chemical synthesis, on the germination and early growth of rice seeds in Bangladesh. Green AgNPs, synthesized using neem extract, showed smaller particle sizes (21.19 nm) and better performance than chemically synthesized AgNPs (27.238 nm). Seeds primed with AgNPs (1–200 mg/L) exhibited enhanced root and shoot growth, with optimal results at 70–160 mg/L. Germination remained high (95–100%) in both treatments, indicating low toxicity. The improved efficacy of green AgNPs is attributed to the presence of neem's bioactive phytochemicals, which also contribute to their environmentally benign synthesis, avoiding hazardous chemicals and minimizing ecological impact. Findings suggest nanopriming as a cost-effective, scalable technique for improving rice productivity. Further field validation and safety assessments are recommended to support their integration into eco-friendly agricultural practices.

1. INTRODUCTION

Rice (*Oryza sativa* L.) is a vital food crop for over half the global population and remains the cornerstone of food and economic security in Bangladesh. However, productivity continues to be challenged by multiple abiotic and biotic stresses, including drought, poor seed vigor, and climate variability. Early seedling establishment, particularly germination success, is crucial for achieving optimal plant density and yield potential in the field.

Seed priming is a proven pre-sowing strategy to improve germination and seedling vigor by modulating metabolic and physiological processes. Nanopriming using nanoparticles (NPs) in priming solutions has emerged as a powerful enhancement of traditional priming, improving water absorption, enzymatic activation, and redox balance [1], while reducing microbial contamination risks [2], [3], [4]. Among various NPs, silver nanoparticles (AgNPs) are particularly promising due to their unique physicochemical and antimicrobial properties, which positively influence germination and early growth [5], [6].

Chemically synthesized AgNPs, such as those produced via sodium borohydride reduction, are effective but may raise cytotoxicity and environmental safety concerns [7], [8]. In contrast, green synthesis using plant extracts offers an eco-friendly, biocompatible approach, leveraging natural reducing and stabilizing agents such as polyphenols and flavonoids [9], [10]. *Azadirachta indica* (neem) is frequently used in green synthesis due to its phytochemical richness and widespread availability [10].

Although increasing interest in AgNPs for agricultural use, comparative studies on green versus chemically synthesized AgNPs in rice seed priming especially for high-yielding Bangladeshi cultivars are still scarce. This study addresses that gap by assessing the effects of both synthesis methods on rice seed germination and early seedling growth, promoting a safer and more sustainable nanotechnology-based approach to rice production in Bangladesh.

2. METHODOLOGY

2.1 Synthesis of Silver Nanoparticles (AgNPs)

AgNPs were synthesized via two different methods: a plant-mediated green approach and a conventional chemical route.

2.1.1 Green Synthesis of AgNPs

Azadirachta indica (neem) was selected for the preparation of green-synthesized AgNPs, due to its high phytochemical content of flavonoids, terpenoids, and alkaloids, which act as both reducing and stabilizing agents. These compounds not only reduce silver ions to form nanoparticles but also provide a dual stabilization mechanism, both electrostatic

*Corresponding author's email: mrislam@duet.ac.bd

and steric, that helps keep the nanoparticles dispersed and prevents their agglomeration.

The green synthesis process is illustrated in Fig. 1, where fresh leaves of neem were rinsed thoroughly with distilled water and air-dried. A total of 25 grams of leaves were boiled in 100 mL of deionized water for 15 minutes to extract bioactive compounds. After filtration, this extract served as a natural reducing and capping agent. It was added dropwise to a 1 mM aqueous solution of silver nitrate ($AgNO_3$) under continuous stirring at ambient temperature. The progression of the reaction was visually confirmed by a color transition from pale yellow to brown, indicating AgNP formation.

(a) (b) (c) (d)

Fig. 1: (a) $AgNO_3$ Solution (b) Adding Neem Extract to the $AgNO_3$ Solution Drop Wise. (c) AgNP Solution after 1 Hour of Stirring (d) AgNP Solution after 24 Hours of Cold Storage

2.1.2 Chemical Synthesis of AgNPs

In chemical synthesis, Trisodium citrate was initially tested as a reducing agent but failed to produce stable AgNPs, causing aggregation. Sodium borohydride ($NaBH_4$) was then chosen for its high reduction efficiency, producing small, uniform, and stable nanoparticles.

The chemical synthesis process is illustrated in Fig. 2, where a 1 mM $AgNO_3$ solution was prepared and trisodium citrate ($Na_3C_6H_5O_7$) solution was added to the silver nitrate ($AgNO_3$) solution. The $NaBH_4$ solution was then slowly added dropwise to the $AgNO_3$ solution, where the solution was initially clear. After 1 mL of $NaBH_4$ was added, the solution was observed to turn pale yellow, indicating the formation of AgNPs. Finally, after 3 mL of $NaBH_4$ was added, the solution turned dark brown, confirming the complete reduction of silver ions to metallic silver and the formation of stable nanoparticles. Trisodium citrate was used as a stabilizing agent in the chemical route to prevent particle agglomeration [8].

After the synthesis procedure, centrifugation was performed to separate nanoparticles from the liquid phase shown Fig. 1(d) & Fig. 2(d). The nanoparticles were then transferred to a petri dish displayed Fig. 3 (a) and air-dried. Once dried, AgNPs from both green and chemical synthesis were obtained in powder form, as shown in Fig. 3. The green-synthesized AgNPs of Fig. 3(b) are finer and more uniform due to neem-based stabilization, while the chemically synthesized AgNPs of Fig. 3(c) show more aggregation, highlighting the superior stability of the green-synthesized nanoparticles. Due to the unclear nature of these figures, higher-magnification FE-SEM images are provided later for a clearer illustration of the physical properties and differences between the two types of nanoparticles.

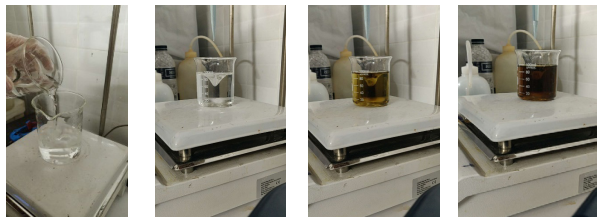

(a) (b) (c) (d)

Fig. 2: (a) Adding $Na_3C_6H_5O_7$ Solution to $AgNO_3$ Solution (b) Before Adding $NaBH_4$ (c) Forming AgNP as Turned Pale Yellow after adding 1ml of $NaBH_4$ (d) AgNP Solution Turned into Dark Brown after Adding 3ml of $NaBH_4$

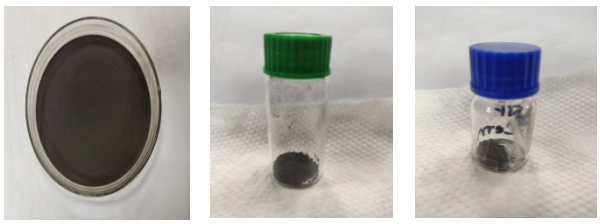

(a) (b) (c)

Fig. 3: (a) AgNPs after Drying (b) Green Synthesized AgNP Powder form (c) Chemical Synthesized AgNP Powder form

2.2 Materials and Reagents

In this study, a variety of chemical reagents, biological materials, and seeds were employed to synthesize and evaluate AgNPs and their effects on rice seed priming. Table 1 provides a comprehensive overview of the raw materials used, including their chemical names.

2.3 Characterization of AgNPs

Optical characteristics and the presence of surface plasmon resonance were analyzed through UV–Visible spectrophotometry. Additionally, Field Emission Scanning Electron Microscopy (FE-SEM) was utilized to evaluate the morphology and estimate particle size distribution. Fourier Transform Infrared Spectroscopy (FTIR) analysis was used to identify the functional groups involved in the reduction and stabilization of AgNPs, confirming the presence of biomolecules or capping agents on their surface.

Table I: Materials and Reagents

Material	CAS Number	Supplier	Country
Azadirachta indica (neem) leaves	-	Local Source	Bangladesh
Silver Nitrate ($AgNO_3$)	7761-88-8	Sigma-Aldrich	USA
Sodium Borohydride ($NaBH_4$)	16940-66-2	Sigma-Aldrich	USA
Trisodium Citrate ($Na_3C_6H_5O_7$)	6132-04-3	Sigma-Aldrich	USA
Deionized Water (DI Water)	-	Labtex	Bangladesh
BRRI-88 Rice Seeds	-	BRRI	Bangladesh

2.4 Seed Priming Procedure

BRRI-88 rice seeds (certified) were used for the study. Various concentrations of AgNPs, ranging from 1 to 200 mg/L, were prepared by diluting the synthesized particles in deionized water. Every 30 rice seeds were soaked in these AgNP solutions for 12 hours, as shown in Fig. 4, at ambient temperature with mild agitation to ensure even treatment. The control treatment consisted of water-only hydropriming, where an equivalent number of seeds were soaked in deionized water for the same duration. After soaking, the seeds were dried under aseptic conditions on Whatman No. 1 filter paper, which has a pore size of 11 µm, and stored in paper bags at room temperature until further use.

Fig. 4: Rice Seed Priming using Different Concentrations of AgNPs and Control Treatments

2.5 Germination Bioassay

After soaking the AgNP-primed seeds, they were transferred into sterile Petri dishes lined with two layers of Whatman No. 1 filter paper (pore size 11 µm), which were moistened with approximately 15–20 mL of normal water so that the seeds were submerged under the water to maintain proper moisture for seed germination. Each dish received thirty seeds, and all treatments were replicated three times. The dishes were incubated in a controlled growth chamber at 25 ± 1°C under a 16-hour light and 8-hour dark photoperiod. Germination was recorded daily for a period of seven days, with seeds considered germinated when the radicle extended at least 2 mm, is illustrated in Fig. 5.

On the final day, both root and shoot lengths were measured from scanned image of Fig. 5(b) captured by microscope using ImageJ software which is shown in Fig. 5(d). To measure the root and shoot length, a scale reference is required, which was also captured at the same height as the seed images using a microscope as shown in Fig. 5(c). Germination rates were calculated, and seedling vigor indices were computed using standard equations based on shoot and root measurements. Statistical analysis was performed to identify significant treatment effects.

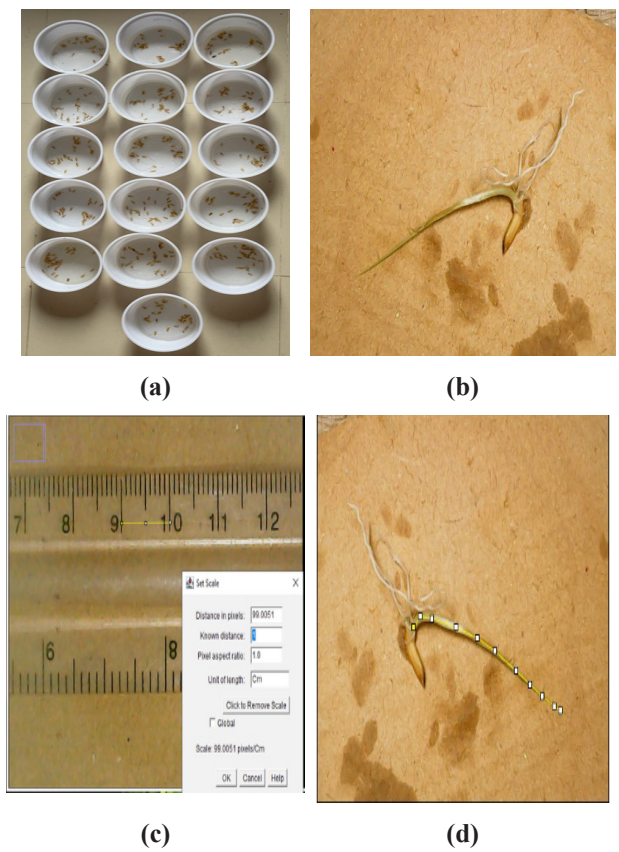

Fig. 5: (a) Performing Germination in Normal Water; (b) Images Captured by a Microscope for Measuring Root and Shoot Lengths ; (c) Scale set-up in Image J (d) Root-Shoot Length Measuring using Image J Software

3. LITERATURE SURVEY

3.1 Rice Production and Climate Stress in Bangladesh

Rice cultivation is the backbone of Bangladesh's agriculture. The widespread adoption of high-yielding modern rice varieties has contributed significantly to national food security [1]. However, the sector faces increasing threats from climate change, including rising temperatures, water scarcity, and erratic weather patterns [3]. These factors, especially during the dry Boro season, result in elevated irrigation demands and reduced productivity [3].

3.2 Nanoparticle Synthesis Approaches

Nanoparticles can be synthesized via top-down or bottom-up methods. The top-down approach (e.g., milling, etching, ablation) breaks bulk materials into nanoparticles but often involves high energy use and toxic byproducts. In contrast, bottom-up methods (e.g., precipitation, sol-gel, pyrolysis) assemble particles atom-by-atom, offering better control over size and morphology, though some processes still involve hazardous chemicals.

The green synthesis approach used in this research follows the bottom-up method shown in Fig. 6. Specifically, it employs biological agents like plant extracts (in this case, *Azadirachta indica*, or neem) to reduce metal ions and form nanoparticles. This method is eco-friendly, non-toxic, and cost-effective, making it highly suitable for sustainable agricultural practices, such as seed priming[11].

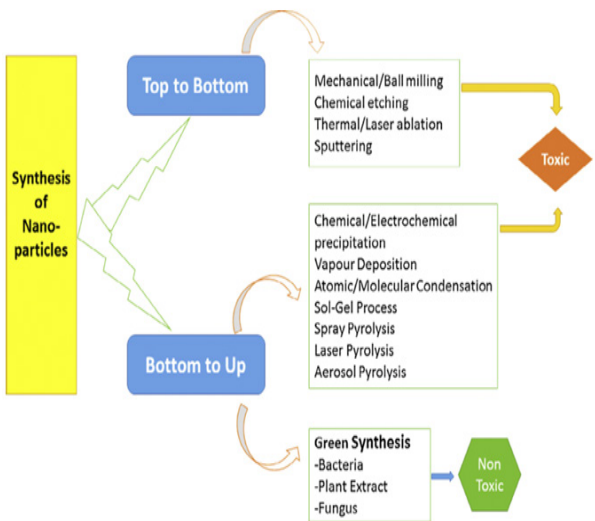

Fig. 6: Different Approaches to the Synthesis of Silver Nanoparticles [11]

3.3 Effect of AgNP Priming on Germination and Root Shoot Growth

Seed priming is a pre-sowing method that activates metabolic processes through controlled hydration, improving seed vigor and stress tolerance. Hydropriming and osmopriming are common in rice and enhance germination, seedling growth, and biochemical activity [1], [12]. However, their effectiveness can be inconsistent under stress. Nano-priming, using nanoparticles like AgNPs and ZnO, offers a more efficient alternative by improving water uptake, enzyme activation, and antioxidant responses [1], [3], [5], [13]. This technique shows great potential for enhancing rice performance under challenging environmental conditions.

Many studies on seed priming, such as those by W. Mahakham [14], have recorded germination over a period of six days and it is shown in Fig. 7. In contrast, the present study monitored germination daily for seven days, as this duration provided sufficient time for seedling development and vigor assessment. While previous studies have attempted seed priming in rice, our research distinguishes itself by comparing green-synthesized AgNPs with chemically synthesized AgNPs in rice seed priming. This comparison, particularly using *Azadirachta indica* (neem) as the source for green synthesis, has not been fully explored in agricultural practices for rice. Our research identifies a specific AgNP concentration range, that optimally promotes root and shoot length in rice seedlings.

While previous studies have attempted seed priming in rice, our research distinguishes itself by comparing green-synthesized AgNPs with chemically synthesized AgNPs in rice seed priming. This comparison, particularly using *Azadirachta indica* (neem) as the source for green synthesis, has not been fully explored in agricultural practices for rice. Our research identifies a specific AgNP concentration range, that optimally promotes root and shoot length in rice seedlings.

3.4 Prospects and Challenges

Green synthesis methods, such as using *Azadirachta indica*, provide safer, eco-friendly alternatives to chemical routes [9], [10]. However, challenges persist, including nanoparticle toxicity, inconsistent results due to variable NP size and concentration, and limited understanding of long-term environmental effects [2], [7], [8]. In addition, future studies could explore multiple rice varieties to compare the effects of AgNP priming across different cultivars.

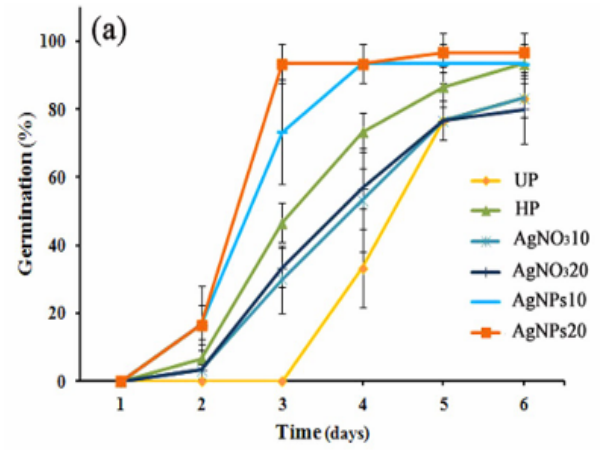

Fig. 7: (a) Germination Rate of Rice Seeds after Priming with Different Priming Agents and Phenotype of Rice Seedlings after 6-Day Germination (B) Data are Presented as Means of three Replicates Containing 10 Seeds Each ± Standard Error of Means [13]

4. RESULTS AND DISCUSSIONS

4.1 Functional Group Analysis Using FTIR

FTIR analysis revealed distinct functional groups responsible for nanoparticle synthesis and stabilization. The FTIR spectrum of green-synthesized AgNPs shows a strong peak between 3430–3600 cm^{-1} for O–H stretching (alcohols and phenols), a weaker peak at 1595 cm^{-1} for N–H stretching (aromatic secondary amines), and a faint band near 1450 cm^{-1} for C=O stretching (likely from flavonoids, aiding stabilization) shown in Fig. 8.

In contrast, the FTIR spectrum of chemically synthesized AgNPs shows a sharp band at 1585 cm^{-1}, indicating C–C aromatic stretching and N–H bending (primary amines) [15]. This suggests less effective interaction between sodium citrate and Ag^{+} ions, possibly due to changes in citrate's structure during or after nanoparticle formation [8].

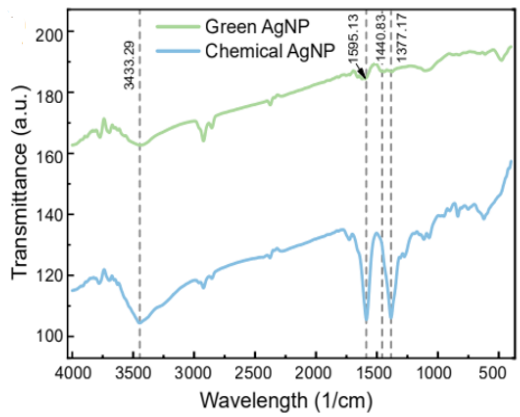

Fig. 8: FT-IR Transmittance Spectra of Green Synthesized AgNP & Chemically Synthesized AgNP

4.2 Optical Properties of AgNPs

UV-Visible spectroscopy was employed to investigate the optical behavior of AgNPs.

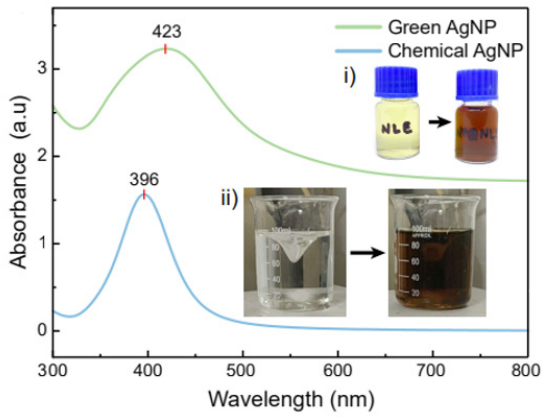

Fig. 9: UV-Vis Absorption Spectra of Green Synthesized AgNP & Chemically Synthesized AgNP

AgNPs were synthesized using both green (neem extract) and chemical (silver nitrate and sodium citrate) methods. The resulting solution underwent a color change from clear to dark brown, indicating successful nanoparticle formation Tests using UV-Vis spectroscopy confirmed that nanoparticles were successfully created in both methods. The green method showed a peak at 423 nm, and the chemical method showed a peak at 396 nm both peaks are signs that the AgNPs formed correctly shown in Fig. 9. Since there were no extra peaks, it also means there were no unwanted substances in the mixtures. However, the peak for the green method was broader, suggesting that the particles were of different sizes. This is likely because the Neem extract has various natural chemicals and the reaction conditions weren't as controlled.

4.3 Particle Morphology (FE-SEM)

Field Emission Scanning Electron Microscopy (FE-SEM) highlighted clear morphological variations between the two synthesis approaches.

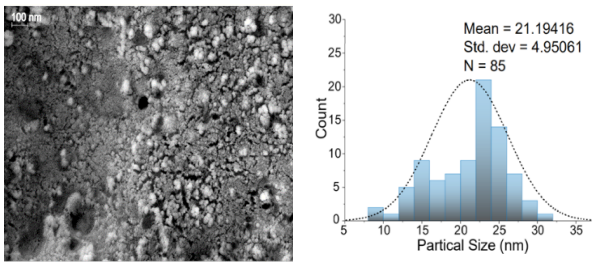

Fig. 10: (a) FE-SEM Image of Green Synthesized AgNPs and (b) Particle Size Distribution for Green Synthesized AgNPs

Fig. 10 represents the Field Emission Scanning Electron Microscopy (FE-SEM) images of AgNPs synthesized through a green method. The analysis reveals that the particles display a diverse array of shapes and are irregularly distributed on the substrate. Measurements taken from 85 individual nanoparticles indicate an average size of 21.19 nm, with a standard deviation of 4.95 nm, emphasizing the structural heterogeneity among the particles.

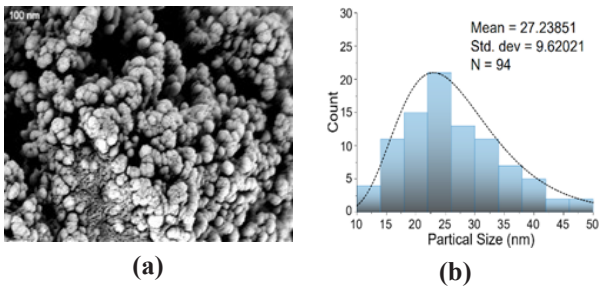

Fig. 11: (a) FE-SEM Image of Chemically Synthesized AgNPs and (b) Particle Size Distribution for Chemically Synthesized AgNPs

In contrast, Fig. 11 shows the FE-SEM images of AgNPs produced via chemical synthesis. This sample comprises a mix of both small and large particles, with an average size of 27.238 nm and a standard deviation of 9.62 nm, based on measurements of 94 nanoparticles. The chemically synthesized particles exhibit a tendency to form agglomerates, resulting in clusters that incorporate a range of particle sizes.

4.4 Effect of AgNPs on Seed Germination Rate

Although the germination percentage was measured for both AgNPs-primed and hydroprimed seeds, no significant difference was observed between the two treatments. Both AgNPs priming and hydropriming resulted in nearly identical germination rates of 95-100%, indicating that AgNPs priming does not negatively affect seed viability or germination.

4.5 Root and Shoot Growth Enhancement

Notable improvement in seedling root and shoot development was recorded following AgNP priming.

4.5.1 Effect of AgNPs on Root Length

The root length response to green-synthesized AgNPs showed variability across three experimental sets that represents in Fig. 12(a), with optimal growth at 130 mg/L in Set 1, 160 mg/L in Set 2, and 70 mg/L in Set 3. Despite these inconsistencies, the concentration range of 70–160 mg/L generally promoted better root growth, suggesting its potential for effective priming.

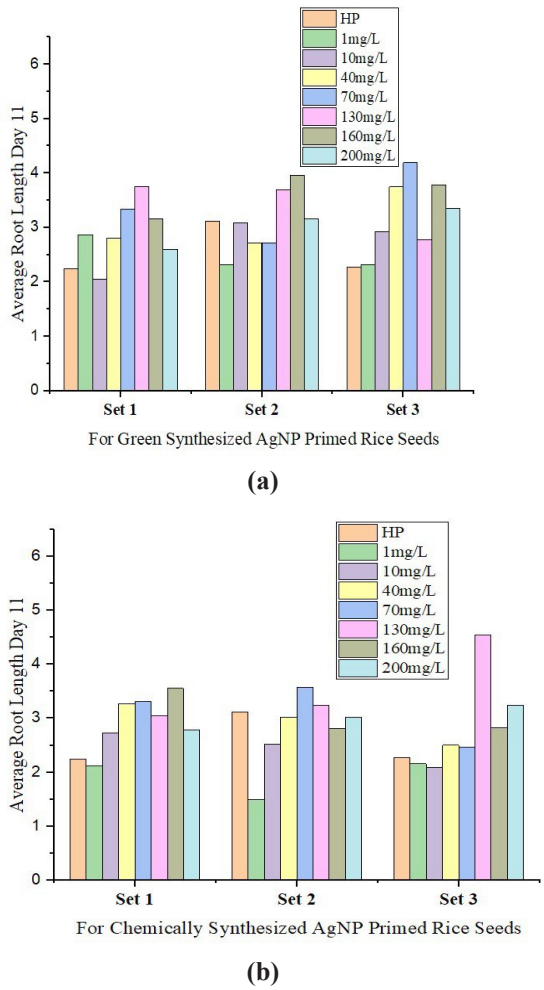

Fig. 12: (a) Impact of Green Synthesized AgNPs and (b) Chemically Synthesized AgNPs on the Root Length (in cm) of Rice Seeds

The results in Fig. 12(b) show that the effect of chemically synthesized AgNPs on root length varies across experimental sets, with Set 1 showing optimal growth at 160 mg/L, Set 2 at 70 mg/L, and Set 3 at 130 mg/L. This inconsistency suggests that the root length response to AgNPs is not dose-dependent or linear. Despite this, the concentration range of 70–160 mg/L appears most effective for promoting root growth. Based on the average results in Fig. 13, chemically synthesized AgNPs showed the highest root length at 130 mg/L, while green synthesized AgNPs reached optimal growth at 70 mg/L. Despite the differences in peak concentrations, both types of AgNPs were most effective within the 70–160 mg/L range, compared to other concentrations. The shoot length response to green synthesized AgNPs in Fig. 14(a) showed no consistent pattern across sets, with optimal concentrations of 130 mg/L, 160 mg/L, and 70 mg/L in Set 1, Set 2, and Set 3, respectively.

4.5.2 Effect of AgNPs on Shoot Length

Despite these variations, the 70–160 mg/L range generally yielded the best results, suggesting it is effective for enhancing shoot growth, though the optimal concentration varies between sets. The shoot length response to chemically synthesized AgNPs in Fig. 14(b) showed no consistent pattern across sets, with peak growth at 130 mg/L in Set 1 and Set 3, and at 200 mg/L in Set 2. However, the optimal shoot length generally fell within the 130–200 mg/L range, indicating this concentration range is most effective for promoting shoot growth.

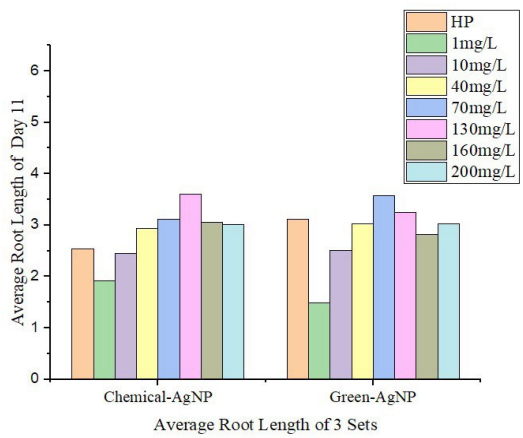

Fig. 13: Impact of Green-synthesized and Chemical- Synthesized AgNPs on the Average Root Length (in cm) of Rice Seeds

In Fig. 15, both chemically synthesized and green synthesized s AgNPs promoted optimal shoot elongation within the 70–200 mg/L range. Chemically synthesized AgNPs showed peak growth at 130 mg/L (130–200 mg/L range), while green synthesized AgNPs were most effective at 160 mg/L (70–160 mg/L range). These results suggest that the 70–200 mg/L range is optimal for enhancing shoot length while minimizing toxicity.

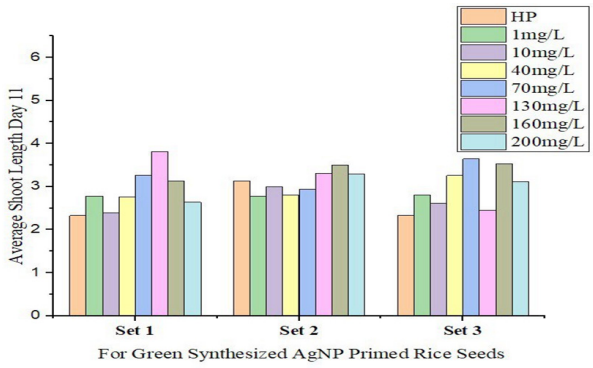

(a)

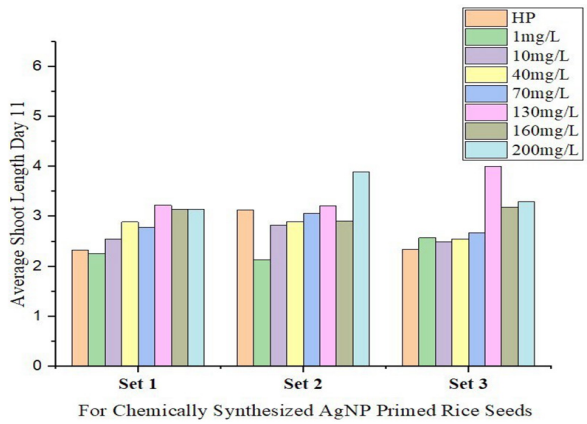

(b)

Fig. 14: (a) Impact of Green Synthesized AgNPs and (b) Chemically Synthesized AgNPs on the Shoot Length (in cm) of Rice Seeds

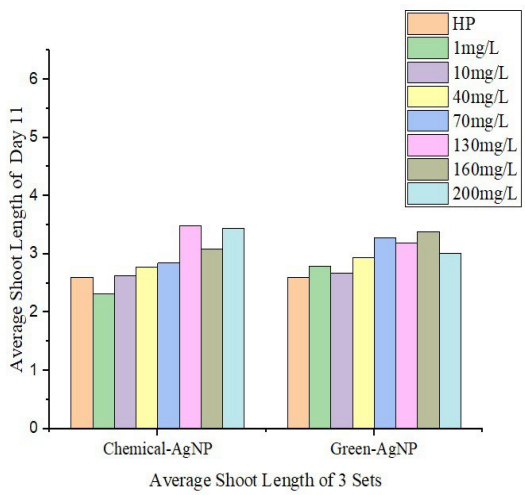

Fig.15: Impact of Green-Synthesized and Chemical-Synthesized AgNPs on the Average Shoot Length (in cm) of Rice Seeds

However, significant differences in the enhancement of root and shoot length were observed between hydropriming and AgNP priming, indicating that AgNP priming had a noticeable impact on seedling growth during the early stages.

5. CONCLUSION

This study demonstrates that both hydropriming and silver nanoparticle (AgNP) treatments significantly enhance rice paddy early seedling development under controlled conditions. Both hydroprimed and AgNP-primed seeds exhibited germination rates of 95-100%, confirming that AgNP priming does not compromise seed viability. AgNP treatments, whether chemically or green synthesized notably improved root and shoot growth. Although the response to AgNP concentration varied across experimental sets, both types showed optimal performance within specific ranges. For root development, the effective concentration window was 70–160 mg/L, while shoot elongation was maximized within 70–200 mg/L. Therefore, based on the range observed for both root and shoot growth, the optimal concentration of AgNPs for maximizing overall seedling growth performance is within the 70–160 mg/L range. These findings indicate that AgNPs, when applied within the appropriate dosage range, can act as potent biostimulants to enhance seedling vigor. However, due to the inconsistent trends across sets, further investigation is needed to elucidate the mechanisms of action and to standardize application protocols for agricultural use.

ACKNOWLEDGEMENT

The authors would like to acknowledge and appreciate UGC and DUET for the contribution of the research grant. The authors would like to thank all individuals who provided support during this research and recognize the assistance of AI tools for writing.

REFERENCES

[1] S. H. Nile et al., "Nano-priming as emerging seed priming technology for sustainable agriculture—recent developments and future perspectives," Journal of Nanobiotechnology 2022 20:1, Vol. 20, No. 1, pp. 1–31, 2022.

[2] R. Javed, M. A. Ahmad, A. Gul, T. Ahsan, and M. Cheema, "Comparison of chemically and biologically synthesized nanoparticles for the production of secondary metabolites, and growth and development of plants," Comprehensive Analytical Chemistry, Vol. 94, pp. 303–329, 2021.

[3] B. Kumar et al., "Nanopriming in sustainable agriculture: recent advances, emerging challenges and future prospective," New and Future Developments in Microbial Biotechnology and Bioengineering: Sustainable Agriculture: Revisiting Green Chemicals, pp. 339–365, 2022.

[4] A. Anandaradje, V. Meyappan, I. Kumar, and N. Sakthivel, "Microbial Synthesis of Silver Nanoparticles and Their Biological Potential," Nanoparticles in Medicine, pp. 99–133, 2020.

[5] S. Khan, M. Zahoor, R. Sher Khan, M. Ikram, and N. U. Islam, "The impact of silver nanoparticles on the growth of plants: The agriculture applications," Heliyon, Vol. 9, No. 6, p. e16928, 2023.

[6] R. Pal et al., "Silver Nanoparticles; Synthesis Characterization Optical properties and Therapeutic Applications," European Chemical Bulletin, Vo. 12, Issue 1, 2023.

[7] S. Iravani, H. Korbekandi, S. V. Mirmohammadi, and B. Zolfaghari, "Synthesis of silver nanoparticles: chemical, physical and biological methods," Res Pharm Sci, Vol. 9, No. 6, p. 385, 2014.

[8] Z. S. Pillai and P. V. Kamat, "What factors control the size and shape of silver nanoparticles in the citrate ion reduction method?" Journal of Physical Chemistry B, Vol. 108, No. 3, pp. 945–951, 2004.

[9] X. Xin, C. Qi, L. Xu, Q. Gao, and X. Liu, "Green synthesis of silver nanoparticles and their antibacterial effects," Frontiers in Chemical Engineering, Vol. 4, p. 941240, 2022.

[10] S. Ahmed, Saifullah, M. Ahmad, B. L. Swami, and S. Ikram, "Green synthesis of silver nanoparticles using Azadirachta indica aqueous leaf extract," J Radiat Res Appl Sci, Vol. 9, No. 1, pp. 1–7, 2016.

[11] S. Ahmed, M. Ahmad, B. L. Swami, and S. Ikram, "A review on plants extract mediated synthesis of silver nanoparticles for antimicrobial applications: A green expertise," J Adv Res, Vol. 7, No. 1, pp. 17–28, 2016.

[12] M. T. MacDonald and V. R. Mohan, "Chemical Seed Priming: Molecules and Mechanisms for Enhancing Plant Germination, Growth, and Stress Tolerance," Curr Issues Mol Biol, Vol. 47, No. 3, p. 177, 2025.

[13] M. Faizan et al., "Nano-priming: Improving plant nutrition to support the establishment of sustainable agriculture under heavy metal stress," Plant Nano Biology, Vol. 10, p. 100096, 2024.

[14] W. Mahakham, A. K. Sarmah, S. Maensiri, and P. Theerakulpisut, "Nanopriming technology for enhancing germination and starch metabolism of aged rice seeds using phytosynthesized silver nanoparticles," Sci Rep, Vol. 7, No. 1, pp. 1–21, 2017.

[15] S. Pasieczna-Patkowska, M. Cichy, and J. Flieger, "Application of Fourier Transform Infrared (FTIR) Spectroscopy in Characterization of Green Synthesized Nanoparticles," Molecules, Vol. 30, No. 3, p. 684, 2025.

Numerical Evaluation of Concrete Filled Steel Box Composite Column

A.K.M. Ruhul Amin, Md. Khasro Miah* and Md. Mozammel Hoque

Department of Civil Engineering, Dhaka University of Engineering & Technology, Gazipur, Bangladesh

ABSTRACT

This study investigates the axial load behavior of concrete-filled fabricated steel box composite (CFSSBC) columns through a detailed parametric analysis. The primary objective is to evaluate how geometric and material parameters such as plate thickness (B/t), length-to-width ratio (L/B), and the compressive strengths of steel and concrete influence the structural performance of CFSSBC columns. A total of sixteen column specimens with varying geometric configurations were analyzed. Finite element analysis (FEA) was conducted using ANSYS software to simulate axial loading conditions, with material properties viz. modulus of elasticity and poison's ratio defined as 200GPa and 0.3 for steel, and 3750√f'c and 0.2 for concrete. Results revealed that increased confinement from steel plates significantly improves axial load capacity. The numerical results aligned closely with analytical predictions, confirming the accuracy of the simulation model. Furthermore, comparisons with design standards revealed that the AISC code offers more conservative estimates. This research provides valuable insights for optimizing CFSSBC column design in structural engineering applications.

1. INTRODUCTION

In recent decades, concrete-filled steel box composite columns have emerged as an essential component in structural engineering due to their superior strength, ductility, and energy dissipation capabilities. Among them, concrete-filled fabricated steel box composite (CFSSBC) columns are particularly promising, combining cast-in-place concrete with prefabricated steel box sections to form a highly efficient structural member. These columns eliminate the need for formwork, reduce construction time, and offer significant improvements in load-carrying capacity and stiffness. They are widely used in the construction of bridges, high-rise buildings, industrial structures, and infrastructures subjected to heavy axial and seismic loads. While CFST (Concrete-Filled Steel Tube) columns have been extensively researched, especially circular and rectangular hollow sections, the fabricated square steel box configuration remains underexplored, particularly with non-conventional materials such as brick aggregate concrete. Most existing studies have concentrated on standardized steel profiles and high-quality concrete mixes, without sufficient investigation into regionally available materials and fabrication-based steel geometries, which are often used in developing countries to reduce construction costs.

Moreover, key geometric parameters, such as the plate width-to-thickness ratio (B/t) and column slenderness ratio (L/B), are known to have a significant influence on both confinement behavior and buckling resistance. However, the combined effect of these parameters on the ultimate axial strength and ductility of CFSSBC columns has not been systematically addressed. In addition, design codes like AISC, ACI, and Eurocode 4 (EC4) provide general design formulations for composite columns, but their accuracy and conservativeness in predicting the axial capacity of fabricated square steel box columns filled with concrete remain questionable.

These research gaps suggest a need for a comprehensive and comparative study focusing on the parametric behavior of CFSSBC columns under axial loading. Understanding how varying the material properties of steel and concrete, along with geometric ratios, impacts the axial capacity and confinement efficiency is critical for advancing design practices and validating or modifying existing code provisions. Fig. 1 shows that the cross section of the composite column.

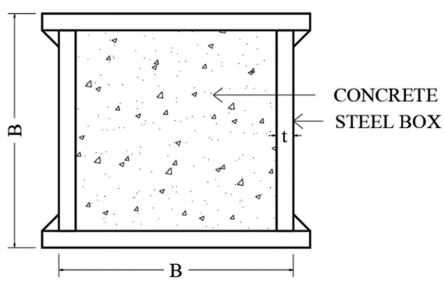

Fig. 1: Concrete Filled Steel Box Section Column

*Corresponding author's email: mkhasro@duet.ac.bd

This study aims to **investigate the axial compressive behavior** of CFSSBC columns through a combination of **numerical modeling and parametric analysis**. A total of 16 (sixteen) square column specimens were considered with varying:

- Plate thickness (B/t);
- Slenderness ratio (L/B);
- Concrete compressive strength;
- Steel yield strength.

Finite element analysis (FEA) was used to simulate the axial loading behavior and to evaluate the confinement effect provided by the fabricated steel box. The study also compares the results with the analytical predictions based on current design codes to assess their level of conservativeness and applicability.

Through this research, **new insights** are provided for:

- Enhancing the axial load design of CFSSBC columns;
- Understanding the confinement mechanisms in fabricated box systems;
- Assessing the suitability of international codes for non-standard columns.

Ultimately, this work aims to contribute toward more efficient and economical composite column designs, particularly in regions where custom-fabricated steel boxes and local aggregate concrete are commonly used.

A numerical investigation using finite element analysis (FEA) of concrete-filled steel box columns was performed. The materials used for the steel plate's strength are Q345, and the compressive strength of the concrete is 46MPa. ANSYS FEA software was used to conduct the finite element (FE) model, employing SOLID45 and SOLID65 elements to represent steel and concrete materials. The cracked and crashed concrete structure was checked using the William-Warnke five parameters rule. The finite element results shows that both the strength increasing coefficient of restrained concrete and the bearing capacity increasing coefficient decrease as the width-to-thickness ratio increases [1]. It was studied numerically using a steel yield strength of 235MPa and a concrete compressive strength of 62.3MPa on a double-skinned composite tube shaft that was put under an axial compressive load [2].

A study was conducted on square CFST columns subjected to concentric loading, using different grades of concrete and varying lengths to width ratios. ANSYS FEM software was used for numerical analysis, and the results show a good match with EC4 (1994) [3]. The behavior of high-strength steel box columns under axial compression is examined using steel plate materials with a strength of 460 MPa. Maximum column strength is affected by initial geometric imperfections and residual stresses [4]. ANSYS finite element analysis software was used to do a numerical study of the cycle behavior of eccentrically compressed steel box columns that were loaded cyclic horizontal loading, [5]. An experimental and numerical investigation on the concrete-filled stainless-steel column exposed to fire. The compressive strength of concrete used 41MPa to 46MPa and the maximum temperature used 800°C. The ABAQUS finite element software was used to conduct the thermal-stress analysis [6].

The eight-node SOLID45 element was used to model steel materials in the 3D numerical model, and the SOLID65 element was used to model concrete materials. The TARGE170 and CONTA173 elements were used to model how steel and concrete interact with each other. In conclusion the finite element model predicts the axial capacity of the columns [7]. A parametric study was conducted on CFST column with the use of different strength steel and concrete using constant height of 400mm with 150mm diameter specimen. The findings were a significant increase of the ultimate capacity of the CFST column by a smaller D/t ratio [8, 9].

A numerical study was done using square concrete-filled double steel tube short columns that were loaded eccentrically. The yield strength of the steel was 345MPa to 412MPa, and the compressive strength of the concrete was 19MPa to 20MPa. [10-12]. A nonlinear numerical analysis was done, and an equation was suggested for the axial loading capacity of a concrete filled steel tube column with initial imperfection [13]. An experimental, parametric and numerical study conclude the capacity due to various L/D ratios of 3, 4, 5 and 6. Local buckling mode of failure observed in all the specimen. ANSYS v18 finite element software was used to model the steel tube columns. A parametric study was conducted to verify the numerical results and the finite element modeling show the efficient comparison with the experimental results [14].

2. PARAMETRIC STUDY

Before conducting the parametric investigation, the finite element (FE) model was validated against experimental data to ensure its accuracy in simulating the axial behavior of concrete-filled fabricated steel box composite (CFSSBC) columns. The comparison focused on ultimate axial load capacity, load–displacement behavior, and failure modes. The results from the FE model closely matched the experimental observations, demonstrating the model's reliability. This validation establishes

confidence in using the FE model for further parametric exploration. Fig. 2 shows the cross section of parametric column specimen.

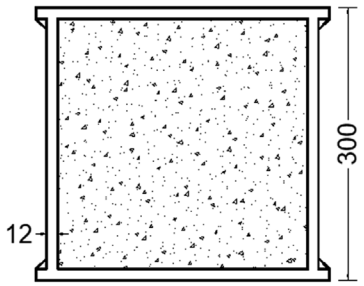

Fig. 2: Cross-section of Parametric Column Specimen

The aim of the parametric study is to systematically investigate how critical design variables influence the axial load behavior of CFSSBC columns. Parameters such as plate thickness (B/t), slenderness ratio (L/B), concrete compressive strength (f'c), and steel yield strength (fy) of sixteen column specimen as shown in Table I, have significant effects on the structural performance of composite columns. Through numerical modeling, the study evaluates how variations in these parameters affect the column's confinement efficiency, load capacity, and buckling behavior. The results also help assess the applicability and conservativeness of existing design standards (e.g., AISC, EC4). The CFSSBC columns were modeled using ANSYS Workbench with the following material properties and modeling techniques:

- **Steel:** Modeled using the 8-node SOLID185 element with bilinear isotropic hardening. The modulus of elasticity was set to 200GPa, and Poisson's ratio was 0.3. Four different yield strengths were used: 250MPa, 345MPa, 415MPa, and 500MPa;
- **Concrete:** Modeled with the SOLID65 element to simulate nonlinear behavior, including the Drucker Prager Damage Plasticity model. The modulus of elasticity was estimated using Ec as $3750\sqrt{fc'}$, and Poisson's ratio was 0.2. Concrete compressive strengths varied from 21MPa to 41MPa;
- **Interaction:** The steel–concrete interface was modeled using surface-to-surface contact with friction to allow for load transfer while capturing interface slip effects. TARGE170 and CONTA173 elements were used to define the contact behavior.

A total of sixteen CFSSBC columns were modeled and grouped into four parametric sets to investigate the effects of different variables:

- **Group G1 (B/t variation):** Explored the influence of plate thickness (6mm, 8mm, 10mm, 12mm), affecting B/t ratios from 50 to 25, while keeping other parameters constant;
- **Group G2 (L/B variation):** Examined the influence of slenderness by varying column lengths (3 m to 6 m), corresponding to L/B ratios of 10 to 20, with constant plate thickness;
- **Group G3 (Concrete strength variation):** Investigated the impact of different concrete compressive strengths (21MPa to 41MPa) on axial capacity;
- **Group G4 (Steel strength variation):** Analyzed the effect of varying steel yield strength (250MPa to 500MPa) on load behavior and confinement.

Table I: Geometric and Materials Parameters of Specimens

SL	SP ID	B (mm)	t (mm)	L (mm)	B/t	L/B	f'c (MPa)	fy (MPa)
1	G106	300	6	3000	50	10	21	250
2	G108	300	8	3000	38	10	21	250
3	G110	300	10	3000	30	10	21	250
4	G112	300	12	3000	25	10	21	250
5	G212L3	300	12	3000	25	10	21	250
6	G212L4	300	12	4000	25	13	21	250
7	G212L5	300	12	5000	25	17	21	250
8	G212L6	300	12	6000	25	20	21	250
9	G312C21	300	12	3000	25	10	21	250
10	G312C28	300	12	3000	25	10	28	250
11	G312C35	300	12	3000	25	10	35	250
12	G312C41	300	12	3000	25	10	41	250
13	G412S250	300	12	3000	25	10	21	250
14	G412S345	300	12	3000	25	10	21	345
15	G412S415	300	12	3000	25	10	21	415
16	G412S500	300	12	3000	25	10	21	500

All models were simulated in ANSYS using displacement-controlled loading under axial compression. Boundary conditions were applied such that:

- One end was fully fixed to prevent displacement and rotation;
- The other end was free in rotation and horizontally restrained, but loaded axially downward.

A nonlinear buckling analysis was also conducted to determine the critical buckling load and to observe post-peak behavior. Numerical results were later compared with analytical predictions to assess the influence of parameters and evaluate code predictions.

2.1 Codes and Standards

Concrete-filled fabricated steel box composite (CFSSBC) columns are governed by several international design standards that provide guidelines for calculating their structural strength and behavior. Among them, the most commonly referenced are:

- **ACI 318-14** Building Code Requirements for Structural Concrete (American Concrete Institute);
- **AISC 360-16** Specification for Structural Steel Buildings (American Institute of Steel Construction);
- **Eurocode 4 (EN 1994-1-1:2004)** – Design of Composite Steel and Concrete Structures (European Committee for Standardization).

These standards outline methods to predict the axial load-bearing capacity of composite columns based on the material properties of concrete and steel, geometric dimensions, and structural interaction. They are widely used in practice due to their reliability and code-based safety factors.

In this study, the results from the finite element analysis (FEA) were compared with predictions derived from AISC 360-16 and Eurocode 4 to assess the conservativeness and applicability of each design approach for CFSSBC columns.

The AISC 360-16 "Specification for Structural Steel Buildings" from the American Institute of Steel Construction (AISC) has the design formulae for steel box composite columns that are filled with concrete. The following equation can be used to find the theoretical axial strength of a steel box composite column filled with concrete:

$$P_n = P_{n0}\left[0.685^{\left(\frac{P_{n0}}{P_e}\right)}\right] \quad (1)$$

$$P_{n0} = \left[A_s f_y + A_{sr}\, f_{ysr} + 0.85\, f_{cu} A_c\right] \quad (2)$$

$$P_e = \pi^2 EI_{eff}/KL^2 \quad (3)$$

$$P_u = A_s f_y + A_c\, f'_c \quad (4)$$

where,

Ac = area of concrete mm2;
Asr = area of continuous reinforcing bars, mm2;
As = area of steel section, mm2;
EIeff = effective moment of inertia rigidity of composite section, Kip-mm2;
fcu = specified minimum concrete compressive strength, MPa;
fy = yield stress of steel section, MPa;
fysr = specific minimum yield stress of reinforcing bars, MPa;
K = effective length factor;
L = laterally unbraced length of the member, mm.

2.2 Uses of Steel Plate

The used adjustable column was 300mm x 300mm, which made a total gross area of 90,000mm^2. Because plates are not all the same width, the areas for steel and concrete are not all the same. The estimated steel area for a 6mm plate is 3,564mm^2, which is 3.96% of the gross area. This is the smallest amount of steel used in the parametric columns. For example, when the plate is 12 mm thick, the steel percentage goes up to 7.84%, which is the highest in this study. These percentages are higher than the minimum standards set by the codes, which say that steel must make up at least 1% of the gross area.

2.3 Concrete Parameters

As part of the parametric study, brick aggregate concrete was used to figure out the factors for the concrete. According to the Bangladesh National Building Code (BNBC 2020), the modulus of elasticity for this concrete can be found using the equation 3750√f'c. The limits for strength ranged from 21Mpa to 41Mpa, and the poison ratio was set at 0.2. For the numerical study, all parametric columns were simulated with the same set of parameters.

3. RESULTS FROM NUMERICAL ANALYSIS

3.1 Effect of B/t Ratio

Although design codes provide general limits for B/t ratios, they do not fully address the nonlinear confinement effects that arise in composite columns with fabricated box sections. Therefore, a detailed parametric study was carried out to evaluate how plate thickness influences axial load capacity beyond simplified code assumptions. The ratio of width to thickness, B/t, is based on the width of the CFFSBC columns and the thickness of the walls or plates used to make the box section. Four different plate thicknesses are used so that the ratios of width to thickness (B/t) stay between 25 and 50. Other factors stay the same, such as the L/B ratio and the strengths of the concrete and steel. As shown in Table II, the B/t ratios were used in four parametric columns in Group G1. Table II also shows the analytical capacity of different methods and the numerical capacity of ANSYS software.

The ultimate capacity of the specimen is calculated from equation 5, the results are defined by $P_{n,\,EC4}$. The effect of B/t ratio on the ultimate capacity of the column is explored in the axial capacity increased as shown in Table II. When the B/t ratio is changed from 50 to 25, the CFFSBC column's maximum vertical capacity goes up by 48%. The $P_{num}/P_{n,EC4}$ ratio shows that the numerical simulation result is well matched with the ultimate capacity of all the specimen from Code provided equation. The load-displacement curve is made from the numerical results for the different plate thicknesses shown in Fig. 3. From Table II, it is observed that the column's axial strength goes down as the B/t ratio goes up. The smaller B/t ratio seen when thicker plates are used, which increases the amount of steel in the column and makes it stronger along its length. The analytical capacity of the column is calculated form the equation:

$$P_{n,Ec4} = A_c f_c + A_s f_y + A_{sr} f_{yr} \tag{5}$$

Raghabendra and Chen [8] did a parametric study with 13 specimens that were all the same size: 400 mm in height and 150 mm wide. Plates of different thicknesses and strengths of steel and concrete were used. The load displacement curve from their work is shown in Fig. 4. The curve shows that the higher the capacity, the lower the D/t ratio. This was also seen in this study.

Table II: Load Carrying Capacity of Specimens Having Different B/t ratios

SL	SP ID	B (mm)	t (mm)	L (mm)	B/t	L/B	$P_{n,ACI}$ (kN)	$P_{n,AISC}$ (kN)	$P_{n,EC4}$ (kN)	P_{Num} (kN)	$P_{Num}/P_{n,EC4}$	Capacity increase
1	G106	300	6	3000	50	10	3299	3149	3560	3618	1.02	1.00
2	G108	300	8	3000	38	10	3872	3706	4126	4145	1.00	1.15
3	G110	300	10	3000	30	10	4449	4265	4696	4718	1.00	1.31
4	G112	300	12	3000	25	10	5032	4825	5272	5295	1.00	1.48

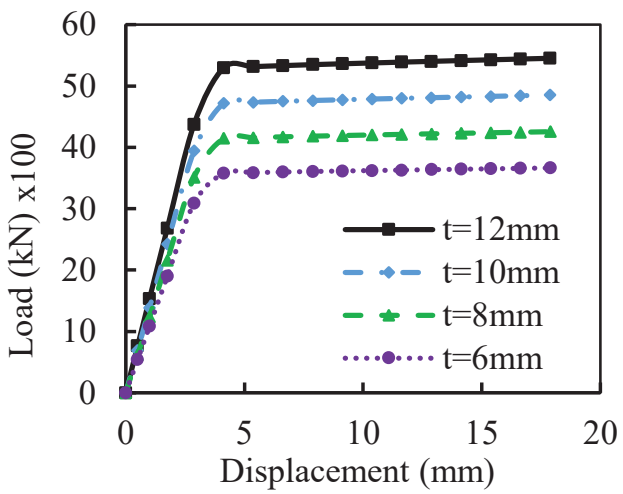

Fig. 3: Load Displacement Curve for Different Plate Thickness

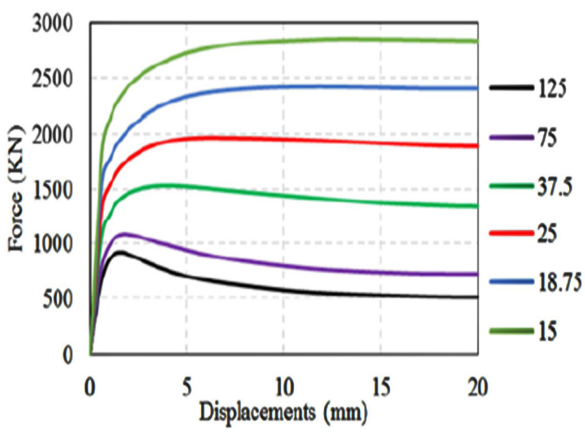

Fig. 4: Load Displacement for Different D/T Ratio [8]

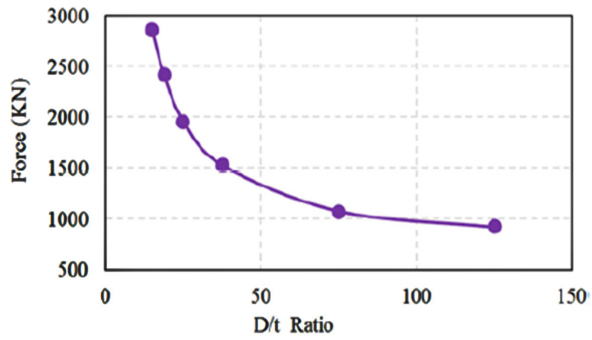

Fig. 5: Capacity Curve for Different B/t Ratios

In this study, Fig. 5 displays the axial strength capacity curve. The analytical capacity was found using the equation given by Eurocode EC 4. The ACI code equation capacity and the numerical capacity from the ANSYS FEM software were also looked into. The number result is very close to the value that the EC 4 code calculated. The capacity curve shows that the higher the B/t ratio, the smaller the capacity. This is also seen in the capacity curve of Raghavendra and Chen, which can be seen in Fig. 6. It is observed that while the numerical results closely match EC4 predictions, the enhanced confinement effect and localized buckling control due to thicker plates are not explicitly captured by the code equations. This highlights the need for such numerical studies to refine design understanding, especially for non-standard configurations.

3.2 Effect of L/B Ratio

Slenderness effects are often underrepresented in current design codes, especially for composite columns. This study examines how varying the L/B ratio affects load behavior, stability, and ductility using validated numerical models. The column specimen's length was varied from 3m to 6m to see how the column's axial strength changed. The L/B ratio factors change when the column length (L) changes. For each L/B ratio, ACI methods were used to figure out the column's axial strength. Fig. 7 displays the load-displacement curves of CFFSBC columns for group G2 that have various L/B ratios. The maximum capacity of the column doesn't change because the code doesn't include the effect of length in its formulas. But there is a change in the displacement; the highest sectional capacity stayed in the same line, but the displacement is changing. This shows that the column's ductility changes. In Table III, one can see the exact results for static analysis and the ACI code analytical results. It was seen that the numerical simulation results were a little higher than the ACI code analysis results. This is because the numerical simulation used the full strength of the materials. It was used a strength reduction factor in the ACI code to lower the strength.

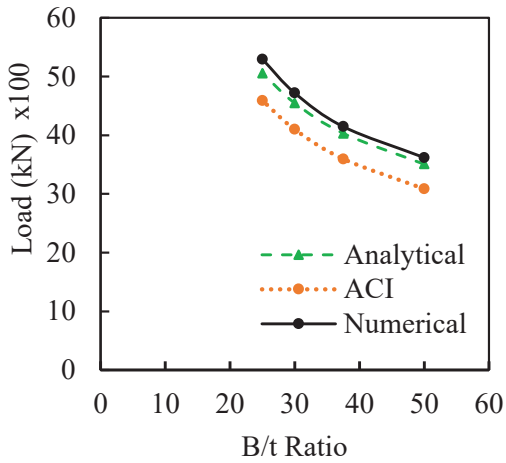

Fig. 6: Capacity Curve for Different D/t Ratios [8]

Table III: Capacity Different L/B (Static Analysis)

SP ID	L/B	$P_{n,ACI}$(kN)	P_{Num}(kN)	P_{Num}/P_{Ana}
G212L3	10	5272	5295	1.00
G212L4	13	5272	5293	1.00
G212L5	17	5272	5293	1.00
G212L6	20	5272	5290	1.00

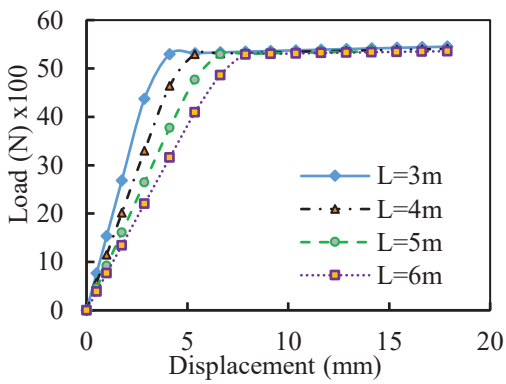

Fig. 7: Load Displacement Curve for Different L/B ratios

The ANSYS WORKBENCH also used the Eigen buckling analysis tool to do the buckling analysis. In group G2, the length of the columns was changed, but all other factors remained the same. The buckling analysis results with various L/B ratios are shown in Table IV. In Fig. 8, the relationship between load capacity and L/B ratios is displayed. The Eigen bending behavior of a numerical

model is shown Fig. 9. In 2014, Bhushan and Mohite did a parametric study on a square CFST column with columns of different lengths. For numerical research, they use Euler's formula and the software ANSYS FEM. Fig. 10 displays the impact of changing L/B on the column's axial capacity, which is in line with this study.

Table IV: Capacity for Diff. L/B (Buckling Analysis)

SP ID	L/B	$P_{e,ACI}$(kN)	P_{Num}(kN)	$P_{Num}/P_{e,ACI}$
G212L3	10	52345	55605	1.06
G212L4	13	29444	31711	1.08
G212L5	17	18844	20720	1.10
G212L6	20	13072	14230	1.09

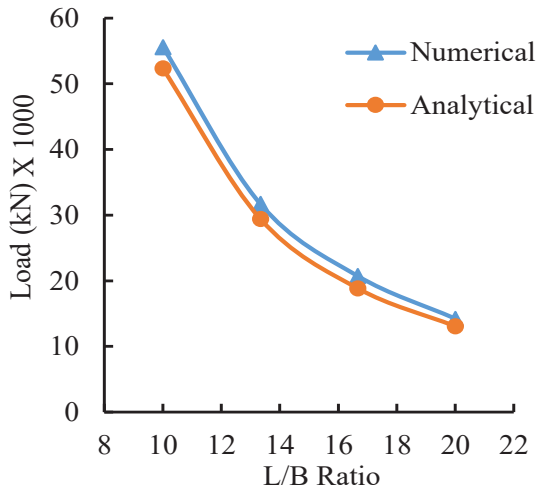

Fig. 8: Effect of L/B Ratio

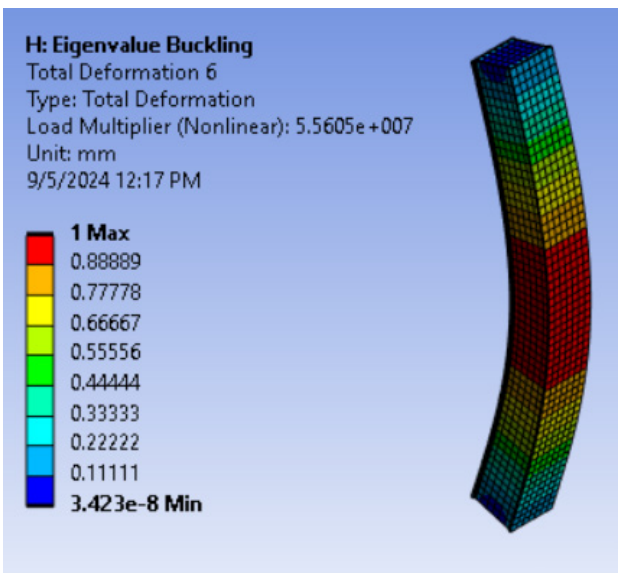

Fig. 9: Eigenvalue Buckling Plot

3.3 Effect of Concrete Strength

While codes assume linear improvements in strength with increasing f'_c, the interaction of high-strength concrete with steel plates in confined sections can exhibit nonlinear gains. Hence, a parametric analysis is essential to understand this behavior. The compressive strength of concrete is a key part of designing and studying composite columns. The compressive strength of concrete is one of the most important factors for the parametric study, and it also has a significant effect on how much load a column can withstand. For composite columns, the compressive strength of the concrete plays a vital role in determining the load-bearing capacity and stability of the column.

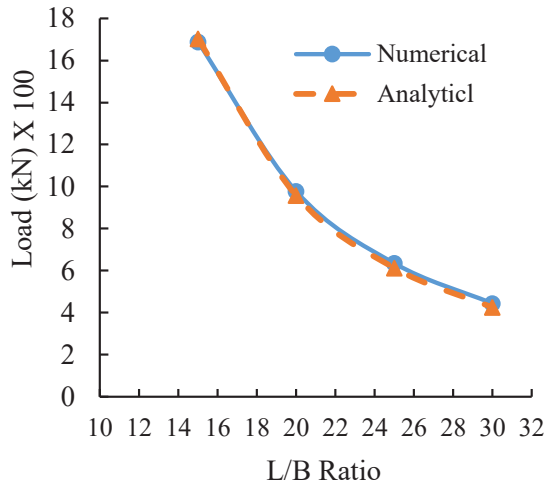

Fig. 10: Effect of L/B ratio (Bushan and Mohite)

Composite columns are made of both concrete and steel. They usually look like a steel section enclosed in concrete or a steel box filled with concrete (CFSB). By putting these two materials together, the column can benefit from both of their strengths: the crushing strength of concrete and the tensile strength and flexibility of steel. Table V shows the effect of changing the strength of concrete. It can be seen in Fig. 11 that the numerical load displacement curve for various f'_c is shown, and in Fig. 12, the capacity curve for various f'_c is shown.

Table V: Capacity of Different f'_c

SP ID	f'_c(MPa)	P_{Ana}(kN)	P_{Num}(kN)
G312C21	21	5272	5292
G312C28	28	5805	5810
G312C35	35	6338	6345
G312C41	41	6795	6814

3.4 Effect of Steel Strength

Design standards include basic provisions for steel yield strength, but do not capture how higher strength steel affects confinement, failure mode, or composite interaction. This study explores these effects numerically for a wide range of f_y values. A very important thing to think about when designing and evaluating composite columns is how strong the steel plates are. The steel's tensile strength is an important factor in parametric studies and has a significant effect on how much load composite columns can carry. The strength of the steel plate in a composite column denotes its capacity to endure compressive loads that aim to diminish its dimensions.

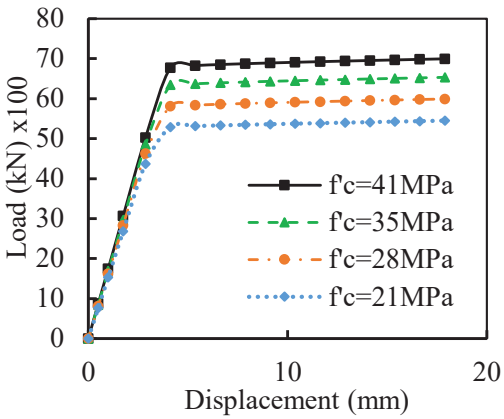

Fig. 11: Load Displacement Curve

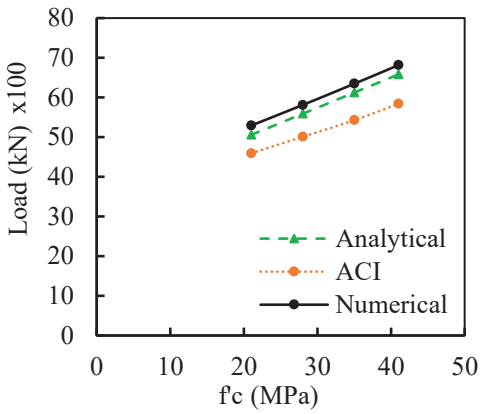

Fig. 12: Capacity Curve for Different $f'c$

Table VI: Capacity of Different f_y

SP ID	fy (MPa)	P_{Ana} (kN)	P_{Num} (kN)
G412S250	250	5272	5302
G412S345	345	6667	6708
G412S415	415	7695	7752
G412S500	500	8944	9013

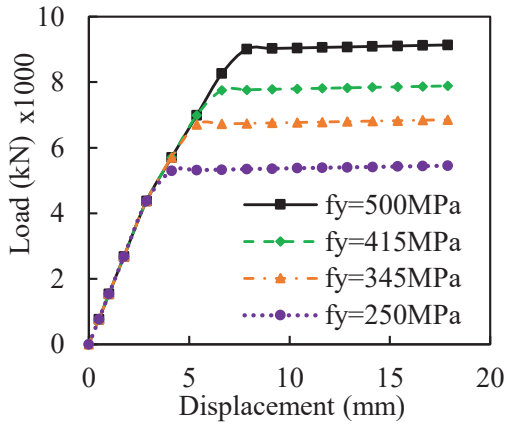

Fig. 13: Load Displacement Curve

The strength of steel plates is a vital consideration in the design and evaluation of composite columns. The tensile strength of the steel in composite columns is important for figuring out how much load they can carry and how stable they are. The results of the steel strength variance are shown in Table VI. Fig. 13 shows the numerical load-displacement curve, and Fig. 14 shows the capacity curve for steels of different strengths.

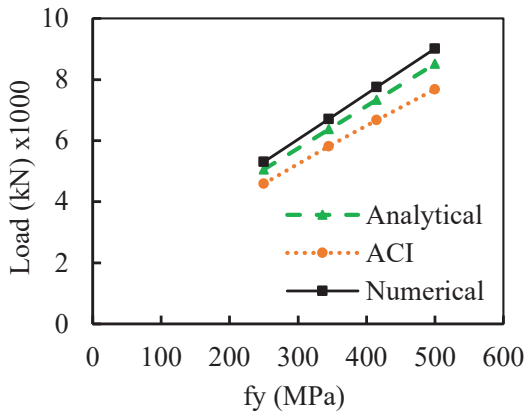

Fig. 14: Capacity Curve for Different f_y

4. CONCLUSION

In conclusion, the parametric study provides a comprehensive evaluation of how geometry and material characteristics influence the axial performance of CFSSBC columns. Although comparisons were made with existing design codes (ACI 318, AISC 360-16, and EC4), these standards have limitations in handling slenderness, local buckling, and high-strength materials. The finite element simulations, validated through experimental data, offer a more refined analysis of composite column behavior, supporting the need for future improvements in code formulations.

Here is a Summary of the Main Findings:

- When the axial capacities were estimated using various design codes, it was found that the AISC code is the most conservative of the bunch;
- Out of all the design codes, EC4 had the highest axial capacity, and the numerical results were very close to those of the EC4 code;
- The ACI code includes a strength reduction factor that makes the calculated capacities lower than the ultimate values. However, compared to the AISC code, they are slightly higher than the real capacities;
- The axial strength of CFFSBC columns increased as the B/t ratio dropped down because the thicker the steel plates made the columns stronger;
- Increasing the axial capacity of the columns happened when the L/B ratio decreasing;
- The numerical simulations closely matched the analytical results, and the variations observed were within acceptable limits.

AKNOWLEDGEMENTS

The authors acknowledge their earnest thankfulness to the Department of Civil Engineering, Dhaka University of Engineering & Technology, Gazipur, for their support and cooperation in conducting the experimental and numerical research works. Without the never-ending support, this research work would not have been finalized.

REFERENCES

[1] J. Zhang, Y. Liu, J. Yang and K. Xu, "Experimental research and finite element analysis of concrete-filled steel box columns with longitudinal stiffeners," Advance Materials Research, Vol. 287-290, pp. 1037-1042. 2011.

[2] W. b. Yuan, and J. j. Yang, "Experimental and numerical studies of short concrete-filled double skin composite tube columns under axially compressive loads," Journal of Construction Steel Research, Vol. 80, pp. 23-31. 2013.

[3] H. Bhushan, and P. M. Mohite, "Parametric study of square concrete filled steel tube columns subjected to concentric loading," International Journal of Engineering Research and Application. Vol. 4, Issue 8, pp. 109-112. 2014.

[4] Y. B. Wang, G. Q. Li, C. Su-Wen and S. Fei-Fei, "Experimental and numerical study on the behaviour of axially compressed high strength steel box-columns," Engineering Structures, 58, 79-91. 2014.

[5] Y. Luo and H. Li, "Experimental and numerical study on cyclic behaviour of eccentrically-compressed steel box columns," Thin-Wall Structures, Vol. 96, pp. 269-285. 2015.

[6] Z. Tao, M. Ghannam, T. Y. Song and L. H. Han, "Experimental and numerical investigation of concrete-filled stainless-steel columns exposed to fire," Journal of Constructional Steel Research, Vol. 118, pp. 120-134. 2016.

[7] P. K. Gupta, Z. Khaudhair and A. K. Ahufa, "3D Numerical Simulation of Concrete-Filled Steel Tubular Columns Using ANSYS," UKIERI Concrete Congress-Innovations in Concrete Construction, 2017.

[8] R. Yadav and B. Chen, "Parametric study on the axial behaviour of concrete filled steel tube (CFST) columns," American Journal of Applied Scientific Research, Vol. 3, No. 4, pp. 37-41. 2017.

[9] K. B. Manikandan and C. Umarani, "Parametric study of CFST columns by numerical mock-up," Materials Today: Proceedings, Vol. 45, Part 7, pp. 6021-6027, 2021.

[10] M. Ahmed, Q. Q. Liang, V. I. Patel and M. N. Hadi, "Experimental and numerical studies of square concrete-filled double steel tubular short columns under eccentric loading," Engineering Structure, Vol. 197, p. 109419. 2019.

[11] K. Y. Ning, L. Yang, H. Y. Ban, and Y. N. Sun, "Experimental and numerical studies on hysteretic behaviour of stainless-steel welded box-section columns," Thin-Walled Structure, Vol. 136, pp. 280-291, 2019.

[12] X. Tang, Y. Yang, W. L. Yang, and Y. F. Chen, "Experimental and numerical investigation on the seismic behaviour of plane frames with special-shaped concrete-filled steel tubular columns," Journal of Building Engineering, Vol. 35, p. 102070, 2021.

[13] H. Ahmad, M. F. Ejaz, and M. Aslam, "Nonlinear numerical analysis and proposed equation for axial loading capacity of concrete filled steel tube column with initial imperfection," Structural Monitoring and Maintenance, Vol. 9, pp. 81-105, 2022.

[14] M. I. S. Shaik, and G. M. Ganesh, "Impact of diameter to thickness D/t on axial capacity of circular CFST column: Experimental, parametric and numerical analysis," International Journal of Applied Science and Engineering, Vol. 19, No. 2, p. 2021486, 2022.

[15] EN 1994-2:2004 Eurocode 4. Design of composite steel and concrete structures – Part 1-1: Genera rules and rules for buildings, 2004.

[16] Building code requirements for structural concrete (ACI 318), American Concrete Institute, 2007.

[17] Specification for structural steel building: Load and resistance factor design (ANSI/AISC 360-16), American Institute of Steel Construction, 2016.

[18] Bangladesh National Building Code, Bangladesh Standard and Testing Institution, 2020.

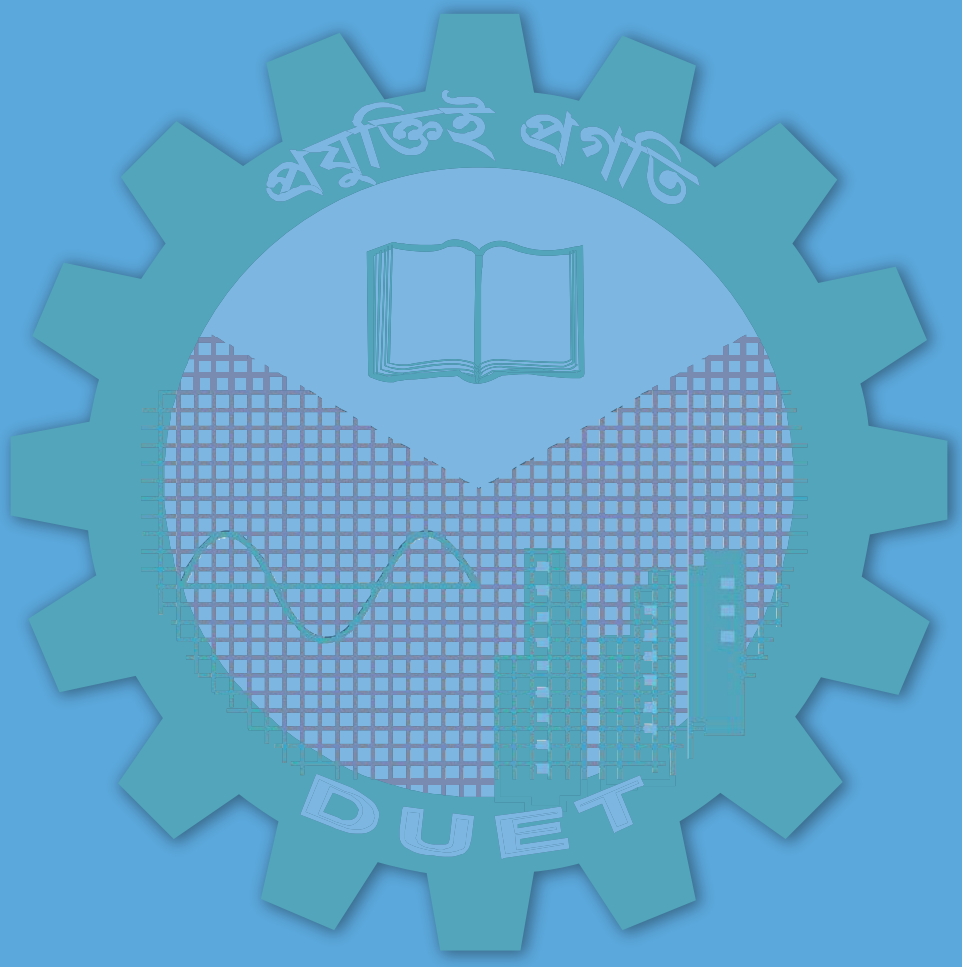

Please visit site: journal.duet.org